Synthesis and Study of the Cyclic Lipopeptide Antibiotics Daptomycin and A54145

by

Ryan Moreira

A thesis
presented to the University of Waterloo
in fulfillment of the
thesis requirement for the degree of
Doctor of Philosophy
in
Chemistry

Waterloo, Ontario, Canada, 2022

Examining Committee Membership

The following served on the Examining Committee for this thesis. The decision of the Examining Committee is by majority vote.

External Examiner
Dr. John Vederas, PhD,
University Professor, University of Alberta
Chemistry

Supervisor
Dr. Scott D. Taylor, PhD
Professor, University of Waterloo
Chemistry

Internal-external member
Dr. Trevor Charles, PhD
Professor, University of Waterloo
Biology

Other Members
Dr. Gary Dmitrienko, PhD
Professor Emeritus, University of Waterloo
Chemistry

Dr. Adrian Schwan, PhD
Professor, University of Guelph
Chemistry

Author's Declaration

This thesis consists of material all of which I authored or co-authored: see Statement of Contributions included in the thesis. This is a true copy of the thesis, including any required final revisions, as accepted by my examiners.

I understand that my thesis may be made electronically available to the public.

Statement of Contributions

Ryan Moreira is the sole author for chapters 1,3,5-7, and 10-11, and is the primary author and contributor for all chapters presented in this thesis. All chapters with the exclusion of chapter 7 are either published at the time of writing or are in-press. Chapter 7 is currently being expanded upon and adapted for publication. All chapters were written under the supervision of Dr. Scott Taylor. Additional details regarding contributions are included in a preface for each chapter when appropriate.

Abstract

Daptomycin (dap) is a clinical antibiotic used to treat infections with multi-drug resistant Gram-positive bacteria. Despite nearly 20 years of clinical use, the action mechanism of this important peptide is not fully understood. However, it is known that dap targets the bacterial membrane to which it binds in a calcium and phosphatidylglycerol (PG, an anionic membrane lipid found in bacteria) dependent manner. More recent works on dap suggested that it may possess a chiral target, but the identity of this chiral target was unknown.

A54145D (A5D) is a peptide natural product related to dap in both structure and function. Like dap, A5D requires calcium and PG for membrane insertion. In contrast to dap, A5D is not as greatly inhibited by lung surfactant (LS) and thus A5D was deemed a lead compound for the development of a treatment for community acquired bacterial pneumonia (CAP). To date no clinical drugs have come out of these efforts and no explanation for the difference in the antagonism of dap and A5D in the presence of lung surfactant has been forthcoming.

To better elucidate the mechanism of action of these peptides, we set out to determine if they have a chiral target and if this chiral target is a stereoisomer of PG. Preliminary investigations done using synthetically accessible dap analogs and stereochemically impure samples of PG suggested that dap and PG may participate in a chiral interaction, warranting further investigation with dap and stereochemically pure samples of PG. To this end, we aimed to synthesize dap, A5D and their unnatural enantiomers, as well as the 4 stereoisomers of PG.

Enroute to a new synthesis of dap and its unnatural enantiomer (ent-dap), we developed a highly efficient, enantiospecific and diastereoselective synthesis of (2S,3R)- and (2R,3S)-methylglutamate (an unusual amino acid found in dap) suitably protected for solid-phase peptide synthesis (SPPS). This route was used to prepare multigram quantities of each aforementioned isomer of methylglutamate.

A new synthesis of dap was developed which overcame many of the shortcomings of pervious routes. Key to the development of this synthesis was the elucidation of an unprecedented side reaction involving a central building block. Modification of this building block rendered it stable to Fmoc SPPS and led to the first truly efficient synthesis of daptomycin. This route was used to prepare dap and ent-dap.

Bioactivity assays of dap and ent-dap revealed that dap is approximately 85-fold more active than ent-dap strongly supporting the proposal that dap interacts with a chiral molecule as part of its mechanism of action. To determine if this molecule is a stereoisomer of PG, we developed a stereospecific synthesis of PG which gave access to all 4 stereoisomers. Using these lipids, we demonstrated that dap recognizes both stereocenters of PG but is more sensitive to the stereocenter at the headgroup of this lipid. Using circular dichroism and fluorescence, we determined that lipid stereochemistry influences the membrane affinity, backbone conformation and oligomerization of dap. Since these are all predictors of antibacterial activity, we concluded that the chiral target of dap is 2R,2'S-PG – the naturally most abundant stereoisomer of this lipid.

The interaction between dap and PG emerged as central to the antibacterial action of dap and thus we set out to establish a structure-activity relationship between these two molecules. To this end, 9 modified PGs were prepared. Modification to the headgroup of PG was found to substantially affect membrane affinity, backbone conformation and oligomerization. The data collected suggests that daptomycin envelops the headgroup of PG and possesses unique binding

sites for each hydroxyl group at the headgroup of this lipid. Shortening the acyl tails of PG demonstrated that PGs containing two saturated, linear tails of 8 carbons in length are needed for binding at micromolar concentrations. Furthermore, these data demonstrate that incorporation of PGs into a lipid membrane and preassembly of PGs are not perquisites for daptomycin-PG interactions.

Dap resistant strains of bacteria often possess mutations to an enzyme involved in the lysinylation of PG converting it to lysyl-PG. Despite considerable efforts by many research groups, it is currently unclear how increased lysyl-PG content can confer dap resistance. Our structure-activity study suggested that lysinylation of PG may confer resistance to dap by effectively masking PG thereby reducing the number of binding sites for dap. To investigate this hypothesis, we developed a stereospecific synthesis of lysyl-PG and explored how the presence of lysyl-PG in PG-containing model membranes affected the affinity and membrane bound state of daptomycin. We found that dap possesses a substantially reduced affinity for lysyl-PG compared to PG confirming the plausibility of the masking hypothesis; however, the collected data does not provide a compelling explanation for observed levels of dap resistance when the quantities of lysyl-PG in resistant strains of bacteria are considered.

We aimed to determine whether A5D targets the same stereoisomer of PG as dap by developing a total synthesis of A5D. We achieved the total synthesis of this natural product and I contributed to this effort by developing new routes to the unusual amino acids present in A5D. Key to the synthesis of these building blocks was the development of conditions for the Sharpless asymmetric aminohydroxylation reaction which allowed for the preparation of Fmoc-protected 1,2-aminoalcohols. Through reaction scoping, we were able to demonstrate that these conditions yield products with enantio- and regioselectivities that rival the classical reaction conditions. The scoping study resulted in the discovery of a substrate well-suited for the synthesis of the unusual amino acids present in the unnatural enantiomer of A5D (ent-A5D).

Bioactivity studies on A5D and ent-A5D revealed that A5D is 32-fold more active than ent-A5D proving that A5D possesses a chiral target. To determine if this chiral target is a stereoisomer of PG, we prepared a fluorescently labelled analog of A5D using some of the synthetic methodology we previously developed. This analog of A5D was found to have nearly identical antimicrobial activity compared to the natural product. Using this analog, it was determined that PG stereochemistry influences the membrane affinity, backbone conformation and oligomerization of A5D. A5D possessed a strong preference for 2R,2'S-PG and thus it was concluded that 2R,2'S-PG is the chiral target of A5D.

LS contains high concentrations of PG; thus, it was hypothesized that PG is responsible for the antagonism of dap and A5D, and the activity difference of these peptides in the presence of LS is due to a difference in how each peptide binds to the different stereoisomers of PG. To investigate this hypothesis, we determined the stereochemical content of PG in mammalian LS using a new approach and found that it consisted solely of 2R,2'S-PG which is preferred by dap and A5D. Binding studies revealed that each peptide binds to this lipid with a μM dissociation constant. Reinvestigation of the claim that dap and A5D possess different activities in the presence of LS were found to contradict previous reports. Indeed, antagonism studies on dap, A5D and analogs thereof demonstrated that each peptide is antagonised equally by LS and the antagonism is fully explained by a sole interaction with PG.

Acknowledgements

This thesis would not be completed in its current form without the assistance of many. I thank Prof. Scott D. Taylor for his example, support and genuine enthusiasm for scientific inquiry. It has been a pleasure to share my excitement for research with him. I thank all the members of my examining committee for their contributions. Dr. Gary Dmitrienko and Dr. Adrian Schwan for providing critical feedback on my work and for insightful discussions throughout. Dr. John Vederas and Dr. Trevor Charles for taking the time to read and discuss this thesis. I extend my gratitude to my former committee members: Dr. Michael Palmer for nurturing my budding interest in biophysical chemistry and Dr. Scott Hopkins for his support and encouragement over the years.

I thank my fellow Taylor lab members: Dr. Braden Kralt for his example, friendship and his tireless perseverance during the harrowing total synthesis of A54145 factor D; Dr. Robert Taylor for his kind nature and advice; Dr. Jacob Soley for providing some healthy competition at the fumehood; Dr. Michael Noden for his ingenuity and positivity; Matthew Diamandas for his passion for organic chemistry; Jeremy Goodyear for his friendship and patience during the most intense portions of my thesis work. I extend my gratitude to other Taylor lab members that I did not have a chance to work with: Yuhan Huang, Ghufran Barnawi and Dr. Bowei Zheng.

I thank the undergraduate students that I had the pleasure of supervising and teaching over the course of my studies, and I thank Julie Goll for giving me the opportunity to learn how to teach.

I thank Dr. Jean Duhamel, Dr. Elizabeth Meiering, Dr. Trevor Charles, Dr. Gary Dmitrienko, Dr. Thorsten Dieckmann and their respective research group members for helping me complete some of the work presented in this thesis. I extend my gratitude to Jan Venne, Dr. Jalil Assoud, Val Goodfellow and Dr. Richard Smith for their technical assistance.

I thank my parents and loved ones for their unwavering support.

I thank Dalia Naser for her love and support. She possesses kindness beyond measure and continually fills my life with her light.

Table of Contents

List of Figures

xv

List of Schemes

List of Tables

List of Abbreviations

2-ClTrt	2-chlorotrityl
2MP	2-methylpiperidine
6-Cl-HOBt	1-hydroxy-6-chloro-benzotriazole
A domain	Adenylation domain
A5	A54145
A54145E	A5 factor E
A5D	A5 factor D
A5DCyh	A5D containing cyclohexylglycine at position 13
A5DCyp	A5D containing cyclopentylglycine at position 13
A5DKyn	A5D containing Kyn13
AABA	2-amino-3-azidobutanoic acid
acrylodan-A5D	A5D labelled at D-Lys8 with acrylodan
acrylodan-Dap	Daptomycin labelled at Orn6 with acrylodan
Agr	A gene found in *S. aureus* that is involved in quorum sensing
alanyl-PG	1,2-acyl-sn-glycero-3-[phospho-rac-(3-alanyl(1-glycerol))]
Alloc	Allyloxycarbonyl
BDMA	Benzaldehyde dimethyl acetal
BLS	Bovine lung surfactant
BnBr	Benzyl bromide
Bobbitt's Salt	4-(acetylamino)-2,2,6,6-tetramethyl-1-oxo-piperidinium tetrafluoroborate
Boc	tert-Butyloxycarbonyl
BODIPY	4,4-difluoro-4-bora-3a,4a-diaza-s-indacene
BOP	Benzotriazol-1-yloxytris(dimethylamino)phosphonium hexafluorophosphate
BTEAC	Benzyltriethylammonium chloride
C domain	Condensation domain
C4PG	PG bearing two fully saturated, unbranched tails containing 4 carbons each
C55P	Undecaprenolphosphate
C55PP	Undecaprenolpyrophosphate
C6PG	PG bearing two fully saturated, unbranched tails containing 6 carbons each
C8PG	PG bearing two fully saturated, unbranched tails containing 8 carbons each
CAP	Community-acquired bacterial pneumonia
Cbz	Carboxybenzyl
CCCP	Carbonyl cyanide m-chlorophenyl hydrazine
CD	Circular dichroism
CDP-DAG	Cytidine diphosphate diacylglycerol
cLPAs	Cyclic lipodepsipeptide antibiotics

CMC	Critical micelle concentration
CSA	Camphorsulfonic acid
Daba	Diaminobutyric acid
Dapa	L-diaminopropionic acid
dap-EW	A daptomycin analog bearing Glu12 and Trp13
DCC	*N,N'*-dicyclohexylcarbodiimide
DCM	Dichloromethane
DDQ	2,3-Dichloro-5,6-dicyano-1,4-benzoquinone
DIBALH	Diisobutylaluminium hydride
DIC	Diisopropylcarbodiimide
DIPEA	Diisopropylethylamine
DiSC3(5)	3,3'-dipropylthiadicarbocyanine iodide
DivIVA	A protein that localizes in areas of negative membrane curvature and recruits cell division proteins
DMAC	Dimethylacetamide
DMAP	*N,N'*-dimethylaminopyridine
DMBA	Dimethylbarbituric acid
DMF	Dimethylformamide
DMPC	1,2-dimyristoyl-sn-glycero-3-phosphocholine
DMPG	1,2-dimyristoyl-sn-glycero-3-phospho-(1'-rac-glycerol)
DNA	Deoxyribonucleic acid
DOPC	1,2-dioleoyl-sn-glycero-3-phosphocholine
DOPE	1,2-dioleoyl-sn-glycero-3-phosphoethanolamine
DOPG	1,2-dioleoyl-sn-glycero-3-phospho-(1'-rac-glycerol)
DptL	Portion of the NRPS system of daptomycin that is responsible for the synthesis of MeGlu
DptJ	Portion of the NRPS system of daptomycin that is responsible for the synthesis of Kyn
DSC	Differential scanning calorimetry
DTT	Dithiothreitol
E domain	Epimerization domain
ent-	Denotes unnatural enantiomer
ESKAPE	*Enterococcus faecium*, *Staphylococcus aureus*, *Klebsiella pneumoniae*, *Acinetobacter baumannii*, *Pseudomonas aeruginosa*, and *Enterobacter* sp
equiv	Equivalent
FASII	Fatty acid synthesis pathway
FmocOSuc	Fmoc *N*-hydroxysuccinimide ester
FRET	Fluorescence resonance energy transfer
GFP	Green fluorescent protein
GUV	Giant unilamellar vesicle
hAsn	Hydroxyasparagine

HATU	1-[Bis(dimethylamino)methylene]-1H-1,2,3-triazolo[4,5-b]pyridinium 3-oxide hexafluorophosphate
HCTU	O-(1H-6-Chlorobenzotriazole-1-yl)-1,1,3,3-tetramethyluronium hexafluorophosphate
HEPES	4-(2-hydroxyethyl)-1-piperazineethanesulfonic acid
HF/pyr	HF-pyridine complex (Olah's reagent)
HFIP	Hexafluoroisopropanol
HOAt	1-Hydroxy-7-azabenzotriazole
HPLC	High-performance liquid chromatography
HRMS	High resolution mass spectrometry
HS-AFM	Highspeed atomic force microscopy
HWE	Horner-Wadsworth-Emmons
ITC	Isothermal titration calorimetery
Kyn	Kynurenine
LPS	Lipopolysaccharides
LptI	Portion of the NRPS system of A5 that is responsible for the synthesis of MeGlu
LptL	Portion of the NRPS system of A5 that is responsible for the synthesis of hAsn
LS	Lung surfactant
LTA	Lipotechoic acid
LUV	Large unilamellar vesicles
lysyl-PG	1,2-acyl-sn-glycero-3-[phospho-rac-(3-lysyl(1-glycerol))]
M domain	Methylation domain
mCPBA	Meta-Chloroperoxybenzoic acid
MeGlu	(2S,3R)-3-methylglutamate
MeOAsp	Methoxyaspartate
MIC	Minimum inhibitory concentration
MoA	Mechanism of Action
MprF	Multi-peptide resistance factor
MraY	Phospho-MurNAc-pentapeptide translocase
mRNA	Messenger RNA
MRSA	Methicillin-resistant *Staphylococcus aureu*s
MS	Mass spectrometry
MurA	An enzyme that catalyses the addition of PEP to NAG-UDP
MurB	An enzyme that reduces PEP attached to NAG creating NAM-UDP
MurC-F	Enzymes responsible for the attachment of the pentapeptide to NAM-UDP
MurG	UDP-N-acetylglucosamine--N-acetylmuramyl-(pentapeptide) pyrophosphoryl-undecaprenol N-acetylglucosamine transferase
NAG	*N*-acetylglucosamine

NAM	*N*-acetylmuarmic acid
NBD	*N*-(7-Nitrobenz-2-oxa-1,3-diazol-4-yl)
NBD-daptomycin	Daptomycin labelled at Orn6 with NBD
NCL	Native chemical ligation
NMM	*N*-methylmorpholine
NMP	*N*-Methyl-2-pyrrolidone
NMR	Nuclear magnetic resonance
NRPS	Non-ribosomal peptide synthetase
Orn	Ornithine
PA	Phosphatidic acid
PBFI	1,3-Benzenedicarboxylic acid, 4,4'-[1,4,10,13-tetraoxa-7,16-diazacyclooctadecane-7,16-diylbis(5-methoxy-6,2-benzofurandiyl)]bis-, tetrakis[(acetyloxy)methyl] ester
PC	Phosphatidylcholine
PEP	Phosphoenolpyruvate
perylene-dap	Daptomycin with a perylene butanoic acid tail
pfp	Pentafluorophenol
PG	Phosphatidylglycerol
Pgs	Phosphatidylglycerolphosphate synthase
PlsX	Phosphate acyltransferase
PMBCl	*p*-Methoxybenzyl chloride
POPC	1-palmitoyl-2-oleoyl-glycero-3-phosphocholine
POPG	1-palmitoyl-2-oleoyl-sn-glycero-3-phospho-(1'-rac-glycerol)
PSM	Phenol soluble modulin
p-TsOH	Para-toluene sulfonic acid
PyAOP	(7-Azabenzotriazol-1-yloxy)tripyrrolidinophosphonium hexafluorophosphate
PyBOP	Benzotriazol-1-yloxytripyrrolidinophosphonium hexafluorophosphate
R-HPLC	Reversed phase high performance liquid chromatography
RIF	Region of increased fluidity
RNA	Ribonucleic acid
SAM	S-adenosyl methionine
Sar	Sarcosine
SAR	Structure-activity relationship
SpoVM	A protein involved in sporulation which localizes in areas of positive membrane curvature
SPPS	Solid-phase peptide synthesis
SUV	Small unilamellar vesicles
SyrP	Portion of the NRPS system of syringomycin that is responsible for the synthesis of β-hydroxyaspartate
T domain	Thiolation domain

TBAF	Tetrabutylammonium fluoride
TBS	tert-Butyldimethylsilyl
Te domain	Thioesterase domain
TEMPO	(2,2,6,6-Tetramethylpiperidin-1-yl)oxyl
TFA	Trifluoroacetic acid
TFE	Trifluoroethanol
THF	Tetrahydrofuran
TIPS	Triisopropylsilane
TMSCl	Trimethylsilyl chloride
Ts	4-Toluenesulfonyl
UDP	Uridine diphosphate
UV/vis	Spectroscopy that employs light in the ultraviolet (UV) and/or visible (vis) range
VREF	Vancomycin- resistant *Enterococcus faecalis*
VRSA	Vancomycin-resistant *Staphylococcus aureus*
α-KG	α-Ketoglutarate

Chapter 1 - Introduction and Literature Review

1   Introduction

Antimicrobials are substances that interact with microbes to arrest their growth and/or kill them. Of all the classes of antimicrobials, antibiotics are arguably the most important since they act against microbes infecting a human host. Many different microbes cause human disease and thus antibiotics against fungi, protozoa and bacteria have been developed. However, the term antibiotic is most often used to refer to antibacterial antibiotics in the scientific literature and here the term will be used thusly.

Although a detailed scientific understanding of antibiotics has only been developing over the past century or so, the history of antibiotics spans millennia.[1,2] The ancient Egyptians and ancient Greeks used various moulds to treat surface infectious and references to similar treatments were made by ancient Nubians, Chinese and Serbians. Tetracycline – an important modern clinical antibiotic – was found in the bones of ancient Sudanese Nubia who lived circa 350 AD and it probably got there through contamination of the beer they drank with *Streptomyces* spp. (the natural producer of tetracycline). Thus, antibiotics had an impact on human civilizations well before the modern antibiotic era.

The modern antibiotic era is thought to have begun in the early 20th century when Paul Ehrlich along with Sahachiro Hata developed the first synthetic antibiotic salvarsan (**1.1,** Figure 1.1) which was the first effective treatment for syphilis.[2] This development was followed by the discovery of prontosil (**1.2**), the first sulfadrug, which greatly widened the success of antimicrobial chemotherapies and led to increased interest in these materials. Four years before the deployment of prontosil, Alexander Fleming made his famous discovery of penicillin (**1.3**); however, it was

Fleming's persistence rather than his keen observational skills that made penicillin a clinical success. Over a 12-year period, Fleming provided the *Penicillium* strain to anyone requesting it with the hope that chemists would become interested in solving problems associated with the purification of the active ingredient. In 1940, Howard Florey and Ernest Chain published a method of purifying the material which gave quantities sufficient for clinical testing. This protocol eventually led to penicillin mass production and distribution in 1945.[3] The success of salvarsan, prontosil and penicillin led to an explosion in antibiotic research between the 1940s and the 1960s which is commonly referred to the golden era of antibiotic discovery. Since the early 1960s, the rate of antibiotic discovery has decreased dramatically.[4] In fact, between 1962 and 2000, no new major classes of antibiotics were approved for clinical use. This dry spell was broken in 2000 with the approval of linezolid (**1.4**)[5] which was followed by the approval of 4 other new classes of antibiotics defined by daptomycin (**1.5**, 2003),[6] retapamulin (**1.7**, 2007),[7] fixadomycin (**1.8**, 2012), and bedaquiline (**1.6**, 2012)[8]. The dearth in the development of new antibiotic classes is concerning due the constant emergence of antibacterial resistance which erodes clinical efficacy eventually resulting in treatment failures.

Bacterial resistance to antibiotics is a ubiquitous phenomenon that develops during the clinical use of an antibiotic.[5] All antibiotics, especially those that are bactericidal, impose a strong evolutionary pressure on bacteria which inevitably leads to the development of resistance through natural selection. The rate at which resistance develops to a given antibiotic is intrinsically tied to the mechanism of the antibiotic and to how often it is used. Thus, the extensive use of antibiotics of the same major class has led to the emergence of multi-drug resistant strains of bacteria. Currently, *Enterococcus faecium*, *Staphylococcus aureus*, *Klebsiella pneumoniae*, *Acinetobacter baumannii*, *Pseudomonas aeruginosa*, and *Enterobacter* sp (ESKAPE pathogens) are the most

concerning due to widespread drug resistance. The impact of these pathogens is substantial -- the World Health Organization deems antibiotic resistance as 'one of the biggest threats to global health, food security and development'. The Center for Disease Control estimated in 2019 that antibiotic resistance will cost the United States of America $55 billion every year.[4]
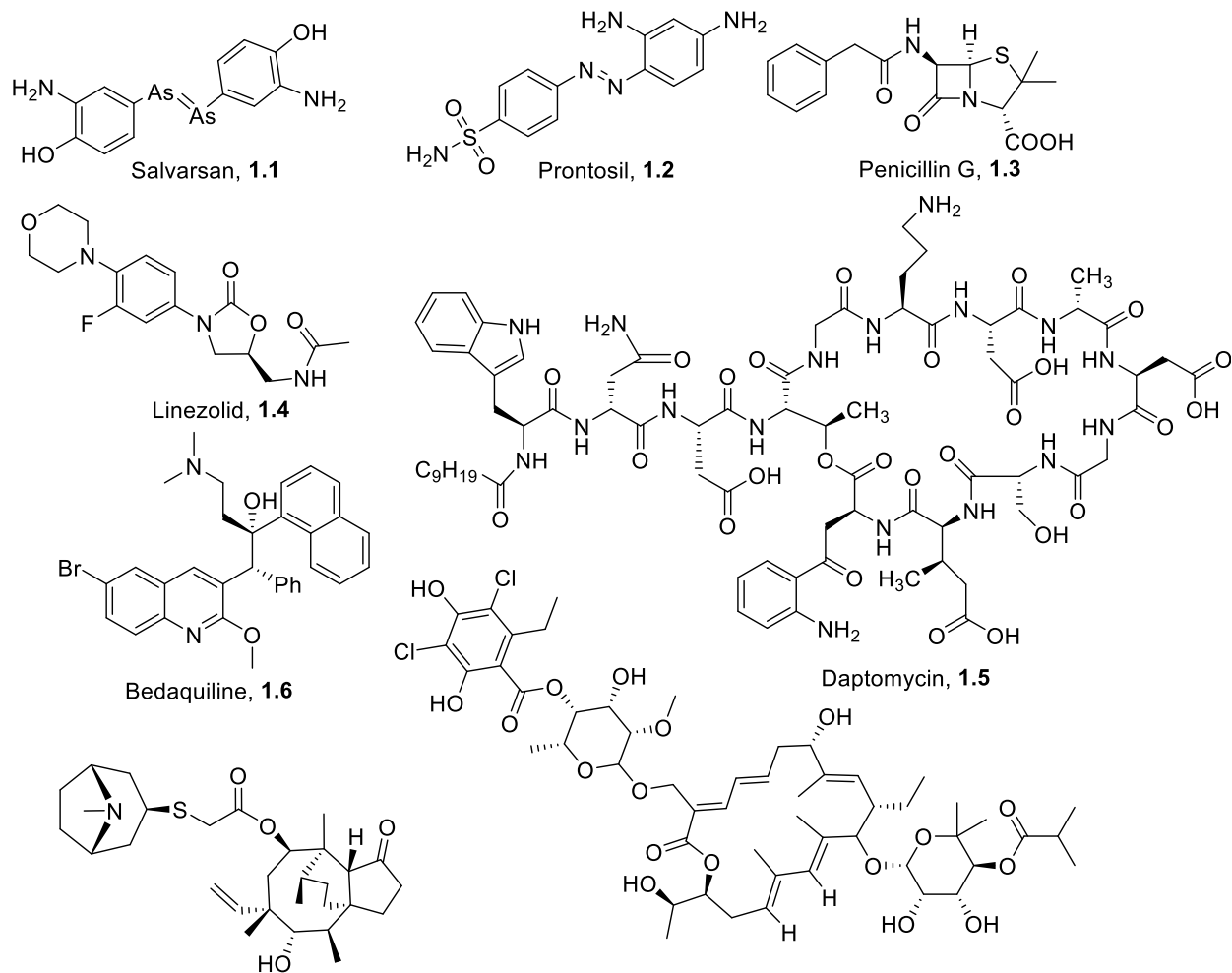
Figure 1.1 Clinical antibiotics old and new

One way to slow antimicrobial resistance is to limit the use of certain antibiotics. To this end, a short list of antibiotics was created which were only to be used as a last resort, thus prolonging their clinical efficacy. One of these last-resort antibiotics is daptomycin.

1.1 Introduction for daptomycin and A54145

Daptomycin (dap, Figure 1.2) is a cyclic lipodepsipeptide produced by a soil dwelling bacteria called *Streptomyces roseoporus*.[6] The producing strain was isolated by researchers at Eli Lily from a soil sample taken from Mount Ararat in Turkey. This strain produced a family of peptides called A21978C which differed only at the lipid tail. A 10-carbon tail was found to be optimal as it gave a desirable mixture of high antimicrobial activity and low host toxicity. Daptomycin was found to be broadly active against Gram-positive organisms but inactive against Gram-negative bacteria.[9] Early studies on the antibacterial activity of daptomycin established a strong correlation between activity and calcium concentration.[9] The antibacterial activity of daptomycin was nearly maximal at a calcium ion concentration of 1.25 mM which is similar to the serum concentration of calcium ions in humans. Initial attempts to develop daptomycin into a clinical drug were halted due to the observation of unacceptable myopathy in phase II. As a result, daptomycin was shelved until the drug was licensed to Cubist for further development in 1997. Through modifying the dosing regime, researchers at Cubist were able to attenuate the adverse effects of daptomycin on the musculoskeletal system, leading to the FDA approval of daptomycin in 2003 for the treatment of skin and skin-structure infections. In 2006, daptomycin was approved for the treatment of bacteremia and right-sided endocarditis caused by methicillin-resistant *Staphylococcus aureus* (MRSA).[10] In addition, daptomycin shows strong *in vivo* activity against clinically important Gram-positive cocci such as vancomycin-resistant *Staphylococcus aureus* (VRSA) and vancomycin- resistant *Enterococcus faecalis* (VREF).[11] Despite showing high activity against *Streptococcus pneumoniae*, daptomycin failed to meet statistical noninferiority criteria in a clinical trial for severe community-acquired pneumonia (CAP) compared to ceftriaxone.[12] It was found later that daptomycin is readily sequestered by lung surfactant (LS).

Daptomycin, **1.5**
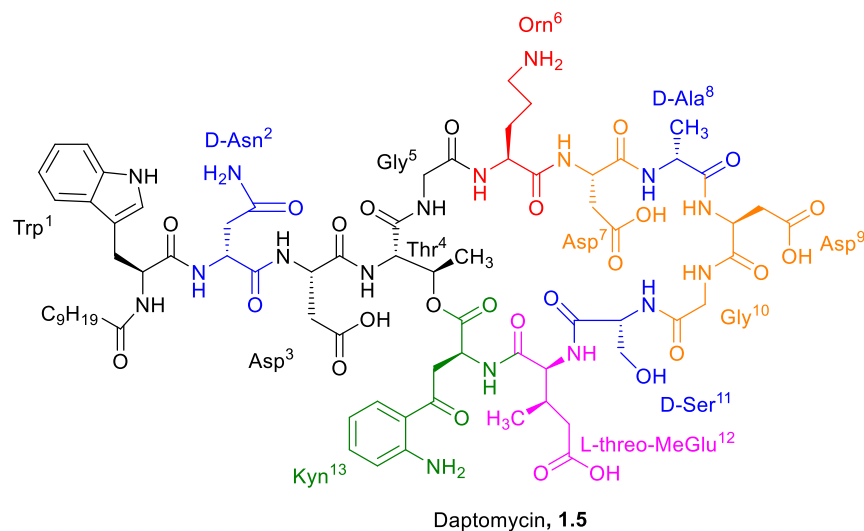
Figure 1.2: The structure of dap. Dap has several uncommon amino acids: kynurenine (Kyn) (green), L-*threo*-MeGlu (magenta), ornithine (red). D-Amino acids are shown in blue. Residues 7-10 (shown in orange with the exception of D-Ala8) make up the DXDG binding motif required for Ca^{2+} binding.

The core structure of daptomycin was deduced in 1987 using primarily chemical methods, mass spectrometry and NMR.[13] Daptomycin possesses 13 amino acids residues, 10 of which comprise a macrocycle that is enclosed by an ester bond between the side chain of Thr4 and the α-COOH of kynurenine (Kyn)13 (Figure 1.2). The remaining amino acids form an exocyclic tripeptide that is acylated at its *N*-terminus with decanoic acid. Daptomycin contains three unusual amino acids: Orn6, (2S,3R)-3-methylglutamate (MeGlu)12 and Kyn13, as well as three D-amino acids: D-Asn2, D-Ala8 and D-Ser11. Daptomycin contains a DXDG motif which is made of up Asp7, D-Ala8, Asp9 and Gly10. These residues are likely involved in daptomycin's interaction with calcium.

A54145 (A5, Figure 1.3) is a family of cyclic lipodepsipeptide antibiotics (cLPAs) comprising 8 different members isolated from *Streptomyces fradiae*.[14] A5 was isolated by researchers at Eli Lilly in 1990 only a few years after daptomycin. Like daptomycin, A5 is active against a broad range of Gram-positive bacteria but is mostly inactive against Gram-negative

bacteria. Additionally, the activity of A5 is strongly dependent on the presence of calcium.[15] No member of the A5 family was developed into a clinical drug probably because they are 2-4 fold less active than daptomycin and are more toxic.[15] However, some members of A5, most notably A5 factor D (A5D), displayed similar animal toxicity and enhanced activity in the presence of LS compared to daptomycin.[16] This prompted researchers at Cubist to make hybrid analogs of daptomycin and A5D in an attempt to find a peptide that would meet statistical noninferiority criteria in a clinical trial for severe CAP (see sections 1.6.1-1.6.3).[16,17] To date, no clinical drugs have come out of these endeavours.

Like daptomycin, the A5 family consist of a 10 amino acid macrocycle closed with an ester (depsi) bond, to which is attached an exocyclic lipidated tripeptide; however, the A5 family differs from daptomycin in amino acids at eight positions. The A5 family also contains the uncommon amino acid L-hydroxyasparagine (L-hAsn) and L-methoxyaspartate (L-MeOAsp) which are not present in daptomycin. The A5 family possess a conserved DXDG motif which is comprised of Asp7, D-Lys8, MeOAsp9, Gly10. This motif is at the same position in daptomycin and is also thought to confer A5's interaction with calcium. The macrocyclic portion of the A5 family differ from each other only at position 12 (Glu or (2S,3R)-3-methylglutamate (MeGlu)) and/or position 13 (Val or Ile). A5 members possessing MeGlu12 are more potent than those possessing Glu12 but are substantially more toxic.[15]

Figure 1.3: The structure of the A5 family. Fully conserved unusual amino acids are colored in red. D-amino acids are colored in blue. Position 12 is colored in magenta since it can contain either MeGlu or Glu.
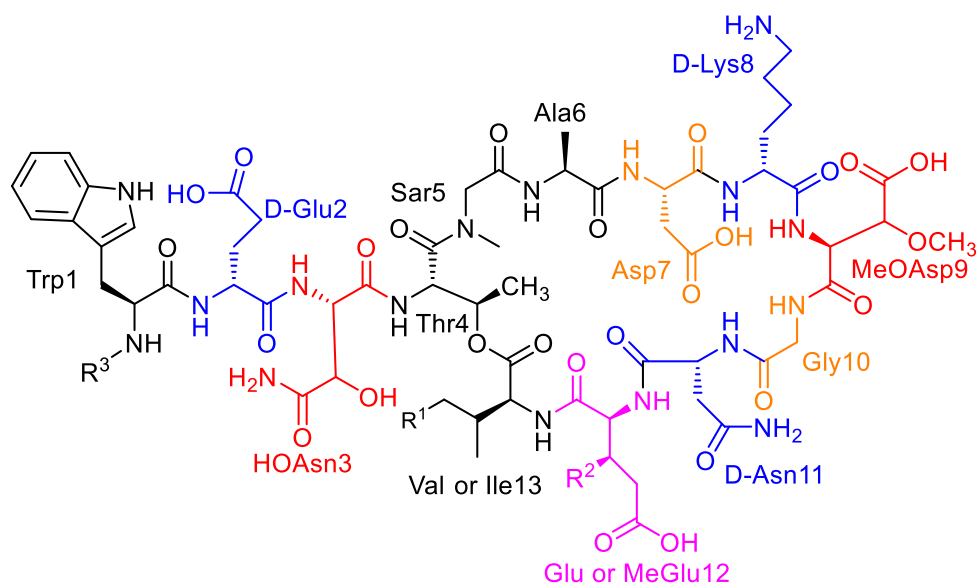
Factor	R^1	R^2	R^3
A	CH_3	H	*iso*-decanoyl (iC_{10})
A_1	CH_3	H	*n*-decanoyl (nC_{10})
B	CH_3	CH_3	*n*-decanoyl (nC_{10})
B_1	CH_3	CH_3	*iso*-decanoyl (iC_{10})
C	H	CH_3	anteiso-undecanoyl (aC_{11})
D	CH_3	H	anteiso-undecanoyl (aC_{11})
E	CH_3	CH_3	anteiso-undecanoyl (aC_{11})
F	H	H	*iso*-decanoyl (iC_{10})

The action mechanism of daptomycin has captured the interest of researchers for about 40 years and the action mechanism of A54145 is thought to be similar. In 1985, Eliopoulos et al. demonstrated that the minimum inhibitory concentration (MIC) of $A21978C_1$, a member of the A21978C family that contains an 8-methyldecanoic acid residue, was strongly correlated to the concentration of calcium present in the growth medium.[9] Other organic or inorganic salts had little effect on the activity of $A21978C_1$. Mechanism of action studies from the same paper demonstrated that $A21978C_1$ did not interact with penicillin binding protein and did not impact the synthesis of DNA, RNA or proteins, but did impact the synthesis of peptidoglycan albeit at concentrations well above the MIC

(100 µg/mL). In the following year, Lakey et al. demonstrated that A21978C increases the conductivity of unnatural bilayers in a calcium-dependent manner.[18] Based on their results, Lakey et al. proposed that the *in-vivo* activity of A21978C could not be fully explained by an ionophore mechanism. Lakey and Ptak would go on to demonstrate that daptomycin inserts into lipid membranes in a calcium-dependent manner.[19] Cell fractionation experiments revealed that daptomycin binds to the cell membrane and cell wall but not to cytosolic constituents.[20] Binding to the cell wall was found to be reversible while binding to the cell membrane was irreversible. In 2003, Silverman et al. demonstrated that the membranes of *S. aureus* cells treated with daptomycin depolarized in a dose-dependent manner.[21] In addition, cell depolarization and cell death were found to be temporally linked.

Many early studies on daptomycin were done on model membranes that do not reflect the composition or properties of bacterial membranes.[22,23] Indeed, these model membranes were composed almost entirely of phosphatidylcholine (PC) and did not possess any anionic lipids like phosphatidylglycerol (PG) or cardiolipin which make up a substantial portion of the bacterial membrane.[23] Using circular dichroism (CD), Hancock and coworkers found that daptomycin undergoes a strong structural transition in the presence of calcium and large unilamellar vesicles (LUVs) containing PG (Figure 1.4).[24] The structural transition was not observed when daptomycin was associated with model membranes that only contained PC in the presence of calcium. In the same study, the researchers found that daptomycin inserts more readily and more deeply into PG-containing membranes in the presence of calcium as indicated by an increase in the fluorescence quantum yield of Kyn13 (Figure 1.4). These results suggested that daptomycin might be forming a specific complex with PG.
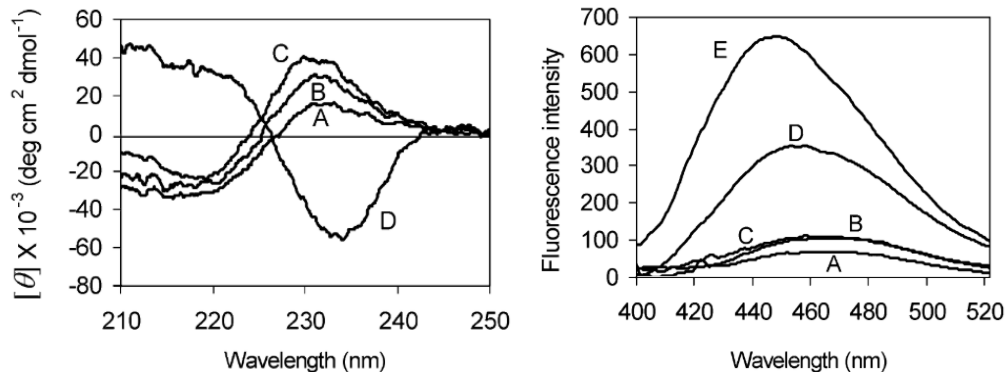
Figure 1.4. (Left) CD traces collected on daptomycin (6 µM) in 20 mM HEPES (pH ~ 7.4) (A) daptomycin in buffer (B) daptomycin in buffer containing 5 mM CaCl₂ (C) daptomycin in buffer containing PG/PC liposomes (180 µM) (D) daptomycin in buffer containing 5 mM CaCl₂ and PG/PC LUVs. (Right) Fluorescence emission of Kyn13 in daptomycin (10 µM) (A) daptomycin in buffer (B) PC liposomes (C) PG/PC liposomes (D) PC liposomes in the presence of 5mM CaCl₂ (E) PC/PG liposomes in the presence of 5 mM CaCl₂. This figure was reproduced from *Chem. Biol.*, 2004, **11**, 949–957 with permission.

Although many details about how daptomycin kills bacteria need to be worked out, these early studies firmly established the calcium dependence of daptomycin and its interaction the bacterial membrane and suggest that daptomycin may be forming a complex with phosphatidylglycerol.

1.2 Introduction for phosphatidylglycerol

Phosphatidylglycerol (PG, Figure 1.5) is an anionic lipid that is abundant in the membranes of Gram-positive organisms. In some strains of *S. aureus*, PG can make up 80% of the phospholipids present by mass.[25] In contrast, most of the PG found in eukaryotic cells is localized to the mitochondria.

The role of PG in bacterial membranes is multi-faceted. Fundamentally, PG is the primary negative charge carrier in the bacterial membrane and helps maintain a high concentration of cations near the membranes surface. Biophysical studies on PG-containing membranes show that the lipid interacts weakly with calcium cations and thus the cations are thought to 'roll' along the membrane following the distribution of PG.[26] Molecular dynamics simulations demonstrate that PG stabilizes lipid membranes by increasing inter-lipid hydrogen bonds.[27] PG plays several roles in bacterial cell division. Confocal microscopy studies on *B subtilis* show that PG forms helices

on the cell membrane (Figure 1.5).[28] These helices coincide with distribution of certain proteins involved in cell wall synthesis. Indeed, the distribution of PG appears to be important for formation of the Z-ring, which is a polymer of protein that forms a ring around the bacterial division site and is required for fission.[29,30] PG is synthesized during cell division and metabolized after fission suggesting that it stabilizes the membrane during this process.[31] It also behaves as a cofactor in cell wall synthesis .[32] In addition to its involvement in cell division, PG interacts with several other protein systems. It is implicated in protein folding[33] and several proteins have binding sites for PG.[34,35] It also activates glycerol phosphate acyl transferase, implying that it is involved in a positive feedback loop that produces phosphatidic acid (PA).[36] PG is also implicated in the transport of proteins across the inner membranes.[37] Thus, PG is an important lipid in the bacterial membrane; its distribution and molecular structure confers the proper function of many protein systems and cellular processes.
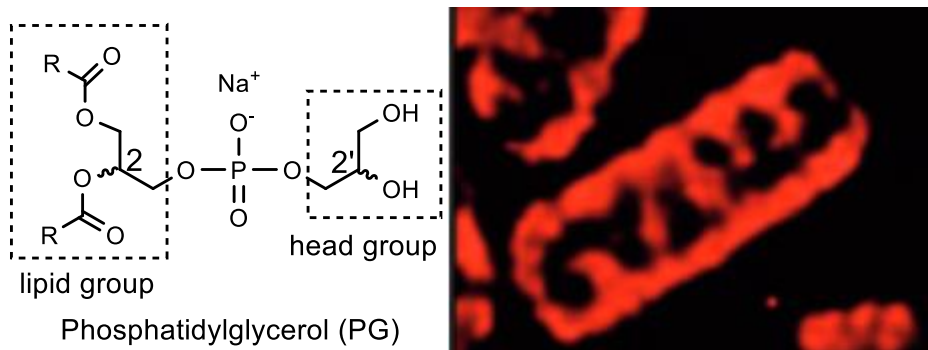
Figure 1.5: (Left) the structure of PG. (Right) Visualization of an anionic lipid specific dye in wild-type B. subtilis. The lipid helices were discerned by assembling a series of Z-stacked images taken in successive planes. This figure was reproduced from *J. Bacteriol.*, 2012, **194**, 4494–4504 with permission.

The structure of PG is shown in Figure 1.5. The molecule can be split into two portions: the lipid group (which bears the acyl tails) and the head group. PG possess 2 stereocenters one at the same position in each group. The stereochemical content of PG in bacteria has not been determined broadly since it was assumed based on enzymatic studies to be entirely of the 2R,2'S

10

configuration. However, Kuksis and coworkers found that 10% of the PG in *E. coli* possessed the 2R,2'R configuration.[38] In addition, non-negligible quantities of 2R,2'R-PG were found in marine bacteria.[39] The primary biosynthetic pathway used to prepare PG is expected to give exclusively 2R,2'S-PG as illustrated in Figure 1.6.[40] Phosphatidic acid (PA) is converted to cytidine diphosphate diacylglycerol (CDP-DAG) by phosphadtidate cytidyltransferase. This activated form of PA is then reacted with glycerol-3-phosphate (which possesses R-absolute configuration) catalyzed by the enzyme phosphatidylglycerolphosphate synthase (Pgs) producing phosphatidylglycerol-3'-phosphoric acid. An unknown phosphatase then removes the phosphate from the 3' position yielding 2R,2'S-PG. PG is the immediate precursor to the lipid cardiolipin which serves an important role in metabolism and has been implicated in daptomycin resistance (see section 1.5.1).[40]
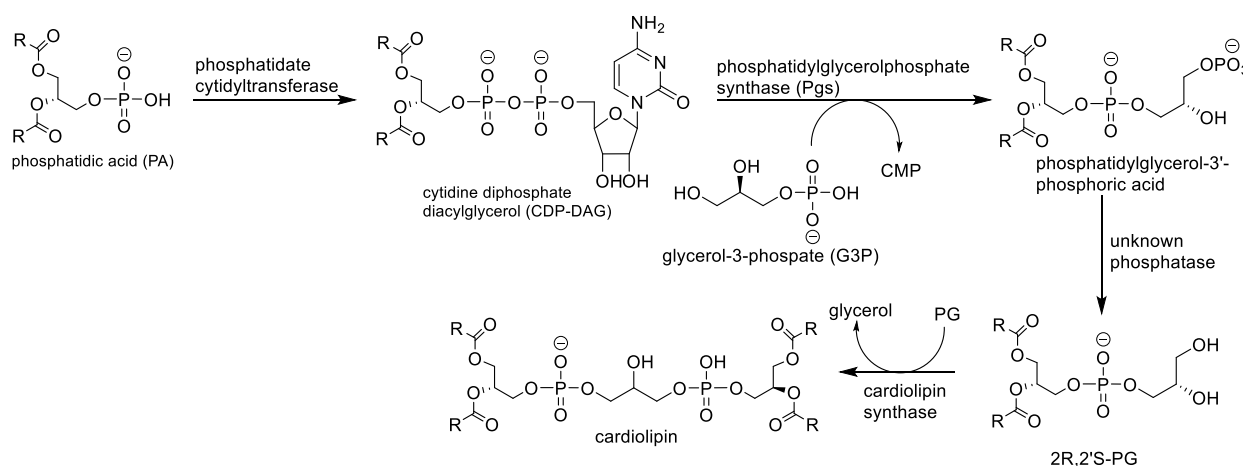
Figure 1.6: Stereospecific biosynthesis of 2R,2'S-PG

A minor pathway to PG is thought to produce 2R,2'S-PG and 2R,2'R-PG in equal quantities via a reaction is called transphosphatidylation which is catalyzed by phospholipase D enzymes (Figure 1.7). Briefly, the enzyme reacts with a phospholipid containing a polar headgroup, like phosphatidylcholine (PC), ejecting the headgroup and creating an activated form of PA which can

react with various alcohols such as glycerol. Transphosphatidylation reactions catalyzed by phospholipase D enzymes were shown to produce both 2R,2'S-PG and 2R,2'R-PG.[38,39,41,42] The prevalence of this pathway in Gram-positive bacteria has not been determined, but gene deletion experiments suggest that only a small fraction of PG is produced this way.[43] Nonetheless, it seems reasonable to conclude that some 2R,2'R-PG is present bacterial membranes.
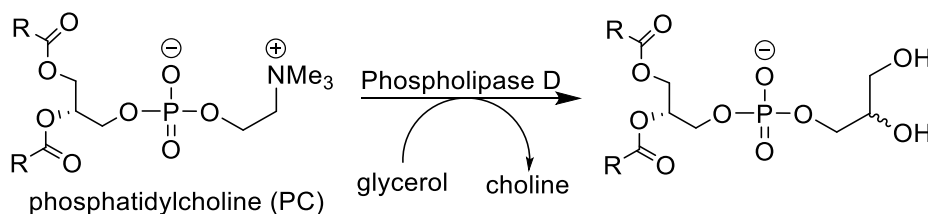
Figure 1.7: Biosynthesis of PG that produces a mixture of 2R,2'R- and 2R,2'S-PG

1.3 Gram staining and cell wall synthesis

Most bacteria can be classified into two broad categories based on their exteriors -- Gram-positive and Gram-negative. They are named based on how they react to the Gram-staining process. The staining procedure involves treating the bacteria with crystal violet which is retained by the peptidoglycan (murein) layer (Figure 1.8). The stain is then removed with ethanol which washes the stain out of the thin peptidoglycan layer found in Gram-negative bacteria but does not remove the stain from the much thicker layer of peptidoglycan that surrounds Gram-positive bacteria. The bacteria are then treated with a counter stain. When the process is complete, Gram-positive bacteria are stained violet while Gram-negative bacteria are counter stained. In addition to possessing a much thinner layer of peptidoglycan, Gram-negative bacteria possess an outer lipid membrane which contains lipopolysaccharides (LPS). LPS stabilizes the membrane architecture and is essential to the survival of these cells. In contrast, Gram-positive organisms do not possess an outer membrane. They are surrounded by a thicker layer of peptidoglycan which is decorated with lipotechoic acids (LTAs).
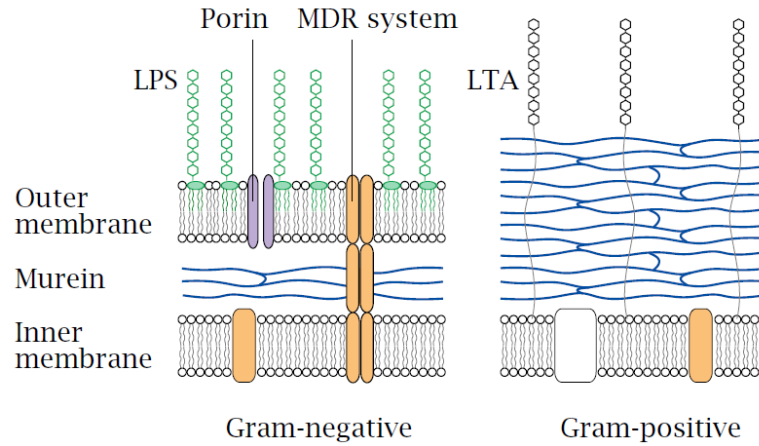
Figure 1.8. Differences in the structure of Gram-positive and Gram-negative bacteria. This figure was used with permission from the author Dr. Michael Palmer.

Peptidoglycan is a polymer of sugars crosslinked by oligopeptides which forms a mesh-like structure that envelopes the bacterial cell. The layer provides structural strength and opposes the osmotic pressure of the cytoplasm. Due to its role as a cellular wall, peptidoglycan is readily synthesized and metabolised in response to cellular processes, mainly cellular division. Figure 1.9 illustrates the process of peptidoglycan synthesis.
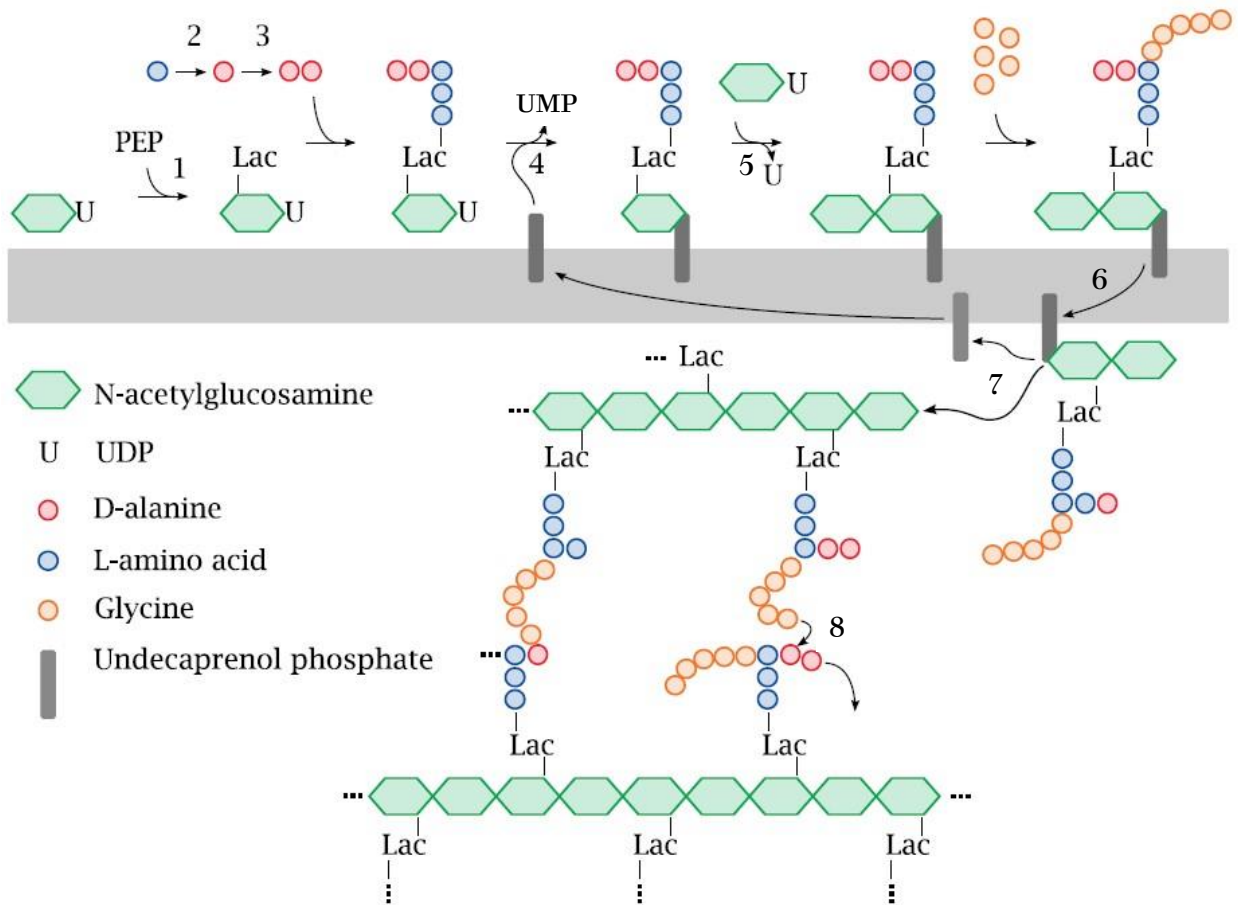
Figure 1.9 Synthesis of peptidoglycan from N-acetylglucosamine (NAG) to crosslinking of lipid II.[44] 1: MurA catalyzes the reaction between phosphoenolpyruvate (PEP) and NAG attached to uridine diphosphate (UDP). MurB reduces the PEP residue to a lactate (Lac) forming the N-acetylmuramic acid residue (NAM). 2: Alanine racemase converts L-Ala to D-Ala. 3: D-Ala residues are assembled into a dimer and attached to a tripeptide of L-amino acids. This pentapeptide is attached to the Lac group via an amide bond and these transformations are catalyzed by MurC-F.[45] 4: MraY then catalyzes the displacement of UDP by undecaprenol phosphate ($C_{55}P$) forming Lipid I and uridine monophosphate (UMP). 5: MurG catalyzes the attachment of NAG to Lipid I through displacement of UDP from UDP-NAG forming lipid II. Elongation of Lipid II with 5 glycine residues occurs in some species of bacteria (e.g., *S. aureus*).[46] 6: The complete lipid II is flipped from the cytosol to the periplasm by an unknown flippase enzyme.[47] 7: once translocated, the peptidoglycan portion of lipid II is transferred to a growing NAM-NAG copolymer via a transglycosylation reaction. 8: transpeptidases then catalyze the crosslinking of the NAM-NAG chains via peptide moieties. This figure was used with permission from the author Dr. Michael Palmer.

Numerous antibiotics target cell wall synthesis in different ways. Penicillin and other β-lactamases inhibit the NAM-NAG crosslinking step by reacting with transpeptidases called *penicillin binding proteins* (Figure 1.9, step 8).[48] The same step is inhibited by vancomycin which binds to the D-Ala-D-Ala portion of the peptidyl substrate.[49] Fosfomycin mimics PEP and reacts

14

with MurA inhibiting the synthesis of NAM (step 1).[50] Cycloserine inhibits alanine racemase and synthesis of the D-Ala dimer (step 2 and 3).[51] Laspartomycin and friulimicin bind directly to $C_{55}P$ in calcium dependent manner (step 4).[52,53] Mureidomycin A is thought to directly inhibit MraY preventing the synthesis of lipid I (step 4).[54] Bacitracin interacts with $C_{55}P$ containing species preventing translocation of lipid II to the outer leaflet of the bacterial membrane (step 6).[55] Many peptide antibiotics are known to bind to lipid II directly preventing step 7. Some of these include nisin,[56] haloduracin,[57] lacticin 3147,[58] teixobactin,[59] and lysobactin[60].

1.4 The action mechanism of daptomycin and A54145

1.4.1 Disruption of the cell wall and cell wall synthesis

The impact of daptomycin on cell wall synthesis has been investigated extensively. Early studies by Eliopoulos et al. suggested that daptomycin might kill bacteria through inhibiting peptidoglycan synthesis, but as mentioned, these studies were performed at concentrations well-above the MIC and, even then, the impact was marginal compared to what was observed with vancomycin under the same conditions. Allen et al. reported essentially the same results under very similar conditions.[61] Heijenoort and coworkers demonstrated that daptomycin inhibits the uptake of (^{14}C)-*N*-acetylgucosamine (NAG) at concentrations approaching the MIC.[62] Based on these results, the authors proposed that daptomycin inhibits a step in lipid II synthesis that is in between glucosamine 6-phosphate and UDP-*N*-acetylglucosamine. This hypothesis was supported by the observation of large distortions in the cell walls of daptomycin treated *S. aureus* observed by scanning electron microscopy.[63] In addition, proteome and transcriptome profiles of bacteria treated with sublethal concentrations of daptomycin are unique, but share similarities with antibiotics that target cell wall synthesis.[64] However, it was found that daptomycin is active against mycoplasms – strains of bacteria that completely lack peptidoglycan.[65] L-forms of *B. subtilis*, which did not express many of the enzymes needed for lipid II synthesis and were

incapable of producing NAM-UDP, are hypersensitive to daptomycin but resistant to vancomycin.[66] In addition, daptomycin is not antagonized by lipid II or lipid II precursors[67] nor does it inhibit lipid II synthesis *in-vitro*.[53] It is possible that daptomycin, like nisin, possess a two- or multifold action mechanism; therefore, activity against cell wall-less bacteria can not rule out a mechanism involving cell wall synthesis, but it does suggest that this is not central to the action of daptomycin.

Daptomycin was found to arrest LTA synthesis in *E. faecium* pre-treated with lysozyme to remove the cell wall which, at the time, was seen as indirect evidence of daptomycin interfering with LTA synthesis.[68] Further investigations by Canepari et al. found that ^{14}C-labelled daptomycin bound to the cell wall and cell membrane but was not present in cytosolic contents.[20] In the same study, the authors found that daptomycin inhibited peptidoglycan synthesis at the MIC of *S. aureus* but not *E. faecium*. In contrast, the incorporation of ^{14}C glycerol in LTA was truncated at the MIC for both strains. A more detailed study by the same authors showed that daptomycin caused the build up of intermediates involved in LTA synthesis suggesting a protein interaction.[69] However, attempts to isolate this protein via an affinity column were unsuccessful. Laganas et al cast doubt on the LTA hypothesis when they showed that daptomycin killed *S. aureus* pre-treated with rifampin. Since rifampin causes the cessation of macromolecular synthesis, including LTA synthesis, through inhibiting RNA polymerase, it was concluded that the target of daptomycin can not be LTA synthesis or any macromolecular synthesis process.[70]

A recent study by Grein et al. has postulated that daptomycin inhibits peptidoglycan synthesis by sequestering lipid II and precursors to lipid II, but only in the presence of PG and calcium.[71] Pre-treatment of strains of *S. aureus* with non-lethal concentrations of teixobactin (a lipid II binder) delayed daptomycin-induced killing suggesting that both compounds have the same

target. Treating *S. aureus* with vancomycin, which causes lipid II accumulation, resulted in hyperaccumulation of a fluorescently labelled form of daptomycin (BODIPY-dap, Figure 1.10). It was found that more BODIPY-dap was bound to PG-containing model membranes that possessed undecaprenol phosphate, undecaprenol pyrophosphate or lipid II. Solutions containing PG, calcium, lipid II and daptomycin were found to form an extraction stable complex only when all these components were present. Additionally, the authors showed that daptomycin inhibits MraY from synthesizing lipid I when daptomycin is present in a 10:1 ratio with respect to lipid I or lipid II, indicating that a daptomycin oligomer is involved in this mechanism. Although the experimental framework presented in this work appears robust, the fact that lipid II has no effect on the heat of binding of daptomycin to PG-containing membranes casts doubt on the conclusions drawn from this work.[72] Indeed, it is possible that daptomycin and these cell wall precursors incidentally colocalize on the cell membrane, which can result in sequestration of these materials or disruption of the intricate enzymatic machinery that assembles the cell wall. Both effects could occur without a strong interaction between daptomycin and an intermediate in cell wall synthesis and there is precedent for mechanisms of this type.[73] However, if this is the case, inhibition of cell wall synthesis is incidental to daptomycin binding to the lipid membrane, oligomerizing and disrupting lipid domains.
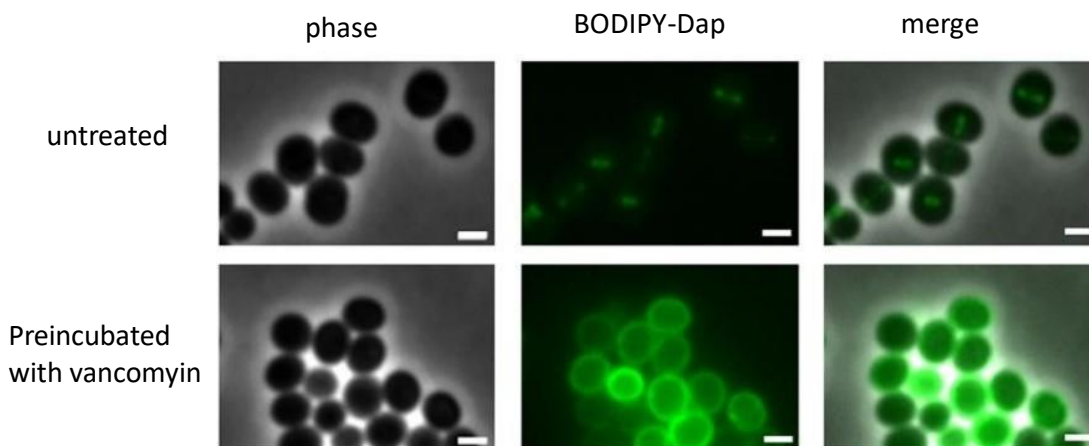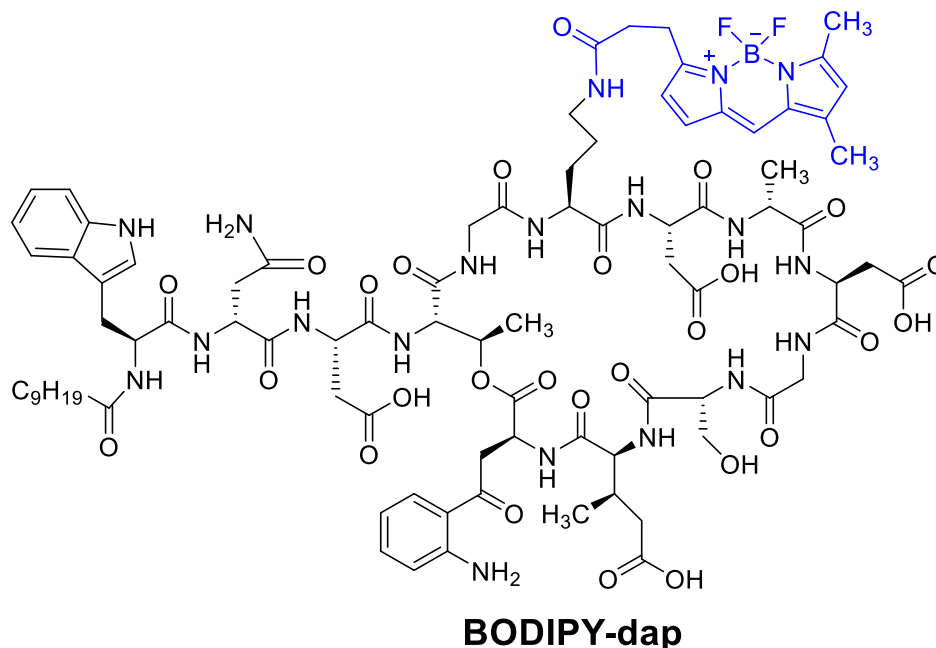
BODIPY-dap

Figure 1.10. (Top) The structure of BODIPY-dap. (Bottom) BODIPY-dap binding to *S. aureus* cells treated with vancomycin (5 μg/mL) followed by washing the cells twice and incubation with daptomycin (mixture of BODIPY-dap and daptomycin) for 10 min in the presence of Ca^{2+}. Lipid II is expected to be dispersed over the entire cell membrane as a consequence of strong accumulation. Figure was reproduced from *Nat. Commun.*, 2020, **11**, 1–11 (open access).

As discussed in sections 1.4.2, the insertion of daptomycin into the bacterial membrane has substantial impacts on membrane integrity and organization, which are closely linked to metabolism and energy production. As a result, it can be difficult to deconvolute the impact daptomycin has on macromolecular synthesis from the impact it has on energy production.[74]

1.4.2 Disruption of the organization and proper function of the cell membrane

A large portion of cell wall synthesis occurs in the cellular membrane. Thus, disruptions in the order and function of the cell membrane could impact cell wall synthesis and explain previous observations. This hypothesis was explored by Pogliano et al who observed the impact of daptomycin on the cell membrane of *B. subtilis* using confocal microscopy.[75] Using a cationic dye called FM4-64, which images anionic membrane constituents selectively, they found that daptomycin forms membrane protrusions after 10 min of treatment at the MIC (Figure 1.11). Combining FM4-64 with sytox green, which selectively stains DNA and is excluded from cells with intact membranes, they showed that the membrane was still intact despite these defects. Only 10% of cells showed bright sytox staining while 90% of these cells showed protrusion. At the 45-60 min mark >90% of cells stained with sytox. These data show that the formation of these membrane protrusions is incipient to cell death. Executing the same studies with BODIPY-dap demonstrated that the peptide localized in the same protrusions imaged with FM 4-64 and the division septum. Interestingly, BODIPY-dap stains incomplete septa selectively suggesting that the peptide targets intermediates or enzymes involved in cell wall synthesis. Treatment of *B. subtilis* cells with sublethal concentrations of daptomycin resulted in morphological changes consistent with aberrant cell wall synthesis. All the observed cells were bent or bulged demonstrating that daptomycin acts to disrupt the cell membrane and cell wall. Repeating this experiment with BODIPY-dap, the authors found that the peptide localized in these bulges and bends. To see if daptomycin treatment affected the distribution of cell wall synthesis proteins, the researchers expressed GFP-DivIVA (a membrane binding protein that gravitates towards area of negative membrane curvature and recruits other proteins to the poles and the division septum[76]) and GFP-SpoVM (a membrane protein that gravitates to areas of positive membrane curvature and anchors the spore coat[77]) and found that their positions were altered by daptomycin treatment.

GFP-DivIVA localized to septal regions and daptomycin-induced membrane bulges. GFP-SpoVM, which is uniformly distributed throughout the cell membrane, was excluded from daptomycin patches. These results show that daptomycin-patches resemble areas of septation and thus recruits cell division proteins to these regions. Staining cells with labelled vancomycin clearly show peptidoglycan biosynthesis is occurring at these daptomycin-patches. From these data it is apparent that daptomycin causes membrane defects which leads to aberrant localization of cell wall synthesis proteins.
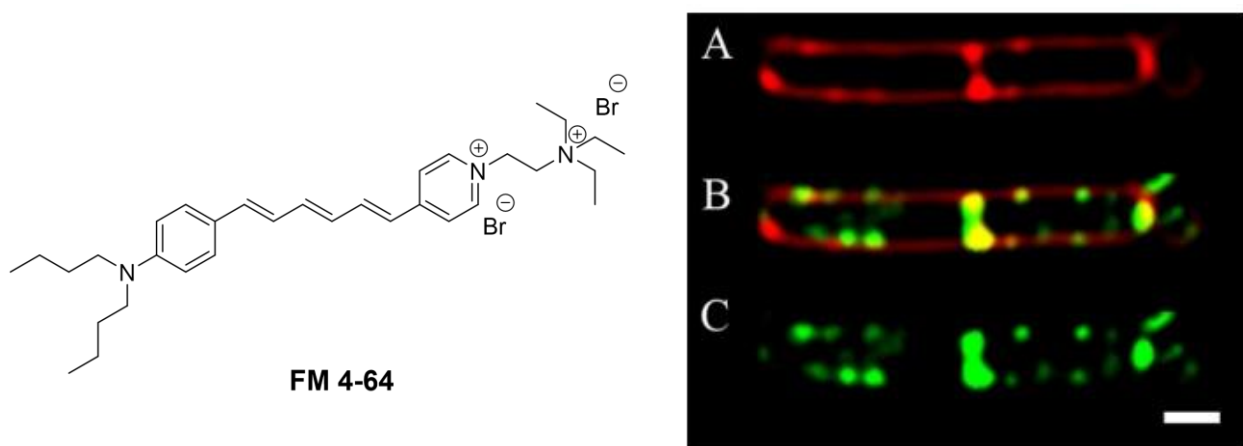
Figure 1.11. Imaging of B. subtilis cells stained with FM 4-64 and BODIPY-daptomycin. (A) FM 4-64 distribution showing the formation of membrane protrusion (B) overlay of (A) and (C). (C) BODIPY-daptomycin distribution showing localization to membrane protrusions and forming septum. Figure was reproduced from *J. Bacteriol.*, 2012, **194**, 4494–4504 with permission.

Müller et al investigated many of the claims made by Pogliano et al.[64] The authors used strains of *B. subtilis* expressing GFP-labelled proteins involved in cell wall, RNA, DNA, protein and cyotoskeleton synthesis, as well as cell division and division site regulation, to observe how treatment with daptomycin affects protein localization. Gradual delocalization was only observed for proteins involved in cell division and cell wall synthesis. Most of these proteins rely on the membrane potential for proper localization, thus it is unclear whether delocalization was caused by the slow dissipation in the membrane potential caused by daptomycin or by a specific

interaction with daptomycin. In contrast, daptomycin caused immediate dissociation of MurG (an essential cell wall synthesis protein) and PlsX (an essential phospholipid synthesis protein) from *B. subtilis* membranes (Figure 1.12). Since the structures of these two proteins are so different, it was proposed that daptomycin causes their dissociation by interfering with regions of increased fluidity (RIFs) to which these proteins, daptomycin, as well as lipid II precursors and LTA precursors preferentially localize. However, the primary experiment used to show that daptomycin disrupts RIFs employed a dye with fluorescence properties that were like Kyn which is present in daptomycin. Therefore, it is unclear whether daptomycin inhibits cellular processes by targeting RIFs.
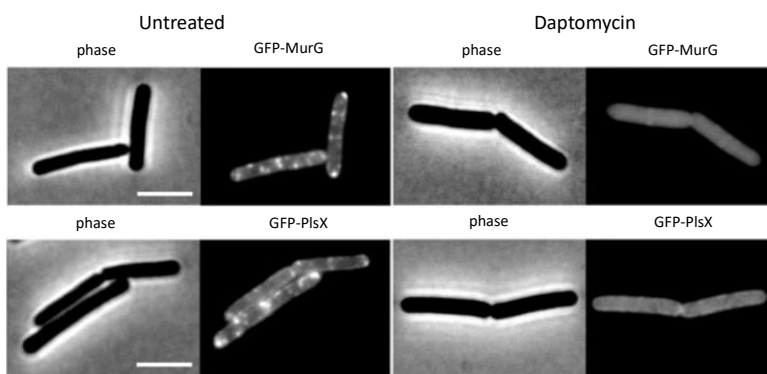
Figure 1.12. Localization of GFP-labelled MurG and GFP-labelled PlsX after treatment with 2 µg/mL daptomycin for 10 min. Figure was reproduced from *Proc. Natl. Acad. Sci.*, 2016, **113**, E7077–E7086 (open access).

Müller et al were critical of some of the conclusions drawn by Pogliano et al.[64] First, they found that daptomycin caused *B. subtilis* cell lysis at 4 µg/mL based on a decrease in optical density. This is in contrast to what was observed by Pogliano et al on *B. subtilis* and Silverman and coworkers on *S. aureus*.[75,78] Second, a more detailed investigation by Müller et al revealed that daptomycin is probably not localizing to membrane invaginations but is causing the local accumulation of lipid material instead. Third, they demonstrate that the localization of GFP-

DivIVA with daptomycin is an experimental artifact caused by the tendency of GFP-labelled proteins to oligomerize.

Evidence supporting the hypothesis that daptomycin disrupts fluid lipid domains has recently been reported, albeit on model membranes. Differential Scanning Calorimetry (DSC) studies done on PG containing LUVs demonstrate that less fluid lipid domains form upon daptomycin insertion.[79] Lee et al showed that daptomycin binding is attenuated by the presence of cholesterol which rigidifies biological membranes.[80] Taylor et al. demonstrated that daptomycin binds more readily to LUVs composed of lipids containing unsaturations which serve to fluidize the membrane.[81] Kreutzberger et al demonstrated that daptomycin induces the formation of PG domains on Giant Unilamellar Vesicles (GUVs) greatly disrupting the distribution of acidic phospholipids in these systems.[82] Based on these and other experiments, Howe and Sofou proposed that daptomycin forms crystalline domains on the membrane and membrane defects are introduced at the interface of these domains and the surrounding lipid material.[79] Since PG is a fluid lipid for which daptomycin appears to have a preference, the binding of daptomycin to RIFs could decrease fluidity in these regions and this could be responsible for the ejection of colocalized proteins observed by Müller et al. Moreover, the formation of membrane defects at the interface of crystalline daptomycin-lipid domain provides a compelling explanation for the gradual dissipation of membrane potential induced by daptomycin.

The binding of daptomycin was thought to impose quite a bit of mechanical strain on the bacterial membrane due to its large size. This mechanical impact was characterized by Chen et al. who demonstrated that the binding of dap to GUVs is accompanied by a lateral expansion of the membrane followed by contraction down to a surface area that is below the initial value, suggesting that lipid material was lost during the contraction event.[83] Later studies by the same authors

demonstrated that this phenomenon is dependent on lipid composition.[80] The contribution of lipid extraction to the action mechanism of daptomycin is not known. Contraction of cells treated with daptomycin is observed but this occurs well after cell death.[71] However, this study does highlight the strain that daptomycin places on the bacterial membranes.

The conclusion from the studies summarized in this section are presented a graphical mechanism in Figure 1.13.
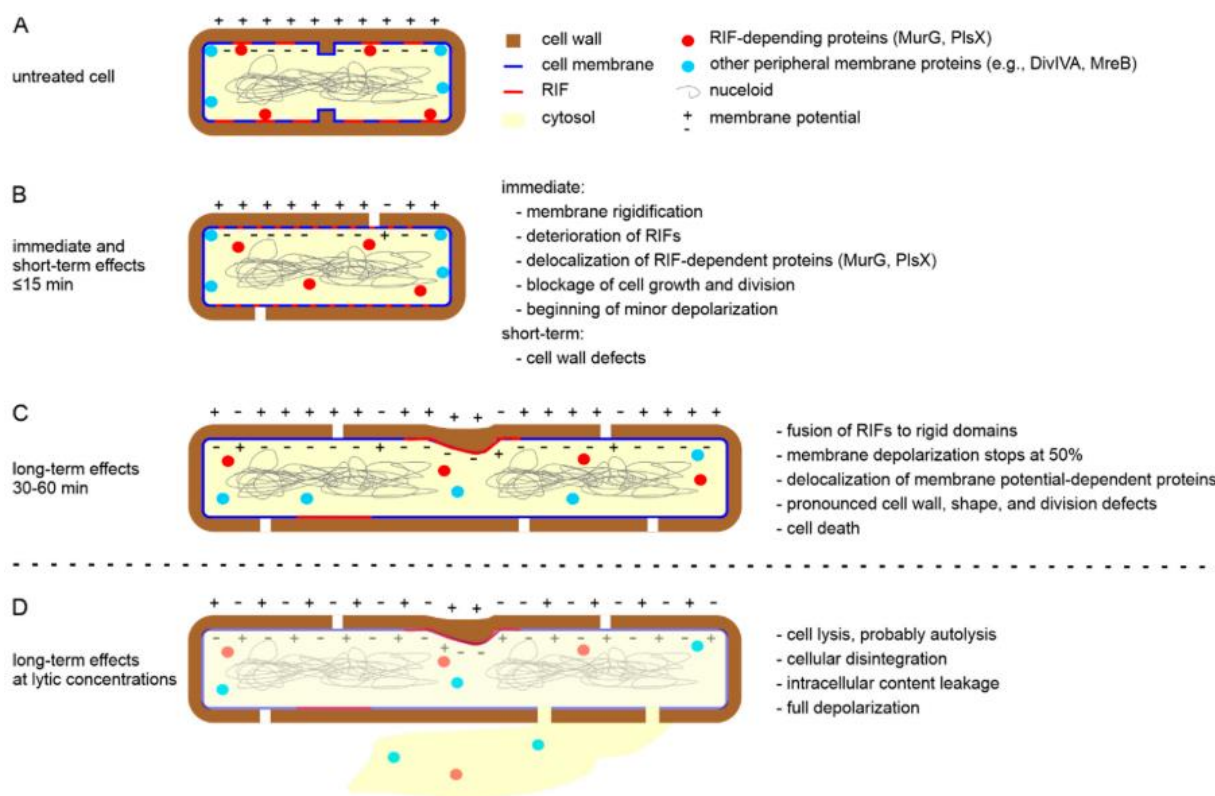
Figure 1.13. A graphical summary of the effects that daptomycin has on the membranes of Gram-positive bacteria. Figure was reproduced from *Antibiotics*, 2020, **9**, 17 (open access).

1.4.3 Oligomerization and pore formation

Allen et al. were the first to demonstrate that daptomycin causes the dissipation of the membrane potential of *S. aureus* cells through the loss of potassium ions.[61] Subsequent studies by the same authors showed that the depolarization of *S. aureus* cells was dependent on calcium and the membrane

potential.[84] Additionally, the authors demonstrated that treatment of *B. megaterium* with daptomycin inhibited active transport systems, including those involved in amino acid transport.[85] Based on this finding, the authors proposed that daptomycin inhibits peptidoglycan synthesis by lowering the availability of the amino acids used to build lipid II. Silverman et al. established a correlation between dissipation of the membrane potential of *S. aureus* and cell death suggesting that this dissipation is central to the action mechanism of daptomycin.[21] Using a potassium sensitive dye called PBFI, the authors demonstrated that, in the presence of calcium, daptomycin caused potassium release from *S. aureus* that was similar to valinomycin, albeit more gradual. The curves in Figure 1.14 describe the $DiSC_3(5)$ emission ratio, which is related to the membrane potential, for a population of bacteria stained with the dye then treated with daptomycin or nisin for a certain time interval before spectroscopic investigation using flow cytometry. These studies showed that daptomycin caused gradual dissipation of the membrane potential over the course of 60 minutes (Figure 1.14). The rate of dissipation was found to be significantly lower than what was observed with nisin. Based on these results, Silverman et al proposed that daptomycin is a pore forming ionophore that forms oligomeric pores on bacterial membranes.
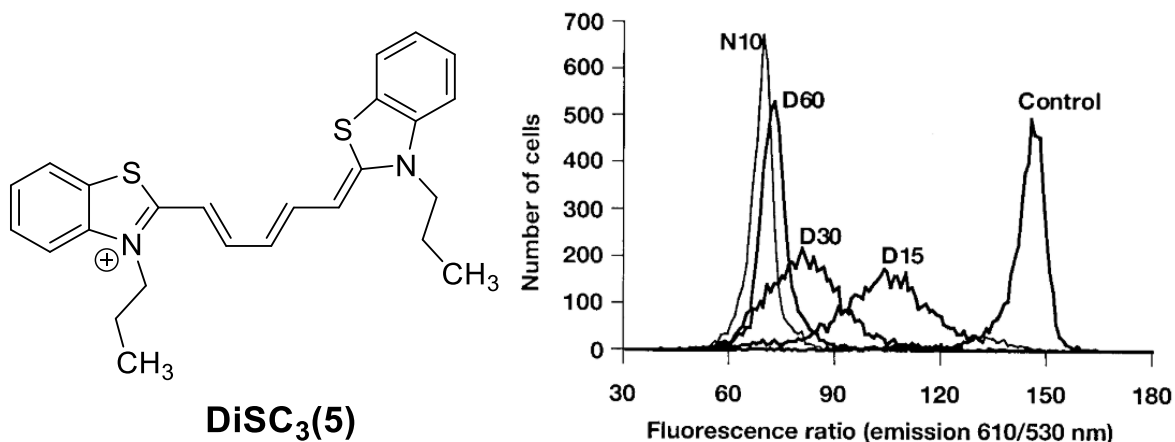
Figure 1.14. The time-dependent depolarization of a population of *S. aureus* cells caused by daptomycin (D) or nisin (N) monitored by $DiSC_3(5)$ fluorescence flow cytometry. Cells were incubated with 5 µg/mL daptomycin for 15 min (D15), 30 min (D30) or 60 min (D60) before measurement. This experiment was repeated with nisin (25 µg/mL) using a 10 min incubation time (N10). Figure was reproduced from *Antimicrob. Agents Chemother.*, 2003, **47**, 2538–2544 with permission.

The Palmer group was the first to show experimentally that daptomycin forms oligomers on bacterial and model membranes. The first study in this line of work was done using NBD-daptomycin (which has Orn6 labelled with an NBD moiety, Figure 1.15) -- a fluorescently labelled daptomycin analog with similar biological activity.[86] It was found that the NBD moiety undergoes self-quenching on PG containing membranes and the self quenching could be decreased by mixing unlabelled daptomycin with NBD-daptomycin indicating oligomer formation. Kyn13 on daptomycin and NBD have overlapping emission and excitation spectra, respectively. Thus, they can be used in fluorescence resonance energy transfer (FRET) experiments. FRET experiments revealed that daptomycin oligomerizes only on PG containing membranes forming oligomers containing 6-7 subunits.[87]
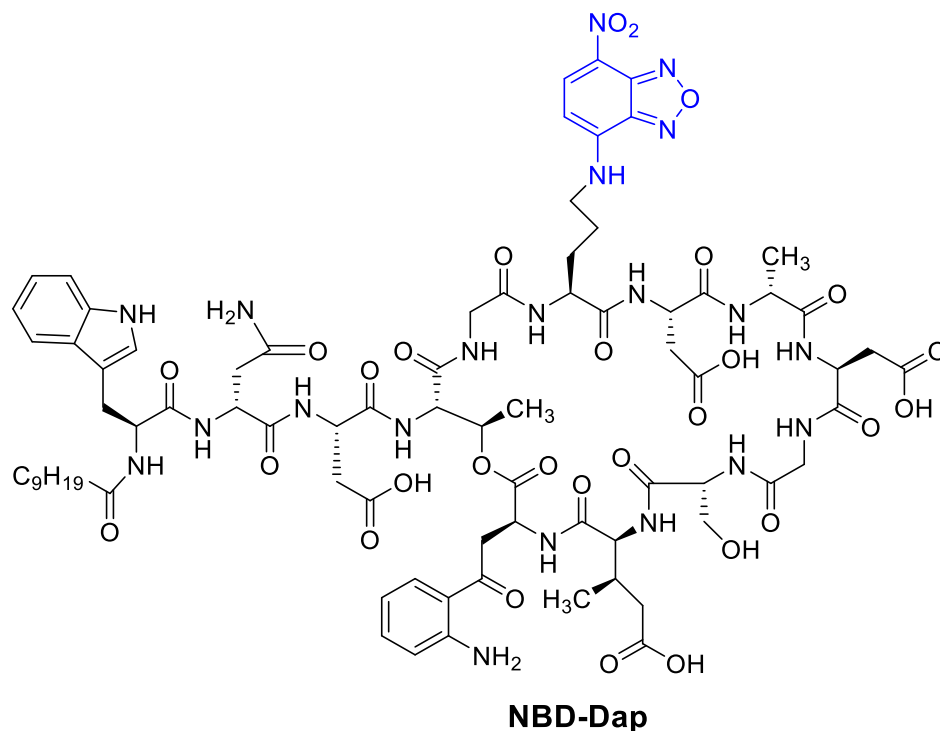
Figure 1.15. Structure of NBD-labelled daptomycin (NBD-Dap)

Palmer and coworkers went on to show that daptomycin forms oligomers using excimer fluorescence.[88] The process of excimer formation is more strictly dependent on the distance between interacting subunits and thus excimer formation is a more stringent indication of oligomer formation compared to FRET. Initially, the authors labelled daptomycin with a pyrene butanoic acid tail but found

25

this approach unsuitable due to FRET between pyrene and Kyn13. Replacement of pyrene with perylene yielded a system with suitable spectroscopic properties for investigations of oligomer formation. Perylene-daptomycin (perylene-dap; Figure 1.16) formed excimers on model and bacterial membranes at concentrations approaching the MIC in the presence of calcium. Excimer formation on model membranes was dependent on the presence of PG and titration of a solution of perylene-dap with PG containing lipid bicelles demonstrated that only a single equivalent of PG is needed to complete the oligomerization event.
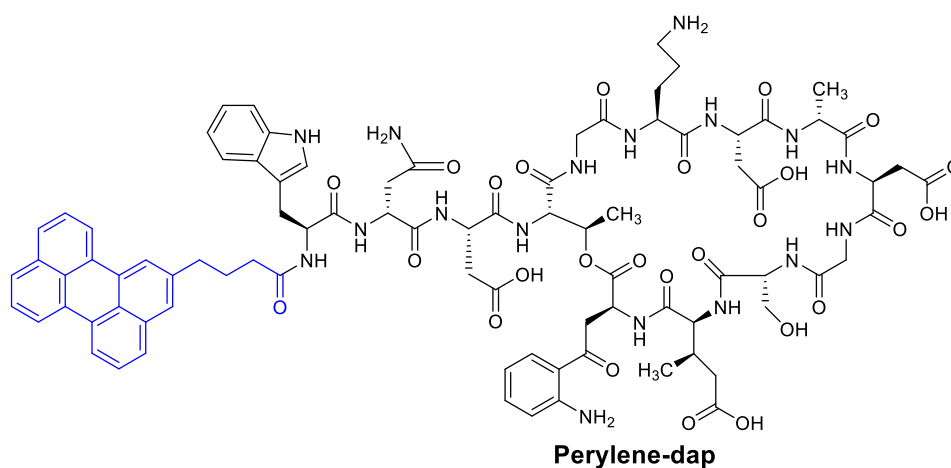
Perylene-dap

Figure 1.16. Daptomycin labelled with a perylene butanoic acid tail (perylene-Dap)

A similar set of experiments was performed on CB-182,462 which is an analog of A54145E containing an isodecyl-carbamate tail.[89] CB-182,462 was labelled at D-Lys8 with NBD and self-quenching was observed on PG containing membranes. The signal could be restored by mixing labelled and unlabelled material together. Interestingly, when daptomycin was mixed with CB-182,462 FRET could be observed between the Kyn13 on daptomycin and Trp1 on CB-182,426 demonstrating that hybrid oligomers were formed. It was shown that hybrid oligomer formation also occurred on *B. subtilis* membranes. Isothermal titration calorimetry studies revealed that daptomycin and CB-182,462 have virtually the same affinity for DOPC/DOPG (dioleoylphosphatidylcholine/dioleoylphosphatidylglycerol) membranes and the exergonicity is not

26

changed under conditions that yield hybrid oligomers, suggesting that pure and hybrid oligomers have similar stability. The antimicrobial activity of these hybrid oligomers was assayed using an isobologram approach which demonstrated that hybrid oligomers are not as active as either of the pure oligomers. This suggests that the structure of the oligomer, and not just the number of oligomers, has an impact on bactericidal activity.

Unlike daptomycin, A54145 does not contain Kyn so its oligomerization can be characterized by pyrene excimer formation which is preferred over perylene since the monomer and excimer emissions are better resolved.[90] An analog of A54145 factor D (A5D) containing a pyrene butanoic acid tail (pyrene-A5D, Figure 1.17) was prepared and found to be similarly active against *B. subtilis*. Pyrene-A5D was found to form excimers in a calcium and PG dependent manner. Quantitative analysis of the fluorescence lifetimes of pyrene-A5D excimers confirmed that pyrene aggregates are present on PG containing membranes. Monitoring excimer formation as a function of calcium concentration revealed that there are two oligomeric states: one at low calcium concentrations and another at higher calcium concentrations. These results suggest that, at low calcium concentrations, smaller oligomers of pyrene-A5D loosely associate with the surface of the membrane. Once physiological calcium concentrations are reached, the peptide inserts into the membrane more deeply and possibly forms larger oligomers.
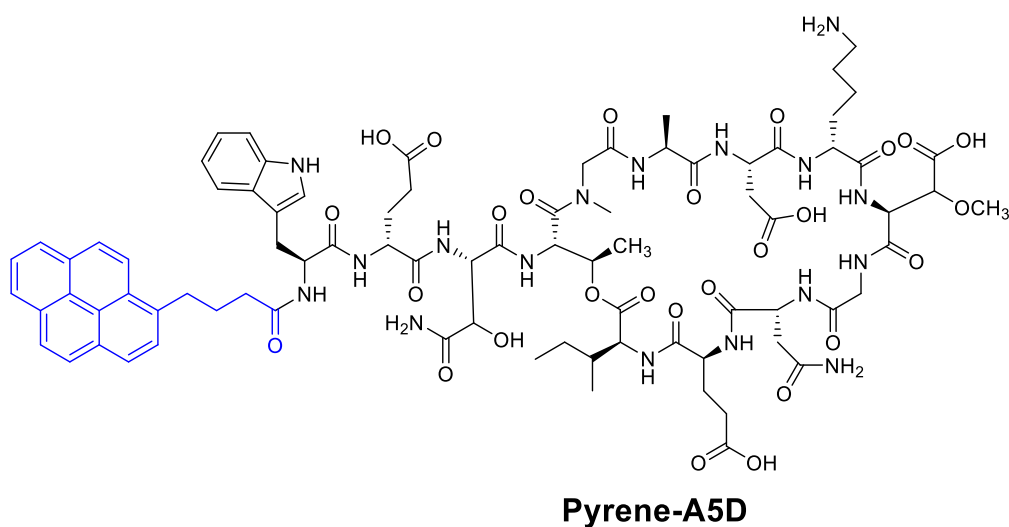
Pyrene-A5D

Figure 1.17. A5D bearing a pyrene butanoic acid tail (pyrene-A5D)

The stepwise nature of the membrane insertion of daptomycin and A54145 was investigated in detail by Taylor et al.[91] ITC studies done on daptomycin in the presence of PG containing model membranes suggested that two successive calcium binding events occur; however, others are skeptical of this claim due to the complexity of interpreting the thermal responses of complex binding events.[92] In any case, daptomycin labelled with acrylodan at Orn6 (acrylodan-Dap) and A5D labelled with acrylodan at D-Lys8 (acrylodan-A5D) were used to determine which portion of the peptide inserts into model membranes first (Figure 1.17). For both peptides, it was found that acrylodan insertion is essentially complete at 0.1 mM $CaCl_2$ while Kyn13 on daptomycin and Trp1 on A5D needed 1 mM $CaCl_2$ to fully insert into the membrane. Based on these and other findings, it seems that daptomycin inserts into the membrane in a stepwise fashion with insertion of the Orn6 residue occurring first. This is followed by insertion of the lipid tail and other hydrophobic residues like Kyn13. An analogous stepwise insertion is proposed for A5D.
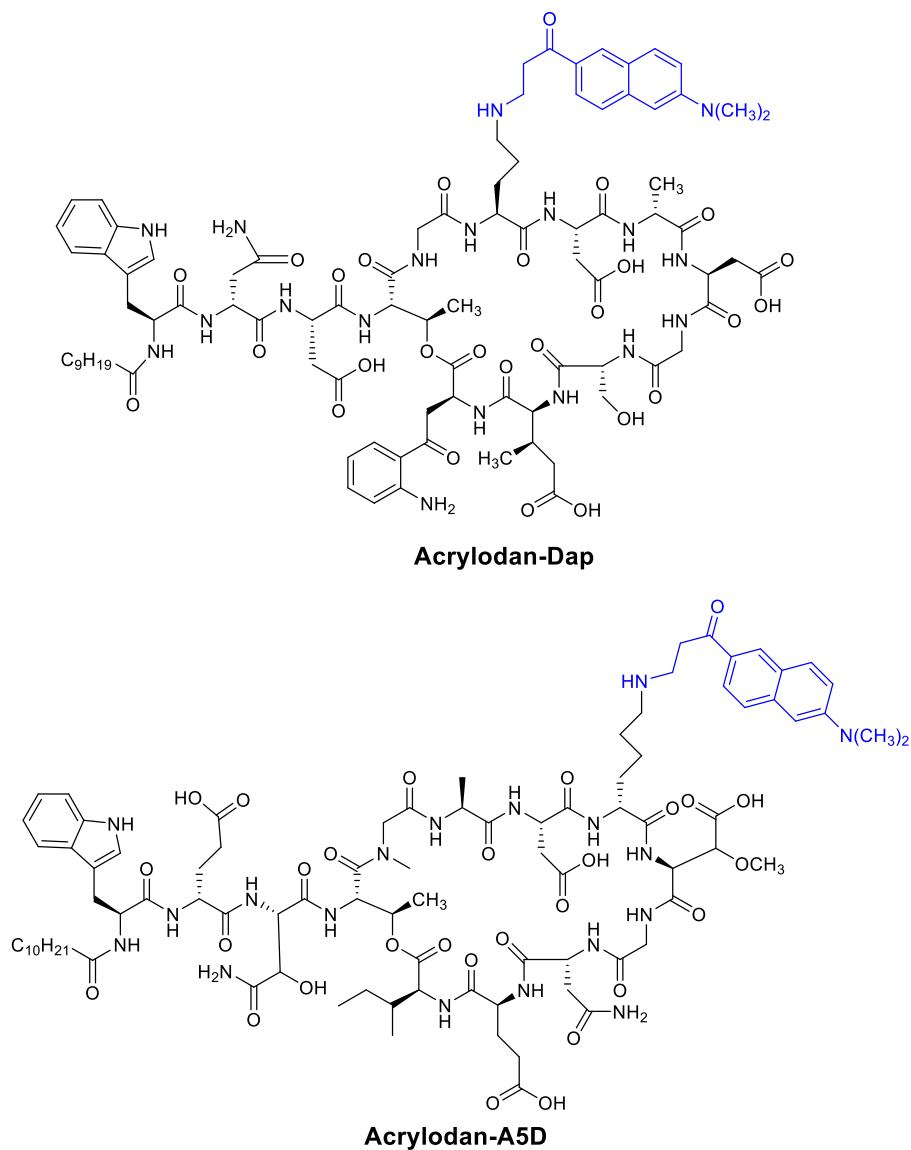
Figure 1.18. Daptomycin and A5D labelled with the environmentally sensitive dye acrylodan

The Palmer group demonstrated that daptomycin formed ion permeable pores in model membranes composed of DMPG/DMPC (dimyristoylphosphatidylcholine/dimyristoylphosphatidylglycerol).[93] To the this end, the Palmer group employed pyranine encapsulated in liposomes. In this experiment, the liposomes are diluted in buffer that contains a high concentration of salt but a low concentration of protons relative to the buffer encapsulated (Figure 1.19). This creates an opposing salt and pH gradient. Pyranine is a pH sensitive fluorophore which emits strongly at pH >7; thus, dissipation of the proton gradient, which is coupled to dissipation of the

salt gradient, results in a large increase in the emission of pyranine. When a proton ionophore called cyanide m-chlorophenyl hydrazone (CCCP) was added to these liposomes diluted in the high salt/low pH buffer, minimal pyranine fluorescence was observed, which is expected since protons effluxed must be replaced with salt cations for continued spontaneous efflux. Daptomycin alone did not increase the pyranine emission substantially implying that the pores formed by daptomycin are impermeable to protons or only allow for cations to be transported into the liposome. When both daptomycin and CCCP are present, the pyranine emission increases steadily indicating that both gradients were dissipating. Conducting this experiment with many different salts demonstrated that daptomycin pores readily transported sodium, potassium, caesium, and magnesium ions, while organic cations such as choline and hexamethonium were transported at a much slower rate and anions were not transported at all. A quantitative analysis of the rate at which daptomycin transports cations showed that it is many orders of magnitude slower than gramicidin.[93]
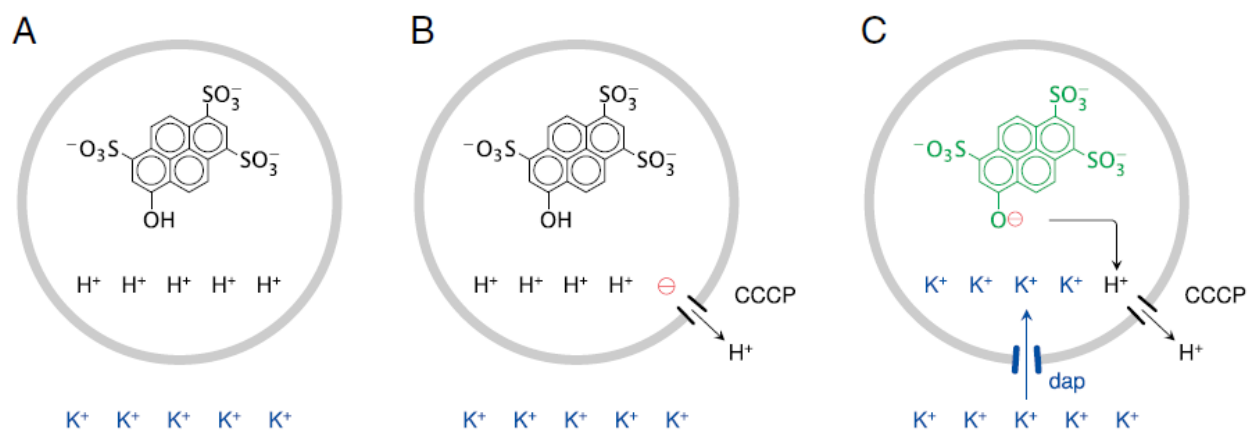
Figure 1.19. (A) Liposomes loaded with pyranine were diluted in buffer creating two opposite ion concentration gradients across the membrane (high potassium concentration outside, high proton concentration on the inside). (B) Application of CCCP alone will create a diffusion potential which will prevent a major efflux of protons. (C) Addition of daptomycin allows for the diffusion of potassium ions into the liposome effectively replacing any protons effluxed. Under these conditions, both gradients can be dissipated. Dissipation of the proton gradient is indicated by a larger increase in the fluorescence of pyranine. This figure was reproduced from *Biochim. Biophys. Acta - Biomembr.*, 2014, **1838**, 2425–2430 with permission.

Follow up studies by Straus and coworkers reported that the DMPC/DMPG systems used by Palmer and coworkers were unstable especially in the presence of CCCP.[94] However, the conditions used by Straus and coworkers differed in some key ways. The authors did not use buffers supplemented with sucrose and the calcium concentration they used was 18.5-fold lower; both changes destabilize DMPC/DMPG model membranes.[95] The model membranes they used contained 3:1 DMPC:DMPG while Palmer and coworkers used 1:1 DMPC:DMPG. Additionally, Straus and coworkers used CCCP concentrations that were two-fold greater.

In the same report, using the pyranine assay described in Figure 1.19, Straus and coworkers found that pore formation did not occur on model membranes composed of POPC/POPG (palmitoyloleoylphosphatidylcholine/palmitoyloleoylphosphatidylglycerol), which are more fluid and more stable than DMPC/DMPG membranes, but did observe potassium transport when the potassium sensitive dye PBFI was used. However, the authors did not consider that the excitation and emission spectra of Kyn and PBFI overlap, thus the jump in PBFI emission observed by Straus and coworkers was caused by the fluorescence emission of daptomycin and was not indicative of PBFI complexing to potassium. This was experimentally demonstrated by Palmer and coworkers in a rebuttal. In the same paper, the authors found that the translocation and pore formation of daptomycin is strongly dependent on lipid acyl tail chain length.[81]

The translocation and pore formation of daptomycin has been characterized using several different models and techniques. On DMPG/DMPC membranes, daptomycin evenly distributes across the inner and outer leaflet while on POPC/POPG or DOPC/DOPG membranes only about 25% of daptomycin translocated to the inner leaflet.[81] In line with this, Kreutzberger et al did not observe daptomycin translocating to inner vesicles when bound to giant multilamellar vesicles (GMVs) composed of POPC/POPC.[82] On POPC/POPG and DOPC/DOPG membranes, Palmer and coworkers observed that daptomycin does not form pores and forms smaller oligomers containing only 3-4 subunits.[81] Lee at el also did not observe daptomycin-induced potassium ion transport across

POPC/POPG membranes.[80] It was later found that only a small fraction of DOPC (10%) is needed to inhibit pore formation on DMPG/DMPC membranes.[96] Based on these and other observations, Palmer and coworkers proposed a pore formation mechanism for daptomycin which is illustrated in Figure 1.20.
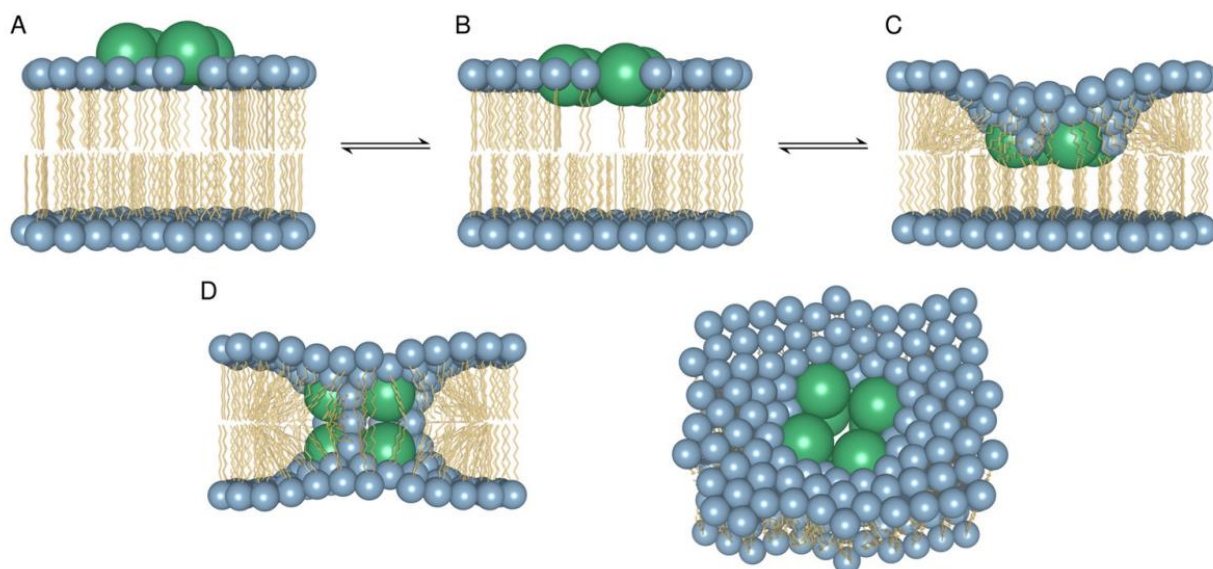
Figure 1.20. Pore formation model proposed by Palmer and coworkers (A) daptomycin forms tetramers in the outer leaflet (B) insertion into the headgroup layer is limited by distension and void creation (C) these voids are then filled by collapse of the lipids surrounding the tetramer forming a half-pore structure (D) the tetramers then translocate and overlap, forming an octameric pore. This was figure was reproduced from *J. Biol. Chem.*, 2014, **289**, 11584–11591 (open access).

The fact that ion transport is only observed on DMPG/DMPC membranes brings many of the conclusions drawn by Palmer and coworkers into question. The applicability of DM membranes as models for bacteria cells is conflicting. On one hand, the DM tail length and lack of unsaturation matches the most common lipids found in bacteria and thus the fluidity of these membranes reflects, but is not identical, to what is found in bacterial membranes.[97] On the other hand, DM lipids are highly crystalline and can be unstable; in fact, Straus and coworkers showed that DMPC/DMPG LUVs rapidly undergo membrane fusion in the presence of daptomycin and calcium.[98] Thus, the applicability of DM lipid is dependent on the experiment one wishes to perform.

Other groups have found that daptomycin forms pores on model membranes. Seydlova et al performed conductance measurements on planar lipid membranes and observed pore formation.[99] In this experiment a lipid bilayer separates two aqueous reservoirs across which an external voltage is applied. Through monitoring changes in current, pore forming events (which increase the current) and pore closing events (which decrease current) can be observed. The authors observed that daptomycin formed pores of various sizes and the sizes of these pores depended on the external voltage applied, suggesting that daptomycin targets potentiated membranes. These studies investigated pore formation on a membrane composed of pure 1,2-diphytanoyl-sn-glycero-3-phospho- (1'-rac- glycerol) which is not a good model of a bacterial membrane. Additionally, high concentrations of daptomycin (10 µg/mL) were used for model membrane and *in-vitro* studies so, although daptomycin causes membrane leakage at these concentrations, this effect may not contribute to killing at its MIC.

A recent study by Zuttion et al. used highspeed atomic force microscopy (HS-AFM) to image the dynamic oligomer formation process of daptomycin on model membranes.[100]. The authors find that daptomycin oligomers of 2 to 6 monomers are formed within milliseconds of binding to pure POPG. At the tens of minutes mark, oligomers begin to interact and form supramolecular structures. The pore forming event is directly observed and characterized by the fusion of two types of oligomers ('elongated hump' and 'dimple') in to an imageable toroidal pore (Figure 1.21). The applicability of these results to bacterial systems is questionable. The membranes investigated in this study were composed of pure POPG, which is unnatural, and the membranes were not potentiated which is known to impact pore formation.[99] Additionally, the timescale of pore formation does not match what is observed *in-vitro*.[21,71]
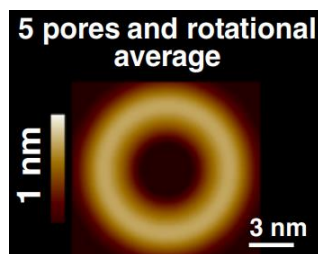
Figure 1.21. HS-AFM image of the toroidal pore formed by daptomycin on model membranes. This figure was reproduced from *Nat. Commun.*, 2020, **11**, 6312 (open access).

In-vitro studies of the pore formation mechanism proposed for daptomycin suggest that this action mechanism is highly concentration-dependent and does not function at the MIC. Studies on *S. aureus* performed by Silverman et al. showed slow dissipation of the membrane potential over the course of 60 minutes at 5-10 times the MIC using two different assays while a similar study by Mensa showed only partial depolarization of *S. aureus* cells over 30 minutes.[21,101,102] Another study showed that leakage of K^+ and membrane depolarization were observed on timescales that did not match the timescale of cell death at 4 times the MIC.[103] Using the membrane potential sensitive dye $DiSC_3(5)$ Müller et al demonstrated that dissipation of the membrane potential of *B. subtilis* cells treated with daptomycin is marginal at the MIC (2 µg/mL) (Figure 1.22). Even at 2 times the MIC, the rate of depolarization is slow and takes about 30 minutes to reach completion. These results are in sharp contrast to what the authors observed with gramicidin which causes immediate and complete depolarization at concentrations approaching the MIC.[104]
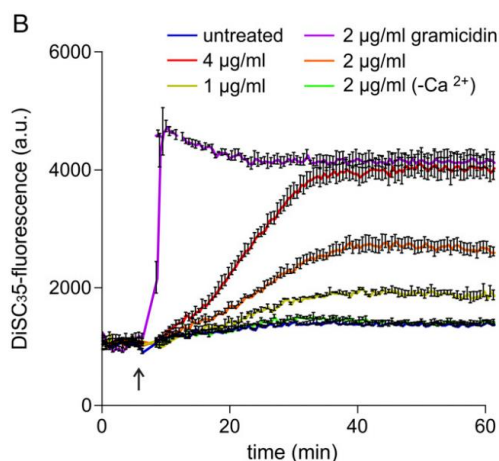
Figure 1.22. Depolarization of B. subtilis cells imaged by DiSC$_3$(5) fluorescence. Figure was reproduced from *Proc. Natl. Acad. Sci.*, 2016, **113**, E7077–E7086 (open access).

Considering the conflicting reports of daptomycin forming pores on model membranes and the apparent concentration and time-dependence of its ability to depolarize bacteria *in-vitro,* it currently appears that pore formation is not central to the action of daptomycin. However, it is apparent that daptomycin does form oligomers and these oligomers can form pores.

1.5   Mechanisms of resistance to daptomycin

Despite limiting the clinical use of daptomycin to last resort circumstances, significant clinical resistance has emerged to the antibiotic.[105–107] This has spurred research into mechanisms of resistance which incidentally provides insight into the action mechanism of daptomycin. Thus, two major classes of daptomycin resistance mechanism will be discussed.

1.5.1   Changes in membrane lipid composition

Since the site of action of daptomycin is the bacterial membrane, it is no surprise that many resistance mechanisms involve changes in lipid content. The lipids most involved in daptomycin resistance are PG, cardiolipin and lysyl-PG (Figure 1.23)
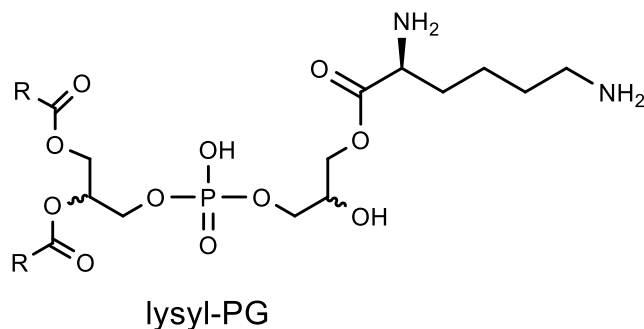
Figure 1.23 Structure of lysyl-PG

A reduction in the content of PG, especially on the outer leaflet, is often observed in resistant strains of *B. subtilis* and *S. aureus*.[108] In addition, the natural daptomycin producing strain, *Streptomyces roseosporus*, likely resists daptomycin by having very low PG content which

is characteristic of *Streptomyces* spp (less than 5% of phospholipids are PG; often the PG content is so low it cannot be detected).[109–112] In *B. subitlis* and *S. aureus*, a reduction in membrane PG content is conferred through a reduction in the activity of the PG synthesis protein Pgs.[113–115] Reducing PG content is thought to reduce the negative charge of the membrane and thus repel daptomycin; however, this hypothesis assumes that daptomycin works like other cationic antimicrobial peptides. Currently, it is unclear whether a reduction in membrane charge or a reduction in the number of binding sites is responsible for the observed resistance.

An increase in cardiolipin[116,117] and lysyl-PG content have also been implicated in daptomycin resistance.[118] Lysyl-PG is an important component of the membranes of Gram-positive bacteria where it comprises 20-50% of all phospholipids by mass.[119] The lipid is synthesized by a protein encoded by the multi-peptide resistance factor gene (*mprF*). This protein (MprF) contains a flippase and lysinylation domain, thus the protein converts PG into lysyl-PG by reacting the former with lysyl-tRNA (Figure 1.22). Once synthesized, the lysyl-PG is translocated to the outer leaflet by the flippase domain. *mprF* confers resistance to many cationic peptides usually through decreasing the negative charge of the outer leaflet effectively repelling the cationic peptide. Although daptomycin is not a cationic peptide, mutations to *mprF* are often observed in daptomycin resistant strains of *S. aureus* and *E. faecalis* but the mechanism of protection provided by these mutations is unclear.[108] An early hypothesis supposed that, upon binding to calcium, daptomycin effectively becomes cationic and thus lysyl-PG confers resistance to daptomycin by electrostatically repelling it from the bacterial membrane.[120] However, an investigation of the affinity of daptomycin for PG containing models membranes in presence of lysyl-PG showed that the effect of this lipid on membrane affinity is marginal and the authors concluded that a charge repulsion mechanism was not sufficient to explain the contribution of lysyl-PG to daptomycin

resistance.[121] Additionally, Mishra et al and Ernst et al did not find a strong correlation between the activity of daptomycin and membrane charge in bacteria.[122,123] Both lysyl-PG and cardiolipin are metabolically linked to PG so it is possible that resistant strains are masking PG through converting it to cardiolipin or lysyl-PG. In line with this hypothesis, daptomycin resistant strains of *E. faecalis* were found to have reduced lysyl-PG and PG content, relative to parent strains that were not resistant to daptomycin.[124] Additionally, alanyl- and lysyl-PG were found to provide equivalent protection from daptomycin despite the former being zwitterionic.[123] It is also hypothesized that lysyl-PG and cardiolipin may confer resistance by stabilizing the membrane to daptomycin once it is bound rather than preventing the peptide from binding. Indeed, Palmer and coworkers showed that the translocation and oligomerization of daptomycin is strongly inhibited by the presence of cardiolipin in DMPC/DMPG LUVs. Kilelee et al. demonstrated that although lysyl-PG could not prevent a cationic peptide from binding to a model membrane it could prevent membrane leakage, and the authors supposed that a similar mechanism might explain how lysyl-PG provides resistance to daptomycin.[125] There is essentially no experimental evidence supporting this hypothesis; however, it has been observed that changes in membrane lipid composition can resist daptomycin by preventing it from accumulating in division septum.[126]
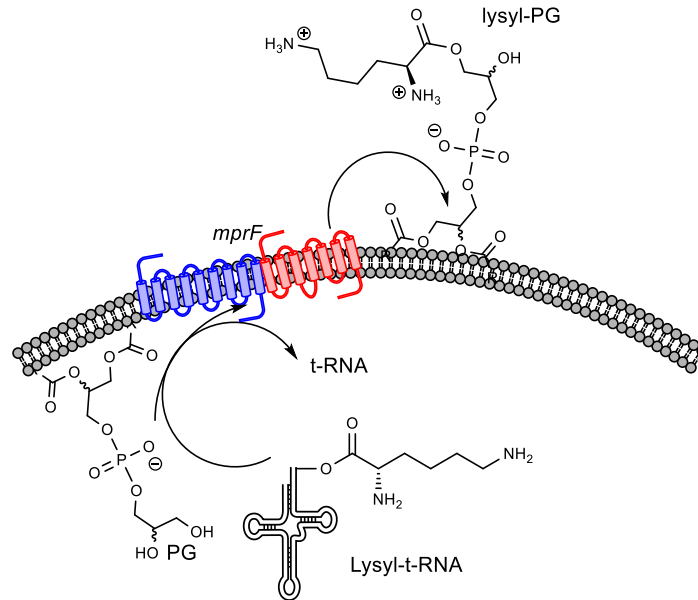
Figure 1.24. MprF synthesizing and translocating lysyl-PG. The lysinylation domain is colored in blue and the flippase domain is colored in red.

Curiously, the impact of *mprF* on daptomycin protection seems to be strongly strain dependent. For example, *E. faecalis* strains not possessing the *mprF* gene, which is responsible for increasing the lysyl-PG content of a bacterial membrane, showed only a marginal change in MIC;[127] however, *mprF* does confer daptomycin resistance in *S. aureus*.[128] The conflicting nature of these observations lead to suggestions that *mprF* confers resistance to daptomycin by some activity that is not related to the synthesis or translocation of lysyl-PG. To investigate this claim, Ernst et al. characterized *mprF* mutations commonly associated with daptomycin resistance in a defined genetic background, controlling for additional mutations.[129] They found that only some of the widely reported mutations can reproducibly cause daptomycin resistance and that these mutations do not impact lysyl-PG synthesis or translocation or any other process controlling cell surface charge. Instead, they found that mutations associated with the intramolecular interaction of the synthase and flippase domains seemed to have the strongest impact on daptomycin resistance, suggesting that the protein is somehow accommodating daptomycin (Figure 1.25). The

plausibility of this hypothesis was supported by Song et al. who showed that daptomycin can fit into an atomistic structure of an MprF determined by cryogenic electron microscopy (Figure 1.25).[130]
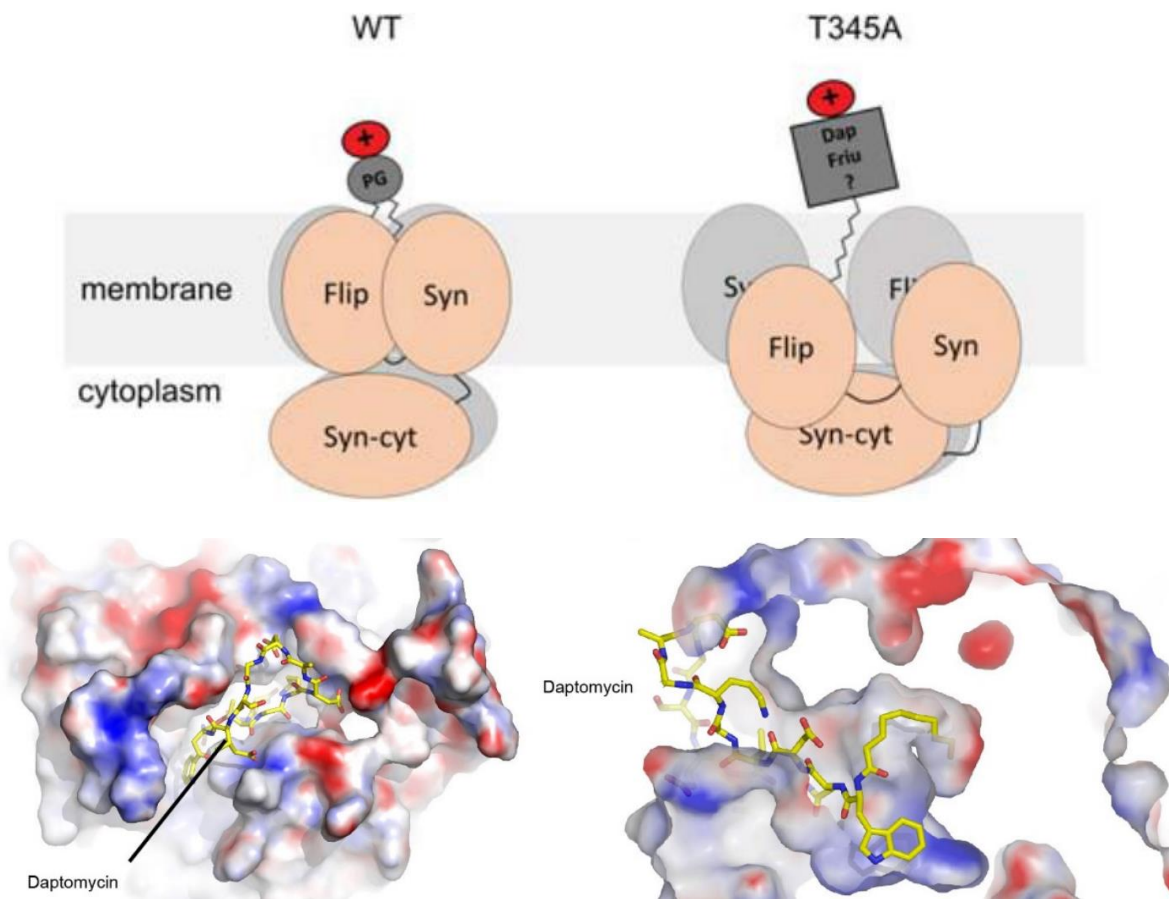
Figure 1.25. (top) *mprF* resistance mechanism proposed by Ernst et al. showing daptomycin interacting with an MprF whose subunits are loosely associated by mutations to the interface joining the two domains. Figure was reproduced from *MBio*, 2018, **9**, e01659-18 (open access). (bottom) docking daptomycin into a cryo-em structure of MprF. Figure was reproduced from *Nat. Commun.*, 2021, **12**, 2927 (open access).

1.5.2 Inactivation of daptomycin via sequestration or chemical modification

In 2016, a novel daptomycin resistance mechanism was proposed for *S. aureus*.[131] The authors observed significant resistance to daptomycin in strains that harboured deletions to *Agr* – a gene involved in quorum sensing. Similar observations were made on clinical isolates with dysfunctional *Agr* systems, and it was found that dysfunctional *Agr* systems predicted *S. aureus*

survival *in-vivo*. To investigate the mechanism of daptomycin inhibition caused by *Agr* system deletion, the authors incubated daptomycin in the supernatant of *Agr* deficient organisms and found that the daptomycin was rapidly inactivated. Analysis of the culture supernatant revealed that daptomycin triggered the release of phospholipids from *Agr* deficient *S. aureus*. TLC confirmed that PG made up most of the released phospholipids and purified PG was found to inhibit daptomycin in a dose dependent manner. 2 equivalents of PG were found to completely inhibit daptomycin (20 µg/mL) at physiological calcium concentrations. Interestingly, lysyl-PG was found to antagonize daptomycin, albeit at much higher concentrations. Other lipid components like PA, cardiolipin and diacylglycerols did not antagonise daptomycin. Based on this, the authors concluded that daptomycin was inhibited solely by the released PG. The authors went on to show that lipid release is an active process (i.e., it is not caused by daptomycin induced lipid extraction), but *Agr* system function did not affect phospholipid release (both wild type and *Agr* dysfunctional organisms released phospholipids similarly). Remarkably, it was found that the *Agr* system abrogates daptomycin resistance by releasing amphiphilic peptides called phenol soluble modulins (PSM) which compete with daptomycin for PG. Indeed, combination of purified PSM with daptomycin protected daptomycin from antagonism by PG. Based on these results, the author proposed that *S. aureus* strains lacking a functional *Agr* system inactivate daptomycin by actively expelling PG into the extracellular space conferring resistance. The authors went on to show that *E. faecalis* also releases phospholipids in response to daptomycin by a similar mechanism.[132] Follow up studies demonstrated that the rate of *S. aureus* phospholipid release can be increased by the supplementation of fatty acids which lead the authors to hypothesize that phospholipid release was promoted by the FASII pathway.[133] They found that co-administration of AFN-1252 (an

inhibitor of FASII) and daptomycin inhibited phospholipid-mediated inactivation of daptomycin, while daptomycin inhibited the emergence of resistance to AFN-1252.

In addition to inactivating daptomycin through sequestration, resistant strains of bacteria are known to inactivate daptomycin through chemical modification. D'Costa et al investigated the resistance mechanisms of soil dwelling bacteria and found that the organisms inactivated daptomycin by removing the tail or by hydrolyzing the ester bond, highlighting the importance of both of these moieties for activity.[134] This resistance mechanism has not been observed in clinical isolates.

1.6   The synthesis of Daptomycin, A54145 and analogs thereof

Many analog studies have been completed on both daptomycin and A54145. These analogs were synthesized using a variety of different approaches. Early studies focused on biosynthetic, semi-synthetic and chemoenzymatic routes, while more recent efforts have focused on developing totally synthetic routes. A recent review of these analog studies reports on 344 analogs of both daptomycin, A54145 and hybrids of the two.[135] Very recently, the Taylor group reported on 40 more analogs of daptomycin.[136] At this point, a detailed structure activity-relationship of daptomycin has emerged and analogs active against daptomycin-resistance strains of bacteria have been discovered. Considering the amount of literature published on this topic, it is not possible to review every paper in this thesis. Instead, discussion will be limited to works that are directly related to subsequent chapters.

1.6.1   The biosynthesis of daptomycin and A54145

Many proteins and peptides are prepared ribosomally meaning their primary sequence is encoded into DNA which is transcribed into mRNA and then translated to the amino acid sequence. Central to this process is the ribosome which is responsible for translating mRNA into the primary sequence. In contrast, daptomycin and A54145 are prepared by non-ribosomal peptide synthetases (NRPSs) which knit together the primary sequence of these peptides by an entirely different

sequence of chemical reactions. The gene map in Figure 1.26 illustrates the organization of NRPSs. They incorporate each amino acid with a set of modules that consists of a condensation domain (C), adenylation domain (A), thiolation domain (T) and, for D-amino acids, an epimerization domain (E). A54145 contains sarcosine which is biosynthesized through *N*-methylation of glycine catalyzed by a methylation domain (M). In both daptomycin and A54145 the final reaction, which cyclizes the peptide and forms the ester bond, is catalyzed by a thioesterase domain (Te).
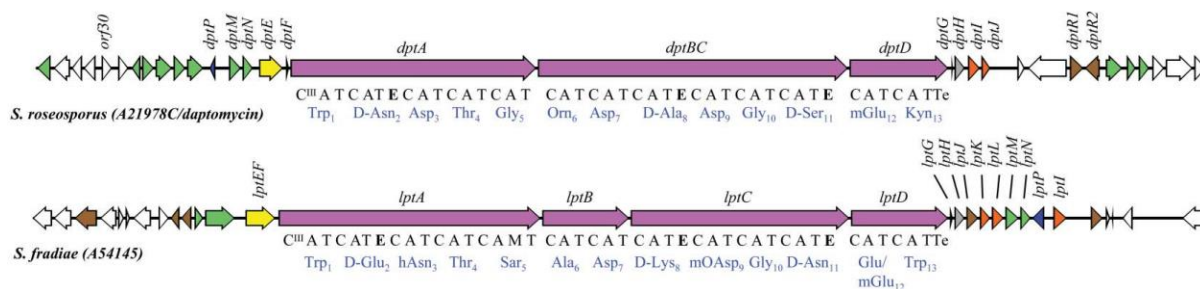
Figure 1.26. biosynthesis gene cluster for daptomycin (dpt) and A54145 (lpt). Catalytic domains (C, A, T, E, M, Te) are denoted below their position in the NRPS genes. Amino acids incorporate by each module at show below in blue. This figure was reproduced from *Nat. Prod. Rep.*, 2005, **22**, 717 with permission.

The mechanism of the C, A and T domains is illustrated in Figure 1.27. First, each amino acid is activated by its respective A domain through a reaction with ATP which allows for thiolation tethering it to the T domain. Once attached to the T domain, the condensation of adjacent amino acid is catalyzed by the C domain. The growing peptide chain is passed along each thiolation site until it reaches the final T domain where it is passed to the Te domain for cyclization.

Daptomycin possesses the unusual amino acids Orn6, MeGlu12 and Kyn13 and A54145 possess Sar5, hAsn3 and MeOAsp9. Except for Sar5, all of these are synthesized prior to incorporation into the growing peptide chain and are not the result of post-NRPS modification. Orn is not directly prepared by any portion of the NRPS and is likely drawn from cytosolic Orn which is an intermediate in Arg biosynthesis.[137] In contrast, DptJ is likely involved in Kyn synthesis since it possesses Trp 2,3-dioxygenase and kynurenine foramidase activity (Scheme

1.1).[137] MeGlu is synthesized by DptL and LptI in daptomycin and A54145, respectively. MeGlu is not synthesize via direct methylation of glutamate; instead, it is prepared via a S-adenosyl methionine (SAM)-dependent α-ketoglutarate (α-KG) methyltransferases that catalyzes stereospecific methylation of α-KG leading to (3R)-3-methyl-2-oxoglutarate (Scheme 1.1).[138] An amino acid transaminase domain then converts this intermediate into MeGlu and this pathway is known to prepare (2S,3R)-MeGlu. Bioinformatic studies demonstrate that LptL shares high sequence homology with a known asparagine oxidase enzyme which produces L-*threo*-hAsn and it is postulated that the same enzyme mechanism is used to prepare hAsn3 in A54145.[139] MeOAsp appears to be formed by hydroxylation of Asp followed by methylation of the installed α-OH and these transformations are thought to be facilitated by LptJ and LptK, respectively.[140] LptJ has high sequence homology with SyrP, which is thought to be responsible for the hydroxylation of Asp in syringomycin and, since this enzyme is known to produce L-t*hreo*-β-hydroxyAsp, it was assumed that L-*threo*-MeOAsp is present in A54145.[141]
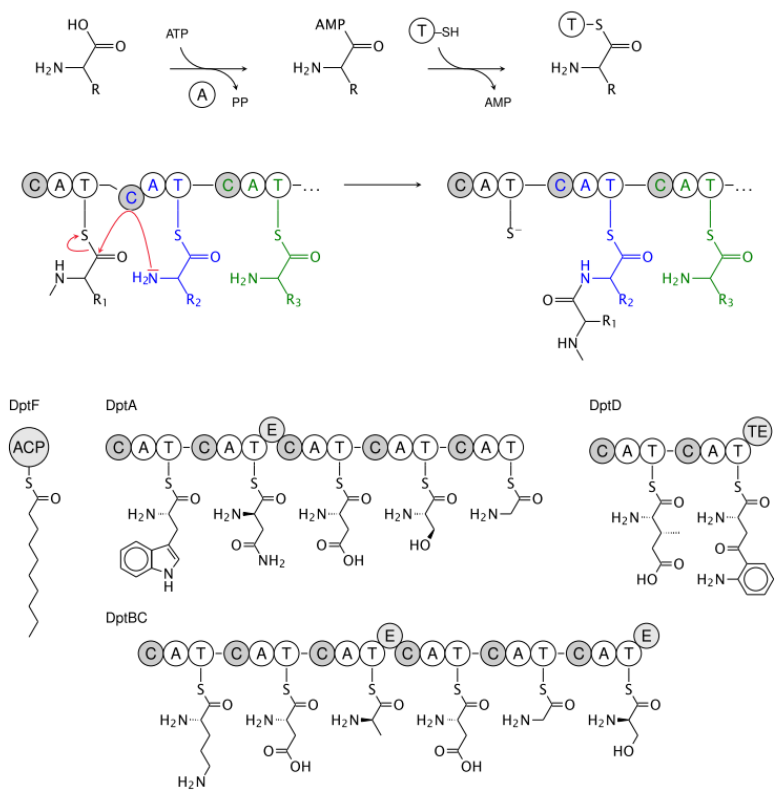
Figure 1.27. Illustration of the biosynthesis of daptomycin. This figure was reproduced from *Bioorg. Med. Chem.*, 2016, **24**, 6253–6268 with permission.
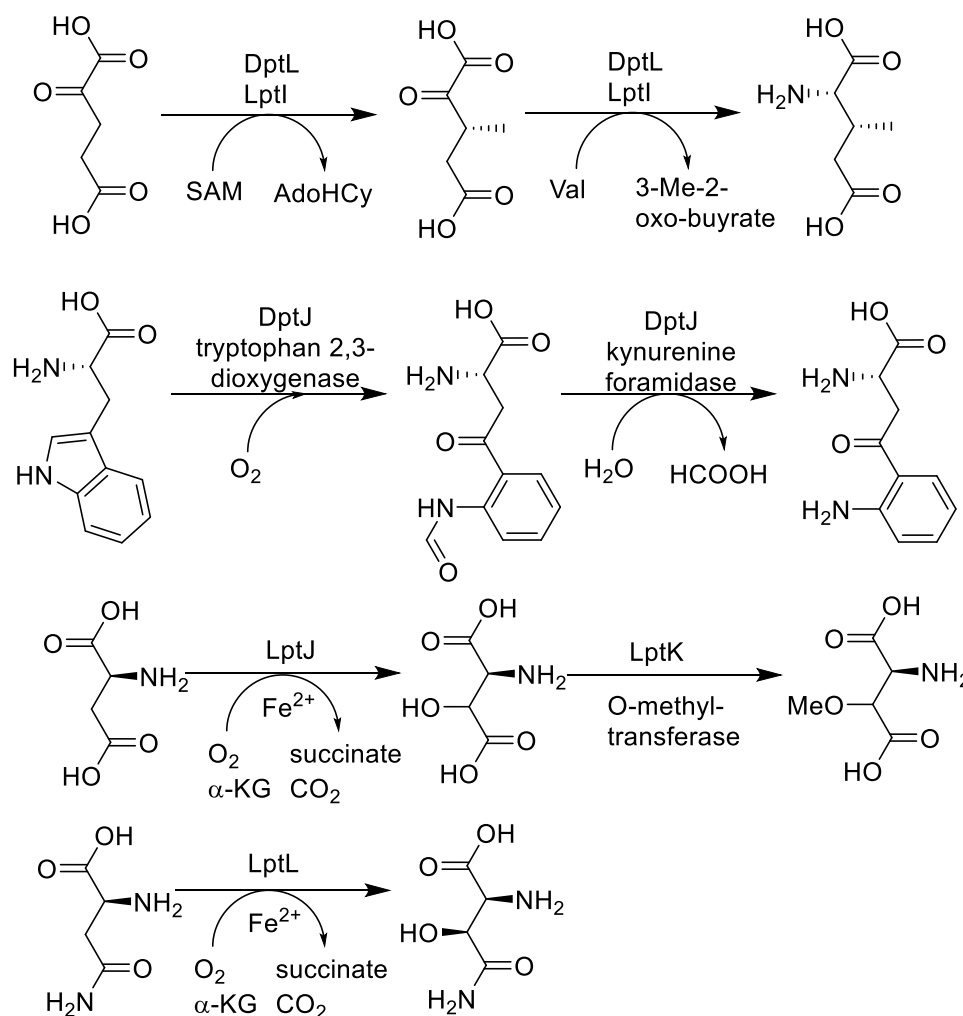
Scheme 1.1 biosynthesis of the unusual amino acids in daptomycin and A54145. Gene locations are denoted above the arrow.

1.6.2 The inhibition of daptomycin by lung surfactant

Many of the analog studies discussed in this section were motivated by the inactivation of daptomycin by lung surfactant (LS) observed by Silverman and coworkers in 2005, just two years after the FDA approval of daptomycin.[142] Before a detailed description of their account is provided, a brief overview of LS is warranted.

LS is a complex mixture of lipids and proteins that serves an essential role in respiration. LS coats the interior surface of the alveoli reducing surface tension at the air-water interface that exists between the alveoli and the surrounding central air space preventing alveolar collapse during

expiration.[143] The main constituents of LS are phospholipids (~80%), surfactant proteins (~10%) and neutral hydrophobic molecules (triacylglycerols, cholesterol etc.; 10%).[143] Approximately 85% of the phospholipids present are phosphotidylcholines, the majority of which are DPPC (dipalmitoylphosphatidylcholine). The remaining fraction is composed mostly of PG (10% of the total phospholipid content) which is also found in high concentrations in bacterial membranes.

Silverman and coworkers revealed that daptomycin had failed to meet statistical non-inferiority criteria in a clinical trial for severe CAP despite displaying potent bactericidal activity against *S. pneumoniae* (MIC_{90} = 0.06 µg/mL).[142] Investigations into the efficacy of daptomycin in treating pulmonary infections in mouse models demonstrated that daptomycin was unable to reduce the bacterial load in the lung tissue after 24 hours. Under identical conditions ceftriaxone reduced the bacterial load by 5 orders of magnitude. The authors proposed that daptomycin is inhibited by insertion into lipid aggregates that are known to comprise LS. Experiments with the bovine derived LS (Survanta®) demonstrated that daptomycin is inhibited by LS in a dose-dependent manner. Fluorescence studies confirmed that daptomycin inserts into surfactant aggregates in a calcium-dependent manner. Curiously, the antagonism of daptomycin by LS could be attenuated by the addition of detergent, further implicating LS aggregates in the mechanism of sequestration. Based on their findings and considering that LS and the bacterial membrane have similar lipid compositions, the authors concluded that daptomycin was incapable of distinguishing between the two resulting in pulmonary-specific inactivation. Despite the uniqueness of this organ specific inactivation, the exact molecular component(s) of LS responsible for the inactivation of daptomycin was never determined and few mechanistic studies describing this phenomenon have been performed.[144]

Soon after reporting that daptomycin was inhibited by LS, researchers at Cubist disclosed that some cofactors of A54145, primarily factor D (A5D), were not as strongly inhibited by LS. This motivated an extensive analog study to find a non-toxic daptomycin-A54145 hybrid that would effectively treat CAP.

1.6.3 Combinatorial biosynthesis of daptomycin and A54145 hybrids

A team at Cubist lead by Richard Baltz characterized, genetically engineered and expressed NRPSs capable of synthesizing analogs of daptomycin, A54145 and hybrids of the two.[145] Their efforts resulted in the preparation of 28 daptomycin-A54145 hybrids some of which displayed potent antibacterial activity against *S. aureus* both in the presence and absence of LS (1% Survanta (v/v)) (Table 1.2).[16,17,145] From these results, a basic structure-activity relationship can be described between these molecular scaffolds and sequestration by LS (which is related to the factor change in the MIC caused by LS). In general, it appears the MeGlu12 contributes strongly to activity and sequestration by LS. It has also been implicated in the toxicity of A54145 cofactors and thus should be avoided.[15] Many analogs based on A5E, which is strongly inhibited by LS, were found to have improved properties (entries 2-13). Replacement of D-Glu2 with D-Asn (entry 3) increased activity in the presence of LS by a factor of 8 while only decreasing activity in the absence of LS by a factor of 2. Replacement of hAsn3 with Asn (entry 5) had no effect on activity but greatly increased sequestration by LS. Replacement of D-Lys8 with D-Ala, D-Ser or D-Asn (entries 8-10) did not result in improved properties. For the A5E scaffold, MeOAsp9 seemed to be involved in sequestration since replacement with Asp (entry 11) greatly improved activity in the presence of LS. Substitutions at position 11 (entries 12 and 13) resulted in marginal reductions in sequestration and did not affect activity substantially. In contrast to A5E, many analogs based on A5D, which is not strongly inhibited by LS, showed diminished antibacterial activity, but marginal changes in sequestration by LS (entries 14-28). Replacement of D-Glu2 with D-Asn (entry 15)

47

decreased activity substantially but did not change sequestration. Replacement of hAsn3 with Asn (entry 17) truncated antibacterial activity but had no effect on sequestration. Replacement of Sar5 with Gly (entry 20) or D-Lys8 with D-Ala, D-Ser, D-Asn (entries 21-23) reduced activity but marginally changed sequestration. In contrast to A5E, replacing MeOAsp9 with Asp truncated activity (entry 25). Replacement of D-Asn11 with D-Ala or D-Ser (entries 26 and 27) reduced activity and did not change sequestration. Promisingly, replacement of Ile13 with Kyn increased activity both in the presence and absence of LS relative to A5D (entry 28).

Cubist did not report a comprehensive study on the *in-vivo* efficacy of their reported analogs. In fact, *in-vivo* testing was only described on CB-182,561 (entry 4) which was able to reduce the bacterial load in lung tissue by a factor of one half to one third.[16] In comparison, under the same conditions, vancomycin reduced the bacterial load by *8 orders of magnitude*. The improvement conferred by CB-182,561 relative to daptomycin, which could not decrease the bacterial load at all, is marginal and is much smaller than predicted by *in-vitro* studies. Additionally, Cubist found CB-182,561 to cause non-lethal toxicity complicating the interpretation of the results of the *in-vivo* testing.

Table 1.2. Antimicrobial activities of daptomycin-A54145 hybrids in the presence and absence of Survanta against *S. aureus* 42 (ATCC 29213). Calcium ion concentration was 50 mg/mL.

entry	peptide	Amino acid position								MIC (µg/mL)	
		2	3	5	8	9	11	12	13	No surfactant	1% surfactant
1	Daptomycin	D-Asn	Asp	Gly	D-Ala	Asp	D-Ser	MeGlu	Kyn	0.5	64
2	A54145E	D-Glu	HOAsn	Sar	D-Lys	MeOAsp	D-Asn	MeGlu	Ile	1	32
3	CB-182,575	D-Asn	HOAsn	Sar	D-Lys	MeOAsp	D-Asn	MeGlu	Ile	2	4
4	CB-182,561	D-Asn	Asp	Sar	D-Lys	MeOAsp	D-Asn	MeGlu	Ile	1	2
5	CB-182,363	D-Glu	Asn	Sar	D-Lys	MeOAsp	D-Asn	MeGlu	Ile	2	16
6	CB-182,597	D-Glu	Asn	Sar	D-Lys	HOAsp	D-Asn	MeGlu	Ile	1	16
7	CB-182,390	D-Glu	Asn	Sar	D-Lys	Asp	D-Asn	MeGlu	Ile	2	2
8	CB-182,571	D-Glu	HOAsn	Sar	D-Ala	MeOAsp	D-Asn	MeGlu	Ile	1	32
9	CB-182,549	D-Glu	HOAsn	Sar	D-Ser	MeOAsp	D-Asn	MeGlu	Ile	1	16

10	CB-182,510	D-Glu	HOAsn	Sar	D-Asn	MeOAsp	D-Asn	MeGlu	Ile	8	64
11	CB-182,443	D-Glu	HOAsn	Sar	D-Lys	Asp	D-Asn	MeGlu	Ile	2	4
12	CB-182,548	D-Glu	HOAsn	Sar	D-Lys	MeOAsp	D-Ala	MeGlu	Ile	1	16
13	CB-182,332	D-Glu	HOAsn	Sar	D-Lys	MeOAsp	D-Ser	MeGlu	Ile	2	16
14	A54145D	D-Glu	HOAsn	Sar	D-Lys	MeOAsp	D-Asn	Glu	Ile	2	4
15	CB-182,444	D-Asn	HOAsn	Sar	D-Lys	MeOAsp	D-Asn	Glu	Ile	8	8
16	CB-182,560	D-Asn	Asp	Sar	D-Lys	MeOAsp	D-Asn	Glu	Ile	8	16
17	CB-182,325	D-Glu	Asn	Sar	D-Lys	MeOAsp	D-Asn	Glu	Ile	32	32
18	CB-182,349	D-Glu	Asn	Sar	D-Lys	HOAsp	D-Asn	Glu	Ile	32	64
19	CB-182,348	D-Glu	Asn	Sar	D-Lys	Asp	D-Asn	Glu	Ile	16	32
20	CB-182,391	D-Glu	HOAsn	Gly	D-Lys	MeOAsp	D-Asn	Glu	Ile	16	32
21	CB-182,567	D-Glu	HOAsn	Sar	D-Ala	MeOAsp	D-Asn	Glu	Ile	4	8
22	CB-182,532	D-Glu	HOAsn	Sar	D-Ser	MeOAsp	D-Asn	Glu	Ile	8	8
23	CB-182,531	D-Glu	HOAsn	Sar	D-Asn	MeOAsp	D-Asn	Glu	Ile	16	16
24	CB-182,350	D-Glu	HOAsn	Sar	D-Lys	HOAsp	D-Asn	Glu	Ile	8	16
25	CB-182,333	D-Glu	HOAsn	Sar	D-Lys	Asp	D-Asn	Glu	Ile	32	64
26	CB-182,509	D-Glu	HOAsn	Sar	D-Lys	MeOAsp	D-Ala	Glu	Ile	8	16
27	CB-182,336	D-Glu	HOAsn	Sar	D-Lys	MeOAsp	D-Ser	Glu	Ile	64	128
28	CB-183,296	D-Glu	HOAsn	Sar	D-Lys	MeOAsp	D-Asn	Glu	Kyn	1	2

1.6.4 Semi-synthetic approach to Trp1 analogs of daptomycin

A second strategy used by Cubist to overcome the sequestration of daptomycin by LS involved the synthesis of daptomycin analogs with various substitutions at Trp1. This position cannot be modified by genetically engineering NRPS because both daptomycin and A54145 contain Trp1. Therefore, Cubist developed a semi-synthetic approach to these analogs (Scheme 1.2). Orn6 is protected with a Cbz group then the lipid tail is removed using a deacylase enzyme giving peptide **1.6**.[146] Edman degradation removed Trp1 exposing the α-amino group of D-Asn2 and yielding peptide **1.7**. Boc-protected amino acids were coupled to **1.8** via the pentafluorophenol (pfp) ester and the decanoic acid tail was reintroduced via the pfp ester yielding daptomycin analogs **1.9** after removal of the Cbz group by hydrogenolysis. Of the 22 analogs of daptomycin prepared, 8 showed substantially improved activities in the presence of 1% LS (Survanta). Promisingly, peptide **1.9a** was found to be unaffected by LS even when 5% Survanta was present. Interestingly, Cubist

reported that the activity of daptomycin against *S. aureus* 42 (ATCC 29213) in the presence of 1% Survanta and 50 mg/mL Ca^{2+} was 16 µg/mL which contradicts previous reports made by them under identical conditions (entry 1, Table 1.2).
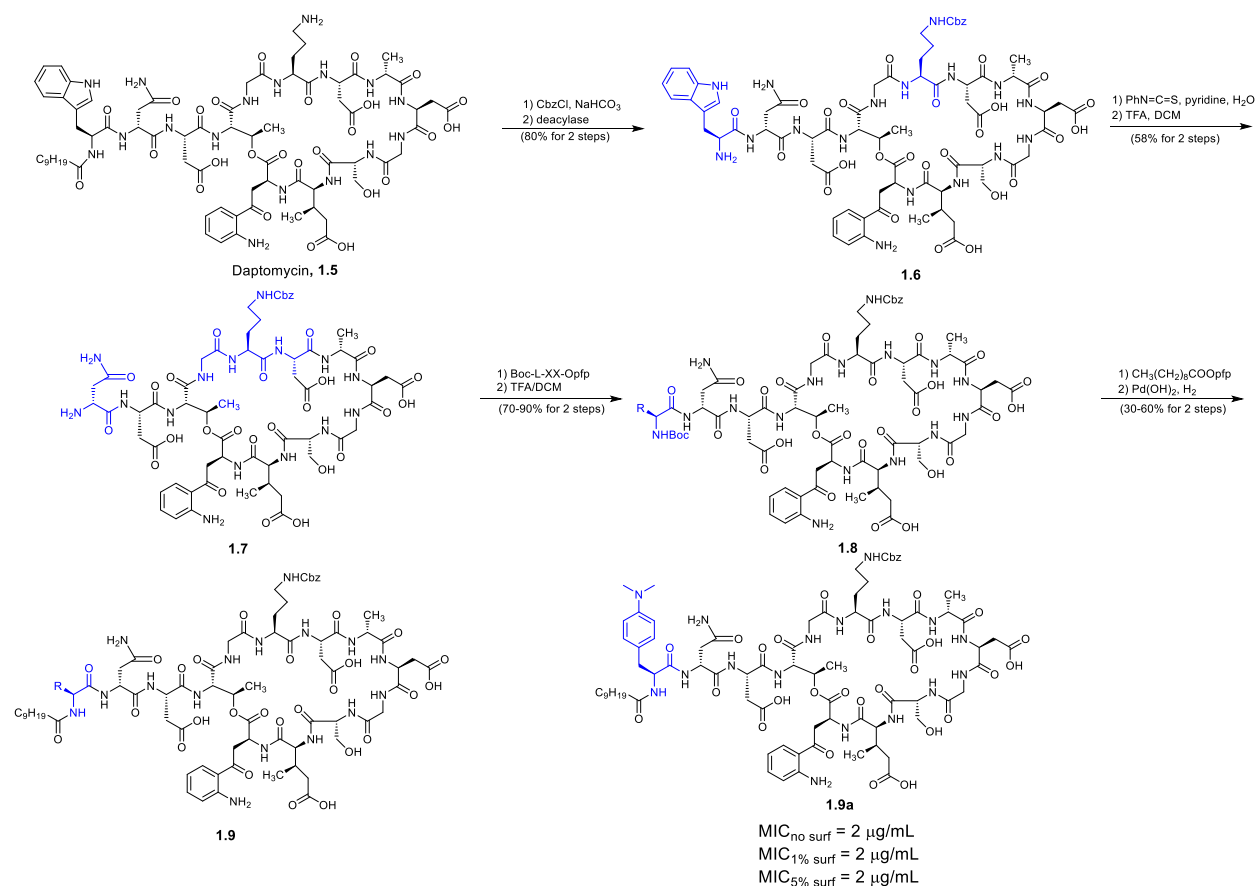
Scheme 1.2 Semi-synthetic route to Trp analogs developed by Cubist. MIC data presented for **1.9a** was collected against *S. aureus* ATCC 29213 in the absence or presence of 1% or 5% Survanta. All MICs were performed with 50 mg/mL calcium ion concentration.

1.6.5 The total synthesis of daptomycin

The total synthesis of daptomycin was first tackled by researchers at Cubist who employed a labor-intensive solution phase approach.[147] Since then, several groups have attempted to develop solid-phase approaches but only three have been successful. Since a new total synthesis of daptomycin comprises a portion of this thesis, the efforts of all four groups will be discussed. First, a brief overview of solid-phase peptide synthesis is warranted.

1.6.5.1   Solid-phase peptide synthesis

The total synthesis of peptide natural products was originally conducted in solution like any other

totally synthetic endeavour.[148] Due to the polymer-like nature of peptides, the process was

iterative and is described in Scheme 1.3. The process requires the synthesis of protected amino

acids with both the α-amino group and any reactive side chains protected orthogonally. These

building blocks are then condensed together forming a peptide bond. The N-terminus of this

peptide is then selectively deprotected allowing for the installation the next protected amino acid.

The process is repeated iteratively for all remaining amino acids until the protected peptide is

formed. Usually, all the remaining protecting groups are removed in a single step called a global

deprotection which yields the desired peptide after purification.
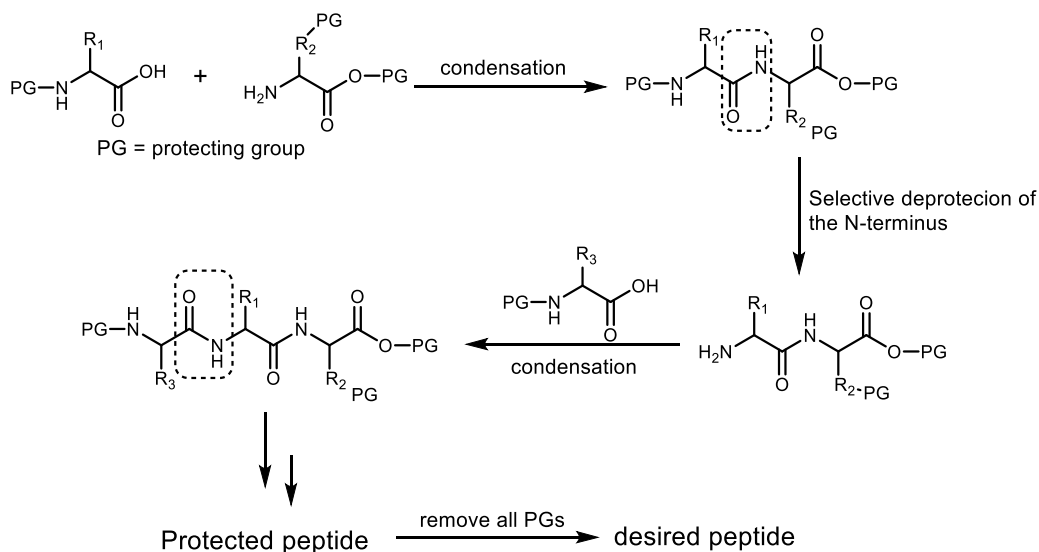
Scheme 1.3 General approach to iterative peptide synthesis

Solution phase peptide synthesis was found to have some distinct limitations.[148,149] First,

each intermediate needs to be purified, often by chromatography, which can be very time

consuming and difficult, especially as the peptide becomes larger than 10 residues. This is because

as the peptide becomes larger, it begins to aggregate in solution decreasing the reactivity of the N-

terminal amino group; thus, excess reagents are needed to push the reaction to completion. Second,

the process is labor intensive and not easily automated. This places an economic limitation on length of peptide that can be synthesized given a finite pool of resources.

To overcome some of these limitation, Robert Merrifield invented solid-phase peptide synthesis (SPPS) which revolutionized peptide and protein synthesis and earned him the Nobel prize in 1984. The process devised by Merrifield is illustrated in Scheme 1.4.[150] Briefly, the C-terminal amino acid is attached to an insoluble polymer support (often made from a cross-linked polystyrene resin) by a reactive group called a linker. The linker functions both as an attachment to the solid-support and a C-terminal protecting group. Once attached to the insoluble resin, the N-terminal protecting group is removed and the next protected amino acid is coupled to the N-terminus. Excess amino acid is needed to push the coupling to >99% completion and this is key to preparing pure peptide especially those that contain 40-50 amino acids.[149] Once the coupling is complete, the remaining amino acid and coupling agent is removed by filtering the insoluble resin and washing it several times with solvent. This process is repeated until the fully protected peptide is formed at which point it is treated with a global deprotection mixture that often cleaves the peptide from the solid support.

When Merrifield developed SPPS, he used a Boc protecting group strategy which employs amino acids protected with Boc at the α-amino group. This strategy works well since the Boc group is deprotected rapidly and with few side reactions; however, the process necessitates the use of side chain protecting groups which are most efficiently removed with liquid hydrofluoric acid. Due to its toxicity, there are many restrictions associated with the use of liquid HF and many researchers interested in peptide synthesis do not have the special equipment required to handle this noxious acid. Additionally, some peptide sequences do not fare well under the harsh global deprotection conditions employed in routine Boc SPPS. These limitations motivated the

development of Fmoc SPPS which was extensively used in some of the total syntheses of daptomycin.
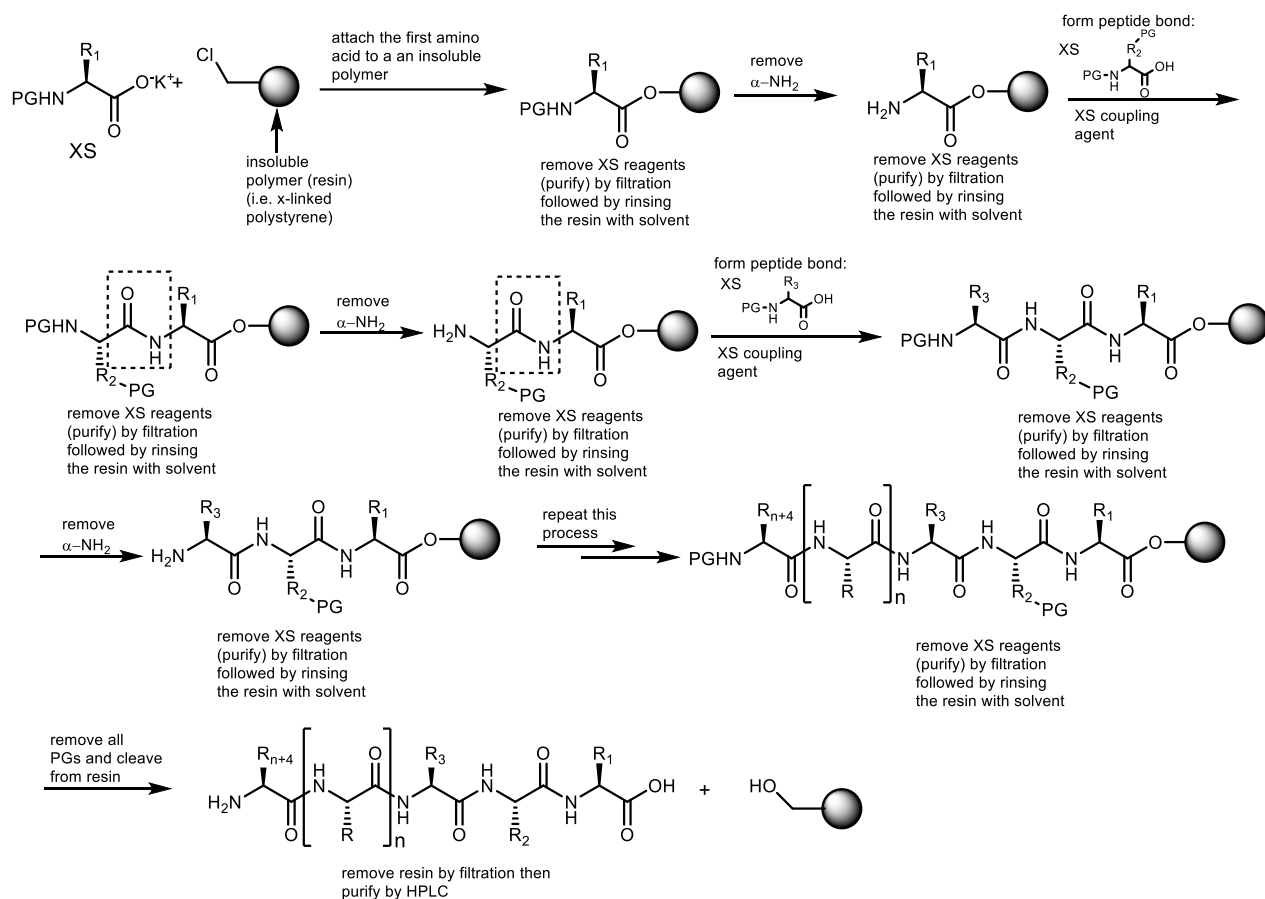
Scheme 1.4 Detailed overview of the process of SPPS developed by Robert Merrifield

The protecting groups commonly used in Fmoc SPPS are illustrated in Figure 1.28.[151] α-Amino protection is achieved by conversion of the amine to an fluorenylmethoxycarbamate (FmocNH-). This group is readily removed by amine bases in polar aprotic solvents such as DMF. When the group was developed for Fmoc SPPS, solutions of piperidine in DMF were commonly used. However, due to restrictions on the availability of piperidine, 2-methylpiperdine and 4-methylpiperidine are often used in its place. Common side chain protecting groups employed in Fmoc SPPS are illustrated in Figure 1.28. Also, included in Figure 1.28 are the azide and alloc

groups which are employed when preparing branched peptide where α-amino deprotection in the presence of an Fmoc group is often required.[152–154]
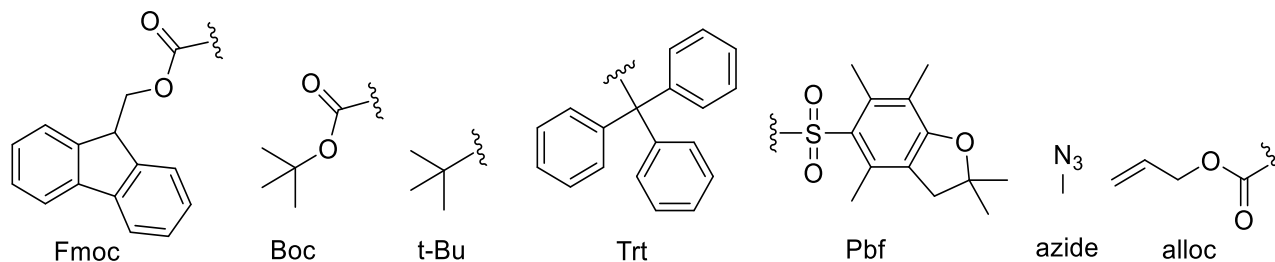
Amino Acid	Side Chain PG	Susceptible to
Lys	Boc	TFA
Arg	Pbf	TFA
Asp and Glu	tBu	TFA
Asn and Gln	Often not protected, Trt used when necessary	TFA
Met	Often not protected	
His	Trt	TFA
Ser, Thr	tBu	TFA
Tyr	tBu	TFA
Trp	Boc	TFA
Cys	Trt	TFA

Figure 1.28 A common protecting group scheme for Fmoc SPPS

Judicious choice of linker is key to the success of a synthesis of a cyclic peptide. Linkers commonly used in SPPS along with deprotection conditions are illustrated in Figure 1.29. The 2-ClTrt linker is commonly used in the Fmoc SPPS of cyclic peptides, because it allows for the linear peptide to be cleaved without removing the protecting group, which is key to the success of an off-

resin cyclization approach. In cases, where an on-resin cyclization approach is taken, a Wang resin, which bears a 4-benzyloxybenzyl alcohol linker, may be used. If the same approach is taken using Boc SPPS, the Merrifield linker or PAM linker is employed. The PAM linker is more acid stable than the Merrifield linker which confers higher yields especially for longer peptides.

2-Chlorotrityl linker (2-ClTrt)
1% TFA/DCM

4-Benzyloxybenzyl alcohol linker
100% TFA

Merrifield linker
liquid HF

PAM linker
liquid HF
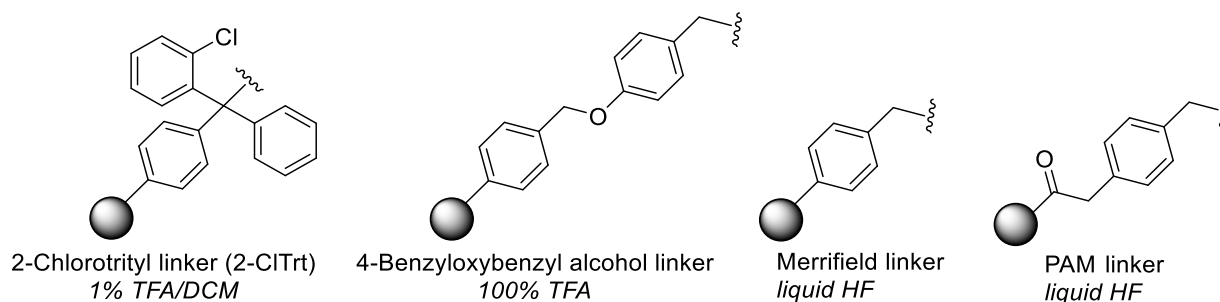
Figure 1.29. Linkers commonly used in SPPS. Common deprotection conditions are denoted in italics.

1.6.5.2   *Total synthesis of daptomycin by the Li group*

The Li group published the first total synthesis of daptomycin involving SPPS in 2013.[155] In their retrosynthetic analysis, the Li group envisioned cyclizing daptomycin using a Ser/Thr native chemical ligation (NCL) strategy which they reported on in 2010.[156] A brief overview of this method is provided in Scheme 1.5. A peptide building block bearing a salicylaldehyde ester is incubated with a peptide possessing an N-terminal Thr or Ser in pyridine/acetic acid forming the hemiaminal. A spontaneous 1,5-O→N acyl shift transfers the acyl group forming the peptide bond between the two peptide fragments. The newly formed hemiaminal is then removed by treatment with TFA. The method provides a selective approach to amide bond formation since, in theory, ligation should only occur at Ser/Thr. It is also an appealing option for peptide cyclization since it can be done at much higher concentration than traditional cyclization methods and should occur without any epimerization. With that said, the method is not without its drawbacks. The multistep approach requires HPLC purification before and after peptide bond formation. As well, the pyridine/acetic acid reaction solvent does not accommodate unprotected peptides with many

hydrophilic residues. The group's decision to cyclize daptomycin via this method forced them to cyclize daptomycin between D-Ser11 and Gly10 (Scheme 1.5).
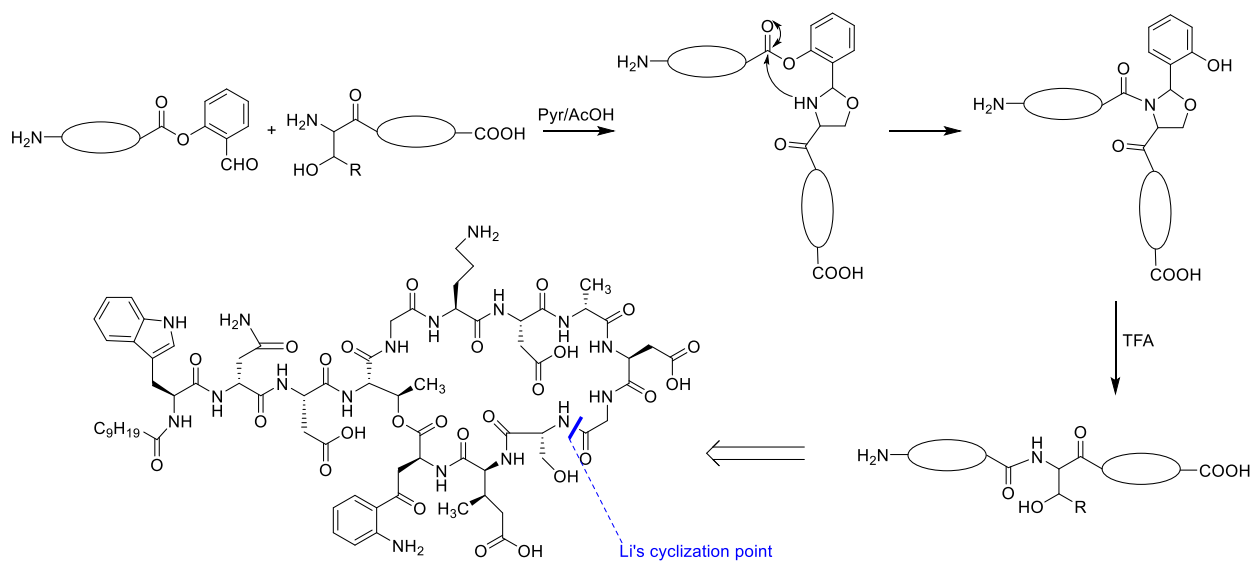
Scheme 1.5 Overview of Ser/Thr NCL approach Li took

To synthesize daptomycin, the Li group needed ample quantities of Fmoc-L-Kyn(PG)-OH and Fmoc-L-MeGlu(t-Bu)-OH. Li and coworkers found that Fmoc-L-Kyn(Boc,CHO)-OH could easily be prepared from the ozonolysis of Fmoc-L-Trp(Boc)-OH. The MeGlu synthon was prepared from intermediate **1.10** which can be synthesized from (S)-pyroglutaminol in 6 steps.[157] **1.10** was converted into Fmoc-L-MeGlu(t-Bu)-OH in 6 steps (Scheme 1.6). Briefly, **1.12** is hydrolyzed with LiOH H_2O/THF then the carboxylic acid is converted to a t-Bu ester using t-BuBr/K_2CO_3/benzyltriethylammonium chloride (BTEAC)/Dimethylacetamide (DMAC) giving **1.12**.[158] TBS removal was achieved using TBAF/THF and the primary alcohol **1.13** was oxidized to the carboxylic acid **1.14** with $NaIO_4$/$RuCl_3$. Finally, the Boc group was removed with HCl/dioxane, and the amino group was protected with FmocOSuc. This yields Fmoc-L-MeGlu(t-Bu)-OH in approximately 12 steps.

Their first approach to daptomycin involved an off-resin cyclization in which the key ester bond would be formed on the resin bound peptide (Scheme 1.7). This approach began with attaching Fmoc-Gly10-OH to a polystyrene solid support via a 2-ClTrt linker and extending the peptide iteratively using standard Fmoc SPPS conditions yielding linear peptide **1.15**. The TBS group on the side chain of Thr4 was deprotected with TBAF/THF but subsequent esterification could not be achieved with Fmoc-L-Kyn(CHO,Boc)-OH.
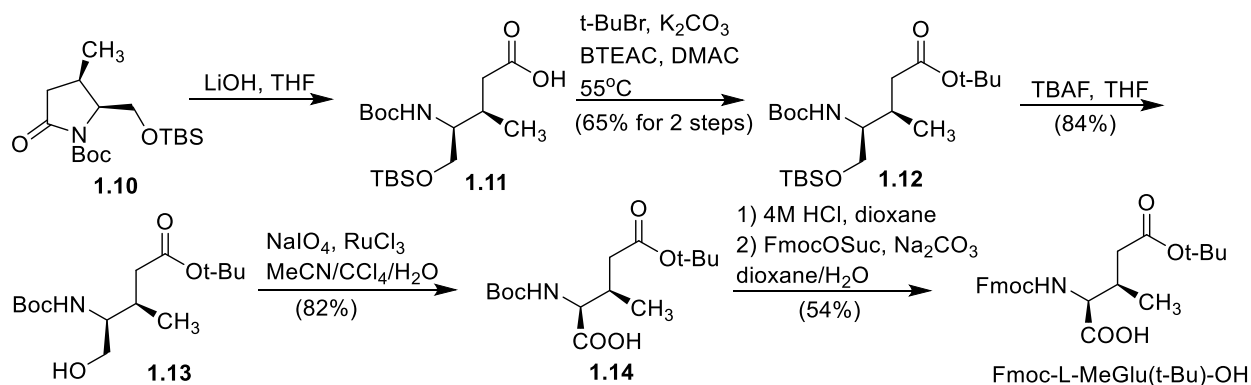
Scheme 1.6 Synthesis of the Fmoc-L-MeGlu(t-Bu)-OH reported by the Li group

To circumvent the difficult ester bond formation, the Li group adopted a hybrid solution phase and solid-phase approach in which the ester bond would be formed in solution on a lipidated pentapeptide **1.17**. However, the key ester bond again could not be formed. The Li group deemed the Fmoc-L-Kyn(Boc,CHO)-OH building block unsuitable for esterification and opted to form the ester bond on a tripeptide **1.19** using Fmoc-L-Trp(Boc)-OH as a synthon. Ozonolysis of depsi peptide **1.20** yielded suitably protected tripeptide **1.21** bearing the sought-after ester bond.

Tetrapeptide **1.21** was coupled to solid-supported pentapeptide **1.22** under standard conditions giving peptide **1.23** (Scheme 1.8). The last two residues making up the macrocyclic portion of the peptide were coupled on yielding peptide **1.24**. The azide group on **1.24** was reduced with DTT/DIPEA and the remaining residues and the lipid tail were attached via Fmoc SPPS

giving peptide **1.25**. Peptide **1.25** was cleaved from the solid support with AcOH/TFE/DCM, reacted with α,α-dimethoxy-salicylaldehyde/PyBOP/DIPEA and then globally deprotected yielding peptide **1.26** after HPLC purification. Purified **1.26** was dissolved in pyridine/AcOH initiating the NCL and yielding peptide **1.27** which was deprotected with TFA/H$_2$O. Purification of the crude material by HPLC yielded daptomycin.
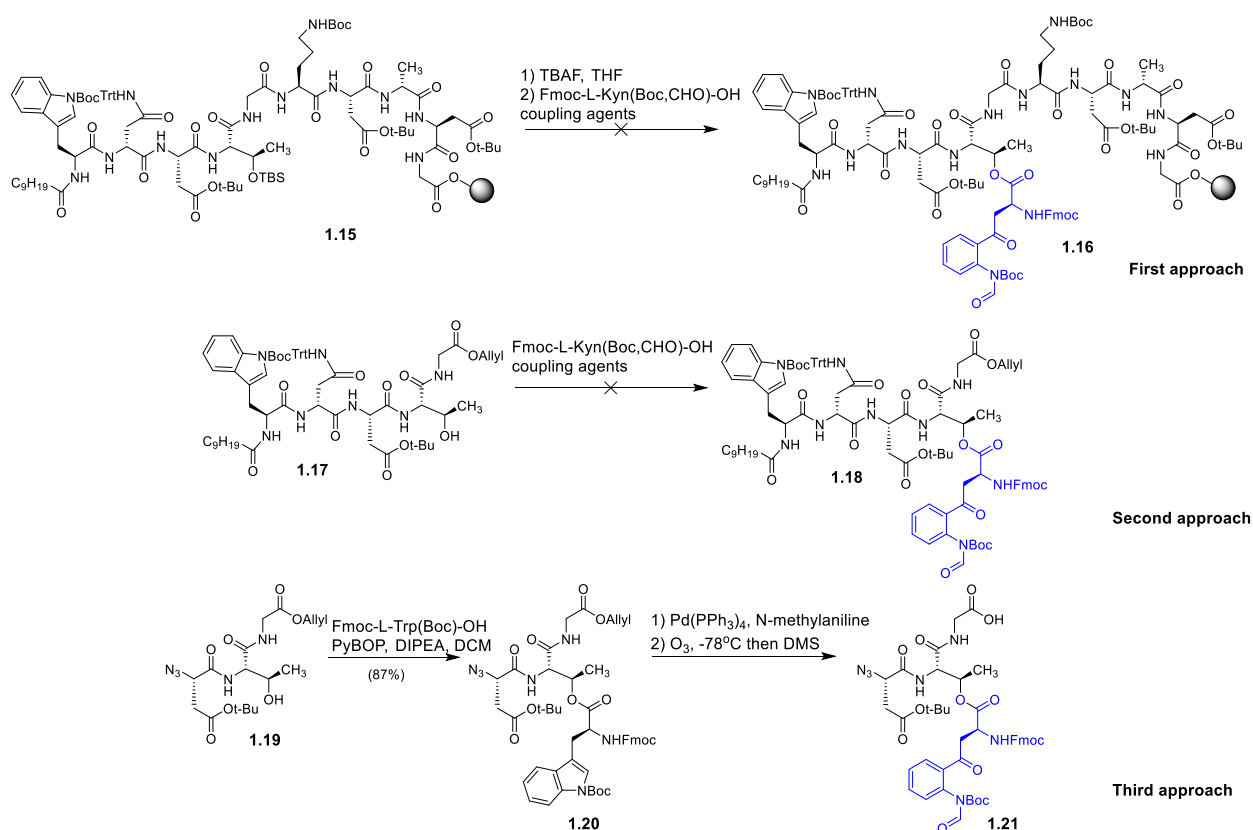
Scheme 1.7. The Li group's first and second approach to daptomycin and the synthesis of **1.21**

Considering the labor intensive nature of the Ser/Thr NCL approach used by Li in their first generation synthesis, it is not surprising that they relied on a more traditional cyclization approach for analog studies.[159] Since publishing their synthesis of daptomycin is 2013, the Li group has prepared approximately 60 analogs of daptomycin and has disclosed a detailed structure-activity relationship for the peptide.[159,160] They have also reported on Kynomycin – an analog of daptomycin which possess a methyl group on the aniline nitrogen of Kyn13. Kynomycin possesses

enhanced activity against daptomycin-resistant strains of *Enterococcus* spp *in-vitro* and *in-vivo*.[161]
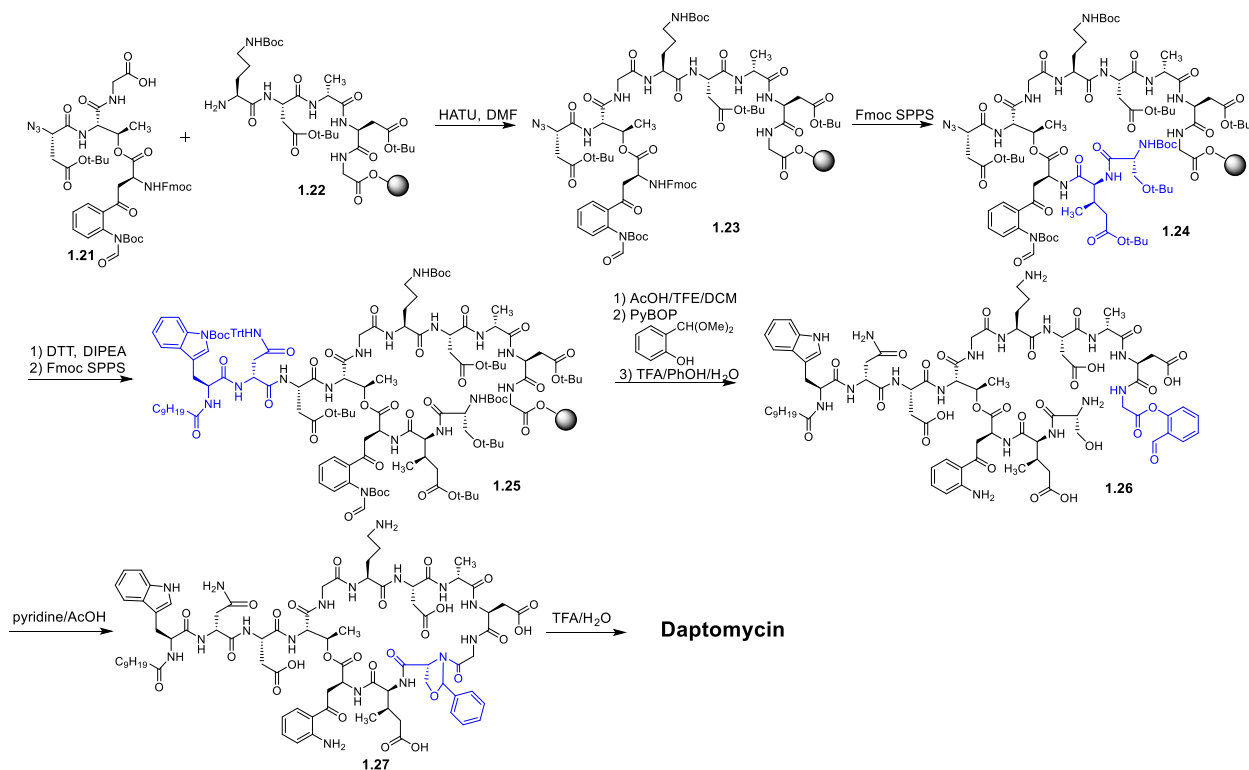
Scheme 1.8 Final approach to the synthesis of daptomycin by the Li group

1.6.5.3   Total synthesis of daptomycin analogs by Martin and coworkers

In 2014, Martin and coworkers disclosed the synthesis of daptomycin analogs in which the ester bond was replaced with an amide bond and MeGlu12 was replaced with Glu12 (dap-Dapa4-Glu12). In their approach, they opted for an off-resin cyclization and thus attached the peptide to a solid-support by the α-COOH of Gly5 with a 2-ClTrt linker (Scheme 1.9). The peptide was extended to the lipid tail using Fmoc SPPS replacing Thr4 with 2,3-diaminopropanoic acid (Dapa) protected at the side chain with an alloc group. Alloc removal from peptide **1.28** yielding **1.29** allowed for iterative attachment of the remaining amino acid residues by Fmoc SPPS giving protected peptide **1.30** which was cleaved from the solid support with HFIP/DCM and cyclized in solution with BOP/DIPEA/DCM. Global deprotection of **1.31** yielded dap-Dapa4-Glu12 which

59

was purified by HPLC. This route was used to prepare the enantiomer of dap-Dapa4-Glu12 (ent-dap-Dapa4-Glu12). The antibacterial activity of each peptide was assayed against *S. aureus*. dap-Dapa4-Glu12 possessed an MIC that was 164-fold greater than daptomycin and ent-dap-Dapa4-Glu12 showed no activity even at concentrations approaching 1 mM. Based on these results, Martin and coworkers suggested that the action mechanism of daptomycin might be dependent on an interaction with a chiral target. However, the massive activity difference between daptomycin and dap-Dapa4-Glu12 suggests that the latter is not a good model of the former rendering their study inconclusive.
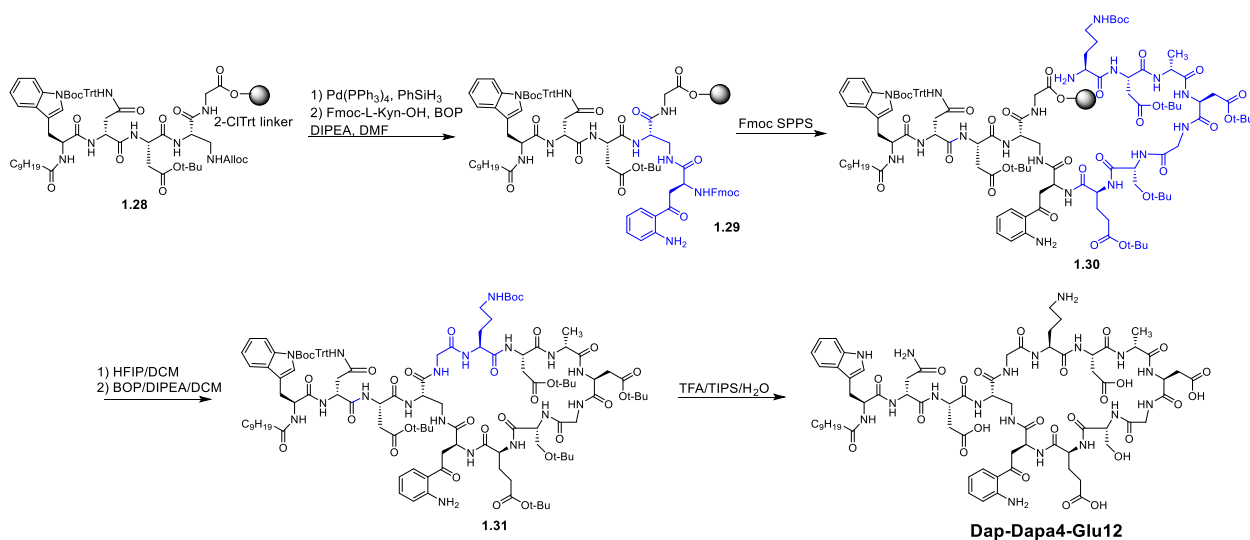
Scheme 1.9 Approach to the synthesis of aza-daptomycin analogs developed by Martin and coworkers

1.6.5.4   *Total synthesis of daptomycin by the Taylor Group*

The total synthesis of daptomycin published by the Li group is not well-suited to the economical preparation of analogs. This is primarily due to the combined solution and solid-phase approach which requires that a significant portion of the peptide be prepared by a multi-step synthesis in solution. Additionally, the need for two HPLC purifications greatly increases the cost per analog. Automated analog preparation would be made far more efficient if the entire synthesis could be done on a solid-support, and this would be conducive to the rapid preparation of a library of

daptomycin analogs by combinatorial techniques. Thus, the Taylor group set out to develop the first total synthesis of daptomycin that would occur completely on the solid-phase.[162]

In their retrosynthetic analysis, the Taylor group envisioned cyclizing the peptide between Ser11 and Gly10 with the peptide attached to the solid support by the side chain of Asp9 linked with 2-ClTrt. To prepare this starting dipeptide, Fmoc-L-Asp-Oallyl was reacted with a 2-ClTrt polystyrene resin giving solid-supported amino acids **1.32** (Scheme 1.10). The allyl ester of **1.32** was removed with $Pd(PPh_3)_4$/dimethylbarbituric acid (DMBA) and the exposed α-COOH was reacted with $TsO^-NH_3^+GlyOallyl$/PyBOP. The resin supported dipeptide **1.33** is an ideal starting point for the solid-phase synthesis of daptomycin. The peptide can be fully elongated by Fmoc SPPS from Asp9 and the cyclization can be initiated on the solid support by deprotecting GlyOallyl. Cyclization then occurs on an achiral residue eliminating any concerns about epimerization. Additionally, since the cyclization occurs on a solid support, the solvent efficiency of the cyclization is increased dramatically due to the pseudo dilution effect.
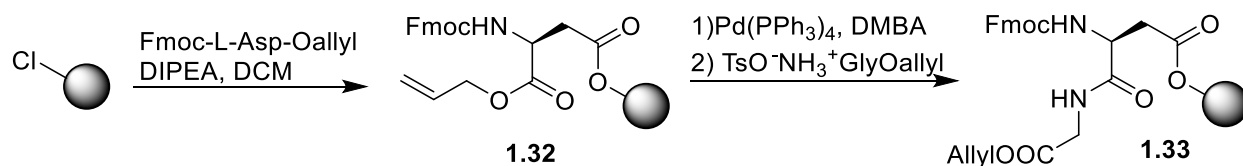
Scheme 1.10 Preparation of the solid support Fmoc-Asp9-Gly10-Oallyl **1.33** starting point used extensively by the Taylor lab for the synthesis of daptomycin and analogs thereof
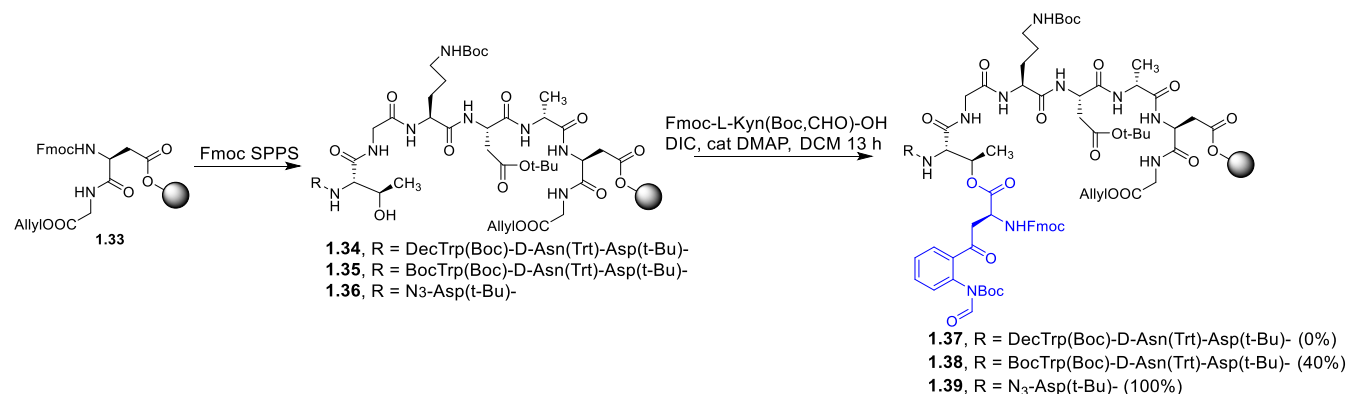
1.34, R = DecTrp(Boc)-D-Asn(Trt)-Asp(t-Bu)-
1.35, R = BocTrp(Boc)-D-Asn(Trt)-Asp(t-Bu)-
1.36, R = N3-Asp(t-Bu)-

Fmoc-L-Kyn(Boc,CHO)-OH
DIC, cat DMAP, DCM 13 h

1.37, R = DecTrp(Boc)-D-Asn(Trt)-Asp(t-Bu)- (0%)
1.38, R = BocTrp(Boc)-D-Asn(Trt)-Asp(t-Bu)- (40%)
1.39, R = N₃-Asp(t-Bu)- (100%)

61

Using this starting point, the Taylor group attempted the total synthesis of daptomycin by extending from Asp9 to the lipid tail then forming the ester bond between the side chain of Thr4 on peptide **1.34** and Fmoc-L-Kyn(CHO,Boc)-OH (Scheme 1.11). Unfortunately, the ester bond resisted formation under a variety of conditions. The Taylor group surmised that the ester bond might be formed on a truncated peptide, so they initiated the esterification on substrates **1.35** and **1.36**. They found that removal of the lipid tail (**1.35**) greatly improved the esterification, but the yield of **1.38** was only 40%. In contrast, the esterification of heptapeptide **1.36** occurred quantitatively giving depsi peptide **1.39**. The azide group on peptide **1.39** was reduced to the amine using PMe$_3$/dioxane/H$_2$O allowing for the attachment of N$_3$-L-Asn(Trt)-OH giving peptide **1.40** (Scheme 1.12). The same azide deprotection and subsequent coupling conditions were used to install N$_3$-Trp(Boc)-OH and the lipid tail giving Fmoc protected depsi peptide **1.41**. Fmoc SPPS was used to attach MeGlu12 (which was prepared using an approach analogous to what is presented in Scheme 1.6) and D-Ser11 giving peptide **1.42**. Peptide **1.43** was then allyl deprotected using Pd(PPh$_3$)$_4$/DMBA and cyclized with PyAOP/HOAt/DIPEA yielding cyclic peptide **1.43**. The cyclization of **1.42** proved challenging, and a number of different solvents were applied to increase the efficiency of the process. The best results were achieved with DMF/DCM/N-Methyl-2-pyrrolidone (NMP) containing 1% Triton X-100 which gave a cyclization efficiency of 40%. Cyclic peptide **1.43** was deprotected with TFA/thioanisole/TIPS/H$_2$O giving crude product which was purified by HPLC yielding daptomycin in a 9% overall yield.
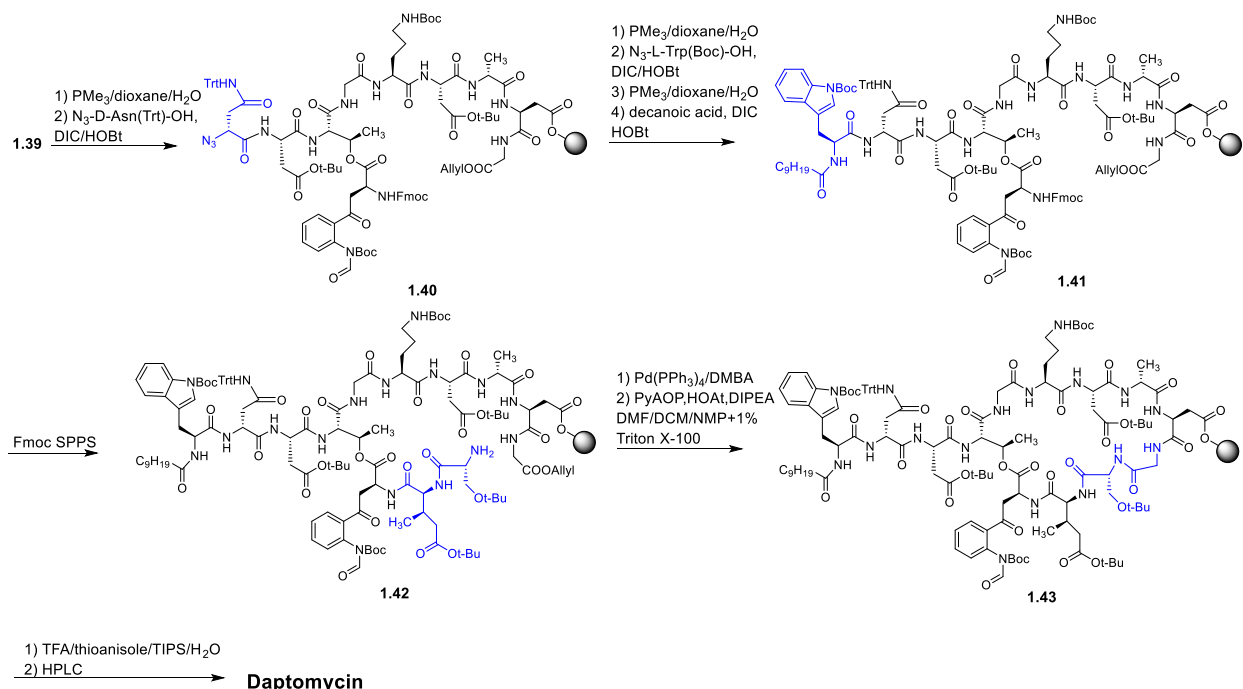
Scheme 1.12 The final route to daptomycin taken by the Taylor group

The Taylor lab used the route outlined in Scheme 1.12 to prepare some analogs of daptomycin. A daptomycin analog that contained (2S,3S)-MeGlu instead of (2S,3R)-MeGlu displayed an MIC that was approximately 50-fold higher than that of daptomycin. Interestingly, a daptomycin analog bearing Glu12 and Trp13 (dap-EW) was found to be almost as active as daptomycin at 5 mM CaCl$_2$ against *B. subtilis*. In contrast, replacement of MeGlu12 with Glu and Kyn13 with Tyr yielded an analog that was significantly less active than daptomycin. In a subsequent publication, a similar approach was used to synthesize analogs of daptomycin in which Thr4 was replaced by Ser.[163] Such an approach required the protection of the Ser side chain with Trt which is removed under conditions that rupture the bond between Asp9 and the 2-ClTrt linker. As a result, a more acid resistant Wang linker was used. Unfortunately, Dap-Ser4-Glu12-Trp13 was 100-fold less active than daptomycin highlighting the importance of Thr4.

63

Although the solid-phase approach developed by the Taylor lab is a step towards a solid-phase synthesis of daptomycin amenable to automation, it suffers from two shortcomings. First, it requires the use of 3 azido acids which are not commercially available. Second, the cyclization efficiency is only modest, thus the conditions developed may not prove general during library synthesis.

The Taylor lab improved on its first synthesis of dap-EW (Scheme 1.13). They aimed at reducing the number of azido acids to one which could be achieved by taking one of two routes. In route A, Asp3 would be installed as an azido acid, allowing formation of the macrocycle by Fmoc SPPS followed by on-resin cyclization. With the macrocycle completed, the azide protecting Asp3 would be reduced, and the remaining amino acids and the lipid tail would be installed using Fmoc SPPS. In route B, the α-azido acid would be used to form the ester bond allowing for installation of Asp3, D-Asn2, Trp1 and the lipid tail by Fmoc SPPS. Route A was hindered by elimination of the azide protecting Asp3 during Fmoc deprotection, which was rather unexpected considering that the Li group also protected Asp3 with an azide and did not report any elimination products.[155] Further experiments demonstrated that this elimination should be problematic with any α-azido acid possessing acidic protons at the β-position, including N_3-Kyn(Boc,CHO)-OH. Thus, route B was further developed which allows for the preparation of Trp13 containing analogs of daptomycin using only a single azido acid.

An all Fmoc approach to synthesizing dap-EW and analogs thereof was eventually disclosed by the Taylor lab (Scheme 1.14). Serendipitously, Barnawi et al found that peptide **1.34**, which bears a lipid tail, could be esterified completely by Fmoc-L-Trp(Boc)-OH using conditions similar to those employed by the Albericio group during their ground-breaking synthesis of pipecolidepsin A.[164] Using this route, the Taylor group performed an alanine scan on dap-EW

and demonstrated that positions 6 and 11 are amenable to substitution. They also disclosed their discovery of dap-Lys6-Glu12-Trp13 – an analog of daptomycin containing only canonical amino acids which is 2-3 fold less active than daptomycin. The Taylor lab has used dap-Lys6-Glu12-Trp13 as a lead structure for a comprehensive analog study exploring substitutions at positions 8 and 11.[136] They found that by substituting these positions with cationic residues (Arg or Lys), they were able to produce analogs with activity that rivalled that of dap-Lys6-Glu12-Trp13. By making the same changes to daptomycin directly using the synthetic developments later disclosed in this thesis, they discovered several analogs of daptomycin that have enhanced activity against various strains of *S. aureus*. To date, the Taylor group has reported on the synthesis and characterization of approximately 50 analogs of daptomycin.
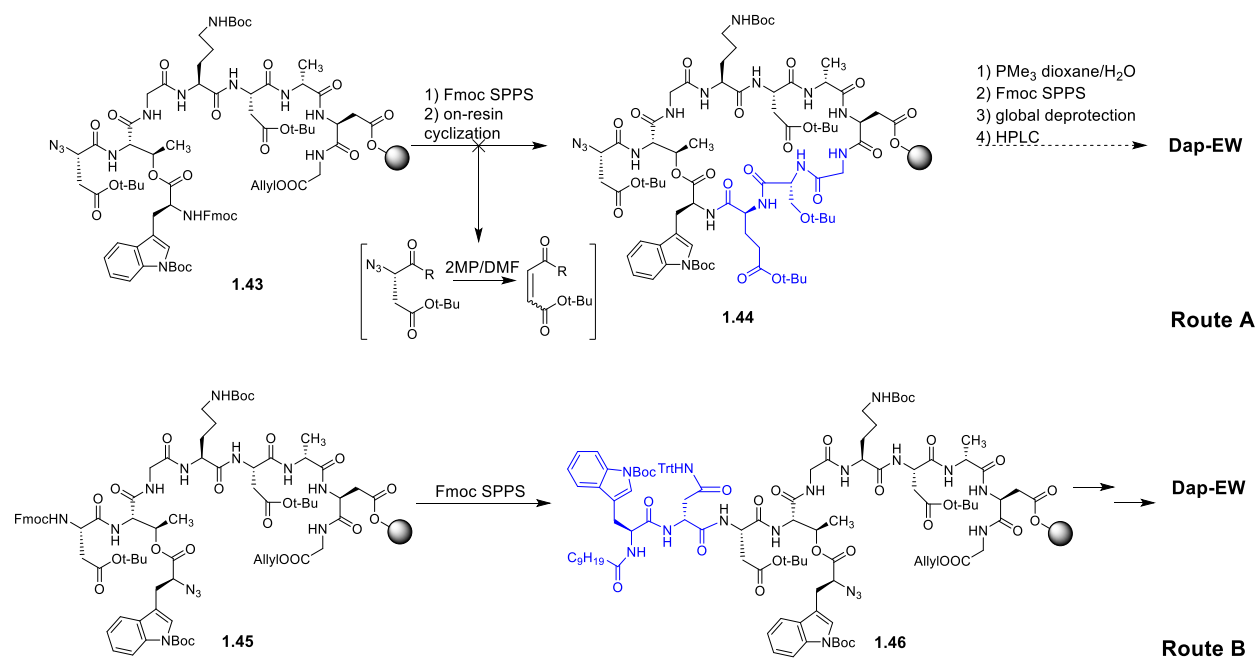
Scheme 1.13 Improved route to dap-EW developed by the Taylor lab
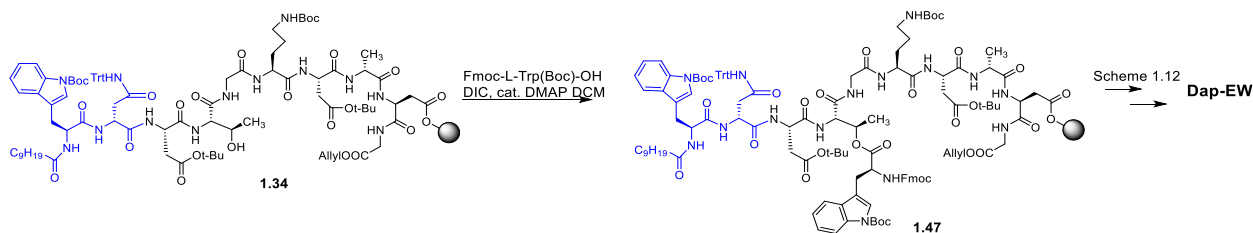
Scheme 1.14 All Fmoc SPPS approach to the synthesis of dap-EW

1.6.5.5 *Total synthesis of daptomycin by the Brimble group*

In 2019, the Brimble group reported on their total synthesis of daptomycin which used a combined

Boc and Fmoc SPPS approach. At the outset, the authors developed a synthesis of Boc-L-

MeGlu(Bn)-OH which starts from chiral iminolactone **1.48** prepared in 3-steps from camphor

quinone (Scheme 1.15).[165] The authors found the transformation of **1.48** to **1.49** to be difficult

and could only get the reaction to work on a 50 mg scale with a modest diastereoselectivity of 3:1

in favour of the desired isomer. Removal of the auxiliary was achieved with 6N HCl yielding the

amino acid **1.50** which was side chain protected as a benzyl ester under acidic conditions. Finally,

the α-amine was protected with a Boc group under standard conditions giving Boc-L-MeGlu(Bn)-

OH (**1.51**) as a 2:1 mixture of (2S,3R):(2S,3S). The authors surmised that they would be able to

separate the two isomers at the end of their synthesis of daptomycin and moved forward with this

mixture of isomers.
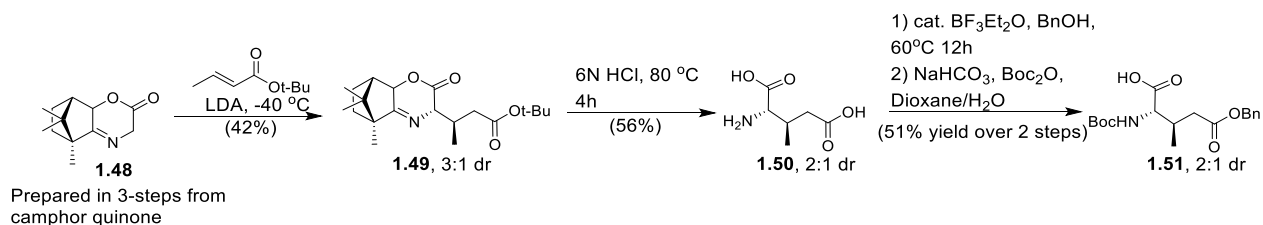
Scheme 1.15 Synthesis of Boc-L-MeGlu(Bn)-OH used by the Brimble group

The Brimble group intended on developing a Boc SPPS approach to daptomycin because

Boc SPPS is faster than Fmoc SPPS and the protecting group scheme helps reduce aggregation.

Additionally, many side reactions in peptide synthesis are catalyzed by base; thus, difficult sequences are more easily prepared using Boc SPPS.

The Brimble group started by attaching Fmoc-L-Asp-Ot-Bu to a PAM linked polystyrene resin (Scheme 1.16). Treatment of **1.52** with TFA/H$_2$O exposed the α-COOH which was reacted with TsO$^-$NH$_3^+$-Gly-OAllyl giving the starting peptide **1.53**. The Brimble group extended from this point to the lipid tail using Boc SPPS giving linear sequence **1.54** but found that the ester bond
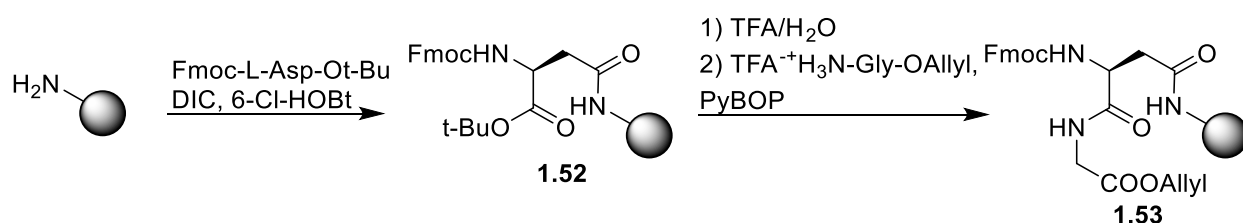
Scheme 1.16 Solid-phase of starting point **1.52** used by the Brimble group to synthesize daptomycin

could not be formed at this stage (Scheme 1.17). The authors then tried to form the ester bond on linear sequence **1.55** which did not contain Trp1 or the lipid tail, however this too failed. In line with what Li and coworkers had proposed for Fmoc-L-Kyn(Boc,CHO)-OH, the authors surmised that Boc-L-Kyn(CHO,CHO)-OH was too unreactive to undergo the desired transformation and decided to use Boc-L-Trp(Boc)-OH as a more reactive Kyn synthon. The Kyn residue would be unmasked via an on-resin ozonolysis reaction first developed by the Li group at a later stage (Scheme 1.18).[166] Esterification of **1.54** with Boc-L-Trp(Boc)-OH occurred without issue yielding peptide **1.58**. The remaining residues in the macrocycle were coupled on with Boc SPPS and the peptide was cyclized on-resin after deprotection of the allyl on Gly10 yielding protected cyclic peptide **1.59**. With the macrocycle complete, the resin-bound peptide was treated with ozone which rapidly converted Trp(Boc)13 to Kyn(CHO,CHO)13 yielding peptide **1.60**. Attempts to elongate **1.60** via Fmoc SPPS were accompanied by rapid conversion of the peptide to an unknown

product. The authors assumed that a base-dependent side reaction involving the ester bond, which is known to be base labile, had occurred and attempted to attenuate this side reaction by modifying the Fmoc deprotection conditions used. They found that this side reaction depended primarily on the strength of the base present and found that 50% morpholine/DMF (2 x 8 min) removed the Fmoc group without causing the side reaction. With these conditions in hand, the Brimble group coupled on the remaining amino acids and the lipid tail without issue. It was noted that treatment of peptide **1.60** with morpholine/DMF removed one of the formyl groups from the side chain of Kyn. Global deprotection of **1.61** was conducted with HF/*p*-cresol. Deformylation of Kyn13 was completed with 1:1 H_2O:MeCN containing 5% TFA. Fortunately, the authors found that daptomycin containing each stereoisomer of MeGlu could be separated by HPLC. The route developed by the Brimble group proceeds with a 6.3% overall yield and was used to prepare 5 analogs none of which were active.
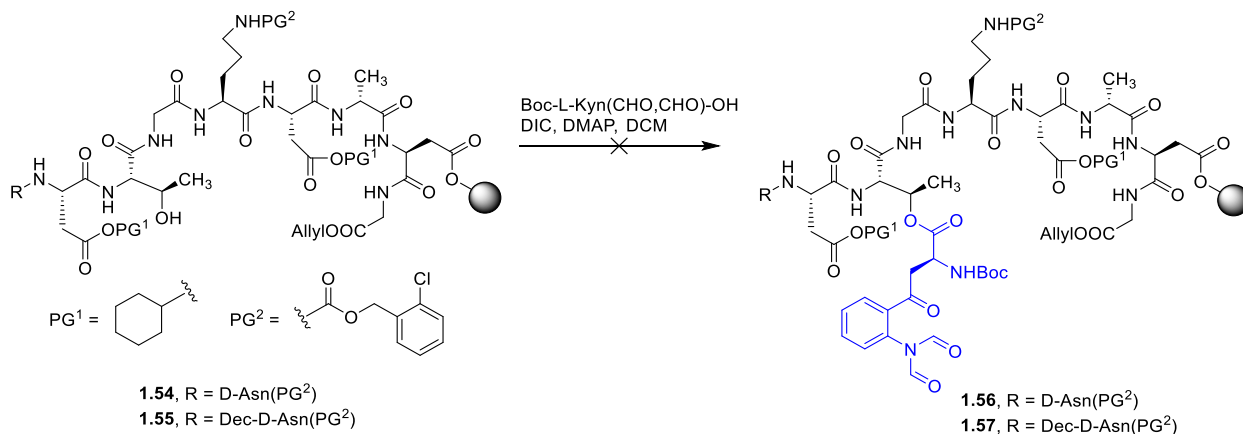
Scheme 1.17 Failed approaches taken by the Brimble group
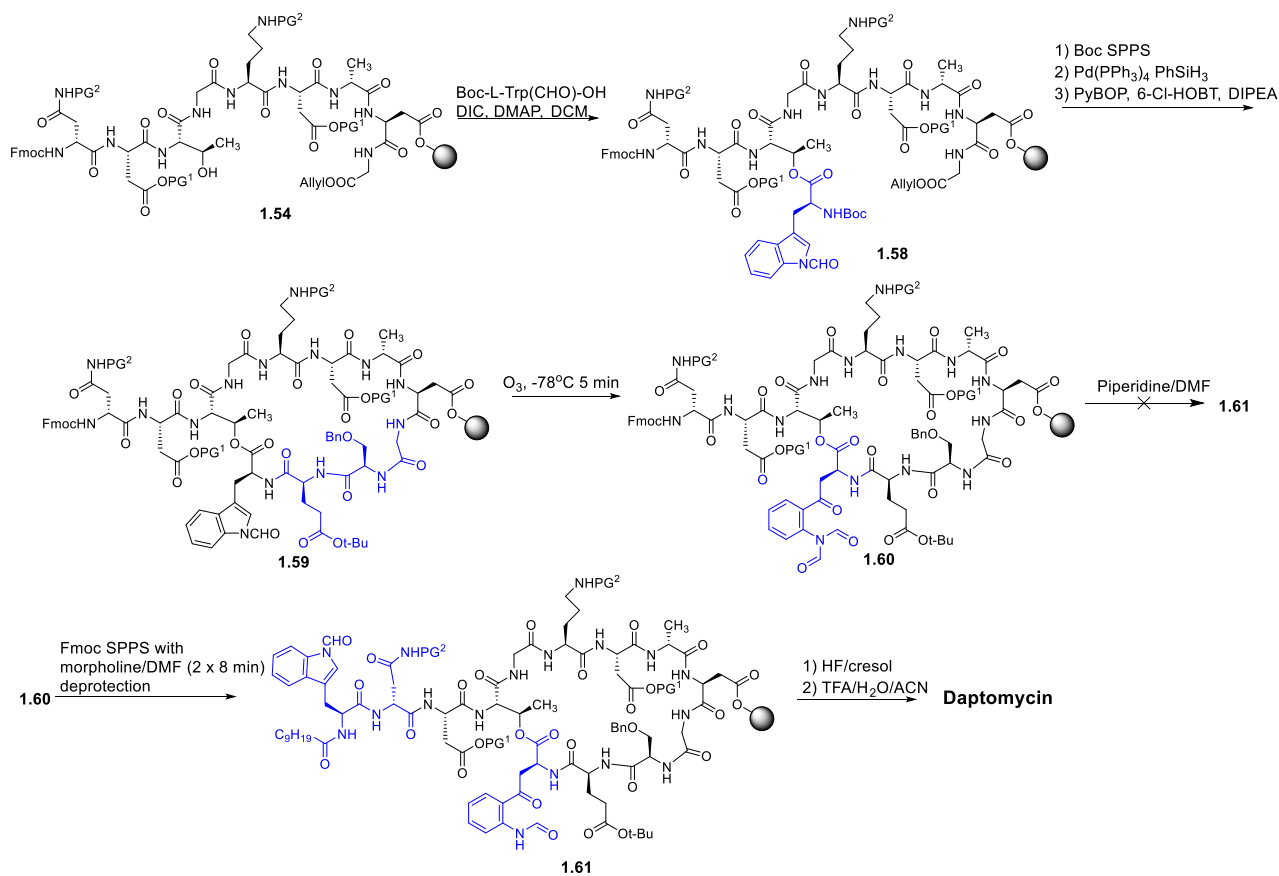
Scheme 1.18 Boc/Fmoc SPPS of daptomycin developed by the Brimble group

1.7 Project goals and overview

The precise molecular target of daptomycin and A54145 is unknown. Recent studies have suggested that daptomycin targets lipid II and its undecaprenol precursors but, as discussed in section 1.4.1, the colocalization of daptomycin with these molecules appears to be coincidental. What seems central to the action of daptomycin is its ability to insert deeply into the bacterial and oligomerize. Since this event appears to be predicated on the presence of PG in the target membrane, it is rational to propose that PG is the molecular target of daptomycin and daptomycin kills bacteria by disrupting the distribution of PG on the bacterial membrane. Considering the critical roles that PG plays (section 1.2) in directing cell wall synthesis and cell division, and its roles as a cofactor in cell wall synthesis, and the fact that it is found in high concentrations in RIFs, this hypothesis accounts for the majority of the effects that daptomycin has on Gram-positive

bacteria. Thus, the first major goal of this work was to determine whether PG is the chiral target of daptomycin and A54145.

The second major goal of this work was to explain why daptomycin and A54145D display different activities in the presence of LS. Considering that both of these antibiotics are thought to function through the same mechanism, and they are both thought to be PG-dependent,[22] the results presented in Table 1.2 can not be explained by the current understanding of these natural products. Indeed, if both peptides bind to PG with similar affinities, as has been suggested by ITC studies done by Palmer and coworkers (discussed in section 1.4.3),[89] then each antibiotic must be sequestered by a different mechanism. One possible explanation for the large activity difference displayed by daptomycin and A5D in the presence of LS is that each peptide targets a different stereoisomer of PG. The plausibility of this hypothesis is predicated on work by Kuksis and coworkers (section 1.2) who discovered that bacteria may contain significant quantities of both 2R,2'S- and 2R,2'R-PG.

The third major goal of this work is to provide rationale for daptomycin resistance mechanisms. As described in section 1.5, it is unclear whether increased lysyl-PG content confers daptomycin resistance by electrostatic repulsion or by masking the PG that is available. The latter hypothesis is predicated on daptomycin being able to recognize the headgroup of PG. Thus, through synthesizing analogs of PG, and analyzing how substitutions affect membrane binding and oligomerization, a rationale for some daptomycin resistance mechanisms will emerge.

This work primarily attempts to explore the validity of the hypothesis that PG is the chiral target of daptomycin and A54145D through experimentally demonstrating that both natural products interact with a chiral target as part of their action mechanism and recognize the stereoisomers PG. To achieve the former, all 4 stereoisomers of PG needed to be synthesized. To

achieve the latter, both the natural and unnatural enantiomers of daptomycin and A54145D needed to be synthesized.

Two minor goals were achieved in chapter 2. The first goal was to conclusively determine the importance of the ester bond in daptomycin through the synthesis of analogs of daptomycin that possess an amide bond in place of the ester bond. The second goal was to determine whether the enantiomer of an active daptomycin analog was active *in-vitro*. This study determined that the ester bond is fundamentally important to the antibacterial activity of daptomycin and that daptomycin probably interacts with a chiral target as part of its MoA.

The goal of Chapter 3 was to develop an efficient, enantioselective synthesis of Fmoc-MeGlu(tBu)-OH that would be used to develop a new route to daptomycin. This synthetic study succeeded in developing a 6-step enantiospecific and diastereoselective synthesis for Fmoc-MeGlu(tBu)-OH which was used to synthesize both the L- and D-isomers of this synthon.

The goal of Chapter 4 was to develop an all Fmoc SPPS approach to daptomycin which would allow for rapid synthesis of the unnatural enantiomer of daptomycin (ent-dap) and analogs of daptomycin. The completion of this study led to the discovery that Fmoc-L-Kyn(CHO,Boc)-OH and Fmoc-L-Kyn(CHO,CHO)-OH are not suitable for Fmoc SPPS due to base instability. Remedying this issue restored the reactivity of this synthon allowing for the first ever all Fmoc SPPS total synthesis of daptomycin.

The goals of Chapter 5 were three-fold. First we wanted to ascertain whether daptomycin interacts with a chiral target by determining the antibacterial activity of ent-daptomycin. Second, the four stereoisomers of PG would be synthesized via a diastereo- and enantiospecific synthesis. Third, the interaction of daptomycin and ent-daptomycin with each of the four stereoisomers of

PG would be probed using a variety of techniques to determine how membrane affinity and membrane bound state are affected by peptide and lipid stereochemistry. These goals were accomplished, and the resulting study unequivocally demonstrated that daptomycin interacts with a chiral target as part of its MoA. PG stereochemistry was found to strongly influence membrane affinity, membrane bound state and oligomerization demonstrating that 2R,2'S-PG is the chiral target of daptomycin.

The goal of Chapter 6 was to develop a structure-activity relationship for the interaction of PG with daptomycin through synthesizing analogs of PG. This would shed light on which portions of PG are recognized by daptomycin and would determine whether PG needs to be in a membrane environment to be recognized by daptomycin. These studies demonstrated that daptomycin interacts with both hydroxyl groups on the headgroup of PG and primarily interacts with the first 7-8 carbons of the lipid tails of PG. Studies with PG bearing fatty acid tails containing only 8 carbons demonstrated that PG does not need to be in a membrane to bind avidly to daptomycin.

The goal of Chapter 7 was to develop a stereoselective synthesis of lysyl-PG and determine how lysyl-PG affects the membrane affinity and membrane bound state of daptomycin. A synthesis for lysyl-PG was successfully developed. Lysinylation was found to effectively mask PG. The affinity of daptomycin for membranes containing PG was virtually unaffected by the presence of lysyl-PG. The membrane bound structure of daptomycin was unperturbed by the presence of lysyl-PG, but the oligomerization event was affected. Based on this study, it seems that the increases in lysyl-PG content observed in the membranes of daptomycin resistant strains of bacteria cannot explain conferred levels of resistance. With that said, it is possible for bacteria to subvert the action of daptomycin by converting a substantial fraction of their PG to lysyl-PG

The goal of chapter 8 was to develop a new, enantio- and diastereoselective synthesis for Fmoc-hAsn(TBS)-OH and Fmoc-MeOAsp(t-Bu)-OH which would facilitate a total synthesis of A5D. The syntheses of Fmoc-L-*threo*-hAsn(TBS)-OH, Fmoc-L-*threo*-MeOAsp(tBu)-OH, and Fmoc-L-*erythro*-MeOAsp(t-Bu)-OH were achieved using a new approach. These building blocks were successfully applied to the development of a synthesis for A5D which demonstrated that the natural product possess L-*erythro*-MeOAsp.

The goals of chapter 9 were to generalize the aminohydroxylation chemistry used in chapter 8 and to find improved substrates for that reaction which could be used for the synthesis of Fmoc-D-*threo*-hAsn(TBS)-OH and Fmoc-D-*threo*-MeOAsp(tBu)-OH; these would later be used to prepare the unnatural enantiomer of A5D. Both of these goals were achieved. The aminohydroxylation reaction was found to function with substrate scope that rivalled that of similar methods. Substrate scoping led to the discovery of a starting material that was well-suited for the aminohydroxylation reaction and gave an Fmoc protected amino alcohol which was efficiently converted to Fmoc-D-*threo*-hAsn(TBS)-OH and Fmoc-D-*threo*-MeOAsp(tBu)-OH.

The first goal of Chapter 10 was to synthesize and determine the antibacterial activity of the unnatural enantiomer of A5D. Second, we would develop a means for assaying the membrane interaction of A5D with model membranes. Third, the interaction of A5D with enantiopure PG would be determined to ascertain how peptide and lipid stereochemistry affect membrane affinity and membrane bound state. Fourth, the antagonism of daptomycin and A5D by each stereoisomer of PG would be determined *in-vitro*. Fifth, the stereochemical content of PG in bovine LS would be determined. This study demonstrated that A5D does interact with a chiral target and this chiral target is 2R,2'S-PG. A5D and daptomycin were equally antagonized by each stereoisomer of PG and had similar affinity for 2R,2'S-PG. A new method for determining the stereochemical content

of PG was developed and this was used to show that LS consists of exclusively 2R,2'S-PG. Further studies demonstrated that daptomycin and A5D are equally antagonized by PG. These studies disproved the hypothesis that A5D is less susceptible to inhibition by lung surfactant and cast doubt on the hypothesis that a daptomycin or A5D analog can be used to treat CAP.

The goal of chapter 11 was to tie the content of previous chapters together by summarizing the most pertinent findings of this thesis and propose future studies which could build on this body of work.

Chapter 2 - The Effect of Replacing the Ester Bond with an Amide Bond and of Overall Stereochemistry on the Activity of Daptomycin

2   Preface and contributions

The work presented in this chapter was completed primarily by me under the supervision of Prof. Scott D. Taylor and Prof. Michael Palmer. The unnatural enantiomer of dap-K6-E12-W13 was prepared by Ghufran Barnawi – a graduate student in the Taylor lab. David Beriashvili, a graduate student in Prof. Palmer's lab, assisted with the membrane binding studies.

The manuscript that this chapter is based on was published in the journal *Bioorganic & Medicinal Chemistry* (*Bioorg. Med. Chem.* **2019**, *27*, 240–246). The manuscript was prepared by Prof. Taylor and me. In accordance with the policies of Elsevier, as an author of this manuscript, I retain the right to include this article in my thesis. The published version of the manuscript was edited to fit within this thesis. Additional supplementary information can be found on the journal's website.

2.1   Introduction

One potentially powerful approach for uncovering daptomycin's mechanism of action (MoA), and for producing novel antibiotics with improved properties, is by performing structure-activity relationship (SAR) studies. However, daptomycin is a complex molecule, which has made the development of an efficient method for preparing daptomycin analogs a challenge (see section 1.6).

Among the questions for which we wished to answer with our SAR studies were: (1) can the ester bond in daptomycin be replaced with an amide bond without significant loss of activity? and, (2) what is the effect of overall stereochemistry on daptomycin's activity?

The answers to the above questions are of some interest. As mentioned in section 1.5.2, a study by D'Costa et al has shown that laboratory isolates of actinomycetes frequently attain resistance to daptomycin by enzymatic hydrolysis of the ester bond and resistance via this mechanism could become clinically relevant in the future.[134] It is possible that this mechanism of resistance could be circumvented by replacing the ester bond with an amide bond. Such an analog would also be expected to be more resistant to hydrolysis than daptomycin in the body. Moreover, it would be expected that the synthesis of such an analog would be less challenging since the formation of the ester bond is often the most difficult step in the chemical synthesis of daptomycin (discussed at length in section 1.6.5).

Comparing both enantiomeric forms of biologically active peptides is a common tactic for determining whether or not the peptide is involved in a chiral interaction with a chiral target.[52,167,168] Studying both enantiomeric forms of daptomycin or a reasonably active daptomycin analog, could determine whether or not a chiral interaction with a chiral target is essential to daptomycin's MoA.

As discussed in Martin and coworkers attempted to answer the first question posed above by replacing Thr4 in Dap-E12-W13 with L-diaminopropionic acid (Dapa), thus replacing the ester bond with an amide bond (Dap-Dapa4-E12-W13).[167] As expected, this analog was much more resistant to degradation than daptomycin in human plasma serum; however, it was 82-fold less active (MIC = 160 µg/mL) against *S. aureus* than daptomycin (MIC = 1.9 µg/mL). It was suggested that the poor activity of Dap-Dapa4-E12-W13 was due to conformational changes/restrictions in the macrocycle that resulted from incorporation of the amide linkage. However, we have found that Dap-S4-E12-W13, in which Thr 4 is replaced with Ser, was at least 29-fold less active (inactive up to 100 µg/mL) than Dap-E12-W13 against *B. subtilis*, indicating that the methyl group

76

on the Thr4 side chain was very important for activity.[169] Therefore, the poor activity of Dap-Dapa4-E12-W13 may be due, in whole or in part, to the lack of a methyl group on the side chain of the Dapa residue rather than being due to the introduction of the new amide bond.

The Martin group attempted to answer the second question by making the enantiomer of Dap-Dapa4-E12-W13 (*ent*-Dap-Dapa4-E12-W13).[167] They reported that *ent*-Dap-Dapa4-E12-W13 was inactive up to 1280 μM. On the basis of these results, they suggested that a specific chiral interaction(s) may be required for daptomycin activity; however, due to the poor activity of Dap-Dapa4-E12-W13, it is not possible to draw a definitive conclusion concerning the effect of overall stereochemistry on the activity of daptomycin. What their results do reveal is that *ent*-Dap-Dapa4-E12-W13 is at least 8-fold less active than Dap-Dapa4-E12-W13. Indeed, since Dap-Dapa4-E12-W13 had such low activity and is probably structurally very different from daptomycin, it is even possible that this analog may not exert its antibacterial action by the same mechanism as daptomycin.

2.1, R^1 = CH_3, R^2 = H
2.2, R^1 = H, R^2 = CH_3
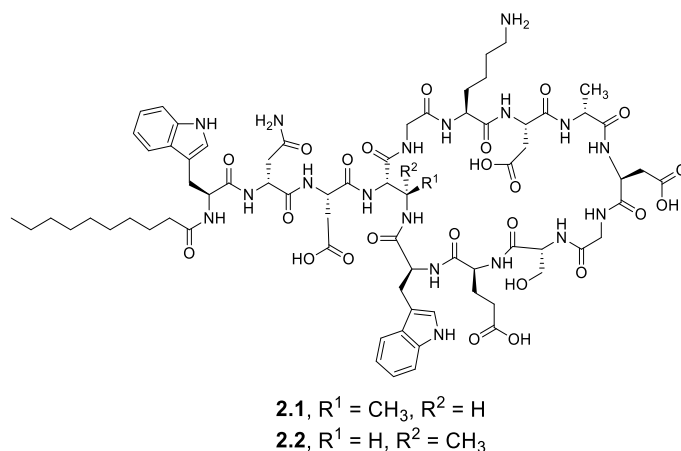
Figure 2.1 The structure of aza-daptomycin analogs **2.1** and **2.2**

In this chapter, more definitive answers to the above questions are provided. This was achieved by preparing peptides **2.1** and **2.2** (Figure 2), which are analogs of Dap-K6-E12-W13 in

which Thr4 is replaced with (2S,3R)-diaminobutyric acid ((2S,3R)-Daba in peptide **2.1**) or its epimer (2S,3S-Daba in peptide **2.2**), as well as *ent*-Dap-K6-E12-W13. The biological activity of these peptides was determined and their interaction with model liposomes in the presence of Ca^{2+} studied.

2.2   Results and discussion

2.2.1   Syntheses

It was decided that Fmoc-protected (2S,3R)- or (2S,3S)-2-amino-3-azidobutanoic acid (FmocAABA) should be used as building blocks for incorporating the Daba residues during Fmoc SPPS of peptides **2.1** and **2.2**. This strategy of using the azido group for protection of the β-amino group in Daba during Fmoc SPPS has recently been employed by Dianati et al. during the SPPS of a peptide-based protease inhibitor.[168] They prepared (2S,3R)- and (2S,3S)-FmocAABA via a 6-step synthesis starting from L-BocThr or L-Boc-*allo*-Thr. Although this procedure was appealing, as it required only three chromatographic purifications, the overall yields were somewhat low (22-23%). Therefore, we decided to prepare these two isomers using a route similar to one that was described in a Pfizer patent for the synthesis of Boc-protected (2S,3R)-AABA benzyl ester.[170] As outlined in Scheme 1, BocThrOtBu[171] was converted to cyclic sulfamidate **2.3** through reaction with $SOCl_2$, followed by oxidation of the resulting sulfamidite with $NaIO_4$ catalyzed by $RuCl_3$. Compound **2.3** was opened by reaction with NaN_3 and the resulting sulfamic acid was hydrolyzed in a mildly acidic solution of aqueous sodium chloride to give compound **2.4**. The amino and COOH groups in **2.4** were deprotected using $TFA:H_2O$ (9:1) and the α-amino group subsequently re-protected with FmocOSu, yielding (2S,3R)-FmocAABA (**2.5**). The same route was used to synthesize (2S,3S)-FmocAABA (**2.8**) starting from L-Boc-*allo*-ThrOtBu. The overall yields of this 6-step process, which required only one chromatographic purification (at the end of each synthesis), were 50% (for **2.5**) and 51% (for **2.8**).
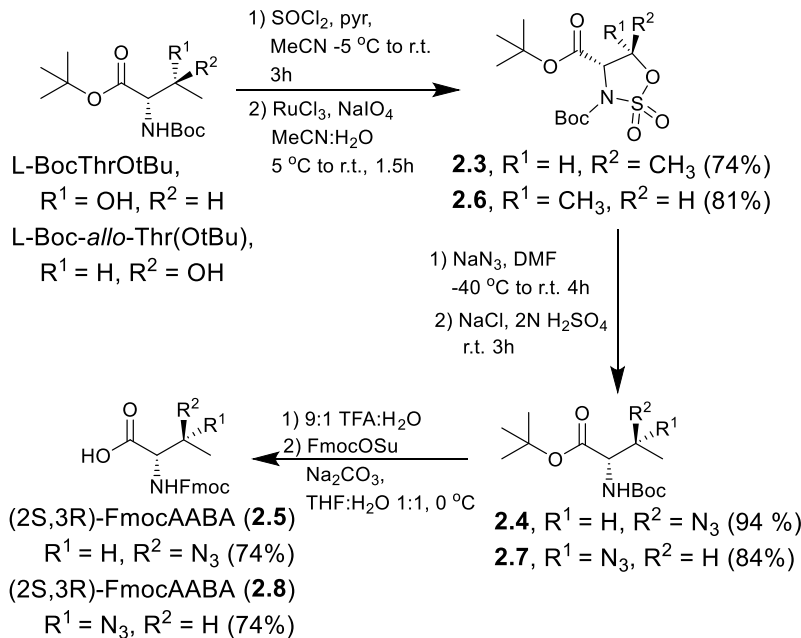
Scheme 2.1 Synthesis of **2.5** and **2.8**

With (2S,3R)-FmocAABA (**2.5**) and (2S,3S)-FmocAABA (**2.8**) in hand, we then prepared

peptides **2.1** and **2.2** using the route outlined in Scheme 2.2 (synthesis of peptide **2.1** shown).

Peptide **2.9**[162] was elongated by Fmoc-SPPS using HCTU/NMM to give peptide **2.10**. The azido

moiety in peptide **2.10** was reduced using DTT/DIPEA in anhydrous DMF to give peptide **2.11**.

Reducing the secondary azide using PMe_3 in 2:1 dioxane:H_2O produced the corresponding

secondary alcohol, likely through phosphine-mediated diazonium formation.[172] The final three

residues – Trp13, Glu12 and D-Ser11 – were coupled on to peptide **2.11** using DIC/HOBt to give

peptide **2.12**. The alloc group in peptide **2.12** was removed using $Pd(PPh_3)_4$/DMBA followed by

removal of the Fmoc group on Ser11 to give peptide **2.13**. Cyclization of peptide **2.13** to give

peptide **2.14** was accomplished using PyAOP/HOAt/2,4,6-collidine in 3:1 DMF:dichloromethane

containing 1% Triton™ X-100. Cleavage from the resin using a TFA:TIPS:H_2O cleavage cocktail

gave peptide **2.1**. The same route was used for peptide **2.2**. Both were purified by reversed-phase

HPLC (Figures A.1 and A.3) and characterized by HRMS (Figures A.2 and A.4).
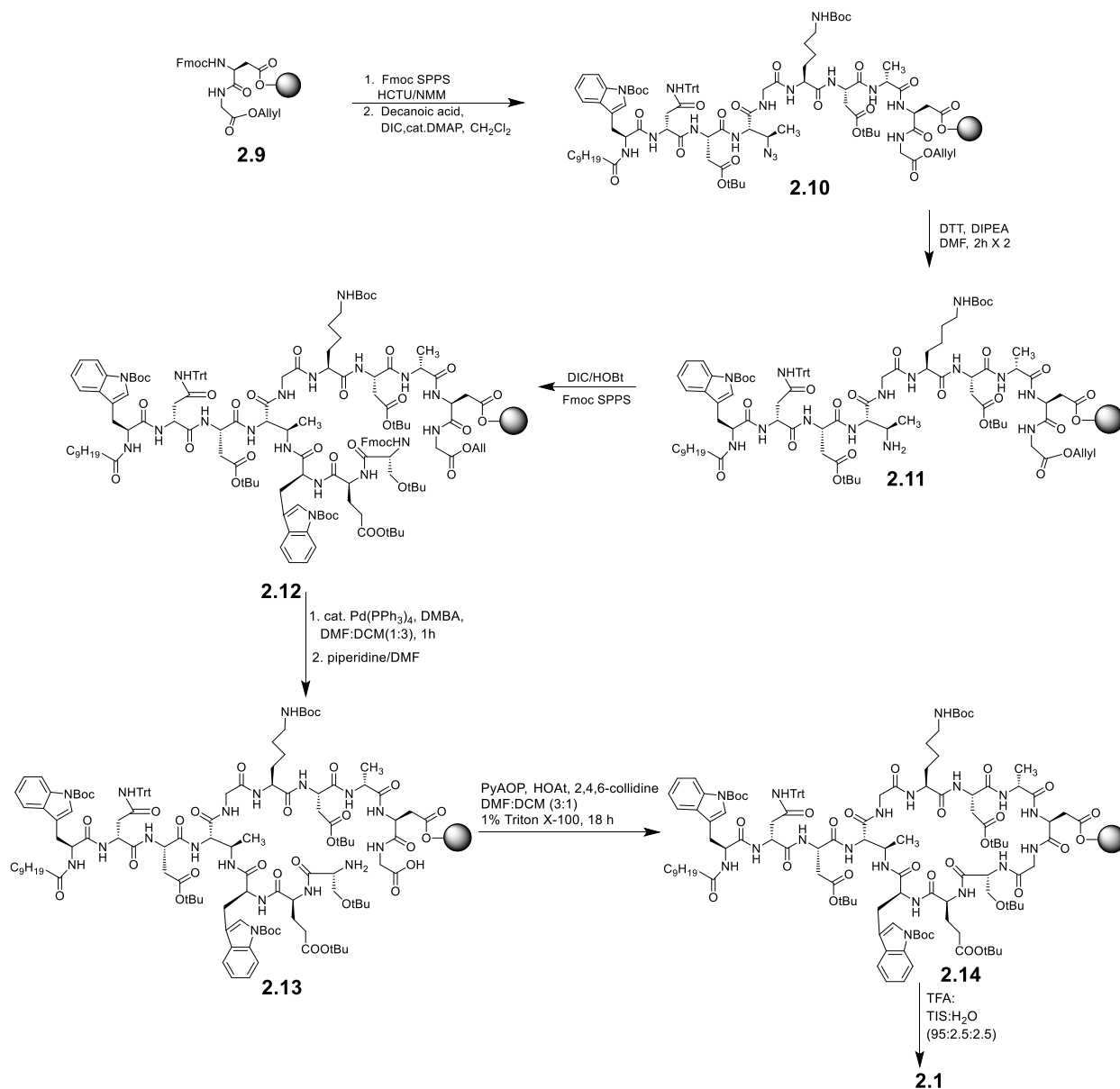
Scheme 2.2. Synthesis of peptide **2.1**. The synthesis of peptide **2.2** was accomplished in an identical manner using (2S,3S)-FmocAABA (**2.8**).

ent-Dap-K6-E12-W13 was prepared in exactly the same manner as Dap-K6-E12-W13, except that the amino acid building blocks employed were of the opposite stereochemisty.[173] The enantiomeric peptides had identical analytical RP-HPLC retention times and the chromatogram resulting from a co-injection of the two peptides exhibited a single peak (See Figure A.6).

Moreover, their circular dichroism spectra further supported their enantiomeric nature (see Figure A.7).

2.2.2 Antibacterial activity of daptomycin analogs

Peptides **2.1** and **2.2** and *ent*-Dap-K6-E12-W13 were assayed against *B. subtilis* 1046 (Table 1). Analogs **2.1** and **2.2** were substantially less active than Dap-K6-E12-W13 at physiological Ca^{2+} concentration, unequivocally demonstrating that, in addition to the methyl group on the Thr side chain, the ester bond in daptomycin is indeed crucial for its activity. Analog **2.1** exhibited greater activity than **2.2** at 1.25 mM Ca^{2+}, indicating that the R-configuration (the same as in the side chain of L-Thr in daptomycin) at the 3-position of the DABA residue is preferred in these analogs. As we have found with other moderately or poorly active daptomycin analogs[20-23] some of the activity of **2.1** and **2.2** could be regained by increasing the Ca^{2+} concentration, suggesting that amide (versus ester) bond and the configuration at the 3-position of the Daba side chain (or Thr in Dap) affects Ca^{2+} binding without changing the nature of the antibiotic substantially.

Table 2.1 MIC values of daptomycin and its analogs against *B. subtilis* 1046.

	MIC (µg/mL)	
peptide	1.25 mM Ca^{+2}	5 mM Ca^{+2}
Dap	0.75	0.5
Dap-K6-E12-W13	1.5	0.5
2.1	50	10
2.2	>100	10
ent-Dap-K6-E12-W13	>200	100

ent-Dap-K6-E12-W13 was at least 133-fold less active than Dap-K6-E12-W13 which strongly indicates that a specific chiral interaction is required for daptomycin's activity. It is

possible that the required chiral interaction involves the chiral lipid PG, whose presence in bacterial membranes is essential for daptomycin's activity. Additionally, recent studies on daptomycin's MoA suggest that a chiral interaction between daptomycin and a membrane bound protein may be required for activity.[64]

2.2.3 Membrane binding of daptomycin analogs

The binding of daptomycin and its analogs to large unilammelar vesicles (LUV) containing PG as a function of Ca^{2+}-concentration can be examined by monitoring the change in the intrinsic fluorescence of the Kyn and/or Trp residue(s).[19,173] Figure 2.2 shows the membrane binding curves for daptomycin, Dap-K6-E12-W13, peptides **2.1** and **2.2**, and *ent*-Dap-K6-E12-W13 using LUVs composed of equimolar quantities of DMPC and DMPG.

For daptomycin and Dap-K6-E12-W13, the fluorescence increased sharply when the concentration of Ca^{2+} exceeded 0.1 mM indicating insertion of the Kyn (daptomycin) or Trp (Dap-K6-E12-W13) residues into the membrane. The signal approaches saturation at approximately 1 mM Ca^{2+}. In contrast, for peptide **2.1**, the fluorescence did not increase sharply until the concentration of Ca^{2+} exceeded 1 mM and did not approach saturation until approximately 10 mM Ca^{2+}. For peptide **2.2**, the fluorescence did not increase sharply from 0 to 10 mM Ca^{2+}. These results suggest that peptides **2.1** and **2.2** have a lower affinity for Ca^{2+} than Dap-K6-E12-W13 and/or the **2.1**-Ca^{2+} and **2.2**-Ca^{2+} complexes have a lower affinity for the liposomes than the Dap-K6-E12-W13-Ca^{2+} complex. In any case, the reduced affinities of these peptides for Ca^{2+} and/or the reduced affinity of their Ca^{2+} complexes for the target membranes may be the reason for the reduced activity of these analogs.
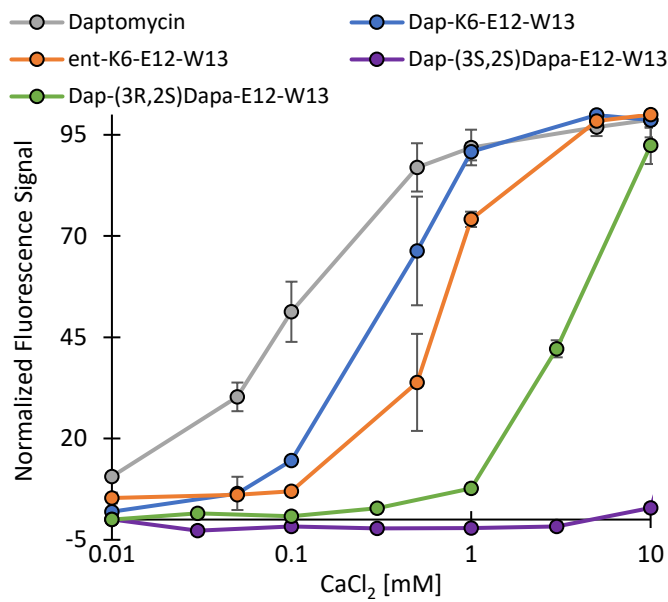
Figure 2.2 The intrinsic fluorescence of daptomycin (grey), Dap-K6-E12-W13 (blue), ent-Dap-K6-E12-W13 (orange) and peptide **2.1** (green), peptide **2.2** (purple) and in the presence of DMPC/DMPG (1:1) LUVs as a function of Ca^{2+} concentration. An increase in the intrinsic fluorescence of the Kyn residue in daptomycin or of the Trp residues in Dap-K6-E12-W13, peptide **2.1**, peptide **2.2** and ent-Dap-K6-E12-W13 indicates insertion of the fluorophore. The data shown was normalized by the maximum emission intensity observed in each titration, with error bars representing the standard deviations of three separate experiments.

The membrane binding curves of Dap-K6-E12-W13 and *ent*-Dap-K6-E12-W13 were similar, but the peptides do have a reproducible difference in membrane affinity. Being enantiomers, the intrinsic affinity of Dap-K6-E12-W13 and *ent*-Dap-K6-E12-W13 for Ca^{2+} must be the same. Hence, the disparity in their membrane binding curves must be due to the difference in the affinity of their Ca^{2+} complexes for PG. This strongly suggests that the stereochemistry of PG effects daptomycin-membrane interactions. It is important to note that the commercial DMPG used in this study, 1,2-dimyristoyl-sn-glycero-3-phospho-(1'-rac-glycerol), was a 1:1 mixture of 2R,2'R and 2R,2'S diastereomers. Therefore, it is possible that the effect of the PG stereochemistry on daptomycin-membrane interactions is even greater than what is shown in Figure 2.2. To the best of our knowledge, the absolute configuration at both stereogenic centers in PG in *B. subtilis*

83

membranes has not been unequivocally established but it is assumed to be 2R,2'S-PG (see section 1.2).

2.3 Conclusions

In this chapter, we have demonstrated that the methyl group on the side chain of Thr4 and the ester bond are crucial for daptomycin's antimicrobial activity. We have also shown that, since the enantiomer of Dap-K6-E12-W13 is inactive, a specific chiral interaction(s) is involved in daptomycin's antibacterial action. Membrane binding studies provide evidence that daptomycin is involved in a chiral interaction with PG.

2.4 Experimental

2.4.1 General Methods

All resins, amino acids and reagents were purchased from commercial suppliers. ACS grade *N,N*-dimethylformamide (DMF) was dried by distillation over calcium hydride under reduced pressure. Dichloromethane and acetonitrile were dried by distillation over calcium hydride under nitrogen. Pyridine was dried by refluxing over potassium hydroxide followed by fractional distillation. Tetrahydrofuran (THF) was distilled from sodium metal in the presence of benzophenone under N_2. Chromatography was preformed using 60 Å silica gel.

All peptide syntheses were performed manually using a rotary shaker for agitation.[23] *ent*-Dap-K6-E12-W13 was prepared using the same procedure that was used for preparing Dap-K6-E12-W13 (see Figure A.5-A.7 for the HRMS, analytical HPLC and CD spectrum of *ent*-Dap-K6-E12-W13).[23] Membrane binding studies and MIC determinations were performed as previously described.[23]

Reversed-phase analytical and semi preparative HPLC were performed using a Waters 600 controller equipped with Waters 2487 dual wavelength detector set to 220 and 260 nm. A Higgins

Analytical Inc. (Mountainview, CA, USA) CLIPEUS C18 column (10 µM, 250 x 4.6 mm) was used for analytical HPLC at a flow rate of 1 mL/min. Reversed-phase semi-preparative HPLC was performed using a Higgins CLIPEUS C18 column (10µM, 250 x 20 mm) at a flow rate of 10.0 mL/min.

Circular dichroism traces were collected using a Jasco J-715 CD spectrometer. The peptide concentration of each solution was 100 µM in 20 mM HEPES buffer (pH 7.4). Samples were measured at room temperature from 210-250 nm at a scan rate of 50 nm min^{-1} and a bandwidth 1 nm. A 1 mm cuvette was used. The outputted data was converted to molar ellipticity in units of deg cm^2 dmol^{-1}.

High resolution positive electrospray (ESI) mass spectra were obtained using an orbitrap mass spectrometer. Samples were sprayed from MeOH: 1% formic acid in H$_2$O. All spectra were collected in the positive mode. ^{1}H- and ^{13}C-NMR were collected using a Bruker Avance-300 spectrophotometer. Chemical shifts (δ) for samples run in CDCl$_3$ are reported in ppm relative to an internal standard (trimethylsilane, δ 0). For ^{13}C-NMR samples run in CDCl$_3$ chemical shifts are reported relative to the solvent peak (77.0 ppm). Chemical shifts (δ) for samples run in CD$_3$OD are reported relative to the solvent peak (δ 3.30). For ^{13}C NMR samples run in CD$_3$OD, chemical shifts are reported relative to the solvent peak (49.15 ppm, central peak).

2.4.2   Syntheses
*Di-tert-butyl (4S,5R)-5-methyl-1,2,3-oxathiazolidine-3,4-dicarboxylate 2,2-dioxide (**2.5**) and di-tert-butyl (4S,5S)-5-methyl-1,2,3-oxathiazolidine-3,4-dicarboxylate 2,2-dioxide (**2.8**).*

Anhydrous acetonitrile (14 mL) and thionyl chloride (1.38 mL, 19.1 mmol, 2.05 equiv) were added to a reaction vessel at -5 °C. Boc-L-ThrOtBu[29] (2.56 g, 9.31 mmol, 1.00 equiv) in anhydrous acetonitrile (7 mL) was added dropwise to the reaction vessel. Anhydrous pyridine (3.75 mL, 46.6 mmol, 5.00 equiv) was then added dropwise to the stirred mixture. After 10 min, cooling was

removed, the reaction was stirred at room temperature for 3 h, then concentrated. The residue was mixed with ethyl acetate (65 mL) and water (18 mL) and stirred at room temperature for 20 min. The aqueous layer was extracted with ethyl acetate (65 mL) once then the combined organic layers were washed with brine (150 mL) 3 times, then concentrated. The residue was dissolved in acetonitrile (18 mL) at room temperature and cooled using an ice bath. Ruthenium (III) chloride was added (4 mg, 0.02 mmol, 0.002 equiv), followed by sodium periodate (3.98 g, 18.6 mmol, 2.00 equiv). After stirring for 10 min, water (18 mL) was added dropwise, cooling was removed, and the mixture was stirred for 1.5 h at room temperature. The mixture was filtered, washed with brine (18 mL) once and extracted with ethyl acetate (18 mL) twice. The organic layer was washed with brine (50 mL) once, dried over Na_2SO_4, filtered over a bed of Na_2SO_4+silica gel+celite then concentrated, yielding **2.3** as an orange oil (2.59 g, 82% yield). ^{1}H NMR (300 MHz, $CDCl_3$) δ 4.81 (1H, q, *J=5.8* Hz) 4.33 (1H, d, *J=5.5* Hz) 1.69 (1H, d, *J=6.4* Hz) 1.55 (9H, s) 1.49 (9H, s). ^{13}C NMR (75 MHz, $CDCl_3$) δ 165.4, 148.2, 85.7, 84.2, 77.5, 64.3, 27.8, 19.1. HRMS-ESI[+] (m/z) calcd for $C_{13}H_{24}NO_7S$ (M+H)[+], 338.12680; found, 338.12632.

2.6 was prepared using the same procedure starting from Boc-L-*allo*-ThrOtBu (74 % yield). ^{1}H NMR (300 MHz, $CDCl_3$) δ 5.05 (1H, q, *J=6.3* Hz) 4.46 (1H, d, *J=6.0* Hz) 1.56-1.44 (21 H, m). ^{13}C NMR (75 MHz, $CDCl_3$) δ 164.8, 148.0, 85.5, 84.0, 76.0, 62.9, 27.8, 15.1. HRMS-ESI[+] (m/z) calcd for $C_{13}H_{27}N_2O_7S$ (M+NH_4)[+], 355.15335; found, 355.15337.

*tert-butyl (2S,3S)-3-azido-2-((tert-butoxycarbonyl)amino)butanoate (**2.4**) and tert-butyl (2R,3S)-3-azido-2-((tert-butoxycarbonyl)amino)butanoate (**2.7**).*

To a solution of **2.3** (2.56 g, 7.67 mmol, 1.00 equiv) in anhydrous DMF (28 mL) at -40 ºC was added sodium azide (650 mg, 9.97 mmol, 1.30 equiv) portion wise. The mixture was allowed to reach room temperature over 4 h, at which point 20% $NaCl_{(aq)}$ (17 mL) and 2 N H_2SO_4 (1.7 mL)

were added. The reaction mixture was stirred at room temperature for 3 h, then partitioned between ethyl acetate (75 mL) and water (200 mL). The aqueous layer was extracted with ethyl acetate (75 mL) once. The combined organic layers were washed with water (150 mL) once and brine (150 mL) once, dried over Na_2SO_4, then concentrated yielding **2.4** as a yellow oil (2.06 g, 84% yield). ^1H NMR (300 MHz, CDCl$_3$) δ 5.28 (1H, br. s.) 4.32-4.29 (1H, m) 3.78 (1H, m) 1.53 (9H, s) 1.45 (9H, s) 1.33 (3H, d, *J=6.8* Hz). ^{13}C NMR (75 MHz, CDCl$_3$) δ 168.5, 155.1, 83.0, 80.2, 58.9, 57.9, 28.2, 27.9, 15.4. HRMS-ESI$^+$ (m/z) calcd for $C_{13}H_{25}N_4O_4$ (M+H)$^+$, 301.18629; found, 301.18629.

2.7 was prepared using the same procedure starting from **2.6** (94 % yield). ^1H NMR (300 MHz, CDCl$_3$) δ 5.10 (1H, d *J=9.1 Hz*) 4.23 (1H, d *J=8.7 Hz*) 4.10-4.08 (1H, m) 1.47 (9H, s) 1.44 (9H, s) 1.33 (3H, d, *J=6.7* Hz). ^{13}C NMR (75 MHz, CDCl$_3$) δ 169.0, 155.8, 82.6, 79.8, 58.9, 57.6, 28.1, 27.8, 16.0. HRMS-ESI$^+$ (m/z) calcd for $C_{13}H_{24}KN_4O_4$ (M+K)$^+$, 339.14166; found, 339.14291.

*(2S,3S)-2-((((9H-fluoren-9-yl)methoxy)carbonyl)amino)-3-azidobutanoic acid (**2.5**) and (2R,3S)-2-((((9H-fluoren-9-yl)methoxy)carbonyl)amino)-3-azidobutanoic acid (**2.8**).*

A reaction vessel containing **2.4** (2.06 g, 6.87 mmol, 1.00 equiv) was cooled in an ice bath then trifluoroacetic acid (15 mL) and water (2 mL) were added dropwise. The ice bath was removed, and the mixture stirred for 2 h. The mixture was concentrated and residual TFA was removed by several rotary evaporations with toluene. The residue was suspended in water (33 mL), then cooled in an ice bath and basified slowly with sodium carbonate to a pH of 8 over a period of 30 min. A solution of *N*-(9-Fluorenylmethoxycarbonyloxy)succinimide (FmocOsu) (2.55 g, 7.56 mmol, 1.10 equiv) in THF (18 mL) was added dropwise to the stirring reaction mixture to avoid clumping of the formed precipitate. Once the addition was complete, the ice bath was removed and the mixture stirred for 16 h. Two-thirds of the solvent was removed and the residue was acidified with concentrated HCl to a pH of 2. Dichloromethane (20 mL) was then added to the residue and the

mixture was stirred for 10 min. The aqueous layer was then extracted with dichloromethane (20 mL) once and the combined organic layers were dried over Na_2SO_4, concentrated and subjected to silica gel column chromatography (98:1:1 dichloromethane:AcOH:MeOH), which gave **2.5** as a colorless powder (1.86 g, 74% yield). NMR data was found to match that reported in literature.[27] ^{1}H NMR (300 MHz, CD_3OD) δ 7.76 (2H, d, *J=7.4* Hz) 7.65 (2H, d, *J=7.4* Hz) 7.39-7.34 (2H, m) 7.31-7.26 (2H, m) 4.44-4.30 (3H, m) 4.22-4.18 (1H, m) 3.89 (1H, quintet, *J=6.3* Hz) 1.29 (3H, d, *J=6.8* Hz). ^{13}C NMR (75 MHz, CD_3OD) δ 174.7, 158.7, 145.4, 145.3, 142.7, 128.9, 128.3, 126.4, 121.1, 68.4, 59.3, 59.2, 48.5, 15.4. HRMS-ESI[+] (m/z) calcd for $C_{19}H_{19}N_4O_4$ (M+H)[+], 367.14008; found, 367.14000.

2.8 was prepared following a similar procedure starting from **2.7** (74% yield). NMR data was found to match that reported in literature.[27] ^{1}H NMR (300 MHz, CD_3OD) δ 7.78 (2H, d, *J=7.4* Hz) 7.68 (2H, d, *J=7.4* Hz) 7.40-7.35 (2H, m) 7.32-7.27 (2H, m) 4.87-4.31 (3H, m) 4.26-4.21 (1H, m) 3.89 (1H, quintet, *J=6.3* Hz) 1.29 (3H, d, *J=6.8* Hz). ^{13}C NMR (75 MHz, CD_3OD) δ 173.1, 159.1, 145.4, 145.2, 142.7, 128.9, 128.3, 126.4, 121.1, 68.3, 59.7, 59.4, 48.5, 16.7. HRMS-ESI[+] (m/z) calcd for $C_{19}H_{19}N_4O_4$ (M-H)[+], 367.14008; found, 367.13998.

*Synthesis of peptides **2.1** and **2.2***.

For the synthesis of peptides **2.1** and **2.2**, in addition to compounds **2.5** and **2.8**, the following protected amino acids were used: FmocAsp(tBu)OH, FmocGlyOH, FmocGlu(tBu)OH, FmocTrp(Boc)OH, Fmoc-D-Ser(tBu)OH, FmocLys(Boc)OH, Fmoc-D-AlaOH, Fmoc-D-Asn(Trt)OH, FmocTrp(Boc)OH. Chlorotrityl chloride Tentagel resin (2ClTrt-TG, 1052 mg, 0.19 mmol/g) was swelled in dichloromethane (3 x 15 min). To the swollen resin was added FmocAspGlyOallyl[23] (4.0 equiv) and diisopropylethylamine (DIPEA) (8.0 equiv) as solution in dichloromethane (3.5 mL). After agitating for 4 hours, the resin was filtered and washed with

dichloromethane (15 min x 3) and the resin was capped using dichloromethane:MeOH: DIPEA (1.5 mL, 17:2:1, 3 x 15 min). The capped resin was washed with dichloromethane (3min x 3) followed by DMF (3 min x 3). Following deprotection using 2-methylpiperidine (20% in DMF, 1 x 5 min, 1 x 15 min) and washing with DMF (3 min x 3), all subsequent residues (5 equiv for each coupling) were coupled on using [(6-chloro-1H-benzotriazol-1-yl)oxy](dimethylamino)-*N,N*-dimethylmethaniminium hexafluoro-phosphate (HCTU) (5 equiv) and *N*-methylmorpholine (5 equiv) as a solution in DMF (3.5 mL). All couplings were found to go to completion after 50 min, at which point the resin was filtered and washed with DMF (3 min x 3). The decanoyl tail was added by coupling decanoic acid (4 equiv) to Trp at position 1 using DIC/HOBt for 13 hours. Once the resin was washed, the azide on the AABA residue at position 4 was reduced to the corresponding amine by agitating the resin in a solution of dithiothreitol (2M) and DIPEA (1M) for 2 hours two times. The remaining residues were coupled onto the resulting amine using DIC/HOBt (5equiv) in DMF (3.5 mL). The allyl group on Gly at position 10 was removed using catalytic Pd(PPh$_3$)$_4$ (0.2 equiv) and 1,3-dimethylbarbituric acid (DMBA, 10 equiv) in DMF:dichloromethane (1.5 mL, 1:3). The resin was washed with dichloromethane (3 x 3 min), then a 1.0 % solution of sodium diethyldithiocarbamate trihydrate in DMF (3 x 3 min) to remove excess Pd catalyst, and then dichloromethane (3 x 3 min) and DMF (3 x 3 min). Following Fmoc-deprotection of Ser at position 11, the linear peptide was cyclized using (7-azabenzotriazol-1-yloxy)tripyrrolidinophosphonium hexafluorophosphate (PyAOP)/1-Hydroxy-7-azabenzotriazole (HOAt)/2,4,6-collidine (4:4:8 equiv) with 1 % Triton-X 100 in DMF (4 mL). The resulting peptide was simultaneously cleaved from the resin and globally deprotected using TFA:triisopropylsilane (TIPS):H$_2$O 95:2.5:2.5. The crude peptide was concentrated under a stream of air and purified by semi-preparatory HPLC. Peptide **1** (16 mg, 10% yield): purified using 65:35 ACN:0.1 % TFA in

H$_2$O for 50 min (t$_r$ = 29.6 min), HRMS-ESI$^+$ (m/z) calcd for C$_{73}$H$_{103}$N$_{18}$O$_{24}$ (M+H$^+$), 1615.7387; found, 1615.7378. Peptide **2** (8 mg, 5%): purified using 65:35 ACN:0.1 % TFA in H$_2$O for 50 min (t$_r$ = 32.6 min), HRMS-ESI$^+$ (m/z) calcd for C$_{73}$H$_{103}$N$_{18}$O$_{24}$ (M+H$^+$), 1615.7387; found, 1615.7392 (See Figures. A.1-A.4 in the SI for analytical HPLC chromatograms and HRMS).

Chapter 3 - Highly Efficient and Enantiospecific syntheses of (2S,3R)-3-Alkyl- and Alkenylglutamates from Fmoc-protected Garner's Aldehyde

3 Preface and contributions

The work presented in this chapter is based on a manuscript published in the journal *Amino Acids* (*Amino Acids* **2020**, *52*, 987–998. Adapted with permission). I completed all the experimental work presented in this chapter and wrote the first draft of the manuscript which was edited and refined by Prof. Taylor. All this work was done under the supervision of Prof. Taylor. Additional supplementary data is available at the journal's website.

3.1 Introduction

As discussed in the introduction, one of the primary goals of this thesis was to determine whether daptomycin interacts with a chiral target as part of its action mechanism. The role of a chiral interaction is most readily determined by probing the biological activity of the unnatural enantiomer of a natural product; thus, we set out to develop a new synthesis of daptomycin and its unnatural enantiomer that would incorporate what we learned from completing the total synthesis of A5D (chapter 8) and build on what was already known from the current routes to daptomycin (section 1.6). Before embarking on this journey, we wanted to develop a more efficient enantiospecific synthesis of Fmoc-MeGlu(t-Bu)-OH that could be used in the synthesis of daptomycin, its unnatural enantiomer and some other natural products that were being investigated by other members of the Taylor lab. What follows is a detailed account of our efforts.

The enantioselective synthesis of nonproteinogenic and unnatural amino acids has long been a topic of considerable interest.[174] Among such amino acids are α-amino acids substituted at the 3-position. Such compounds have been found in a variety of natural products and have also

been used as tools to elucidate mechanisms of biological processes[175] and for the development peptide and peptidomimetic therapeutic agents.[176,177]

We are specifically interested in the preparation of the nonproteinogenic amino acid (*2S,3R*)-3-methylglutamate (3MeGlu) as well as other 3-substituted glutamate derivatives. 3MeGlu occurs in a number of natural products such as the clinically important antibiotic daptomycin as well as several other antibiotics such as some of the A54145 factors and some of the calcium-dependent antibiotic (CDAs) factors.[178] 3MeGlu itself is also a selective inhibitor of excitatory amino acid transporters GLT-1, EAAT2, and EAAT4 and is used as a key tool in the study of general EAAT function.[179]

For the synthesis of daptomycin, the Li group[155] and the Taylor group[162] developed a synthesis of 3MeGlu protected for Fmoc SPPS (Fmoc-(2S,3R)-3MeGlu(tBu)-OH, (**3.1**, Figure 3.1) starting from (S)-pyroglutaminol.[180] However, the synthesis was lengthy (12-steps) and the overall yield was low. As one of the goals of our work on daptomycin and the A54145 series of antibiotics[181] is to prepare analogs with improved properties, we required a more efficient synthesis of 3MeGlu as well as other 3-substituted glutamate derivatives suitably protected for Fmoc SPPS.
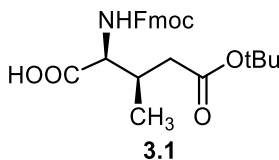
Figure 3.1 Structure of Fmoc-(2S,3R)-3MeGlu(tBu)-OH (**3.1**)

In addition to the above-mentioned route, several other asymmetric syntheses of both protected and unprotected 3MeGlu have been reported. The majority of these routes employ a conjugate addition of chiral glycine derivatives to a crotonate ester as the key step.[182–184] Other

routes include employing an Arndt-Eistert homologation of protected (2S,3S)-3-methylaspartic acid as a key step[185] and a stereoselective 1,4-addition of Me$_2$CuLi to a 3,4-unsaturated pyroglutamate 2,6,7-trioxabicyclo[2.2.2]octane (OBO) ester derivative.[186] Prof Hruby's group investigated stereoselective 1,4 additions on glutamic acid synthons and although this approach is quite appealing due to its high selectivity, it can only access (2S,3S) and (2R,3R) 3alkylGlu [187–190]. Lou et al reported the synthesis of Boc-(2S,3R)-3MeGlu(Me)-OEt by alkylation of a glycine-derived imine with a secondary brosylate.[191] The Brimble group has recently reported the synthesis of Boc-(2S,3R)-3MeGlu(Bn)OH, as a 2:1 mixture of diastereomers, employing a conjugate addition of an iminolactone chiral glycine derivative to tert-butyl crotonate as the key step.[192] Very recently, the Li group reported the synthesis of **3.1** based on a C-H activation strategy;[193] however, the procedure was still rather lengthy (10 steps) and the overall yield was less than 17%.

In 1991, Mann and coworkers reported the 1,4-addition of lithium dialkylcuprates on enoate **3.2**, which was prepared via a Horner-Wadsworth-Emmons (HWE) reaction on Boc-protected Garner's aldehyde (Scheme 3.1).[194] The yields were good and the dr's reasonable (4:1) to very good (19:1). Later studies by others demonstrated that, under the right conditions, that 1,4-addition reactions of metal dialkylcuprates on alkenes derived from Cbz or Boc-protected Garner's aldehyde usually proceed in good yield and often in high dr.[195–200] The high yield and dr's of this reaction prompted us to investigate this approach as an efficient route to amino acid **3.1** as well as other *3R*-substituted L-glutamate derivatives suitable protected for Fmoc SPPS.[201]
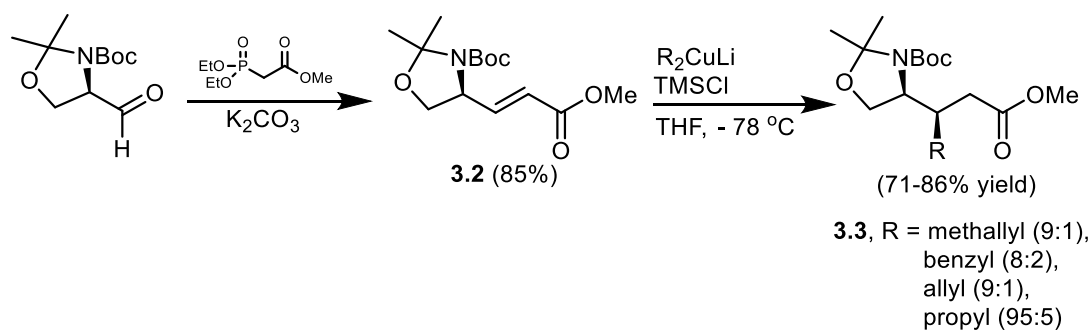
Scheme 3.1 Structure of Fmoc-(2S,3R)-3MeGlu(tBu)-OH (**3.1**)

3.2 Results and discussion

Our investigation began with Cbz-protected Garner's aldehyde (**3.4**) which is commercially available but very expensive; therefore, we opted to prepare **3.4** starting from L-CbzSer-OMe using a 2-step literature procedure (Scheme 3.2).[202] The aldehyde was converted to **3.5** in an 87 % yield via a HWE reaction with *tert*-butyldiethylphosphonoacetate and sodium hydride.[202] Methylation of enone **3.5** was performed using the conditions initially described by Hanessian on **3.2**.[198,199] We were pleased to find that the reaction proceeded to completion almost immediately at -73 °C (internal temperature), giving **3.6** in a 79% yield with a dr of >20:1. Opening of the oxazolidine and oxidation of the resulting alcohol was achieved in a single step and a 69% yield with Jones reagent.[197] We found that concomitant removal of the *tert*-butyl ester could be suppressed by adding the Jones reagent over 3.5 hours at room temperature. Attempts to further suppress *tert*-butyl ester removal by diluting the Jones reagent were unsuccessful. With ester **3.7** in hand, the final product was prepared by removing the Cbz protecting group via hydrogenolysis followed by Fmoc protection using standard conditions. The purification of **3.1** by chromatography was challenging as the amphiphilic building block does not interact with silica strongly and has unusual solubility properties. This amounts to **3.1** streaking on the column and eluting much earlier than predicted by the TLC. Nevertheless, we found that recrystallization of the mixed fraction

containing trace FmocOSuc and **3.1** in ethyl acetate/hexanes provided pure **3.1** in 78 % yield which

matched previously reported spectra.[155,162,193]
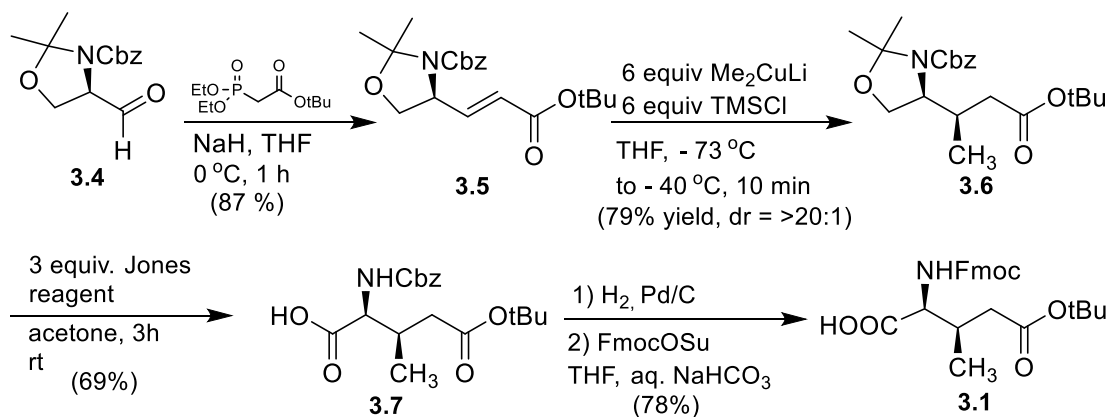
Scheme 3.2 Synthesis of **3.1** Starting with Cbz-Protected Garner's Aldehyde **3.4**

Although the route outlined in Scheme 3.2 is the most efficient synthesis of **3.1** to date, we

postulated that an even more efficient synthesis could be developed starting with Fmoc-protected

Garner's aldehyde (Scheme 3.3). Surprisingly, we could find only one report in the literature where

Fmoc-protected Garner's aldehyde has been used as a chiral synthon in an enantioselective

synthesis. In 2006, Bertozzi and coworkers described a 3-step synthesis of Fmoc-protected

Garner's aldehyde by subjecting Fmoc-Ser-OMe to dimethoxypropane to give the oxazolidine

followed by reduction of the ester with LiBH$_4$ and oxidation of the resulting alcohol with

TEMPO/NaOCl.[203] The resulting Fmoc-protected Garner's aldehyde was then used to prepare

Fmoc-protected L-formyl glycine as its ethyl acetal.[203] We prepared Fmoc-protected Garner's

aldehyde in just two steps by first converting Fmoc-L-Ser-OMe to oxazolidine 3.**8** using

dimethoxy propane and BF$_3$•Et$_2$O.[203] We found that **3.8** could be reduced to **3.9** in a very high

yield using DIBALH so long as the reaction was quenched through slow addition of MeOH cooled

to -73 °C (dry ice/acetone) to maintain an internal temp < -65 °C. This procedure is reproducible

on scales as large 5g. Initially, we were concerned that the basic conditions required for the HWE

reaction would not be compatible with the Fmoc group in **3.9**. However, we found that the olefination of **3.9** proceeded to completion within 10 min at -10 °C using NaH as a base, though careful control of temperature and reaction time was crucial. Under these conditions, very little Fmoc removal could be detected by TLC or by ^{1}H NMR of the crude product. Methylation of **3.10** proceeded with a nearly quantitative yield under the reaction conditions used for the Cbz analogue. NMR analysis of the crude **3.11** at room temperature (rt) was complicated by the presence of rotamers. This problem was resolved by performing the NMR analysis in DMSO-d_6 at 60 °C, and, under these conditions, we could not observe the other diastereomer and concluded that the dr must be >20:1. The oxidation-cleavage step proved to be challenging. Unfortunately, the Jones oxidation proceeded with only a moderate yield due to the increased stability of the Fmoc acetonide. After extensive optimization, the highest yield achieved was only 48% (route A). However, the product was easy to isolate by chromatography and none of the anti-diastereomer could be detected in the final product, proving that the methylation of **3.10** indeed proceeded with a very high dr.[155,193] To improve the yield of this transformation, we attempted to remove the acetonide selectively using cat. TsOH in methanol at 0 °C or bismuth nitrate in DCM,[204] but both reactions failed. Interestingly, we found that Bobbit's salt in 9:1 MeCN:H_2O cleaved the acetonide and partially oxidized the liberated alcohol;[205] however, concomitant removal of the t-Bu ester was observed. Finally, we found that $BiBr_3$ in dry MeCN with a stoichiometric amount of water was able to cleanly remove the acetonide without compromising the *tert*-butyl ester (route B).[206,207] After workup, the crude alcohol was oxidized via TEMPO oxidation and purification was easily achieved via chromatography (79% over two steps). This highlights one of the technical advantages of starting from **3.8** rather than **3.4**. The final product contained solely the syn isomer,

suggesting that the dr of the methylation was as high as previous reports had found with **3.2**.[198,199]

The overall yield was 61% when using route B in the final two steps.
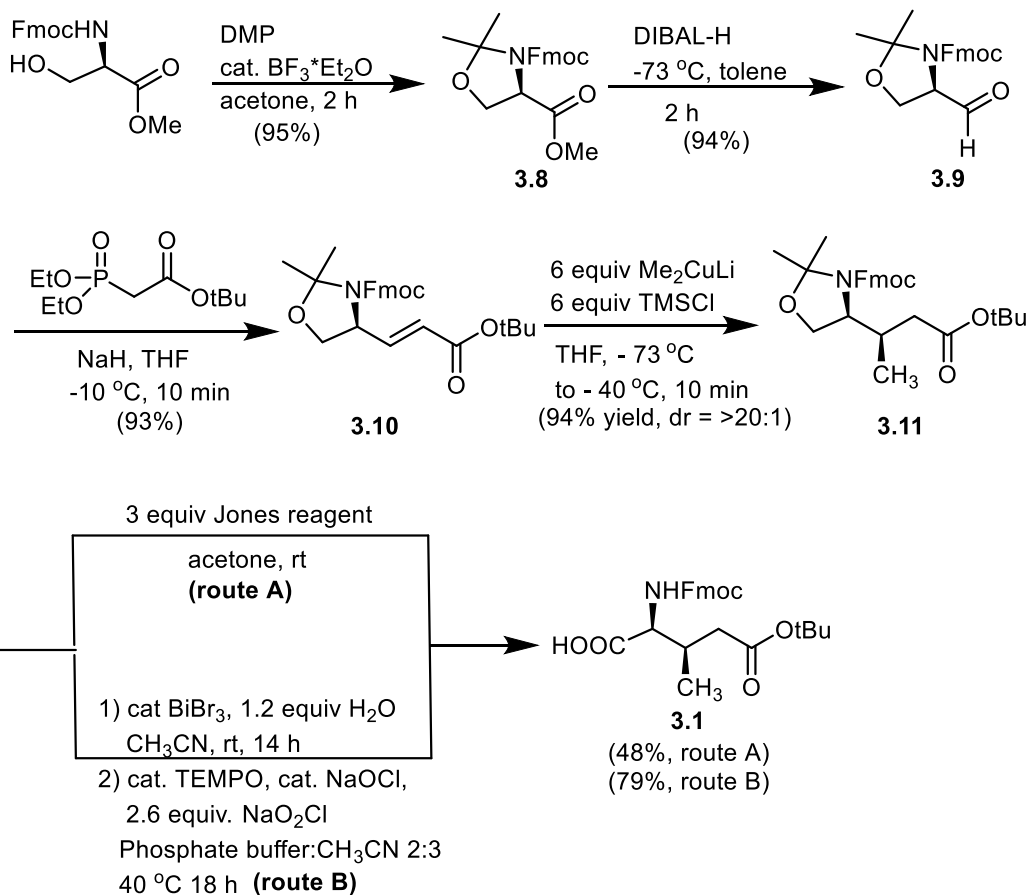
Scheme 3.3 Synthesis of **3.1** using Fmoc-protected Garner's Aldehyde **3.9**

     We were initially surprised to find that the conditions used to methylate **3.10** were not nearly as effective for the ethylation reaction. Although the ethylation proceeded to completion when EtLi/CuI/TMSCl was used, a significant amount of decomposition was observed and only a 58% yield of the desired product **3.12** was achieved (entry 1). These results motivated us to develop a more robust set of alkylation/alkenylation conditions based on the current understanding of 1,4-additions with cuprates. The results of this study are summarized in Table 3.1. Switching from EtLi to EtMgBr made the reaction more sluggish and reduced reaction yield, highlighting the

97

importance of lithium salts (entry 2).[208,209] Since we considered decomposition of the starting material to proceed through a radical pathway,[210,211] we attempted to attenuate this by reducing reaction temperature (entry 3), but this reduced conversion. We then attempted the alkylation using CuCN as a copper source but found that both stoichiometric and catalytic[208,212] amounts of cuprate derived from CuCN caused intractable decomposition of the starting material (entry 4). It is known that transmetalations with CuBr*DMS are more reproducible compared to CuI.[213] CuBr*DMS can attenuate radical formation[210] and the addition of lithium salts can improve yield and diastereoselectivity.[208] Under conditions described by Mann (CuBr*DMS and LiBr)[194], using THF as a solvent, we found that the yield of this reaction was marginally better than entry 2, but the product after chromatography was exceptionally pure and the reaction went to completion with only 3 equiv of cuprate. This suggested that the alkylation pathway was selectively accelerated over the decomposition pathway under these conditions (entry 5). Based on these results, we reasoned that by reducing the reaction temperature (entry 6) and the number of equivalents of cuprate (entry 7) we could improve the yield. Finally, we found that careful control of the reaction temperature during the addition followed by gradual warming to room temperature provided **3.12** in a good yield with very high diastereomeric purity (entry 8). While executing these reactions, we found that ethyl cuprate is only stable up to -18 °C (its breakdown is accompanied by the formation of colloidal copper that quickly turns the reaction solution black) and thus careful control of transmetalation temperature is key to reproducibility.[214] This may have contributed to the poor results observed in entries 1-3 and may explain why they deviated so greatly from literature. It also may explain why some authors found vinylation procedures on similar compounds difficult to reproduce.[215]

Table 3.1 Optimization Study on the Ethylation of **3.10**
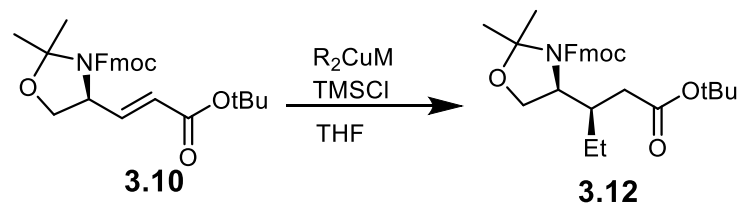
entry	RM	Copper (I) Source	Cuprate/ TMSCl (equiv)	Temp (°C)[e] and Time[g]	Yield (%)[c]
1[a]	EtLi	CuI	6	-73 then -40 for 10 min	58
2[a]	EtMgBr	CuI	6	-73 then -40 for 10 min	52[d]
3[a]	EtMgBr	CuI	6	-73 for 3h	44[d]
4[b]	Et Li*2MgBr$_2$	CuCN	6	-73 then -40 for 10 min	ND[f]
5[b]	Et Li*2MgBr$_2$	CuBr*DMS	3	-40 for 1h	54
6[b]	Et Li*2MgBr$_2$	CuBr*DMS	3	-73 then -40 for 10 min	58
7[b]	Et Li*2MgBr$_2$	CuBr*DMS	1.5	-73 then -40 for 10 min	64[d]
8[b]	Et Li*2MgBr$_2$	CuBr*DMS	1.5	-73 to 15 °C about 1 h[h]	76

[a]Transmetalation was done at -5 °C. [b]Transmetalation was done at -40 °C. [c]Isolated yield. [d]Did not go to completion. [e]Internal reaction temperature. [f]Significant decomposition. [g]The reaction was quenched with sat. aq. NH$_4$Cl:NH$_4$OH 9:1 after this time. [h] Reaction time depends on the scale and flask used. We found that the reaction always proceeded better on a larger scale (1.5 g vs 100 mg) due to more gradual warming to rt.

We were pleased to find that the conditions described in entry 8 of Table 3.1 also worked well for other alkylation/alkenylation reactions (Table 3.2). Propylation of **3.11** gave **3.13** in a nearly quantitative yield with high diastereomeric purity (Table 3.2, entry 2). The butylation reaction also went very cleanly under these conditions, although 3 equivalents of cuprate were needed to get **3.14** in a quantitative yield with high diastereomeric purity (entry 3). Interestingly, we found that the dibutyl cuprate was much more thermally stable than diethyl or dipropyl (both of which began to decompose at -18 °C) and only began to decompose at 8 °C. These conditions

are also suitable for the benzylation reaction (**3.15**, entry 4), although the reaction of dibenzyl cuprate with the alkene proceeded much more slowly than with any of the dialkyl cuprates. In fact, it was necessary to warm the solution of the cuprate and alkene to room temperature in stages to afford a nearly quantitative yield of the desired product which was formed with a high dr (93:7 syn:anti). With 6 equivalents of vinyl cuprate, the vinylation reaction proceeded to completion upon warming to room temperature, giving **3.16** in a good yield with very high dr (entry 5).

Table 3.2 Yield and Diastereoselectivity of 1,4-Addition Reactions to Alkene **3.10**
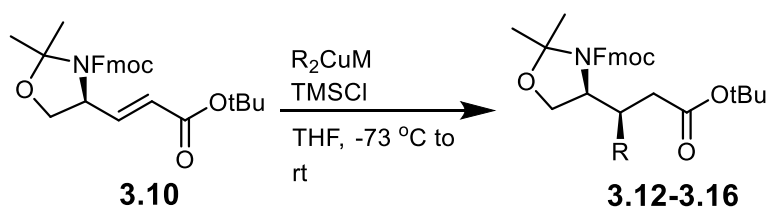
entry	R	M	Cuprate/TMSCl (equiv)	Yield (%)[a]	Dr[b]
1	Et (**3.12**)	Li*2MgBr$_2$	1.5	76	>20:1
2	Pr (**3.13**)	Li*2MgBr$_2$	1.5	94	>20:1
3	Bu (**3.14**)	Li*2MgBr$_2$	3	99	>20:1
4	Bn (**3.15**)	Li*2MgCl$_2$	3	94	>13:1
5	Vinyl (**3.16**)	Li*2MgBr$_2$	6	89	>20:1[c]

[a]Isolated yield. [b]Determined by ^{1}H-NMR in DMSO-d_6 at 60 °C. [c]Determined by ^{1}H-NMR in DMSO-d_6 at 100 °C.

The catalytic BiBr$_3$/MeCN/H$_2$O cleanly deprotected each acetonide without issue (Table 3.3). The crude alcohol, in each case, was easily converted to the final amino acid building block through a TEMPO oxidation. In fact, this two-step sequence was so effective that all the final products could be purified through a simple plug column to remove any leftover acetonide and TEMPO, giving pure **3.17**-**3.21**.

Table 3.3 Yields of the Two-step Deprotection and Oxidation of **3.12-3.16**
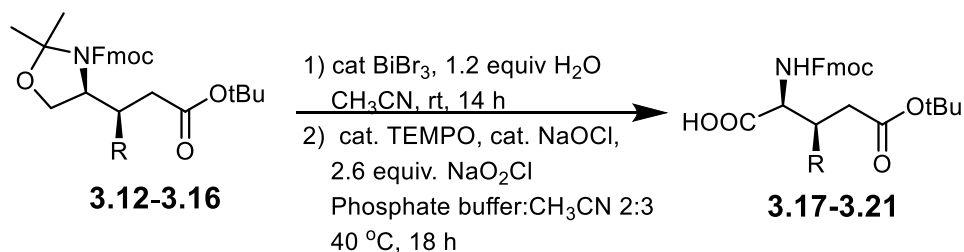
entry	R	Yield (%)
1	Et (**3.17**)	82
2	Pr (**3.18**)	83
3	Bu (**3.19**)	78
4	Bn (**3.20**)	80
5	Vinyl (**3.21**)	79

3.3 Conclusions

In conclusion, we have developed an operationally simple, enantiospecific and diastereoselective synthesis of Fmoc-(2S,3R)-3MeGlu(tBu)-OH in 5- or 6-steps from commercially available D-FmocSer-OMe. This is only the second example in the literature where Fmoc-protected Garner's aldehyde has been used as a chiral synthon in an enantioselective synthesis, and it is by far the most efficient and high yielding synthesis of enantiopure Fmoc-3MeGlu(tBu)-OH reported to date. We have also shown that the key 1,4-addition reaction works well (good yield and excellent dr) with other lithium dialkyl and divinyl cuprates. The products of these transformations were easily converted into Fmoc-(*2S,3R*)-3-alkyl- or 3-vinylGlu(tBu)-OH. The described route to this class of compounds is very appealing since it allows for the rapid synthesis of 3-substituted glutamates protected for Fmoc SPPS via a single mid-stage olefin.

3.4 Experimental
General Methods.

All reagents and solvents were purchased from commercial suppliers. Methylene chloride (DCM) and acetonitrile (MeCN) were dried by distillation over calcium hydride under nitrogen.

Tetrahydrofuran (THF) was distilled from sodium metal in the presence of benzophenone under N_2. Chromatography was preformed using 60 Å silica gel. CuBr*DMS and CuI were freshly prepared according to procedures described by House.[216] The purity of stored copper (I) salts was evaluated before use by dissolving in dimethylsulfide (DMS). EtMgBr, nPrMgBr, and nBuMgBr were prepared immediately before use in the usual way. MeLi, VinylMgBr and BnMgCl were purchased from a commercial supplier. All organometallics were titrated (menthol/1,10-phenanthroline in THF) immediately before use. VinylMgBr was titrated in the same way using diethyl ether as a solvent.

High resolution positive electrospray (ESI) mass spectra were obtained using an orbitrap mass spectrometer. Samples were sprayed from MeOH: 1% formic acid in H_2O. All spectra were collected in the positive mode. ^{1}H- and ^{13}C-NMR were collected using a Bruker Avance-300 spectrophotometer. Variable temperature NMR experiments were performed on a 500 MHz spectrophotometer. Proton Chemical shifts (δ) for samples run in $CDCl_3$ are reported in ppm relative to an internal standard (tetramethylsilane, 0 ppm). For samples run in DMSO-d_6 or CD_3OD, δ was relative to the l solvent peak (2.50 ppm or 3.31 ppm, respectively). For ^{13}C-NMR samples run in $CDCl_3$ chemical shifts are reported relative to the solvent peak (77.0 ppm). For samples run in DMSO-d_6 or CD_3OD, δ was relative to the solvent peak (39.5 ppm or 49.2 ppm, respectively).

Determining Diastereomeric Purity.

Data was collected on each sample at room temperature in DMSO-d_6. In each case, two or three distinct species can be observed by NMR. To determine if these species were rotameric, the samples were heated to a higher temperature (~60 °C or ~100 °C) and analyzed a second time. Peaks that coalesced were indicated with a bracket on the room temperature spectrum. The

spectrum was closely analyzed for any remaining peaks consistent with diastereomeric species. In many cases, diastereomeric peaks were not observed. We corroborated our analysis by converting **3.6**, **3.12-3.16** to **3.1**, **3.17-3.21**. In each case, this almost completely eliminated the rotameric effects observed, allowing for another detailed analysis of the NMR data. Since the **3.1, 3.17-3.21** are purified by a plug column, it is not possible for the diastereomers to be resolved during this separation; thus, the diastereomeric purity of the final product should reflect that of the psuedoproline SM. Using this analysis, we were only able to detect the presence of a diastereomer in product **3.15** and **3.20**. As expected, the relative amount of this building block is the same in **3.15** and **3.20**. A caption below each low temperature spectrum explicitly states the conclusions from our analysis.

Benzyl (S,E)-4-(3-(tert-butoxy)-3-oxoprop-1-en-1-yl)-2,2-dimethyloxazolidine-3-carboxylate (3.5).

To a suspension of sodium hydride (60% in mineral oil; 848 mg, 21.2 mmol, 1.20 equiv) in dry THF (35 mL) cooled (ice-water bath) to 3 °C was added *tert*-butyl diethylphosphonoacetate (5.19 mL, 22.1 mmol, 1.25 equiv) dropwise. The solution was stirred vigorously for 30 min, then a solution of benzyl (S)-4-formyl-2,2-dimethyloxazolidine-3-carboxylate[2] (4.65 g, 17.7 mmol, 1.00 equiv) in THF (37 mL) was added dropwise to the vigorously stirred solution. After 1 h, the reaction was quenched with saturated aqueous NH_4Cl (100 mL). The layers were separated, and the aqueous layer was extracted with EtOAc (100 mL x 3). The combined organic layers were dried with brine and $MgSO_4$ before filtrating and concentrating. The crude product was purified by silica gel column chromatography (20% EtOAc/80% hexanes) yielding **3.5** as a colorless oil (5.58 g, 87% yield). $[\alpha]^{22}_D = +57.0$ (c 0.162, $CHCl_3$). NMR spectra indicated that **3.5** exists as a mixture of two rotamers in $CDCl_3$. ^{1}H NMR (300 MHz, $CDCl_3$) δ 7.34-7.30 (5H, m) 6.72 (1H, dd,

$J = 7.7, 15.8$ Hz) 5.90 and 5.74 (1H, d, $J = 15.8$ Hz) 5.10 (2H, m) 4.58-4.46 (1H, m) 4.09 (1H, dd,

$J = 6.0, 9.0$ Hz) 3.82 (1H, d, $J = 9.0$ Hz) 1.66-1.47 (15H, m). ^{13}C NMR (75 MHz, CDCl$_3$) δ 165.4,

152.3, 144.3, 143.9, 136.4, 128.6, 128.2, 128.1, 124.7, 95.8 and 94.5, 80.8, 67.8 and 67.5, 67.0,

58.6 and 57.9, 31.7 and 28.3, 27.5 and 26.5, 23.6 and 22.8. HRMS-ESI+ (*m/z*): [M + H]$^+$ calculated

for C$_{20}$H$_{34}$O$_5$N, 362.19620; found, 362.19693.

*Benzyl (S)-4-((S)-4-(tert-butoxy)-4-oxobutan-2-yl)-2,2-dimethyloxazolidine-3-carboxylate (**3.6**).*

To a colorless suspension of freshly purified CuI (6.34 g, 33.3 mmol, 6.3 equiv) in dry THF (63.2

mL) at 3 °C (ice-water bath) under N$_2$ was added MeLi (1.6 M in diethyl ether, 41.6 mL, 66.6

mmol, 12.6 equiv) dropwise. During the addition the solution went from orange to colorless. The

solution was then cooled to -73 °C (dry ice/acetone bath) and TMSCl (4.22 mL, 33.3 mmol, 6.30

equiv) was added. When the solution temperature had returned to -73 °C, a solution of **5** (2.00 g,

5.30 mmol, 1.00 equiv) in dry THF (108 mL) was added such that the internal temperature of the

reaction mixture was kept < -65 °C. After the addition, the solution was brought to -40 °C (dry

ice/MeCN slurry) and stirred until the bright orange color had dissipated and the solution was

colorless (about 10 min). The reaction was then quenched by pouring the reaction mixture carefully

into a flask containing ice-cold 9:1 sat. aq. NH$_4$Cl:NH$_4$OH (160 mL). Once the addition was

complete, the solution was stirred in open air until all the solid had dissipated and the solution was

deep blue. The layers were then separated, and the aqueous layer was extracted with EtOAc (160

mL x 2). The combined organic layers were dried with sat. brine and MgSO$_4$ before filtering and

concentrating. The crude oil was purified by silica gel column chromatography (20% EtOAc/80%

hexanes) yielding **3.6** as a colorless oil (1.65 g, 79%). [α]^{22}$_D$ = +23.4 (c 0.223, CH$_2$Cl$_2$). NMR

spectra indicated that **3.6** exists as a mixture of two rotamers in CD$_3$OD. ^{1}H NMR (300 MHz,

CD$_3$OD): δ 7.37-7.32 (5H, m) 5.12 (2H, m) 3.98-3.84 (3H, m) 2.50-2.36 (2H, m) 1.98-1.90 (1H,

m) 1.59-1.42 (15H, m) 0.89-0.87 (3H, m). ^{13}C NMR (75 MHz, CD$_3$OD) δ 175.6, 156.7 and 156.2, 139.4 and 139.2, 131.1 and 130.8, 130.6 and 130.4, 97.2 and 96.9, 83.1, 69.9 and 69.4, 66.8 and 66.6, 64.6 and 63.8, 40.2, 35.4 and 35.1, 29.9 and 29.4, 28.8 and 28.0, 25.8 and 24.3, 18.4. HRMS-ESI+ (*m/z*): [M + H]$^+$ calculated for C$_{21}$H$_{32}$O$_5$N, 378.22750; found, 378.22626.

(2S,3R)-2-(((benzyloxy)carbonyl)amino)-5-(tert-butoxy)-3-methyl-5-oxopentanoic acid (3.7).

To a room temperature solution of **3.6** (1.79 g, 4.75 mmol, 1 equiv) in acetone (47.5 mL) was added freshly prepared Jones reagent (2.67 M CrO$_3$/5.34 M H$_2$SO$_4$, 5.34 mL, 3 equiv) over 3.5 hours via a syringe pump. Once the addition was complete, the solution was cooled (ice-water bath) and iPrOH (6 mL) was added. Cooling was removed and the solution was stirred for 30 min. At this point, celite was added to the stirred solution and the mixture was filtered over celite. The celite was washed with DCM (20 mL) and MeOH (20 mL) until all the product was removed. The filtrate was then dried over MgSO$_4$, filtered and then concentrated. The crude oil was purified by silica gel column chromatography (40% EtOAc/59% hexanes/1% AcOH) yielding **3.7** as a colorless solid (1.15 g, 69% yield). ^{1}H NMR (300 MHz, CDCl$_3$): δ11.27 (1H, br. s) 7.33-7.30 (5H, m) 6.43 and 5.48 (1H, d, *J* = 8.7 Hz) 5.10 (2H, m) 4.56-4.51 (1H, m) 2.61 (1H, m) 2.47-2.40 (1H, m) 2.10 (1H, dd, *J* = 6.6, 15.9 Hz) 1.44 (9H, s) 0.91 (3H, d, *J* = 6.4 Hz). ^{13}C NMR (75 MHz, CDCl$_3$): δ 176.1, 171.9, 156.6, 136.2, 128.7, 128.4, 128.3, 81.1, 67.4, 57.3, 39.4, 33.0, 28.2, 14.8. HRMS-ESI+ (*m/z*): [M + H]$^+$ calculated for C$_{18}$H$_{26}$O$_6$N, 352.17546; found, 352.17520.

(2S,3R)-2-(((((9H-fluoren-9-yl)methoxy)carbonyl)amino)-5-(tert-butoxy)-3-methyl-5

oxopentanoic acid (3.1).

A suspension of **3.7** (968 mg, 2.76 mmol, 1.00 equiv) and Pd/C (10% w/w; 387 mg, 0.364 mmol, 0.13 equiv) was stirred under an atmosphere of hydrogen gas for 2 hours at room temperature. The

suspension was then filtered over celite and the celite pad was extracted with methanol several times. The filtrate was concentrated and the residue was suspended in THF (26 mL) with gentle warming to maximize dissolution. Once the suspension had cooled to room temperature, an aqueous solution of Na_2CO_3 (0.0983 g/mL, 14.9 mL, 13.8 mmol, 5.00 equiv) was added and the mixture was stirred vigorously until all the solid had dissolved. The resulting solution was cooled (ice-water bath) and a solution Fmoc *N*-hydroxysuccinimide ester (1.12 g, 3.31 mmol, 1.20 equiv) in THF (10.8 mL) was added dropwise. Cooling was removed and the solution was stirred vigorously overnight. The reaction was then diluted with H_2O (100 mL), cooled (ice-water bath) and acidified to pH ca. 2 with 1M HCl. This was extracted with EtOAc (100 mL x 4) and the combined organic layer was dried with $MgSO_4$ and filtered. After concentration, the crude reside was purified by silica gel column chromatography (25% EtOAc/74% hexanes/1% AcOH) and any mixed fractions were further purified by recrystallization in EtOAc/hexanes. This yielded **3.1** as a colorless solid (957 mg, 79% yield). The optical rotation and NMR data matched those previously reported in literature.[6,7] $[\alpha]^{22}_D$ = +8.4 (c 0.268, CH_2Cl_2). ^{1}H NMR (300 MHz, $CDCl_3$) 11.17 (1H, br. s) 7.75 (2H, d, *J* = 7.2 Hz) 7.59 (2H, m) 7.41-7.28 (4H, m) 6.16 and 5.47 (1H, d, *J* = 9.0 Hz) 4.57-4.40 (3H, m), 4.22 (1H, app t, *J* = 6.4 Hz) 2.63-2.41 (2H, m) 2.17-2.09 (1H, m) 1.45 (9H, m) 0.95 (3H, d, *J* = 5.8 Hz). ^{13}C NMR (75 MHz, $CDCl_3$): δ 176.3, 172.0, 156.6, 144.0, 143.9, 141.5, 127.9, 127.3, 125.2, 120.2, 81.3, 67.4, 57.4, 47.3, 39.5, 33.0, 28.2, 15.1. HRMS-ESI+ (*m/z*): [M + H]$^+$ calculated for $C_{25}H_{30}O_6N$, 440.20676; found, 440.20702.

*(9H-fluoren-9-yl)methyl (R)-4-formyl-2,2-dimethyloxazolidine-3-carboxylate (**3.9**).*

A solution of 3-((9H-fluoren-9-yl)methyl) 4-methyl (R)-2,2-dimethyloxazolidine-3,4-dicarboxylate[19] (**3.8**) (3.23 g, 8.47 mmol, 1.00 equiv) in dry toluene (16.2 mL) was cooled to -73 °C (acetone/dry ice) under N_2. DIBAL-H (1M in toluene; 12.7 mL, 12.7 mmol, 1.50 equiv) was

added via a syringe pump such that the internal temperature < -65 °C. Once the addition was complete, the solution was stirred for 30 min then another portion of DIBAL-H (1M in toluene; 4.23 mL, 4.23 mmol, 0.50 equiv) was added in the same way. The solution was stirred for 30 min, then MeOH (3.9 mL), cooled in a separate flask to -73 °C (dry ice/acetone bath), was transferred via cannula to the reaction mixture. The addition rate was adjusted such that the internal temperature did not exceed -65 °C. Once the addition was complete, the solution was poured into a flask containing ice-cold 1M HCl (74 mL). The solution was stirred vigorously for a short period of time and then separated. The aqueous layer was extracted with EtOAc (100 mL x 3). The combined organic layer was washed with sat. brine, dried with $MgSO_4$, filtered and then concentrated on to silica. The crude product adhered to silica was purified by silica gel column chromatography (30% EtOAc/70% hexanes). The product containing fractions were concentrated then redissolved in Et_2O and diluted with a large amount of hexanes. Upon concentration of this solution, **3.9** formed as a colorless, chalky solid (2.80 g, 94% yield). $[\alpha]^{22}_D$ = +69.2 (c 0.200, $CHCl_3$).[22] The NMR spectra indicated that **3.9** exists as a mixture of two rotamers in $CDCl_3$. ^{1}H NMR (300 MHz, $CDCl_3$) δ 9.44 and 9.13 (1H, s) 7.75-7.31 (8H, m) 4.80 (1H, m) 4.56 (1H, dd, *J* = 4.6, 13.1 Hz) 4.23-3.92 (4H, m) 1.58 and 0.91 (3H, s) 1.47 and 0.85 (3H, s). ^{13}C NMR (75 MHz, $CDCl_3$) δ 199.2 and 199.0, 153.4 and 152.0, 143.8, 141.7, 141.5, 127.9, 127.3, 124.8 and 124.7, 124.5 and 124.3, 120.1, 95.5 and 94.8, 77.4, 66.8 and 65.0, 64.4 and 63.6, 47.4, 25.8, 23.7 and 23.5. HRMS-ESI+ (*m/z*): [M + H]+ calculated for $C_{21}H_{22}O_4N$, 352.15433; found, 352.15356.

*(9H-fluoren-9-yl)methyl (S,E)-4-(3-(tert-butoxy)-3-oxoprop-1-en-1-yl)-2,2-dimethyloxazolidine-3-carboxylate (**3.10**).*

To a suspension of sodium hydride (60% in mineral oil; 212 mg, 5.31 mmol, 1.1 equiv) in dry THF (14 mL) cooled (ice-water bath) to 3 °C was added *tert*-butyl diethylphosphonoacetate (1.36

mL, 5.79 mmol, 1.2 equiv) dropwise. The solution was stirred vigorously for 30 min, then cooled to -10 °C (dry ice/ethylene glycol bath). A solution of **3.9** (1.70 g, 4.83 mmol, 1 equiv) in THF (14 mL), also cooled to -10 °C (dry ice/ethylene glycol bath), was transferred via cannula to the vigorously stirred solution. The addition rate was adjusted such that the internal temperature of the reaction vessel was <-5 °C throughout the reaction. Once the addition was complete, the solution was vigorously stirred until TLC showed that the reaction had reached completion (about 10 min). The reaction was then quenched with saturated aqueous NH_4Cl (34 mL). The layers were separated, and the aqueous layer was extracted with EtOAc (50 mL x 3). The combined organic layers were dried with brine and $MgSO_4$ before filtrating and concentrating. The crude product was purified by silica gel column chromatography (23% EtOAc/77% hexanes) yielding **3.10** as a colorless solid (2.03 g, 93% yield). $[\alpha]^{22}_D = +40.4$ (c 0.275, CH_2Cl_2). The NMR spectra indicated that **3.10** exists as a mixture of two rotamers in $CDCl_3$. ^1H NMR (300 MHz, $CDCl_3$) δ 7.75 (2H, d, J = 7.4 Hz) 7.55-7.53 (2H, m) 7.40-7.28 (4H, m) 6.67-6.62 (1H, m) 5.79 and 5.52 (1H, d, J = 15.4 Hz) 4.74 (1H, m) 4.55-4.41 (2H, m) 4.20 (2H, m) 3.99-3.97 (1H, m) 3.77-3.68 (1H, m) 1.62 and 0.92 (3H, s) 1.46 (9H, s) 1.46 and 0.80 (3H, s). ^{13}C NMR (75 MHz, $CDCl_3$) δ 165.5 and 165.3, 152.8 and 152.4, 144.4 and 144.1, 144.1 and 143.8, 141.7 and 141.6, 141.5 and 141.4, 127.8, 127.2, 125.1 and 124.9, 124.5 and 124.2, 120.1 and 120.0, 94.9 and 94.3, 80.7, 68.0 and 67.3, 66.8 and 66.3, 58.3 and 57.7, 47.5 and 47.4, 28.2, 26.4, 23.6 and 23.3. HRMS-ESI+ (*m/z*): [M + Na]$^+$ calculated for $C_{27}H_{31}O_5NNa$, 472.20944; found, 472.20880.

(9H-fluoren-9-yl)methyl (S)-4-((R)-4-(tert-butoxy)-4-oxobutan-2-yl)-2,2-dimethyloxazolidine-3-carboxylate (3.11).

3.11 was prepared following the same procedure used for the preparation of **3.6** (921.5 mg, 93% yield). $[\alpha]^{22}_D = +22.0$ (c 0.270, CH_2Cl_2). NMR spectra indicated that **3.11** exists as a mixture of

two rotamers in CDCl$_3$. ^{1}H NMR (300 MHz, CDCl$_3$) δ 7.74 (2H, d, J = 7.4 Hz) 7.58 (2H, m) 7.40-7.30 (4H, m) 4.76-4.68 and 4.47-4.43 (2H, m) 4.21-4.20 (1H, m) 3.78-3.69 and 3.41 (3H, m) 2.29-2.23 (2H, m) 1.84-1.81 (1H, m) 1.58 and 0.90 (3H, s) 1.41 (9H, s) 1.34 and 0.77 (3H, s) 0.83 and 0.68 (3H, d, J = 6.5 Hz). ^{13}C NMR (75 MHz, CDCl$_3$) δ 172.2, 153.5 and 153.0, 144.2 and 144.0, 143.9 and 143.7, 141.6 and 141.3, 127.6, 127.1 and 127.0, 124.8 and 124.7, 124.4 and 124.2, 119.9 and 119.8, 94.3 and 93.9, 80.0, 66.0 and 65.8, 64.1 and 63.9, 61.5 and 60.9, 47.4, 37.9 and 37.2, 32.5, 28.0, 25.8, 22.9 and 22.3, 16.3 and 16.1. HRMS-ESI+ (*m/z*): [M + H]$^+$ calculated for C$_{28}$H$_{36}$O$_5$N, 466.25732; found, 466.25732.

*(9H-fluoren-9-yl)methyl (R)-4-((S)-1-(tert-butoxy)-1-oxopentan-3-yl)-2,2-dimethyloxazolidine-3-carboxylate (**3.12**).*

To a homogeneous solution of CuBr*DMS (690 mg, 3.33 mmol, 1.50 equiv) and dry LiBr (580 mg, 6.66 mmol, 3.00 equiv) in dry THF (40 mL) cooled to -40 °C (internal temperature; dry ice/MeCN bath) under N$_2$ was added a freshly prepared solution of EtMgBr (1.25M in THF; 5.30 mL, 6.66 mmol, 3.00 equiv). The addition rate was adjusted such that the internal temperature < -35 °C. The resulting light lavender suspension was stirred for 30 min at -40 °C and then cooled to -73 °C. To this solution was added a solution of TMSCl (0.430 mL, 3.33 mmol, 1.50 equiv) in THF (15 mL). The addition rate was adjusted such that the reaction temperature < -40 °C. Once the reaction mixture had cooled back down to -73 °C, a solution of **3.10** (1.00 g, 2.22 mmol, 1.00 equiv) in THF (20 mL) was added via a syringe pump such that the internal temperature did not exceed -70 °C. Once the addition was complete, cooling was removed, and the solution was allowed to reach 15 °C at which point it was poured into a flask containing ice-cold 9:1 saturated aqueous NH$_4$Cl:NH$_4$OH (60 mL). The mixture was stirred vigorously under air until all the solid had dissipated and the mixture was a deep blue color (about 30 min, but it depends on the

cuprate/alkyl copper present). The layers were separated, and the aqueous layer was extracted with EtOAc (60 mL x 2). The combined organic layers were washed with brine, then dried with $MgSO_4$ before filtering and concentrating. The crude oil was purified via silica gel column chromatography (20% EtOAc/80% hexanes) yielding **3.12** as a colorless syrup (809 mg, 76%). $[\alpha]^{22}_D = +20.5$ (c 0.079, CH_2Cl_2). NMR spectra indicated that 3.**12** exists as a mixture of two rotamers in $CDCl_3$. ^1H NMR (300 MHz, $CDCl_3$) δ 7.74 (2H, d, $J = 7.4$ Hz) 7.63-7.57 (2H, m) 7.40-7.27 (4H, m) 4.73 and 4.45 (2H, m) 4.22 (1H, m) 3.95 and 3.75-3.68 (3H, m) 2.31-2.26 (2H, m) 1.92 (1H, dd, $J = 9.2, 14.6$ Hz) 1.64-0.75 (20H, m). ^{13}C NMR (75 MHz, $CDCl_3$) δ 172.7, 153.3, 144.5 and 144.1, 143.8, 141.6, 141.5, 127.8, 127.3, 125.1 and 124.9, 124.6 and 124.4, 120.1 and 120.0, 94.6 and 94.0, 80.2, 66.2, 64.0, 59.8 and 59.0, 47.8 and 47.4, 38.6 and 38.3, 35.8 and 35.6, 28.2 and 25.9, 25.0 and 24.6, 23.0 and 22.5, 11.9. HRMS-ESI+ (*m/z*): $[M + H]^+$ calculated for $C_{29}H_{38}O_5N$, 480.27445; found, 480.27422.

*(9H-fluoren-9-yl)methyl (S)-4-((R)-1-(tert-butoxy)-1-oxohexan-3-yl)-2,2-dimethyloxazolidine-3-carboxylate (**3.13**).*

3.13 was prepared following the procedure used for the preparation of **3.12**. nPrMgBr (solution in THF) was used instead of EtMgBr (1.030 g, 94% yield). $[\alpha]^{22}_D = +22.2$ (c 0.085, CH_2Cl_2). NMR spectra indicated that **3.13** exists as a mixture of two rotamers in $CDCl_3$. ^1H NMR (300 MHz, $CDCl_3$) δ 7.74 (2H, d, $J = 7.4$ Hz) 7.60-7.57 (2H, m) 7.39-7.30 (4H, m) 4.74 and 4.44 (2H, m) 4.21 (1H, m) 3.93 and 3.75-3.62 (3H, m) 2.37-2.32 (2H, m) 1.91 (1H, dd, $J = 9.3, 15.2$ Hz) 1.61-0.74 (22H, m). ^{13}C NMR (75 MHz, $CDCl_3$) δ 172.7, 153.5 and 153.2, 144.4 and 144.1, 143.7, 141.7 and 141.6, 141.6 and 141.4,127.7, 127.2, 125.1 and 124.9, 124.5 and 124.3, 120.0 and 119.9, 94.6, 94.0, 80.2, 66.1, 64.0 and 63.8, 59.8 and 59.1, 47.7 and 47.4, 36.8, 36.0 and 35.7, 34.4 and 33.9,

28.2, 25.9, 22.9 and 22.4, 20.3, 14.5 and 14.3. HRMS-ESI+ (*m/z*): [M + H]$^+$ calculated for C$_{30}$H$_{40}$O$_5$N, 494.29010; found, 494.28878.

(9H-fluoren-9-yl)methyl (S)-4-((R)-1-(tert-butoxy)-1-oxoheptan-3-yl)-2,2-dimethyloxazolidine-3-carboxylate (3.14).

3.14 was prepared following the procedure used for the preparation of **3.12**, 3 equiv of cuprate were used instead of 1.5 equiv. BuMgBr (solution in THF) was used instead of EtMgBr (1.116 g, 99% yield). [α]^{22}$_D$ = +11.6 (c 0.160, CH$_2$Cl$_2$). NMR spectra indicated that **3.14** exists as a mixture of two rotamers in CDCl$_3$. ^{1}H NMR (300 MHz, CDCl$_3$) δ 7.75 (2H, d, *J* = 7.4 Hz) 7.60-7.57 (2H, m) 7.40-7.28 (4H, m) 4.72 and 4.43 (2H, m) 4.23-4.22 (1H, m) 3.94 and 3.77-3.69 (3H, m) 2.37-2.32 (2H, m) 1.92 (1H, dd, *J* = 9.2, 15.0 Hz) 1.61-0.74 (24H, m). ^{13}C NMR (75 MHz, CDCl$_3$) δ 172.7, 153.5 and 153.2, 144.4 and 144.1, 143.7, 141.7 and 141.6, 141.6 and 141.4, 127.7, 127.2, 125.1 and 124.9, 124.5 and 124.3, 120.0 and 119.9, 94.7, 94.0, 80.2, 66.3 and 66.1, 64.0 and 63.8, 59.9 and 59.2, 47.7 and 47.4, 37.0, 36.2 and 36.0, 35.8, 32.0 and 31.5, 29.4, 28.2, 25.9 23.1 and 22.9, 22.5, 14.1. HRMS-ESI+ (*m/z*): [M + H]$^+$ calculated for C$_{31}$H$_{42}$O$_5$N, 508.30575; found, 508.30516.

(9H-fluoren-9-yl)methyl (S)-4-((R)-4-(tert-butoxy)-4-oxo-1-phenylbutan-2-yl)-2,2-dimethyloxazolidine-3-carboxylate (3.15).

3.15 was prepared following the procedure used for the preparation of **3.12**. However, 3 equiv of cuprate were used instead of 1.5 equiv. BnMgCl (solution in THF) was used instead of EtMgBr and, after the addition of alkene, the reaction mixture was brought to -40 °C (dry ice/MeCN bath) and allowed to react at this temperature for 1 hour before cooling was removed (1.690 g, 94% yield). [α]^{22}$_D$ = +22.9 (c 0.272, CH$_2$Cl$_2$). NMR spectra indicated that **3.15** exists as a mixture of

two rotamers in CDCl$_3$. ^{1}H NMR (300 MHz, CDCl$_3$): δ 7.75 (2H, m) 7.57-7.51 (2H, m) 7.38-7.10 (10H, m) 4.75-4.72 (1H, m) 4.39 (1H, m) 4.19 (1H, m) 3.81-3.71 (3H, m) 2.93-2.65 (2H, m) 2.48-2.28 (2H, m) 2.16-2.08 (1H, m) 1.70 and 0.88 (3H, s) 1.41 (9H, s) 1.41 and 0.70 (3H, s). ^{13}C NMR (75 MHz, CDCl$_3$) δ 172.7, 153.2, 144.3 and 144.1, 143.9 and 143.8, 141.4 and 141.2, 139.4 and 139.1, 129.1, 128.5, 127.7, 127.2 and 127.2, 126.3, 125.2 and 125.0, 124.5 and 124.2, 119.9, 94.7 and 94.0, 80.4 and 80.3, 67.0 and 66.0, 63.9 and60.0, 59.2 and 58.4, 47.5 and 47.3, 38.8, 37.8 and 37.4, 35.4 and 34.9, 28.1 and 28.1, 25.9, 22.9 and 22.4. HRMS-ESI+ (*m/z*): [M + H]$^+$ calculated for C$_{34}$H$_{40}$O$_5$N, 542.29010; found, 542.28845.

*(9H-fluoren-9-yl)methyl (S)-4-((S)-5-(tert-butoxy)-5-oxopent-1-en-3-yl)-2,2-dimethyloxazolidine-3-carboxylate (**3.16**).*

3.16 was prepared following the procedure used for the preparation of **3.12**. However, 6 equiv of cuprate were used instead of 1.5 equiv. VinylMgBr (solution in THF) was used instead of EtMgBr (1.410 g, 89% yield). [α]^{22}$_D$ = +21.3 (c 0.320, CH$_2$Cl$_2$). NMR spectra indicated that **3.16** exists as a mixture of two rotamers in CDCl$_3$. ^{1}H NMR (300 MHz, CDCl$_3$): δ 7.74 (2H, d, *J* = 7.3 Hz) 7.62-7.56 (2H, m) 7.38-7.31 (4H, m) 5.64 and 5.33 (1H, m) 5.06-4.69 (4H, m) 4.21 (1H, m) 3.91-3.54 (3H, m) 2.97-2.86 (1H, m) 2.31-2.03 (2H, m) 1.66-0.78 (15H, m) ^{13}C NMR (75 MHz, CDCl$_3$) δ171.5, 153.5 and 152.9, 144.3 and 144.0, 144.0 and 143.7, 141.5 and 141.4, 137.2, 127.7, 127.2 and 127.1, 124.9 and 124.8, 124.5 and 124.3, 120.0 and 119.9, 118.1 and 117.1, 94.7 and 94.1, 80.3, 66.1, 64.7, 60.2 and 59.4, 47.6 and 47.3, 42.7, 35.8 and 35.3, 28.1, 26.1 and 25.9, 23.1 and 22.5. HRMS-ESI+ (*m/z*): [M + H]$^+$ calculated for C$_{29}$H$_{36}$NO$_5$, 478.25880; found, 478.25718.

General Procedure used for Acetonide Deprotection and Crude Alcohol Oxidation.

BiBr$_3$ (0.15 equiv) was added to a solution of acetonide in dry acetonitrile (0.1 M acetonide concentration). This mixture was stirred under N$_2$ for 30 min, then H$_2$O (1.2 equiv) was added, and the flask was sealed. After 18 hours of stirring at room temperature, the reaction was quenched with saturated aqueous NaHCO$_3$ (5 mL/mmol). The layers were separated, and the aqueous layer was extracted with EtOAc (10 mL/mmol x 3). The combined organic layers were washed with brine and dried with MgSO$_4$ prior to filtering and concentrating. The crude alcohol was then dissolved in MeCN (12 mL/mmol) at room temperature. To this solution was added TEMPO (0.1 equiv), phosphate buffer (0.67M, pH ca. 6.7; 8 mL/mmol) and NaO$_2$Cl (2 M solution in water; 2.6 equiv or 1.3 mL/mmol). The resulting mixture was brought to 40 °C then NaOCl (0.81 M; 0.060 equiv) diluted in H$_2$O (1.6 mL/mmol) was added over 1 hour via a syringe pump. The resulting solution was sealed and stirred for 18 hours. The final mixture was quenched with saturated aqueous Na$_2$SO$_3$ (5 mL/mmol) and the layers were separated. The aqueous layer was cooled (ice-water) and acidified to a pH ca. 3 with 1M HCl. The aqueous layer was then extracted with EtOAc (x3) and the combined organic layers were washed with brine and dried with MgSO$_4$ prior to filtering and concentrating on to silica. The crude product adhered to silica was purified via loading onto a short pad of silica and eluting all impurities (20% EtOAc/80% hexanes) and then flushing the column (98% EtOAc/2% AcOH) to recover the purified product, which was concentrated from heptane to remove trace acetic acid.

(2S,3R)-2-((((9H-fluoren-9-yl)methoxy)carbonyl)amino)-5-(tert-butoxy)-3-ethyl-5-oxopentanoic acid (3.17). **3.17** was prepared from **3.12** following the General Procedure. This yielded **3.17** as a colorless solid (981 mg, 82% yield). [α]^{22}$_D$ = +0.35 (c 0.257, CH$_2$Cl$_2$). ^{1}H NMR (300 MHz, CD$_3$OD): δ 7.76 (2H, d, *J* = 7.4 Hz) 7.67-7.64 (2H, m) 7.38-7.26 (5H, m) 4.43-4.20 (4H, m) 2.36-2.24 (3H, m) 1.42-1.26 (11H, m) 0.92 (3H, t, *J* = 7.2 Hz). ^{13}C NMR (75 MHz, DMSO-*d$_6$*): δ 176.4,

174.6, 159.7, 147.1, 144.0, 131.0, 130.4, 128.7, 128.5, 123.4, 83.1, 69.1, 59.0, 50.0, 41.3, 39.2, 31.0, 25.6, 14.7. HRMS-ESI+ (m/z): [M + H]$^+$ calculated for $C_{26}H_{32}NO_6$, 454.22241; found, 454.22058.

(2S,3R)-2-(((((9H-fluoren-9-yl)methoxy)carbonyl)amino)-3-(2-(tert-butoxy)-2-oxoethyl)hexanoic acid (3.18). **3.18** was prepared from **3.13** following the General Procedure. This yielded **3.18** as a colorless solid (647 mg, 83% yield). [α]^{22}$_D$ = +8.25 (c 0.0824, CH_2Cl_2). ^{1}H NMR (300 MHz, CDCl$_3$): 7.75 (2H, d, *J* = 7.4 Hz) 7.60-7.58 (2H, m) 7.41-7.28 (4H, m) 5.96 and 5.58 (1H, d, *J* = 8.3 Hz) 4.57 (1H, app d, *J* = 8.3 Hz) 4.41-4.39 (2H, m) 4.21 (1H, app t, *J* = 6.8 Hz) 2.43-2.26 (3H, m) 1.46-1.24 (13H, m) 0.90 (3H, m). ^{13}C NMR (75 MHz, DMSO-*d$_6$*): δ 173.5, 171.7, 156.9, 144.3, 141.2, 128.1, 127.5, 125.9, 125.8, 120.6, 80.2, 66.3, 56.5, 47.1, 36.9, 36.7, 32.1, 28.2, 20.0, 14.5. HRMS-ESI+ (m/z): [M + H]$^+$ calculated for $C_{27}H_{34}NO_6$, 468.23806; found, 468.23748.

(2S,3R)-2-(((((9H-fluoren-9-yl)methoxy)carbonyl)amino)-3-(2-(tert-butoxy)-2-oxoethyl)heptanoic acid (3.19). **3.19** was prepared from **3.14** following the General Procedure. This yielded **3.19** as a colorless solid (827 mg, 78% yield). [α]^{22}$_D$ = +3.58 (c 0.120, CH_2Cl_2). ^{1}H NMR (300 MHz, DMSO-*d$_6$*): 7.85 (2H, d, J = 7.4 Hz) 7.74-7.53 (3H, m) 7.39 (2H, app t, *J* = 7.3 Hz) 7.30 (2H, app t, *J* = 7.2 Hz) 4.28-4.19 (4H, m) 2.28-2.11 (3H, m) 1.34-1.15 (15H, m) 0.82 (3H, m). ^{13}C NMR (75 MHz, DMSO-*d$_6$*): δ 173.2, 171.3, 156.4, 143.8, 140.7, 127.6, 127.1, 125.4, 125.3, 120.1, 79.7, 65.8, 56.2, 46.7, 36.5, 29.1, 28.6, 27.7, 22.2, 13.8. HRMS-ESI+ (m/z): [M + H]$^+$ calculated for $C_{27}H_{34}NO_6$, 482.25426; found, 482.25283.

(2S,3R)-2-(((((9H-fluoren-9-yl)methoxy)carbonyl)amino)-3-benzyl-5-(tert-butoxy)-5-oxopentanoic acid (3.20). **3.20** was prepared from **3.15** following the General Procedure. This yielded **3.20** as a colorless solid (1.260 g, 80% yield). [α]^{22}$_D$ = +10.6 (c 0.110, CH_2Cl_2). ^{1}H NMR (300 MHz, DMSO-*d$_6$*): 7.87 (2H, d, *J* = 7.4 Hz) 7.74-7.65 (3H, m) 7.40-7.13 (9H, m) 4.35-4.22

(4H, m) 2.62-2.56 (2H, m) 2.30-2.22 (1H, m) 1.99-1.88 (1H, m) 1.32-1.28 (9H, m). ^{13}C NMR (75 MHz, DMSO-d_6): δ 172.9, 170.8, 156.5, 143.8, 143.8, 140.7, 139.4, 129.0, 128.5, 128.3, 127.7, 127.1, 126.2, 125.4, 125.3, 120.1, 79.9, 65.8, 55.5, 46.7, 38.6, 35.4, 35.1, 27.6. HRMS-ESI+ (*m/z*): [M + H]$^+$ calculated for $C_{31}H_{34}NO_6$, 516.23806; found, 516.23562.

(2S,3S)-2-((((9H-fluoren-9-yl)methoxy)carbonyl)amino)-3-(2-(tert-butoxy)-2-oxoethyl)pent-4-enoic acid (3.21). **3.21** was prepared from **3.16** following the General Procedure. This yielded **3.21** as a colorless solid (1.260 g, 80% yield). $[\alpha]^{22}_D$ = +10.8 (c 0.096, CH_2Cl_2). ^{1}H NMR (300 MHz, CDCl$_3$): 11.00 (1H, br. s) 7.75 (2H, d, *J* = 7.4 Hz) 7.58 (2H, app d, *J* = 7.0 Hz) 7.41-7.28 (4H, m) 5.66-5.56 (1H, m) 5.86 and 5.29 (1H, d, *J* = 9.9 Hz) 5.20-5.15 (2H, m) 4.62 (1H, dd, *J* = 3.3, 9.1 Hz) 4.50-4.39 (2H, m) 4.21 (1H, app t, *J* = 6.9 Hz) 3.22-3.00 (1H, m) 2.55-2.31 (2H, m) 1.44 (9H, s). ^{13}C NMR (75 MHz, CDC1$_3$): δ175.8, 171.1, 156.5, 144.0, 143.8, 141.5, 134.5, 127.9, 127.3, 125.2, 120.2, 119.2, 81.4, 67.4, 56.6, 47.3, 42.3, 36.9, 28.2. HRMS-ESI+ (*m/z*): [M + H]$^+$ calculated for $C_{26}H_{30}NO_6$,452.20676; found, 452.20560.

Chapter 4 - A High-yielding Solid-Phase Total Synthesis of Daptomycin using a Fmoc SPPS Stable Kynurenine Synthon.

4   Preface and contributions

This chapter is based on a manuscript published in *Organic & Biomolecular Chemistry* (Reproduced from *Org. Biomol. Chem.* **2021**, *19*, 3144–3153.). I completed almost all the experimental work present in this chapter. Jacob Wolfe (an undergraduate student in the Taylor lab) helped with the MS-MS analysis and resynthesis of a key side product. I prepared the first draft of this manuscript which was lightly edited by Prof. Taylor. All work presented in this chapter was done under the supervision of Prof. Taylor. Additional supplementary information is available on the journal's website.

4.1   Introduction

With ample quantities of both enantiomers of Fmoc-MeGlu(t-Bu)-OH in hand, we turned our attention towards the synthesis of the unnatural enantiomer of daptomycin. Although we could have used an approach previously described by the Taylor lab, we were interested in developing an even more efficient approach based on what we had learned synthesizing A5D (chapter 8). We ended up finding out that many of the difficulties experienced by the Taylor, Li and Brimble groups while developing routes to daptomycin were caused by the instability of commonly used Kyn building blocks. A detailed account of this work is provided here-in.

As discussed in the introduction, many researchers have attempted to explore dap's structure-activity relationship (SAR) to overcome bacterial resistance, understand dap's mode of action and mitigate dap's inhibition by pulmonary surfactant.[135] Early attempts at preparing analogs of daptomycin utilized chemoenzymatic[217,218] and combinatorial biosynthetic[16,219] approaches but these methods produced less than two dozen analogs. Modern biosynthetic approaches have produced more analogs in a much shorter period of time but have focused on

manipulating Trp1.[220,221] In contrast, total chemical synthesis has allowed for the preparation of approximately 150 analogs of daptomycin to date.

Several syntheses for daptomycin and analogs of daptomycin have been developed by our group and others (see Figure 4.1). The first synthesis of daptomycin was achieved by Cubist Pharmaceuticals in 2006 using a labor intensive solution-phase segment coupling approach.[201] The first partially solid-phase synthesis of daptomycin was reported by the Li group in 2013.[155] Li and coworkers elected to use a convergent synthesis to daptomycin and formed the key ester bond in solution on a branched tetrapeptide which is prepared in 12 steps. The authors exposed intermediates containing azide protected Asp3 to several treatments with piperidine/DMF despite the fact that this moiety undergoes elimination under these conditions.[154] The peptide was cyclized in the solution-phase using a serine chemical ligation strategy which required two HPLC purifications to isolate dap. Considering the inefficiencies of their original synthesis, it is not surprising that the Li group opted to prepare all but 3 of the ~80 daptomycin analogs they have reported to date via a different approach. The synthetic efforts of the Li group have led to the discovery of Kynomycin -- an analog of daptomycin with improved biological properties.[159,161] The second solid-phase synthesis of daptomycin was reported by the Taylor group in 2015 which allowed for the preparation of daptomycin totally on a solid-support, including an on-resin cyclization, with a 9% isolated yield.[162] Since this report, we have prepared >20 daptomycin analogs including an active analog of daptomycin that possess only proteinogenic amino acids.[169,222,223] Finally, in 2019 Brimble and coworkers disclosed a Boc/Fmoc solid-phase synthesis of daptomycin which proceeded with a 9% isolated yield.[192] Their synthesis employed an on-resin cyclization followed by an on-resin ozonolysis of Trp at position 13 to install the key Kyn13 residue. The aforementioned reaction sequence was required to overcome the low reactivity

of Boc-L-Kyn(CHO,CHO)-OH observed during ester bond formation. Following on-resin ozonolysis, Brimble and coworkers found the cyclic peptide underwent a side reaction when exposed to base/DMF deprotection mixtures commonly employed in Fmoc-SPPS. They overcame this side reaction by using a less basic deprotection mixture but did not elucidate the side reaction or the identity of the observed side products. Herein, we report a high-yielding and straightforward SPPS of daptomycin which was achieved through characterizing the base instability of Kyn(CHO,CHO) or Kyn(Boc,CHO) containing peptides.

Li and coworkers 2013

Highlights:
-Tetrapeptide used to make ester bond in solution
-Cyclized via serine ligation in solution requiring two HPLC purifications
-one azido acid used

Taylor and coworkers 2015

Highlights:
-Totally on-resin synthesis
-three azido acids used
-Incomplete on-resin cyclization
-9% isolated yield

Brimble and coworkers 2019

Highlights:
-Boc/Fmoc synthesis
-Totally on-resin synthesis
-On-resin ozonolysis to install Kyn13
-Base instability of key intermediate
-9% isolated yield

This work

Highlights:
-High-yielding off-resin cyclization
-Only Fmoc amino acids used
-Early stage esterification
-Base stable Kyn containing intermediates
-22% isolated yield
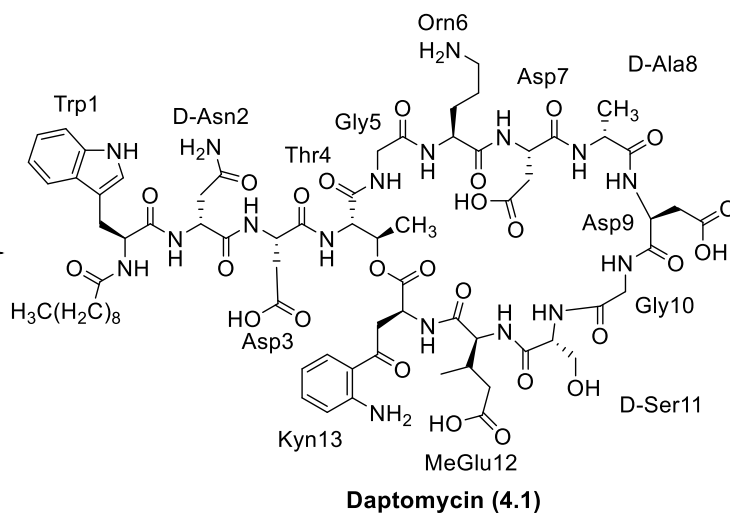
Daptomycin (4.1)

Figure 4.1 Summary of the total chemical synthesis routes to daptomycin.

118

4.2 Results and discussion

The main shortcomings of our initial synthesis of daptomycin were the need to use 3 azido acids that are not commercially available and incomplete on-resin cyclization. We postulated that a more efficient and high-yielding synthesis of dap, and its analogs, could be developed following a route similar to the one we used to prepare A54145D, a Ca^{2+}-dependent cyclic lipodepsipeptide antibiotic that shares some structural features with dap.[181] We envisioned reducing the number of azido acids to one by starting from Gly5 (Scheme 4.1) and forming the ester bond on pentapeptide **4.2**. From **4.3a**, the decanoyl tail would be installed following azide reduction, and then the remaining residues would be coupled using DIC (diisopropylcarbodiimide)/HOBt (1-hydroxybenzotriazole). After cleavage from the 2'-Cl-Trt resin, the protected peptide would be cyclized, globally deprotected and purified.
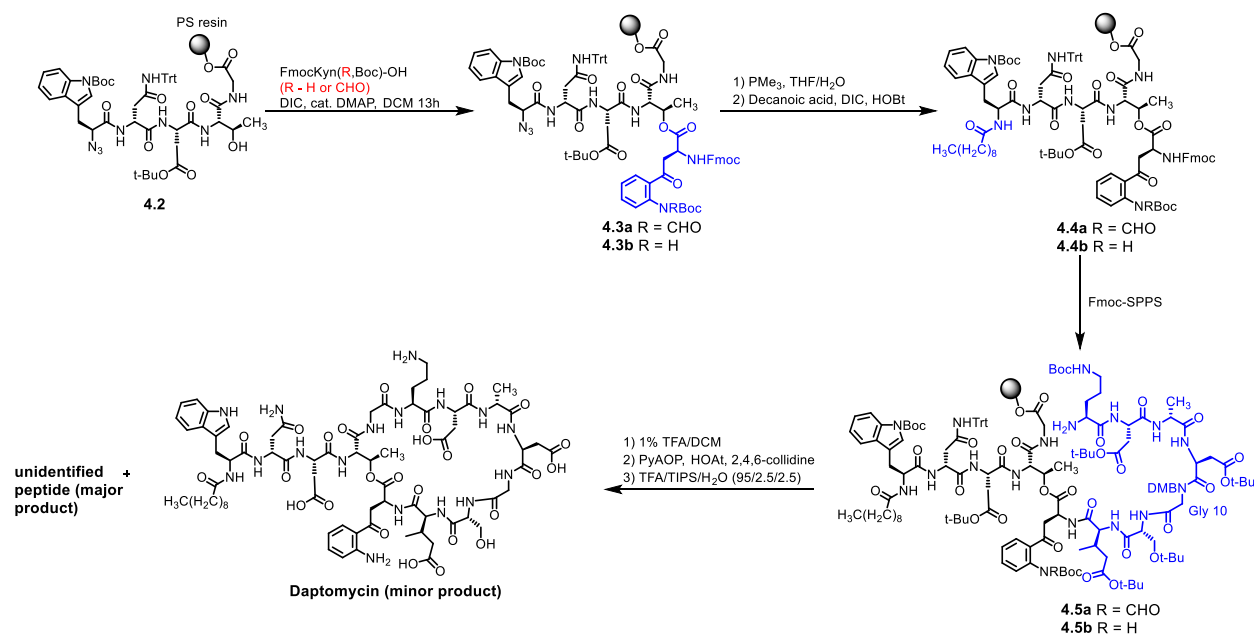
Scheme 4.1 Synthesis of daptomycin using a single azido acid and an off-resin cyclization

Starting from a commercially available Fmoc-Gly-loaded polystyrene resin with a 2'-Cl-Trt linker, we extended to D-Asn(Trt) using standard Fmoc SPPS, and then coupled on azido-L-Trp(Boc)-OH giving peptide **4.2**.[224] Formation of the ester bond between **4.2** and Fmoc-L-

Kyn(Boc,CHO)-OH[155] occurred smoothly via the symmetric anhydride conditions that we reported previously, giving peptide **4.3a**.[162] No epimerization was observed by HPLC at this stage, further demonstrating that the difficulty of this esterification reaction depends strongly on peptide length.[162,181] Reduction of the azido group with PMe_3/THF/H_2O followed by coupling on the decanoic acid tail proceeded cleanly, yielding peptide **4.4a**. Unfortunately, attempts to elongate **4.4a** using Fmoc SPPS were accompanied by intractable decomposition that worsened with each peptide coupling reaction. We were surprised by this outcome considering that this sequence and similar sequences have been prepared under similar conditions.[167,181,225] To determine the source of this decomposition, we decided to continue the synthesis from **4.4a** and try to isolate and characterize any discrete side products after cyclization. To this end, **4.4a** was elongated to **4.5a** using DIC/HOBt couplings. Attempts to monitor this part of the synthesis using HPLC/MS were complicated by an unusual fragmentation pathway that was common to each intermediate which resulted in each intermediate giving the same *m/z* value during mass analysis. We were initially concerned that these data indicated that the peptide had undergone a terminating side reaction, but ninhydrin testing indicated that the peptide was still being elongated. Cyclization of **4.5a** was found to be highly solvent dependent and proceeded reproducibly and with high efficiency using PyAOP (7-azabenzotriazol-1-yloxy)tripyrrolidinophosphonium hexafluorophosphate)/HOAt (1-hydroxy-7-azabenzotriazole)/2,4,6-collidine in dry DMF. Attempts to execute this cyclization in dry DCM or a 3:1 DCM/DMF mixture gave unsatisfactory results that were difficult to reproduce. After cyclization, the peptide was globally deprotected using TFA/TIPS/H_2O and purified by preparative HPLC. During the purification, we found that this synthesis had produced very little daptomycin(<1 mg on a 0.1 mmol scale). The major product of this pathway was an unidentified peptide which had a *m/z* that was 10 amu greater than that of dap.

Our efforts to characterize the unidentified by-product began with determining if the by-product contained an ester bond. After subjecting it to aq. LiOH for 2 h at room temperature, a new compound that had an *m/z* that was 18 amu greater was obtained, indicating that it did indeed possess an ester bond. MS-MS sequencing of the hydrolyzed peptide (see Table B.1) showed that all residues were intact and in their expected position except for Kyn. Thus, the Kyn residue must have been converted to a residue that was 10 amu heavier during the synthesis. Based on these data, we initially proposed that the unidentified peptide could be the isocyanide containing peptide **4.6** which may have formed under the strongly dehydrating cyclization conditions (Figure 4.2). To test this hypothesis, we coupled Fmoc-L-Kyn(Boc,CHO)-OH on to a Fmoc-Gly-loaded polystyrene resin with a 2-Cl Trt linker yielding dipeptide **4.8** which was cleaved from the solid-support using 1% TFA/DCM and exposed to PyAOP/HOAt/2,4,6-collidine in DMF with BnNH$_2$ (Scheme 4.2). After stirring at room temperature for 48 h, the peptide was concentrated and then worked up. After deprotection using TFA/TIPS/H$_2$O, the crude peptide was analyzed via HPLC/MS which showed almost exclusively peptide **4.9**. In addition, exposing **4.11** or **4.12** to the cyclization conditions did not result in any isocyanide formation making **4.6** an unlikely candidate for the unidentified peptide.
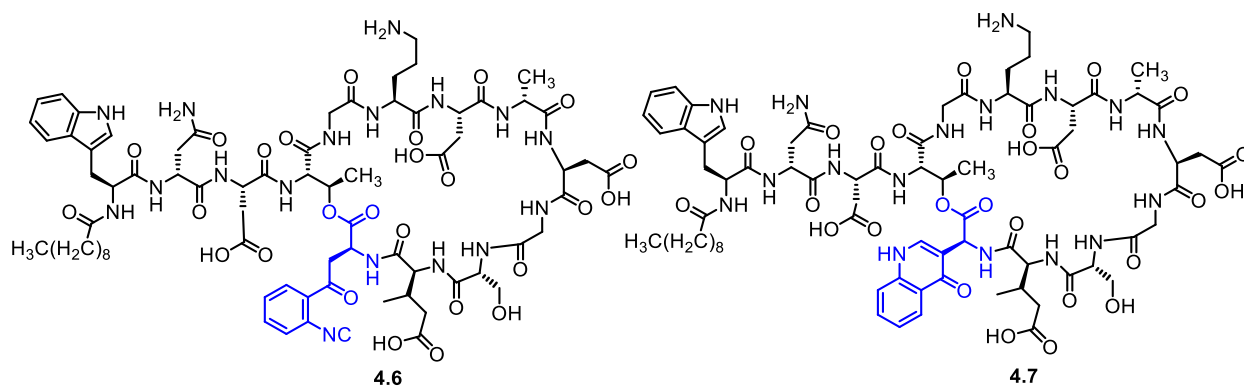
Figure 4.2 Proposed structures of the unidentified peptide
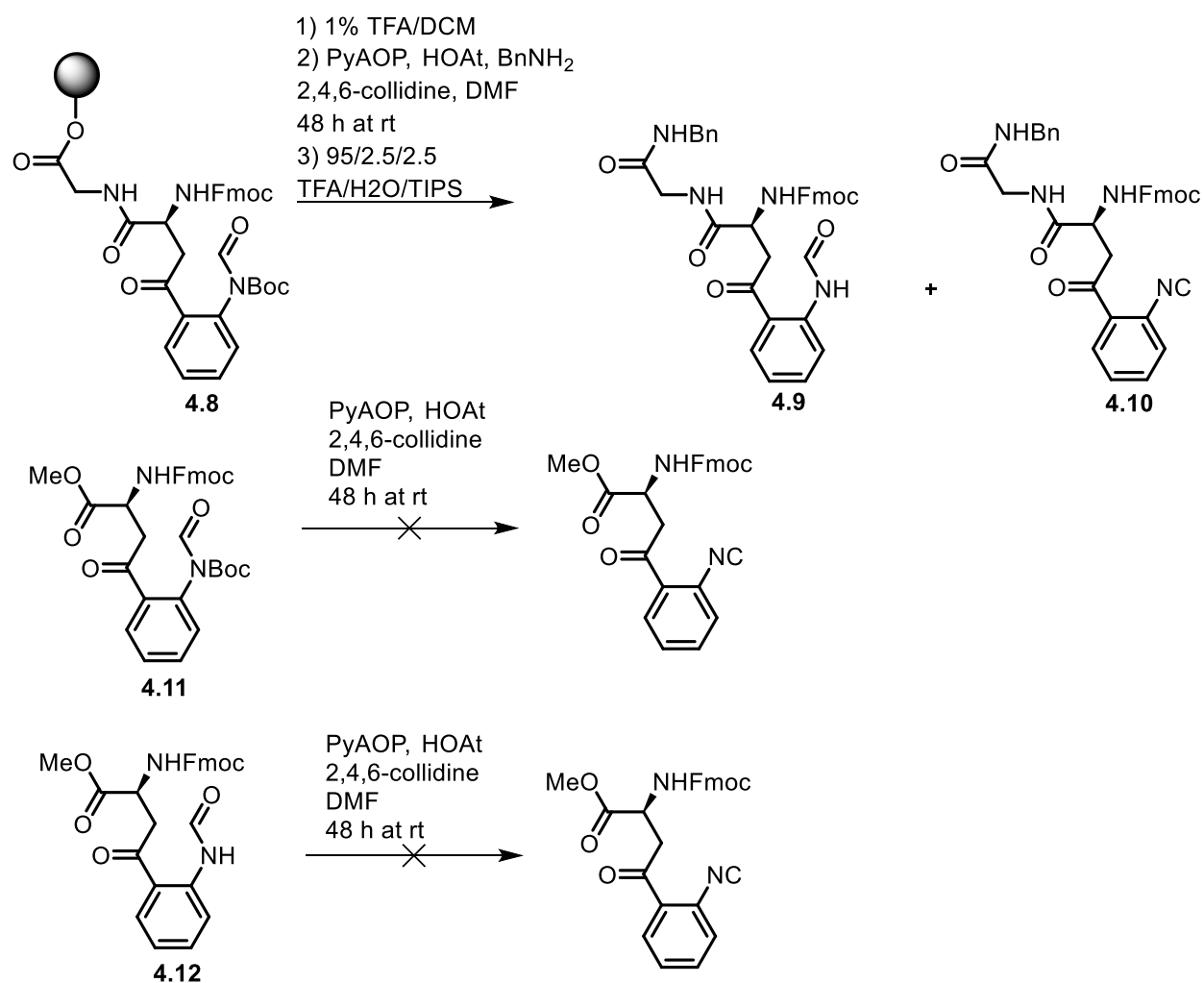
Scheme 4.2 Investigating the stability of Kyn(CHO,Boc) to PyAOP/HOAt/2,4,6-collidine in DMF

During our HPLC purification of the unidentified peptide, we noticed that it did not absorb strongly at 365 nm indicating that the electronic structure of the Kyn aromatic system was significantly altered. With this in mind, we proposed that the quinoline-bearing peptide **4.7** was a likely candidate for the structure of the unidentified by-product. This hypothesis was supported by UV/Vis analysis of the by-product (see Figure B.16) which showed a strong absorption peak at 330 nm indicating the presence of a quinolone residue.[226] The 1D NMR spectrum of the by-product showed that the aromatic Kyn C-H peaks found in daptomycin had shifted downfield which is consistent with peptide **4.7** (see Figure B.10). Finally, 2D NMR analysis of the by-product (see Figures B.11-B.15 and Table B.2) showed carbon and proton signals that were consistent with **4.7.**

Peptide **4.7** was not very active against *B. subtilis* 1046 at 1.25 mM $CaCl_2$ having a MIC of 64 μg/mL. Since **4.7** possessed a shorter RP-HPLC retention time compared to daptomycin(Figures B.1 and B.3), we propose that substitution of Kyn with the 4-quinolone residue disrupts the hydrophobic surface of the peptide, lowering its ability to bind to and disrupt the bacterial cell membrane.[227]

We postulated that peptide **4.7** was formed via a Camps cyclization reaction initiated by treatment of the Kyn(Boc,CHO) containing protected peptide with 20% 2-methylpiperidine (2MP)/DMF (Scheme 4.3).[228] Since we were able to isolate some daptomycin at the end of this synthesis, the Camps cyclization must only occur to a small extent with each treatment with 2MP/DMF. This explains why Fmoc-L-Kyn(Boc,CHO)-OH was an effective building block in the Taylor group's original synthesis of daptomycin but not an effective building block in this synthesis.[162] In addition, the synthesis of **4.7** did not proceed cleanly and many unidentifiable side products formed as the synthesis proceeded. We surmised that enolate formation at the side chain

of Kyn(Boc,CHO) is responsible for both the Camps cyclization and competing decomposition (see Scheme 4.4). This explanation aligns well with the observed relationship between peptide decomposition and base strength described by the Brimble group when exposing a Kyn(CHO,CHO) containing daptomycin precursor to base/DMF mixtures.[192] It also may explain why late-stage on resin ozonolysis of Trp is often needed to complete the synthesis Kyn containing peptides via Fmoc-SPPS.[166,192]
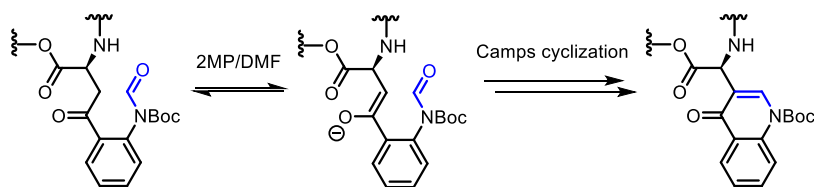
Scheme 4.3 Proposed pathway for the formation of **4.7**

Generally, Camps cyclization requires strongly basic conditions and elevated temperature to proceed to completion.[228] However, in some cases, the reaction was found to proceed well in polar, protic solvents with weak bases.[229] To show that this reaction can proceed on this system under these mild conditions, we prepared compounds **4.13-4.15** and subjected them to 20% 2MP/DMF at room temperature (Table 4.1). Indeed, **4.13** was slowly converted to **4.16** under these conditions over the course of 16 h (entry 1), fully supporting the reaction pathway outlined in Scheme 4.3. Interestingly, compound **4.14** was fully converted to **4.17** in a matter of minutes which is consistent with the observations reported by the Brimble group (entry 2).[192] In contrast, **4.15** was stable under these conditions for 48 h at room temperature (entry 3), demonstrating that the removal of one of the electron withdrawing groups on the side chain of Kyn(Boc,CHO) should yield a Kyn synthon that is stable to Fmoc SPPS. The presence of two electron withdrawing groups on the aniline nitrogen of the Kyn residue increase the acidity of the β-protons on the Kyn side

chain which may promote the enolization process depicted in Scheme 4.3. It is also possible that the acidic NH hydrogen ($pK_a < 16$) on compound **4.15** prevents enolization.

Table 4.1 Investigating the stability of various Kyn synthons in 20% 2MP/DMF at room temperature
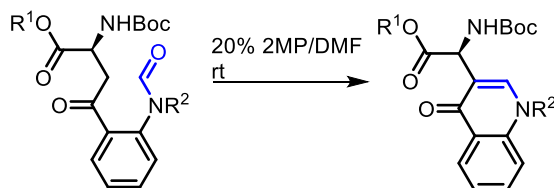
Entry	Starting Material	Product	Reaction Time	% Yield
1	**4.13** (R^1 = t-Bu, R^2 = Boc)	**4.16** (R^1 = t-Bu, R^2 = H)	16 h	61
2	**4.14** (R^1 = Me, R^2 = CHO)	**4.17** (R^1 = Me, R^2 = H)	5 min	74
3	**4.15** (R^1 = Me, R^2 = H)	**4.17** (R^1 = Me, R^2 = H)	48 h	NR

Armed with this new information, we anticipated that the synthesis disclosed in Scheme 4.1 could be achieved with an appropriately protected Kyn building block. To this end, we prepared Fmoc-L-Kyn(Boc)-OH (**4.18**) through mild hydrolysis of Fmoc-L-Kyn(Boc,CHO)-OH using LiOH/THF. We proposed that **4.18** would eliminate the Camps cyclization pathway and increase the quality of the synthesis by limiting enolate formation. We were pleased to find that ester bond formation proceeded cleanly between **4.2** (Scheme 4.1) and **4.18** using the aforementioned conditions giving **4.3b**. Conversion of **4.3b** to **4.4b** proceeded smoothly and elongation of **4.4b** under standard conditions proceeded without any notable decomposition or side reaction giving access to **4.5b**. The linear precursor was successfully cleaved from the solid support and cyclized giving daptomycin in an unprecedented 15% yield after global deprotection followed by

purification via preparative HPLC. The synthetic daptomycin was identical to authentic daptomycin in every respect (HPLC (Figure B.1), HRMS (Figure B.4) and NMR (Figures B.7 and B.8) including biological activity.

The ease with which the ester bond was formed between Kyn synthon **4.18** and peptide **4.2** suggested to us that it may be possible to make the ester bond on a resin-bound peptide that bears the lipid tail. This would enable us to eliminate the need for an azido acid and prepare daptomycin using entirely Fmoc chemistry. Towards this end, peptide **4.19** was prepared using standard Fmoc SPPS (Scheme 4.4). Ester bond formation between synthon **4.18** and peptide **4.19** proceeded cleanly in one overnight coupling using DIC/DMAP in CH_2Cl_2 to give peptide **4.4b** without epimerization as determined by HPLC analysis. Interestingly, we were unable to form the ester bond between Fmoc-L-Kyn(Boc,CHO)-OH and peptide **4.19**. Peptide **4.4b** was converted into daptomycin using the route outlined in Scheme 4.1. The yield was an outstanding 22 % after HPLC purification and the material was identical to authentic daptomycin in every respect (HPLC (Figure B.2), HRMS (Figure B.5) and NMR (Figure B.9)).
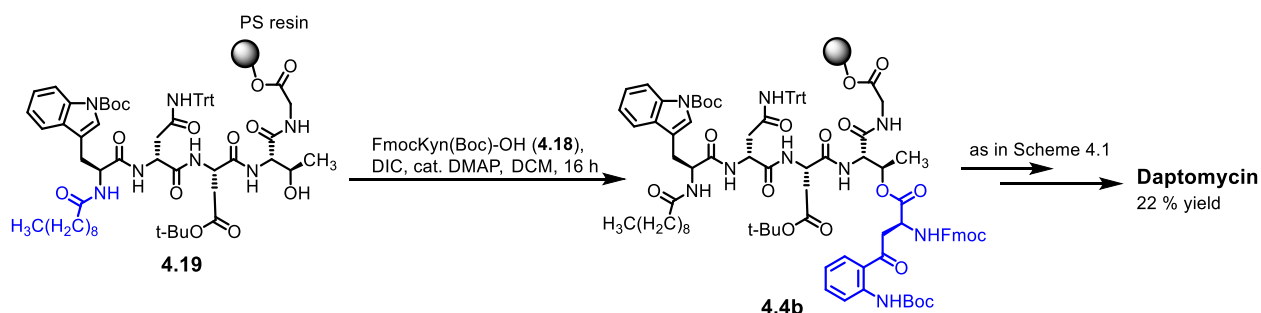
Scheme 4.4 An entirely Fmoc approach to daptomycin

4.3 Conclusions

We have succeeded in developing the highest yielding synthesis of daptomycin to date. Integral to the development of this synthesis was the characterization of an unprecedented side reaction observed when using Fmoc-L-Kyn(Boc,CHO)-OH, which is a common Fmoc SPPS Kyn

building block. This side reaction was found to convert the Kyn(Boc,CHO) containing peptide into a 4-quinolone containing peptide (**4.7**) which was characterized by UV/vis, HRMS and NMR. **4.7** was found to be inactive against *B. subtilis* 1046. It was shown that Boc-L-Kyn(Boc,CHO)-Ot-Bu and Boc-L-Kyn(CHO,CHO)-OMe undergo a Camps cyclization when treated with the 20% 2MP/DMF Fmoc deprotection mixture at room temperature. Thus peptide **4.7** must be formed during repeated treatments of Kyn(Boc,CHO) containing intermediates with 2MP/DMF. In contrast, Boc-L-Kyn(CHO)-OMe was found to be stable under these conditions, suggesting that removal of one of the protecting groups on the side chain of Fmoc-L-Kyn(Boc,CHO)-OH could yield an Fmoc SPPS stable Kyn building block. Indeed, we found that replacing Fmoc-L-Kyn(Boc,CHO)-OH with Fmoc-L-Kyn(Boc)-OH, which is prepared from the former building block in a single step, greatly improved the quality of the synthesis and allowed for the preparation of daptomycin in a 22% overall yield using only Fmoc building blocks. We expect that the synthesis of Kyn containing peptides, such as Kyn containing analogs of dap, will be significantly simplified through the use of suitably protected Kyn synthons that are stable to Fmoc SPPS, such as Fmoc-L-Kyn(Boc)-OH.

4.4   Experimental

General Methods. All reagents and solvents were purchased from commercial suppliers. Methylene chloride (DCM) and acetonitrile (MeCN) were dried by distillation over calcium hydride under nitrogen. Tetrahydrofuran (THF) was distilled from sodium metal in the presence of benzophenone under N_2. 2-methylpiperidine (2MP) was dried over calcium hydride then distilled to give a colorless liquid. Dimethylformamide (DMF) was dried over calcium hydride and distilled under vacuum such that the temperature of the solution remained below 60 °C throughout the course of the distillation. Chromatography was performed using 60 Å silica gel.

Analytical and semi preparative R-HPLC was performed using a Waters 600 controller equipped with Waters 2487 dual wavelength detector set to 220 and 365 nm. A Higgins Analytical Inc. (Mountainview, CA, USA) CLIPEUS C18 column (10 µM, 250 x 4.6 mm) was used for analytical HPLC at a flow rate of 1.0 mL/min. A Higgins CLIPEUS C18 column (10 µM, 250 x 20 mm) was used for semi preparative HPLC at a flow rate of 8.0 mL/min.

High resolution positive electrospray (ESI) mass spectra were obtained using an orbitrap mass spectrometer. Samples were sprayed from MeOH: 1% formic acid in H_2O. All spectra were collected in the positive mode. ^{1}H- and ^{13}C-NMR of **4.11-4.12, 4.14-4.17** and **4.18** were collected using a Bruker Avance-300 spectrophotometer. ^{1}H- and ^{13}C-NMR of **4.13** were collected using a Bruker Avance-500 spectrophotometer. ^{1}H-NMR of daptomycin was collected on a Bruker 600 NMR. ^{1}H-NMR and 2D NMR ([1]H-^{13}C) of 4.**7** were collected on a Bruker 600 NMR. Proton chemical shifts (δ) for samples run in $CDCl_3$ are reported in ppm relative to an internal standard (trimethylsilane, 0 ppm). For samples run in CD_3OD, δ was relative to the residual solvent peak (3.31 ppm). For samples run in DMSO-d_6 chemical shifts are reported relative to the solvent peak (2.50 ppm). For ^{13}C-NMR samples run in $CDCl_3$, δ are reported relative to the solvent peak (77.0 ppm). For samples run in CD_3OD, δ was relative to the solvent peak (49.2 ppm). For samples run in DMSO-d, δ was relative to the solvent peak (39.5 ppm). MIC determinations were performed as previously described.[223]

Fmoc-DMB-Gly-OH was prepared from Fmoc-Gly-OH according to the procedure of Martin and coworkers.[167] Fmoc-(2S,3R)MeGlu(tBu)-OH was prepared according to our procedure (see chapter 4).[230] Fmoc-L-Kyn(Boc,CHO)-OH was prepared according to the procedure of Lam et al.[155] N_3-L-Trp(Boc)-OH was prepared according to the procedure of Lundquist and Pelletier.[231]

*Fmoc-L-Kyn(Boc,CHO)-OMe (**4.11**).*

Fmoc-L-Kyn(Boc,CHO)-OH (500 mg, 0.895 mmol, 1.00 equiv.) was dissolved in MeOH at room temperature and the resulting solution was cooled (ice-water bath) before the addition of thionyl chloride (71.0 µL, 0.984 mmol, 1.10 equiv.). After stirring for 1 hour, the cooling bath was removed, and the reaction mixture was stirred for an additional 3 h at room temperature. The reaction mixture was quenched with saturated aqueous $NaHCO_3$ (50 mL) and extracted with EtOAc (20 mL x 3). The combined organic fractions were washed with brine, dried with $MgSO_4$, filtered and then concentrated. The crude residue was purified by silica gel column chromatography (25% EtOAc / 75% Hexanes) giving Fmoc-L-Kyn(Boc,CHO)-OMe as a colorless foam (62% yield, 318 mg). NMR spectra indicated that **4.11** exists as a mixture of two rotamers in $CDCl_3$.^{1}H NMR (300 MHz, $CDCl_3$): δ 9.31 (1H, s) 9.28 (1H,s) 7.87 (1H, d, J = 7.9 Hz,) 7.83 (1H, d, J = 7.7 Hz) 7.74 (2H, d, J = 7.4 Hz) 7.60-7.58 (3H, m) 7.49 (1H, dd, J = 7.5, 7.6 Hz) 7.39-7.35 (2H, m) 7.31-7.26 (2H, m) 7.18 (1H, d, J = 7.3 Hz) 5.82 (1H, d, J = 8.7 Hz) 4.70 (1H, m) 4.47-4.19 (3H, m) 3.77-3.64 (4H, m) 3.47 (1H, dd, J = 1.5, 18.2 Hz) 1.45 (9H, s). ^{13}C NMR (75 MHz, $CDCl_3$): δ 198.2, 197.7, 171.5, 171.4, 163.2, 163.1, 156.1, 151.8, 143.9, 143.7, 141.3, 134.1, 133.5, 133.4, 133.3, 133.1, 131.0, 130.9, 130.1, 129.6, 129.1, 127.7, 127.1, 125.2, 120.0, 120.1, 84.7. 84.6, 67.3, 67.3, 52.8, 52.7, 50.0, 47.1, 42.4, 42.3, 27.9, 27.9. HRMS-ESI+ (*m/z*): $[M + Na]^+$ calculated for $C_{32}H_{32}O_8N_2Na$, 595.20509; found, 595.20219.

*Fmoc-L-Kyn(CHO)-OMe (**4.12**).*

To a cooled (ice-water bath) solution of Fmoc-L-Kyn(Boc,CHO)-OMe (200 mg, 0.349 mmol, 1.00 equiv.) in dry DCM (10 mL) was added trifluoroacetic acid (3 mL). Cooling was removed and resulting solution was stirred for 2 h at room temperature before dilution with toluene (100 mL) and concentration *in-vacuo*. This yielded Fmoc-L-Kyn(CHO)-OMe (**4.12**) as a pale yellow foam

which was used without further purification (97% yield, 160 mg). ^{1}H NMR (300 MHz, CDCl$_3$): δ 11.40 (1H, s) 8.80 (1H, d, J = 8.3 Hz) 8.51 (1H, s) 7.93 (1H, d, J = 8.0 Hz) 7.78-7.74 (2H, m) 7.65-7.60 (3H, m) 7.43-7.30 (4H, m) 7.20 (1H, dd, J = 7.6, 7.6 Hz) 5.84 (1H, d, J = 7.6 Hz) 4.78 (1H, m) 4.51-4.40 (2H, m) 4.26-4.21 (1H, m) 3.87-3.65 (5H,m). ^{13}C NMR (75 MHz, CDCl$_3$): δ 201.7, 171.6, 159.9, 156.1, 143.8, 143.6, 141.3, 140.2, 135.9, 131.0, 127.1, 125.1, 123.3, 121.8, 121.0, 120.0, 120.0, 67.1, 52.9, 50.0, 47.2, 42.1. HRMS-ESI+ (m/z): [M + H]$^+$ calculated for C$_{27}$H$_{25}$O$_6$N$_2$, 473.17071; found, 473.16888.

*Boc-L-Kyn(Boc,CHO)-Ot-Bu (**4.13**).*

L-Trp-Ot-Bu*HCl (1.00 g, 3.84 mmol, 1.00 equiv.) was suspended in dry DCM (40 mL) and dissolved through the addition of triethylamine (1.28 mL, 9.22 mmol, 2.40 equiv.). To this solution was added di-tert-butyl dicarbonate (1.00 g, 4.61 mmol, 1.20 equiv.). After stirring for 16 h at room temperature, the reaction solution was washed with 0.1 N HCl (40 mL) then brine (40 mL). The organic layer was then dried with MgSO$_4$, filtered and concentrated. The residue was dissolved in dry DCM (15.4 mL) then triethylamine (551 µL, 3.96 mmol, 1.03 equiv.), 4-dimethylaminopyridine (47 mg, 0.384, 0.100 equiv.) and di-tert-butyl dicarbonate (1.00 g, 4.61 mmol, 1.20 equiv.) were added. After stirring the mixture for 2 h at room temperature, the reaction mixture was washed with 0.1 N HCl (20 mL), saturate aqueous NaHCO$_3$ (20 mL) and brine (20 mL). The organic layer was dried with MgSO$_4$ and then concentrated. The residue was dissolved in dry DCM (15 mL) and the solution was cooled (dry ice acetone bath). After bubbling ozone through the solution for 8 min, the reaction was quenched with dimethyl sulfide (3.20 mL, 43.7 mmol, 11.4 equiv.) and cooling was removed. After stirring for 1 hour, the solution was concentrated and Boc-L-Kyn(Boc,CHO)-Ot-Bu (**4.13**) was isolated via silica gel column chromatography (30% EtOAc/ 70% Hexanes) giving **4.13** as a colorless foam (1.23 g, 65% yield

over 3 steps). NMR spectra indicated that **4.13** exists as a mixture of two rotamers in CDCl$_3$. ^{1}H NMR (500 MHz, CDCl$_3$): δ 9.27 (1H, m) 7.86-7.82 (1H, m) 7.58 (1H, t, *J* = 7.6 Hz) 7.48 (1H, t, *J* = 7.6 Hz) 7.17 (1H, d, *J* = 7.5 Hz) 5.48-5.43 (1H, m) 4.47-4.45 (1H, m) 3.66-3.28 (2H, m) 1.47-1.41 (27H, s). ^{13}C NMR (125 MHz, CDCl$_3$): δ 198.2, 198.0, 170.3, 170.1, 163.1, 163.0, 155.6, 151.9, 151.8, 134.4, 134.3, 133.2, 133.1, 133.0, 130.8, 129.8, 129.6, 129.0, 84.5, 84.4, 82.0, 81.9, 79.6, 79.6, 50.2, 50.1, 42.5, 42.3, 28.3, 27.9, 27.9, 27.9. HRMS-ESI+ (*m/z*): [M + H]$^+$ calculated for C$_{25}$H$_{37}$O$_8$N$_2$, 493.25444; found, 493.25450.

*Boc-L-Kyn(CHO,CHO)-OMe (**4.14**).*

Boc-L-Trp(CHO)-OH (1.00 g, 3.00 mmol, 1.00 equiv.) was added to a cooled (ice-water bath) suspension of potassium carbonate (624 mg, 4.51 mmol, 1.50 equiv.) in dry DMF (10 mL) and the resulting suspension was stirred for 1 hour before the addition of MeI (374 µL, 6.00 mmol, 2.00 equiv.). After cooling was removed, the solution was stirred at room temperature for 16 h then diluted with EtOAc (100 mL) and washed with water (100 mL) then brine (100 mL). The organic layer was dried with MgSO$_4$, filtered and then concentrated. The residue was dissolved in dry DCM (12 mL) and the solution was cooled (dry ice acetone bath) and then ozone was bubbled through the solution for 5 min. After quenching the reaction with dimethyl sulfide (2.50 mL, 34.2 mmol, 11.4 equiv.), cooling was removed, and the solution was stirred for 1 hour before it was concentrated. The crude residue was purified by silica gel column chromatography (30% EtOAc / 70% Hexanes to 40 % EtOAc / 60% Hexanes) giving Boc-L-Kyn(CHO,CHO)-OMe (**4.14**) as a pale yellow foam (743 mg, 65% yield over 2 steps). ^{1}H NMR (300 MHz, CDCl$_3$): δ 9.03 (2H, s) 7.90 (1H, d, *J* = 7.5 Hz) 7.67 (1H, dd, *J* = 1.2, 7.5, 7.6 Hz) 7.58 (1H, dd, *J* = 7.5, 7.5 Hz) 7.25 (1H, d, *J* = 7.4) 5.54 (1H, d, *J* = 8.0 Hz) 4.64-4.61 (1H, m) 3.82-3.47 (5H, m) 1.45 (9H, s). ^{13}C NMR

(75 MHz, CDCl$_3$): δ198.6, 171.7, 163.3, 155.5, 133.6, 130.5, 130.0, 129.9, 80.1, 52.7, 49.5, 42.5, 28.3. HRMS-ESI+ (*m/z*): [M + H]$^+$ calculated for C$_{18}$H$_{23}$O$_7$N$_2$, 379.14998; found, 379.15012.

*Boc-L-Kyn(CHO)-OMe (**4.15**).*

4.15 was prepared starting from Boc-L-Trp-OH (1.00 g, 3.29 mmol, 1.00 equiv.) following the same procedure used for the preparation of Boc-L-Kyn(CHO,CHO)-OMe. This yielded Boc-L-Kyn(CHO)-OMe (**4.15**) as a colorless foam (601 mg, 52% yield over 2 steps). ^{1}H NMR (300 MHz, CDCl$_3$): δ11.38 (1H, s) 8.74 (1H, d, *J* = 8.4 Hz) 8.47 (1H, s) 7.90 (1H, dd, *J* = 8.1, 1.3 Hz) 7.58 (1H, m) 7.17 (1H, t, *J* = 7.7 Hz) 5.57 (1H, d, *J* = 8.2 Hz) 4.70 (1H, m) 3.81-3.59 (5H, m) 1.43 (9H, s). ^{13}C NMR (75 MHz, CDCl$_3$): δ 201.9, 171.9, 159.9, 155.5, 140.1, 135.7, 131.0, 123.2, 121.7, 121.1, 80.1, 52.7, 49.5, 42.3, 28.3. HRMS-ESI+ (*m/z*): [M + H]$^+$ calculated for C$_{17}$H$_{23}$O$_6$N$_2$, 351.15506; found, 351.15598.

General procedure for the Camps cyclization.

To a solution of starting material (0.400 mmol) in dry DMF (2.24 mL) was added 2-methylpiperidine (0.560 mL). The reaction was then monitored by TLC until all the starting material was consumed. The reaction mixture was then diluted with EtOAc (30 mL) and washed with 0.1 N HCl (30 mL) followed by brine (30 mL). The organic fraction was dried with MgSO$_4$, filtered and then concentrated. The crude residue was purified by silica gel column chromatography.

*tert-butyl (S)-2-((tert-butoxycarbonyl)amino)-2-(4-oxo-1,4-dihydroquinolin-3-yl)acetate (**4.16**).*

4.16 was prepared from **4.13** following the general procedure for Camps cyclization. The crude residue was purified by silica gel column chromatography (40% EtOAc/ 59% Hexanes / 1% AcOH then 80% EtOAc/ 19% Hexanes / 1% AcOH) giving **4.16** as a colorless solid (61% yield, 92 mg).

^{1}H NMR (300 MHz, CD$_3$OD): δ 8.26 (1H, d, J = 8.1 Hz) 8.07 (1H, br. s) 8.50 (1H, d, J = 8.5 Hz) 7.73 (1H, dt, J = 1.2, 8.3 Hz) 7.58 (1H, d, J = 8.3 Hz) 7.43 (1H, app t, J = 8.0 Hz) 5.20 (1H, s) 1.46 (9H, s) 1.43 (9H, s). ^{13}C NMR (75 MHz, CDCl$_3$): δ175.3, 168.9, 154.8, 138.3, 137.7, 130.7, 123.5, 123.3, 122.4, 116.5, 80.1, 77.9, 52.0, 25.8, 25.3. HRMS-ESI+ (*m/z*): [M + H]$^+$ calculated for C$_{20}$H$_{27}$O$_5$N$_2$, 375.19145; found, 375.19132.

*methyl (S)-2-((tert-butoxycarbonyl)amino)-2-(4-oxo-1,4-dihydroquinolin-3-yl)acetate (**4.17**).*

4.17 was prepared from **4.14** following the general procedure for Camps cyclization. The crude residue was purified by silica gel column chromatography (40% EtOAc/ 59% Hexanes / 1% AcOH then 80% EtOAc/ 19% Hexanes / 1% AcOH) giving **4.17** as a colorless solid (74% yield, 98 mg).). ^{1}H NMR (300 MHz, CDCl$_3$): δ11.69 (1H, br. s) 8.27 (1H, d, J = 8.1 Hz) 8.04 (1H, d, J = 5.3 Hz) 7.66-7.54 (2H, m) 7.32 (1H, t, J = 7.4 Hz) 6.37 (1H, d, J = 7.9 Hz) 5.25 (1H, d, J = 8.2) 3.64 (3H, s) 1.37 (9H, s). ^{13}C NMR (75 MHz, CDCl$_3$): δ177.2, 172.0, 155.8, 140.0, 139.5, 132.3, 125.5, 125.3, 124.2, 118.8, 117.9, 79.9, 53.9, 52.8, 28.3. HRMS-ESI+ (*m/z*): [M + H]$^+$ calculated for C$_{17}$H$_{21}$O$_5$N$_2$, 333.14450; found, 333.14356.

*Fmoc-L-Kyn(Boc)-OH (**4.18**).*

Fmoc-L-Kyn(Boc,CHO)-OH (1.26 g, 2.26 mmol, 1 equiv.) was dissolved in THF (23 mL) and cooled in an ice-water bath. Freshly prepared and titrated aqueous LiOH (1.00 M; 5.86 mL, 5.86 mmol, 2.6 equiv.) was added dropwise to the stirring solution of starting material in THF over 30 min. Once the addition was complete, the solution was neutralized with aqueous HCl (1M, 6 mL) and extracted with EtOAc (3 x 50 mL). The combined organic layer was dried with brine then MgSO$_4$, filtered and then concentrated. The crude residue was purified by silica gel column chromatography (40% EtOAc / 59% Hexanes / 1% AcOH) giving Fmoc-L-Kyn(Boc)-OH (**4.18**)

as a colorless foam (970 mg, 81% yield). ^{1}H NMR (300 MHz, CDCl$_3$): δ10.72 (1H, s) 9.33 (1H, br. s) 8.50 (1H, d, J = 8.5 Hz) 7.82 (1H, d, J = 7.7 Hz) 7.73-7.71 (2H, m) 7.58-7.50 (3H, m) 7.38-7.24 (4H, m) 7.01 (1H, dd, J = 7.7, 7.3 Hz) 5.88 (1H, d, J = 8.4 Hz) 4.81 (1H, m) 4.47-4.35 (3H, m) 4.23-4.20 (1H, m) 3.84 (1H, d, J = 17 Hz) 3.58 (1H, d, J = 16.8 Hz) 1.52 (9H, s). ^{13}C NMR (75 MHz, CDCl$_3$): δ176.0, 156.3, 153.0, 143.8, 143.6, 142.3, 141.3, 135.7, 131.0, 127.8, 127.1, 125.1, 121.2, 120.1, 120.0, 119.4, 81.0, 67.3, 49.8, 47.2, 41.8, 28.3. HRMS-ESI+ (m/z): [M + H]$^+$ calculated for C$_{30}$H$_{31}$O$_7$N$_2$, 531.21258; found, 531.21118.

Fmoc solid-phase synthesis of daptomycin via Scheme 4.1. The 2-chlorotrityl resin loaded with Fmoc-Gly (444 mg, 0.2 mmol) was swollen in DMF (30 min) and then Fmoc-deprotected with 2-methylpiperidine (2MP)/DMF (20%; 3 x 8 min). After washing the resin with DMF (3 x 5min), a solution of Fmoc-L-Asp(t-Bu)-OH (3 equiv.), Hydroxybenzotriazole (HOBt, 3 equiv.) and diisopropylcarbodiimide (DIC, 3 equiv.) in DMF (4 mL) was added to the resin. After rotary agitation for 3 h at room temperature, the resin containing cartridge was drained and the resin was washed with DMF (3 x 5min). All subsequent Fmoc deprotections and couplings, with the exclusion of the ester bond and the cyclization, were performed in this way. Once N$_3$-L-Trp(Boc)-OH was incorporated, the ester bond was formed by first activating Fmoc-L-Kyn(Boc)-OH (10 equiv.) with DIC (10 equiv.) in dry DCM for 30 min and filtering the solution into the cartridge containing the resin. A precisely measured amount of DMAP (0.1 equiv.) was then added as a solution in DCM and the resulting mixture was agitated for 18 h at room temperature. After washing the resin with DCM (5 x 3 min) and DMF (5 x 3min), the azido group was reduced over the course of 1 hour at room temperature with PMe$_3$ (1M in THF, 1.20 mL) in a solution of dioxane (2.40 mL) and H$_2$O (1.20 mL). The resin was then washed with dioxane (3 x 3min), DMF (3 x 3 min) and DCM (3 x 3min). The decanoic acid tail and the remaining amino acid residues were

incorporated using DIC/HOBt/DMF as previously described. Once Fmoc-L-Orn(Boc)-OH was coupled on and Fmoc-deprotected with 2MP /DMF (20%), the peptide was removed from the resin by swelling in DCM (10 min) and then treating with 1% TFA/DCM (6 x 1 min) followed by 1% MeOH/DCM (3 x 1 min). A ninhydrin test was used to determine when all the peptide was removed from the resin. The peptide containing solution was then diluted with toluene and concentrated. The residue was dissolved in dry DMF (200 mL) and to this was added a solution of (7-Azabenzotriazol-1-yloxy)tripyrrolidinophosphonium hexafluorophosphate (PyAOP, 5 equiv.), 1-Hydroxy-7-azabenzotriazole (HOAt, 5 equiv.) and 2,4,6-collidine (10 equiv.) in DMF (5 mL). After stirring at room temperature for 48 h, the cyclization was determined to be complete by TLC (90:10:1 DCM:MeOH:AcOH). The cyclization solution was concentrated *in-vacuo* and the residue was dissolved in EtOAc (200 mL) and then washed with $NaHSO_4$ (1M, 2 x 200 mL), saturated aqueous $NaHCO_3$ (2 x 200 mL) and brine (2 x 200 mL). After drying the organic layer with $MgSO_4$, filtering it and concentrating the filtrate, the residue was cooled (ice-water bath) and suspended in TFA:TIPS:H_2O (95:2.5:2.5). Cooling was removed immediately after the addition and the resulting solution was stirred for 1.5 h at room temperature. At this time, the solution was concentrated with a stream of dry N_2. The deprotected peptide was precipitated from the oily residue through the addition of cold diethyl ether. The solid was washed with diethyl ether 3 times before being dissolved in 3:2 H_2O:MeCN. Pure daptomycin was isolated from this solution by semi-preparative HPLC employing a linear gradient of 35:65 MeCN: H_2O (0.1% TFA) to 50:50 MeCN: H_2O (0.1% TFA) over 60 min. Daptomycin-containing fractions were combined, concentrated *in-vacuo* and lyophilized from milli-Q H_2O to give daptomycin as a colorless powder (49 mg, 15 % yield based on resin loading). HRMS-ESI+ (*m/z*): $[M + H]^+$ calculated for $C_{72}H_{102}O_{26}N_{17}$, 1620.71764; found, 1620.71631. See Figures B.1 for the analytical HPLC

chromatograms of dap. See Figure B.4 for the HRMS of dap. See Figures B.7 and B.8 for the ^{1}H-NMR spectrum of dap.

Fmoc solid-phase synthesis of peptide 4.7.

4.7 was prepared following the same procedure outlined for the synthesis of daptomycin except Fmoc-L-Kyn(Boc)-OH was replaced with Fmoc-L-Kyn(Boc,CHO)-OH. Pure **4.7** was isolated from the 3:2 H_2O:ACN solution by semi preparative HPLC employing a linear gradient of 30:70 MeCN: H_2O (0.1% TFA) to 45:55 MeCN: H_2O (0.1% TFA) over 60 min. **4.7** containing fractions were combined, concentrated *in-vacuo* and lyophilized from milli-Q H_2O to give **4.7** as a colorless powder (6 mg, 2 % yield based on resin loading). HRMS-ESI+ (*m/z*): [M + H]$^+$ calculated for $C_{73}H_{100}O_{26}N_{17}$, 1630.70199; found, 1630.70788. [M + 2H]$^{2+}$ calculated for $C_{73}H_{101}O_{26}N_{17}$, 815.85463; found, 815.85333. See Figure B.3 for the analytical HPLC chromatogram of **4.7**. See Figure B.6 for the HRMS of **4.7**. See Table B.1 for the MS-MS analysis of hydrolyzed **4.7**. See Figure B.10 for the ^{1}H NMR of **4.7**. See Figure B.11-B.15 for the 2D NMR spectra of **4.7**. See Table B.2 for chemical shift assignment of **4.7**. See Figure B.16 for the UV-Vis spectrum of **4.7**.

Fmoc solid-phase synthesis of daptomycin via Scheme 4.4

Daptomycin was synthesized via Scheme 4.4 following the same coupling and deprotection procedures outlined for the synthesis of daptomycin via Scheme 1. Fmoc-L-Trp(Boc)-OH was used in place of N_3-L-Trp(Boc)-OH. Once the decanoic acid tail was coupled on using DIC/HOBt, the ester bond was formed as described for the synthesis of daptomycin via Scheme 1. The rest of the peptide was synthesized following the procedures outlined for the synthesis of daptomycin via Scheme 1. The same purification procedure was used to isolate daptomycin as a colorless powder (71 mg, 22% based on resin loading). HRMS-ESI+ (*m/z*): [M + H]$^+$ calculated for $C_{72}H_{102}O_{26}N_{17}$,

1620.71764; found, 1620.71167. See Figures B.2 for the analytical HPLC chromatograms of daptomycin prepared this way. See Figure B.5 for the HRMS of daptomycin prepared this way. See Figures B.9 for the ^{1}H-NMR spectrum of daptomycin prepared this way.

Chapter 5 - The Chiral Target of Daptomycin is the 2R,2'S Stereoisomer of Phosphatidylglycerol

5 Preface and contributions

The work presented in this chapter is based on a manuscript published in the journal *Angewandte Chemie International Edition* (*Angew. Chemie Int. Ed.* **2022**, *61*, e202114858. Adapted with permission from the publisher). The experimental work was done entirely by me. I also contributed greatly to writing the manuscript which was edited by Prof. Taylor. All the work described in this chapter was done under the supervision of Prof. Taylor. Additional supplementary information is available on the journal's website.

5.1 Introduction

As discussed in the chapter 1, the high efficacy of daptomycin and the lack of widespread resistance to this antibiotic may be due to its unique action mechanism which is not fully understood.[74,232] It is known that daptomycin primarily acts on the bacterial membrane and that phosphatidylglycerol (PG), a major component of most Gram-positive bacterial membranes, must be present.[24,113,114,122] Circular dichroism (CD) studies have shown that, in the presence of Ca^{2+}, daptomycin undergoes a conformational change upon binding to liposomes containing PG.[24,80,92] In the presence of Ca^{2+}, daptomycin has been shown to form oligomers/aggregates in model membrane systems[79,86,88,233,234] that contain PG, as well as isolated Gram-positive bacterial membranes.[88] In addition, daptomycin forms distinct daptomycin–PG domains on model membranes and localizes to PG-rich regions on cells in-vitro.[64,75]

How daptomycin exerts its antibacterial effect upon binding to the membrane has been the subject of much debate. Early studies on *S. aureus* suggested that daptomycin forms pores that cause the selective leakage of potassium ions which results in a decrease in membrane potential eventually causing cell death.[21,84] This has been supported by studies that show that daptomycin

forms cation selective pores and discrete toroidal pores in model membranes.[99,100,235,236] However, studies on bacteria suggest ion leakage and membrane depolarization only occur after prolonged treatment with daptomycin concentrations that are much higher than the MIC and are bacteriolytic.[64] Several other mechanisms have been proposed such as daptomycin-induced lipid extraction,[83] and daptomycin-promoted release of MurG from the membrane, inhibiting cell wall synthesis.[64] Grein et al very recently showed that daptomycin can form a complex with Ca^{2+}, PG and lipid II potentially disrupting cell wall synthesis.[71] At this point, it seems appropriate to conclude that daptomycin's mechanism of action is multi-faceted.

Although the details about how daptomycin kills bacteria are unclear, it is apparent that daptomycin's killing action is dependent on the presence of PG in the membrane. Daptomycin's requirement for PG is rather unique, in fact, the only other known natural product that shares this requirement is A54145 – a cyclic lipopeptide antibiotic closely related to daptomycin in both structure and function.[14,15,181,193] In addition, since PG is found in high concentrations in the membranes of Gram-positive bacteria, where it may comprise 80% of the phospholipids present by mass, but in much lower concentrations in eukaryotic cells, it is likely that daptomycin's requirement for PG is important for its ability to selectively bind to bacterial membranes.[22,25] Daptomycin's interaction with PG is not only interesting because it is unique and fundamental to its killing action, but it is also thought to be responsible for the inhibition of daptomycin in the presence of lung surfactant, rendering it ineffective for the treatment of community acquired bacterial pneumonia (CAP).[142]

Studies by us and others using analogs of the unnatural enantiomer of daptomycin suggested that daptomycin has a chiral target and our studies suggested that the chiral target may be a stereoisomer of PG (chapter 2).[167,222] These results prompted us to initiate a study of how the

overall configuration of daptomycin itself affects biological activity, and if daptomycin is capable of distinguishing between the various stereoisomers of PG, and if the configuration of PG affects the subsequent conformational change and oligomerization of dap. Here we report the results of these studies.

5.2   Results and discussion

The unnatural enantiomer of daptomycin (ent-daptomycin) was prepared according to a new and highly efficient route to daptomycin that we recently developed (chapters 3 and 4) .[237,238] The CD spectrum of ent-daptomycin was equal but opposite to that of daptomycin (Figure C.6; see Figures C.4 and C.5 for additional characterization data). The minimum inhibitory concentration (MIC) of ent-daptomycin was determined using a broth microdilution assay at physiological calcium concentration (1.25 mM).[239] Ent-daptomycin was found to be 85-fold less active against *B. subtilis* 1046 ($MIC_{ent\text{-}daptomycin}$ = 64 µg/mL, $MIC_{daptomycin}$ = 0.75 µg/mL) unequivocally demonstrating that daptomycin has a chiral target(s).

Commercial PG is racemic at the headgroup, and therefore, is not suitable for studying the stereochemical dependence of PG-daptomycin interactions. To fully probe the effects that PG configuration has on the bactericidal activity, membrane binding, conformation, and oligomerization of daptomycin all four stereoisomers of PG were required. PG has been synthesized via chemoenzymatic routes utilizing phospholipase D-catalysed transphosphatidylation to exchange the headgroup of PC for enantiomerically pure protected glycerol.[39,240] In addition, many totally chemical syntheses of PG have been reported. Several routes utilized $POCl_3$ as an electrophilic phosphorous centre and these routes are appealing since they allow for control of the absolute configuration at each stereocenter.[241–244] Indeed, Baer and Buchnea used this route to prepare all four stereoisomers of dioleoylPG (DOPG).[241] However, it

can be difficult to control the number of additions to the highly electrophilic phosphorus centre and acyl migration can be a concern when coupling the 1,2-diacyl glycerol under basic and acidic conditions.[245] Others have prepared PG via esterification of naturally sourced phosphatidic acid using trisylCl as a coupling agent, but this route does not allow for control of the configuration at the tail group.[246] We chose to use phosphoramidite chemistry as this has been used by others to prepare PGs and allows for facile control over the additions to the phosphorous centre without acyl migration (Scheme 6.1).[247–252] The two enantiomers of alcohol **5.5** were prepared based upon a procedure reported by Lee et al.[253] Commercially available chiral alcohols **S-5.1** or **R-5.1** were treated with benzyl bromide (BnBr)/sodium hydride (NaH) to give benzyl ethers **5.2**, and then the acetal in **5.2** was hydrolyzed to give diols **5.3**. Myristic acid was then coupled to the hydroxy groups in **5.3** using N,N'-dicyclohexylcarbodiimide (DCC)/4-dimethylaminopyridine (DMAP) to give esters **5.4**. The benzyl group in **5.4** was removed by hydrogenolysis to give alcohols **S-5.5** and **R-5.5** in 59% and 65% yield respectively over these four steps. The two enantiomers of alcohol **5.9** were prepared based upon a procedure reported by Fukase et al.[254] Alcohols **S-5.1** or **R-5.1** were converted to para-methoxybenzyl (PMB) ethers **5.6** using NaH/PMBCl and then acetals in **5.6** were hydrolyzed to give diols **5.7** using aqueous AcOH. Diols **5.7** were converted to benzylidene acetals **5.8** using benzaldehyde dimethyl acetal (BDMA) and camphorsulfonic acid (CSA). The PMB groups in **5.8** were removed using 2,3-dichloro-5,6-dicyano-1,4-benzoquinone (DDQ) in dichloromethane and water to give alcohols **S-5.9** and **R-5.9** in 40% and 39% yield respectively over these four steps. The enantiomeric purities of **S-5.5**, **R-5.5**, **S-5.9** and **R-5.9** were determined by conversion to the Mosher's ester and analysis by ^{19}F NMR (>91% ee, Figures C.1 and C.2). Alcohols **S-5.5** and **R-5.5** were coupled to phosphoramidite **5.10** to give phosphoramidites **5.11** in outstanding yield using standard phosphoramidite coupling conditions.

Phosphoramidites **5.11** were coupled to alcohols **S-5.9** or **R-5.9** using the same coupling conditions, and, after oxidation with meta-chloroperoxybenzoic acid (mCPBA), gave benzyl esters **5.12** in good yield. Removal of the benzyl and benzylidene protecting groups in **5.12** via hydrogenolysis followed by conversion of the resulting acids to their sodium salts and lyophilization provided all four stereoisomers of dimyristoylPG (DMPG) as colorless powders. The benzylidene/benzyl protecting groups were chosen for this synthesis due to the fact that they can be removed under hydrogenation conditions at the end of the synthesis, inhibiting phosphate migration that is observed under acidic or basic conditions.[244,255] The synthesized lipids were converted to boronic esters containing a chiral appendage (Scheme 5.3, see experimental) and analyzed using ^{31}P NMR.[256] No erosion of the stereochemical purity at the headgroup of PG could be detected (Figure C.3).
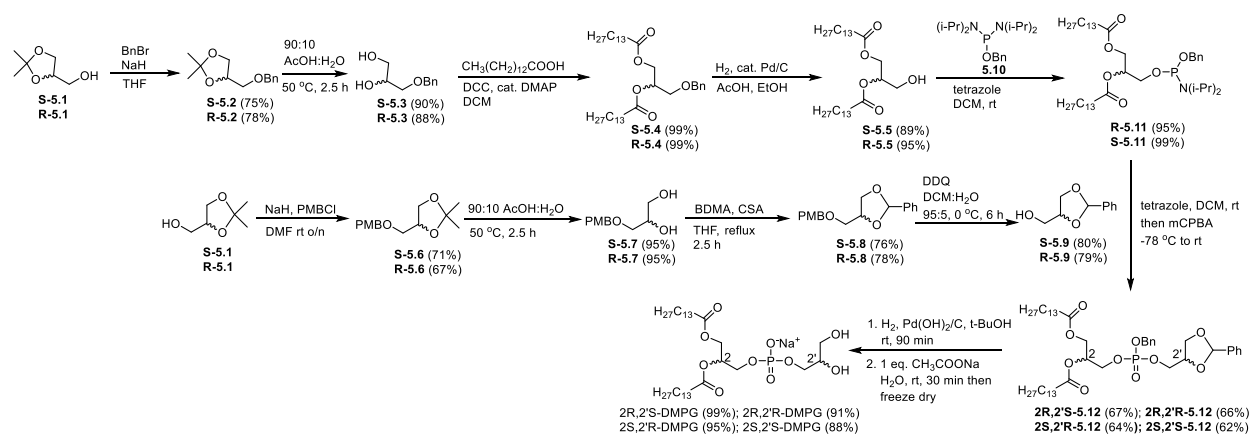
Scheme 5.1 Synthesis of the four stereoisomers of DMPG

Calcium-dependent binding of daptomycin to liposomes can be monitored by titrating in calcium and observing the resulting increase in fluorescence of Kyn13.[19,24] To study the effect of DMPG configuration on this phenomenon, large unilamellar vesicles (LUVs) containing 1,2-dimyristoyl-sn-glycero-3-phosphocholine (DMPC) and one of the four stereoisomers of DMPG (1:1) were prepared. Initially, we compared the membrane binding results between our synthetic DMPG and commercial DMPG. LUVs consisting of 1:1 DMPG:DMPC with the DMPG content

composed of a 1:1 mixture of synthetic 2R,2'S-DMPG and 2R,2'R-DMPG gave similar results to LUVs composed of 1:1 DMPG:DMPC made using commercial DMPG, which is racemic at the headgroup (Figure 5.1A).
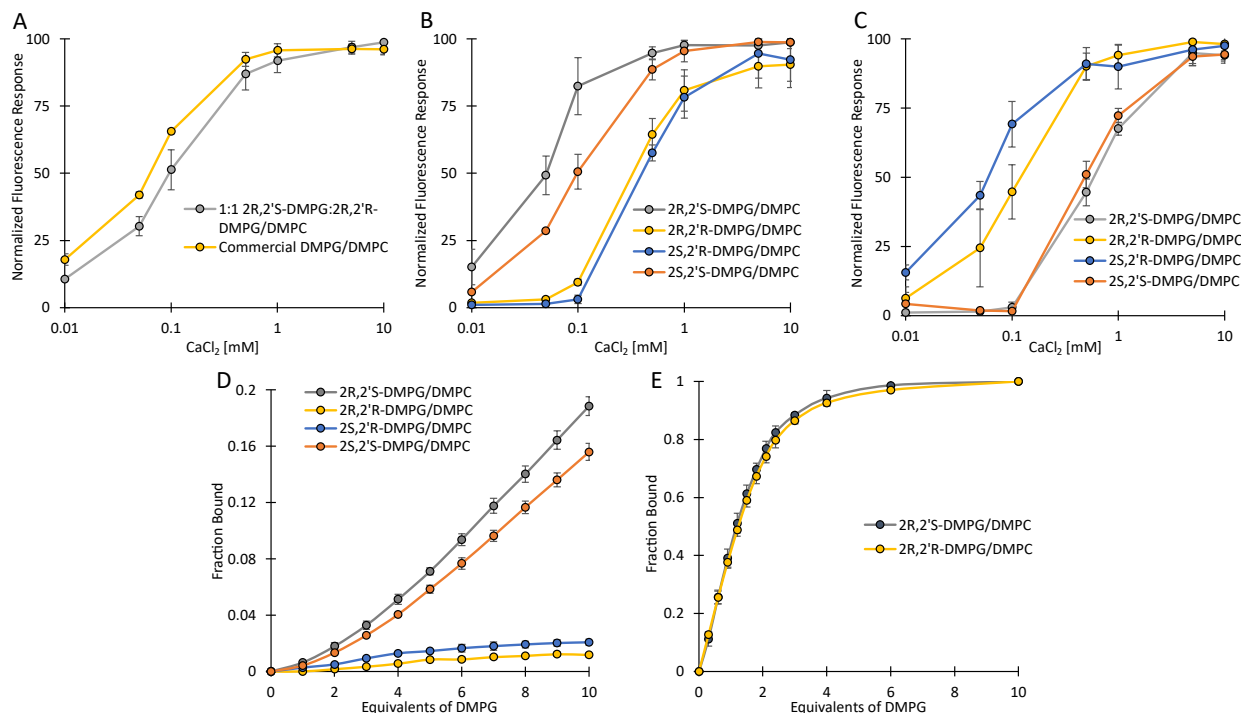
Figure 5.1 Membrane binding curves using daptomycin or ent-daptomycin and LUVs composed of 1:1 DMPG:DMPC at 37 °C in 20 mM HEPES, 150 mM NaCl (pH 7.4). (A) Calcium was titrated into a solution of daptomycin (3 µM) and LUVs (250 µM) containing either a 1:1 mixture of 2R,2'S-DMPG and 2R,2'R-DMPG or commercial DMPG. (B) The same titration described for (A), but the DMPG component is one of the four stereoisomers of DMPG. (C) The same titration described for (A), but with ent-daptomycin and the DMPG component is one of the four stereoisomers of DMPG. (D) LUVs containing one of the four stereoisomers of PG were titrated into a solution of daptomycin (15 µM) at 0.1 mM CaCl$_2$. The fully bound state was achieved by increasing the CaCl$_2$ concentration to 5 mM at the end of the titration. (E) The same titration described for (D) done at 5 mM CaCl$_2$ for LUVs containing 2R,2'S-DMPG and 10 mM CaCl$_2$ for LUVs containing 2R,2'R-DMPG

Studies using enantiomerically pure DMPGs revealed that the binding of daptomycin into LUVs in response to Ca^{2+} depends upon the configuration of the PG (Figure 5.1B). Binding occurs most readily (at lower Ca^{2+} concentrations) with LUVs composed of 2R,2'S-DMPG reaching maximal fluorescence at approximately 0.5-1.0 mM Ca^{2+} (Figure 5.1B). Liposomes composed of

PG that have the opposite configuration at the head group (2R,2'R or 2S,2'R) required an approximately 10-fold higher concentration of Ca^{2+} to reach maximal fluorescence (Figure 5.1B). Surprisingly, the configuration at the tail of PG had a much smaller effect on daptomycin insertion as the liposomes consisting of 2S,2'S-DMPG reached maximal fluorescence at approximately 1 mM Ca^{2+}. These studies reveal that daptomycin has a preference for binding to PG with the S-configuration at the head group and is somewhat insensitive to the configuration at the lipid tail group. The effect of DMPG configuration on ent-daptomycin insertion was equal but opposite to that of daptomycin (Figure 5.1C). These results indicate that the observed changes in daptomycin membrane affinity are due a chiral interaction and not due to differences in the bulk properties of the model membranes. Further evidence that daptomycin's interaction with PG is significantly affected by the PG head group configuration was obtained by monitoring the increase in fluorescence upon titrating a solution of liposomes into a solution of daptomycin at a fixed Ca^{2+} concentration. At 0.1 mM Ca^{2+}, daptomycin inserts readily into 2R,2'S-DMPG and 2S,2'S-DMPG liposomes. In contrast, little insertion is observed into 2R,2'R-DMPG and 2S,2'R liposomes even up to 10 equiv 2R,2'R-DMPG (Figure 5.1D). These experiments were also performed at high Ca^{2+} concentration to determine if the PG stoichiometry remained the same when titrating in LUVs containing either 2R,2'S-DMPG or 2R,2'R-DMPG liposomes. At high Ca^{2+} (concentrations at which daptomycin inserts completely into both of these two chiral liposomes as shown in Figure 5.1), the plot of fraction bound vs. equiv. of DMPG (Figure 5.1E) demonstrates that the stoichiometry of the binding event is the same for both LUVs; thus, the differences observed at 0.1 mM Ca^{2+} are due to a difference in daptomycin's affinity for 2R,2'S-DMPG and 2R,2'R-DMPG.

A plot of the raw fluorescence intensity as a function of DMPG concentration shows that the change in the quantum yield of the Kyn residue depends strongly on DMPG head group configuration (Figure C.4). Indeed, when fully bound to the membrane, the greatest increase in quantum yield is observed with 2R,2'S-DMPG LUVs. Additionally, the emission of the Kyn residue experiences a greater blueshift when bound to membranes containing 2R,2'S-DMPG compared to membranes containing 2R,2'R-DMPG (Figure C.8). These results are fully consistent with the data presented in Figure 5.1 and show that the state of the Kyn in the membrane-bound peptide depends on DMPG configuration.

CD studies have shown that daptomycin undergoes a large conformational change in the presence of Ca^{2+} and PG-containing liposomes.[24,80,92] To determine if this conformational change is affected by the configuration of PG, CD studies were performed using chiral liposomes consisting of all four stereoisomers of DMPG and DMPC (1:1). 5 mM Ca^{2+} was used in these experiments as the membrane insertion studies presented above (Figures 5.1B and 5.1C) revealed that daptomycin inserts almost completely into all four chiral liposomes at this Ca^{2+} concentration.
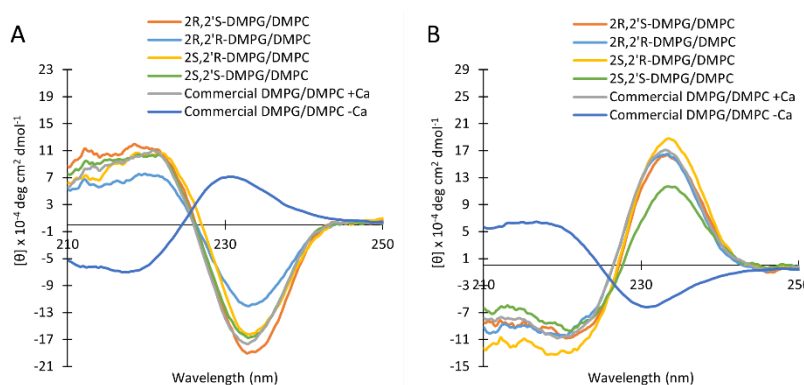
Figure 5.2 CD spectra of daptomycin or ent-daptomycin (15 μM) in the presence of 5 mM Ca^{2+} and LUVs composed of 1:1 DMPG:DMPC at 37 °C in 20 mM HEPES (pH 7.4). (A) Using daptomycin and the DMPG component is one of the four stereoisomers of DMPG. The spectrum of daptomycin in the presence of LUVs containing commercial DMPG both in the presence and absence of Ca^{2+} are also shown for comparison. (B) Using ent-daptomycin and the DMPG component is one of the four stereoisomers of DMPG.

Using LUVs consisting of commercial DMPG:DMPC (1:1) in the presence of 5mM Ca^{2+}, a CD spectrum was obtained that is identical to that reported by Lee et al using DMPG/DMPC and was very similar to those collected in the presence of POPG/POPC or DOPG/DOPE liposomes in that they exhibited the same negative ellipticity maximum at approximately 232 nm and a switch from positive to negative ellipticity at 225 nm (Figure 5.2A).[80,257] When the same experiment was conducted using LUVs in which the DMPG component is one of the four stereoisomers of DMPG we found that all four LUVs gave a similar wave-like CD spectra (Figure 5.2A). The amplitude of these spectra varied little with the exception being the 2R,2'R-DMPG liposomes which exhibited a decrease in amplitude compared to the three other stereoisomers liposomes. The decrease in the amplitude of the curve suggests that a weaker coupling interaction between Kyn 13 and Trp 1 occurs on these membranes; however, it is not known whether this coupling interaction is intermolecular or intramolecular.[257] Repeating the CD studies with ent-daptomycin yielded curves of the opposite sign but of similar amplitude (Figure 5.2B). Based on these data, it appears that the configuration of the head group of PG can influence the backbone conformation of membrane-bound daptomycin but the effect does not appear to be large.

Daptomycin is known to oligomerize on model and bacterial membranes and oligomer formation is an essential part of its killing action. To investigate how the configuration of PG affects daptomycin's ability to oligomerize in model membranes we used daptomycin with a perylene-labelled tail (perylene-daptomycin, Figure 1.16). It has been shown that the oligomerization of perylene-daptomycin on model membranes and bacterial cell membranes is accompanied by excimer formation which emits maximally at 520 nm.[88] Thus, by comparing the fluorescence intensity at 455 nm (where the monomer emission dominates) to the fluorescence

intensity at 560 nm (where excimer emission dominates) the extent of oligomerization can be evaluated.[235]
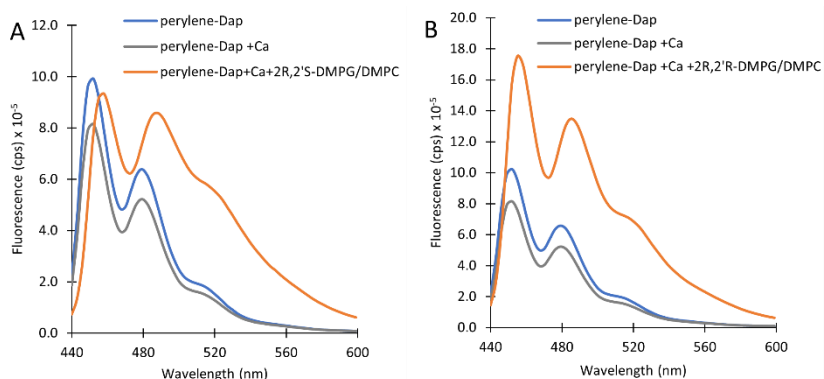
Figure 5.3 Fluorescence spectra of perylene-daptomycin (2.5 µM) in the presence of 5 mM Ca^{2+} and LUVs composed of 1:1 DMPG:DMPC at 37 °C in 20 mM HEPES, 150 mM NaCl (pH 7.4). (A) The DMPG component is 2R,2'S-DMPG. (B) The DMPG component is 2R,2'R-DMPG.

Table 5.1 I_{560}/I_{455} Ratios obtained from the fluorescence spectra of perylene-daptomycin in the presence of 5 mM Ca^{2+} and LUVs composed of DMPC and one of the stereoisomers of DMPG (1:1).[a]

PG stereoisomer	I_{560}/I_{455}
Commercial DMPG	0.170 ± 0.001
2R,2'S	0.21 ± 0.02
2R,2'R	0.12 ± 0.01
2S,2'R	0.156 ± 0.003
2S,2'S	0.223 ± 0.004

[a]Errors are the standard deviation between 3 separate trials.

Figures 5.3A and 5.3B shows the fluorescence spectra of perylene-daptomycin in the presence of 5 mM Ca^{2+} and LUVs consisting of a 1:1 mixture of DMPC and either 2R,2'S-DMPG (Figure 5.3A) or 2R,2'R-DMPG (Figure 5.3B). Perylene excimer formation, and hence oligomerization, as determined by the I_{560}/I_{455} ratio, decreased by 43 % when using LUVs consisting of 2R,2'R-DMPG compared to LUV consisting of 2R,2'S-DMPG. Clear variations in the extent of oligomerization are also observed with the other stereoisomeric LUVs as evidenced by the differences in the I_{560}/I_{455} ratio (Table 5.1). Perylene-daptomycin oligomerizes to the same extent on membranes containing either 2R,2'S-DMPG or 2S,2'S-DMPG demonstrating that the

configuration at the headgroup of PG has a much stronger effect on the extent of oligomerization compared to the configuration at the tail position. Using LUVs containing commercial DMPG, we get an extent of oligomerization that is very close to the average of 2R,2'S-DMPG or 2R,2'R-DMPG. The combination of 2S,2'R-DMPG and perylene-daptomycin should model the combination of 2R,2'S-DMPG and the unnatural enantiomer of perylene-daptomycin (as shown in the membrane binding studies, the stereochemistry of DMPC has little effect on daptomycin or ent-daptomycin). Thus, although ent-daptomycin can bind to bacterial membranes at physiological calcium concentrations, it can not oligomerize to the same extent as dap.

5.3   Conclusions

In conclusion, our finding that ent-daptomycin is 85-fold less active than daptomycin against *B. subtilis* proves unequivocally that daptomycin interacts with a chiral target as part of its mechanism of action. Our membrane binding studies demonstrate that at least one chiral target of daptomycin is PG, and that daptomycin preferentially binds to PG having the 2R,2'S configuration. Daptomycin-PG interactions are particularly sensitive to the configuration at the head group position but, surprisingly, are not very sensitive to the configuration at the tail group position. Although it is known that intrinsic membrane chirality can effect peptide binding,[258–260] we believe that this is the first example whereby the activity of a antibiotic depends upon the configuration of a membrane lipid head group.

It is possible that daptomycin, in addition to PG, interacts with another chiral target such as another chiral lipid or membrane associated protein. It has recently been shown that dap, in the presence of Ca^{2+}, forms a tripartite complex with PG and lipid II which contains multiple stereocenters.[71] They also demonstrated that in the presence of Ca^{2+}, lipid II enhances daptomycin's affinity for PG-containing membranes. However, this same study also showed that

just undecaprenylpyrophosphate ($C_{55}PP$, a component of lipid II) and undecaprenylphosphate ($C_{55}P$), which do not have any stereocenters, also enhance daptomycin's affinity for PG membranes as well as or better than lipid II. This result suggests that it is the achiral undecaprenyl group and/or phosphate portion of lipid II that daptomycin is recognizing. However, we have found that the Ca^{2+}-dependent insertion of daptomycin into 2R,2'S-DMPG:DOPC (2:98) LUVs or C55P:2R,2'S-DMPG:DOPC (2:2:96) LUVs, is essentially the same when monitored using dap's intrinsic Kyn fluorescence (Figure C.9). The same outcome was observed when 2R,2'R-DMPG was used (Figure C.9). These results are inline with a recent study by Kotsogianni et al who found that the presence of Gram-positive lipid II in DOPG/DOPC LUVs did not cause a change in the heat of the binding event as measured by isothermal titration calorimetry.[72] Moreover, it has been shown that PG antagonizes the activity of daptomycin while lipid II does not.[261] These observations suggests that daptomycin does not specifically interact with lipid II, but rather disrupts areas of the membrane that lipid II incidentally localizes to and possibly sequesters the material into daptomycin-PG oligomers.

In 2000, Boaretti and Canepari reported the isolation of two proteins that bound to daptomycin from the cell membranes of *Enterococcus hirae* using affinity chromatography.[262] However, they never identified these proteins. Recent studies by Po et al using a daptomycin photoaffinity probe suggest that daptomycin might interact with the universal stress response protein, Usp2.[263] However, the affinity of this protein for daptomycin was modest ($K_D = 68$ mM, ~40 fold higher than dap's K_D for POPG/POPC membranes at 5 mM $CaCl_2$)[72] and a K_D in the presence of both PG and Ca^{2+} was not reported.

We have shown that the configuration of PG does not have a significant effect upon the ability of daptomycin to undergo a backbone conformational change; however, it does strongly

affect dap's ability to oligomerize. In line with the trends observed in the membrane binding studies, maximal oligomerization occurred with liposomes consisting of the 2R,2'S-PG isomer and the configuration at the tail position had almost no effect on oligomerization while the configuration of the head group had a significant effect. Although ent-daptomycin can bind to 2R,2'S-DMPG/DMPC membranes at physiological Ca^{2+} concentrations, it has a lower affinity for 2R,2'S liposomes than daptomycin and cannot oligomerize to the same extent as daptomycin, and this is likely the reason why ent-daptomycin is considerably less active than dap.

As discussed in section 1.3, most of the PG in bacteria is synthesized through the CDP-diacylglycerol pathway which gives exclusively 2R,2'S-PG (Figure 1.5). However, some of the PG in bacteria is prepared through a transphosphatidylation pathway (Figure 1.6) that is known to prepare equal quantities of 2R,2'S- and 2R,2'R-PG. Indeed, 2R,2'R-PG has been detected in marine bacteria[39] and *E. coli* where it was found to comprise 10% of the PG present.[38] Therefore, it may be possible for bacteria to develop resistance to daptomycin by altering the configuration of the PG head group. However, since PG is known to interact with several proteins that are essential to bacterial survival, this resistance mode would be slow to emerge.[264]

5.4 Experimental
General Methods.

All reagents and solvents were purchased from commercial suppliers. 1,2-dimyristoyl-sn-glycero-3-phospho-(1'-rac-glycerol)(sodium salt), 1,2-dioleoyl-sn-glycero-3-phospho-(1'-rac-glycerol)(sodium salt)) and (1,2-di[(8Z)octadecenoyl]-sn-glycero-3-phosphocholine) were purchased from Avanti Polar Lipids. Methylene chloride (DCM) was dried by distillation over calcium hydride under nitrogen. Acetonitrile (MeCN) was dried by passing it through silica gel then distilling over calcium hydride. Tetrahydrofuran (THF) was distilled from sodium metal in

the presence of benzophenone under N_2. 2-Methylpiperidine was dried over calcium hydride then distilled to give a colorless liquid. Dimethylformamide (DMF) was dried over calcium hydride and distilled under vacuum such that the temperature of the solution remained below 60 °C throughout the course of the distillation. Chromatography was preformed using 60 Å silica gel.

High resolution positive electrospray (ESI) mass spectra were obtained using an orbitrap mass spectrometer. Samples were sprayed from MeOH: 1% formic acid in H_2O. ^{1}H- and ^{13}C-NMR were collected using a Bruker Avance-300, a Bruker Avance-500 or a Bruker Avance-600 spectrophotometer. Proton Chemical shifts (δ) for samples run in $CDCl_3$ are reported in ppm relative to an internal standard (trimethylsilane, 0 ppm). For samples run in CD_3OD, δ was relative to the solvent peak (3.31 ppm). For ^{13}C-NMR samples run in $CDCl_3$ chemical shifts are reported relative to the solvent peak (77.0 ppm). For samples run in CD_3OD, δ was relative to the solvent peak (49.2 ppm).

Compounds **5.2-5.5** were prepared according to procedures reported by Lee at al.[253] Compounds **5.6-5.8** were prepared according to Fukase et al.[254] Fmoc-D-Kyn(Boc)-OH was prepared as previously described.[238] Fmoc-(2R,3S)MeGlu(t-Bu)-OH was prepared as previously described.[230] Fmoc-DMB-Gly-OH was prepared using the procedure reported by Hart et al.[167] The enantiomer of daptomycin was prepared according to our procedure, the absolute configuration at every stereocenter was inverted.[238] Mosher's esters of **5.5** and **5.9** were prepared according to the procedure disclosed by Lindberg et al.[265] $C_{55}P$ was prepared according to the procedure described by Cochrane et al.[266] **5.13** was prepared according to the procedure disclosed by Anslyn and coworkers.[267] MIC determinations were performed as previously described.[223]

Syntheses

(S)-(2-phenyl-1,3-dioxolan-4-yl)methanol (**S-5.9**).

To a cooled (ice-water bath) solution of **S-5.8** (3.65 g, 12.2 mmol, 1.00 equiv) in dichloromethane (47.4 mL) was added distilled water (2.55 mL) followed by freshly recrystallized 2,3-dichloro-5,6-dicyano-1,4-benzoquinone (3.04 g, 13.4 mmol, 1.10 equiv). The solution was stirred at 0 °C for 8 hours then filtered and extracted with saturated aqueous $NaHCO_3$ (50 mL). The aqueous layer was extracted with DCM three times and the combined organic layer was washed with saturated aqueous $NaHCO_3$ and brine. The organic layer was dried with $MgSO_4$, filtered, and then concentrated without heating the rotovap bath. The crude residue was purified via silica gel column chromatography (1:1 pentane:diethyl ether). Product containing fractions were concentrated without the use of high vacuum to prevent loss of product. This yielded **S-5.9** as a colorless oil (1.76 g, 80% yield). $[\alpha]^{22}_D = +7.4$ (c 0.184, CH_2Cl_2). ^{1}H NMR (300 MHz, $CDCl_3$): δ 7.48-7.46 (2H, m) 7.39-7.37 (3H, m) 5.96 and 5.83 (1H, s) 4.41-4.34 (1H, m) 4.22-4.19 and 3.88-3.83 (1H, m) 4.13-4.08 and 4.04-3.99 (1H, m) 3.83-3.65 (2H, m) 1.89 and 1.83 (1H, dd, $J = 6.2$, 5.0 Hz). ^{13}C NMR (75 MHz, $CDCl_3$): δ 140.7, 139.9, 132.4, 132.2, 131.4, 131.3, 129.4, 129.2, 107.2, 106.7, 69.8, 69.6, 66.2, 65.6. HRMS-ESI+ (*m/z*): [M + H]$^+$ calculated for $C_{10}H_{13}O_3$, 181.08592; found, 181.08670.

(R)-(2-phenyl-1,3-dioxolan-4-yl)methanol (**R-5.9**)

R-5.9 was prepared according to the procedure described for **S-5.9** using **R-5.8** in place of **S-5.8** (1.75 g, 79% yield). $[\alpha]^{22}_D = -8.0$ (c 0.206, CH_2Cl_2). The ^{1}H NMR data of **R-5.9** matched that collected for **S-5.9**.

1-(benzyloxy)-N,N,N',N'-tetraisopropylphosphanediamine (**5.10**)

To a cooled (ice-water bath) solution of 1-chloro-*N,N,N',N'*-tetraisopropylphosphanediamine (2.0 g, 7.49 mmol, 1.00 equiv) in dry diethyl ether (40 mL) was added a solution of freshly distilled

and dry BnOH (730 mg, 6.75 mmol, 0.900 equiv), triethylamine (1.20 mL, 8.61 mmol, 1.15 equiv.) in diethyl ether (20 mL) via a syringe pump (0.5 mL/min). After the addition was complete, the resulting suspension was stirred for 4 hours with cooling (ice-water bath). After this time, the suspension was diluted with ice cold hexanes (20 mL), filtered, and then concentrated. The residue was then suspended in cold hexanes (20 mL), filtered and concentrated. The crude residue was purified via silica gel column chromatography (3% triethylamine/hexanes) yielding **5.10** as a colorless oil (69-85% yield). NMR spectra matched those previously reported.[268]

(2R)-3-(((benzyloxy)(diisopropylamino)phosphanyl)oxy)propane-1,2-diyl   ditetradecanoate (**R-5.11**)

Oven dried 4 Å powdered molecular sieves (ca. 500 mg), a stir bar and an oven dried flask were placed under high vacuum and further dried heating with a flame for a few minutes. The hot flask was then allowed to cool to room temperature under vacuum and then it was back filled with N_2 and charged with **S-5.5** (500 mg, 0.975 mmol, 1.00 equiv). In a separate dried flask under N_2, a solution of **5.10** (660 mg, 1.95 mmol, 2.00 equiv.) in freshly distilled dichloromethane (10.4 mL) was prepared. This was transferred by cannula to the flask containing the sieves using a flow of dry N_2. The suspension was allowed to stir over the sieves for 5 min at room temperature. Tetrazole (0.450 M in acetonitrile; 4.33 mL, 1.95 mmol, 2.00 equiv) was added dropwise and the solution was stirred at room temperature for 4 hours. At this point, the solution was diluted with dry dichloromethane (20 mL) and quenched with saturate aqueous $NaHCO_3$ (30 mL). The aqueous layer extracted with dichloromethane three times. The combined organic layer was washed with brine, dried over $MgSO_4$, filtered and the concentrated. The crude residue was purified via silica gel column (gravity; 3% TEA/97% hexanes) chromatography giving **R-5.11** as a colorless oil (727 mg, 99% yield). $[\alpha]^{22}_D = +12.8$ (c 0.153, CH_2Cl_2). ^{1}H NMR (300 MHz, $CDCl_3$): δ 7.33-7.32 (5H,

m) 5.18 (app quintet, J = 5.1 Hz) 4.76-4.60 (2H, m) 4.37-4.29 (1H, m) 4.19-4.12 (1H, m) 3.82-3.56 (4H, m) 2.28 (4H, t, J = 7.4 Hz) 1.59 (4H, m) 1.24-1.15 (52H, m) 0.86 (6H, m). ^{31}P NMR (122 MHz, CDCl$_3$) 150.0, 149.8. ^{13}C NMR (75 MHz, CDCl$_3$): δ 173.4, 173.0, 139.4, 139.3, 128.3, 128.2, 127.3, 127.2, 127.0, 126.9, 70.8, 70.8, 70.7, 65.5, 65.5, 65.3, 65.3, 62.5, 62.5, 61.9, 61.7, 61.6, 61.5, 43.2, 43.0, 34.3, 34.2, 31.9, 29.7, 29.7, 29.5, 29.4, 29.3, 29.1, 29.1, 24.9, 24.9, 24.7, 24.6, 24.5, 24.5, 22.7, 14.1. HRMS-ESI+ (*m/z*): [M + H]$^+$ calculated for C$_{44}$H$_{81}$O$_6$NP, 750.57960; found, 750.57780.

(2S)-3-(((benzyloxy)(diisopropylamino)phosphanyl)oxy)propane-1,2-diyl   ditetradecanoate (**S-5.11**)

S-5.11 was prepared by the procedure described for **R-5.11** using **R-5.5** in place of **S-5.5** (698 mg, 95% yield).. $[\alpha]^{22}_D$ = -13.4 (c 0.174, CH$_2$Cl$_2$). The ^{1}H NMR data of **S-5.11** matched that of **R-5.11**.

(2R)-3-(((benzyloxy)((((4S)-2-phenyl-1,3-dioxolan-4-yl)methoxy)phosphoryl)oxy)propane-1,2-diyl ditetradecanoate (**2R,2'S-5.12**)

Oven dried 4 Å powdered molecular sieves (ca. 500 mg), a stir bar and an oven dried flask were placed under high vacuum and further dried by heating with a flame for a few minutes. The hot flask was then allowed to cool to room temperature under vacuum and then it was back filled with N$_2$. In a separate dried flask under N$_2$, a solution of **R-5.11** (450 mg, 0.667 mmol, 1.50 equiv.) and **R-5.9** (0.720 mg, 0.444 mmol, 1.00 equiv.) in dry dichloromethane (13.5 mL) was prepared. This solution was transferred via cannula into the flask containing the sieves and then stirred over the sieves for 5 min at room temperature. Tetrazole (0.450 M in acetonitrile; 1.77 mL, 0.888 mmol, 2.00 equiv) was added to this stirring solution dropwise at room temperature. After 16 hours, the reaction mixture was cooled (dry ice acetone bath) and freshly purified mCPBA (153 mg, 0.888

mmol, 2.00 equiv.) in dry dichloromethane (2 mL) was added. The solution was stirred for 10 min then brought to room temperature and stirred for 1 hour. After diluting with dry dichloromethane (15 mL), the suspension was vacuum filtered over a cotton plug and then quenched with saturate aqueous $NaHCO_3$ (20 mL). The aqueous layer was extracted three times with dichloromethane then the combined organic layer was washed with brine, dried over $MgSO_4$ and concentrated. The crude residue was purified by silica gel column chromatography (25% EtOAc/ 75% hexanes) yielding **2R,2'S-5.12** as colorless oil (227 mg, 67% yield). $[\alpha]^{22}_D$ = -3.3 (c 0.110, CH_2Cl_2). ^{1}H NMR (300 MHz, $CDCl_3$): δ 7.43-7.33 (10H, m) 5.89 and 5.77 (1H, s) 5.18-5.03 (3H, m) 4.41-3.79 (9H, m) 2.27 (4H, app t, J = 6.6 Hz) 1.57 (4H, m) 1.24 (40H, m) 0.86 (6H, app t, J = 5.7 Hz). ^{31}P NMR (122 MHz, $CDCl_3$) δ 0.19, 0.05. ^{13}C NMR (75 MHz, $CDCl_3$): δ 173.1, 172.8, 137.5, 136.8, 135.6, 135.5, 129.5, 129.3, 128.8, 128.7, 128.7, 128.6, 128.4, 128.0, 126.6, 126.4, 104.7, 104.0, 74.4, 74.3, 74.2, 69.8, 69.8, 69.4, 69.3, 69.3, 69.2, 67.6, 67.6, 67.5, 67.5, 67.3, 67.3, 66.8, 65.6, 65.6, 61.6, 34.1, 34.0, 31.9, 29.7, 29.7, 29.5, 29.4, 29.3, 29.1, 29.1, 24.8, 22.7, 14.1. HRMS-ESI+ (*m/z*): [M + H]$^+$ calculated for $C_{48}H_{78}O_{10}P$, 845.53271; found, 845.53613. *(2R)-3-(((benzyloxy)(((4R)-2-phenyl-1,3-dioxolan-4-yl)methoxy)phosphoryl)oxy)propane-1,2-diyl ditetradecanoate* (**2R,2'R-5.12**)

2R,2'R-5.12 was prepared by the procedure described for **2R,2'S-5.12** using **S-5.9** in place of **R-5.9** (223mg, 66% yield). $[\alpha]^{22}_D$ = +5.4 (c 0.100, CH_2Cl_2). ^{1}H NMR (300 MHz, $CDCl_3$): δ 7.44-7.34 (10H, m) 5.90 and 5.78 (1H, s) 5.18-5.04 (3H, m) 4.40-3.76 (9H, m) 2.28 (4H, app t, J = 6.0 Hz) 1.57 (4H, m) 1.24 (40H, m) 0.87 (6H, t, J = 6.2 Hz). ^{31}P NMR (122 MHz, $CDCl_3$) δ 0.19, 0.05. ^{13}C NMR (75 MHz, $CDCl_3$): δ 173.1, 172.8, 137.3, 136.7, 135.5, 135.4, 129.5, 129.2, 128.7, 128.7, 128.6, 128.3, 128.0, 126.6, 126.3, 104.6, 103.9, 74.3, 74.2, 74.1, 69.7, 69.3, 69.2, 67.5, 67.4, 67.2,

66.7, 65.5, 61.5, 34.0, 33.9, 31.8, 29.6, 29.4, 29.3, 29.2, 29.0, 29.0, 24.7, 22.6, 14.0. HRMS-ESI+ (*m/z*): [M + H]$^+$ calculated for $C_{48}H_{78}O_{10}P$, 845.53271; found, 845.53528.

(2S)-3-(((benzyloxy)(((4R)-2-phenyl-1,3-dioxolan-4-yl)methoxy)phosphoryl)oxy)propane-1,2-diyl ditetradecanoate (**2S,2'R-5.12**)

2S,2'R-5.12 was prepared by the procedure described for **2R,2'S-5.12** using **S-5.11** in place of **R-5.11** and **S-5.9** in place of **R-5.9** (215 mg, 64%). $[\alpha]^{22}_D$ = +3.4 (c 0.110, CH_2Cl_2). ^{1}H NMR and ^{31}P NMR matched that of **2R,2'S-5.12**.

(2S)-3-(((benzyloxy)(((4S)-2-phenyl-1,3-dioxolan-4-yl)methoxy)phosphoryl)oxy)propane-1,2-diyl ditetradecanoate (**2S,2'S-5.12**)

2S,2'S-5.12 was prepared by the procedure described for **2R,2'S-5.12** using **S-5.11** in place of **R-5.11** (210 mg, 63%). $[\alpha]^{22}_D$ = -5.9 (c 0.110, CH_2Cl_2). ^{1}H NMR and ^{31}P NMR matched that of **2R,2'R-5.12**.

sodium (R)-2,3-bis(tetradecanoyloxy)propyl ((S)-2,3-dihydroxypropyl) phosphate (**2R,2'S-DMPG**)

2R,2'S-5.12 (117 mg, 0.138 mmol, 1.00 equiv.), Pd(OH)$_2$/C (20% w/w; 58 mg, 0.80 equiv.) and t-BuOH (2.8 mL) were combined at room temperature and stirred under H$_2$ (1 atm) for 90 min. The reaction solution was filtered over celite and the celite pad was rinsed with CHCl$_3$. The solution was then concentrated and then the residue was suspended in MilliQ water (4.61 mL) containing sodium acetate (11.3 mg, 0.138 mmol, 1.00 equiv.) and stirred for 30 min at room temperature giving an emulsion. Vortexing was used to loosen any material stuck to the base of the glass vial. The solution was then freeze-dried overnight giving **2R,2'S-DMPG** as a colorless powder (94 mg, 99% yield). $[\alpha]^{22}_D$ = -5.6 (c 0.141, CHCl$_3$). ^{1}H NMR (300 MHz, CDCl$_3$): δ 5.22

(1H, m) 4.40-4.36 (1H, m) 4.18-4.12 (1H, m) 3.96-3.82 (5H, m) 3.68-3.57 (2H, app q, J = 7.4 Hz) 1.56 (4H, m) 1.24 (40H, m) 0.87 (6H, app t, J = 6.1 Hz). ^{31}P NMR (122 MHz, 95:5 CDCl$_3$) δ 0.41. ^{13}C NMR (75 MHz, 95:5 CDCl$_3$:CD$_3$OD): δ 173.7, 173.3, 69.6, 67.9, 64.9, 62.4, 62.0, 34.1, 34.0, 31.9, 29.6, 29.4, 29.3, 29.2, 29.1, 29.0, 24.8, 22.6, 14.0. HRMS-ESI- (*m/z*): [M - H]$^-$ calculated for C$_{34}$H$_{66}$O$_{10}$P, 665.43991; found, 665.43908.

sodium (R)-2,3-bis(tetradecanoyloxy)propyl ((R)-2,3-dihydroxypropyl) phosphate (**2R,2'R-DMPG**)

2R,2'R-DMPG was prepared by the procedure described for **2R,2'S-DMPG** using **2R,2'R-5.12** in place of **2R,2'S-5.12** (161 mg, 91% yield). [α]^{22}$_D$ = +8.0 (c 0.121, CHCl$_3$). ^{1}H NMR (300 MHz, CDCl$_3$): ^{1}H NMR (300 MHz, CDCl$_3$): δ 5.22 (1H, m) 4.40-4.36 (1H, m) 4.18-4.12 (1H, m) 3.96-3.82 (5H, m) 3.68-3.57 (2H, m) 2.27 (4H, app q, J = 7.4 Hz) 1.56 (4H, m) 1.24 (40H, m) 0.87 (6H, app t, J = 6.1 Hz).^{31}P NMR (122 MHz, CDCl$_3$) δ 0.37.^{13}C NMR (75 MHz, 95:5 CDCl$_3$:CD$_3$OD): δ 173.8, 173.5, 70.8, 70.4, 66.9, 65.0, 63.6, 62.6, 34.2, 34.1, 31.9, 29.7, 29.6, 29.6, 29.3, 29.2, 29.1, 24.9, 24.8, 22.6, 14.0. HRMS-ESI- (*m/z*): [M - H]$^-$ calculated for C$_{34}$H$_{66}$O$_{10}$P, 665.43991; found, 665.43890.

sodium (S)-2,3-bis(tetradecanoyloxy)propyl ((R)-2,3-dihydroxypropyl) phosphate (**2S,2'R-DMPG**)

2S,2'R-DMPG was prepared by the procedure described for **2R,2'S-DMPG** using **2S,2'R-5.12** in place of **2R,2'S-5.12** (161 mg, 95% yield). [α]^{22}$_D$ = +5.5 (c 0.089, CHCl$_3$). NMR data matched that of **2R,2'S-DMPG**.

sodium (S)-2,3-bis(tetradecanoyloxy)propyl ((S)-2,3-dihydroxypropyl) phosphate (**2S,2'S-DMPG**)

2S,2'S-DMPG was prepared by the procedure described for **2R,2'S-DMPG** using **2S,2'S-5.12** in place of **2R,2'S-5.12** (150 mg, 88% yield). $[\alpha]^{22}_D = -7.8$ (c 0.134, CHCl$_3$). NMR data matched that of **2R,2'R-DMPG**.

Undecaprenol phosphate

Undecaprenol phosphate (C$_{55}$P) was prepared from undecaprenol extracted from powder bay leaves according to the procedure of Cochrane and coworkers.[266] ^{1}H NMR (600 MHz, CDCl$_3$): δ 5.39 (1H, m) 5.14 (10H, m) 4.41 (2H, m) 2.09-2.00 (40H, m) 1.70-1.62 (36H, m) ^{31}P NMR (243 MHz, CDCl$_3$) δ -0.39. ^{13}C NMR (150 MHz, CDCl$_3$): δ135.3, 135.1, 134.9, 134.9, 131.2, 125.1, 125.0, 124.4, 124.3, 124.2, 61.6, 39.8, 39.7, 32.2, 32.0, 26.8, 26.7, 26.4, 25.7, 23.5, 23.4, 17.7, 16.0. HRMS-ESI- (*m/z*): [M - H]⁻calculated for C$_{55}$H$_{90}$O$_4$P, 845.65712; found, 845.66.099.

Determining the Stereochemical Integrity at the Headgroup of the Synthesized DMPGs
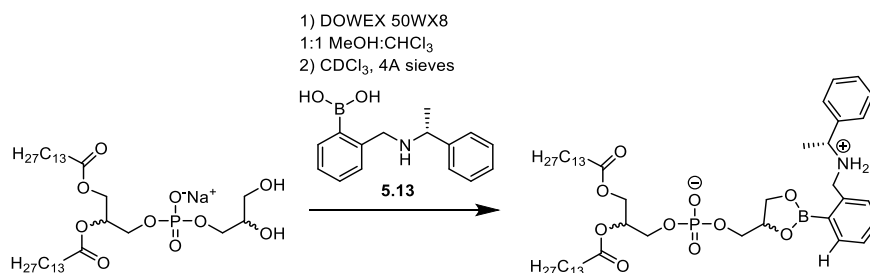
Scheme 5.3 Forming boronic esters with DMPG

This procedure is based on the work of Kelly et al.[256] To a solution of the sodium salt of DMPG (5.0 mg, 7.3 µmol, 1 equiv.) dissolved in 1:1 MeOH:CHCl$_3$ (1 mL) was added DOWEX 50WX8 resin (100 mg, hydrogen form). The resin was removed by filtration and the filtrate was concentrated then dried through repeated concentrations from benzene. The solid product was then dissolved in dry CDCl$_3$ (750 µL) containing **5.13**[267] (1.85 mg, 7.3 µmol, 1 equiv.) and allowed to

stand over 4A molecular sieves for 5 min at room temperature. The samples were then analyzed using ^{31}P NMR (202 MHz, CDCl$_3$). See Figure C.3.

Liposome preparation.

Large unilamellar vesicles were prepared as previously described.[86] DMPC and DMPG were combined in a 1:1 molar ratio in chloroform. The chloroform was removed under an N$_2$ stream leaving a thin film of lipid coating the interior of a round-bottom flask. Trace chloroform was removed under high vacuum then the lipids were hydrated with a pH 7.4 buffer (20 mM HEPES, 150 mM NaCl). Extrusion through a 100 nm polycarbonate filter yielded a solution of LUVs with a total lipid concentration of 5 mM.

For membrane binding studies involving C$_{55}$P, LUVs consisting of C$_{55}$P/DMPG/DOPC were used. DOPC was used as the major component of these LUVs to make the experimental conditions similar to those used by Grein et al and to facilitate the binding of daptomycin to DMPG at <1 mM CaCl$_2$ as daptomycin binds more readily to DOPC/DOPG membranes than DMPC/DMPG membranes.[81] The concentration of DMPG was raised by a factor of 10 relative to what Grein et al used such that 1.67 equivalents of DMPG were present during the titration relative to concentration of daptomycin. To prepare the LUVs containing C$_{55}$P, commercial DOPC (1,2-di[(8Z)octadecenoyl]-sn-glycero-3-phosphocholine), C$_{55}$P and DMPG, were dissolved separately in chloroform, then added to a flask and concentrated under an N$_2$ stream. The lipid film was hydrated and extruded as before which gave a solution of LUVs with a total lipid concentration of 5 mM. To control for the change in membrane charge that occurs when C$_{55}$P is added to a DMPG-containing membrane, data was collected using LUVs containing 4% C$_{55}$P/DOPC and pure DOPC.

Membrane binding assay using kynurenine fluorescence.

This procedure was adapted from the assay described by Taylor et al.[81] Fluorescence was measured in Corning Costar half-area flat bottom black polystyrene 96-well plates using a Tecan Infinite M1000 instrument. 100 µM peptide stocks were diluted with pH 7.4 buffer (20 mM HEPES, 150 mM NaCl) and preheated to 37°C before adding the above-mentioned liposome solution and immediately dispensing 90 µL aliquots into wells pre-loaded with 10 µL of buffer containing $CaCl_2$ at 10x the desired calcium concentration (plate had also been preheated to 37°C) giving a final volume of 100 µL in each well. The final concentrations in each well were 3 µM of peptide, and 250 µM of lipid. Fluorescence measurements were timed to allow for a 3-4 minute incubation period at 37°C. Emission spectra were acquired for kynurenine (Excitation: 365 nm, 5 nm bandwidth) intrinsic fluorescence using 100 flashes at 400 Hz and a step size of 3 nm. Emission spectra for blanks containing 250 µM lipid in buffer and 3 µM peptide were also collected and subtracted from the traces obtained. The signal was normalized according to the maximum emission observed for each trail.

Circular dichroism studies.

Circular dichroism (CD) traces were collected using a Jasco J-815 CD spectrometer. The peptide concentration of each solution was 15 µM in 20 mM HEPES buffer (pH 7.4). Samples were measured at room temperature from 210-250 nm at a scan rate of 10 nm min^{-1} with a digital integration time of 2 seconds and a bandwidth 1 nm. A 1 mm quartz cuvette was used. The outputted data was converted to molar ellipticity in units of deg cm^2 dmol^{-1}. For CD traces collected on peptides in the presence of large unilamellar vesicles (LUVs) a LUV concentration of 180 µM and a $CaCl_2$ concentration of 5 mM was used. For these studies, samples were measured 3 min after mixing.

Oligomerization studies.

Perylene-daptomycin was prepared according to a previously described procedure.[88] Emission spectra were collected using a QuantMaster 4 spectrophotometer (Photon Technology International, London, ON). Samples were excited at 430 nm and the emission between 440 nm and 600 nm was recorded. Bandpasses for emission and excitation were set to 3 nm. Emission spectra were corrected for wavelength-dependent instrument response using a quinine sulfate standard.

Peryelene-daptomycin (2.5 µM) was incubated in pH 7.4 buffer (20 mM HEPES, 150 mM NaCl) at 37 °C. To this was added $CaCl_2$ in the same buffer until the desired calcium concentration was achieved (5 mM was used most often). Once the sample had achieved thermal equilibrium, LUVs were added such that a 250 µM total lipid concentration was achieved. This sample was mixed for 3 min then the emission spectra was recorded. All reported extents of oligomerization are based on at least three replications of this experiment.

Titrating daptomycin with LUVs

Daptomycin (15 µM) was incubated in pH 7.4 buffer (20 mM HEPES, 150 mM NaCl) at 37 °C. To this was added $CaCl_2$ in the same buffer until the desired calcium concentration was achieved (0.1, 5 and 10 mM $CaCl_2$ were used). Once the sample had achieved thermal equilibrium, an aliquot of LUV was added, and the sample was mixed for 3 min then the emission spectra was recorded. Samples were excited at 365 nm and the emission between 400 nm and 600 nm was recorded. Bandpasses for emission and excitation were set to 2.5 nm. Emission spectra were corrected for wavelength-dependent instrument response using a quinine sulfate standard. This

161

process was repeated until 10 equivalents of DMPG were added (total lipid concentration 300 µM).

Chapter 6 - Establishing the Structure−Activity Relationship between Phosphatidylglycerol and Daptomycin

6   Preface and contributions

This chapter is based on a manuscript published in the journal *ACS Infectious Disease* (*Reprinted (adapted) with permission from ACS Infect. Dis.* **2022**, DOI 10.1021/acsinfecdis.2c00262. *Copyright 2022 American Chemical Society*). I completed all the experimental work presented in this chapter and wrote the first draft of the manuscript which was refined and elaborated upon by Prof. Taylor. All this work was done under supervision of Prof. Taylor. Additional supplementary information is available on the journal's website.

6.1   Introduction

One of the major goals of this thesis was to provide rationale for daptomycin resistance mechanisms that involve modification of PG (see section 1.5.1). Chapter 5 revealed that daptomycin recognizes a specific stereoisomer of PG implying that these peptides form a tight complex with this lipid. Therefore, it seemed likely that modifications to the headgroup of PG could have a substantial impact on this central interaction thus conferring resistance. Based on this hypothesis, we set out to establish a structure-activity relationship between daptomycin and PG.

Until recently, it was unknown whether daptomycin was interacting specifically with PG or simply recognizing the negative charge on this acidic lipid. Many genetic analyses of daptomycin resistance implicated the *mprF* gene which encodes for the enzyme responsible for the synthesis and translocation of lysyl-PG to the outer membrane.[120] Since *mprF* confers resistance to cationic peptides, usually through a charge repulsion mechanism, it was thought that daptomycin functions like a cationic peptide gaining its positive charge through binding to calcium before inserting into the membrane.[269] Thus, it was thought that modified-PGs conferred

resistance to daptomycin through decreasing membrane charge and repelling calcium-bound daptomycin from the target membrane, but more recent works have not found evidence of this on model membranes [121] or in bacteria [129]. Instead, it seems more likely that daptomycin specifically recognizes the headgroup of PG rather than just its negative charge and resistance is conferred by PG modification through masking the headgroup of PG. In line with this hypothesis, employing ITC and model liposomes, Kotsogianni et al demonstrated that daptomycin has a considerably greater affinity for dioleoylphosphatidyl glycerol than it does for cardiolipin, dioleoylphosphatidyl serine, or dioleoylphosphatidyl propanol. We recently showed that the interaction of daptomycin with PG is strongly influenced by the configuration of PG and that daptomycin has a considerable preference the 1,2-diacyl-sn-glycero-3-phospho-1'-sn-glycerol stereoisomer (2R,2'S configuration), the most common stereoisomer of PG in bacterial membranes (chapter 5). It was also revealed that daptomycin is more sensitive to the configuration at the head group (2' position) of PG compared to the lipid group (2 position). These two studies reveal that the head group of PG is important for daptomycin-PG interactions. Despite the importance and uniqueness of the interaction of daptomycin with PG, no other studies have been undertaken to ascertain which components of PG are essential for daptomycin-PG interactions. Here we report the first detailed structure-activity relationship study between daptomycin and PG through the synthesis and study of PG analogs.

6.2   Results and Discussion

To investigate the role of the PG hydroxy groups in daptomycin-PG interactions we synthesized dimyristoyl PGs (DMPG), in which one or both hydroxy groups were converted to methyl ethers (**6.12**, **6.17**, **6.18**) or one hydroxy group was removed (**6.15** and **6.16**) (Scheme 6.1). Modified glycerols **6.1**-**6.5** were prepared (Scheme 6.3 see experimental) and reacted with phosphoramidite **6.6** under standard conditions to give phosphotriesters **6.7**-**6.11**. Deprotection of **6.7** and **6.11** via

hydrogenolysis gave 2',3'-dimethyl-DMPGs (**6.12**) and 2'-deoxy-DMPG (**6.16**). Of note is the synthesis of 3'-deoxy-DMPG (**6.15**) which we found could be obtained in a single step via hydrogenolysis of epoxide **6.10**. Removal of the TBS group in **6.8** using TBAF provided alcohol **6.13**. Attempts to remove the TBS group in **6.9** using TBAF gave a mixture of products. Fortunately, using HF/pyr, the TBS group in **6.9** could be removed to give alcohol **6.14** in a satisfactory yield. Subjecting compounds **6.13** and **6.14** to hydrogenolysis gave 2'-methyl-DMPG and 3'-methyl-DMPG (**6.17** and **6.18**) in good yield.
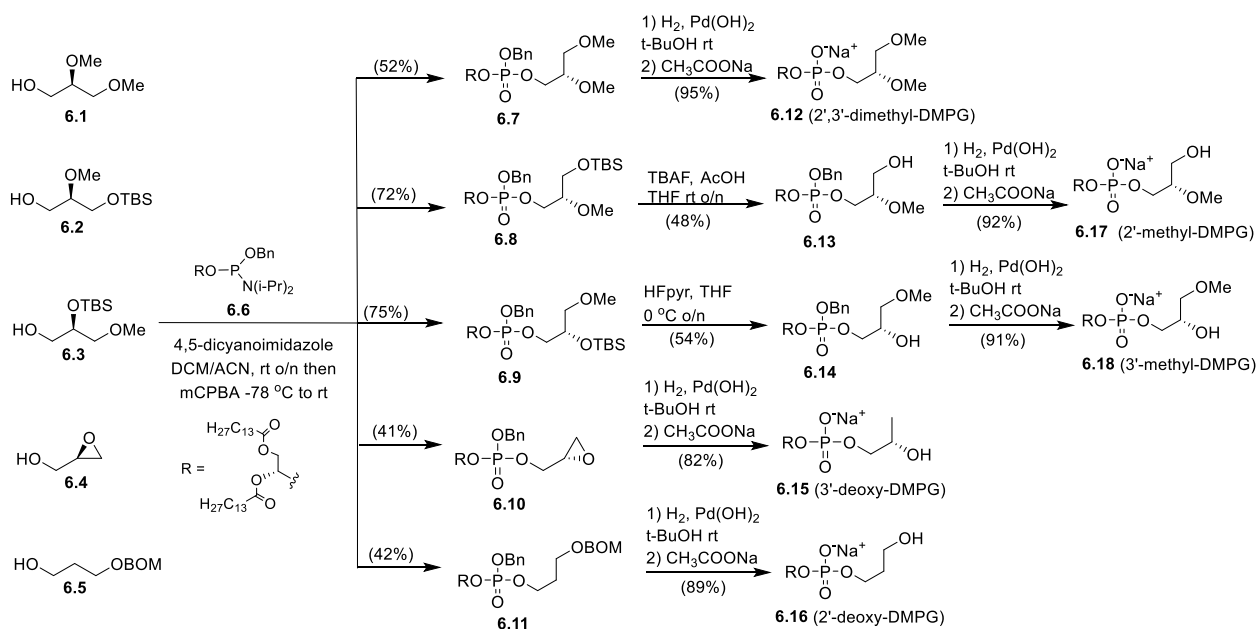
Scheme 6.1 Synthesis of PGs with modified headgroups

The insertion of daptomycin into liposomes is easily monitored by observing the fluorescence of the environmentally sensitive, fluorescent amino acid kynurenine (Kyn) at position 13.[19,24] Thus, large unilamellar vesicles (LUVs) composed of equal parts DMPC and modified DMPG were prepared by extrusion as described previously and incubated with daptomycin. Upon titrating in calcium, the fluorescence intensity of Kyn increases substantially indicating that the residue is entering the membrane environment. By plotting normalized fluorescence intensity,

which is representative of the fraction of peptide bound to the LUV, as a function of calcium concentration, a binding curve is obtained which can be used to determine the relative affinity of daptomycin for each modified lipid.

Figure 6.1A presents the binding curves describing the interaction of daptomycin with each modified lipid. With liposomes containing unmodified PG (2R,2'S-DMPG), maximal membrane insertion was observed at 0.5-1.0 mM Ca^{2+}. Although daptomycin seems to tolerate some modifications to PG, all the liposomes that contained a modified PG required higher Ca^{2+} concentrations to achieve maximal membrane insertion compared to unmodified PG. Complete membrane insertion with liposomes containing 2',3'-dimethyl-DMPG or 2'-methyl-DMPG was not observed even at 10 mM Ca^{2+}. In contrast, with liposomes containing 3'-methyl-DMPG, almost complete insertion was observed at 1.0 mM Ca^{2+}; however, this analog was much less responsive to Ca^{2+} than unmodified PG at lower Ca^{2+} concentrations.

Daptomycin exhibited an equal ability to insert into liposomes containing either 2'- and 3'-deoxy PGs demonstrating that each hydroxyl group is required for membrane insertion. In contrast, daptomycin required much more Ca^{2+} for insertion into liposomes containing 2'-methyl-DMPG compared to liposomes containing 3'-methyl-DMPG. Combined, these results suggest that the binding pocket surrounding each hydroxyl group is distinct. The pocket appears to be tight around the 2'-OH group and is thus significantly perturbed by methylation at this position. In contrast, the binding pocket around the 3'-OH group is spacious and some of the interaction energy lost by destroying a hydrogen bond is gained by the methyl group extending into and filling the gap. This may explain why daptomycin possesses a preference for the 3'-methyl headgroup over the 3'-deoxy headgroup.

Circular dichroism (CD) has been used to demonstrate that daptomycin undergoes a large conformational change in the presence of calcium and membranes containing PG.[24,80,257] The impact of headgroup modification on the conformation of membrane-bound daptomycin was analyzed using CD. On the basis of the data in Figure 6.1A, calcium concentrations were selected such that at least 90% of the daptomycin present was bound to the LUV containing the modified PG. Thus, CD studies were done at Ca^{2+} concentrations that yielded the same degree of binding for each LUV used. In solution, daptomycin possess a wave-like CD trace which inverts and increases in amplitude upon insertion into a PG-containing membrane in the presence of calcium. [24,80,257] Figure 6.1B shows the CD traces collected on daptomycin bound to each modified PG. Methylation of either hydroxyl group substantially impacts the CD trace; however, methylation at the 2' position seemed to cause the greatest perturbation. Methylation at both positions greatly disturbed the backbone conformation. In comparison, deoxygenation had a stronger impact on the backbone conformation than monomethylation but a weaker impact than dimethylation. These data clearly show that the backbone conformation of daptomycin is sensitive to the headgroup of DMPG and both hydroxyl groups are needed to achieve the natural state.
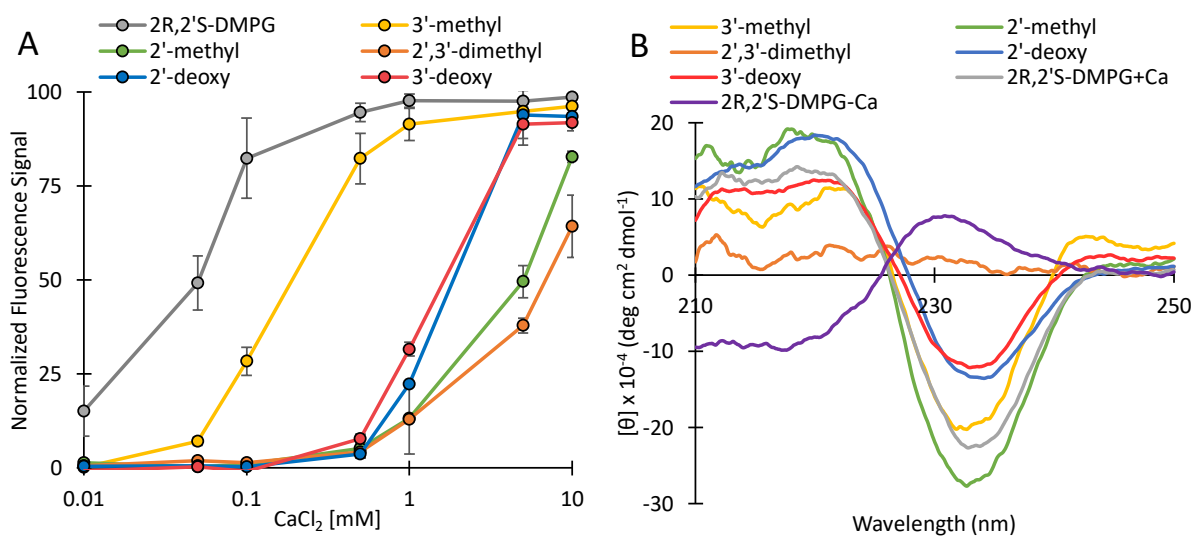
Figure 6.1 (A) Membrane binding curves for daptomycin using LUVs composed of 1:1 modified-DMPG:DMPC at 37 °C in 20 mM HEPES, 150 mM NaCl (pH 7.4). The membrane binding curve for daptomycin using LUVs composed of 2R,2'S-DMPG:DMPC (1:1) is shown for comparison. (B) CD spectra of daptomycin (15 µM) in the presence of LUVs (180 µM) composed of equal parts DMPC and modified-DMPG. A calcium concentration of 5 mM was used when the DMPG component was 2R,2'S-DMPG, 3'-methyl-DMPG, 3'-deoxy-DMPG or 2'-deoxy-DMPG. A calcium concentration of 50 mM was used when the DMPG component was 2',3'-dimethyl-DMPG or 2'-methyl-DMPG.

Daptomycin is known to oligomerize on PG containing membranes in the presence of calcium and this self-association is implicated in its action mechanism. One method that has been used for monitoring the oligomerization of daptomycin employs a daptomycin analog that possesses a perylene tail instead of a decanoic acid tail.[88] When two perylene units come into close contact with one another, excimer emission (520 nm) can be observed which is readily distinguished from the monomer emission (455 nm). Thus, by comparing the emission spectra of perylene-daptomycin bound to various unusual DMPGs, the influence of each lipid modification on the oligomerization event can be determined.

The extent of oligomerization of perylene daptomycin bound to each membrane is presented in Table 6.3 (see Figure D.3 for spectrograms). As in the CD experiments, the calcium concentration was modified such that perylene-daptomycin was fully bound to each membrane during analysis. The extent of oligomerization is described by a ratio in the intensity at 560 nm (where excimer emission is dominant) to 455 nm (where the monomer emission is dominant). Dimethylation of the headgroup and monomethylation at the 2'-OH greatly impeded oligomerization while monomethylation of the 3'-OH gave intermediate results. Interestingly, deoxygenation at the 2' or 3' position increased excimer formation suggesting that deoxygenation influences the structure of the oligomer.

Table 6.3 I_{560}/I_{455} Ratios Obtained from the Fluorescence Spectra of Perylene-daptomycin in the Presence of Ca^{2+} and LUVs Composed of equal parts DMPC and modified DMPGs.

PG	I_{560}/I_{455} ([CaCl$_2$])

2R,2'S-DMPG	0.21 ± 0.02 (5 mM)
2',3'-dimethyl-PG	0.054 ± 0.001 (50 mM)
2'-methyl-DMPG	0.058 ± 0.001 (50 mM)
3'-methyl-DMPG	0.110 ± 0.002 (5 mM)
3'-deoxy-DMPG	0.32 ± 0.02 (5 mM)
2'-deoxy-DMPG	0.260 ± 0.008 (5 mM)

[a]errors are the standard deviation between 3 separate trials

To investigate the minimal lipid length in PG that is required for daptomycin-PG interactions, we prepared several PGs with linear saturated lipids having 4, 6 or 8 carbons (Scheme 6.2). This was readily achieved by reacting the appropriate acyl glycerol (**6.19**-**6.21**, Scheme 6.4 in the experimental) with bis(diisopropylamino)benzyl phosphoramidite yielding phosphoramidites **6.22**-**6.24**. These materials were reacted with a benzylidene-protected glycerol **R**-**6.33** or **S**-**6.33** yielding the phosphotriesters **6.25**-**6.28** after oxidation. The desired PG, **6.29**-**6.32**, were obtained by subjecting **6.25**-**6.28** to hydrogenolysis followed by conversion to their sodium salts.
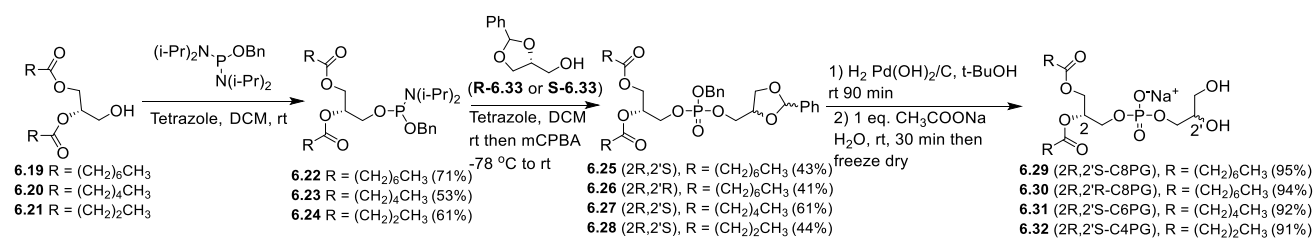
Scheme 6.2 Synthesis of PGs with short lipids.

Titrating Ca^{2+} into a solution of daptomycin and 250 μM 2R,2'S-C4PG resulted in no change in fluorescence even at 10 mM Ca^{2+}. With 250 μM 2R,2'S-C6PG (Figure 6.2A) only a very modest increase in fluorescence was observed as the Ca^{2+} concentration increases from 1-10 mM. However, with 250 μM 2R,2'S-C8PG, the fluorescence readily increased with Ca^{2+} concentration and maximal fluorescence was observed at 0.5-1.0 mM Ca^{2+}. The absolute increase in fluorescence

was only slightly less than that observed when using liposomes consisting of 2R,2'S-DMPG:DMPC (1:1) or just 250 μM 2R,2'S-DMPG (Figure 6.2A). In the case of 250 μM 2R,2'S-DMPG, the fluorescence signal reached a maximum at a much lower calcium concentration compared to what was observed using 2R,2'S-C8PG or LUVs containing 2R,2'S-DMPG/DMPC, but the absolute change in fluorescence intensity was similar. Commercial DMPG has a critical micelle concentration (CMC) of only 11 μM in water and this value would be expected to be considerably lower in saline buffer in the presence of Ca^{2+}.[270] Therefore, it is likely that daptomycin, in the presence of 250 μM 2R,2'S-DMPG and Ca^{2+}, is interacting with a bilayer form of DMPG. Commercial C6PG and C8PG have CMCs of 11 mM and 1.2 mM respectively in water.[270] Using 1-pyrenecarboxyaldehyde fluorescence, we determined the CMC of 2R,2'S-C8PG in the presence of 5 mM Ca^{2+} in 20 mM HEPES buffer, (pH 7.4) to be 300 μM (Figure D.2) which is greater than the concentration of 2R,2'S-C8PG (250 μM) used in Figure 6.2A. 2R,2'S-C6PG and 2R,2'S-C4PG would be expected to have higher CMCs.

The state of daptomycin bound to 2R,2'S-C8PG was studied using the same techniques used above for studying daptomycin bound to methylated and deoxygenated PGs. To determine if daptomycin prefers the S configuration at the head group of C8PG, Ca^{2+} was titrated into a solution of daptomycin and 250 μM 2R,2'R-C8PG and the change in fluorescence was monitored (Figure 6.2A). Maximal fluorescence was not achieved until 10 mM Ca^{2+} and the absolute fluorescence intensity observed at this calcium concentration was ~40% less than what was observed using with 2R,2'S-C8PG at the same calcium concentration. Titrating a solution of C8PG into a solution of daptomycin in the presence of 0.1 mM $CaCl_2$ shows that significantly more 2R,2'R-C8PG is needed to desolvate Kyn13 to the same extent as 2R,2'S-C8PG (Figure 6.2B). Repeating this experiment at 5 mM $CaCl_2$ demonstrates that both isomers bind to daptomycin in a stoichiometric

fashion (Figure 6.2C). In contrast, two equivalents of DMPG are needed to saturate daptomycin under the same conditions when the DMPG is incorporated into an LUV. This is probably because daptomycin can only access the outer leaflet of the LUV.
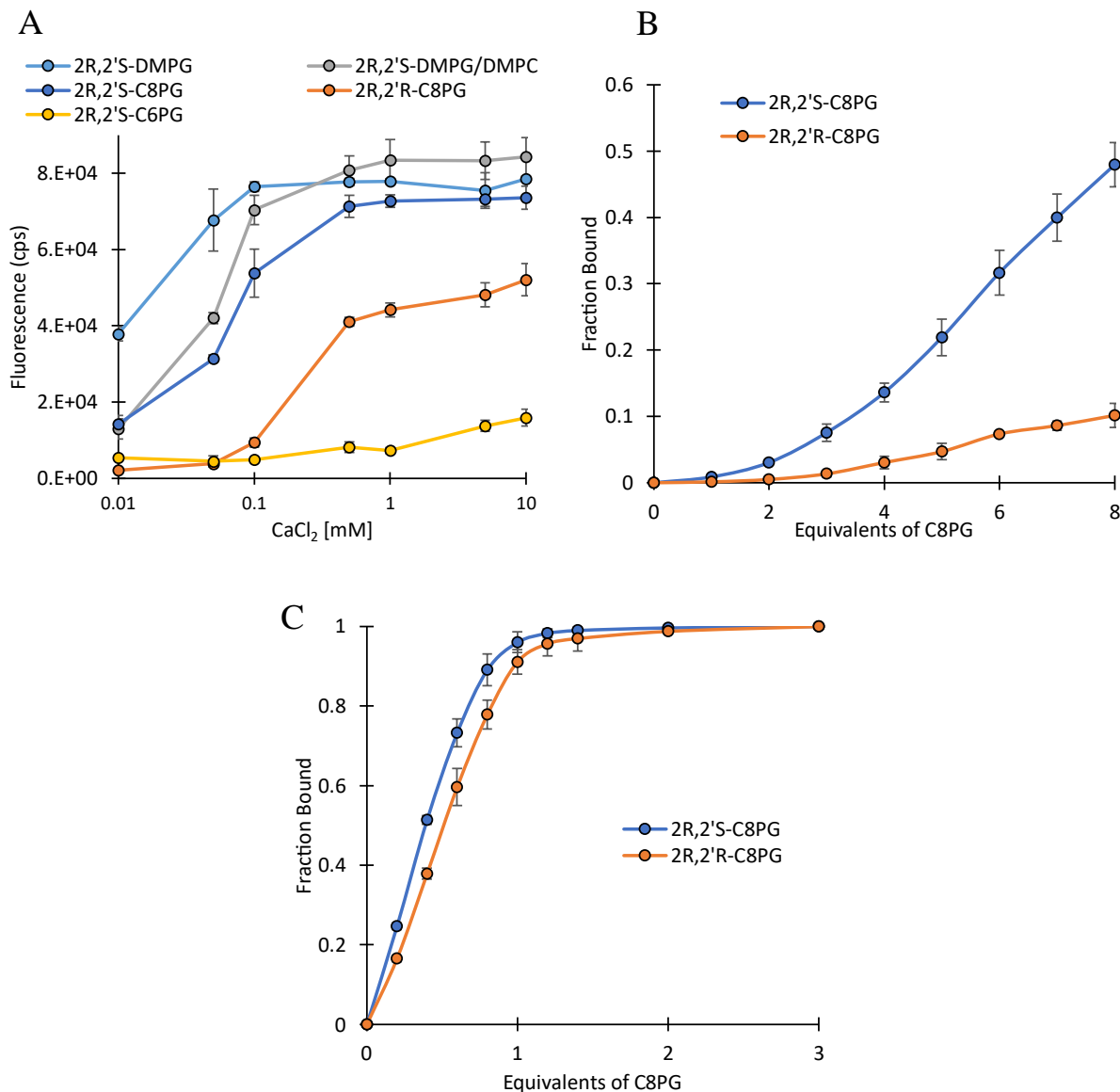

Figure 6.2 Monitoring the change in the fluorescence of Kyn as a function of [$CaCl_2$] or equivalents of PG. (A) The fluorescence intensity of daptomycin (3 µM) bound to PG-lipids (total lipid concentration is 250 µM) with various PG lipid lengths and in various states. (B) The binding of daptomycin (15 µM) to C8PG at 0.1 mM $CaCl_2$. The fully bound state was achieved by increasing the $CaCl_2$ concentration to 5 mM at the end of the titration (C) The binding of daptomycin (15 µM) to C8PG at 5 mM $CaCl_2$

To determine if daptomycin in the presence of the short chain PGs undergoes the same structural transitions that occur when daptomycin interacts with a PG-containing bilayer, we obtained the CD spectra of daptomycin in the presence of stoichiometric amounts of C8PG, C6PG and C4PG (Figure 4A). A stoichiometric amount of 2R,2'S-C6PG was found to give a partial CD response indicating that some of the daptomycin was bound under these conditions; however, the binding was weak, and 6 equivalents of lipid were needed to achieve a complete response. With 2R,2'S-C4PG no CD response was observed even in the presence of 100 equivalents of 2R,2'S-C4PG and 10 mM $CaCl_2$. In contrast, we observed a complete CD transition with just 1 equivalent of 2R,2'S-C8PG and a nearly complete transition with 2R,2'R-C8PG.
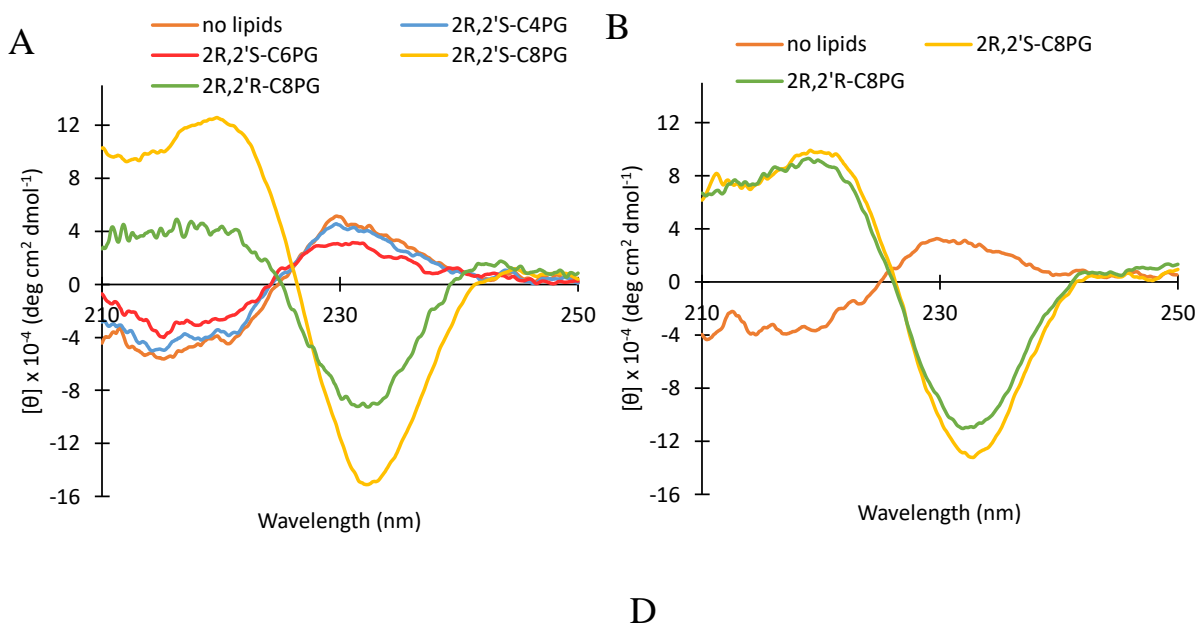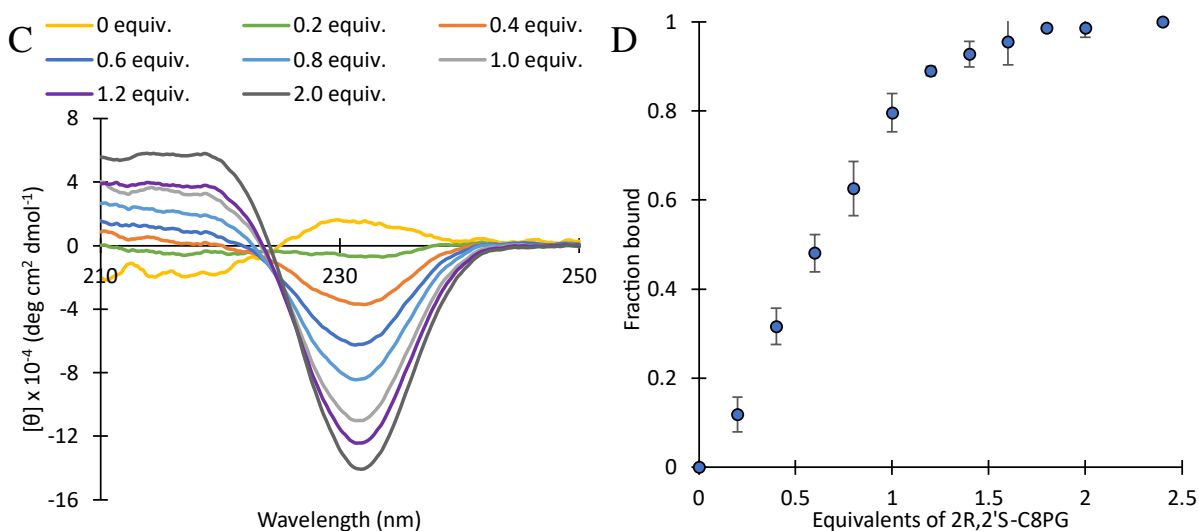
Figure 6.3 CD traces presented as $[\theta] \times 10^{-4}$ (deg cm^2 dmol^{-1}) vs. wavelength (nm) plots. For A-C the buffer was 20 mM HEPES pH = 7.4. The calcium concentration was adjusted to 5 mM and then the analysis was performed after a 3 min mixing time. (A) CD traces of daptomycin (15 μM) in solution with or without stoichiometric amounts of 2R,2'S-C8PG, 2R,2'R-C8PG, 2R,2'S-C6PG or 2R,2'S-C4PG. (B) CD traces of daptomycin (15 μM) in solution or bound to 2R,2'S-C8PG or 2R,2'R-C8PG (180 μM total lipid concentration). (C) CD traces of daptomycin (15 μM) in the presence of various concentrations of 2R,2'S-C8PG (D) Fraction of daptomycin (15 μM) bound to 2R,2'S-C8PG as a function of equivalents of 2R,2'S-C8PG present. This titration was performed in triplicate, the average of these three trials is presented.

Figure 6.3B shows the CD trace of daptomycin in the presence of excess C8PG. The CD trace of daptomycin bound to 2R,2'S-C8PG is very similar to the CD trace of daptomycin bound to LUVs containing 2R,2'S-DMPG/DMPC indicating that the state of daptomycin is similar in these two environments. This is rather unexpected since the lipid concentration (180 μM) is well below the CMC for C8PG at 5 mM CaCl₂ (300 μM) and the complexes must be formed in the absence of a membrane. In addition, the curve for daptomycin bound to 2R,2'R-C8PG is similar to 2R,2'S-C8PG implying that the backbone conformation of daptomycin is marginally influenced by the headgroup configuration of PG which is consistent with previous observations made on daptomycin bound to PG-containing LUVs.

Previously, Lee at al. used CD and model membranes containing PG to determine the daptomycin-calcium-PG ratio.[257] They concluded that daptomycin binds to PG stoichiometrically

173

assuming that daptomycin can only access the PG on the outer leaflet of the membrane bilayer. It is unclear whether daptomycin can translocate on small unilamellar vesicles (SUVs) composed of POPG/POPC which is what Lee et al used in their studies. Kruetzberger et al did not observe the transfer of daptomycin from the outer membrane of giant unilamellar vesicles (GUVs) to inner vesicles suggesting that translocation does not occur. In contrast, Taylor et al found that a significant fraction (~25%) of labelled daptomycin was protected from quenching when bound to POPC/POPG LUVs suggesting that partial translocation does occur, but this effect is strongly influenced by lipid tail length and can not be deconvoluted from the changes in membrane stability caused by altering the lipid tail. To determine the ratio between daptomycin and PG in the absence of a membrane, we titrated daptomycin with 2R,2'S-C8PG at 5 mM $CaCl_2$ and found that 80% of daptomycin was bound when 1 equivalent of 2R,2'S-C8PG was present indicating that the interaction with daptomycin is likely stoichiometric (Figures 6.3C and 6.3D).

Based on the results of the fluorescence (Figure 6.2) and CD (Figure 6.3) studies, the affinity of daptomycin for short chain lipids appears to be dependent on acyl tail chain length and at least 7-8 carbons are required for stoichiometric binding at micromolar peptide concentrations.

We investigated the oligomeric state of daptomycin bound to 2R,2'S-C8PG or 2R,2'R-C8PG using perylene excimer formation. It was found that perylene-daptomycin oligomerizes much more readily when in the presence of excess 2R,2'S-C8PG compared to 2R,2'R-C8PG; however, in both cases the extent of oligomerization was as high if not higher than what was observed with PG/PC LUVs (Figure 6.4).
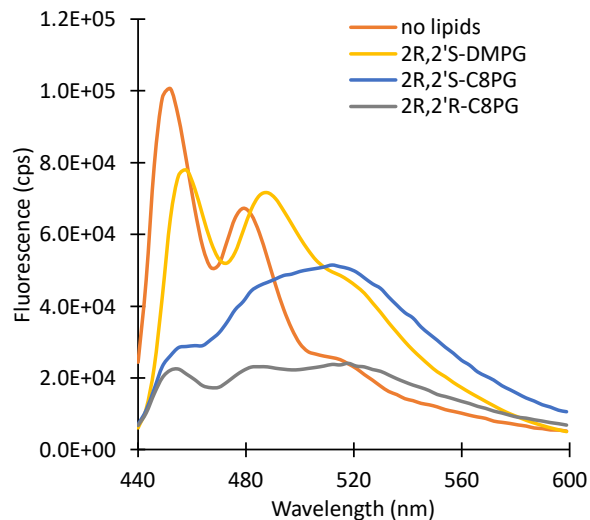
Figure 6.4 Fluorescence of perylene-daptomycin (2.5 μM) in the presence of 250 μM 2R,2'S-C8PG or 2R,2'R-C8PG and 5 mM $CaCl_2$ at 25 °C. A spectrum of perylene-daptomycin (2.5 μM) bound to a LUV containing 2R,2'S-DMPG:DMPC 1:1 in the presence of 5 mM $CaCl_2$ at 25 °C is shown for comparison.

CD and fluorescence studies suggest that daptomycin binds avidly and stoichiometrically to 2R,2'S-C8PG at micromolar concentrations. To confirm this, and to determine the dissociation constant (K_D) of daptomycin for 2R,2'S-C8PG, we used isothermal titration calorimetry (ITC). In this experiment, a solution of daptomycin and calcium was titrated with a concentrated solution of 2R,2'S-C8PG in the same buffer. This gave a titration curve which was fit using Microcal's Origin single binding site model. Figure 6.5 shows a representative curve for the titration of daptomycin with 2R,2'S-C8PG at 5 mM $CaCl_2$. We find that daptomycin possesses a single binding site for 2R,2'S-C8PG (N = 1.0 ± 0.1) to which it binds with an apparent dissociation constant of $K_D = 3.1 ± 0.9$ μM. This K_D value is very similar to the K_D value of 1.7 μM that was reported for daptomycin binding to LUVs consisting of 25% DOPG/75% DOPC in the same buffer system at 5 mM Ca^{2+} using a one-site binding model.[72]
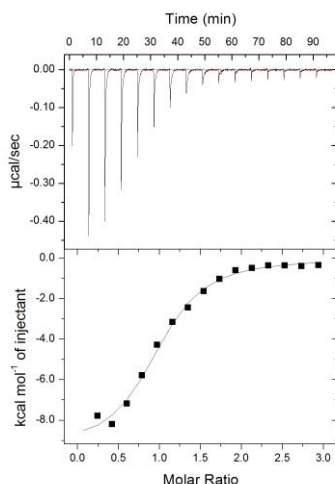
Figure 6.5 A representative thermogram obtained from titrating a solution of daptomycin (23 μM) with 2R,2'S-C8PG at 5 mM CaCl$_2$. Top panels show the raw ITC heat signals. Bottom panels show the integrated isotherms. The solid line shows the best-fit curve determined by Microcal's Origin single binding site model. This titration was performed 4 times (see Figure D.1).

6.3 Conclusions

Through the synthesis of nine modified PGs and studying their interactions with daptomycin we have ascertained details about the interaction of these two molecules. We found that both the 2' and 3' hydroxyl groups of PG influence the membrane affinity, membrane bound structure and oligomerization of daptomycin. The binding pocket surrounding each hydroxyl group is unique with modification at the 3' position being more tolerated than the same modification at the 2' position.

It is known that daptomycin resistant strains of *S. aureus* subvert the action of daptomycin through conversion of PG to alanyl- or lysyl-PG and it has been speculated that this resistance mechanism functions by reducing the negative charge on PG. Our results show that just simple methylation of either hydroxyl in the head group impedes the ability of daptomycin to interact with PG. This suggests that 3' acylation with alanine or lysine should impede the interaction of

daptomycin with the lipid and that this resistance mechanism may not necessarily function solely by reducing membrane charge.

Studies on PGs with unnaturally short lipids revealed that 7-8 carbons are needed for stoichiometric binding at micromolar peptide concentrations and 5 mM $CaCl_2$. Under these conditions, 2R,2'S-C8PG does not form micelles. Thus, studies with 2R,2'S-C8PG allow for the investigation of daptomycin-PG interactions in the absence of a membrane bilayer. Our studies show that daptomycin interacts with 2R,2'S-C8PG in essentially the same manner as when the PG is incorporated into an LUV, and thus preassembly of individual PG moieties is not a prerequisite for binding, structural transition, and oligomerization.

Previous attempts to ascertain daptomycin-PG stoichiometry have been complicated by the fact that daptomycin can not readily access both leaflets of a membrane bilayer. Studies using C8PG reveal that the structural transition, heat of binding and Kyn13 insertion of daptomycin are all saturated with a single equivalent of 2R,2'S-C8PG. These results conclusively demonstrate that daptomycin forms a complex with a single equivalent with PG and this complex can form in outside of a membrane bilayer.

In closing, these studies help to build a more detailed picture of daptomycin's interaction with PG and further define daptomycin as a PG-targeting antibiotic.

6.4 Experimental
General Methods.

All reagents and solvents were purchased from commercial suppliers. Methylene chloride (DCM) was dried by distillation over calcium hydride under nitrogen. Acetonitrile (MeCN) was dried by distilling over P_2O_5 then CaH_2 and allowing to stand over 4A sieves overnight. Tetrahydrofuran

(THF) was distilled from sodium metal in the presence of benzophenone under N_2. Chromatography was preformed using 60 Å silica gel.

High resolution positive electrospray (ESI) mass spectra were obtained using an orbitrap mass spectrometer. Samples were sprayed from MeOH: 1% formic acid in H_2O. All spectra were collected in the positive mode. ^{1}H- and ^{13}C-NMR were collected using either a Bruker Avance-300 or a Bruker Avance-500 spectrophotometer. Proton Chemical shifts (δ) for samples run in $CDCl_3$ are reported in ppm relative to an internal standard (trimethylsilane, 0 ppm). For samples run in CD_3OD, δ was relative to the solvent peak (3.31 ppm). For ^{13}C-NMR samples run in $CDCl_3$ chemical shifts are reported relative to the solvent peak (77.0 ppm). For samples run in CD_3OD, δ was relative to the solvent peak (49.2 ppm).

6.33 and **6.34** were prepared according to the procedure disclosed by Denny et al (Scheme 6.3).[271] Methyl ether **6.35** was prepared according to the procedure by Goddard et al.[272] Alcohol **6.1** was prepared according to the procedure by Fischer and coworkers.[273] **6.36** was prepared according to the procedure by Tateishi et al (Scheme 6.3).[274] **6.37** was prepared according to a patent by Duclos.[275] **6.6** was prepared according to Townsend and coworkers.[268] **6.19** was prepared according the procedure of Conway et al.[276] **6.20** and **6.21** were prepared from ethers **6.38** and **6.39** which were prepared according to the procedure disclosed by Martin et al (Scheme 6.4).[277] **R-6.33** and **S-6.33** were prepared via our procedure.[278]

MIC determinations were performed as previously described.[223]

Determining critical micelle concentration via 1-pyrenecarboxyaldehyde fluorescence.

Critical micelle concentrations of short chains lipids were determined as previously described.[279] Briefly, C8PG was added incrementally to a solution of 1-pyrenecarboxaldehyde (1 µM) in buffer

(20 mM HEPES, 150 mM NaCl, 5 mM CaCl$_2$, 1% DMSO (v/v), pH = 7.4). After each addition, the solution was thoroughly mixed and the emission spectrum was collected (λ_{ex} = 356 nm, λ_{em} = 400-600 nm). The wavelength of maximum emission was determined from each spectrum and plotted as a function of [C8PG].

Liposome preparation.

Large unilamellar vesicles were prepared as previously described.[86] DMPC (1,2-dimyristoyl-sn-glycero-3-phosphocholine) and commercial DMPG (1,2-dimyristoyl-sn-glycero-3-phospho-(1'-rac-glycerol)(sodium salt)) were purchased from Avanti Polar Lipids. DMPC and a second lipid component were combined in a 1:1 molar ratio in chloroform. The chloroform was removed under an N$_2$ stream leaving a thin film of lipid coating the interior of a round-bottom flask. Trace chloroform was removed under high vacuum then the lipids were hydrated with a pH 7.4 buffer (20 mM HEPES, 150 mM NaCl). Extrusion through a 100 nm polycarbonate filter yielded at a total lipid concentration of 5 mM.

Kynurenine fluorescence.

This procedure was adapted from the assay described by Taylor et al.[81] Fluorescence was measured in Corning Costar half-area flat bottom black polystyrene 96-well plates using a Tecan Infinite M1000 instrument. 100 µM peptide stocks were diluted with pH 7.4 buffer (20 mM HEPES, 150 mM NaCl) and preheated to 37°C before adding the above-mentioned liposome solution and immediately dispensing 90 µL aliquots into wells pre-loaded with 10µl of buffer containing CaCl$_2$ at 10x the desired calcium concentration (plate had also been preheated to 37°C) giving a final volume of 100 µL in each well. The final concentrations in each well were 5 µM of peptide, and 250 µM of lipid. Fluorescence measurements were timed to allow for a 3-4 minute

incubation period at 37°C. Emission spectra were acquired for kynurenine (Excitation: 365 nm, 5 nm bandwidth) intrinsic fluorescence using 100 flashes at 400 Hz and a step size of 3 nm. Emission spectra for blanks containing 250 µM lipid in buffer and 5 µM peptide were also collected.

Circular dichroism studies.

Steady State CD Studies

Circular dichroism (CD) traces were collected using a Jasco J-815 CD spectrophotometer. The peptide concentration of each solution was 15 µM in 20 mM HEPES buffer (pH 7.4). Samples were measured at room temperature from 210-250 nm at a scan rate of 10 nm min^{-1} with a digital integration time of 2 seconds and a bandwidth 1 nm. A 1 mm quartz cuvette was used. The outputted data was converted to molar ellipticity in units of deg cm^2 dmol^{-1}. For traces collected using C4, C6, C8PG a total lipid concentration of 180 µM was used. Calcium concentrations were varied across experiments as denoted in each figure description.

Titrating Daptomycin with Lipids

Dap was titrated with 2R,2'S-C8PG by mixing a sample of dap in 20 mM HEPES (pH =7.4) with an amount of 2R,2'S-C8PG dissolved in the same buffer. Additional buffer and CaCl$_2$ dissolved in the same buffer were then added to achieve a final peptide concentration of 15 µM and a final calcium concentration of 5 mM. This solution was then mixed for 3 min before collecting a CD trace using the same parameters described above. Each point was collected in triplicate. The fraction bound was determined from the molar ellipticity at 232 nm.

Perylene Studies

Perylene-daptomycin was prepared according to a previously described procedure.[88] Emission spectra were collected using a QuantMaster 4 spectrophotometer (Photon Technology International, London, ON). Samples were excited at 430 nm and the emission between 440 nm and 600 nm was recorded. Bandpasses for emission and excitation were set to 3 nm. Emission spectra were corrected for wavelength-dependent instrument response using a quinine sulfate standard.

Peryelene-dap (2.5 µM) was incubated in pH 7.4 buffer (20 mM HEPES, 150 mM NaCl) at 37 °C. To this was added $CaCl_2$ in the same buffer until the desired calcium concentration was achieved (5 mM was used most often). Once the sample had achieved thermal equilibrium. LUVs or lipids were added such that a 250 µM total lipid concentration was achieved. This sample was mixed for 3 min then the emission spectra was recorded. All reported extents of oligomerization are based on at least three replications of this experiment.

Isothermal titration calorimetry.

ITC studies were conducted using a MicroCal ITC200 microcalorimeter (Malvern Panalytical Ltd., Malvern, UK). All solutions were degassed for at least 30 minutes prior to loading into the calorimeter. A concentrated stock solution of C8PG (5 mM) was prepared in buffer without calcium (150 mM NaCl, 20 mM HEPES pH =7.4). Before the titration, the lipid stock was diluted with HEPES buffer, degassed for 30 min then a small volume of calcium chloride dissolved in the same HEPES buffer was added just before starting the titration such that the $CaCl_2$ concentration in the syringe was 5 mM. The concentration of C8PG in the ITC syringe was 0.33 mM. The cell was filled with a solution of daptomycin (23 µM) in buffer which included $CaCl_2$ (20 mM HEPES, 150 mM NaCl, 5 mM $CaCl_2$, pH = 7.4). Titrations were conducted at 25 °C with constant stirring

(1000 rpm). The volume of the first injection was 1.0 µL, all subsequent injections were 2.5 µL with a 360 s delay between each injection.

The ITC data was post-processed by the proprietary Origin software provided by Microcal. Binding constants were determined from a least-squares analysis of the integrated heat signals using Origin's one-site binding model. Four runs in total were collected. Heats of dilution were small and constant. These were compared to but not subtracted from the collected data.[72]

Scheme 6.3 Synthesis of modified glycerol **6.2,6.3** and **6.5**
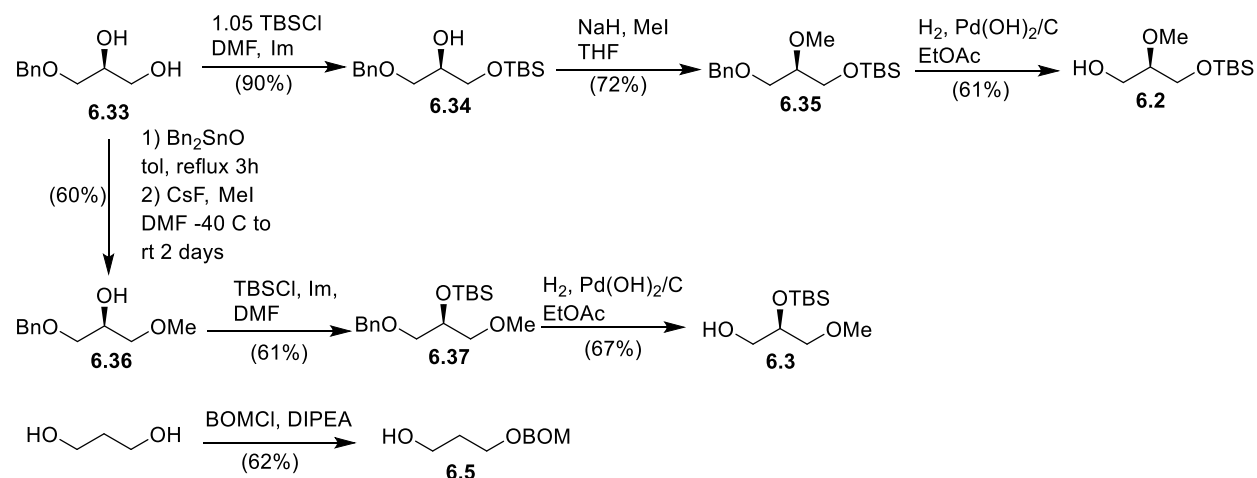
Scheme 6.4 Preparation of **6.20** and **6.21**

6.38 R = (CH$_2$)$_4$CH$_3$
6.39 R = (CH$_2$)$_2$CH$_3$

6.20 R = (CH$_2$)$_4$CH$_3$ (53%)
6.21 R = (CH$_2$)$_2$CH$_3$ (61%)
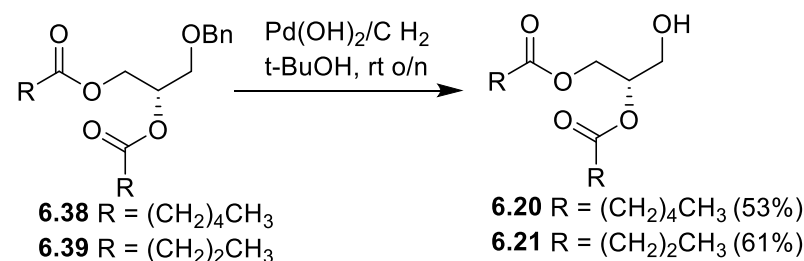
General procedure A for phosphoramidite coupling

P(OBn)(N(iPr)$_2$)$_2$ (2 equiv.) was combined with alcohol (1.00 equiv.) in dry dichloromethane (0.100 M substrate concentration) and this solution was stirred over 4A molecular sieves for 15

min under argon. To this solution 4,5-dicyanoimidazole (2.00 equiv.) dissolved in dry acetonitrile (0.450 M imidazole concentration) was added. The resulting solution was stirred overnight at room temperature and then filtered over celite that was pre-treated with 3% triethylamine / 97% hexanes. The filtrate was concentrated and purified by silica gel column chromatography. The silica was pre-neutralized with triethylamine.

General procedure B for phosphoramidite coupling

Phosphoramidite (0.667 mmol, 1.00 equiv.) was combined with alcohol (0.667 mmol, 1.00 equiv.) in dry dichloromethane (13.5 mL) and stirred over 4A powdered molecular sieves under argon for 15 min. A solution of 4,5-dicyanoimidazole (105 mg, 0.888 mmol, 1.33 equiv.) in dry acetonitrile (5 mL) was added dropwise at room temperature and resulting solution was stirred at room temperature for 18 hours. The reaction mixture was cooled (dry ice-acetone bath) and meta-chloroperoxybenzoicacid (230 mg, 1.33 mmol, 2.00 equiv.) dissolved in dichloromethane (3 mL) was added dropwise. Cooling was removed and the solution was stirred for 2 hours. The sieves were then removed by filtering the reaction mixture over celite. The filter cake was extracted several times with dichloromethane and the filtrate was washed with saturated aqueous $NaHCO_3$ and then dried over $MgSO_4$. After concentration, the phosphotriester was isolated by silica gel column chromatography.

General procedure C for hydrogenolysis of protected phosphatidylglycerols

Phosphotriester (1.00 equiv.) was combined with $Pd(OH)_2/C$ (20% w/w, 0.80 equiv. of $Pd(OH)_2$) in tert-butanol (0.0500 M substrate concentration) at room temperature and stirred under an atmosphere of hydrogen until TLC showed that the reaction had proceeded to completion (usually less than 2 hours). The reaction mixture was filtered over celite and the celite was rinsed with

chloroform several times. The solvent was removed under high vacuum at <35 $^{\circ}$C. The residue was concentrated from chloroform several times and then suspended in an aqueous solution of sodium acetate (0.0300 M, 1.00 equiv.). The suspension was vortexed and then stirred for 30 min at room temperature. The solution was frozen (dry ice-acetone bath) and then lyophilized.

(R)-2,3-dimethoxypropan-1-ol (**6.1**)

6.1 was prepared as described previously.[273] ^{1}H NMR (300 MHz, CDCl$_3$): 3.74 (1H, dd, $J = 4.1$, 11.6 Hz) 3.62 (1H, dd, $J = 5.3$, 11.6 Hz) 3.51-3.37 (8H, m) 2.90 (1H, br. s). ^{13}C NMR (75 MHz, CDCl$_3$): δ 80.0, 72.3, 62.2, 59.3, 57.7. HRMS-ESI+ (*m/z*): [M + H]$^+$ calculated for C$_5$H$_{13}$O$_3$, 121.08592; found, 121.08585.

(R)-3-((tert-butyldimethylsilyl)oxy)-2-methoxypropan-1-ol (**6.2**)

A solution of **6.35** (2.82 g, 3.17 mmol) and Pd(OH)$_2$/C (20% w/w, 563 mg) in EtOAc (40 mL) was stirred under H$_2$ for 16 hours at room temperature. The solution was then filtered over celite and the EtOAc was removed by concentrating under a stream of N$_2$ at room temperature. This yielded pure 2 as a colorless oil (1.34 g, 67% yield). ^{1}H NMR (300 MHz, CDCl$_3$): 3.82-3.75 (2H, m) 3.70-3.62 (2H, m) 3.49 (3H, s) 3.39-3.33 (1H, m) 2.14 (1H, dd, $J = 5.0$, 5.8 Hz) 0.92 (9H, m) 0.1 (6H, m). ^{13}C NMR (75 MHz, CDCl$_3$): δ81.3, 62.7, 62.6, 57.9, 25.8, 18.2, -5.5. HRMS-ESI+ (*m/z*): [M + H]$^+$ calculated for C$_{10}$H$_{25}$O$_3$Si, 221.15675; found, 221.15763.

(R)-2-((tert-butyldimethylsilyl)oxy)-3-methoxypropan-1-ol (**6.3**)

6.3 was prepared from **6.37** following the same procedure outlined for the synthesis of **6.2**. This yielded **6.3** as a colorless oil (916 mg, 61% yield). ^{1}H NMR (300 MHz, CDCl$_3$): 3.90 (1H, tt, $J = 5.9$, 4.6 Hz) 3.63 (2H, m) 3.43-3.40 (2H, m) 3.38 (3H, s) 2.07 (1H, dd, $J = 5.6$, 6.6 Hz) 0.92 (9H,

s) 0.12 (6H, m). ^{13}C NMR (75 MHz, CDCl$_3$): δ74.5, 71.2, 64.8, 59.2, 25.8, 18.1, -4.6, -4.9. HRMS-ESI+ (*m/z*): [M + H]$^+$ calculated for C$_{10}$H$_{25}$O$_3$Si, 221.15675; found, 221.15585.

3-((benzyloxy)methoxy)propan-1-ol (**6.5**)

1,3-propandiol (1.00g, 13.14 mmol, 1.00 equiv.) was diluted in dry dichloromethane (12.5 mL) and the solution was cooled (ice-water bath). To this cooled solution was added diisopropylethylamine (3.45 mL, 19.80 mmol, 1.50 equiv) followed by freshly distilled BOMCl (2.38g, 15.17 mmol, 1.15 equiv.). Cooling was removed and the reaction was stirred under argon overnight at room temperature. The reaction mixture was concentrated and purified by silica gel column chromatography (50% ethyl acetate/50% hexanes) yielding **6.5** as a colorless oil (1.60g, 62% yield). ^{1}H NMR (500 MHz, CDCl$_3$): 7.39-7.29 (5H, m) 4.78 (2H, s) 4.63 (2H, s) 3.79-3.76 (4H, m) 2.38 (1H, br. s) 1.88 (2H, app quintet, *J* = 5.9 Hz). ^{13}C NMR (125 MHz, CDCl$_3$): δ137.8, 128.5, 127.9, 127.8, 94.7, 69.5, 66.3, 61.1, 32.2 HRMS-ESI+ (*m/z*): [M + Na]$^+$ calculated for C$_{11}$H$_{16}$O$_3$Na, 219.09917; found, 219.09827.

(2R)-3-(((benzyloxy)((S)-2,3-dimethoxypropoxy)phosphoryl)oxy)propane-1,2-diyl

ditetradecanoate (**6.7**)

7 was prepared according to general procedure B using phosphoramidite **6.6** and alcohol **6.1**. Crude **7** was purified by silica gel column chromatography (30% ethyl acetate/70% hexanes to 40% ethyl acetate/60% hexanes). This yielded **7** as a colorless oil (180 mg, 52% yield). ^{1}H NMR (300 MHz, CDCl$_3$): 7.38-7.36 (5H, m) 5.20 (1H, m) 5.10-5.06 (2H, m) 4.32-4.27 (1H, m) 4.15-4.00 (5H, m) 3.49-3.42 (6H, m) 3.34-3.33 (3H, m) 2.31-2.26 (4H, m) 1.59 (4H, m) 1.25 (40H, m) 0.87 (6H, m). ^{31}P NMR (122 MHz, CDCl$_3$) δ 1.0. ^{13}C NMR (125 MHz, CDCl$_3$): δ 173.1, 172.8, 135.7, 135.6, 128.6, 128.0, 127.9, 78.6, 78.5, 71.0, 69.5, 69.5, 69.4, 69.3, 66.6, 66.5, 65.4, 61.6, 59.3, 58.0, 34.1,

34.0, 31.9, 29.6, 29.5, 29.3, 29.3, 29.1, 29.1, 24.8, 22.7, 14.1. HRMS-ESI+ (*m/z*): [M + H]$^+$ calculated for C$_{43}$H$_{78}$O$_{10}$P, 785.53271; found, 785.53375.

(2R)-3-(((benzyloxy)((S)-3-((tert-butyldimethylsilyl)oxy)-2-

methoxypropoxy)phosphoryl)oxy)propane-1,2-diyl ditetradecanoate (**6.8**)

6.8 was prepared according to general procedure B starting from phosphoramidite **6.6** and alcohol **6.2**. Crude **6.8** was purified by silica column chromatography (10% ethyl acetate/90% hexanes to 20% ethyl acetate/80% hexanes). This yielded **6.8** as a colorless oil (282 mg, 72% yield). ^{1}H NMR (300 MHz, CDCl$_3$): 7.40-7.36 (5H, m) 5.21 (1H, m) 5.12-5.08 (2H, m) 4.34-4.02 (6H, m) 3.71-3.60 (2H, m) 3.44-3.40 (4H, m) 2.33-2.28 (4H, m) 1.63-1.58 (4H, m) 1.27 (40H, m) 0.90 (15H, m) 0.07 (6H, m). ^{31}P NMR (122 MHz, CDCl$_3$) δ -0.92, -0.95.^{13}C NMR (125 MHz, CDCl$_3$): δ 173.2, 172.8, 135.8, 135.7, 128.6, 127.9, 127.9, 80.3, 80.2, 69.5, 69.4, 69.3, 66.8, 66.7, 65.4, 61.7, 61.4, 58.1, 34.1, 34.0, 31.9, 29.7, 29.5, 29.4, 29.3, 29.1, 29.1, 25.8, 24.8, 22.7, 18.2, 14.1, -5.5. HRMS-ESI+ (*m/z*): [M + H]$^+$ calculated for C$_{48}$H$_{90}$O$_{10}$PSi, 885.60354; found, 885.60669.

(2R)-3-(((benzyloxy)((S)-2-((tert-butyldimethylsilyl)oxy)-3-

methoxypropoxy)phosphoryl)oxy)propane-1,2-diyl ditetradecanoate (**6.9**)

6.9 was prepared following the same procedure reported for the synthesis of **6.8** replacing **6.2** with **6.3**. This yielded **6.9** as a colorless oil (300 mg, 75% yield). ^{1}H NMR (300 MHz, CDCl$_3$): 7.38-7.37 (5H, m) 5.19 (1H, m) 5.10-5.06 (2H, m) 4.33-4.27 (1H, m) 4.15-4.05 (4H, m) 3.96-3.91 (2H, m) 3.36-3.32 (4H, m) 2.31-2.26 (4H, m) 1.62-1.57 (4H, m) 1.26 (40H, m) 0.89 (15H, m) 0.08 (6H, m). ^{31}P NMR (122 MHz, CDCl$_3$) δ -1.1.^{13}C NMR (125 MHz, CDCl$_3$): δ 173.1, 172.7, 135.7, 135.7, 128.6, 127.9, 127.9, 73.6, 70.3, 70.2, 69.5, 69.4, 69.3, 69.1, 69.0, 65.3, 61.6, 59.2, 34.1, 34.0, 31.9,

29.6, 29.5, 29.4, 29.3, 29.1, 29.1, 25.7, 24.8, 22.7, 18.1, 14.1, -4.8. HRMS-ESI+ (*m/z*): [M + H]$^+$ calculated for C$_{48}$H$_{90}$O$_{10}$PSi, 885.60354; found, 885.61091.

(2R)-3-(((benzyloxy)(((S)-oxiran-2-yl)methoxy)phosphoryl)oxy)propane-1,2-diyl ditetradecanoate (**6.10**)

6.10 was prepared according to general procedure B using (S)-glycidol and phosphoramidite **6.6**. Crude **6.10** was purified by silica gel column chromatography (30% ethyl acetate/hexanes to 50% ethyl acetate/hexanes). This yielded **6.10** as a colorless oil (103 mg, 41% yield). ^{1}H NMR (500 MHz, CDCl$_3$): 7.41-7.38 (5H, m) 5.22 (1H, m) 5.11 (2H, dab, *J* = 8.1 Hz) 4.32-4.12 (5H, m) 3.96-3.89 (1H, m) 3.23-3.17 (1H, m) 2.84-2.82 (1H, m) 2.65-2.63 (1H, m) 2.32-2.31 (4H, m) 1.62-1.60 (4H, m) 1.27 (40H, m) 0.91-0.88 (6H, m) ^{31}P NMR (202 MHz CDCl$_3$) δ 0.12.^{13}C NMR (125 MHz, CDCl$_3$): δ 173.2, 172.8, 135.5, 135.5, 128.7, 128.7, 128.0, 69.7, 69.7, 69.7, 69.7, 69.3, 69.3, 68.3, 68.3, 68.2, 65.6, 65.5, 61.6, 49.8, 49.8, 44.4, 44.4, 34.1, 34.0, 31.9, 29.7, 29.7, 29.6, 29.5, 29.4, 29.3, 29.1, 29.1, 24.8, 22.7, 14.1. HRMS-ESI+ (*m/z*): [M + H]$^+$ calculated for C$_{41}$H$_{72}$O$_9$P, 739.49085; found, 739.48815.

(2R)-3-(((benzyloxy)(3-((benzyloxy)methoxy)propoxy)phosphoryl)oxy)propane-1,2-diyl ditetradecanoate (**6.11**)

6.11 was prepared according to general procedure B using alcohol **6.11** and phosphoramidite **6.6**. Crude **6.11** was purified by silica gel column chromatography (20% ethyl acetate/80% hexanes to 30% ethyl acetate/70% hexanes) yielding **6.11** as a colorless oil (186 mg, 42% yield). ^{1}H NMR (300 MHz, CDCl$_3$): 7.39-7.29 (10H, m) 5.21-5.19 (1H, m) 5.1-5.07 (2H, m) 4.73 (2H, s) 4.59 (2H, m) 4.32-4.29 (1H, m) 4.19-4.11 (5H, m) 3.67-3.65 (2H, m) 2.30 (4H, m) 1.94 (2H, m) 1.61 (4H, m) 1.28 (40H, m) 0.91-0.89 (6H, m). ^{31}P NMR (202 MHz, CDCl$_3$) δ 0.28.^{13}C NMR (125 MHz, CDCl$_3$): δ 173.2, 172.8, 137.8, 135.7, 135.7, 128.6, 128.4, 127.9, 127.8, 127.7, 94.6, 69.5, 69.4, 69.4, 69.4, 69.3, 65.3, 65.3, 65.2, 65.1, 63.6, 61.6, 34.1, 34.0, 31.9, 30.5, 30.5, 29.7, 29.7, 29.6,

29.5, 29.4, 29.3, 29.1, 29.1, 24.8, 22.7, 14.1. HRMS-ESI+ (*m/z*): [M + H]$^+$ calculated for C$_{49}$H$_{82}$O$_{10}$P, 861.56401; found, 861.56455.

sodium (R)-2,3-bis(tetradecanoyloxy)propyl ((S)-2,3-dimethoxypropyl) phosphate (**6.12**)

6.12 was prepared according to general procedure C starting from **6.7** (161 mg, 99% yield). ^{1}H NMR (300 MHz, 95:5 CDCl$_3$:CD$_3$OD): 5.25-5.18 (1H, m) 4.36 (1H, dd, *J* = 12.0, 2.9 Hz) 4.14 (1H, dd, *J* = 12.0, 6.6 Hz) 3.92-3.89 (4H, m) 3.52-3.43 (6H, m) 3.34 (3H, m) 2.31-2.24 (4H, m) 1.57-1.55 (4H, m) 1.23 (40H, m) 0.87-0.83 (6H, m). ^{31}P NMR (122 MHz, 95:5 CDCl$_3$:CD$_3$OD) δ 1.1.^{13}C NMR (125 MHz, 95:5 CDCl$_3$:CD$_3$OD): δ 173.7, 173.5, 79.1, 79.0, 71.5, 70.5, 70.4, 64.5, 63.4, 62.6, 59.1, 57.6, 34.2, 34.0, 31.9, 29.6, 29.5, 29.3, 29.1, 24.9, 24.8, 22.6, 14.0. HRMS-ESI+ (*m/z*): [M + H]$^+$ calculated for C$_{36}$H$_{72}$O$_{10}$P, 695.48576; found, 695.48618.

(2R)-3-(((benzyloxy)((S)-3-hydroxy-2-methoxypropoxy)phosphoryl)oxy)propane-1,2-diyl

ditetradecanoate (**6.13**)

To a solution of **6.8** (295 mg, 0.333 mmol) in dry THF (6.7 mL) at room temperature under Ar was added acetic acid (38 µL, 0.666 mmol, 2 equiv.) followed by Tetrabutylammonium fluoride (1M in THF dried over 3A sieves for 2 days; 666 µL, 0.666 mmol, 2 equiv.). After mixing for 16 hours, the reaction was quenched through the addition of silica and the solvent was removed. **6.13** was isolated via silica gel column chromatography (70% EtOAc / 30% hexanes) this gave **6.13** as colorless oil (136 mg, 53% yield). ^{1}H NMR (300 MHz, CDCl$_3$): 7.40-7.36 (5H, m) 5.21 (1H, app sextet, J = 5.5 Hz) 5.10 (2H, m) 4.30 (1H, dd, J = 4.3, 11.9 Hz) 4.17-4.09 (5H, m) 3.71 (1H, dd, J = 2.3, 5.0, 11.8 Hz) 3.69 (1H, dd, J = 5.0, 11.8 Hz) 3.43-3.42 (4H, m) 2.47 (1H, app triplet, J = 7.5 Hz) 2.29 (4H, m) 1.62-1.57 (4H, m) 1.26 (40H, m) 0.90-0.86 (6H, m). ^{31}P NMR (122 MHz, CDCl$_3$) δ -0.4.^{13}C NMR (75 MHz, CDCl$_3$): 173.2, 172.8, 135.5, 128.7, 128.7, 128.0, 79.7, 79.6, 69.7, 69.7,

69.3, 69.3, 65.7, 65.7, 65.6, 65.5, 61.6, 60.5, 60.5, 57.8, 34.1, 34.0, 31.9, 29.6, 29.5, 29.3, 29.3, 29.1, 29.1, 24.8, 22.7, 14.1, 14.0. HRMS-ESI+ (*m/z*): [M + H]$^+$ calculated for C$_{42}$H$_{76}$O$_{10}$P, 771.51706; found, 771.51672.

(2R)-3-(((benzyloxy)((S)-2-hydroxy-3-methoxypropoxy)phosphoryl)oxy)propane-1,2-diyl

ditetradecanoate (**6.14**)

To a solution of **6.9** (182 mg, 0.206 mmol, 1.00 equiv.) in THF (5.4 mL) cooled in an ice-water bath was added HF·pyridine (620μL, 3.00 mL/mmol). The reaction vessel was sealed and allowed to stir overnight in a 0 ^{o}C fridge. After 16 hours of stirring, the reaction mixture was diluted with diethyl ether (20 mL) and washed with saturated aqueous NaHCO$_3$ twice. The organic layer was dried with MgSO$_4$, filtered, and then concentrated. The residue was purified via silica-gel column chromatography (50% Ethyl acetate / 50% Hexanes). This yielded **6.14** as a colorless oil (78 mg, 54% yield). ^{1}H NMR (300 MHz, CDCl$_3$): 7.35 (5H, m) 5.17 (1H, app sextet, J = 4.8 Hz) 5.07 (2H, m) 4.26 (1H, dd, J = 4.2, 12.0 Hz) 4.12-3.92 (6H, m) 3.39-3.30 (5H, m) 2.90 (1H, m) 2.30-2.24 (4H, m) 1.59-1.54 (4H, m) 1.23 (40H, m) 0.87-0.83 (6H, m). ^{31}P NMR (122 MHz, CDCl$_3$) δ 0.9. ^{13}C NMR (75 MHz, CDCl$_3$): δ 173.2, 172.9, 135.6, 135.5, 128.7, 128.7, 128.0, 72.7, 69.8, 69.7, 69.4, 69.3, 69.2, 69.1, 65.6, 65.5, 61.6, 59.2, 34.1, 34.0, 31.9, 29.7, 29.5, 29.4, 29.3, 29.1, 29.1, 24.8, 22.7, 14.1. HRMS-ESI+ (*m/z*): [M + H]$^+$ calculated for C$_{42}$H$_{76}$O$_{10}$P, 771.51706; found, 771.51848.

sodium (R)-2,3-bis(tetradecanoyloxy)propyl ((S)-2-hydroxypropyl) phosphate (**6.15**)

6.15 was prepared using general procedure C starting from **6.10**. Crude **6.15** was isolated by silica gel column chromatography (90:10:0.1 CHCl$_3$:MeOH:NH$_4$OH to 77.5:17.5:2.5:0.1 CHCl$_3$:MeOH:H$_2$O:NH$_4$OH). This yielded the ammonium salt which was converted to the acid form by incubating the purified material over DOWEX 50 (acid form) in a 1:1 mixture of

CHCl$_3$:MeOH. The resin was filtered off and the resulting solution was concentrated under high vacuum at <35 °C. The residue was suspended in aqueous sodium acetate (0.0300 M; 1.00 equiv) and then frozen and lyophilized. This yielded **6.15** as a colorless powder (155 mg, 82% yield). ^{1}H NMR (300 MHz, 95:5 CDCl$_3$:CD$_3$OD): 5.20 (1H, m) 4.37-4.34 (1H, m) 4.16-4.12 (1H, m) 3.92 (3H, m) 3.80-3.76 (1H, m) 3.64-3.60 (1H, m) 2.30-2.26 (4H, m) 1.57 (4H, m) 1.23 (40H, m) 1.11 (3H, d, J = 5.9 Hz) 0.87-0.84 (6H, m). ^{31}P NMR (122 MHz, 95:5 CDCl$_3$:CD$_3$OD) δ 1.6.^{13}C NMR (125 MHz, 95:5 CDCl$_3$:CD$_3$OD): δ 173.7, 173.4, 70.9, 70.4, 70.3, 66.6, 63.5, 62.6, 34.2, 34.0, 31.9, 29.6, 29.5, 29.3, 29.1, 24.9, 24.8, 22.6, 18.7, 14.0. HRMS-ESI+ (*m/z*): [M + H]$^+$ calculated for C$_{34}$H$_{68}$O$_9$P, 651.45955; found, 651.45649.

sodium (R)-2,3-bis(tetradecanoyloxy)propyl (3-hydroxypropyl) phosphate (**6.16**)

6.16 was prepare following general procedure C starting from **6.11**. Reaction times of up to 8 hours are required to ensure complete removal of the BOM group. (152 mg, 89% yield). ^{1}H NMR (500 MHz, CDCl$_3$): 5.24 (1H, m) 4.44-4.42 (1H, m) 4.23-4.19 (1H, m) 4.01-3.95 (4H, m) 3.73 (2H, m) 2.34-2.29 (4H, m) 1.78 (2H, m) 1.60 (4H, m) 1.28 (40H, m) 0.92-0.89 (6H, m). ^{31}P NMR (202 MHz, 95:5 CDCl$_3$:CD$_3$OD) δ 2.66.^{13}C NMR (125 MHz, 95:5 CDCl$_3$:CD$_3$OD): δ 173.8, 173.6, 70.6, 70.5, 63.5, 62.6, 58.2, 34.2, 34.1, 32.8, 32.7, 31.9, 29.7, 29.7, 29.6, 29.5, 29.3, 29.3, 29.2, 29.1, 24.9, 24.8, 22.7, 14.1. HRMS-ESI+ (*m/z*): [M + H]$^+$ calculated for C$_{34}$H$_{68}$O$_9$P, 651.45955; found, 651.45647.

sodium (R)-2,3-bis(tetradecanoyloxy)propyl ((S)-3-hydroxy-2-methoxypropyl) phosphate (**6.17**)

6.17 was prepared according to general procedure C starting from **6.13** (110 mg, 95% yield). ^{1}H NMR (300 MHz, CDCl$_3$): 5.20 (1H, m) 4.36 (1H, dd, J = 2.7, 12.2 Hz) 4.14 (1H, dd, J = 6.7, 12.0 Hz) 3.99-3.90 (4H, m) 3.74-3.62 (2H, m) 3.41 (3H, s) 3.34-3.32 (1H, m) 2.31-2.24 (4H, m) 1.60-

1.55 (4H, m) 1.23 (40H, m) 0.88-0.83 (6H, m).^{31}P NMR (122 MHz, CDCl$_3$) δ 1.5.^{13}C NMR (75 MHz, CDCl$_3$): δ 173.7, 173.5, 79.8, 70.5, 70.4, 63.6, 63.5, 63.4, 63.4, 62.6, 59.4, 57.2, 34.2, 34.0, 31.9, 29.7, 29.5, 29.3, 29.1, 24.9, 24.8, 22.6, 14.0. HRMS-ESI+ (*m/z*): [M + H]$^+$ calculated for C$_{35}$H$_{70}$O$_{10}$P, 681.47011; found, 681.47022.

sodium (R)-2,3-bis(tetradecanoyloxy)propyl ((S)-2-hydroxy-3-methoxypropyl) phosphate (**6.18**)

6.18 was prepared according to general procedure C starting from **6.14** (58 mg, 94% yield). ^{1}H NMR (300 MHz, 95:5 CDCl$_3$:CD$_3$OD): 5.20 (1H, m) 4.38-4.34 (1H, m) 4.16-4.13 (1H, m) 3.90-3.82 (4H, m) 3.40-3.11 (6H, m) 2.30-2.23 (4H, m) 1.56 (4H, m) 1.22 (40H, m) 0.86-0.82 (6H, m). ^{31}P NMR (122 MHz, 95:5 CDCl$_3$:CD$_3$OD) δ 1.7.^{13}C NMR (125 MHz, 95:5 CDCl$_3$:CD$_3$OD): δ 173.7, 173.4, 73.3, 70.5, 70.4, 69.2, 67.3, 63.5, 62.6, 59.0, 34.2, 34.0, 31.9, 29.6, 29.5, 29.3, 29.1, 24.9, 24.8, 22.6, 14.0 HRMS-ESI+ (*m/z*): [M + H]$^+$ calculated for C$_{35}$H$_{69}$O$_{10}$PNa, 703.45206; found, 703.45223.

S)-3-hydroxypropane-1,2-diyl dihexanoate (**6.20**)

A solution of **6.38** (1.20 g, 3.17 mmol) and Pd(OH)$_2$/C (20% w/w, 240 mg) in t-BuOH was stirred under H$_2$ for 16 hours at room temperature. The solution was then filtered over celite and the t-BuOH was removed by concentrating from benzene once. This yielded pure **6.20** as a colorless oil (480 mg, 53% yield). ^{1}H NMR data matched that previously reported.[277]

(S)-3-hydroxypropane-1,2-diyl dibutyrate (**6.21**)

6.21 was prepared from **6.39** following the same procedure used to prepare **6.20**. This yielded **6.21** as a colorless (220 mg, 61% yield). ^{1}H NMR data matched that previously reported.[280]

(2R)-3-(((benzyloxy)(diisopropylamino)phosphaneyl)oxy)propane-1,2-diyl dioctanoate (**6.22**)

6.22 was prepared according to general procedure A. The alcohol was used was **6.19** (856 mg, 76% yield). $[\alpha]^{22}_D = +5.1$ (c 0.140, CH_2Cl_2). ^{1}H NMR (300 MHz, $CDCl_3$): 7.33-7.27 (5H, m) 5.19 (1H, app quint, J = 4.9 Hz) 4.81-4.60 (1H, m) 4.38-4.30 (1H, m) 4.20-4.13 (2H, m) 3.83-3.56 (4H, m) 2.31-2.26 (4H, m) 1.60 (4H, m) 1.26-1.16 (28H, m) 0.89-0.84 (6H, m).^{31}P NMR (122 MHz, $CDCl_3$) 149.9, 149.8. ^{13}C NMR (75 MHz, $CDCl_3$): δ 173.3, 173.0, 139.4, 139.3, 128.3, 128.3, 127.3, 127.2, 127.0, 126.9, 126.9, 70.9, 70.9, 65.5, 65.3, 62.5, 61.7, 61.5, 43.2, 43.0, 34.3, 34.1, 31.7, 29.1, 29.1, 28.9, 24.9, 24.7, 24.6, 24.5, 22.6, 14.0. HRMS-ESI+ (*m/z*): [M + H]$^+$ calculated for $C_{32}H_{57}O_6NP$, 582.39180; found, 582.39273.

(2R)-3-(((benzyloxy)(diisopropylamino)phosphaneyl)oxy)propane-1,2-diyl dihexanoate (**6.23**)

6.23 was prepared according to general procedure A starting from **6.20**. The crude material was purified by silica gel column chromatography (3% triethylamine/97% hexanes to 3% triethylamine/20% ethyl acetate/77% hexanes) yielding **6.23** as a colorless oil contaminated with P(OBn)(N(i-Pr)$_2$)$_2$ (443 mg, 51% crude yield). Crude **6.23** was used without further purification.

(2R)-3-(((benzyloxy)(diisopropylamino)phosphaneyl)oxy)propane-1,2-diyl dibutyrate (**6.24**)

6.24 was prepared according to general procedure A starting from **6.21**. The crude material was purified by silica gel column chromatography (3% triethylamine/97% hexanes to 3% triethylamine/20% ethyl acetate/77% hexanes) yielding **6.21** as a colorless oil contaminated with P(OBn)(N(i-Pr)$_2$)$_2$ (438 mg, 53% crude yield). Crude **6.21** was used without further purification.

(2R)-3-(((benzyloxy)(((4S)-2-phenyl-1,3-dioxolan-4-yl)methoxy)phosphoryl)oxy)propane-1,2-diyl dioctanoate (**6.25**)

6.25 was prepared according to general procedure B. The phosphoramidite was **6.22**, the alcohol was **R-6.33** (131 mg, 43% yield). $[\alpha]^{22}_D = -2.7$ (c 0.091, CH_2Cl_2). ^{1}H NMR (300 MHz, $CDCl_3$):

7.44-7.35 (10H, m), 5.90 and 5.78 (1H, s) 5.19-5.03 (3H, m) 4.42-3.80 (9H, m) 2.29-2.24 (4H, m) 1.57 (4H, m) 1.25 (16H, m) 0.85 (6H, m). ^{31}P NMR (122 MHz, CDCl$_3$) δ 0.19, 0.05.^{13}C NMR (75 MHz, CDCl$_3$): δ 173.1, 172.7, 137.3, 136.6, 135.4, 135.3, 129.5,129.2, 128.7, 128.6, 128.6, 128.3, 127.9, 126.6, 126.3, 104.6, 103.9, 74.2, 74.1, 69.6, 69.1, 67.4, 67.2, 66.7, 65.5, 61.5, 71.3, 68.2, 65.5, 64.8, 34.0, 33.9, 31.5, 28.9, 18.9, 28.8, 24.7, 22.5, 14.0. HRMS-ESI+ (*m/z*): [M + H]$^+$ calculated for C$_{36}$H$_{54}$O$_{10}$P, 677.34491; found, 677.34425.

(2R)-3-(((benzyloxy)(((4R)-2-phenyl-1,3-dioxolan-4-yl)methoxy)phosphoryl)oxy)propane-1,2-diyl dioctanoate (**6.26**)

6.26 was prepared according to the procedure described for **6.25** using **S-6.33** in place of **R-6.33** (102 mg, 41% yield). [α]$^{22}_D$ = +3.5 (c 0.089, CH$_2$Cl$_2$). ^{1}H NMR (300 MHz, CDCl$_3$): 7.43-7.35 (10H, m) 5.90 and 5.78 (1H, s) 5.20-5.04 (3H, m) 4.40-3.80 (9H, m) 2.28-2.24 (4H, m) 1.57 (4H, m) 1.25 (16H, m) 0.86-0.84 (6H, m). ^{31}P NMR (122 MHz, CDCl$_3$) δ 0.19 and 0.04.^{13}C NMR (75 MHz, CDCl$_3$): δ 173.1, 172.7, 137.3, 136.6, 135.4, 135.4, 129.5, 129.2, 128.7, 128.7, 128.6, 128.3, 127.9, 126.6, 126.3, 104.6, 103.9, 74.2, 74.1, 69.6, 69.1, 67.4, 67.2, 66.7, 65.5, 61.5, 34.0, 33.89, 31.6, 28.9, 28.9, 28.8, 24.7, 22.5, 14.0. HRMS-ESI+ (*m/z*): [M + H]$^+$ calculated for C$_{36}$H$_{54}$O$_{10}$P, 677.34491; found, 677.34232.

(2R)-3-(((benzyloxy)(((S)-2-phenyl-1,3-dioxolan-4-yl)methoxy)phosphoryl)oxy)propane-1,2-diyl dihexanoate (**6.27**)

6.27 was prepared according to general procedure B using phosphoramidite **6.23** and alcohol **R-6.33**. It was purified by silica gel column chromatography (5% EtOAc / 95% DCM to 10% EtOAc / 90% DCM). This yielded **6.27** as a colorless oil (311 mg, 61% yield). ^{1}H NMR (300 MHz, CDCl$_3$) 7.49-7.36 (10H, m) 5.92 and 5.80 (1H, m) 5.14-5.06 (3H, m) 4.41-3.82 (9H, m) 2.30 (4H, m) 1.61

(4H, m) 1.29 (8H, m) 0.89 (6H, m).^{31}P NMR (122 MHz, CDCl$_3$) δ -1.0, -1.12.^{13}C NMR (75 MHz, CDCl$_3$): δ 173.2, 172.8, 137.5, 136.8, 135.5, 135.5, 129.5, 129.3, 128.7, 128.4, 128.0, 126.7, 126.4, 104.6, 104.0, 74.4, 74.3, 74.2, 69.8, 69.7, 69.4, 69.25, 67.6, 67.5, 67.2, 66.7, 65.6, 62.7, 61.6, 34.1, 33.9, 31.2, 31.2, 24.5, 22.3, 13.9.HRMS-ESI+ (*m/z*): [M + H]$^+$ calculated for C$_{32}$H$_{46}$O$_{10}$P, 621.28231; found, 621.27997.

(2R)-3-(((benzyloxy)(((S)-2-phenyl-1,3-dioxolan-4-yl)methoxy)phosphoryl)oxy)propane-1,2-diyl dibutyrate (**6.28**)

6.28 was prepared according to general procedure B using phosphoramidite **6.24** and alcohol **R-6.33** (5% EtOAc / 95% DCM). This yielded **6.28** as a colorless oil (84 mg, 44% yield). ^{1}H NMR (300 MHz, CDCl$_3$): 7.48-7.39 (10H, m) 5.93 and 5.82 (1H, m) 5.24-5.20 (1H, m) 5.15-5.08 (2H, m) 4.47-4.44 (1H, m) 4.33-3.81 (8H, m) 2.30 (4H, m) 1.66 (4H, m) 0.95 (6H, m). ^{31}P NMR (122 MHz, CDCl$_3$) δ 0.2, 0.08, 0.05.^{13}C NMR (125 MHz, CDCl$_3$): δ 173.0, 172.6, 137.4, 136.7, 135.5, 135.5, 129.6, 129.3, 128.8, 128.8, 128.7, 128.7, 128.4, 128.1, 128.0, 126.7, 126.4, 104.7, 104.0, 74.4, 74.3, 74.3, 74.2, 69.8, 69.7, 69.3, 69.3, 67.6, 67.5, 67.3, 66.8, 65.6, 65.6, 61.5, 36.0, 35.9, 18.3, 13.6, 13.6. HRMS-ESI+ (*m/z*): [M + H]$^+$ calculated for C$_{28}$H$_{38}$O$_{10}$P, 565.21971; found, 565.21698.

sodium (R)-2,3-bis(octanoyloxy)propyl ((S)-2,3-dihydroxypropyl) phosphate (**6.29**)

6.29 was prepared according to general procedure C starting from **6.25**. (73 mg, 94% yield). ^{1}H NMR (300 MHz, 95:5 CDCl$_3$:CD$_3$OD): 5.18 (1H, s), 4.36 (1H, m) 4.16-3.60 (9H, m) 2.30- 2.3 (4H, m) 1.56 (4H, m) 1.24 (16H, m) 0.84 (6H, m). ^{31}P NMR (122 MHz, 95:5 CDCl$_3$:CD$_3$OD) δ 1.5.^{13}C NMR (125 MHz, 95:5 CDCl$_3$:CD$_3$OD): δ 173.7, 173.4, 70.7, 70.4, 70.4, 68.8, 63.5, 62.6,

34.1, 33.9, 31.6, 29.0, 28.9, 28.8, 28.8, 24.8, 24.7, 22.5, 13.9. HRMS-ESI+ (*m/z*): [M + H]$^+$ calculated for $C_{22}H_{43}O_{10}NaP$, 521.24861; found, 521.24752.

sodium (R)-2,3-bis(octanoyloxy)propyl ((S)-2,3-dihydroxypropyl) phosphate (**6.30**)

6.30 was prepared according to general procedure C starting from **6.26** (67 mg, 85% yield). ^{1}H NMR (300 MHz, 95:5 CDCl$_3$:CD$_3$OD): 5.19 (1H, s), 4.37 (1H, m) 4.16-3.60 (9H, m) 2.30- 2.26 (4H, m) 1.56 (4H, m) 1.25 (16H, m) 0.85 (6H, m). ^{31}P NMR (122 MHz, 95:5 CDCl$_3$:CD$_3$OD) δ 1.5.^{13}C NMR (125 MHz, 95:5 CDCl$_3$:CD$_3$OD): δ 173.7, 173.5, 70.8, 70.4, 70.4, 68.9, 63.5, 62.6, 34.1, 34.0, 31.6, 29.0, 29.0, 28.9, 28.9, 24.8, 24.8, 22.5, 13.9 HRMS-ESI+ (*m/z*): [M + H]$^+$ calculated for $C_{22}H_{43}O_{10}NaP$, 521.24861; found, 521.24703.

sodium (R)-2,3-bis(hexanoyloxy)propyl ((S)-2,3-dihydroxypropyl) phosphate (**6.31**)

6.31 was prepared according to general procedure C starting from **6.27** (117 mg, 96% yield). ^{1}H NMR (300 MHz, 95:5 CDCl$_3$:CD$_3$OD): 5.15 (1H, m) 4.31-3.54 (11H, m) 2.23 (4H, m) 1.52 (4H, m) 1.22 (8H, m) 0.81 (6H, m). ^{31}P NMR (122 MHz, 95:5 CDCl$_3$:CD$_3$OD) δ 2.7. ^{13}C NMR (125 MHz, 95:5 CDCl$_3$:CD$_3$OD): δ173.8, 173.5, 70.8, 70.4, 70.3, 66.6, 63.5, 62.5, 34.1, 33.9, 31.1, 24.4, 22.1, 13.7. HRMS-ESI+ (*m/z*): [M + H]$^+$ calculated for $C_{18}H_{35}O_{10}NaP$, 465.18600; found, 465.18413.

sodium (R)-2,3-bis(butyryloxy)propyl ((S)-2,3-dihydroxypropyl) phosphate (**6.32**)

6.32 was prepared according to general procedure C starting from **6.28** (117 mg, 96% yield). ^{1}H NMR (300 MHz, 95:5 CDCl$_3$:CD$_3$OD): 5.22 (1H, m) 4.38 (1H, m) 4.24-4.14 (3H, m) 3.93-3.83 (5H, m) 3.62-3.58 (2H, m) 2.30-2.25 (4H, m) 1.64-1.58 (4H, m) 0.94-0.90 (6H, m).^{31}P NMR (122 MHz, 95:5 CDCl$_3$:CD$_3$OD) δ 1.6.^{13}C NMR (125 MHz, 95:5 CDCl$_3$:CD$_3$OD): δ173.7, 173.4, 70.8,

70.5, 70.4, 66.9, 63.6, 62.6, 36.0, 35.9, 18.3, 18.2. HRMS-ESI+ (*m/z*): [M + H]$^+$ calculated for C$_{14}$H$_{26}$O$_{10}$NaP, 409.12340; found, 409.12145.

Chapter 7 - An Enantiospecific Synthesis of lysyl-PG and its Interaction with Daptomycin

7   Introduction

One of the goals of this thesis was to provide rationale for the supposed resistance to daptomycin conferred by increased lysyl-PG content. As mentioned in the introduction, many resistant strains of *S. aureus* contain increased lysyl-PG content.[122,126] The protein responsible for the synthesis and translocation of lysyl-PG is MprF and strains of *Staphlococcus* spp. without a functioning lysyl-PG synthesis pathway are hypersusceptible to daptomycin.[108,128] Thus, the presence of MprF confers a basal level of resistance in *S. aureus*, but the mechanism of resistance is not entirely clear. First it was hypothesized that increased lysyl-PG content served to decrease the negative charge of the bacterial membrane effectively repelling calcium bound daptomycin conferring resistance.[269] Studies employing *S. aureus* strains show hypersusceptibility to daptomycin and decreased cytochrome c binding when MprF is knocked out compared to the parent strain, supporting the charge repulsion mechanism.[281] However, a charge repulsion mechanism was found to be insufficient on both model membranes[121] and in bacteria[122,123,128,129] suggesting that MprF and/or lysyl-PG play other roles in daptomycin resistance.

A second hypothesis suggests that increased lysyl-PG content confers resistance by decreasing PG content thus reducing the number of binding sites for daptomycin. In line with this, zwitterionic alanyl-PG is as effective as lysyl-PG at conferring resistance to daptomycin in *S. aureus*.[123] Additionally, reductions in membrane PG content often accompany increases in lysyl-PG content in both *S. aureus* and *B. subtilis*.

It can be difficult to correlate changes in lysyl-PG content and changes in daptomycin susceptibility if there are other simultaneous genetic difference in the assayed organisms. For

example, MprF deletion provides marginal resistance in *E. faecalis*[124] but substantial resistance in *S. aureus*[128]. The importance of controlling for genetic differences while studying MprF conferred resistance in *S. aureus* was highlighted in a work by Ernst and coworkers who demonstrated that increased lysyl-PG or alanyl-PG content could only provide protection from daptomycin if these lipids were effectively translocated to the outer membrane.[123] In another work by Ernst et al, the authors characterized *mprF* from daptomycin resistant strains of *S. aureus* with a consistent genetic background and found that only some of these genes conferred resistance despite all of them possessing equivalent lysyl-PG synthesis and translocation activity.[129] This led the authors to formulate a third hypothesis which states that certain mutations to *mprF* confer resistance to daptomycin by a specific interaction between the peptide and MprF.[129] Although the plausibility of this hypothesis was supported by a structural study done on the MprF, no direct experimental evidence of this interaction is forthcoming.[130]

A fourth hypothesis proposes that, rather than preventing binding, lysyl-PG alters the membrane in a way that resists the natural action of daptomycin. Recent studies on the action mechanism of daptomycin have demonstrated that daptomycin prefers to bind to regions of increased fluidity and may alter the fluidity of these domains resulting in cell membrane disorganization.[64,79,82] Alterations in membrane fluidity are often accompanied by daptomycin resistance in *S. aureus*; however, the relationship between cell membrane fluidity and daptomycin susceptibility appears to be complicated by additional mutations.[122,282,283] In cases where lysyl-PG content is significantly increased, an increase in membrane fluidity is often observed, but it not clear whether lysyl-PG confers this change in fluidity.[122,282] It has been shown that changes in lipid composition, including an increase in lysyl-PG content, can alter the distribution of daptomycin bound to *E. faecalis* in a manner that is thought to confer resistance.[126] Additionally,

although not much is known about how lysyl-PG impacts the properties of a bacterial membrane, lysyl-PG alters the lamellar phase behaviour of model membranes through the formation of lysyl-PG/PG ion pairs which may confer changes in membrane fluidity and organization.[284]

To date, only a single study has described the interaction of daptomycin with model membranes containing lysyl-PG. This was completed Pokorny and coworkers in 2016 who tested two membrane compositions: 70:30 POPC:POPG and 70:10:20 POPC:POPG:lysyl-POPG.[121] The authors found that the dissociation constant increased by a factor of 4 when the lysyl-POPG containing LUV was used. Analysis of on and off kinetics suggested that the membrane bound state of daptomycin was disproportionately destabilized compared to the transition state of the binding event. However, it is unclear whether the decrease in affinity was due to a change in membrane charge, decrease in PG content and/or an alteration in membrane fluidity, and no information regarding how lysyl-PG influenced the membrane bound state of daptomycin was collected.

We aimed to determine whether lysyl-PG can influence the affinity and/or membrane bound state of daptomycin in a way that explains the putative correlation between lysyl-PG content and daptomycin resistance while controlling for PG content and charge. With the methodology described in chapters 5 and 6, we supposed that we could easily synthesize ample quantities of enantiomerically pure lysyl-DMPG allowing for detailed studies in model membranes.

Although commercially available, lysyl-DMPG is expensive and is not available as a single isomer. In fact, commercial lysyl-DMPG is racemic at the headgroup and can possess up to 15% of the 2'-isomer. The results in chapter 5 and 6 demonstrate the importance of studying daptomycin using isomerically pure lipids, thus we set out to develop a synthesis of isomerically pure lysyl-DMPG. Lysyl-PG has been made twice in the past. The first synthesis was by Bonsen et al. in

1967,[285] the second synthesis was published in the following year by Molotovsky et al.[286] Both syntheses disconnect lysyl-PG at the same position yielding an alkyl iodide bearing the protected 3'-lysyl glycerol and a phosphatidic acid diester silver salt bearing the tail group (Scheme 7.1). A modified approach via the same disconnection was employed by Tocanne et al. in 1974 to synthesize 2'- and 3'-lysyl-PG.
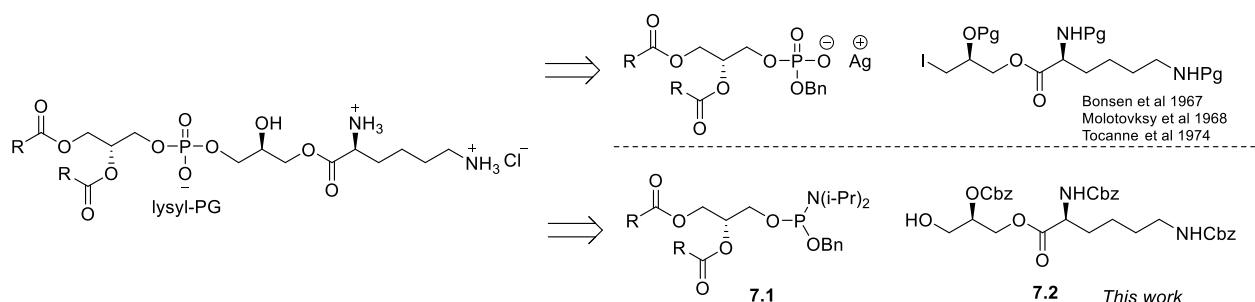
Scheme 7.1. Past and present disconnections applied to the synthesis of lysyl-PG

We surmised that lysyl-DMPG could be rapidly accessed using phosphoramidite chemistry, essentially reversing the polarity of the disconnection used almost 50 years ago. This disconnection was particularly appealing since we had already developed a robust route to **7.1** which makes up a significant portion of the molecule. Thus, we could focus our attention on preparing alcohol **7.2** and then feed this material into the pathways presented in chapters 5 and 6 to rapidly access stereochemically pure lysyl-DMPG. The results of our efforts are reported here-in.

7.1 Results and discussion

The synthesis of alcohol **7.2** proved treacherous because the Cbz-protected lysine unit was more prone to migration than a simple aliphatic acyl group, which precluded approaches used to prepare lipid tail groups with mixed fatty acid chains.[244,277,287,288] In line with Tocanne et al,[289] we also found the final product to be quite fragile, necessitating a swift and clean deprotection under mild conditions, the consideration of which is reflected in the protecting group scheme. Our route to

lysyl-DMPG is disclosed in Scheme 7.2. Commercially available isopropylidene **7.3** is PMB-protected yielding ether **7.4** which was deprotected under known conditions giving diol **7.5**. The diol **7.5** was regioselectively tosylated with 4-toluenesulfonyl chloride (TsCl)/triethylamine (TEA) using catalytic dibutyl tin(IV) oxide at 0°C yielding monotosylate **7.6**.[290,291] The regioselectivity of this reaction was determined by inverse gated ^{13}C NMR to be 33:1. The secondary alcohol was protected with benzyl chloroformate (CbzCl)/tetramethylethylenediamine (TMEDA)[292] giving **7.7**. The tosylate was displaced by refluxing **7.7** with NaI in acetone yielding the corresponding alkyl iodide which was immediately reacted with Cbz-Lys(Cbz)-OCs in DMF for 72 hours giving **7.8** in a satisfactory yield as a single regioisomer. PMB deprotection of **7.8** went smoothly giving alcohol **7.1**, no carbonate migration was observed under these conditions.[293]
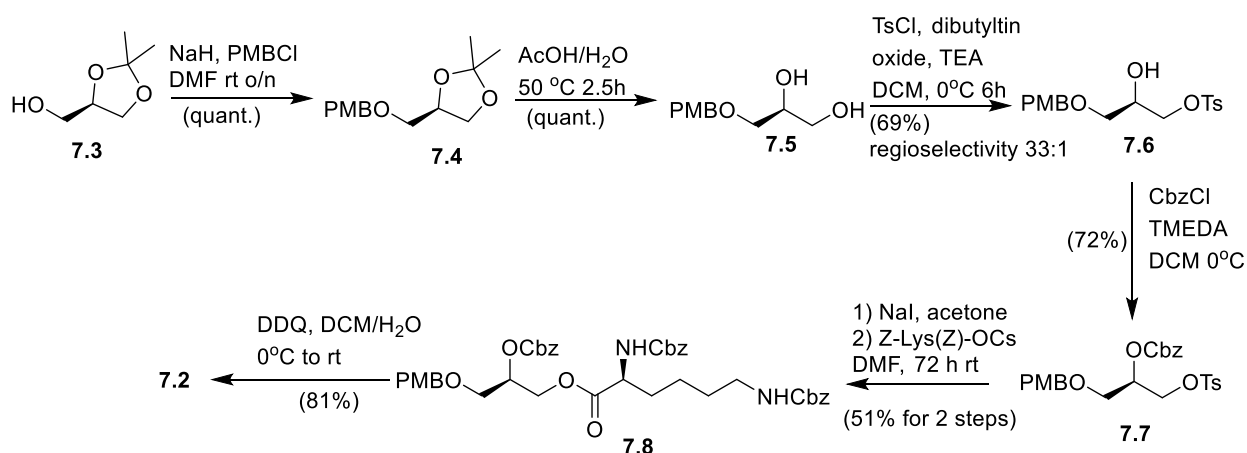
Scheme 7.2 Synthesis of alcohol **7.2**

Phosphoramidite **7.1** was prepared using our previously described approach (chapter 5). Alcohol **7.2** was reacted with **7.1** using 4,5-dicyanoimidazole[294] as an activator yielding protected phosphotriester **7.9** after oxidation of the *in-situ* formed phosphite with mCPBA (Scheme 7.2). Clean deprotection of **7.9** proved to be a difficult step. We found that H_2/Pd(OH)$_2$/C in t-BuOH was unable to remove the all of the protecting groups. Using conditions described by Tocanne et

201

al,[289] we were able to rapidly and cleanly deprotect **7.9**, convert it to its HCl salt and lyophilize it. This yielded lysyl-DMPG as a colorless powder which was fully characterized by NMR.
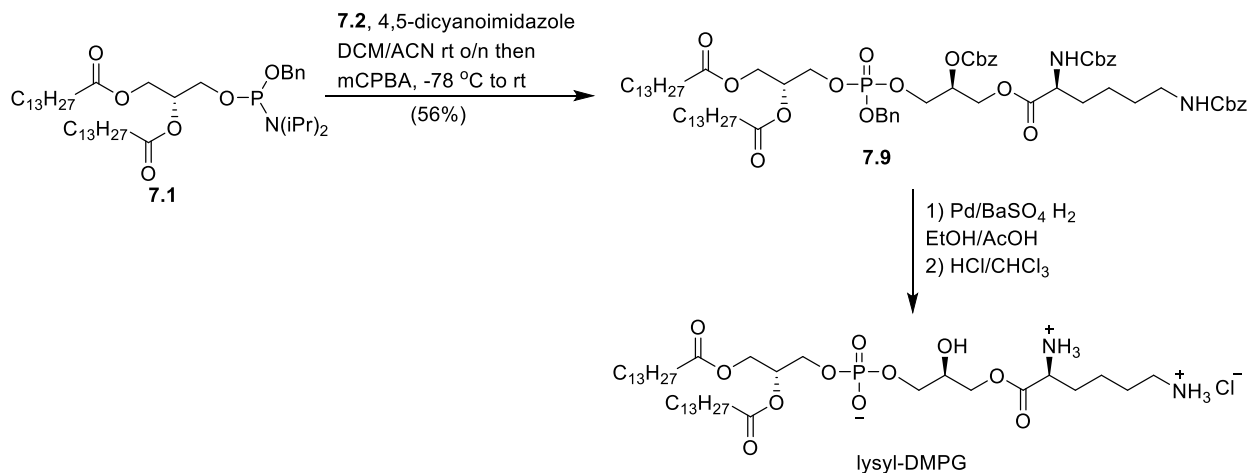
Scheme 7.3 Synthesis of lysyl-DMPG from **7.1** and **7.2**

With ample quantities of lysyl-DMPG in hand, we investigated how the presence of this lipid influences the membrane affinity of daptomycin. Lysyl-DMPG was incorporated into LUVs containing DMPC with or without DMPG (Figure 7.1A). Daptomycin displayed significantly reduced affinity for membranes containing 75:25 DMPC:lysyl-DMPG compared to membranes containing 75:25 DMPC:DMPG. These results demonstrate that at physiological calcium concentrations and micromolar daptomycin concentrations the peptide would not readily bind to lysyl-DMPG. Daptomycin possessed nearly identical affinity for a LUV containing 50:25:25 DMPC:DMPG:lysyl-DMPG compared to a LUV containing 75:25 DMPC:DMPG showing that the peptide is not particularly sensitive to alterations in membrane charge. Repeating this experiment on multiple LUVs containing the same fraction DMPG but incrementally increasing fractions of lysyl-DMPG demonstrates that lysyl-DMPG can impede the binding of daptomycin, but the effect is marginal. Considering that resistant strains of *S. aureus* possess approximately 16-35% lysyl-PG content and 52-81% PG content, it is unlikely that lysyl-PG would effectively

202

prevent daptomycin from binding to the bacterial membrane and thus resistance must primarily be conferred by some other action.[122]
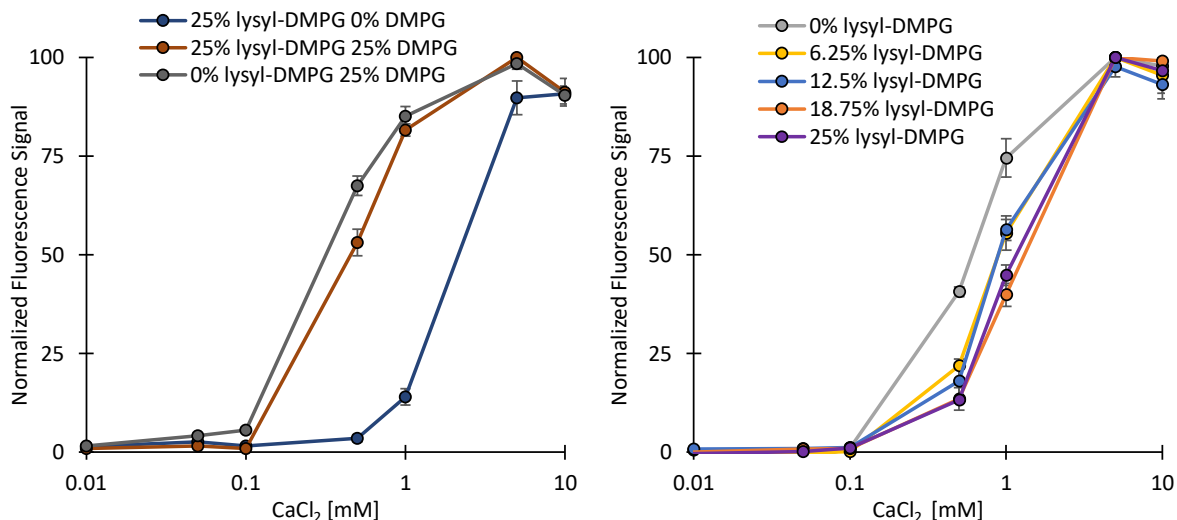
Figure 7.1 Membrane binding curves for daptomycin (3 μM) using 37 °C in 20 mM HEPES, 150 mM NaCl (pH 7.4). (A) daptomycin binding to LUVs (250 μM total lipid concentration) containing DMPG:lysyl-DMPG:DMPC. The legend denotes the % molar concentration of lysyl-DMPG and DMPG while DMPC makes up the remaining fraction. (B) the same experiment described for (A) but with LUVs containing 12.5% DMPG. The legend denotes the composition of lysyl-DMPG while DMPC makes up the remaining lipid fraction.

To investigate the impact of lysyl-DMPG on the membrane bound state of daptomycin we employed circular dichroism (CD). CD was first applied by Hancock and coworkers to monitor the membrane insertion and membrane bound state of daptomycin.[24] It has since been used by Huang and coworkers to ascertain the impact of changes in membrane lipid composition on the backbone structure of daptomycin[80] and to determine the stoichiometry of membrane bound Daptomycin:calcium:PG.[257] We have used CD extensively to study the interaction of daptomycin and the related natural product A54145D with PG.[278] The CD trace of daptomycin in solution possesses an S-like shape (Figure 7.2). In the presence of 5 mM CaCl$_2$ and LUVs containing 87.5:12.5 DMPC:DMPG, the trace inverts signaling the complexation of daptomycin with calcium and PG. Incrementally increasing the lysyl-DMPG content in membranes containing identical

concentrations of DMPG (12.5 mol%) demonstrated that lysyl-DMPG is unable to significantly perturb the backbone confirmation of calcium-PG bound daptomycin. Indeed, all the collected traces were within standard error of one another.
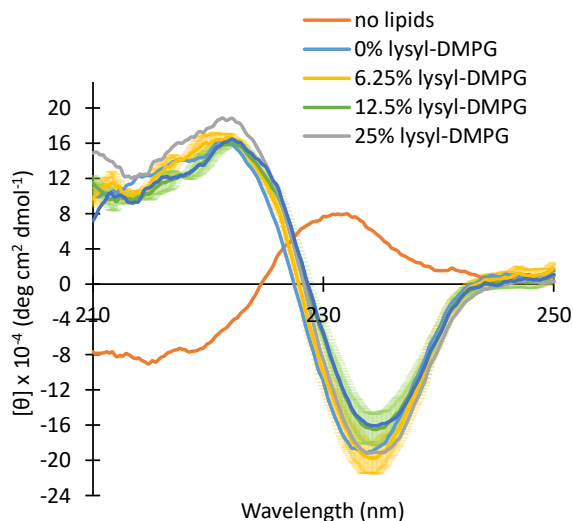
Figure 7.2. CD spectra of dap (15 µM) in the presence of 5 mM Ca^{2+} and LUVs composed of DMPG:DMPC:lysyl-DMPG at 37 °C in 20 mM HEPES (pH 7.4). Each LUV contained 12.5% DMPG; the legend denotes the lysyl-DMPG content, and the remaining fraction was made up of DMPC. Error bars represent the standard deviation of at least three trials.

It is known that daptomycin forms oligomers on model membranes containing PG and on bacterial membranes. One method for monitoring the oligomerization of daptomycin is through monitoring the excimer formation of daptomycin bearing a perylene tail (perylene-dap; Figure 1.16). The fluorescence properties of perylene monomers and excimers differ greatly and these differences were carefully characterized by Palmer and coworkers.[88] The perylene-dap monomer emits maximally at 455 nm while the excimer emits maximally at 520 nm. Thus, by comparing the intensity at 455 nm to the intensity at 560 nm where the excimer dominates, the extent of oligomerization can be determined. We found that the extent of oligomerization increased with increasing lysyl-DMPG content, and this affect was saturable (Figure 7.3). It is unclear why lysyl-

DMPG would increase the extent of oligomerization, but these results hint that lysyl-DMPG could affect oligomer structure or localization in a manner that confers resistance.
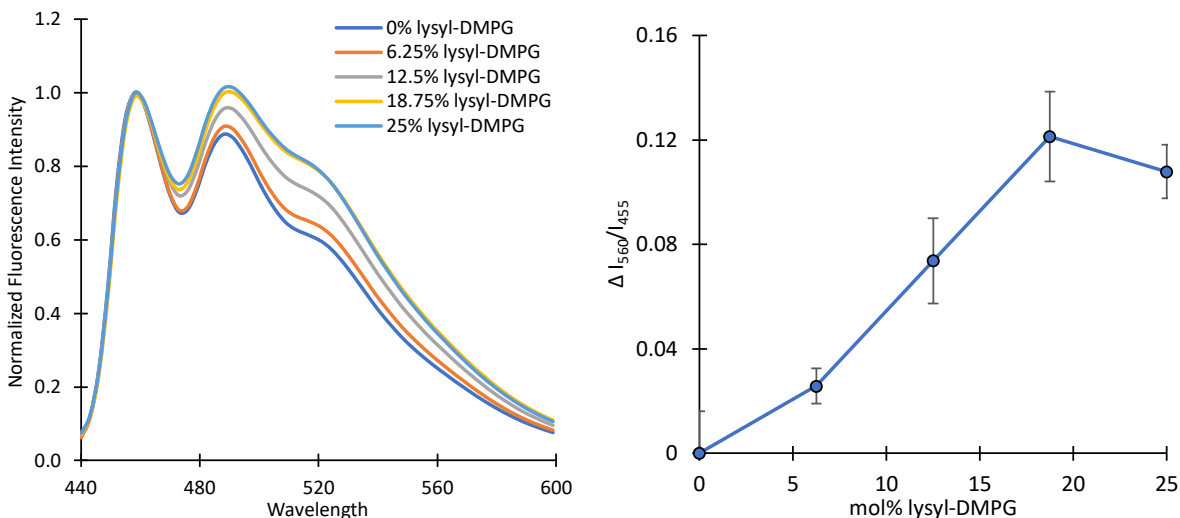
Figure 7.3 Increases in lysyl-DMPG content increases the extent of oligomerization of daptomycin. (A) Fluorescence spectra of perylene-dap (2.5 μM) in the presence of 5 mM Ca^{2+} and LUVs (250 μM total lipid concentration) composed of DMPG, DMPC, and lysyl-DMPG at 37 °C in 20 mM HEPES, 150 mM NaCl (pH 7.4). DMPG content was 12.5 mol% in all cases. The lysyl-DMPG content is reported in the legend and DMPC made up the remaining fraction. (B) a plot of the increment in the ratio of emissions at 560 nm and at 455 nm is plotted as a function of the mol% lysyl-DMPG in each LUV.

7.2   Conclusions

We succeeded in developing a stereospecific synthesis of lysyl-DMPG which allowed for a detailed investigation of the interaction between this lipid and daptomycin in the presence of PG. Membrane binding studies demonstrate that daptomycin has a significantly reduced affinity for lysyl-PG compared to PG and this result is in line with Chapter 6. Through incrementally increasing lysyl-DMPG content while holding the PG content constant, we found that lysyl-DMPG does prevent the binding of daptomycin, but the effect is marginal. Considering that daptomycin resistant strains of bacteria contain far higher concentrations of PG (>50%) compared to the LUVs used in these experiments, and often only contain on average ~20% lysyl-PG, it is unlikely that the observed increases in MIC_{dap} are due to changes in bacterial membrane affinity conferred by

increased lysyl-PG content. CD studies demonstrate that increases in lysyl-PG content are not able to detectably change the backbone conformation of daptomycin bound to calcium and PG. Perylene-excimer studies show that increases in lysyl-DMPG content cause increases in excimer formation suggesting that lysyl-PG can affect oligomerization. It is not clear why the presence of lysyl-DMPG confers an increase in oligomer formation, but it is possible that the presence of this lipid in the membrane changes the structure of the oligomer in a way that increases its size or improves its stability. Previous studies by Palmer and coworkers demonstrated that antibacterial activity is dependent on the precise structure of the oligomer, thus the putative structural impacts of lysyl-PG on the oligomer could result in changes in antibacterial activity.[89] Lysyl-PG may also change the lipid environment that surrounds each daptomycin oligomer which could have concomitant impacts on oligomer stability and on the localization of membrane bound daptomycin. Since changes in the localization of daptomycin on bacterial membranes have been implicated in daptomycin resistance, it is possible that lysyl-PG confers resistance by preventing daptomycin from accumulating in certain areas of the membrane where proteins sensitive to the membrane impacts of daptomycin are localized.[126] In summary, our study demonstrates that increases in lysyl-PG content do not confer resistance to daptomycin by preventing binding or significantly perturbing backbone structure, but they may impact the oligomeric state of daptomycin in a way that confers resistance.

7.3 Experimental

Methods

All reagents and solvents were purchased from commercial suppliers. Methylene chloride (DCM) was dried by distillation over calcium hydride under nitrogen. Acetonitrile (MeCN) was dried by distilling over P_2O_5 then CaH_2 and allowing to stand over 4A sieves overnight. Tetrahydrofuran

(THF) was distilled from sodium metal in the presence of benzophenone under N_2. Chromatography was preformed using 60 Å silica gel.

High resolution positive electrospray (ESI) mass spectra were obtained using an orbitrap mass spectrometer. Samples were sprayed from MeOH: 1% formic acid in H_2O. All spectra were collected in the positive mode. ^{1}H- and ^{13}C-NMR were collected using either a Bruker Avance-300 or a Bruker Avance-500 spectrophotometer. Proton Chemical shifts (δ) for samples run in CDCl$_3$ are reported in ppm relative to an internal standard (trimethylsilane, 0 ppm). For samples run in CD$_3$OD, δ was relative to the solvent peak (3.31 ppm). For ^{13}C-NMR samples run in CDCl$_3$ chemical shifts are reported relative to the solvent peak (77.0 ppm). For samples run in CD$_3$OD, δ was relative to the solvent peak (49.2 ppm).

7.1 and **7.5** were prepared as described in chapter 5.

Liposome preparation.

Large unilamellar vesicles were prepared as previously described.[86] DMPC (1,2-dimyristoyl-sn-glycero-3-phosphocholine) and commercial DMPG (1,2-dimyristoyl-sn-glycero-3-phospho-(1'-rac-glycerol)(sodium salt)) were purchased from Avanti Polar Lipids. Lysyl-DMPG was prepared as described. Solutions of each lipid in chloroform were combined in a thoroughly cleaned and dried round bottom flask. The chloroform was removed under an N_2 stream leaving a thin film of lipid coating the interior of a round-bottom flask. Trace chloroform was removed under high vacuum then the lipids were hydrated with a pH 7.4 buffer (20 mM HEPES, 150 mM NaCl). Extrusion through a 100 nm polycarbonate filter yielded at a total lipid concentration of 5 mM.

Kynurenine fluorescence.

This procedure was adapted from the assay described by Taylor et al.[81] Fluorescence was measured in Corning Costar half-area flat bottom black polystyrene 96-well plates using a Tecan Infinite M1000 instrument. 100 µM peptide stocks were diluted with pH 7.4 buffer (20 mM HEPES, 150 mM NaCl) and preheated to 37°C before adding the above-mentioned liposome solution and immediately dispensing 90 µL aliquots into wells pre-loaded with 10µl of buffer containing CaCl$_2$ at 10x the desired calcium concentration (plate had also been preheated to 37°C) giving a final volume of 100 µL in each well. The final concentrations in each well were 5 µM of peptide, and 250 µM of lipid. Fluorescence measurements were timed to allow for a 3-4 minute incubation period at 37°C. Emission spectra were acquired for kynurenine (Excitation: 365 nm, 5 nm bandwidth) intrinsic fluorescence using 100 flashes at 400 Hz and a step size of 3 nm. Emission spectra for blanks containing 250 µM lipid in buffer and 5 µM peptide were also collected.

Circular dichroism studies.

Circular dichroism (CD) traces were collected using a Jasco J-815 CD spectrophotometer. The peptide concentration of each solution was 15 µM in 20 mM HEPES buffer (pH 7.4). Samples were measured at room temperature from 210-250 nm at a scan rate of 10 nm min^{-1} with a digital integration time of 2 seconds and a bandwidth 1 nm. A 1 mm quartz cuvette was used. The outputted data was converted to molar ellipticity in units of deg cm^2 dmol^{-1}. For traces collected using C4, C6, C8PG a total lipid concentration of 180 µM was used. Calcium concentrations were varied across experiments as denoted in each figure description.

Perylene Studies

Perylene-daptomycin was prepared according to a previously described procedure.[88] Emission spectra were collected using a QuantMaster 4 spectrophotometer (Photon Technology

International, London, ON). Samples were excited at 430 nm and the emission between 440 nm and 600 nm was recorded. Bandpasses for emission and excitation were set to 3 nm. Emission spectra were corrected for wavelength-dependent instrument response using a quinine sulfate standard.

Peryelene-dap (2.5 µM) was incubated in pH 7.4 buffer (20 mM HEPES, 150 mM NaCl) at 37 °C. To this was added CaCl$_2$ in the same buffer until the desired calcium concentration was achieved (5 mM was used most often). Once the sample had achieved thermal equilibrium. LUVs or lipids were added such that a 250 µM total lipid concentration was achieved. This sample was mixed for 3 min then the emission spectra was recorded. All reported extents of oligomerization are based on at least three replications of this experiment.

(R)-2-hydroxy-3-((4-methoxybenzyl)oxy)propyl 4-methylbenzenesulfonate (**7.6**)

A solution of **7.5** (5.68 g, 26.8 mmol, 1.00 equiv.), triethylamine (3.70 mL, 26.8 mmol, 1.00 equiv.) and dibutyltin(IV) oxide (133 mg, 0.535 mmol, 0.0200 equiv.) was stirred with cooling (ice-water) for 10 min before the addition of 4-toluenesulfonyl chloride (5.10g, 26.8 mmol, 1.00 equiv.). The resulting suspension was stirred for 8 hours. The solution was then concentrated and the residue was suspended in 1:1 ethyl acetate:hexanes and filtered. The filtrate was concentrated, and the residue was purified by silica gel column chromatography (40% ethyl acetate/60% hexanes). This yielded **7.6** as a colorless oil (6.74g, 69% yield). NMR data matched that previously reported.[291]

^{1}H NMR (300 MHz, CDCl$_3$): 7.82 (2H, d, *J* = 8.3 Hz) 7.36 (2H, d, *J* = 8.0 Hz) 7.22 (2H, d, *J* = 8.7 Hz) 6.90 (2H, d, *J* = 8.7 Hz) 4.45 (2H, m) 4.07 (3H, m) 3.83 (3H, s) 3.51 (2H, m) 2.47 (3H, s) 2.38 (1H, d, *J* = 5.5 Hz). ^{13}C NMR (75 MHz, CDCl$_3$): δ159.3, 145.1, 132.6, 130.0, 129.7, 129.4, 128.0, 113.9, 73.1, 70.9, 69.9, 68.3, 55.3, 21.6.

(R)-2-(((benzyloxy)carbonyl)oxy)-3-((4-methoxybenzyl)oxy)propyl   *4-methylbenzenesulfonate*
(**7.7**)

To a cooled (ice-water) solution of **7.6** (6.74g, 18.4 mmol, 1.00 equiv.) and benzyl chloroformate

(2.89 mL, 20.2 mmol, 1.10 equiv.) in dry DCM (100 mL) was added Tetramethylethylenediamine

(1.66 mL, 11.0 mmol, 0.600 equiv.). The resulting suspension was stirred for 30 min then washed

with H_2O, dried over $MgSO_4$ and concentrated. The residue was purified by silica gel column

chromatography (20% ethyl acetate/80% hexanes to 30% ethyl acetate/70% hexanes). This yielded

7.7 as a colorless oil (6.63 g, 72% yield). ^{1}H NMR (300 MHz, CDCl$_3$): 7.78 (2H, d, J = 8.3 Hz)

7.39 (5H, m) 7.31 (2H, d, J = 8.0 Hz) 7.20 (2H, d, J = 8.7 Hz) 6.89 (2H, d, J = 8.7 Hz) 5.16 (2H,

m) 5.06-5.00 (1H, m) 4.42 (2H, d$_{AB}$, J_{AB} = 11.6 Hz) 4.33-4.22 (2H, m) 3.82 (3H, s) 3.60 (2H, m)

2.43 (3H, s). ^{13}C NMR (75 MHz, CDCl$_3$): 159.4, 154.3, 145.0, 134.9, 132.6, 129.9, 129.5, 129.4,

128.7, 128.3, 128.0, 113.9, 73.8, 73.1, 70.0, 67.8, 67.0, 55.3, 21.7. HRMS-ESI+ (*m/z*): [M + NH$_4$]$^+$

calculated for C$_{26}$H$_{32}$O$_8$NS, 518.18431; found, 518.18420.

(R)-2-(((benzyloxy)carbonyl)oxy)-3-((4-methoxybenzyl)oxy)propyl   *N2,N6-*
bis((benzyloxy)carbonyl)-L-lysinate (**7.8**)

A solution of **7.7** (6.41g, 12.8 mmol, 1.00 equiv.) and freshly dried sodium iodide (5.75g, 38.4

mmol, 3.00 equiv.) was refluxed in dry acetone (100 mL) in the dark for 24 hours. The solution

was cooled to room temperature, filtered, concentrated then suspended in diethyl ether, filtered

and concentrated. The reside was purified by silica gel column chromatography (10% ethyl

acetate/90% hexanes and 20% ethyl acetate/80% hexanes) and the isolated alkyl iodide was

dissolved in dry DMF (16 mL). Lyophilized Cbz-Lys(Cbz)-OCs prepared by the method outlined

by Lajoie and coworkers[295] was added to this solution and the mixture was stirred in the dark at

room temperature for 3 days. The reaction mixture was diluted with ethyl acetate (160 mL) and

washed with brine then dried over MgSO$_4$, filtered and concentrated. The residue was purified by silica gel column chromatography (30% ethyl acetate/70% hexanes to 50% ethyl acetate/50% hexanes). This yielded **7.8** as a colorless oil (4.95 g, 52% yield). ^{1}H NMR (300 MHz, CDCl$_3$): 7.36-7.24 (17H, m) 6.90 (2H, d, $J = 8.4$ Hz) 5.59 (1H, app t, $J = 7.6$ Hz) 5.18-5.11 (8H, m) 4.56-4.25 (5H, m) 3.81 (3H, s) 3.62-3.61 (2H, m) 3.15-3.14 (2H, m) 1.80-1.65 (2H, m) 1.44-1.34 (4H, m).^{13}C NMR (125 MHz, CDCl$_3$)172.1 and 172.0, 159.4, 156.6, 156.1, 154.6 and 154.6, 136.8, 136.3, 135.1 and 135.1, 129.6 and 129.4, 129.4, 128.7, 128.6, 128.5, 128.4, 128.3, 128.2, 128.1, 128.1, 113.9, 74.3, 73.1, 69.9 and 69.9, 67.5 and 67.5, 67.0, 66.6, 63.7 and 63.5, 55.3, 53.8 and 53.7, and 40.5, 31.9 and 31.8, 29.3, 22.3 and 22.2. HRMS-ESI+ (*m/z*): [M + H]$^+$ calculated for C$_{41}$H$_{47}$O$_{11}$N$_2$, 743.31744; found, 743.31558.

(R)-2-(((benzyloxy)carbonyl)oxy)-3-hydroxypropyl N2,N6-bis((benzyloxy)carbonyl)-L-lysinate (**7.2**)

2,3-Dichloro-5,6-dicyano-1,4-benzoquinone (1.15g, 5.08 mmol, 1.10 equiv.) was added to a cooled (ice-water) solution of **7.7** (3.43g, 4.62 mmol, 1.00 equiv.) dissolved in dry DCM (18.5 mL) containing H$_2$O (0.966 mL). The solution was stirred for 4 hours then brought to room temperature and stirred for an additional 1 hour. The reaction mixture was diluted with ethyl acetate (50 mL), washed with saturate aqueous NaHCO$_3$ and brine. The organic layer was dried with MgSO$_4$, filter and concentrated. The crude residue was purified by silica gel column chromatography (50% ethyl acetate/50% hexanes to 70% ethyl acetate/30% hexanes). This yielded **7.2** as a colorless oil. ^{1}H NMR (300 MHz, CDCl$_3$): 7.35-7.34 (15H, m) 5.78 (1H, d, $J = 6.3$ Hz) 5.26 (1H, m) 5.26-5.08 (6H, m) 4.99 (1H, m) 4.54-4.23 (3H, m) 3.79 (2H, m) 3.38 (1H, m) 3.13-3.12 (2H, m) 1.78-1.65 (2H, m) 1.43-1.33 (4H, m).^{13}C NMR (125 MHz, CDCl$_3$) 172.4 and 172.3, 156.8, 156.3, 154.7, 136.7, 136.3, 135.0, 128.7, 128.6, 128.5, 128.4, 128.3, 128.2, 128.1, 76.0,

70.0, 67.1, 66.7, 63.2 and 63.0, 60.7, 53.9, 40.4, 31.7, 29.3, 22.3. HRMS-ESI+ (*m/z*): [M + H]⁺ calculated for $C_{33}H_{39}O_{10}N_2$, 623.25992; found, 623.25968.

(2R)-3-(((benzyloxy)((S)-2-(((benzyloxy)carbonyl)oxy)-3-((N2,N6-bis((benzyloxy)carbonyl)-L-lysyl)oxy)propoxy)phosphoryl)oxy)propane-1,2-diyl ditetradecanoate (**7.9**)

Freshly activated 4A powdered molecular sieves were added to dried flask and the flask was placed under dry argon. To this flask, a solution of **7.1** (650 mg, 0.869 mmol, 1.30 equiv.) and alcohol **7.2** (415 mg, 0.666 mmol, 1.00 equiv.) in dry DCM (13.5 mL) was added and the formed suspension was stirred for 15 min at room temperature. A solution 4,5-dicyanoimidazole (118 mg, 0.999 mmol, 1.50 equiv.) in dry acetonitrile (5 mL) was added to the suspension and the reaction mixture was stirred overnight at room temperature. The solution was then cooled (dry ice acetone) and a solution of meta-Chloroperoxybenzoic acid (234 mg, 1.33 mmol, 2.00 equiv.) in DCM (3 mL) was added. Cooling was removed and the reaction mixture was stirred for 90 minutes. The molecular sieves were removed by filtered in the reaction mixture over a pad of celite. The celite pad was extracted with DCM. The filtrate was washed with saturate aqueous NaHCO₃ and brine then dried over MgSO₄, filtered and concentrated. The crude residue was purified by silica gel column chromatography (35% ethyl acetate/65% hexanes). This yielded **7.9** as a colorless oil (486 mg, 56% yield). ¹H NMR (500 MHz, CDCl₃): 7.36-7.35 (20H, m) 5.55 (1H, m) 5.17-5.06 (11H, m) 4.46-4.10 (9H, m) 3.16 (2H, m) 2.31-2.28 (4H, m) 1.82 (1H, m) 1.66-1.28 (49H, m) 0.91 (6H, m). ³¹P NMR (202 MHz, CDCl₃) 0.10, 0.05. ¹³C NMR (125 MHz, CDCl₃) 173.2, 172.8, 171.9 and 171.8, 156.6, 156.1, 156.0, 154.2 and 154.2, 136.7, 136.3, 135.4 and 135.3, 134.8 and 134.7, 128.8, 128.7, 128.7, 128.5, 128.5, 128.4, 128.3, 128.2, 128.1, 128.1, 128.0, 73.3 and 73.2, 70.2 and 70.2, 69.9-69.8, 69.3 and 69.2, 67.0, 66.5, 65.7, 65.1, 62.3, 61.6 and 61.6, 53.7 and 53.6, 40.4, 34.1,

34.0, 31.9, 29.7, 29.7, 29.5, 29.4, 29.3, 29.1, 29.1, 24.8, 22.7, 22.2 and 22.2, 14.1 HRMS-ESI+ (*m/z*): [M + H]$^+$ calculated for $C_{71}H_{104}O_{17}N_2P$, 1287.70671; found, 1287.70336.

(R)-2,3-bis(tetradecanoyloxy)propyl ((S)-3-(((S)-2,6-diammoniohexanoyl)oxy)-2-hydroxypropyl)

phosphate chloride (lysyl-DMPG)

Pd/BaSO$_4$ (5% Pd loading; 400 mg) was suspended in dry ethanol containing 4% acetic acid by volume (2.0 mL) and stirred under an atmosphere of H$_2$ until the catalyst had turned black (about 15 min). A solution of **7.9** (178mg, 0.138 mmol, 1.00 equiv.) in dry ethanol containing 4% acetic acid by volume (1.5 mL) was added and the suspension was stirred for 4 hours at room temperature under a H$_2$ atmosphere. The reaction mixture was centrifuged to remove Pd/BaSO$_4$ and the pellet was extracted once with ethanol containing 4% acetic acid by volume (3.5 mL). The solvent was removed at room temperature under high vacuum. The residue was concentrated from toluene and then chloroform three times each at room temperature. The residue was dissolved in of dry chloroform (3.5 mL) and cooled (ice water) before CHCl$_3$*HCl (prepared by bubbling dry HCl gas through chloroform (0.16 M); 0.864 mL, 0.138 mmol, 1.00 equiv.) was added. Immediately following the addition, the solvent was removed at 0 ^{o}C under high vacuum. The residue was concentrated from CHCl$_3$ twice at 0°C, then suspended in MQ H$_2$O (3.0 mL) and lyophilized. This yielded lysyl-DMPG as a colorless powder. ^{1}H NMR (300 MHz, CD$_3$OD): 5.27 (1H, app sextet, *J* = 5.3 Hz) 4.47-3.99 (10H, m) 3.00 (2H, app t, *J* = 7.3 Hz) 2.40-2.32 (4H, m) 2.10-1.96 (2H, m) 1.79-1.65 (8H, m) 1.31 (40H, m) 0.94-0.90 (6H. m).^{31}P NMR (121 MHz, CD$_3$OD) -0.5. ^{13}C NMR (125 MHz, CD$_3$OD) 171.9, 171.6, 167.2 and 167.2, 68.6 and 68.6, 66.0 and 65.9, 65.0 and 64.9, 64.6 and 64.5, 62.7 and 62.7, 60.5, 50.9, 37.4, 32.2, 32.0, 30.2, 27.9, 27.9, 27.8, 27.8, 27.6, 27.3, 27.3, 25.0, 23.1, 23.1, 20.8, 20.1 and 20.1, 11.6. HRMS-ESI+ (*m/z*): [M + H]$^+$ calculated for $C_{40}H_{80}O_{11}N_2P$, 795.54942; found, 795.54731.

8   Preface and contributions

This chapter is divided into two parts (section 8.1 and section 8.2). The first part focuses entirely on the development of a new enantioselective and diastereospecific synthesis of Fmoc-*threo*-hAsn(TBS)-OH and Fmoc-*threo*-MeOAsp(tBu)-OH. The second part presents the total synthesis of A54145 factor D which employs the building blocks prepared in the first two parts. All this work was done under the supervision of Prof. Scott D. Taylor

Section 8.1 is based on a manuscript published in the journal *Organic Letters* (*Reprinted (adapted) with permission from Org. Lett.* **2018***, 20, 7717–7720. Copyright 2018 American Chemical Society*) The experimental work presented in this section was completed entirely by me. I also assisted in preparation of the manuscript as it pertained to the oxidative cleavage reaction. Additional supplementary data is available on the journal's website.

Section 8.2 is based on a manuscript published in *The Journal of Organic Chemistry* (*Reprinted (adapted) with permission from J. Org. Chem.* **2019***, 84,* 12021–12030.*Copyright 2019 American Chemical Society*). The Fmoc SPPS route to A54145 factor D was developed primarily by Braden Kralt, a graduate student in the Taylor Lab. My contributions included the synthesis of Fmoc-L-*erythro*-MeOAsp(t-Bu)-OH and (R)-2-Methylbutanal. In Section 8.2, I will provide a detailed account of my contributions to the total synthesis of A54145 factor D and will overview the route developed by other members of the Taylor. Additional supplementary data is available on the journal's website.

8.1   Asymmetric synthesis of Fmoc-protected β-hydroxy and β-methoxy amino acids via a Sharpless aminohydroxylation reaction using FmocNHCl

As stated in chapter 1, one of the primary goals of this thesis was to determine whether the chiral target of A5D is a stereoisomer of PG. To complete this goal, we needed to develop a synthesis of A5D that could later be applied to the synthesis of the unnatural enantiomer of A5D. This is no small task: A5D possesses more unusual amino acids than daptomycin and an ester bond that is arguably more difficult to form. In addition, when we embarked on this project, no attempts on the total synthesis of A5D had been published.

As discussed in section 1.1, A5D possesses the unusual amino acids hAsn and MeOAsp, which are not found at any position in daptomycin.[14,15] Both of the amino acids are known to possess the S-absolute configuration at the α-position, while the absolute configurations at the β-position are not as well established. LptL, the portion of NRPS that synthesizes hAsn3 in A5D, possesses high sequence homology with an asparagine oxidase enzyme known to synthesized L-*threo*-hAsn.[139] In contrast, LptJ, which is responsible for the hydrolyxation step during the biosynthesis of MeOAsp9, is rather unique, but does bear some resemblance to an enzyme known to produce L-*threo*-hAsp (section 1.6.1).[141,296] Based on these studies, it was assumed that A5D contained L-*threo*-hAsn3 and L-*threo*-MeOAsp9. Thus, we focused on developing a synthesis for Fmoc-L-*threo*-hAsn(TBS)-OH (**8.1**) and Fmoc-L-*threo*-MeOAsp(t-Bu)-OH (**8.2**) which would later be applied to the development of an Fmoc SPPS of A5D (Figure 8.1).
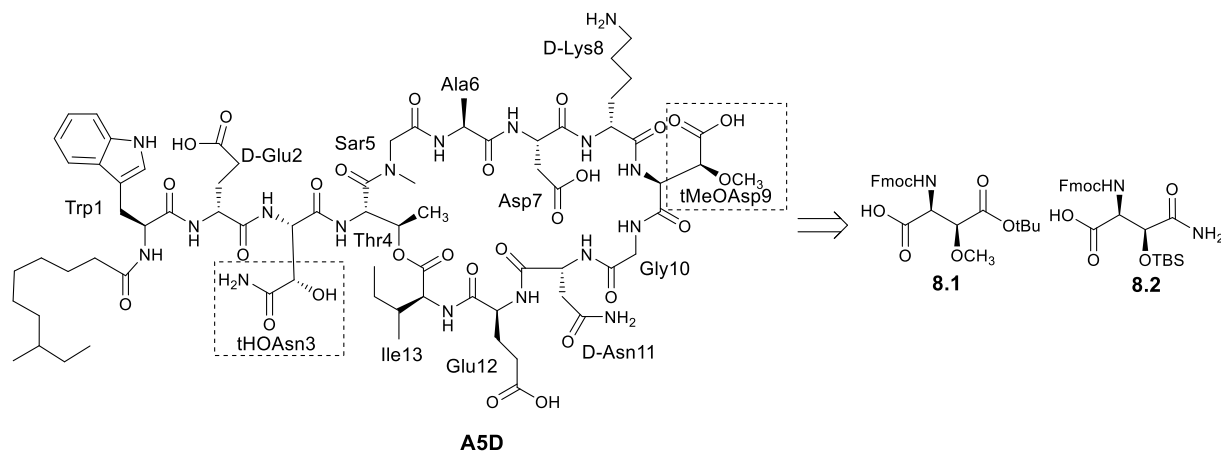
Figure 8.1 Fmoc-L-*threo*-hAsn(TBS)-OH (**8.1**) and Fmoc-L-*threo*-MeOAsp(tBu)-OH (**8.2**)

A thorough literature search revealed a multitude of approaches to **8.1** and **8.2**. Shimamoto et al reported a synthesis of unprotected L-*threo*-MeOAsp starting from Garner's aldehyde;[297] however, the synthesis was lengthy (13 steps) and required the separation of diastereomeric intermediates. Several enantioselective syntheses of protected and unprotected L-*threo*-β-hydroxyaspartate,[298–302] and a synthesis of protected L-*threo*-β-methoxyasparagine[303] have been reported. Although it would be possible to adapt these approaches to achieve a synthesis of compound **8.1**, we believed that a shorter and more efficient route could be developed.

threo-hAsn is found in a number of other natural products,[304] and several enantioselective syntheses of it, protected[305–307] and unprotected,[308] have been reported. Guzmán-Martínez and Van Nieuwenhze reported the synthesis of Fmoc-L-*threo*-hAsn(Trt)-OH.[307] In their route, L-threo-β-hydroxyaspartic acid, which was prepared in three steps from L-dimethyl aspartate using the procedure of Cardillo et al.,[302] was subjected to eight reactions to give Fmoc-L-*threo*-hAsn(Trt)-OH. Boger and coworkers reported a 5-step synthesis of Boc-L-*threo*-hAsn(Trt)-OH.[305,306] The first step in their synthesis was a Sharpless asymmetric aminohydroxylation (SAAH) of the methyl ester of (*E*)-4-methoxycinnamate utilizing benzyloxycarbamate as the nitrogen source. Among the subsequent steps of their synthesis were the substitution of the Cbz

216

group with a Boc group, a 10-14 day aminolysis of the methyl ester to give the carboxamide side chain and a RuCl$_3$/NaIO$_4$ oxidation of the *p*-methoxyphenyl group to give the α-COOH group. A similar approach has been used to prepare Boc-L-*erythro*-hAsn(TBS)-OH.[309]

We decided to employ Boger's strategy of using the SAAH reaction as the initial and key step in the synthesis of both **8.1** and **8.2**; however, we wished to avoid the removal and installation of several amino protecting groups, a lengthy aminolysis reaction (for preparing compound **8.2**), and the use of the *p*-methoxyphenyl group as a masking group for α-COOH group, as the RuCl$_3$/NaIO$_4$ oxidation of this group often proceeds in only moderate yields and requires careful attention to the reaction conditions to achieve consistent results.[303,305,306,309]

To avoid the removal and installation of several amino protecting groups, we envisioned installing the Fmoc-protected amino group at the beginning of the synthesis by performing a SAAH reaction on alkene **8.3** to give compound **8.4** which would be used to prepare both compounds **8.1** and **8.2** (Scheme 8.1).
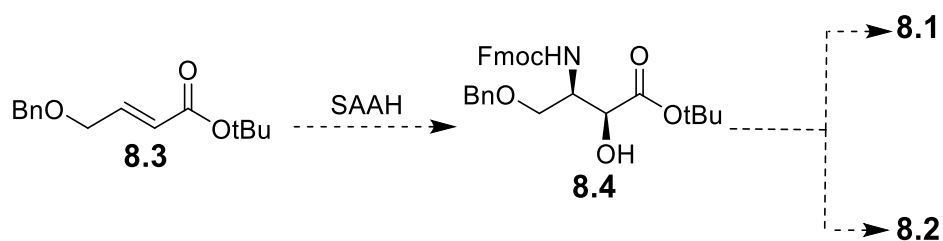
Scheme 8.1 Proposed route to compounds **8.1** and **8.2**

A search of the literature revealed that no reports have appeared describing any attempts to perform SAAH reactions using fluorenylcarbamate (FmocNH$_2$). The reason for this is probably because it has been assumed that the Fmoc group is too base-labile to survive the basic conditions that are usually used for SAAH reactions. Harris et al developed carbamate **8.5** for use in base-free SAAH reactions (Scheme 8.2).[310] We attempted the SAAH reaction on alkene **8.3**[311] using

8.5 under the conditions reported by Harris et al. This gave a mixture of the desired compound **8.4a** and the undesired regioisomer **8.4b** in a 4:1 ratio and in an overall yield of 62%. The isomers could be easily separated by flash chromatography. Compound **8.4a** was isolated in a 48% yield with an enantiomeric ratio (er) of 3:2 as determined by chiral stationary phase HPLC.
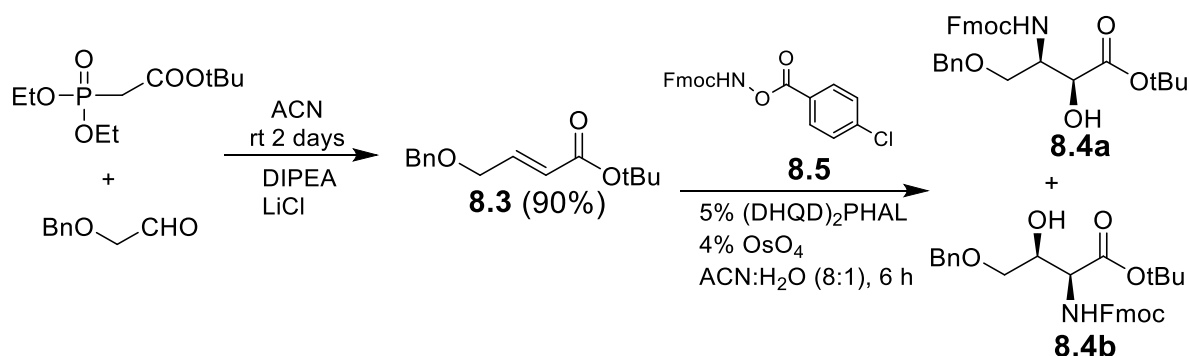
Scheme 8.2 SAAH reaction on compound **8.3** using compound **8.6** as the nitrogen source

Our limited success with reagent **8.5** prompted us to look at other Fmoc-based nitrogen donors for the SAAH reaction. As mentioned earlier, the base-lability of the Fmoc group suggests that performing a SAAH reaction using $FmocNH_2$ under standard (basic) conditions would not be very successful. Indeed, when we attempted the reaction of **8.3** with $FmocNH_2$ under the SAAH conditions used by Boger et al (H_2O:nPrOH (1:1), 4 % $K_2OsO_2(OH)_4$, 5 % $(DHQD)_2PHAL$, 2.3 equiv. NaOH, 2.5 equiv. $FmocNH_2$, 1.02 equiv. t-BuOCl, rt then 0 °C)[305] we were able to isolate only trace amounts of the SAAH reaction products. We noticed that $FmocNH_2$ was not very soluble under these reaction conditions and in H_2O/alcohol mixtures in general, and this may have contributed, at least in part, to the failure of the reaction in that the required *N*-chlorofluorenyl carbamate (FmocNHCl, **8.6**, Figure 8.2) may not have been formed or was forming very slowly. Therefore, we decided to prepare **8.6** and examine it as a nitrogen source in the SAAH reaction, anticipating that the much lower pK_a of the *N*-chlorocarbamate moiety in **8.6** compared to that in $FmocNH_2$ would allow for the dissolution of **8.6** under the basic conditions.[312]

8.6
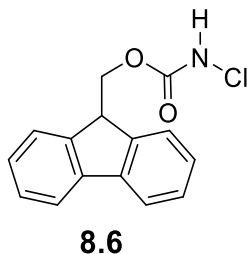
Figure 8.2. N-chlorofluorenyl carbamate (FmocNHCl, **8.6**).

Recently, Gwon et al reported the isolation of **8.6** in a 41% yield by reacting FmocNH$_2$ with trichloroisocyanuric acid (TCAA), an inexpensive chlorinating agent, in MeOH.[313] By making some minor modifications to Gwon et al's procedure, we were able to obtain **8.6** in 70-95 % yields in multigram quantities. Compound **8.6** is stable white powder and can be stored at room temperature.

We performed SAAH reactions on **8.3** using **8.6** and focused on obtaining conditions that provided compound **8.4a** with an er suitable for our purpose. Toward this end, a series of reactions were run using 2 equiv. of **8.6** and 1.7 equiv. NaOH in nPrOH/H$_2$O mixtures in the presence of different amounts of ligand and osmate and in varying ratios of nPrOH to water at 0 °C. After 4 h, the reactions were quenched regardless of whether they were complete or not, and compound **8.4a** was isolated, and its er and yield determined (Table 8.1).

We first attempted the reaction using 5 and 4 mol % ligand and osmate respectively in nPrOH:H$_2$O, 1:1. This provided **8.4a** in a 42% yield with an er of 87:13 (entry 1). We attempted to improve the yield and er by increasing the amount of ligand and osmate to 12 and 8 mol % respectively; however, this resulted in only minor improvements to both yield and er (entry 2). We noticed that the dissolution of **8.6** in nPrOH:H$_2$O, 1:1 was limited so we increased the proportion of nPrOH (nPrOH:H$_2$O, 3:2), but decreased the amount of ligand and osmate to 9 and 8 mol % respectively. This resulted in an increase in yield to 65%, but not er (entry 3). However, when

219

performing the reaction in this solvent mixture and using 12 and 8 mol % of ligand and osmate respectively, all of alkene **8.3** was consumed after 4 h, the yield increased to a respectable 70% and the er improved to 95:5 (entry 4, see Figure F.1) which was acceptable to us for the synthesis of **8.1** and **8.2**. ^{1}H-NMR analysis of the crude reaction mixture after workup revealed that the ratio of **8.4a**:**8.4b** was 12.5:1. It is worth noting that, so long as the reaction was maintained at 0 °C, we were unable to detect (by TLC) dibenzofulvene or fluorenol during the reaction, which suggests that decomposition of **8.6** via base-promoted elimination processes did not occur. A further increase in the proportion of nPrOH resulted in a decrease in yield, but no decrease in er (entries 5 and 6). Performing the reaction under the conditions outlined in entry 4 using FmocNH$_2$ and t-BuOCl gave **8.4a** in just a 15% yield and an er of 94:6 (entry 7).

Table 8.1. Results of the SAAH reaction on compound **8.3** using compound **8.7**
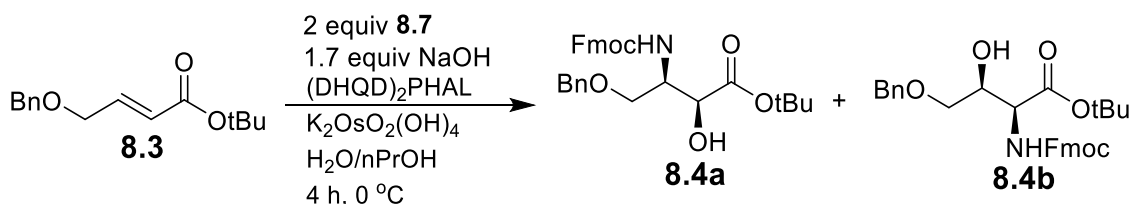
Entry	Ratio nPrOH:H$_2$O	Ligand[a] (mol %)	Osmate (mol %)	**8.4a** (% yield)[b]	Er[c,d]
1	1:1	5	4	42	87:13
2	1:1	12	8	45	90:10
3	3:2	9	8	65	90:10
4	3:2	12	8	70	95:5
5	3:1	12	8	48	95:5
6	4:1	12	8	54	95:5
7[e]	3:2	12	8	15	94:6

[a](DHQD)$_2$PHAL. [b]Isolated yield. [c]Absolute configuration was determined by ^{1}H NMR analysis of the (R)- and (S)-Mosher's esters. [d]Determined by chiral stationary phase HPLC. [e]Using 2 equiv FmocNH$_2$ and t-BuOCl.

Compound **8.4a**, obtained using the conditions outlined in entry 4 in Table 1, was used to prepare compounds **8.1** and **8.2**. To obtain compound **8.1** (Scheme 8.3), the hydroxy group in **8.4a** was methylated using MeI/Ag$_2$O to give compound **8.7** in 88% yield. We were unable to remove

the benzyl group by hydrogenolysis without losing the Fmoc protecting group (See Table F.1).We attempted to do a one-pot conversion of **8.7** into **8.1** using 4-acetylamino-2,2,6,6-tetramethylpiperidine-1-oxoammonium tetrafluoroborate (Bobbitt's salt) as described by Pradhan et al (3 equiv. Bobbitt's salt, 9:1 MeCN:H_2O, rt).[205] Under these conditions, almost all of **8.7** was converted to alcohol **8.8** after 18 h, but the reaction did not proceed any further, and even after 48 h, only small amounts of the corresponding aldehyde and **8.1** were evident. Since these types of oxidations appear to proceed best under neutral or basic conditions,[314] we added a neutral phosphate buffer to the acidic reaction mixture after all of **8.7** was converted to **8.8** (18 h). However, only small amounts of **8.1** were obtained after 24 h. A sodium chlorite test[314] performed immediately after the addition of the buffer revealed that almost no Bobbitt's salt was present, suggesting that it had probably decomposed to 4-acetamidoTEMPO and/or the corresponding hydroxylamine.[315] We reasoned that 4-acetamidoTEMPO and/or the corresponding hydroxylamine could be converted back to the corresponding oxoammonium salt with NaOCl.[314] Therefore, compound **8.7** was subjected to a concentrated solution of 3 equiv. of Bobbitt's salt for 18 h at rt to give mainly **8.8**. The mixture was cooled to 0 ℃ and then a phosphate buffer was added, followed by $NaClO_2$ and NaClO. This resulted in the rapid oxidation of **8.8**, and compound **8.1** was obtained in a 90% yield.

To obtain **8.2**, the t-butyl group in **8.4a** was first removed using TFA (Scheme 8.4). We attempted to convert the resulting crude acid to the primary amide using 1.3 equiv. $(Boc)_2O$/1.2 equiv. NH_4HCO_3 according to the procedure of Pozdenev.[316] However, this provided a mixture of the desired compound **8.9** and the t-butyl carbonate **8.10**. We were unable to develop conditions that prevented the formation of the t-butyl carbonate moiety. Therefore, we used 3 equiv. $(Boc)_2O$ and 1.7 equiv. NH_4HCO_3 to quantitatively convert **8.4** into **8.10**. Treating crude **8.10** with TFA for

60 min resulted in quantitative removal of the Boc group, and the resulting crude alcohol was reacted with TBSCl to give **8.11** in an 81% yield over 4 steps (one chromatographic purification). Attempts to convert **8.11** into compound **8.12** or amino acid **8.2** using the conditions outlined in Scheme 8.3 (**8.7** to **8.8** or **8.7** to **8.1**) resulted in a complex mixture of products. Nevertheless, we found that the benzyl group could be removed using BCl_3 in the presence of pentamethylbenzene (PMB) which gave alcohol **8.12** in an 82% yield.[317] Oxidation of **8.12** with TEMPO/$NaClO_2$/NaClO gave **8.2** in a 95% yield.
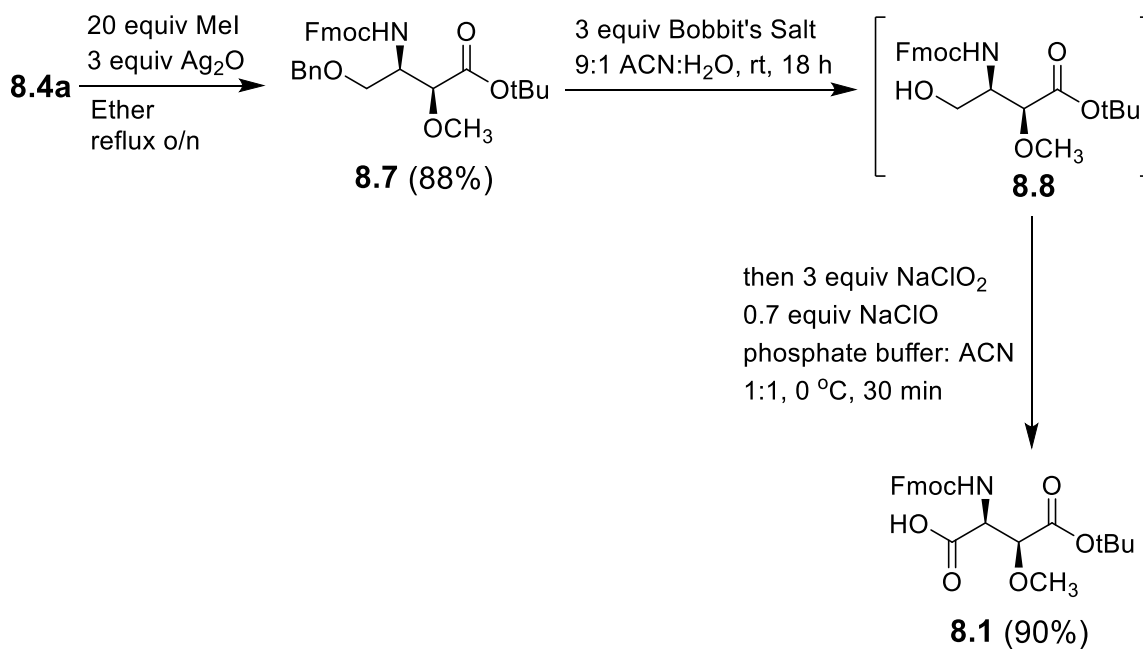
Scheme 8.3 Synthesis of amino acid **8.1** from compound **8.4**.
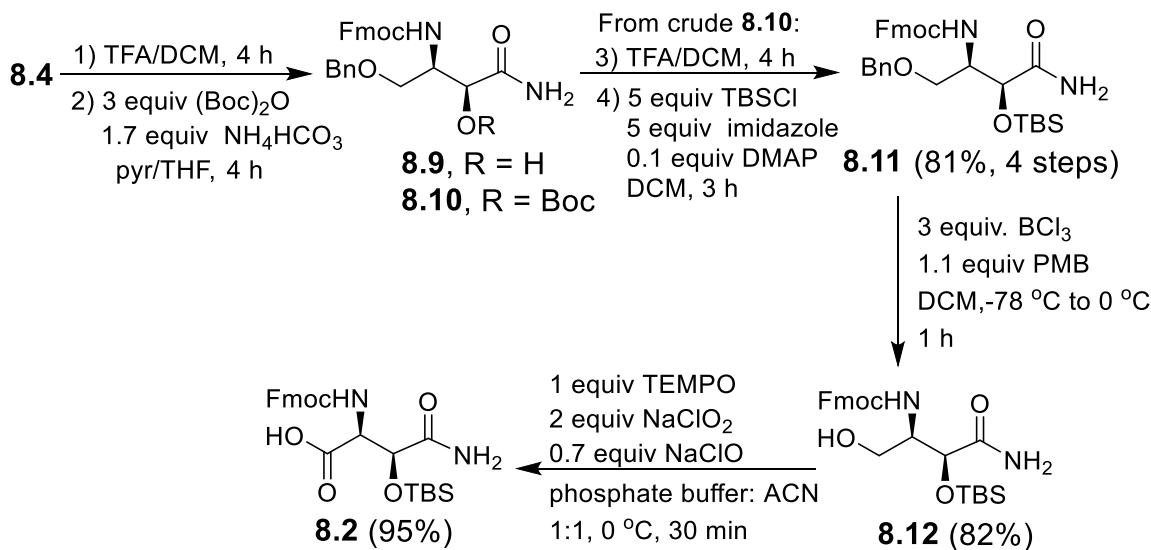
Scheme 8.4 Synthesis of amino acid **8.2** from compound **8.4.**

In summary, we succeeded in developing efficient asymmetric syntheses of Fmoc-L-*threo*-MeOAsp(t-Bu)-OH (**8.1**) and Fmoc-L-*threo*-hAsn(TBS)-OH (**8.2**). The key step was a SAAH reaction on alkene **8.3** using FmocNHCl, a readily prepared and storable nitrogen source. We also demonstrated, contrary to expectations, that the Fmoc group can survive the basic conditions that are often employed for SAAH reactions, and that the Fmoc-protected product can be obtained in good yield and stereoselectivity. We also showed that FmocNHCl can be prepared in a single step, in very high yield, and in multigram quantities, and is a stable solid and storable at room temperature, making this reagent a very convenient one for SAAH reactions where the installation of an Fmoc-protected amine is desired.

8.2   The Solid-phase Synthesis of A54145D

Before, embarking on the synthesis of A5D, we need ample quantities of the 8-methyl decanoic acid lipid tail. (±)-8-methyldecanoic acid ((±)-**8.15**) was prepared follow the sequence in Scheme 8.5. This was achieved by performing a Wittig reaction between phosphonium salt **8.13**[318] and (±)-2-methylbutanal which gave alkene (±)-**8.14** in 66% yield. Fatty acid (±)-**8.15** was obtained in good yield by subjecting (±)-**8.14** to hydrogenolysis and then NaOH.

223
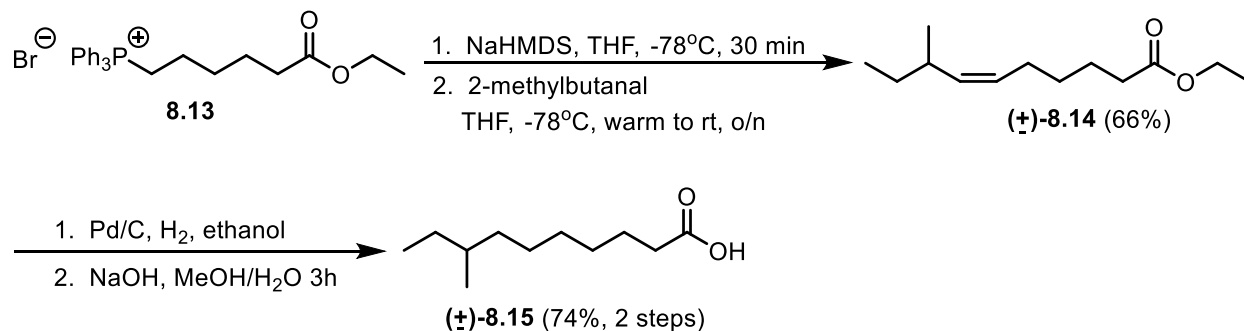
Scheme 8.5. Synthesis of (±)-8-methyldecanoic acid ((±)-**8.15**)

Several difficulties were encountered when developing the total synthesis of A5D which are discussed in detail both in the manuscript associated with this section and in Braden Kralt's thesis.[181,319] The final synthesis is presented in Scheme 8.6 which starts with attachment of Fmoc-Sar-OH to a polystyrene resin via a 2-ClTrt linker. After removing the Fmoc group from Sar, Fmoc-L-Thr-OH is coupled on with *N,N'*-diisopropylcarbodiimide (DIC)/hydroxybenzotriazole (HOBt) to the free α-amine giving resin bound dipeptide **8.16**. To prevent diketopiperazine formation, Thr4 is Fmoc deprotected with 2 x 1 min treatments with 20% 2-MP/DMF and Fmoc-*threo*-hAsn(OTBS)-OH is immediately coupled to the unmasked α-amine with DIC/HOBt yielding tripeptide **8.17**. The ester bond was formed on **8.17** with one overnight treatment with 10 equiv. N3-Ile-OH, 10 equiv. DIC, 0.1 equiv. DMAP giving depsi peptide **8.18**. Peptide **8.18** was elongated to Trp1 using Fmoc SPPS at which point we attached a racemic 8-methyldecanoic acid tail giving lipopeptide **8.19**. At this stage, TBAF/AcOH was used to remove the TBS group on hAsn3 and then the α-azide of Ile was reduced under conditions developed by the Taylor lab which prevent triazole formation that generally occurs upon reduction of azides α to ester bonds.[320] Reversing the order of these reactions, gave a complex mixture of products highlighting an incompatibility between silyl groups and phosphines. This reaction sequence successfully synthesized peptide **8.20** which was elongated by Fmoc SPPS to Ala6 giving peptide **8.21**.

Cleavage from the solid-support was achieved with 1% TFA/DCM yielding peptide **8.22** which was cyclized in solution at a concentration of 1 mM with PyAOP/HOAt/2,4,6-collidine in DMF. Cyclic peptide **8.23** was then globally deprotected giving crude A5D containing L-*threo*-MeOAsp9 (A5D-tMeOAsp) which was isolated by HPLC in an 8% overall yield.

The antimicrobial activity of the synthesized material was found to be 64-fold higher than a sample of the authentic material suggesting that the configuration at the β-positions of hAsn3 or MeOAsp9 was incorrect in our synthesis (Table 8.2). As discussed in section 1.6.1, the configuration assigned to the β-position of hAsn3 is based on homology between the NRPSs of A54145D. Crystallographic data unequivocally proved that the enzyme responsible for the β-oxidation of Asn in CDA gives exclusively L-*threo*-hAsn. In contrast, the enzymes responsible for the synthesis of MeOAsp are less well-known; thus, we concluded that the configuration at β-position of MeOAsp is probably incorrect and started to develop a synthesis for Fmoc-L-*erythro*-MeOAsp(t-Bu)-OH (**8.27**). While this synthesis was in development, the Li lab disclosed the first total synthesis of A54145A, A1, B, B1 and F which confirmed that A5 contains L-*threo*-hAsn and L-*erythro*-MeOAsp.
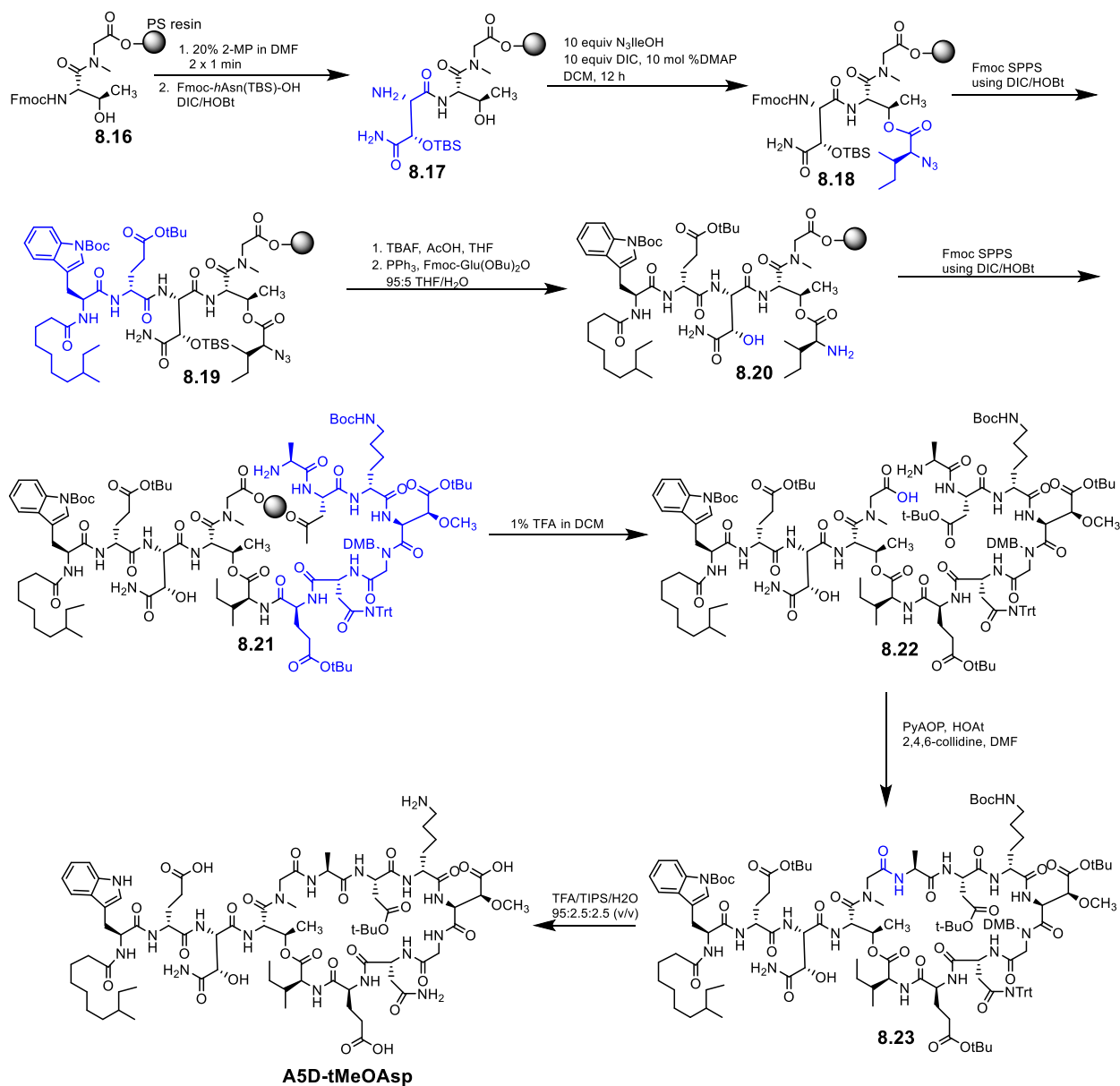
Scheme 8.6 Synthesis of A5D-tMeOAsp

Our approach to **8.27** was inspired Wong et al. who used a Mitsunobu reaction sequence to invert the configuration of the β-hydroxy group and establish the absolute configuration of Boc-L-*erythro*-hAsn(TBS)-OH (Scheme 8.7).[309] Our synthesis began with **8.4** which was reacted with DIAD/PPh₃/*p*-nitrobenzoic acid (PNBCOOH) yielding ester **8.24** which was purified by recrystallization. The PNB ester was readily azidolyzed under neutral conditions which gave **8.25**

in an excellent yield.[309] Chiral stationary phase HPLC analysis of **8.25** showed that the recrystallization of **8.24** had increased the er to 97:3 (Figure F.2). Methylation with MeI/Ag$_2$O gave **8.26** which was oxidatively-cleaved with Bobbit's salt as done in Scheme 8.3, yielding **8.27**
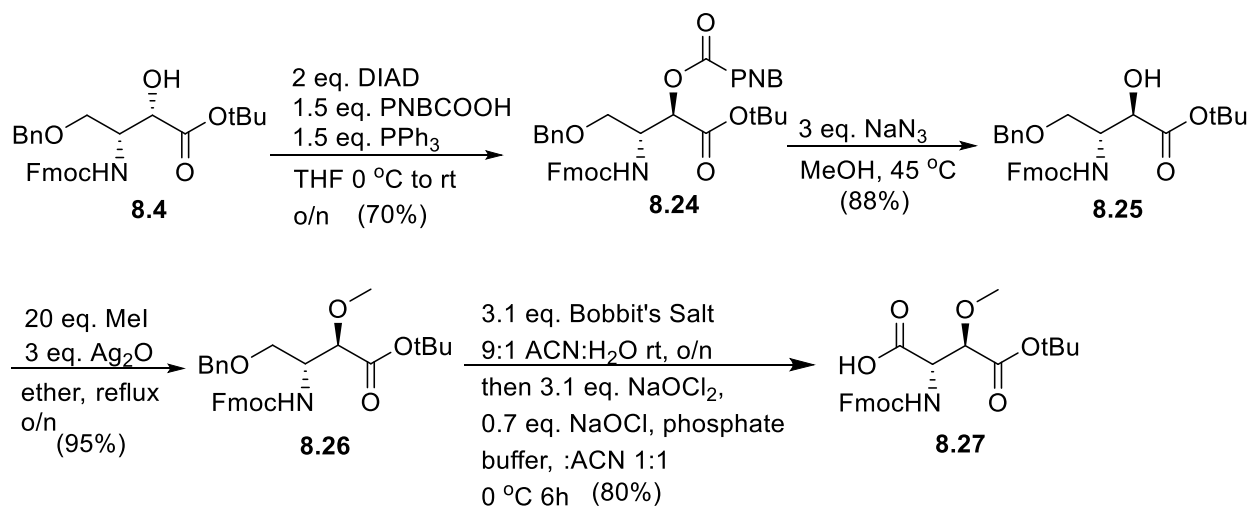
Scheme 8.7 Synthesis of Fmoc-L-*erythro*-MeOAsp-OH

A5D-*e*MeOAsp was prepared using the same route (Scheme 8.6) that was used for the A5D-*t*MeOAsp isomer. The biological activity of A5D-*e*MeOAsp was the same as authentic A5D (Table 8.2). The HPLC chromatogram and NMR spectra of synthetic A5D-*e*MeOAsp were also identical to authentic A5D. These results indicated that the MeOAsp residue in A5D has the *2S,3R* (L-*erythro*) configuration and strongly suggested that the hAsn residue is indeed the L-*threo* isomer.

Table 8.2 MIC's of A5D peptides

entry	peptide	MIC (µg/mL)[a]
1	Authentic A5D	0.5
2	A5D-*t*MeOAsp	>32
3	A5D-*e*MeOAsp	0.5

| 4 | A5D-(R)-anteiso | 0.5 |
| 5 | A5D-(S)-anteiso | 0.5 |

[a]Against *B. subtilis* 1046. 1.25 mM Ca^2 present.

Although the configuration of the *anteiso*-lipid in A5D has never been determined, Kaneda has reported that *anteiso*-lipids in Gram-positive bacteria have the *S*-configuration.[321] The fact that our synthetic A5D, which contained a racemic lipid, exhibited the same activity as authentic A5D suggests that the stereochemistry of the lipid does not affect activity or that the lipid in A5D is actually racemic. To determine if this is indeed the case, we prepared A5D (containing the correct L-*erythro*-MeOAsp isomer) bearing either (*R*)-8-methyldecanoic or (*S*)-8-methyldecanoic acid (A5D-(8*R*)-anteiso and A5D-(8*S*)-anteiso). (8*R*)- and (8*S*)-methyldecanoic acid were prepared using the same route used to prepare (±)-8-methyldecanoic (Scheme 8.5) except (*R*) or (*S*)-2-methylbutanal was used instead of (±)-2-methylbutanal. (*S*)-2-Methylbutanal was readily prepared by TEMPO oxidation of commercially available (*S*)-2-methylbutanol.[322] However, (*R*)-2-methylbutanol and (*R*)-2-methylbutanal are either not commercially available or very expensive. We prepared (*R*)-2-methylbutanal using a route similar to that developed by Yang et al for the synthesis of (*R*)-2-methylpentanal (Scheme 8.8).[323] (1*S*)-2,10-Camphorsultam was treated with butyryl chloride in the presence of TEA and DMAP which gave sulfonamide **8.28** in 69% yield. Methylation at the 2-position of the butyryl portion of **8.28** with NaHMDS/MeI gave compound **8.29** in 79 % yield. A crystal structure of **8.29** was used to establish the absolute configuration at the α-position (Figure F.3 and Table F.2). Treatment of **8.29** with DIBAL gave (*R*)-2-methylbutanal (**8.30**) in 33 % yield.
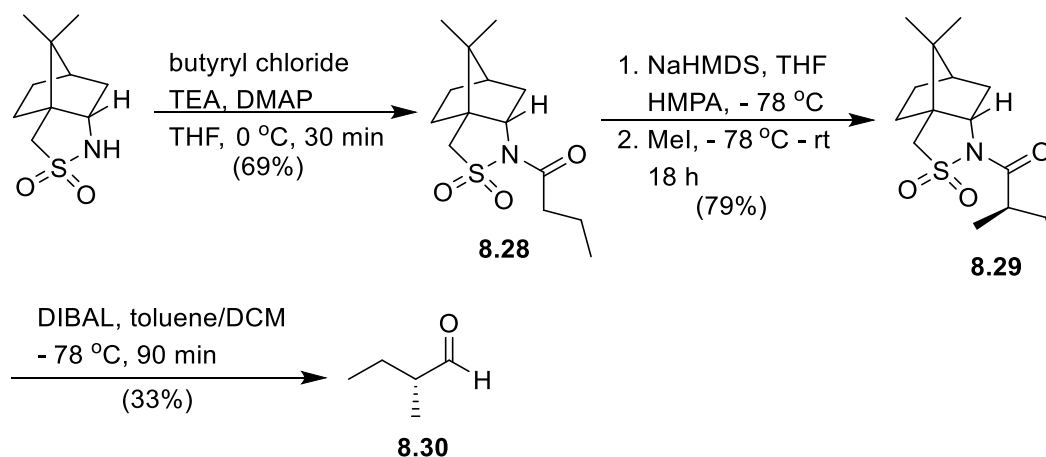
Scheme 8.8 Synthesis of (R)-2-methylbutyraldehyde

A5D-(8*R*)-anteiso and A5D-(8*S*)-anteiso were prepared using the same route outlined in Scheme 8.8 except Fmoc-L-*erythro*-MeOAsp(tBu)OH, and (8*R*)- or (8*S*)-methyldecanoic acid was used. The biological activities of A5D-(8*R*)-anteiso and A5D-(8*S*)-anteiso were determined against *B. subtilis* (Table 8.2), and it was found that the biological activities of A5D-(*R*)-anteiso and A5D-(*S*)-*anteiso* were identical to those of authentic A5D and A5D-*e*MeOAsp.

8.3 Conclusions

In closing, we succeeded in developing a total synthesis of the natural product A5D. Key to the success of this synthesis was the development of an efficient route to the unusual amino acids present in A5D which gave rapid access to both the *threo* and *erythro* isomers. The work presented in this chapter was later used to synthesize the unnatural enantiomer of A5D which was one of the major goals of this thesis (see chapter 10).

It is important to note that while the work described here was nearing completion, Chen et al reported the total synthesis of A54145A, A1, B, B1 and F, the stereochemical revision of the MeOAsp, and confirmed that the hAsn residue is the L-*threo* isomer.[193] Their approach was to attach the peptide to the resin via Gly10; however, the yields were low (3 %). Our studies suggest that the low yields may have been due to one of the side reactions we observed while using this

attachment point. Their having to make the ester bond on a 10-mer containing the lipid tail may also have contributed to the low yields. In contrast, we have devised a more efficient synthesis of A5D. Consistent with the studies of Chen et al,[193] we found that the MeOAsp residue has the *2S,3R* configuration. Additionally, we show that the stereochemistry of the lipid does not affect biological activity. This opens the door for a detailed investigation into the action mechanism of A5D and its supposed activity in the presence of lung surfactant.

8.4 Experimental

General Information.

All reagents were purchased from commercial suppliers. ACS grade n-propanol (nPrOH), Toluene and trifluoroacetic acid (TFA) were used without further purification. Methylene chloride (DCM) and acetonitrile (ACN) were dried by distillation over calcium hydride under nitrogen. Pyridine was dried by refluxing over potassium hydroxide followed by fractional distillation. Tetrahydrofuran (THF) was distilled from sodium metal in the presence of benzophenone under N_2. Chromatography was preformed using 60 Å silica gel.

Reversed-phase analytical chiral HPLC was performed using a CHIRAL PAK AS-RH 5 µm 4.6 mm x 150 mm column with a flow rate of 0.5 mL/min.

High resolution positive electrospray (ESI) mass spectra were obtained using an orbitrap mass spectrometer. Samples were sprayed from MeOH: 1% formic acid in H_2O. All spectra were collected in the positive mode. ^{1}H- and ^{13}C-NMR were collected using a Bruker Avance-300 spectrophotometer. ^{1}H NMR chemical shifts (δ) are reported in ppm relative to an internal standard (trimethylsilane, 0 ppm). ^{13}C-NMR chemical shifts are reported relative to the solvent peak (77.0 ppm for $CDCl_3$, 49.2 ppm for CD_3OD).

*FmocNHCl (**8.6**).*

Modified from Gwon et al.[313] FmocNH$_2$ (12 g, 50 mmol, 1.0 equiv) was dissolved with heating in MeOH (750 mL). When the reaction mixture had cooled to 35 °C, pulverized trichloroisocyanuric acid (3.86 g, 16.7 mmol, 1/3 equiv) was added in a single portion. After stirring for 18 h at room temperature the resulting solid was suspended in hot toluene. The cloudy suspension was filtered while hot. FmocNHCl crystallized from the filtrate upon cooling. (13 g, 95%). Characterization data was found to match those reported by Gwon et al.

tert-butyl (2S,3R)-3-(((((9H-fluoren-9-yl)methoxy)carbonyl)amino)-4-(benzyloxy)-2-hydroxybut-anoate (8.4a). To a cooled (ice bath) slurry of FmocNHCl (11.0 g, 40.2 mmol, 2.00 equiv) in n-PrOH (90 mL) was added a solution of sodium hydroxide (1.20 g, 30.0 mmol, 1.50 equiv) in water (150 mL). A solution of (DHQD)$_2$PHAL (1.40 g, 1.80 mmol, 12.0 mol %) in nPrOH (75 mL) and a solution of **8.3**[311] (5.00 g, 20.1 mmol, 1.00 equiv) in nPrOH (150 mL) were added immediately after. The reaction was allowed to cool (ice bath), then a solution of potassium osmate (594 mg, 1.61 mmol, 8 mol %) and sodium hydroxide (153 mg, 3.83 mmol, 0.190 equiv) in water (65 mL) was added. The cooled reaction was stirred for 4 h, at which point TLC had indicated that the reaction was complete. The mixture was neutralized with 1N HCl and the resulting slurry was filtered. The filter cake was washed several times with 3:2 nPrOH:H$_2$O. The filtrate was concentrated and then partitioned between ethyl acetate (EtOAc, 100 mL) and water (100 mL). The aqueous layer was extracted twice, and the combined organic layer was washed with 1 N HCl (300 mL), sat. NaHCO$_3$ (300 mL) and brine (300 mL). The resulting organic layer was dried with MgSO$_4$, filtered and concentrated. The crude oil was subjected to silica gel column chromatography (12.5% EtOAc/77.5% benzene) which provided **8.4a** as a clear viscous oil (7.09 g, 70% yield). ^{1}H NMR (300 MHz, CDCl$_3$): δ 7.68 (2H, d, J = 7.5 Hz) 7.48 (2H, m) 7.34-7.22 (9H, m) 5.05 (1H, d, J = 9.7 Hz) 4.48 (2H, d, J_{AB} = 12.1 Hz) 4.30-4.25 (4H, m) 4.13-4.08 (1H, dd,

J = 7.2, 7.2 Hz) 3.51-3.46 (2H, m) 1.36 (9H, s).^{13}C NMR (75 MHz, CDCl$_3$): δ 172.5, 155.7, 143.8, 143.7, 141.2, 137.7, 128.3, 128.2, 127.7, 127.7, 127.6, 127.0, 125.0, 119.9, 119.9, 83.4, 73.2, 69.5, 68.9, 66.8, 52.2, 47.0, 27.6. HRMS-ESI+ (m/z): [M + H]$^+$ calculated for C$_{30}$H$_{34}$O$_6$N, 504.23806; found, 504.23984.

For chiral HPLC studies, the enantiomer of **8.4** (**ent-8.4**) was prepared following a similar procedure but (DHQ)$_2$PHAL was used in place of (DHQD)$_2$PHAL. ^{1}H and ^{13}C NMR spectra were identical to **8.4**.

tert-butyl (2S,3R)-3-((((9H-fluoren-9-yl)methoxy)carbonyl)amino)-4-(benzyloxy)-2-methoxybut-anoate (8.8). Freshly prepared, dry Ag$_2$O (3.45g, 14.9 mmol, 3.00 equiv) and MeI (6.19 mL, 49.6 mmol, 20.0 equiv) were added to solution of compound **8.4a** (2.50 g, 4.97 mmol, 1.00 equiv) in ether (100 mL) at room temperature. The mixture was vortexed briefly until a suspension was formed. The mixture was then brought to reflux and allowed to react for 18 h, with vigorous stirring, under an inert atmosphere. The mixture was cooled to room temperature, filtered and concentrated. The residue was subjected to silica gel column chromatography (25% EtOAc/75% hexanes) which provided **8.8** as a colorless, vicious oil (2.25 g, 88% yield). ^{1}H NMR (300 MHz, CDCl$_3$): δ 7.67 (2H, d, J = 7.4 Hz) 7.49 (2H, d, J = 7.2 Hz) 7.34-7.20 (9H, m) 5.10 (1H, d, J = 9.5 Hz) 4.50 (2H, d, J_{AB} = 11.9 Hz) 4.33-4.08 (4H, m) 3.93 (1H, s) 3.45-3.43 (2H, m) 3.37 (3H, s) 1.36 (9H, s). ^{13}C NMR (75 MHz, CDCl$_3$): δ 169.5, 155.6, 143.7, 143.5, 141.0, 141.0, 137.7, 128.2, 127.5, 127.4, 126.8, 124.9, 124.9, 119.7, 81.8, 77.9, 72.8, 68.0, 66.7, 58.6, 52.1, 46.9, 27.7. HRMS-ESI+ (m/z): [M + H]$^+$ calculated for C$_{31}$H$_{36}$O$_6$N, 518.25371; found, 518.25386.

(2S,3S)-2-((((9H-fluoren-9-yl)methoxy)carbonyl)amino)-4-(tert-butoxy)-3-methoxy-4-oxobutanoic acid (8.1). Bobbit's salt (2.90 g, 9.70 mmol, 3.00 equiv) was added portion wise over 30 min to a stirred solution of **8.8** (1.28 g, 3.22 mmol, 1.00 equiv) in freshly prepared 9:1 ACN:H$_2$O

(12.9 mL) then stirred for 18 h at room temperature. The mixture was diluted with phosphate buffer (0.67 M, pH ca. 7; 21.5 mL) at room temperature and the mixture was neutralized with 1N NaOH. The neutralized mixture was diluted with ACN (20.5 mL) and cooled (ice bath). An aqueous solution of $NaClO_2$ (80% w/w; 1.13 g, 9.98 mmol, 3.10 equiv) was added and the mixture was stirred for 10 min. An aqueous solution of NaOCl (6.0 %; 2.8 mL, 2.3 mmol, 0.70 equiv) was added dropwise to the stirred reaction mixture over 30 min. Once the addition was complete, the mixture was stirred for 30 min then quenched with saturated aqueous Na_2SO_3. The resulting suspension was filtered, the filtrate concentrated to half volume, cooled (ice-water bath), and then acidified slowly with 12 N HCl (pH ca. 2). The aqueous layer was extracted with DCM (3 x 50 mL) and the combined organic layer was dried with $MgSO_4$. The residue was adhered to silica and subjected to silica gel column chromatography (40 % EtOAc/59% hexanes/1% AcOH), which provided **8.1** as a white solid (985 mg, 90% yield). $[\alpha]_D^{22} = -13.1$ (c 0.068, CH_3OH); ^1H NMR (300 MHz, $CDCl_3$): δ 10.44 (1H, br. s) 7.72 (2H, d, J = 7.4 Hz) 7.60-7.55 (2H, m) 7.39-7.24 (4H, m) 5.77 (1H, d, J = 10.0 Hz) 4.96 (1H, dd, J = 9.9, 1.2 Hz) 4.34-4.32 (3H, m) 4.19 (1H, t, J = 6.6 Hz) 3.47 (3H, s) 1.44 (9H, s). ^{13}C NMR (75 MHz, $CDCl_3$): δ 174.3, 168.0, 156.4, 143.7, 143.6, 141.2, 127.6, 127.6, 127.1, 125.2, 125.1, 119.9, 83.2, 79.6, 67.5, 59.3, 56.3, 46.9, 27.8. HRMS-ESI+ (m/z): [M + H]$^+$ calculated for $C_{24}H_{28}O_7N$, 442.18603; found, 442.18605.

(9H-fluoren-9-yl)methyl ((2R,3S)-4-amino-1-(benzyloxy)-3-((tert-butyldimethylsilyl)oxy)-4-oxobutan-2-yl)carbamate (**8.11**). TFA (36 mL) was added dropwise to a stirred, cooled (ice bath) solution of compound **8.4a** (3.00 g, 5.96 mmol, 1.00 equiv) in dry DCM (36 mL). After the addition, the mixture was stirred for 30 min then brought to room temperature and stirred for 4 h. Toluene (36 mL) was added then the mixture was concentrated by rotary evaporation. TFA was removed by rotary evaporation (3x) in the presence of toluene until a white solid formed. The solid

was dissolved in THF (60 mL) and the mixture cooled (ice bath). Di-tert-butyl-dicarbonate (7.75 g, 35.5 mmol, 3.00 equiv), ammonium bicarbonate (812 mg, 10.3 mmol, 1.70 equiv) and pyridine (2.89 mL, 35.5 mmol, 3.00 equiv) were added to the stirred mixture. The mixture was stirred for 30 min and then warmed to room temperature and stirred for 4 h. The mixture was concentrated, the residue was dissolved in EtOAc (75 mL) and washed with 1N HCl (50 mL). The aqueous layer was extracted with EtOAc (1x) and the combined organic layer was washed with brine and then dried with MgSO$_4$ and concentrated. The reside was dissolved in DCM (36 mL), then cooled (ice bath), then TFA (36 mL) was added dropwise to the stirred solution. After 30 min, the reaction mixture was brought to room temperature and stirred for 1 h. Toluene (36 mL) was added, and the solution was concentrated. The residue was dissolved in DCM (50 mL) and washed with sat. NaHCO$_3$ (3x) then brine (1x). The organic layer was dried with Na$_2$SO$_4$ then concentrated. The residue was dissolved in dry DCM (60 mL), cooled (ice bath) and imidazole (2.00 g, 29.8 mmol, 5.00 equiv) followed by *tert*-butyldimethylsilyl chloride (TBSCl, 4.49 g, 29.8 mmol, 5.00 equiv) were added. After stirring for 5 min, dimethylaminopyridine (DMAP, 73 mg, 0.60 mmol, 0.10 equiv) was added and the resulting mixture was stirred for 3 h. After 3 h the reaction was quenched with 0.2 N HCl (60 mL) while cold. The aqueous layer was extracted with DCM (60 mL) twice and the combined organic layer was washed with sat. NaHCO$_3$, brine and then dried with Na$_2$SO$_4$. The organic layer was concentrated and subjected to silica gel flash column chromatography (30 % to 50 % EtOAc/Hexanes) which provided **8.11** as a white solid (2.70 g, 81 % yield). ^{1}H NMR (300 MHz, CDCl$_3$): δ 7.68 (2H, d, *J* = 7.4 Hz) 7.52 (2H, d, *J* = 7.2 Hz) 7.33-7.18 (9H, m) 6.33 (1H, br. s) 6.20-5.75 (1H, br. m) 5.60 (1H, d, *J* = 9.3 Hz) 4.44-4.29 (2H, m) 4.23-4.21 (2H, m) 4.17-4.16 (1H, m) 4.11-4.09 (2H, m) 3.55-3.53-3.29 (2H, m) 0.84 (9H, s) 0.06-0.05 (6H, m). ^{13}C NMR (75 MHz, CDCl$_3$): δ 175.0, 155.9, 144.0, 143.9, 141.3, 141.2, 137.9 128.3, 127.6, 127.5,

127.0, 125.1, 119.9, 83.4, 73.1, 71.4, 67.7, 66.9, 53.5, 47.2, 25.7, 17.9, -5.1, -5.3. HRMS-ESI+ (m/z): [M + H]$^+$ calculated for $C_{32}H_{41}O_5N_2Si$, 561.27902; found, 561.27758.

(9H-fluoren-9-yl)methyl ((2R,3S)-4-amino-3-((tert-butyldimethylsilyl)oxy)-1-hydroxy-4-oxobutan-2-yl)carbamate (8.12). Compound **8.11** (2.59 g, 4.62 mmol, 1.00 equiv) and pentamethyl benzene (685 mg, 4.62 mmol, 1.10 equiv) were dissolved in dry DCM (46 mL) under an inert atmosphere. The mixture was cooled to -78 °C (dry ice acetone bath) and BCl_3 (1 M in DCM, 13.9 mL, 13.9 mmol, 3.00 equiv) was added dropwise over 10 min. The dry ice bath was removed and replaced with an ice bath. The mixture was stirred for 1 h and then quenched by the dropwise addition of saturate aqueous $NaHCO_3$ (75 mL). After 10 min of stirring, the mixture was extracted with EtOAc (2 x 75 mL). The combined organics were washed with brine, dried with $MgSO_4$ and concentrated. The crude oil was subjected to silica gel column chromatography (50% EtOAc/49% hexane/1% AcOH to 60% EtOAc/39% hexane/1% AcOH) which provided **8.12** as a colorless foam (1.72 g, 82%). ^1H NMR (300 MHz, $CDCl_3$): δ 7.73 (2H, d, *J* = 7.5 Hz) 7.57 (2H, d, *J* = 7.4 Hz) 7.41-7.27 (4H, m) 6.53 (1H, br. s) 5.83-5.80 (2H, m) 4.37 (2H, d, *J* = 7.1 Hz) 4.26-4.18 (2H, m) 4.00-3.96 (1H, m) 3.76-3.64 (2H, m) 2.53 (1H, br. s) 0.92 (9H, s) 0.15-0.12 (6H, m). ^{13}C NMR (75 MHz, $CDCl_3$): δ 175.7, 156.3, 143.8, 143.8, 141.2, 141.2, 127.6, 127.0, 125.0, 119.8, 71.5, 66.9, 61.0, 55.7, 47.0, 25.6, 17.9, -5.2, -5.4. HRMS-ESI+ (m/z): [M + H]$^+$ calculated for $C_{25}H_{35}O_5N_2Si$, 471.23098; found, 471.23093.

(2S,3S)-2-(((((9H-Fluoren-9-yl)methoxy)carbonyl)amino)-4-amino-3-((tert-butyldimethylsilyl)oxy) -4-oxobutanoic acid (8.2).

TEMPO (449 mg, 2.79 mmol, 1.50 equiv) was added to a stirred, cooled solution (ice bath) of compound **8.12** (875 mg, 1.86 mmol, 1.00 equiv) in acetonitrile (26 mL). $NaClO_2$ (591 mg, 5.23 mmol, 2.80 equiv) in cold phosphate buffer (0.67 M, pH = 7; 17.5 mL) was added dropwise to the

stirred reaction mixture. An aqueous solution of NaOCl (1.6 mL, 1.3 mmol, 0.70 equiv) was added

dropwise over 30 min. Once the addition was complete, the reaction was stirred for 3 h and then

quenched with sat. Na_2SO_3 (10 mL) and brought to room temperature. The reaction mixture was

acidified with 12 N HCl (pH ca. 2) and the aqueous layer was extracted with DCM (3 x 100 mL).

The combined organic layer was dried with $MgSO_4$, filtered and concentrated. The residue was

subjected to silica gel column chromatography (40% EtOAc/59% hexanes/1% AcOH) which

provided **8.2** as a colorless solid (863 mg, 95% yield). $[\alpha]_D^{22} = -16.4$ (c 0.072, CH_3OH); ^1H NMR

(300 MHz, CD_3OD): δ 7.64-7.61 (2H, m) 7.51-7.41 (2H, m) 7.25-7.12 (4H, m) 6.71-6.68 and 6.15-

6.12 (1H, d, J = 9.3 Hz) 4.57-4.50 (3H, m) 4.24-4.07 (3H, m) 0.80 (9H, s) -0.005- -0.017 (6H, m).

^{13}C NMR (75 MHz, CD_3OD): δ 176.0, 172.9, 158.7, 145.3, 142.6, 128.9, 128.3, 126.4, 121.0, 75.4,

68.5, 58.8, 48.3, 26.4, 19.2, -4.8, -5.0. HRMS-ESI+ (m/z): $[M + H]^+$ calculated for $C_{25}H_{33}O_6N_2Si$,

485.21024; found, 485.21012.

tert-Butyl   (2S,3R)-3-((((9H-fluoren-9-yl)methoxy)carbonyl)amino)-4-(benzyloxy)-2-

*hydroxybutanoate (**8.24**).*

Compound **8.4** (er = 95:5, 3.09 g, 6.14 mmol), *p*-nitrobenzoic acid (1.54 g, 9.20 mmol, 1.50 equiv)

and triphenylphosphine (2.41 g, 9.20 mmol, 1.50 equiv) were dissolved in THF (31 mL) and this

solution was cooled (ice-water bath). Diisopropyl azodicarboxylate (1.81 mL, 9.20 mmol, 1.50

equiv) was added and the solution was left for 24 h at room temperature under an inert atmosphere.

After concentrating the reaction mixture, a single re-crystallization of the crude solid in MeOH

afforded **8.24** as a colorless, crystalline solid (3.52 g, 88% yield). ^1H NMR (300 MHz, $CDCl_3$): δ

8.20 (2H, d, J = 8.4 Hz), 8.10 (2H, d, J = 8.4 Hz), 7.75 (2H, m), 7.58 (2H, m), 7.41-7.25 (9H, m),

5.37-5.29 (2H, m), 4.58-4.42 (5H, m), 3.72-3.64 (2H, m) 1.45 (9H, s); ^{13}C NMR (75 MHz, $CDCl_3$):

166.3, 163.8, 155.7, 150.6, 143.7, 141.3, 137.3, 134.5, 131.0, 128.5, 128.0, 127.7, 127.0, 125.0,

124.9, 123.5, 120.0, 83.3, 73.3, 67.8, 67.0, 51.1, 47.1, 27.9; HRMS-ESI$^+$ (m/z): [M + H]$^+$ calcd for C$_{40}$H$_{35}$O$_6$N$_3$, 653.2520; found, 653.2507.

tert-Butyl (2R,3R)-3-((((9H-fluoren-9-yl)methoxy)carbonyl)amino)-4-(benzyloxy)-2-hydroxybutanoate (8.25).

Compound **8.24** (1.95 g, 3.00 mmol) and NaN$_3$ (584 mg, 9.00 mmol) were suspended in MeOH (50 mL) at room temperature. The colorless suspension was stirred at 45 °C for 4 hours. The homogenous mixture was concentrated, and the crude residue subjected to silica gel column chromatography (20% ethyl acetate/80% hexanes) which provided pure **8.25** as a colorless foam (1.45 g, 95% yield). The er was determined to be 97:3 by chiral RP-HPLC (see figure F.2) ^{1}H NMR (300 MHz, CDCl$_3$): δ 7.76 (2H, d, J = 6.9 Hz), 7.60 (2H, d, J = 6.9 Hz), 7.42-7.25 (9H, m), 5.45 (1H, m), 4.48-4.40 (4H, m), 4.23-4.22 (3H, m), 3.56-3.35 (3H, m), 1.44 (9H, s); ^{13}C NMR (75 MHz, CDCl$_3$): 171.4, 155.8, 143.8, 141.3, 137.4, 128.4, 127.9, 127.9, 127.7, 127.0, 119.9, 83.0, 73.4, 71.7, 68.4, 66.9, 52.4, 47.1, 27.9; HRMS-ESI$^+$ (m/z): [M + H]$^+$ calcd for C$_{30}$H$_{34}$O$_6$N, 504.2381; found, 504.2374.

tert-Butyl (2R,3R)-3-((((9H-fluoren-9-yl)methoxy)carbonyl)amino)-4-(benzyloxy)-2-methoxybutanoate (8.26).

To a solution of **8.25** (1.20 g, 2.38 mmol) in diethyl ether (48 mL) was added freshly prepared, dry silver oxide (1.65 g, 7.15 mmol) and MeI (2.97 mL, 47.7 mmol). The suspension was vortexed briefly then refluxed overnight. The suspension was cooled to room temperature and then filtered through Celite. The filtrate was concentrated which provided pure **8.26** as a white foam (1.18 g, 96% yield). ^{1}H NMR (300 MHz, CDCl$_3$): δ 7.76 (2H, d, J = 7.5 Hz), 7.60 (2H, d, J = 7.5 Hz), 7.40 (2H, t, J = 7.2 Hz), 7.33-7.25 (9H, m), 5.28-5.25 (1H, m), 4.51 (2H, m), 4.38 (2H, m), 4.23 (2H,

m), 3.82 (1H, d, J = 5.7 Hz), 3.62 (1H, dd, J = 5.1, 9.6 Hz) 3.50-3.41 (5H, m), 1.43 (9H, s); ^{13}C NMR (75 MHz, CDCl$_3$): 169.4, 155.8, 143.9, 141.3, 137.9, 128.4, 127.7, 127.7, 127.7, 127.0, 125.1, 120.0, 82.1, 80.4, 73.1, 68.0, 68.8, 58.7, 52.2, 47.2, 27.9; HRMS-ESI$^+$ (m/z): [M + H]$^+$ calcd for C$_{31}$H$_{36}$O$_6$N, 518.2537; found, 518.2539.

Fmoc-L-erythro-MeOAsp(tBu)-OH (**8.27**).

Bobbit's salt (2.33 g, 7.79 mmol, 3.10 equiv) was added to a solution of **8.26** (1.30 g, 2.51 mmol, 1.00 equiv) in MeCN (9 mL) and H$_2$O (1 mL) and the mixture was stirred overnight. The mixture was cooled (ice-water bath) and diluted with a solution of NaOCl$_2$ (80% w/w; 880 mg, 7.78 mmol, 3.00 equiv.) in phosphate buffer (0.67 N, pH ca. 7; 16.8 mL). The pH of the resulting solution was adjusted to 7 with 1 N NaOH, at which point MeCN (15.7 mL) was added, followed by a dropwise addition of NaOCl (0.81 M bleach; 2.2 mL, 1.8 mmol, 0.70 equiv) over 30 min. After 8 hours, sat. aqueous NaSO$_3$ was added until the dark red color faded to a pale orange. The two layers were separated, and the aqueous layer was acidified to pH 2 with conc. aqueous HCl and extracted with DCM (50 mL) three times. The combined organic layer was dried over MgSO$_4$, filtered and concentrated. The crude residue was subjected to FC (40% ethyl acetate/59% hexanes/1% AcOH) which provided pure **8.27** as a colorless foam (891 mg, 80% yield). $[\alpha]^{22}_D$ = 44.8^0 (c. 0.800, CH$_2$Cl$_2$). ^{1}H NMR (300 MHz, CDCl$_3$): δ 11.30 (1H, br. s), 7.76 (2H, d, J = 7.5 Hz), 7.61 (2H, d, J = 7.2), 7.40 (2H, t, J = 7.5 Hz), 7.31 (2H, t, J = 7.5 Hz), 6.16 and 5.78 (1H, d, J = 8.4 Hz), 4.94 and 4.67 (1H, dd, J = 2.4, 8.4 Hz), 4.52-4.37 (2H, m), 4.25 (1H, t, J = 6.9 Hz), 4.07 (1H, d, J = 2.4 Hz), 3.53 and 3.46 (3H, s), 1.51 (9H, s); ^{13}C NMR (75 MHz, CDCl$_3$): 172.7, 168.0, 155.9, 143.7, 143.5, 141.2, 127.6, 127.0, 125.0, 119.9, 83.1, 80.7, 67.3, 59.6, 55.8, 46.9, 27.8; HRMS-ESI$^+$ (m/z): [M + H]$^+$ calcd for C$_{24}$H$_{28}$O$_7$N, 442.1860; found, 442.1857.

*1-((3aR,6R)-8,8-Dimethyl-2,2-dioxidotetrahydro-3H-3a,6-methanobenzo[c]isothiazol-1(4H)-yl)butan-1-one (**8.28**).*

(1S)-(−)-2,10-Camphorsultam (10.0 g, 46.4 mmol, 1.00 equiv) and DMAP (624 mg, 5.11 mmol, 0.110 equiv) were dissolved in dry THF (60 mL) at room temperature. The solution was cooled (ice bath) and triethylamine (7.04 mL, 69.7 mmol, 1.50 equiv) was added followed by the dropwise addition of butyryl chloride (5.30 mL, 51.1 mmol, 1.10 equiv). The formed suspension was stirred for 30 min then quenched with 1N HCl (20 mL) and extracted with ethyl acetate (3 x 60 mL). The combined organic layer was washed once with 1N NaOH (100 mL), dried over $MgSO_4$ and filtered. The filtrate was concentrated, and the crude solid was purified by a single recrystallization in methanol, yielding **8.28** as a colorless, crystalline solid (9.2 g, 69% yield). ^{1}H NMR (300 MHz, $CDCl_3$): δ 3.83 (1H, dd, J = 5.7, 6.9 Hz), 3.47 (1H, d, J = 13.8 Hz), 3.39 (1H, d, J = 13.8 Hz), 2.74-2.57 (2H, m), 2.06-2.01 (2H, m), 1.86-1.83 (2H, m), 1.68 (2H, sext, J = 7.2 Hz), 1.41-1.28 (2H, m), 1.12 (3H, s), 0.95-0.90 (6H, m); ^{13}C NMR (75 MHz, $CDCl_3$): 171.9, 65.1, 52.9, 48.3, 47.7, 44.6, 38.5, 37.3, 32.8, 26.4, 20.8, 19.8, 17.9, 13.5; HRMS-ESI^{+} (m/z): [M + H]$^{+}$ calcd for $C_{14}H_{24}O_3NS$, 286.1471; found, 286.1465.

*S(2R)-1-((3aR,6R)-8,8-Dimethyl-2,2-dioxidotetrahydro-3H-3a,6-methanobenzo[c]isothiazol-1(4H)-yl)-2-methylbutan-1-one (**8.29**).*

NaHMDS (40.1 mL, 1M in THF, 40.1 mmol, 1.30 equiv) was added dropwise to a solution **8.28** (8.81 g, 30.9 mmol, 1.00 equiv) in dry THF (221 mL) cooled to -78 °C, under an inert atmosphere. The resulting solution was stirred for 1 h, then dry HMPA (16.1 mL) and MeI (5.76 mL, 92.6 mmol, 2.30 equiv) were added, and cooling was removed. The solution was stirred at room temperature for 18 h, then quenched with sat. aqueous NH_4Cl (40 mL) and extracted with ethyl acetate (3 x 100 mL). The combined organic layer was dried with $MgSO_4$, filtered and

concentrated. The crude solid was purified by a single recrystallization in methanol which yielded **8.29** (7.30 g, 79% yield) as a colorless, crystalline solid. ^{1}H NMR (300 MHz, CDCl$_3$): δ 3.85 (1H, t, J = 6.3 Hz), 3.47 (1H, d, J = 13.5 Hz), 3.39 (1H, d, J = 13.8 Hz), 2.93 (1H, sex., J = 6.9 Hz), 2.01-1.99 (2H, m), 1.89-1.70 (4H, m), 1.40-1.27 (3H, m), 1.16-1.11 (6H, m), 0.93-0.84 (6H, m); ^{13}C NMR (75 MHz, CDCl$_3$): 176.2, 64.9, 53.1, 48.1, 47.6, 44.5, 41.7, 38.4, 32.7, 26.3, 25.6, 20.7, 19.8, 18.5, 11.7; HRMS-ESI[+] (m/z): [M + H][+] calcd for C$_{14}$H$_{24}$O$_3$NS, 300.1628; found, 300.1621. The absolute configuration was confirmed by X-ray crystallography (see figure F.3).

*(R)-2-Methylbutanal (**8.30**).*

DIBAL (1M in toluene; 36.6 mL, 36.6 mmol, 1.50 equiv) was added dropwise to a solution of **8.29** (7.31 g, 24.4 mmol, 1.00 equiv) in dry DCM at -78 °C under an inert atmosphere. The resulting solution was stirred for 90 min, then quenched with a solution of NaHSO$_3$ (8.77 g) in H$_2$O (90 mL) and allowed to come to room temperature. The mixture was extracted with pentane (3 x 100 mL) and the combined organic layer concentrated by rotary evaporation (no heating) until only toluene remained. The residue was subjected to FC (30% DCM/70% pentane then 45%DCM/55% pentane). The combined fractions that contained **8.29** were carefully concentrated by rotary evaporation (no heating) until only a solution of **8.29** in DCM remained (40% w/w). The ^{1}H-NMR spectrum was identical to that of 2-methylbutyraldehyde. This solution was used immediately for the synthesis of (R)-methyldecanoic acid which was prepared as described by Braden Kralt in Scheme 8.5.

Chapter 9 - Synthesis of Fmoc-protected Amino Alcohols via the Sharpless Asymmetric Aminohydroxylation Reaction using FmocNHCl as the Nitrogen Source.

9   Preface and contributions

The work presented in this chapter is based on a paper published in *The Journal of Organic Chemistry* (*Reprinted (adapted) with permission from J. Org. Chem.* **2019**, *84*, 15476–15485 *Copyright 2019 American Chemical Society*). Almost all the experimental work done in this chapter was completed by me. Matthew Diamandas, a graduate student in the Taylor lab, assisted with the purification and characterization of **9.23**. He also assisted with the Mosher's ester analysis of **9.8B**, **9.14A**, **9.18A** and **9.23A'**. I prepared the first draft of this manuscript which was refined and edited by Prof. Taylor. All the work done in this chapter was done under the supervision of Prof. Taylor. Additional supplementary data is available on the journal's website.

9.1   Introduction

The Sharpless asymmetric aminohydroxylation (SAAH) reaction is perhaps the most powerful and direct approach for preparing vicinal amino alcohols in an enantioselective manner.[1] *N*-Chlorinated derivatives of benzyl (CbzNHCl) and *tert*-butyl carbamates (BocNHCl), which are usually generated *in situ* from the corresponding carbamates and *tert*-butylhypochlorite, have been widely used as the nitrogen source in the SAAH reaction.[324] In contrast, until very recently, fluorenylmethyl (Fmoc) carbamates, such as FmocNHCl (**9.1**, Figure 9.1), had never been used as a nitrogen source in SAAH reactions. The reason for this is probably because it had been assumed that the Fmoc group was too bulky to allow for high enantioselectivity[325] and too base labile to survive the basic conditions normally employed in the SAAH reaction. The latter problem was circumvented in 2011 by Harris et al., who reported that fluorenylmethylcarbamate **9.2** (Figure 9.1), could be used as a nitrogen source for the SAAH reaction under base free conditions.[310]

9.1   **9.2**
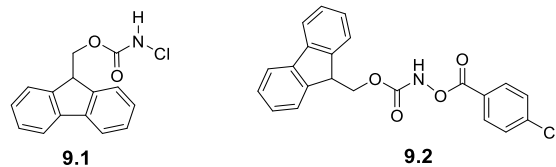
Figure 9.1 Reagents used for Introducing Fmoc-Protected Amines in the SAAH Reaction.

Recently, we reported that Fmoc-protected amino alcohol **9.4** could be prepared in good yield and enantioselectivity from alkene **9.3** via a SAAH reaction under classic (ie. basic) SAAH reaction conditions using **9.1** as the nitrogen source (Scheme 9.1).[181,326] We showed that the reaction proceeded much better when **9.1** was introduced into the reaction mixture as a reagent rather than being generated *in situ* from FmocNH$_2$ and *tert*-butylhypochlorite. Multigram quantities of reagent **9.1** were prepared in a single step and in high yield by reacting FmocNH$_2$ with trichloroisocyanuric acid, an inexpensive chlorinating agent, and **9.1** is a stable, easily-handled solid, and is storable at room temperature.[326] Compound **9.4** was used to achieve concise syntheses of L-*threo*-β-hydroxyasparagine, L-*threo*-β-methoxyaspartate, and L-*erythro*-β-methoxyaspartate, suitably protected for Fmoc solid phase peptide synthesis (**9.5**, **9.6a** and **9.6b** respectively in Scheme 9.1).[181,326] Amino acids **9.5** and **9.6b** were used to achieve the total synthesis of A54145 factor D, a complex cyclic lipodepsipeptide antibiotic.[181] Overall, these studies suggested that reagent **9.1** could be a very useful and general reagent for SAAH reactions and natural product synthesis.
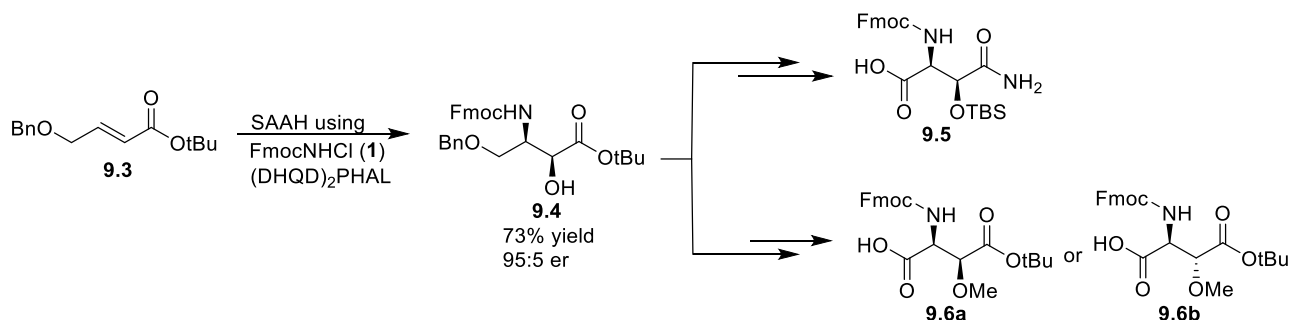
Scheme 9.1 Synthesis of Fmoc-Protected Amino Alcohol **9.4** using Reagent **9.1**.

Here we report the results of our investigations on the scope of the SAAH reaction using reagent **9.1** as the nitrogen source both in the absence of a chiral ligand, and in presence of the chiral ligands (DHQD)$_2$PHAL (DHQD) and (DHQ)$_2$PHAL (DHQ). These studies enabled us to develop an efficient synthesis of highly enantiomerically enriched **ent-9.5** and **ent-9.6a** (D-*threo*-β-hydroxyasparagine and D-*threo*-β-methoxyaspartate respectively), which could not be achieved starting from **9.3**.

9.2   Results and discussion

We first explored the effectiveness of FmocNHCl as a nitrogen source for the amino hydroxylation on some common olefins in the absence of chiral ligands. We began this study by subjecting styrene (**9.7**) to **9.1**/NaOH/8% osmate in nPrOH/H$_2$O (Table 9.1, entry 1). Although the regioselectivity was excellent in that the ratio of the resulting amino alcohols, (±)-**9.8A**:(±)-**9.8B**, was 1:19, the isolated yield of the major product, (±)-**9.8B**, was only a moderate 45%. We noticed that this reaction produced significant amounts of FmocNH$_2$, suggesting that competing hydrolysis of the *in situ* formed FmocNOsO$_3$ was having a deleterious effect on reaction efficiency.[327] This prompted us to investigate the stability of FmocNHCl which we found to spontaneously convert to FmocNH$_2$ in nPrOH/H$_2$O at 0 ºC (Scheme G.1); however, the conversion is much faster in the presence of osmate and an alkene (Table G.5). The hydrolysis could be suppressed to an extent by lowering the catalyst loading to 4% (Table G.5), which gave (±)-**9.8B** in an isolated yield of 56% (entry 2). Further reduction of the catalyst loading to 2% did not result in an increase in the yield of (±)-**9.8B** even if the reaction time was doubled (entry 3).

It is well-known that some simple, achiral tertiary amine base ligands accelerate the osmium catalyzed dihydroxylation process.[328] Therefore, we considered that the addition of a

catalytic amount of achiral amine base ligand could suppress unwanted hydrolysis by accelerating the osmylation step in the aminohydroxylation process.[328] Only a few reports have appeared describing the effects of simple, achiral tertiary amine base ligands on the aminohydroxylation process. The most notable examples were described by Angelaud et al[329] and Donohoe et al.[330,331] Angelaud et al[329] reported that the addition of quinuclidine or DIPEA greatly affected the regioselectivity of the aminohydroxylation process. Unfortunately, no data on reaction yield was provided. Donohoe et al explored the effects of quinuclidine and DIPEA on the tethered aminohydroxylation reaction and found that DIPEA enhanced the rate of the reaction substantially and increased the yield.[330,331] Interestingly, quinuclidine was found to slow the reaction down and greatly decreased reaction yield. The mixed results observed by Donohoe et al maybe explained by the fact that the ligand can accelerate the osmylation step but hinder the rate controlling hydrolysis step.[328] With this in mind, we screened a series of tertiary amine bases to determine if any were capable of improving the efficiency of the aminohydroxylation reaction on styrene (Table 9.1).

For its historical significance,[328] we first tried pyridine which we found to inhibit catalytic turnover almost immediately (the solution quickly turned from green to bright yellow, indicating that the dioxo osmium(VI) monoazaglycolate species was no longer present).[332] After 4 hours, the reaction was worked-up and the small amount of product that was recovered had a regioselectivity of 1:10 (entry 4). The same turnover-inhibiting effect was observed when pyridyl acrylates were subjected to SAAH with *in-situ* generated CbzNHCl.[333] We found that the *N*-methylmorpholine (NMM) decreased reaction yield and altered the regioselectivity to 1:7 (entry 5). Similar results were observed with 1,4-diazabicyclo[2.2.2]octane (DABCO), although the regioselectivity was 1:10 (entry 6). It should be noted that turnover with DABCO was quickly

inhibited, which maybe explained by the formation of an unreactive bridged DABCO-imidoosmium complex.[334] The results observed with triethylamine (TEA) as a ligand are perplexing (entry 7). We found TEA to substantially increase overall yield (76%) and the isolated yield of (±)-**9.8B** (69%) even though the regioselectivity decreased to 1:10 and reaction took twice as long to stop turning over (as evidenced by dissipation in the green color). We initially thought that TEA was stabilizing the imidoosmium complex, decreasing reaction rate but incongruently preventing hydrolysis of the imidoosomium complex. However, closer analysis of the FmocNHCl, FmocNH$_2$ and (±)-**9.8B** produced under ligand and ligand-free conditions (Table G.5) suggest that TEA stabilizes osmium species in solution preventing the catalyst from decomposing into osmic acid; thus, catalytic turnover is possible at higher levels of conversion compared to the ligand free condition and this is primarily responsible for the increase in yield. Compared to TEA, similar effects were observed with *N,N*-diisopropylethylamine (DIPEA), although the observed regioselectivity is lower (1:6.2, entry 8). These results show that the observed effects on regioselectivity are not due to small changes in pH since TEA and DIPEA have the same pK$_a$, and thus the two ligands must be forming a complex with FmocNOsO$_3$ in solution.[335] 1,8-diazabicyclo(5.4.0)undec-7-ene (DBU) gave results that are almost identical to those observed with DIPEA.

Table 9.1 The Effect of a Catalytic Amount of an Achiral Ligand on the Yield and Regioselectivity of the Aminohydroxylation Reaction using Styrene as a Substrate.

245
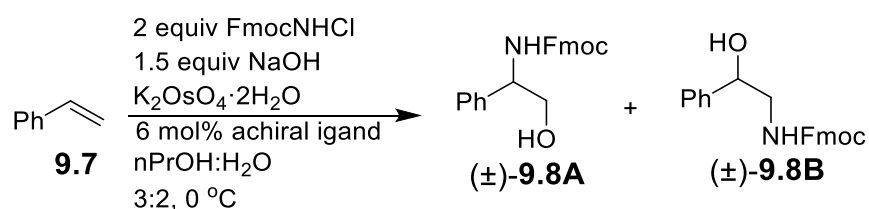
entry	achiral ligand (6 mol%)	mol % $K_2OsO_4 \cdot 2H_2O$	time (h)	% yield $(\pm)$-**9.8B**[a]	regioselectivity[b]
1	none	8	3	45	1:19
2	none	4	3	56	1:19
3	none	2	6	56	1:10
4	pyridine	4	4	18	1:10
5	NMM	4	4	30	1:7
6	DABCO	4	1	36	1:7
7	TEA	4	6	69	1:10
8	DIPEA	4	4	61	1:6.2
9	DBU	4	6	62	1:7

[a]Isolated yield of $(\pm)$-**9.8B**. [b] $(\pm)$-**9.8A**:$(\pm)$-**9.8B** Determined by ^{1}H NMR of mixture of $(\pm)$-**9.8A** and $(\pm)$-**9.8B**

Using 4 mol % osmate catalyst, we examined several other common alkenes as substrates (Table 9.2). Like styrene, the regioselectivity of the reaction with alkene **9.9** was very high and the yield of the major product, $(\pm)$-**9.10B**, was a modest 55% (entry 3). To our surprise, we found that the addition of TEA reduced the yield of $(\pm)$-**9.10B** to 43% (entry 4). Adding DIPEA in place of TEA gave $(\pm)$-**9.10B** in a 46% yield and caused no change in regioselectivity, suggesting that this effect is not due to sterics alone.

Initial attempts at converting alkene **9.11** to $(\pm)$-**9.12** were unsuccessful due to the alkenes poor solubility in the aqueous alcohol solvent system. When aqueous acetonitrile was used, **9.11** was converted to $(\pm)$-**9.12** in a 47% yield (entry 5). Under these conditions, the addition of catalytic TEA dramatically improved the yield of $(\pm)$-**9.12** to 84% (entry 6).

The reaction using alkene **9.13** produced amino alcohols $(\pm)$-**9.14A** and $(\pm)$-**9.14B** which were difficult to separate by column chromatography, and so were characterized as a 1:2 mixture

(($\pm$)-**9.14A**:($\pm$)-**9.14B**; Figure G.13). The yield of major product, ($\pm$)-**9.14B**, was estimated using ^{1}H NMR on the isolated mixture to be only 18 % (entry 7). In the presence of catalytic TEA, the yield of ($\pm$)-**9.14B** was improved to 33% (entry 8) although the regioselectivity was not substantially affected (1:2.4).

The reaction using isopropylcinnamate (**9.15**) produced products ($\pm$)-**9.16A** and ($\pm$)-**9.16B** as a 1:1.9 mixture (($\pm$)-**9.16A**:($\pm$)-**9.16B**), entry 9). The regioselectivity of this entry matched that reported by Harris et al under base-free conditions using reagent **9.2**.[310] These two amino alcohols were also difficult to separate by column chromatography and so were characterized as a 1:1.9 mixture (Figure G.12). The yield of major product, ($\pm$)-**9.16B**, was estimated using ^{1}H NMR on the isolated mixture to be 46 % (entry 9), which is quite high compared to the previous entries despite the reaction having to proceed for 60 h. The yield of ($\pm$)-**9.16B** was improved to 55% by the addition of catalytic TEA while the regioselectivity was almost unaffected (1:2) (entry 10). In this case, TEA also reduced the reaction time to 48 hours.

The reaction with cyclohexene (**9.17**) gave amino alcohol ($\pm$)-**9.18** in a meager 18% yield after 24 h (entry 11). The addition of catalytic TEA was found to almost completely inhibit conversion of this starting material (entry 12). Attempts to convert **9.19** to its amino alcohol proved unfruitful (entry 13) even in the presence of achiral bases (TEA) and even chiral ligands (DHQ)$_2$PHAL or (DHQD)$_2$PHAL.

Table 9.2 Aminohydroxylation Reactions using FmocNHCl.
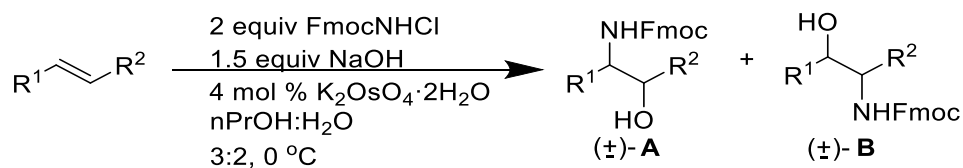
entry	alkene	mol % TEA	time (h)	major product	product ratio[a]	yield (%)[b]
1	**9.7** (R^1 = Ph, R^2=H)	0	3	(±)-**9.8B**	1:19	56
2	**9.7**	6	6	(±)-**9.8B**	1:19	69
3	**9.9** (R^1 = PhCH$_2$, R^2 = H)	0	15	(±)-**9.10B**	1:20	55
4	**9.9**	6	15	(±)-**9.10B**	1:20	43, 46[g]
5[e]	**9.11** (R^1=R^2=Ph)	0	18	(±)-**9.12**	NA[c]	47
6[e]	**9.11**	6	18	(±)-**9.12**	NA[c]	84
7	**9.13** (R^1 = 4-MeOPh, R^2 = CO$_2$Me)	0	36	(±)-**9.14B**	1:2	18[f]
8	**9.13**	6	36	(±)-**9.14B**	1:2.4	33[f]
9	**9.15** (R^1 = Ph, R^2 = CO$_2$iPr)	0	60	(±)-**9.16B**	1:1.9	46[f]
10	**9.15**	6	48	(±)-**9.16B**	1:2	55[f]
11	cyclohexene (**9.17**)	0	24	(±)-**9.18**	NA[c]	18
12	**9.17**	6	24	(±)-**9.18**	NA[c]	0
13	**9.19**	0/6	24	NR[d]	NR[d]	NR[d]

[a]Ratio of **A:B** determined using ^{1}H NMR. [b]Isolated yield of major product. [c]NA = not applicable. [d]NR = no reaction. [e]3:2 MeCN:H$_2$O was used as a solvent. [f]Yield of major product estimated using ^{1}H NMR. [g]6 mol % DIPEA in place of TEA

Next, we explored the reaction in the presence of chiral ligands (DHQD)$_2$PHAL (DHQD) and (DHQ)$_2$PHAL (DHQ) (Table 9.3). With styrene (**9.7**), we found that the presence of either ligand significantly increased the overall reaction yield, but since little regioselectivity was observed, the isolated yields of the major products, **9.8B** and **9.8B'**, were modest (entries 1 and 2). Poor regioselectivity is often observed when using styrene and *in situ*-generated CbzNHCl[336] or BocNHCl. in the SAAH reaction. The er values using reagent **9.1** are slightly less than those reported for the same reaction and ligands using *in situ*-generated CbzNHCl[336] or BocNHCl.[337]

The presence of a chiral ligand dramatically increased the rate of the reaction with cyclohexene (**9.17**) (entries 3 and 4).[328] Using DHQD, amino alcohol **9.18A** was obtained in a reasonable yield and with excellent enantioselectivity (entry 3). The er values using reagent **9.1** are considerably superior, while the yield of the major product is similar to those reported for the same reaction and ligand but using other nitrogen sources.[310,327,338] The reaction was slower with DHQ, but the yield of the major product, **9.18A'**, was higher while the er was lower (entry 4) compared to the corresponding DHQD reaction. The er values using DHQ and reagent **9.1** are slightly better than those reported for the same reaction and ligand using other nitrogen sources. [310,327,338]

The reaction with alkene ester **9.15** also proceeded faster in the presence of the ligands, and in good yield, with high regioselectivity and enantioselectivity with either ligand (entries 5 and 6). The reaction in the presence of a ligand favored the formation of **9.16A** and **9.16A'**, while in the absence of an alkaloid ligand **9.16B** was favored (entries 9 and 10, Table 9.2).

Substituting the isopropyl group in **9.15** with a methyl group (**9.20**, entries 7 and 8) resulted in only a small decrease in regioselectivity, and the enantioselectivity was still excellent. Ester **9.20** has been examined by Harris et al as a substrate in the SAAH reaction using reagent **9.2** under base-free conditions using both DHQD and DHQ as ligands.[310] They obtained the same regioisomers (**9.21A** and **9.21A'**) as the major products and in similar yields and enantioselectivities to those reported here; however, their regioisomeric ratios were significantly less (approximately 6:1 for both ligands).[310]

The reaction using the *p*-methoxyphenyl derivative of **9.20**, compound **9.13**, and the DHQD ligand proceeded with excellent regioselectivity and provided amino alcohol **9.14A** as the major product in good yield and enantioselectivity (entry 9). The er obtained with reagent **9.1** is

slightly lower than those reported for the same reaction using the DHQD ligand and *in situ-*generated CbzNHCl.[305,306] The reaction using the DHQ ligand also proceeded with excellent regioselectivity and enantioselectivity; however, the yield of the major regioisomer, **9.14A'**, was modest (entry 10).

Using the DHQD ligand, indole alkene **9.22** afforded **9.23A** as the major regioisomer in a good yield with excellent regioselectivity and enantioselectivity (entry 11). Likewise, the reaction with the DHQ ligand proceeded with high regioselectivity and excellent enantioselectivity providing **9.23A'** in a similar yield (entry 12). Although the regioselectivity using the DHQ ligand is poorer than that previously reported with a very similar substrate and *in situ* generated CbzNHCl, the enantioselectivity using either the DHQD or DHQ ligand and **9.1** as a nitrogen source is superior.[333]

Table 9.3 Asymmetric Aminohydroxylation Reactions using FmocNHCl.
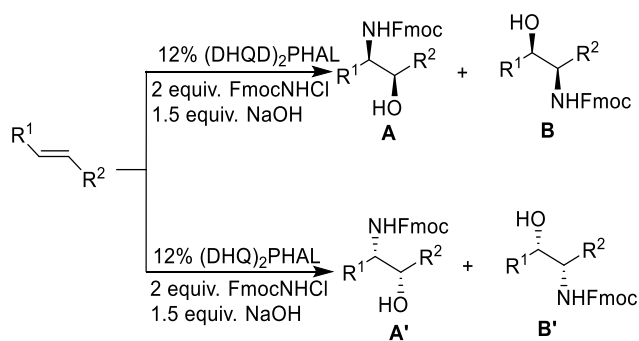
entry	alkene	solvent[a]	ligand[b]	time (h)	major product	product ratio[c]	yield (%)[d]	er[e]
1	**9.7** (R¹ = Ph, R² = H)	nPrOH/H₂O	DHQD	3	**9.8B**	47:53	45	93:7
2	**9.7**	nPrOH/H₂O	DHQ	18	**9.8B'**	49:51	41	89:11
3[f,g]	cyclohexene (**9.17**)	nPrOH/H₂O	DHQD	20	**9.18A** (**1R,2S**)	-	62	98:2
4[f,g]	**9.17**	nPrOH/H₂O	DHQ	36	**9.18A'** (**1S,2R**)	-	73	84:16
5	**9.15** (R¹ = Ph, R² = CO₂iPr)	nPrOH/H₂O	DHQD	3	**9.16A**	>20:1	81	98:2
6	**9.15**	nPrOH/H₂O	DHQ	3	**9.16A'**	>20.1	71	99.5:0.5

250

7	**9.20** (R^1 = Ph, R^2 = CO$_2$Me)	nPrOH/H$_2$O	DHQD	2	**9.21A**	15:1	67	97:3
8	**9.20**	nPrOH/H$_2$O	DHQ	2	**9.21A'**	15:1	86	94:6
9	**9.13** (R^1 = 4-MeOPh, R^2 = CO$_2$Me)	nPrOH/H$_2$O	DHQD	2.5	**9.14A**	>20:1	67	95:5
10	**9.13**	nPrOH/H$_2$O	DHQ	3	**9.14A'**	>20.1	46	98:2
11	**9.22** (R^1 = N-tBoc-3-indol, R^2 = CO$_2$Me)	nPrOH/H$_2$O	DHQD	4	**9.23A**	20:1	65	98:2
12	**9.22**	nPrOH/H$_2$O	DHQ	23	**9.23A'**	8.4:1	59	>99
13	**9.3** (R^1 = BnOCH$_2$, R^2 = CO$_2$tBu)	nPrOH/H$_2$O	DHQD	3	**9.4A**	12:1	70	95:5
14	**9.3**	MeCN/H$_2$O	DHQD	5	**9.4A**	4:1	56	96:4
15	**9.3**	nPrOH/H$_2$O	DHQ	8	**9.4A'**	ND	51	92:8
16	**9.3**	MeCN/H$_2$O	DHQ	18	**9.4A'**	ND	25	92.5:7.5
17	**9.24** (R^1 = 4-MeOBnOCH$_2$ R^2 = CO$_2$Me)	nPrOH/H$_2$O	DHQD	3	**9.25A**	15:1	73	89:11
18	**9.24**	MeCN/H$_2$O	DHQD	4	**9.25A'**	5:1	45	93:7
19	**9.24**	nPrOH/H$_2$O	DHQ	2	**9.25A'**	15:1	73	96:4

[a]Ratio of nPrOH/H$_2$O or MeCN/H$_2$O was 3:2. [b]12 mol% ligand used, 8 mol% K$_2$OsO$_4$·2H$_2$O used in all reactions. [c]Product ratio = A:B or A':B' determined by ^{1}H NMR [d]Isolated yield of major product. [e]er = enantiomeric ratio of major product as determined by chiral HPLC. [f]The general scheme does not apply to this cis alkene. [g]The configuration of the product is indicated under the major product column. Carbon 1 bears the installed alcohol. Carbon 2 bears the installed carbamate.

We previously reported that the SAAH reaction of alkene **9.3** with the DHQD ligand proceeded with very good regioselectivity and provided amino alcohol **9.4A** (compound **9.4** in Scheme 9.1) in good yield and enantioselectivity (entry 13).[326] Changing the solvent to MeCN/H$_2$O resulted in a decrease in regioselectivity and yield of **9.4A**, but with almost identical enantioselectivity (entry 14). To our surprise, the reaction was slower with the DHQ ligand, and the major product, **9.4A'**, was produced in lower yield and er compared to the reaction using DHQD regardless of whether the solvent was nPrOH/H$_2$O or MeCN/H$_2$O (entries 15 and 16).

Previous work by Janda and McLeod showed that *p*-methoxyphenyl ethers are strong directing groups for the SAAH reaction.[339–341] The reaction on the *p*-OMe analog (**9.24**[342]) of compound **9.3** proceeded with a better regioselectivity compared to the reaction using alkene **3**,

and the yield of the major products, **9.25A** or **9.25A'**, was also better, regardless of the ligand used (entries 17 and 19). However, with the DHQD ligand, the er of **9.25A** was less than that of compound **9.4A**, while with the DHQ ligand, the er of amino alcohol **9.25A'** was greater than that of **9.4A'**. Performing this reaction with the DHQD ligand in MeCN/H$_2$O resulted in a decrease in regioselectivity and yield of the major product, though the er did not change significantly (entry 18).

As part of our work on the synthesis of lipopeptide antibiotics,[181,326] we wished to prepare the enantiomers of protected amino acids **9.5** and **9.6a**. For these syntheses, it would have been preferable to start with compound **9.4A'** (entry 15, Table 9.2), which is the enantiomer of **9.4A** (compound **9.4** in Scheme 9.1), as this would have allowed us to use the identical route that we developed for the syntheses of **9.5** and **9.6a** (**ent-9.5** and **ent-9.6a**, respectively).[326] Unfortunately, the er of **9.4A'** was not quite high enough for this purpose. Since the er of **9.25A'** (entry 19, Table 9.2) was high enough we decided to develop a synthesis of **ent-9.5** and **ent-9.6a** starting with **9.25A'**.

To prepare **ent-9.5**, we first hydrolyzed the methyl ester of **9.25A'** with aqueous lithium hydroxide in the presence of a high concentration of calcium chloride (Scheme 9.2).[343] After aqueous work up, the crude material was amidated using BOP/DIPEA/NH$_4$Cl[344] yielding **9.26** in a 62% yield over two steps. Silylation of **9.26** using TBSCl/imidazole and catalytic DMAP gave **9.27** in a 74 % yield. Attempts to remove the PMB group in **9.27** using Bobbitt's salt were unsuccessful.[326] We also tried to remove the PMB group in **9.27** using DDQ in aqueous DCM; however, these conditions provided **9.28** in low yield due to concomitant removal of the TBS group.[345] However, **9.28** could be obtained in an 86% yield using BCl$_3$ with pentamethylbenzene as a scavenger.[317] Oxidation of **9.28** using TEMPO/NaClO$_2$/NaOCl provided **ent-9.5** in very high

yield; although a stoichiometric amount of TEMPO was required to prevent chlorination of the amide nitrogen. The NMR data of **ent-9.5** was identical to that reported for **9.5** and possessed an optical rotation equal and opposite to that reported for **9.5**.[326]
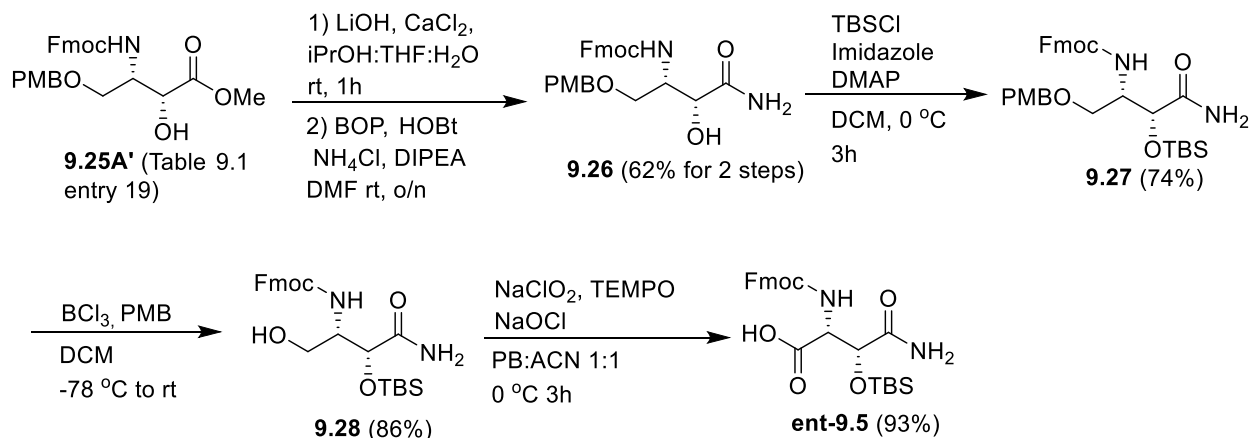
Scheme 9.2 Synthesis of **ent-9.5**

To prepare **ent-9.6a**, **9.25A'** was methylated with MeI/Ag$_2$O to give **9.29** in an 88 % yield (Scheme 9.3). We found that the hydrolysis of the ester in **9.29** was too slow using aqueous lithium hydroxide to allow for selective deprotection of the acid in the presence of the Fmoc group, even at high calcium concentrations. After trying trimethyl tin hydroxide[346] and AlCl$_3$/DMA,[347] we found that efficient deprotection of **9.29** could be achieved in good yield using LiI in ethyl acetate at 80 °C.[348] The free acid **9.30** was converted to *t*-butyl ester **9.31** in excellent yield using *t*-butyltrichloroacetimidate catalyzed by BF$_3$·Et$_2$O. However, we found that these results were difficult to reproduce at larger scales (> 1 g) due to concomitant removal of the PMB group, which yielded a mixture of **9.31** and **9.32**. We saw this as potentially advantageous since **9.32** could simply be added to the subsequent oxidation, after the cleavage was complete, reducing that amount of Bobbit's salt needed to afford **ent-9.6a**. As suspected, the PMB group of **9.31** was easily removed and the resulting *in-situ* generated primary alcohol was oxidized via a two-stage, one-pot reaction employing 1.1 equiv of Bobbit's salt followed by treatment with

TEMPO/NaClO$_2$/NaOCl.[326] This provided **ent-9.6a** in an 80% yield The NMR data of **ent-9.6** was identical to that reported for **9.6** and possessed an optical rotation equal and opposite to that reported for **9.6**.[326]
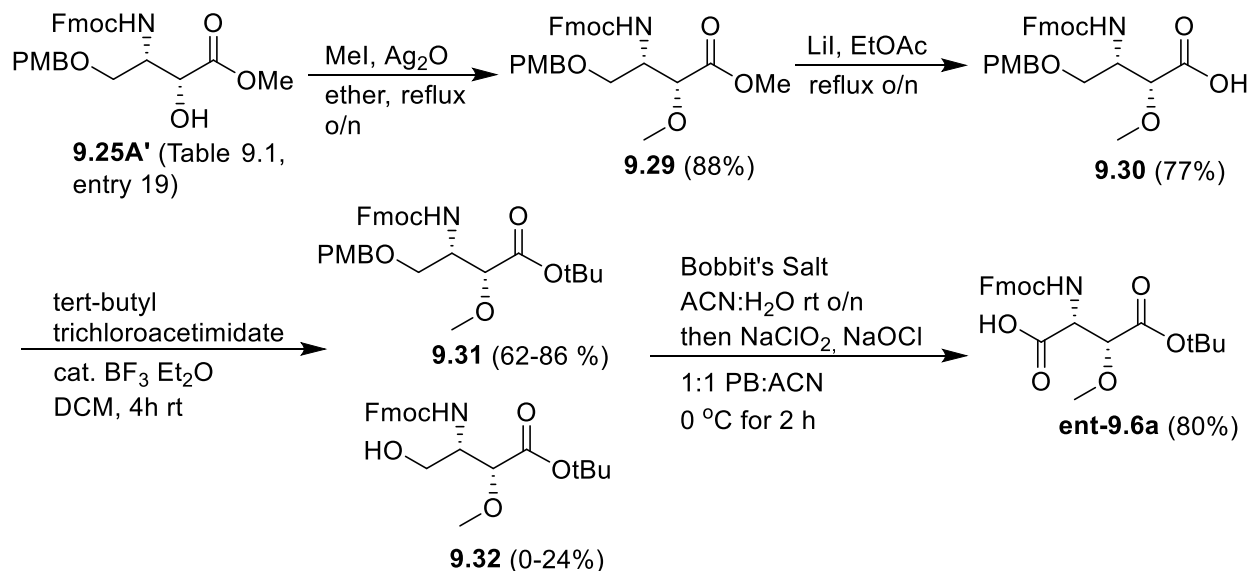
Scheme 9.3 Synthesis of **ent-9.6a.**

9.3   Conclusions

In summary, we have shown that FmocNHCl (**9.1**) is an effective nitrogen source for the SAAH reaction. In the absence of a ligand, the reaction usually provided Fmoc-protected amino alcohols in modest yields but with excellent regioselectivity. However, in some instances, both the yields and the regioselectivities could be altered by the addition of a catalytic amount of TEA. In the presence of a chiral ligand, the reactions proceeded more readily. In general, yields, regio- and enantioselectivities were like those reported using other carbamate nitrogen sources. Remarkably, the enantioselectivity of all but two examples exceed an er of 90:10 with many examples giving er of 95:5 or higher. A practical application of this chemistry was demonstrated by the synthesis of D-*threo*-β-hydroxyasparagine and D-*threo*-β-methoxyaspartate, suitably protected for Fmoc solid phase peptide synthesis.

9.4 Experimental

General Experimental Information. All reagents were purchased from commercial suppliers. ACS grade n-propanol (nPrOH), toluene and were used without further purification. Methylene chloride (CH_2Cl_2) and acetonitrile (ACN) were dried by distillation over calcium hydride under nitrogen. Pyridine was dried by refluxing over potassium hydroxide followed by fractional distillation. Tetrahydrofuran (THF) was distilled from sodium metal in the presence of benzophenone under N_2. Chromatography was preformed using 60 Å silica gel. All reported enantiomeric ratios (Ers) were determined by chiral HPLC. Reversed-phase analytical chiral HPLC was performed using a CHIRAL PAK AS-RH 5 µm 4.6 mm x 150 mm column with a flow rate of 0.5 mL/min. Normal-phase analytical chiral HPLC was performed using a CHIRAL PAK OD-H 5 µm 4.6 mm x 250 mm column with a flow rate of 0.4 mL/min. Analytical samples were prepared by dissolving a small amount of pure sample in 1 mL of mobile phase. For some samples run on the normal phase column which were not very soluble in the mobile phase, the solid was first dissolved in MeCN (50 µL) before being diluted with 90:10 iPrOH:hexanes. High resolution positive electrospray (ESI) mass spectra were obtained using an orbitrap mass spectrometer. Samples were sprayed from MeOH: 1% formic acid in H_2O. All spectra were collected in the positive mode. ^1H- and ^{13}C-NMR were collected using a Bruker Avance-300 spectrophotometer. ^1H-NMR chemical shifts (δ) are reported in ppm relative to an internal standard (trimethylsilane, 0 ppm). $^{13}C\{^1H\}$-NMR chemical shifts are reported relative to the solvent peak (77.0 ppm for $CDCl_3$, 49.2 ppm for CD_3OD, 39.5 ppm for DMSO-d_6). The configurations of **9.8B**, **9.14A**, **9.18A** and **9.23A'** were determined using Mosher's ester (Figure G.8-G.11 and Table G.1-G.4).[349]

Improved Procedure for Preparing FmocNHCl. FmocNH$_2$ (12 g, 50.15 mmol, 1 eq.) was dissolved with heating in MeOH (750 mL). When the reaction mixture had cooled to 35 °C, pulverized trichloroisocyanuric acid (3.86 g, 16.72 mmol, 1/3 equiv.) was added in a single

portion. The reaction was stirred for 14 hours at room temperature in a dark fumehood, then re-heated to 35 °C and another portion of pulverized trichloroisocyanuric (386 mg, 1.66 mmol, 0.03 equiv.) was added. After stirring at room temperature for an additional 4 hours, the reaction mixture was concentrated, and the resulting solid was suspended in hot toluene and then filtered while hot. Crystals form in the filtrate as the filtrate cools. Pure FmocNHCl (13.0 g, 70-95%) was obtained by heating the filtrate till the crystals redissolved and then allowing the filtrate to cool slowly during which pure FmocNHCl crystallized out of solution. The resulting crystals (FmocNHCl) were obtained by filtration then freed from solvent under high vacuum.

General Procedure for Sharpless Aminohydroxylation Reactions using FmocNHCl. To a suspension of FmocNHCl (221 mg, 0.804 mmol, 2.00 equiv) in nPrOH (1.75 mL) cooled in an ice-water bath, was added NaOH (24 mg, 0.60 mmol, 1.5 equiv) in H_2O (3 mL). This was followed by the addition of a solution of (DHQD)$_2$PHAL, (DHQ)$_2$PHAL (38 mg, 0.048 mmol, 12 mol%) or triethylamine (6 mol%) fully dissolved in nPrOH (3 mL) and a solution of alkene (0.402 mmol) in nPrOH (1.5 mL). $K_2[OsO_2(OH)_4]$ (12 mg, 0.032 mmol, 8 mol%) dissolved in H_2O (1.25 mL, a couple drops of the NaOH solution were added to the solution of $K_2[OsO_2(OH)_4]$ in H_2O) was added to the reaction mixture and, at this point, the reaction solution was deep-green and homogeneous. The cooled (ice-water bath) reaction mixture was stirred until the green color had dissipated or until TLC had indicated complete conversion of the alkene. The reaction was extracted with EtOAc (20 mL) twice and this organic layer was washed with aqueous sat. NaHCO$_3$ (30 mL) and brine. The organic layer was dried with Na$_2$SO$_4$ and concentrated. The crude residue was purified by silica-gel column chromatography.

(9H-Fluoren-9-yl)methyl (R)-(2-hydroxy-2-phenylethyl)carbamate (9.8B) and (9H-fluoren-9-yl)methyl (S)-(2-hydroxy-2-phenylethyl)carbamate (9.8B'). **9.8B** was prepared from **9.7** following

the general procedure using (DHQD)$_2$PHAL as a ligand. It was isolated by silica gel column chromatography (5% EtOAc/95% CH$_2$Cl$_2$) which yielded **9.8B** as a colorless, crystalline solid (65 mg, 45%). $[\alpha]^{22}_D$ = -18.2^0 (c. 0.560, CH$_2$Cl$_2$). Er = 94:6 (Figure G.1). **9.8B'** was prepared from **9.7** following the general procedure using (DHQ)$_2$PHAL as a ligand. It was isolated by silica gel column chromatography (5% EtOAc/95% CH$_2$Cl$_2$) which yielded **9.8B'** as a colorless, crystalline solid (54 mg, 37%). $[\alpha]^{22}_D$ = 15.9^0 (c. 0.324, CH$_2$Cl$_2$). Er = 88:11 (Figure G.1). NMR data matched those previously reported.[350] The ^{1}H NMR spectra of (±)-**9.8B**, **9.8B** and **9.8B'** were identical. ^{1}H NMR (300 MHz, CDCl$_3$): δ 7.68 (2H, d, J = 7.5 Hz), 7.49 (2H, m), 7.34-7.16 (9H, m), 5.14 (1H, m), 4.73 (1H, d, J = 9.3 Hz), 4.34-4.32 (2H, m), 4.12 (1H, dd, J = 6.9, 6.9 Hz), 3.48-3.44 (1H, m), 3.25-3.16 (1H, m), 2.78 (1H, br. s). ^{13}C{^{1}H} NMR (75 MHz, CDCl$_3$): 157.1, 143.8, 141.5, 141.3, 128.5, 127.9, 127.7, 127.0, 125.9, 125.0, 120.0, 73.6, 66.8, 48.5, 47.2. HRMS-ESI+ (m/z): [M + H]+ calculated for C$_{23}$H$_{22}$O$_3$N, 360.1594; found, 360.1594.

*(9H-Fluoren-9-yl)methyl (2-hydroxy-3-phenylpropyl)carbamate((±)-**9.10B***).

(±)-**9.10B** was prepared from **9.9** following the general procedure (no ligand was added). It was isolated by silica gel column chromatography (5% EtOAc/95% CH$_2$Cl$_2$) which yielded (±)-**9.10B** as a colorless, crystalline solid (83 mg, 55%). ^{1}H NMR (300 MHz, CDCl$_3$): δ 7.68 (2H, d, J = 7.8 Hz), 7.51 (2H, m), 7.34-7.11 (9H, m), 4.35 (1H, m), 4.12 (1H, dd, J = 6.3, 6.3 Hz), 3.85 (1H, m), 3.36 (1H, m), 3.03 (1H, m), 2.74-2.57 (2H, m), 2.15 (1H, br. s). ^{13}C{^{1}H} NMR (75 MHz, CDCl$_3$): 157.0, 143.8, 141.3, 137.4, 129.3, 128.7, 127.7, 127.0, 126.7, 125.0, 120.0, 72.0, 66.7, 50.7, 47.2, 46.2, 41.2. HRMS-ESI+ (m/z): [M + H]+ calculated for C$_{24}$H$_{24}$O$_3$N, 374.1751; found, 374.1746.

(9H-Fluoren-9-yl)methyl (2-hydroxy-1,2-diphenylethyl)carbamate **((±)-9.12).** **(±)-9.12** was prepared from **9.11** following the general procedure using MeCN in place of nPrOH and triethylamine as a ligand. It was isolated by silica gel column chromatography (2.5%

EtOAc/97.5% CH$_2$Cl$_2$ to 5% EtOAc/95% CH$_2$Cl$_2$) which yielded (±)-**9.12** as a colorless, crystalline solid (147mg, 84% yield). ^{1}H NMR (300 MHz, DMSO-d_6): δ7.89-7.66 (5H, m) 7.41-7.17 (14H, m) 5.52 (1H, d, J = 4.8 Hz), 4.79-4.74 (2H, m), 4.20-4.12 (3H, m). ^{13}C{^{1}H} NMR (75 MHz, DMSO-d_6): 155.7, 143.9, 143.7, 143.0, 141.5, 140.6, 127.7, 127.6, 127.3, 127.0, 127.0, 126.8, 126.6, 126.6, 125.3, 125.2, 120.0, 75.5, 65.5, 61.3, 46.6. HRMS-ESI+ (m/z): [M + H]+ calculated for C$_{29}$H$_{26}$O$_3$N, 436.1907; found, 436.1910.

Methyl (2S,3R)-3-(((((9H-fluoren-9-yl)methoxy)carbonyl)amino)-2-hydroxy-3-(4-methoxyphenyl)propanoate **(9.14A)** *and methyl (2R,3S)-3-(((((9H-fluoren-9-yl)methoxy)carbonyl)amino)-2-hydroxy-3-(4-methoxyphenyl)propanoate* **(9.14A').** **9.14A** was prepared from **9.13** following the general procedure using (DHQD)$_2$PHAL as a ligand. It was isolated by silica gel column chromatography (25% EtOAc/75% hexanes to 20% EtOAc/80% hexanes) which yielded **9.14A** as a colorless, crystalline solid (119 mg, 67%). [α]$^{22}_D$ = -19.5^0 (c. 0.868, CH$_2$Cl$_2$). Er = 97:3 (Figure G.2). **9.14A'** was prepared from **9.13** following the general procedure using (DHQ)$_2$PHAL as a ligand. It was isolated by silica gel column chromatography (25% EtOAc/75% hexanes) which yielded **9.14A'** as a colorless, crystalline solid (83 mg, 46%). [α]$^{22}_D$ = 21.3^0 (c. 0.952, CH$_2$Cl$_2$). Er = 99:1 (Figure G.2). The ^{1}H NMR spectra of **9.14A** and **9.14A'** were identical. ^{1}H NMR (300 MHz, CDCl$_3$): δ 7.67 (2H, d, J = 7.2 Hz), 7.47 (2H, m), 7.33-7.16 (6H, m), 6.79 (2H, d, J = 8.7 Hz), 5.63 (1H, d, J = 9.3 Hz), 5.13 (1H, d, J = 9.6 Hz), 4.39-4.08 (4H, m), 3.73-3.70 (6H, m), 3.22 (1H, d, J = 4.2 Hz). ^{13}C{^{1}H} NMR (75 MHz, CDCl$_3$): 173.3, 159.2, 155.7, 143.7, 141.2, 130.9, 127.9, 127.7, 127.0, 120.0, 114.0, 73.4, 66.9, 55.9, 55.3, 53.1, 47.1. HRMS-ESI+ (m/z): [M + H]+ calculated for C$_{26}$H$_{26}$O$_6$N, 448.1755; found, 448.1746.

Isopropyl (2S,3R)-3-(((((9H-fluoren-9-yl)methoxy)carbonyl)amino)-2-hydroxy-3-phenylpropanoate (9.16A) and isopropyl (2R,3S)-3-(((((9H-fluoren-9-yl)methoxy)carbonyl)amino)-2-hydroxy-3-phenylpropanoate (9.16A').

9.16A was prepared from **9.15** following the general procedure using (DHQD)$_2$PHAL as a ligand. It was isolated by silica gel column chromatography (10% EtOAc/90% hexanes to 20% EtOAc/80% hexanes) which yielded **9.16A** as a colorless, crystalline solid (145 mg, 81%). $[\alpha]^{22}_D$ = -17.2^0 (c. 0.744, CH$_2$Cl$_2$). Er = 98:2 (Figure G.3). **9.16A'** was prepared from **9.15** following the general procedure using (DHQ)$_2$PHAL as a ligand. It was isolated by silica gel column chromatography (10% EtOAc/90% hexanes to 20% EtOAc/80% hexanes) which yielded **9.16A'** as a colorless, crystalline solid (128 mg, 71%). $[\alpha]^{22}_D$ = 21.2^0 (c. 0.712, CH$_2$Cl$_2$). Er = 99:1 (Figure G.3). NMR data matched those previously reported.[2] The ^{1}H NMR spectra of **9.16A** and **9.16A'** were identical. ^{1}H NMR (300 MHz, CDCl$_3$): δ 7.67 (2H, d, J = 7.2 Hz), 7.48 (2H, m), 7.34-7.22 (9H, m), 5.64 (1H, d, J = 9.3 Hz), 5.22 (1H, d, J = 9.0 Hz), 5.07 (1H, sept, J = 6.0 Hz), 4.40-4.09 (4H, m), 3.18 (1H, br. s), 1.23-1.16 (6H, m). ^{13}C{^{1}H} NMR (75 MHz, CDCl$_3$): 172.3, 155.6, 143.9, 143.8, 141.3, 139.0, 128.6, 127.8, 127.7, 127.1, 126.7, 125.0, 120.0, 73.5, 70.9, 67.0, 56.3, 47.2, 21.7, 21.6. HRMS-ESI+ (m/z): [M + H]+ calculated for C$_{27}$H$_{28}$O$_5$N, 446.1962; found, 446.1951.

(9H-Fluoren-9-yl)methyl ((1S,2R)-2-hydroxycyclohexyl)carbamate (9.18A) and (9H-fluoren-9-yl)methyl ((1R,2S)-2-hydroxycyclohexyl)carbamate (9.18A'). **9.18A** was prepared from **9.17** following the general procedure using (DHQD)$_2$PHAL as a ligand. It was isolated by silica gel column chromatography (5% EtOAc/95% CH$_2$Cl$_2$) which yielded **9.18A** as a colorless, crystalline solid (113 mg, 75%). $[\alpha]^{22}_D$ = -17.4^0 (c. 0.800, CH$_2$Cl$_2$). Er = 98.5:1.5 (Figure G.4). **9.18A'** was prepared from **9.17** following the general procedure using (DHQ)$_2$PHAL as a ligand. It was isolated by silica gel column chromatography (5% EtOAc/95% CH$_2$Cl$_2$) which yielded **9.18A'** as

a colorless, crystalline solid (102 mg, 68%). $[\alpha]^{22}_D = 15.6^0$ (c. 0.904, CH_2Cl_2). Er = 84:16 (Figure G.4). The ^1H NMR spectra of **9.18A** and **9.18A'** were identical. ^1H NMR (300 MHz, $CDCl_3$): δ 7.66 (2H, d, J = 7.5 Hz), 7.49 (2H, d, J = 7.5 Hz), 7.30 (2H, dd, J = 7.2, 7.2 Hz), 7.21 (2H, dd, J = 7.2, 7.2 Hz), 5.18 (1H, d, J = 7.5 Hz), 4.30 (2H, m), 4.11 (1H, dd, J = 6.9, 6.9 Hz) 3.55 (1H, m) 2.11 (1H, br. s), 1.65-1.18 (8H, m). $^{13}C\{^1H\}$ NMR (75 MHz, $CDCl_3$): 156.1, 143.9, 141.2, 127.6, 127.0, 125.0, 119.9, 68.8, 66.5, 52.5, 47.2, 31.7, 27.2, 23.7, 19.6. HRMS-ESI+ (m/z): [M + H]+ calculated for $C_{21}H_{24}O_3N$, 338.1751; found, 338.1748.

Methyl (2S,3R)-3-((((9H-fluoren-9-yl)methoxy)carbonyl)amino)-2-hydroxy-3-phenylpropanoate (9.21A) and methyl (2R,3S)-3-((((9H-fluoren-9-yl)methoxy)carbonyl)amino)-2-hydroxy-3-phenylpropanoate (9.21A'). **9.21A** was prepared from **9.19** following the general procedure using $(DHQD)_2PHAL$ as a ligand. It was isolated by silica gel column chromatography (5% EtOAc/95% CH_2Cl_2) which yielded **9.21A** as a colorless, crystalline solid (113 mg, 67%). $[\alpha]^{22}_D = -9.9^0$ (c. 0.728, $CHCl_3$). Er = 97:3 (Figure G.5). **9.1A'** was prepared from **9.19** following the general procedure using $(DHQ)_2PHAL$ as a ligand. It was isolated by silica gel column chromatography (5% EtOAc/95% CH_2Cl_2) which yielded **9.21A'** as a colorless, crystalline solid (145 mg, 86%). $[\alpha]^{22}_D = 10.5^0$ (c. 0.852, $CHCl_3$). Er = 94:6 (Figure G.5). NMR spectra matched those previously reported.[2] The ^1H NMR spectra of **9.21A** and **9.21A'** were identical. ^1H NMR (300 MHz, $CDCl_3$): δ 7.67 (2H, d, J = 6.7 Hz), 7.48 (2H, d, J = 7.2Hz), 7.31-7.10 (9H, m), 5.65 (1H, d, J = 9.0 Hz), 5.19 (1H, d, J = 9.6 Hz), 4.43-4.12 (4H, m), 3.74 (3H, s), 3.18 (1H, br. s). $^{13}C\{^1H\}$ NMR (75 MHz, $CDCl_3$): δ173.1, 155.6, 143.6, 143.6, 141.2, 138.7, 128.6, 127.8, 127.6, 127.0, 124.9, 118.9, 73.3, 66.9, 56.3, 53.1, 47.0. HRMS-ESI+ (m/z): [M + H]+ calculated for $C_{25}H_{24}O_5N$, 418.1649; found, 418.1639.

*(2R,3S)-tert-Butyl 3-(1-(((((9H-fluoren-9-yl)methoxy)carbonyl)amino)-2-hydroxy-3-methoxy-3-oxopropyl)-1H-indole-1-carboxylate (**9.23A**) and (2R,3S)-tert-butyl 3-(1-(((((9H-fluoren-9-yl)methoxy)carbonyl)amino)-2-hydroxy-3-methoxy-3-oxopropyl)-1H-indole-1-carboxylate*

(**9.23A'**). **9.23A** was prepared from **9.22**[351] following the general procedure using (DHQD)$_2$PHAL as a ligand. It was isolated by silica gel column chromatography (20% EtOAc/80% hexanes) which yielded **9.23A** as a colorless, crystalline solid (148 mg, 65%). $[\alpha]^{22}_D$ = -17.3^0 (c. 0.808, CH$_2$Cl$_2$). Er = 98:2 (Figure G.6). **9.23A'** was prepared from **9.22** following the general procedure using (DHQ)$_2$PHAL as a ligand. It was isolated by silica gel column chromatography (20% EtOAc/80% hexanes) which yielded **9.23A'** as a colorless, crystalline solid (134 mg, 59%). $[\alpha]^{22}_D$ = 20.8 (c. 0.903, CH$_2$Cl$_2$). Er = >99.5:0.5 (Figure G.6). The ^{1}H NMR spectra of **9.23A** and **9.23A'** were identical. ^{1}H NMR (300 MHz, CDCl$_3$): δ 8.15 (1H, d, J = 6.5 Hz), δ 7.80-7.49 (6H, m), δ 7.43-7.21 (6H, m), δ 5.83-5.40 (2H, m), δ 5.66 (1H, br s), δ 4.50-4.10 (3H, m), δ 3.86 (3H, s), δ 3.52 (1H, br s), δ 1.67 (9H, s). ^{13}C{^{1}H} NMR (75 MHz, CDCl$_3$): δ 176.2, 158.6, 152.5, 146.7, 146.6, 144.1, 138.4, 131.6, 130.6, 130.0, 128.0, 127.7, 126.9, 125.8, 122.9, 122.2, 121.6, 118.3, 86.9, 75.1, 70.1, 56.2, 52.8, 50.0, 31.1. HRMS-ESI+ (m/z): [M + H]+ calculated for C$_{32}$H$_{33}$O$_7$N$_2$, 557.2282; found, 557.2301.

*Methyl (2S,3R)-3-(((((9H-fluoren-9-yl)methoxy)carbonyl)amino)-2-hydroxy-4-((4-methoxybenzyl)oxy)butanoate (**9.25A**).* **9.25A** was prepared from **9.24**[342] following the general procedure using (DHQD)$_2$PHAL as a ligand. It was isolated by silica gel column chromatography (30% EtOAc/70% hexanes to 40% EtOAc/70% hexanes) which yielded **9.25A** as a colorless, crystalline solid (144 mg, 73%). $[\alpha]^{22}_D$ = +2.4^0 (c. 0.704, CH$_2$Cl$_2$). Er = 91:9 (Figure G.7). ^{1}H-NMR spectrum was identical to that of **9.25A'**.

Methyl (2R,3S)-3-(((((9H-fluoren-9-yl)methoxy)carbonyl)amino)-2-hydroxy-4-((4-methoxybenzyl)oxy)butanoate (9.25A'). To a cooled (ice bath) slurry of FmocNHCl (8.9 g, 32.5 mmol, 2.0 equiv) in nPrOH (71 mL) was added a solution of sodium hydroxide (975 mg, 24.4 mmol, 1.5 equiv) in water (121 mL). A solution of (DHQ)$_2$PHAL (1.52 g, 1.95 mmol, 12 mol %) in nPrOH (121 mL) and a solution of alkene **9.24** (3.84 g, 16.3 mmol, 1.0 equiv) in nPrOH (61 mL) were added immediately after. The reaction mixture was cooled (ice bath) and at this point it was homogeneous, then a solution of potassium osmate (479 mg, 1.30 mmol, 8 mol %) and sodium hydroxide (61 mg, 1.525 mmol, 0.09 equiv) in water (51 mL) was added. The cooled reaction was stirred for 3 h, at which point TLC had indicated that the reaction was complete. The mixture was neutralized with 1N HCl and the resulting slurry was filtered. The filter cake was washed several times with 3:2 nPrOH:H$_2$O. The filtrate was concentrated and then partitioned between ethyl acetate (EtOAc, 100 mL) and water (100 mL). The aqueous layer was extracted twice and the combined organic layer was washed with 1 N HCl (300 mL), sat. NaHCO$_3$ (300 mL) and brine (300 mL). The resulting organic layer was dried with MgSO4, filtered and concentrated. The crude oil was suspended in CH$_2$Cl$_2$, filtered and concentrated. This process was repeated three times, then the crude oil was purified by silica gel column chromatography (30% EtOAc/70% hexanes to 40% EtOAc/60% hexanes) yielding **9.25A'** as a colorless foam (5.53 g, 73% yield). $[\alpha]^{22}_D$ = -3.0^0 (c. 0.801, CH$_2$Cl$_2$). Er = 96:4 (Figure G.7). ^{1}H NMR (300 MHz, CDCl$_3$): δ 7.76 (2H, d, *J* = 7.2 Hz), 7.61 (2H, m) 7.43-7.28 (6H, m) 6.88 (2H, d, *J* = 8.1 Hz), 5.66 (1H, d, *J* = 9.6 Hz) 4.53-4.20 (7H, m) 3.89-3.55 (9H, m). ^{13}C{^{1}H} NMR (75 MHz, CDCl$_3$): 173.5, 158.9, 155.8, 143.6, 143.4, 140.9, 129.4, 129.1, 127.3, 126.7, 124.8, 124.7, 119.6, 113.4, 72.5, 69.3, 52.4, 46.7. HRMS-ESI+ (m/z): [M + H]+ calculated for C$_{28}$H$_{30}$O$_7$N, 492.2017; found, 492.2011.

(9H-Fluoren-9-yl)methyl((2S,3R)-4-amino-3-hydroxy-1-((4-methoxybenzyl)oxy)-4-oxobutan-2-yl)carbamate (9.26). To a solution of **9.25A'** (2.88 g, 5.86 mmol, 1 equiv) in THF (40 mL) and isopropanol (133 mL) was added pulverized $CaCl_2$ (10.66 g, 96.08 mmol, 16.4 equiv). The resulting suspension was cooled (ice-water bath) and ice-cold LiOH (0.28N, 41.8 mL, 2.0 equiv) was added dropwise. After stirring for 15 min more ice cold LiOH (0.28 N, 33.5 mL, 1.6 equiv) was added dropwise to the suspension. Cooling was removed, and once it had reached room temperature, the reaction mixture was stirred for 45 min, at which point it was extracted with diethyl ether (100 mL). The aqueous layer was acidified with 1N HCl (pH ca. 2) and extracted with EtOAc (100 mL) three times. The combined organic layer was washed with 0.1 N HCl (300 mL) twice, dried over $MgSO_4$, filtered and concentrated. The crude residue was dissolved in DMF (117 mL) and reacted with benzotriazol-1-yloxytris(dimethylamino)phosphonium hexafluorophosphate (BOP; 3.89 g, 8.79 mmol, 1.5 equiv) for 5 min at room temperature. NH_4Cl (627 mg, 11.7 mmol, 2.0 equiv) and DIPEA (3.06 mL, 17.58 mmol, 3 equiv) were then added and the resulting suspension was stirred at room temperature for 2 hours. The reaction mixture was then diluted with EtOAc (1200 mL) and washed with 1N HCl (800 mL), sat. $NaHCO_3$ (800 mL) and brine (800 mL) twice. The organic layer was dried with Na_2SO_4, concentrated and subjected to silica gel flash column chromatography (80% EtOAc/19% hexanes/1% AcOH then 98% EtOAc/2% AcOH) yielding **9.26** as a colourless oil (1.73 g, 62% for two steps). ^{1}H NMR (300 MHz, $CDCl_3$): δ 7.60 (2H, d, *J* = 7.5 Hz), 7.44-7.40 (2H, m) 7.27-7.22(2H, m) 7.17-7.12 (2H, m) 7.05 (2H, d, *J* = 8.4 Hz) 6.70 (2H, d, *J* = 8.7 Hz) 6.66 (1H, br. s) 6.13(1H, br. s) 5.81 (1H, d, *J* = 9.0 Hz) 4.35-3.99 (8H, m) 3.70-3.50 (5H, m).^{13}C{^{1}H} NMR (75 MHz, $CDCl_3$): δ 175.3, 159.3, 156.6, 143.8, 143.6, 141.2, 129.4, 129.2, 127.6, 127.0, 125.0, 125.0, 119.9, 113.8, 73.1, 72.3, 70.3,

66.9, 55.1, 52.0, 46.9. HRMS-ESI+ (m/z): [M + H]+ calculated for $C_{27}H_{29}O_6N_2$, 477.2020; found, 477.2005.

(9H-Fluoren-9-yl)methyl((2S,3R)-4-amino-3-((tert-butyldimethylsilyl)oxy)-1-((4-methoxybenzyl)oxy)-4-oxobutan-2-yl)carbamate (9.27). To a cool (ice bath) solution of **9.26** (1.069 g, 2.24 mmol, 1.00 equiv) in dry CH_2Cl_2 (22.5 mL) was added Imidazole (764 mg, 11.2 mmol, 5.00 equiv) and TBSCl (1.69 g, 11.2 mmol, 5.00 equiv). After 5 min of stirring, DMAP (27 mg, 0.22 mmol, 0.10 equiv) was added and the suspension was stirred for 3 hours. After this time, the reaction was quenched with 0.2 N HCl (22 mL) while cold. The aqueous layer was then extracted with CH_2Cl_2 (22 mL) three times and the combined organic layer was washed with sat. $NaHCO_3$ (100 mL), brine (100 mL) and dried over Na_2SO_4 and concentrated. The crude residue was subjected to silica gel flash column chromatography (30% EtOAc/70% hexanes then 50% EtOAc/50% hexanes) yielding **9.27** as a colorless oil (979 mg, 74%). ^{1}H NMR (300 MHz, CDCl3): δ 7.65 (2H, d, *J* = 8.4 Hz), 7.53-7.50 (2H, m) 7.29 (2H, t, *J* = 7.5 Hz) 7.22-7.12 (6H, m) 6.75 (2H, d, *J* = 8.4 Hz), 6.32 (1H, br. s), 6.04 (1H, br. s) 5.56 (1H, d, *J* = 9.3 Hz) 4.36-4.11 (7H, m) 3.68 (3H, s) 3.50-3.23 (2H, m) 0.830 (9H, s) 0.049-0.031 (6H, m).^{13}C{^{1}H} NMR (75 MHz, CDCl3): δ175.1, 159.1, 155.8, 143.9, 143.9, 141.2, 129.9, 129.2, 127.6, 127.0, 125.1, 119.9, 113.6, 72.6, 71.3, 67.3, 66.8, 55.2, 53.4, 47.1, 25.6, 17.9, -5.1, -5.4. HRMS-ESI+ (m/z): [M + H]+ calculated for $C_{33}H_{43}O_6N_2Si$, 591.2885; found, 591.2891.

(9H-fluoren-9-yl)methyl((2S,3R)-4-amino-3-((tert-butyldimethylsilyl)oxy)-1-hydroxy-4-oxobutan-2-yl)carbamate (9.28). **9.27** (1.1 g, 1.9 mmol, 1.0 equiv) and pentamethylbenzene (306 mg, 2.06 mmol, 1.10 equiv) were dissolved in dry CH_2Cl_2 (20 mL) under an inert atmosphere. The reaction mixture was cooled to -78 °C and BCl_3 (1M in CH_2Cl_2, 5.62 mL, 5.62 mmol, 3.00 equiv) was added dropwise over 10 min. After the addition, the reaction mixture was warmed in an ice-

water bath. The resulting mixture was stirred for 1 hr and then quenched by the dropwise addition of sat. NaHCO$_3$ (40 mL). After 10 min of stirring, the reaction mixture was brought to room temperature and the aqueous layer was extracted with EtOAc (40 mL) twice. The organic layers were combined, washed with brine, dried with MgSO$_4$ and concentrated. The crude oil was purified by silica gel column chromatography (50% EtOAc/49% hexanes/1% AcOH to 60% EtOAc/39% hexanes/1% AcOH) yielding **9.28** (759 mg, 86%) as a colorless foam. Characterization data matched that previously reported.[3] ^{1}H NMR (300 MHz, CDCl$_3$): δ 7.73 (2H, d, *J* = 7.5 Hz) 7.59 (2H, m) 7.40-7.26 (4H, m) 6.06 (2H, m) 5.86 (1H, d, *J* = 9.3 Hz) 4.37-4.35 (2H, m) 4.29 (1H, d, *J* = 3.6 Hz) 4.20 (1H, dd, *J* = 6.9, 6.9 Hz) 4.00 (1H, m) 3.79-3.62 (2H, m), 0.93 (9H, s) 0.16-0.12 (6H, m).^{13}C{^{1}H} NMR (75 MHz, CDCl$_3$): δ 175.9, 156.3, 143.8, 143.8, 141.2, 141.2, 127.6, 126.6, 125.1, 119.8, 71.5, 66.9, 61.0, 55.7, 47.1, 25.6, 17.9, -5.2, -5.4. HRMS-ESI+ (m/z): [M + H]+ calculated for C$_{25}$H$_{35}$O$_5$N$_2$Si, 471.2310; found, 471.2309.

*(2R,3R)-2-(((((9H-Fluoren-9-yl)methoxy)carbonyl)amino)-4-amino-3-((tert-butyldimethylsilyl)oxy)-4-oxobutanoic acid (**ent-9.5**).* **9.28** (786 mg, 1.67 mmol, 1 equiv) was dissolved in ACN (23.4 mL) and cooled in an ice-water bath. TEMPO (392 mg, 2.88 mmol, 1.50 equiv) was added to the stirring reaction mixture. NaClO$_2$ (80% w/w; 529 mg, 4.68 mmol, 2.80 equiv) was dissolved in cold phosphate buffer (0.67 N, pH = 7; 15.8 mL) and added dropwise to the stirring reaction mixture. NaOCl (6% bleach; 1.44 mL, 1.17 mmol, 0.70 equiv) was added dropwise over 30 min. Once the addition was complete, the reaction was stirred for 3 hrs and then quenched with sat. Na$_2$SO$_3$ (10 mL) and brought to room temperature. The reaction mixture was acidified with 12 N HCl (pH ca. 2) and the aqueous layer was extracted with CH$_2$Cl$_2$ (75 mL) three times. The combined organic layer was dried with MgSO$_4$ and filtered. After concentrating, the residue was subjected to silica gel column chromatography (40% EtOAc/60% hexanes/1% AcOH)

allowing for the isolation of **ent-9.5** (721 mg, 92% yield) as a colorless solid. (635 mg, 92%).

NMR data matched those previously reported for its enantiomer.[3] $[\alpha]^{22}_D = 16.3^0$ (c 0.744, CH$_3$OH)

^{1}H NMR (300 MHz, CD$_3$OD): δ 7.62-7.40 (4H, m) 7.24-7.12 (4H, m), 6.73 (1H, d, J = 8.7 Hz)

4.61-4.55 (2H, m) 4.23-4.04 (3H, m) 0.81 (9H, s) 0.00 (6H, m). ^{13}C{^{1}H} NMR (75 MHz, CD$_3$OD):

δ 175.9, 172.9, 158.6, 145.3, 142.6, 128.9, 128.3, 126.4, 121.0, 75.4, 68.4, 58.9, 26.4, 19.2, -4.7, -

5.0. HRMS-ESI+ (m/z): [M + H]+ calculated for C$_{25}$H$_{33}$O$_6$N$_2$Si, 485.2102; found, 485.2105.

(2R,3S)-3-(((((9H-Fluoren-9-yl)methoxy)carbonyl)amino)-2-methoxy-4-((4-

methoxybenzyl)oxy)butanoate (9.29). **9.25A'** (1.70 g, 3.46 mmol, 1.00 equiv) was dissolved in

ether (69 mL) at room temperature. Freshly prepared, dry Ag$_2$O (2.40g, 10.4 mmol, 3 equiv)

followed by MeI (4.31 mL, 69.2 mmol, 20.0 equiv) were added to the flask. The reaction mixture

was vortexed briefly until a suspension was formed. The reaction mixture was then brought to

reflux and allowed to react for 18 hrs, with vigorous stirring, under an inert atmosphere. The

reaction mixture was cooled to room temperature, filtered, and concentrated. The residue was

purified by silica gel column chromatography (20% EtOAc/80% hexanes) allowing for the

isolation of **9.29** (1.54 g, 88% yield) as a colorless, vicious oil. ^{1}H NMR (300 MHz, CDCl$_3$): δ

7.74 (2H, d, J = 7.2 Hz) 7.59 (2H, m) 7.41-7.28 (6H, m) 6.88 (2H, d, J = 8.1 Hz) 5.40 (1H, d, J =

9.6 Hz) 4.53-4.13 (7H, m) 3.76-3.71 (6H, m) 3.55-3.45 (5H, m). ^{13}C{^{1}H} NMR (75 MHz, CDCl$_3$):

δ 171.0, 159.0, 155.6, 143.7, 143.5, 141.0, 129.6, 129.1, 127.4, 126.8, 124.9, 124.8, 119.7, 113.5,

77.6, 72.5, 67.3, 66.7, 58.6, 54.9, 52.1, 51.8, 46.8. HRMS-ESI+ (m/z): [M + H]+ calculated for

C$_{29}$H$_{32}$O$_7$N, 506.2173; found, 506.2172.

Preparation of (2R,3S)-3-(((((9H-Fluoren-9-yl)methoxy)carbonyl)amino)-2-methoxy-4-((4-

methoxybenzyl)oxy)butanoic acid (9.30). To a solution of **9.29** (1.03 g, 2.04 mmol, 1.00 equiv) in

degassed ethyl acetate (14.6 mL) was added LiI (1.36g, 10.2 mmol, 5.00 equiv) at room

temperature. The reaction vessel was then sealed, brought to 80 °C and stirred for 18 hrs. Once the reaction mixture had cooled to room temperature, it was diluted with ethyl acetate (50 mL) and washed with 0.1 N HCl (50 mL), dried over $MgSO_4$ and concentrated. The crude residue was subjected to silica gel column chromatography (40% EtOAc/59% hexanes/1% AcOH) yielding **9.30** as a colorless oil (800 mg, 80%). ^1H NMR (300 MHz, CDCl$_3$): δ 11.0 (1H, br. s), 7.73 (2H, d, J = 7.5 Hz), 7.58 (2H, m), 7.40-7.22 (6H, m), 6.85 (2H, d, J = 8.4 Hz), 4.53-4.26 (5H, m), 4.21-4.12 (2H, m), 3.78 (3H, s), 3.52-3.38 (5H, m). $^{13}C\{^1H\}$ NMR (75 MHz, CDCl$_3$): δ 174.5, 159.1, 156.3, 143.9, 143.5, 141.2, 141.1, 129.7, 129.3, 127.6, 127.0, 125.2, 125.1, 119.8, 113.7, 72.6, 67.5, 67.2, 59.0, 55.1, 52.1, 52.1, 46.9. HRMS-ESI+ (m/z): [M + H]+ calculated for $C_{28}H_{30}O_7N$, 492.2017; found, 492.2027.

*(2R,3S)-3-(((((9H-Fluoren-9-yl)methoxy)carbonyl)amino)-2-methoxy-4-((4-methoxybenzyl)oxy)butanoic acid (**9.31**).* To a solution of **9.30** (1.00 g, 2.05 mmol, 1.00 equiv) in CH_2Cl_2 (26 mL) cooled in an ice-water bath were added tert-Butyl 2,2,2-trichloroacetimidate (1.83 mL, 10.25 mmol, 5.00 equiv) and BF$_3$·Et$_2$O (29 µL, 0.21 mmol, 0.10 equiv). The resulting suspension was stirred for 1 hr at room temperature then concentrated. The crude residue was dissolved in CH_2Cl_2 (50 mL) and washed with 1N NaOH (50 mL), H_2O (50 mL), brine (50 mL), dried over $MgSO_4$ and concentrated. The crude residue was purified by silica gel column chromatography (20% EtOAc/80% hexanes then 40% EtOAc/59% Hexanes/1% AcOH) yielded **9.31** as a colorless oil (966 mg, 86%). ^1H NMR (300 MHz, CDCl$_3$): δ 7.75 (2H, d, J = 7.5 Hz), 7.57 (2H, d, J = 7.2 Hz), 7.39 (2H, dd, J = 7.2, 7.2 Hz), 7.32-7.28 (2H, m), 6.91 (2H, d, J = 6.9 Hz) 5.19 (1H, d, J = 9.3 Hz) 4.54-4.16 (6H, m) 3.99 (1H, br. s) 3.79 (3H, m) 3.50-3.44 (5H, m), 1.44 (9H, s). $^{13}C\{^1H\}$ NMR (75 MHz, CDCl$_3$): δ 169.8, 159.2, 155.8, 143.9, 143.7, 141.2, 141.2,

130.0, 129.4, 127.6, 127.0, 125.1, 125.1, 119.9, 113.7, 82.1, 78.0, 72.7, 67.9, 66.9, 58.9, 55.2, 52.3, 47.1, 27.9. HRMS-ESI+ (m/z): [M + H]+ calculated for $C_{32}H_{38}O_7N$, 548.2643; found, 548.2650.

tert-Butyl (2R,3S)-3-((((9H-fluoren-9-yl)methoxy)carbonyl)amino)-4-hydroxy-2-methoxybutanoate (9.32). **9.32** was recovered from the silica gel column used to purify **9.31**. This yielded **9.32** as a colorless foam (0-24% yield). ^{1}H NMR (300 MHz, CDCl₃): δ 7.64 (2H, d, *J* = 7.2 Hz), 7.28, (2H, d, *J* = 6.9 Hz), 7.28 (2H, t, *J* = 6.9 Hz), 7.20 (2H, t, *J* = 7.5 Hz), 5.36 (1H, d, *J* = 9.0 Hz), 4.31-4.08 (4H, m), 3.92 (1H, m) 3.71-3.53 (2H, m), 3.37 (3H, s), 1.35 (9H, s). ^{13}C{^{1}H} NMR (75 MHz, CDCl₃): δ 169.6, 156.2, 143.7, 143.6, 141.1, 141.1, 127.6, 126.9, 125.0, 119.8, 82.3, 79.1, 67.0, 62.2, 58.7, 54.2, 47.0, 27.8. HRMS-ESI+ (m/z): [M + H]+ calculated for $C_{24}H_{30}NO_6$, 428.2073; found, 428.2080.

(2R,3R)-2-((((9H-Fluoren-9-yl)methoxy)carbonyl)amino)-4-(tert-butoxy)-3-methoxy-4-oxobutanoic acid (ent-9.6a). **9.31** (883 mg, 1.61 mmol, 1.00 equiv) was dissolved in freshly prepared 9:1 ACN:H_2O (6.5 mL) and Bobbit's Salt (532 mg, 1.77 mmol, 1.10 equiv) was added to the stirring solution. The reaction mixture was sealed and allowed to stir for 18 hrs at room temperature. The resulting solution was cooled in an ice-water bath (any recovered **9.32** was added at this point and the amount of primary oxidant was scaled accordingly), diluted with a solution of $NaClO_2$ (80% w/w; 547 mg, 4.84 mmol, 3.00 equiv) in phosphate buffer (0.67 M, pH ca. 7; 10.75 mL) and then the mixture was neutralized with 1N NaOH. The neutralized mixture was diluted with ACN (9.65 mL) followed by a dropwise addition of NaOCl (6% bleach; 1.40 mL, 1.13 mmol, 0.70 equiv) over 30 min. Once the addition was complete, the reaction proceeded to completion in 4h at which point it was quenched with saturated aqueous Na_2SO_3. The organic layer was separated, and the aqueous layer was acidified slowly with 12 N HCl (pH ca. 2). The aqueous layer was extracted with CH_2Cl_2 (50 mL) three times and the combined organic layer was dried with

MgSO$_4$. The residue was purified by silica gel column chromatography (40 % EtOAc/59% hexanes/1% AcOH), allowing for the isolation of **ent-9.6a** as a colorless solid (569 mg, 80%). NMR data matched those previously reported for its enantiomer.[3] $[\alpha]^{22}_D = 14.3^0$ (c. 0.628, CH$_3$OH). ^{1}H NMR (300 MHz, CDCl$_3$): δ 11.11 (1H, br. s) 7.73 (2H, d, J = 7.2 Hz) 7.61-7.56 (2H, m) 7.40-7.26 (4H, m) 5.76 (1H, d, J = 10.2 Hz) 4.96 (1H, d, J = 9.9 Hz) 4.35-4.32 (3H, m) 4.20 (1H, dd, J = 7.2 Hz) 3.48 (3H, s) 1.45 (9H, s). ^{13}C{^{1}H}NMR (75 MHz, CDCl$_3$): δ174.5, 168.0, 156.4, 143.7, 143.6, 141.2, 127.7, 127.1, 125.2, 125.2, 119.9, 83.2, 79.6, 77.4, 67.6, 59.3, 56.4, 46.9, 27.9. HRMS-ESI+ (m/z): [M + H]+ calculated for C$_{24}$H$_{28}$O$_7$N, 442.1860; found, 442.1852.

Chapter 10 - A54145 Factor D is Not Less Susceptible to Inhibition by Lung Surfactant than Daptomycin

10 Preface and contributions

This chapter is based on an article published in the journal *ACS Infectious Disease* (*Reprinted (adapted) with permission from ACS Infect. Dis.* **2022**, *8* (9), 1935–1947. *Copyright 2022 American Chemical Society*). All the experimental work was completed by me under the supervision of Prof. Scott Taylor. I wrote the first draft of the manuscript which was expanded upon by Prof. Taylor. Additional supplementary data is available on the journal's website.

10.1 Introduction

With the chiral target of daptomycin established (chapter 5) we wished to determine whether A5D possessed a chiral target and whether this chiral target was 2R,2'S-PG. We also set out to determine the absolute configuration of PG in mammalian lung surfactant. It was our intention to use these pieces of information to determine if the difference in the activity of A5D and daptomycin in the presence of LS could be fully accounted for by a difference in PG affinity, or if another molecule that only antagonises daptomycin must be present. However, we discovered that some of the claims made about the activity of A5D in the presence of LS did not hold up under scrutiny. A detailed account of this work is provided here-in.

As discussed in chapter 1, one limitation of daptomycin is that it cannot be used for treating community acquired bacterial pneumonia (CAP) due to sequestration by lung surfactant.[12] For example, researchers at Cubist Pharmaceuticals reported that daptomycin's MIC increases 128-fold against *S. aureus* (0.5 µg/mL to 64 µg/mL) in the presence of bovine lung surfactant (BLS).[16] This is the only example of a pulmonary-specific mechanism resulting in the failure of an antibiotic in a clinical trial, and was the first report of organ-specific inactivation of an antibacterial agent.

In contrast, A5D, which was reported to have a 4-fold greater MIC than daptomycin against *S. aureus*, exhibited only a 2-fold increase in MIC in the presence of BLS, suggesting that A5D is less susceptible to inhibition by lung surfactant than daptomycin.[16] This finding prompted researchers at Cubist Pharmaceuticals to expend a considerable amount of resources attempting to create a non-toxic A5/daptomycin hybrid that is highly active in the presence of lung surfactant and could be used for treating CAP.[16,17,145] However, no clinical antibiotics came out of these endeavors.

The effect of lung surfactant on daptomycin activity was first described by Silverman et al at Cubist Pharmaceuticals who proposed that daptomycin is inserting into PG-containing lipid aggregates in a calcium-dependent manner resulting in inhibition.[12] Indeed, this hypothesis was supported by Martin and coworkers who found that daptomycin is fully antagonized by two equivalents of 1-palmitoyl-2-oleoyl-sn-glycero-3- phospho-(1'-rac-glycerol) (POPG).[52] Although this explanation describes one possible mode of daptomycin sequestration, it fails to explain the *apparent difference* in the activity of daptomycin and A5D in the presence of lung surfactant.

One possible explanation for the apparent difference in the activity of daptomycin and A5D in the presence of lung surfactant is that A5D has a much lower affinity for PG or some other component of BLS than daptomycin. We recently showed that the interaction between daptomycin and PG is a chiral recognition event which is strongly impacted by the absolute configuration of both PG and peptide (chapter 5).[278] These studies revealed that the chiral target of daptomycin is 1,2-diacyl-sn-glycero-3-phospho-1'-sn-glycerol stereoisomer (2R,2'S configuration). If PG in lung surfactant consists of mainly the 2R,2'S stereoisomer and bacteria may possess 2R,2'S-PG and 2R,2'R-PG,[38] it is also possible that the difference between the activity of A5D and daptomycin may be due to each peptide targeting a different stereoisomer of PG. Therefore, we set out to

determine if A5D also interacts preferentially with a specific stereoisomer of PG and establish the absolute configuration of PG in lung surfactant. We also aimed to determine if A5D and daptomycin exhibit different affinities for their respective PG stereoisomers and, if so, whether this difference in affinity can account for the apparent difference in their inhibition by lung surfactant.

10.2 Results and discussion

To determine if A5D interacts with a chiral target, the unnatural enantiomer of A5D (ent-A5D) was required. For the synthesis of ent-A5D, Fmoc-D-threo-hAsn(TBS)-OH was prepared according to our previously reported procedure (chapter 8).[352] Fmoc-D-erythro-MeOAsp(t-Bu)-OH was prepared using a route analogous to our previously disclosed routes (see section 10.5, Scheme 10.7).[181,326,352]

The natural enantiomer of A5D and the unnatural enantiomer of A5D (ent-A5D) were prepared according to our previously reported synthetic route.[181] The synthesized ent-A5D possessed an equal but opposite CD spectrum compared to A5D (Figure H.1) and co-eluted with A5D (Figure H.2). The minimum inhibitory concentration (MIC) of ent-A5D was 32-fold greater than the natural isomer ($MIC_{ent-A5D} = 128$ µg/mL, $MIC_{A5D} = 4$ µg/mL) against *B. subtilis* 1046 at 1.25 mM $CaCl_2$, unequivocally demonstrating that A5D interacts with a chiral target as part of its action mechanism.

To determine if A5D engages in a chiral recognition with PG, we first needed a robust means of assaying the membrane insertion of A5D. Monitoring the membrane insertion of A5D has been done by observing the blue shift in the emission of Trp1 which occurs upon membrane binding.[91] Although this appears to be a satisfactory method for monitoring the insertion of A5D into model membranes in some cases, we found it to be too insensitive for our purposes.

Considering that the membrane insertion of daptomycin can be measured with high sensitivity by monitoring Kyn13 fluorescence,[19] we surmised that placing a Kyn residue at the same position in A5D could yield an analog whose membrane insertion could be easily monitored. Baltz and coworkers have reported that an A5D analog called CB-183,296, which bears a Kyn at the13 position (referred to as A5DKyn henceforth), exhibited a 2-fold lower MIC (1 µg/mL) against a strain of *S. aureus* than A5D, and whose MIC increases only 2-fold in the presence of BLS.[145] Since this analog has very similar biological properties to A5D, its membrane binding profiles and lipid interactions should be very similar to that of native A5D. Therefore, we synthesized A5DKyn using the route outlined in Scheme 10.1. Dipeptide **10.1** was prepared by coupling on Fmoc-L-Thr-OH using DIC/HOBt to a polystyrene resin-bound Sar residue attached to a 2-Cl Trt linker. **10.1** was carefully deprotected using 2 x 1 min treatments with 20% 2-methylpiperidine (2-MP)/DMF to mitigate DKP formation, as reported previously.[181] After coupling on Fmoc-L-*threo*-hAsn(TBS)-OH using DIC/HOBt, the peptide was elongated to pentapeptide **10.2**. Ester bond formation at this stage proceeded smoothly via the symmetric anhydride of Fmoc-L-Kyn(Boc)-OH.[238] Removal of the Alloc group from hexapeptide **10.3** was achieved with 1,3-dimethylbarbituric acid/Pd(PPh$_3$)$_4$ which allowed for addition of the (±)-8-methyldecanoic acid tail giving **10.4**. To keep our synthesis consistent with Kralt et al, we removed the TBS group from peptide **10.4** with TBAF/THF and then elongated to Ala 6 using Fmoc SPPS with DIC/HOBt couplings. Peptide **10.5** was cleaved from the solid-support using 1% TFA/DCM giving peptide **10.6** which was cyclized over a 48-hour period at room temperature using PyAOP/HOAt/2,4,6-collidine in DMF. After the cyclization, peptide **10.7** was globally deprotected using TFA/TIPS/H$_2$O. A5DKyn was isolated via semi-preparative R-HPLC in a 6% overall yield. The final peptide was sequenced by MS-MS (Figure H.8) and assigned by 1D and 2D NMR (see

Figures H.11-H.15 and Table H.1). Antibacterial studies revealed that A5DKyn and A5D possess an identical MIC against *B. subtilis* 1046 at 1.25 mM $CaCl_2$ (MIC_{A5DKyn} = 4 µg/mL).
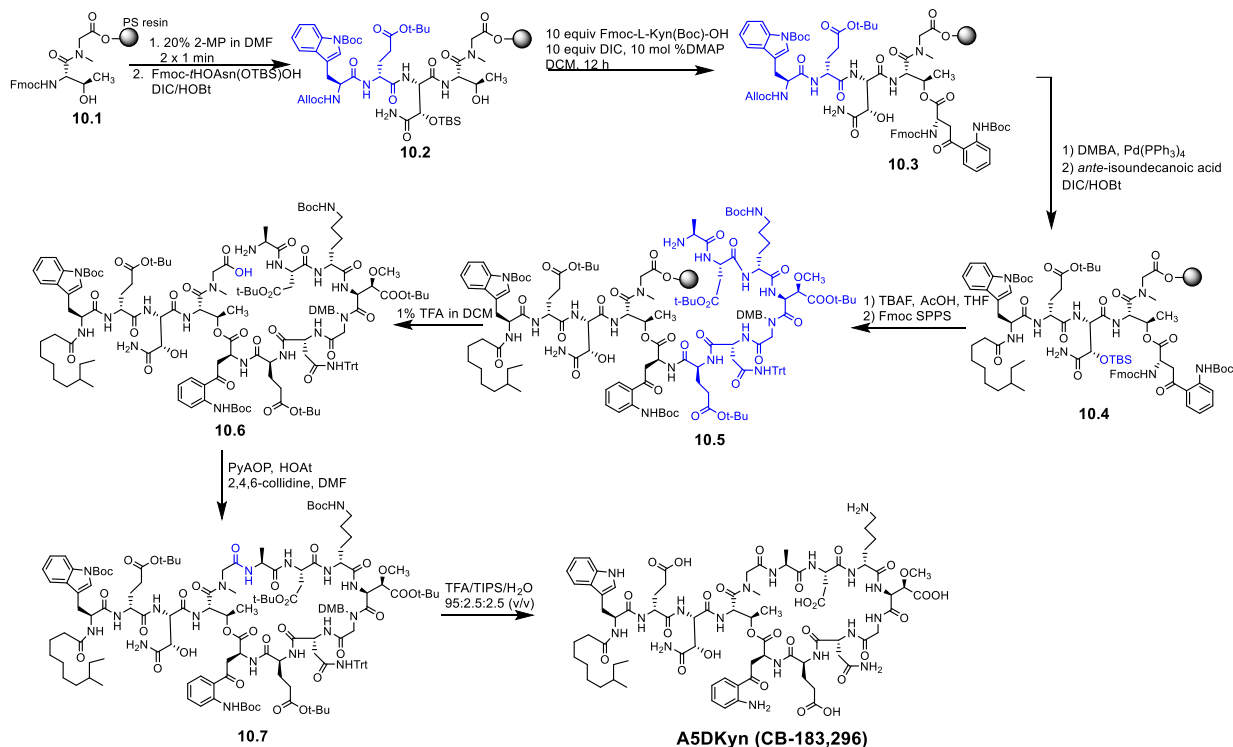
Scheme 10.1 Fmoc SPPS of A5DKyn

As with daptomycin, we observe that the insertion of A5DKyn into model membranes is accompanied by a large increase in the emission intensity of Kyn13 and a modest blue shift. These properties make it suitable for the determination of the relative affinity that A5DKyn has for each stereoisomer of DMPG. All four stereochemically pure DMPG isomers, which were synthesized using our previously reported route,[278] were used to prepare large unilamellar vesicles (LUVs). Titrating calcium into a solution of A5DKyn and LUVs containing one of the four stereoisomers of DMPG, we observe calcium-dependent membrane insertion that is influenced by the absolute configuration of the DMPG present (Figure 10.1A). Like daptomycin, A5DKyn prefers 2R,2'S-DMPG since half-maximal insertion occurs at a calcium concentration that is approximately 3-4 times

lower than with the other isomers. Similar to daptomycin, A5DKyn is very sensitive to the absolute configuration at the headgroup of PG; however, A5DKyn is more sensitive to the absolute configuration at the lipid group than daptomycin. Indeed, half-maximal insertion is achieved at nearly the same calcium concentration for 2R,2'R-DMPG, 2S,2'S-DMPG and 2S,2'R-DMPG.
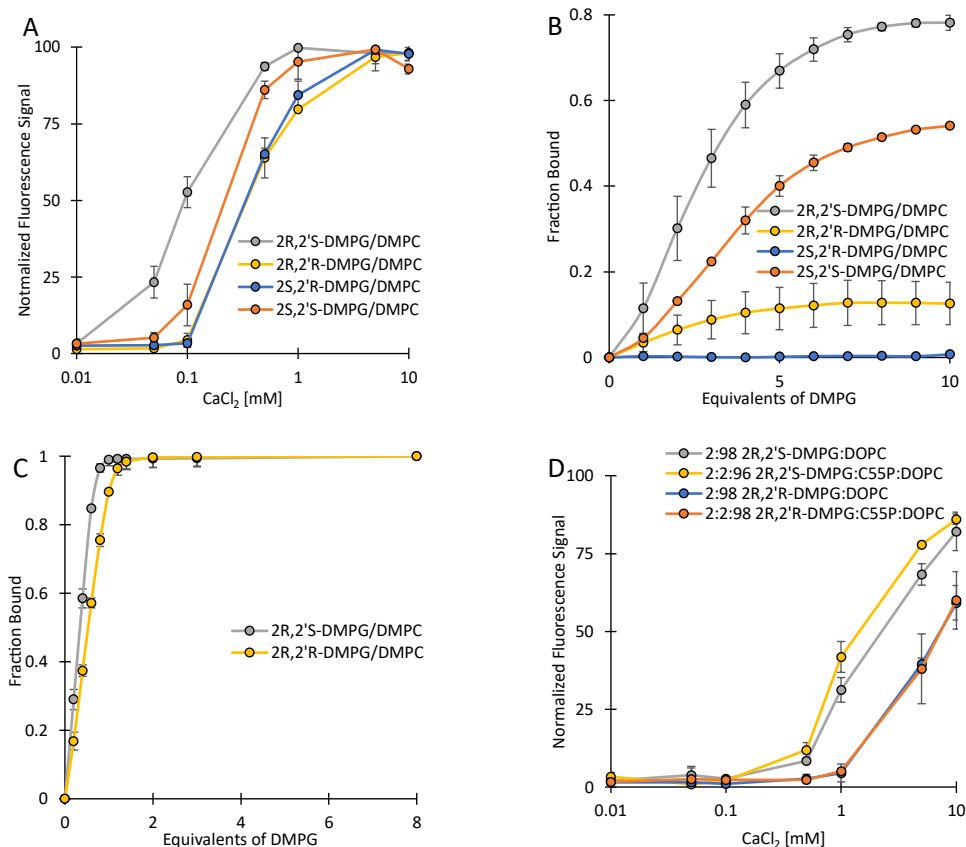
Figure 10.1 Membrane binding curves using A5DKyn and LUVs composed of 1:1 DMPG:DMPC at 37 °C in 20 mM HEPES, 150 mM NaCl (pH 7.4). (A) Calcium was titrated into a solution of A5DKyn (3 μM) and LUVs (250 μM) containing one of the stereoisomers of DMPG. (B) LUVs containing one of the four stereoisomers of PG were titrated into a solution of A5DKyn (15 μM) at 0.1 mM CaCl$_2$. The fully bound state was achieved by increasing the CaCl$_2$ concentration to 5 mM at the end of the titration. (C) The same titration described for (B) using 5 mM CaCl$_2$ for LUVs containing (2R,2'S)-DMPG and 10 mM CaCl$_2$ for LUVs containing (2R,2'R)-DMPG. (D) The same titration described for (A) but with LUVs containing 2:98 DMPG:DOPC or 2:2:96 DMPG:C$_{55}$P:DOPC.

Titrating LUVs into solutions of A5DKyn at fixed calcium concentrations paints a more detailed picture of the interaction of this peptide with the different stereoisomers of DMPG (Figure 10.1B-C). At 0.1 mM CaCl$_2$, A5DKyn readily distinguishes between the

four isomers of DMPG and displays a strong preference for 2R,2'S-DMPG (Figure 10.1B). Inverting the absolute configuration of the lipid group to give 2S,2'S-DMPG results in a modest decrease in membrane affinity while inverting the headgroup absolute configuration to give 2R,2'R-DMPG truncates affinity. Interestingly, no membrane insertion is observed with 2S,2'R-DMPG, indicating that ent-A5D would not be able to insert into a membrane containing only 2R,2'S-DMPG at 0.1 mM $CaCl_2$.

At high calcium concentration (5-10 mM), the insertion of A5DKyn can be pushed to completion allowing for the evaluation of binding stoichiometry (Figure 10.1C). Under these conditions we observed stoichiometric binding between DMPG and A5DKyn regardless of the headgroup configuration. These results indicate that the differences in the binding curves presented in Figures 10.1A-C are due to a change in the binding constant and are not caused by a change in binding stoichiometry. It is surprising that only a single equivalent of DMPG is needed to saturate A5DKyn since 2 equivalents are needed to saturate daptomycin under identical conditions. Considering the similarity of these natural products, we do not think that they possess different binding stoichiometries, instead it seems more likely that A5DKyn is able to access both leaflets of the LUV while daptomycin can only access one.[257]

Recently, Grein et al reported that daptomycin has enhanced affinity for model membranes that contain both PG and undecaprenol phosphate ($C_{55}P$).[71] To investigate whether or not A5D participates in such an interaction and to determine how this interaction is influenced by PG stereochemistry, we probed the binding of A5DKyn to model membranes containing semi-synthetic $C_{55}P$,[266] DMPG and DOPC (Figure 10.1D). In line

with our findings on daptomycin, A5DKyn is unaffected by $C_{55}P$ in the presence of PG and calcium. Similar findings were reported by Martin and coworkers using ITC.[72]

Several enlightening investigations of daptomycin have employed circular dichroism to assay the membrane bound state of daptomycin.[24,80,257] In each of these studies, the authors report that solution-phase daptomycin display a wave-like CD curve which is inverted upon insertion into a PG-containing membrane in the presence of calcium. The wave-like shape of the CD traces is thought to be caused by an interaction between Trp1 and Kyn13.[257] Therefore, CD analysis of A5DKyn, which contains Trp1 and Kyn13, would provide information about how the state of this peptide is affected by the stereochemistry of DMPG and how this state compares to daptomycin.
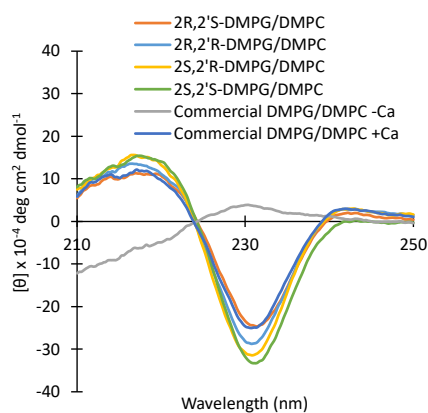
Figure 10.2. CD traces presented as $[\theta]$ x 10^{-4} (deg cm^2 dmol^{-1}) vs. wavelength (nm) plots. 15 µM peptide was incubated with 180 µM LUV at 5 mM CaCl$_2$ in 20 mM HEPES pH = 7.4 for 3 minutes before analysis at room temperature.

The results of our CD study are presented in Figure 10.2. A5DKyn displays a wave-like CD curve in solution that is similar to those reported for daptomycin.[24,80,257] In the presence of calcium and PG-containing LUVs, A5DKyn experiences a strong structural change which is indicated by an inversion in the sign of the wave and an increase in its amplitude. This behaviour is remarkably similar to that reported for daptomycin and it strongly suggests that the state of these two peptides is similar when bound to a PG-containing membrane. The membrane bound state of A5DKyn is

affected by the absolute configuration of the DMPG to which it is bound, although only small changes in amplitude are observed.

Previous studies on A5D and analogs of A5D have shown that it oligomerizes on model membranes.[89,90] One of the key experiments in this line of work was done using a pyrene-labelled A5D (referred to by pyrene-A5D henceforth).[90] When two pyrene units come into close contact with one another they form an excimer which emits maximally at 475 nm while the monomer emits maximally at 375 nm. Therefore, oligomer formation should be accompanied by an increase in the fluorescence intensity observed at 475 nm.

Figure 10.3 show the fluorescence emission of pyrene-A5D bound to LUVs composed of DMPG/DMPC at 1.25 mm $CaCl_2$. In all cases, an increase monomer emission is observed indicating that the pyrene unit has entered the non-polar membrane environment.[90] However, excimer formation is only observed when pyrene-A5D is bound to 2R,2'S- or 2S,2'S-DMPG. Remarkably, very little excimer formation is observed when pyrene-A5D is bound to 2S,2'R-DMPG. Thus, although ent-A5D can likely bind to a bacterial membrane at physiological calcium concentrations, it cannot oligomerize to same extent as a5d explaining its inactivity.

Isothermal titration calorimetry (ITC) was used to determine the affinity of daptomycin and A5D for 2R,2'S-DMPG incorporated into LUVs at 1.25 mm Ca^{2+} (Figures 10.4, H.9 and H.10).[72,89] at physiological calcium concentrations, we found daptomycin to have a $K_D = 0.25 \pm 0.04$ µM and binding stoichiometry of 1:2 daptomycin:2R,2'S-DMPG (number of sites = 2.4 ± 0.1). These values are very similar to those reported by Palmer and co-workers using LUVs composed of equimolar concentrations of DOPG/DOPC at 1 mM $CaCl_2$.[89] In contrast, A5D had a $K_D = 7.5 \pm 0.6$ µM but interacted stoichiometrically with 2R,2'S-dmpg (number of sites = 0.93 ± 0.1). These data reveal that A5D has a lower affinity for these 2R,2'S-DMPG-containing

liposomes than daptomycin, but still binds avidly to this molecule at low micromolar concentrations.
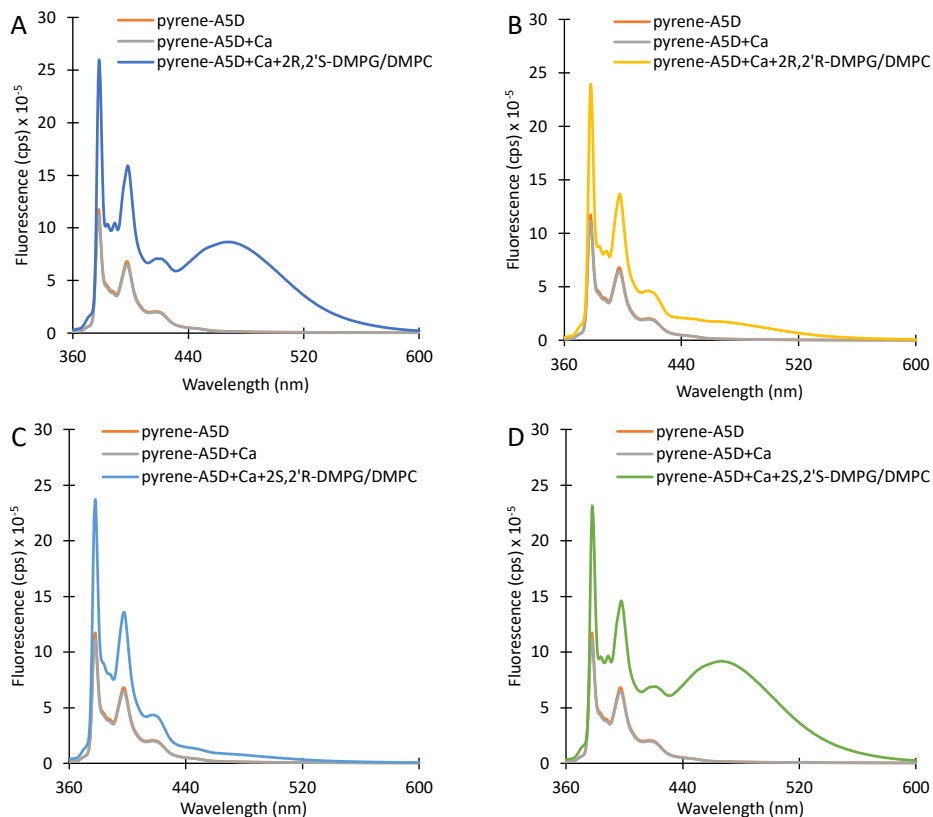
Figure 10.3 Fluorescence spectra of pyrene-A5D (2.5 µM) in the presence of 1.25 mM Ca^{2+} and LUVs composed of 1:1 DMPG:DMPC at 37 °C in 20 mM HEPES, 150 mM NaCl (pH 7.4). (A) The DMPG component is 2R,2'S-DMPG. (B) The DMPG component is 2R,2'R-DMPG. (C) The DMPG component is 2S,2'R-DMPG. (D) The DMPG component is 2S,2'S-DMPG.
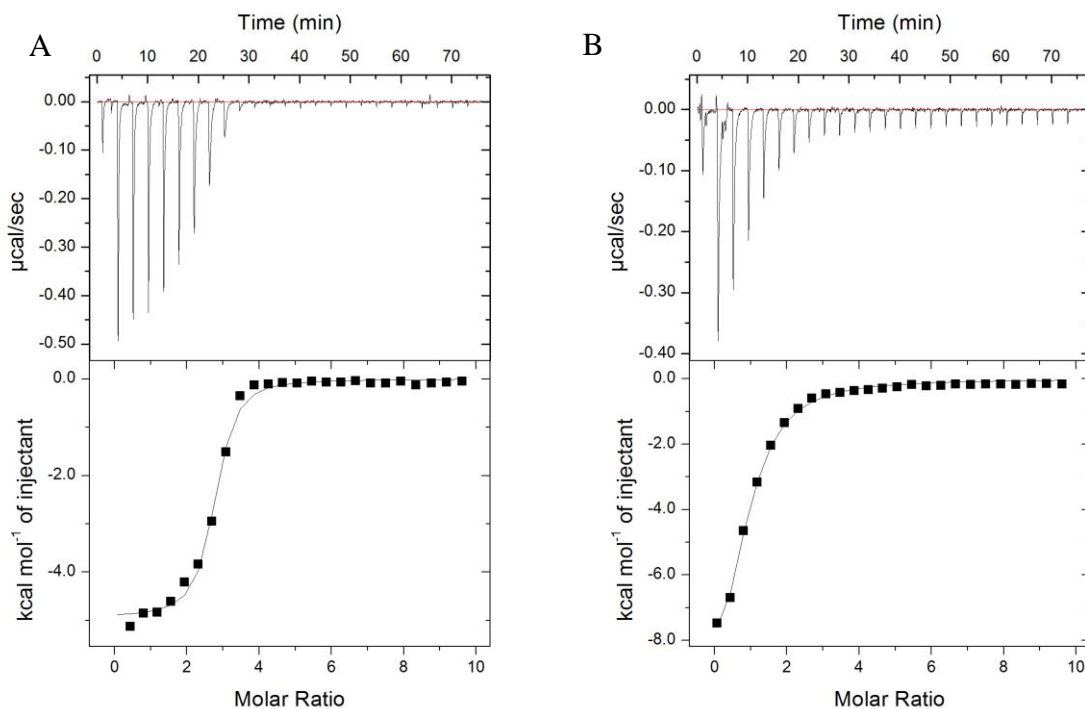
Figure 10.4 Representative binding isotherms for the titrations of LUVs (25:75 2R,2'S-DMPG:DOPC) into a solution of daptomycin (20 µM) (Panel A) or A5D (20 µM) (Panel B) in buffer consisting of 20 mM HEPES, 150 mM NaCl and 1.25 mM CaCl$_2$, pH 7.4. Data was collected in triplicate. See Figure H.9 and H.10 for the remaining thermograms.

The ability of each stereoisomer of DMPG to inhibit daptomycin and A5D against *B. subtilis* was determined at eight times the MIC (8 µg/ mL and 32 µg/mL of daptomycin and A5D respectively) of each peptide. The results of this study are summarized in Table 10.1. Incomplete antagonism of daptomycin occurred with just one equivalent of commercial DMPG (which contains both 2R,2'S- and 2R,2'R-DMPG[38]), 2R,2'S-DMPG or 2S,2'S-DMPG; however, complete antagonism occurred with 2 equivalents of commercial DMPG, 2R,2'S-DMPG or 2S,2'S-DMPG. 2R,2'R-DMPG exhibited incomplete inhibition at 2 equivalents but was completely inhibited at 4 equivalents while 2S,2'R-DMPG exhibited incomplete inhibition at 4 equivalents but complete inhibition at 6 equivalents. The results with the 2R,2'S-DMPG and 2S,2'S-DMPG stereoisomers may

280

seem at odds with the seemingly equivalent antagonism using commercial DMPG, but this is not the case since complete antagonism at 2 equivalents means that complete antagonism occurs at greater than 1 but less than or equal to 2 equivalents of 2R,2'S -DMPG and 2S,2'S-DMPG. Considering these ranges, it is expected that a sample containing stoichiometric amounts of 2R,2'S-DMPG and 2R,2'R-DMPG (which is the composition of commercial DMPG) would fully antagonize dap when 1.5-2.5 equivalents are present.

As was the case with daptomycin, no antagonism of A5D occurred with just one equivalent of commercial DMPG, 2R,2'S- DMPG or 2S,2'S-DMPG; however, surprisingly, complete antagonism occurred when 2 equivalents of commercial DMPG, 2R,2'S-DMPG or 2S,2'S-DMPG were present. Similar to daptomycin, 4 equivalents of 2R,2'R-DMPG and 8 equivalents 2S,2'R-DMPG completely inhibited A5D.

A5D has a considerably lower affinity for 2R,2'S-DMPG than daptomycin when determined in the context of the liposomes used for the ITC studies. Using the K_D value (7.5 µM) determined from the ITC studies described in Figure 10.4, it can be calculated that in the presence of two equivalents of PG and at a peptide concentration of 32 µg/mL, 76% of A5D should have been bound to PG, leaving 7.7 µg/mL of A5D still available to inhibit bacterial growth.[353] Our finding that two equivalents of PG completely inhibit A5D, suggests that A5D has a higher affinity for 'free' PG compared to when PG is incorporated into the liposomes used for the ITC studies.

Table 10.1 Antagonism of Daptomycin and A5D with DMPG.[a]

Peptide	Equivalents of DMPG				
	commercial DMPG	2R,2'S-DMPG	2R,2'R-DMPG	2S,2'R-DMPG	2S,2'S-DMPG
Daptomycin	2	2	4	6	2
A5D	2	2	4	8	2

To ascertain the role PG in lung surfactant plays on the inhibition of daptomycin and A5D, it was necessary to determine the absolute configuration of PG in BLS. PG derived from BLS (which will be referred to as BLS-PG) contains a variety of different fatty acid tail groups[354] so determining the absolute configuration of its headgroup cannot be done via chiral boronic ester formation.[256] To determine the absolute configuration of BLS-PG, we isolated the PG from BLS and hydrolyzed it using KOH in MeOH (Scheme 10.2). This yielded phosphatidylglycerol **10.8** which was converted to bis-ketal **10.9** using D-camphor dimethylketal/p-toluene sulfonic acid (p-TsOH) in acetonitrile.[355] Analyzing the crude material by ^{1}H NMR yielded a spectrum that closely resembled the spectrum reported by Tan et al for the sn-3,1' isomer indicating that the starting material is 2R,2'S-PG (Figure H.16).[355]
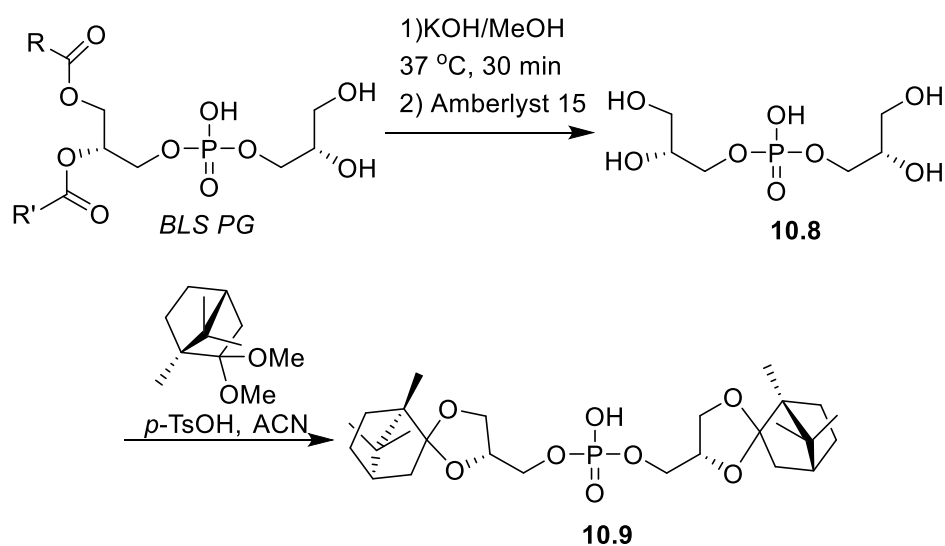
Scheme 10.2 Synthesis of compound **10.9** from BLS PG.

To support the conclusion that BLS-PG has the 2R,2'S configuration, we synthesized an enantiomerically pure sample of **10.9** (Scheme 10.3). Alcohol **S-10.11** was converted to phosphotriester **10.14** via phosphoramidites **10.12** and **10.13** using standard

phosphoramidite chemistry. Phosphotriester **10.14** was deprotected with H_2/Pd(OH)$_2$

yielding **10.8** which was converted to its sodium salt and fully characterized (see appendix).

10.8 was converted back to the acid form with amberlyst 15/MeOH and reacted with

camphor dimethylketal/p-toluene sulfonic acid yielding an enantiomerically pure sample

of **10.9**. The ^{1}H NMR spectrum of compound **10.9** prepared by this route matched

compound **10.9** derived from lung surfactant indicating that the majority of BLS-PG

possess the 2R,2'S absolute configuration (Figure H.16). However, due to the complexity

of the spectra for **10.9**, it was difficult to determine the relative amounts of 2R,2'S-PG and

2R,2'R-PG from these spectra.
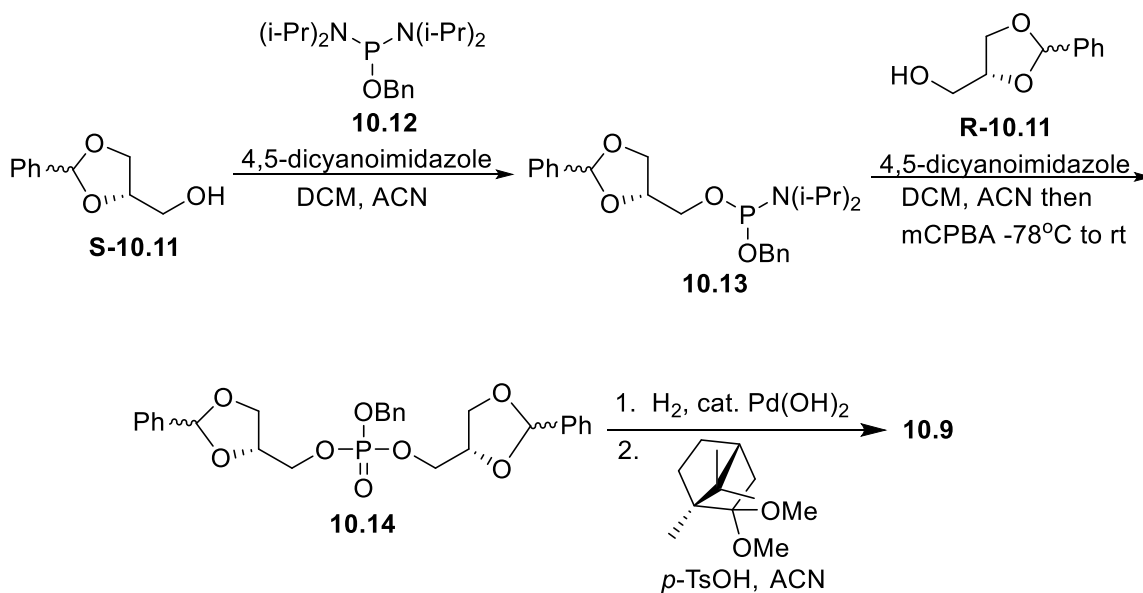
Scheme 10.3 Synthesis of compound **10.9** from **S-10.11**

Since the chiral boronic acid assay is insensitive to the absolute configuration at the

lipid group (Chapter 5, Figure C.3), we reasoned that the relative amounts of 2R,2'S-PG

and 2R,2'R-PG could be determined using this method. BLS-PG was converted to boronic

ester **10.16** using racemic or optically pure boronic acid **10.15** (Scheme 10.4). When BLS-

PG was reacted with racemic **10.15**, the two key peaks at 7.71 and 7.61 ppm in the ^{1}H NMR

spectrum of the resulting boronic esters **10.16** were well-resolved (Figure H.17). Ester

formation with samples of optically pure **10.15** each yielded individual peaks in the same region, indicating that BLS-PG is composed of exclusively 2R,2'S-PG.
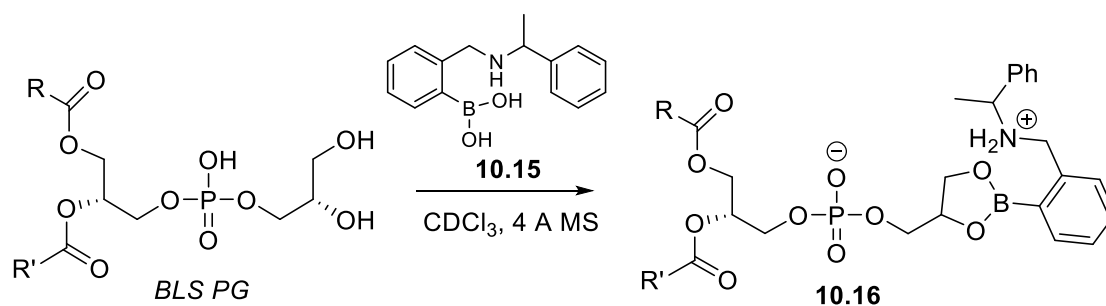
Scheme 10.4 Synthesis of compound **10.16** from BLS-PG.

Since 1-2 equivalents of 2R,2'S-DMPG can completely inhibit the activity of daptomycin and A5D, and lung surfactant PG is composed of exclusively 2R,2'S-PG, then it would be expected that the complete inhibition of these peptides by lung surfactant should occur when enough BLS is present such that the molar quantity of PG in the BLS is 1-2 times the molar quantity of peptide. To determine if this is indeed the case, we evaluated the effect of varying amounts of BLS on the activity of daptomycin and A5D at fixed concentrations of peptide. The results are given in Table 10.2 in terms of the equivalents of PG in BLS to peptide (the concentration of PG in the BLS used in our studies is approximately 4.9 ± 0.6 mM based on a PG content of 3.5 mg/mL (13% of total phospholipids present by mass[356] and an average molecular weight of 719 g/mol[354]). As expected, complete inhibition occurred when enough BLS was added such that the molar quantity of PG in the BLS was approximately 1-2 times the molar quantity of peptide.

Table 10.2 Antagonism of Daptomycin and A5D by PG in BLS against *B. subtilis* 1046.[a]

Equiv	Dap (μg/mL)			A5D (μg/mL)
PG[b]	8	16	32	32
1/8	nd	nd	NG	nd
1/4	nd	NG	NG	NG
1/2	NG	NG	NG	NG
1	NG	NG	NG	NG
2	G	G	G	G

[a]NG = no growth. G = growth. G/NG were determined visually after incubating for 18-20 hours at 37 °C. Assignments were confirmed by plating each well onto agar made from the growth medium and incubating 18-20 hours at 37 °C. nd = not determined. [b]Molar equivalents of PG in BLS compared to peptide.

We also determined the MIC values of daptomycin, A5D, A5DKyn, as well as two other A5D analogs, A5DCyh and A5DCyp, (Figure 6), against *B. subtilis* and two strains of *S. aureus* (one MSSA and one MRSA) in the presence and absence of 0.185 % BLS (v/v) at 1.25 mM CaCl$_2$ (Table 3). A5DCyh and A5DCyp, which were prepared using the route outlined in Scheme 10.1, contain L-cyclohexylglycine or L-cyclopentylglycine in place of Ile13. In the absence of BLS, A5DCyh and A5DCyp are two-fold more potent than A5D against *B. subtilis* while A5DKyn, A5DCyh and A5DCyp are 4-fold more potent than A5D against both strains of *S. aureus*.

In the presence of BLS, the MIC values were 8-16 μg/mL for all of the peptides and bacteria. Under the conditions that were used to obtain the data in Table 10.3 (0.185% BLS in the assay), it can be calculated that the MIC of daptomycin in the presence of BLS should be approximately 10-11 μg/mL against both *B. subtilis* and *S. aureus* assuming 1.5 equivalents of PG is needed to inhibit the peptide. For A5D and A5DKyn, it can be calculated that the MIC in the presence of BLS should be approximately 13 μg/mL against *B. subtilis* and 16 μg/mL (for A5D) and 12 μg/mL (for A5DKyn) against *S. aureus*. For A5DCyh and A5DCyp the calculated MIC values should be 12 μg/mL against *B. subtilis* and both strains of *S. aureus*. All calculated MIC values are within the experimental MIC range of 8-16 μg/mL. These results, along with those

presented in Table 2, suggest that the antagonism of daptomycin and A5D by BLS is mainly due to their interaction with PG and that A5D is not less susceptible to inhibition by lung surfactant than daptomycin.

Table 10.3 The MICs of daptomycin, A5D and A5D analogs in the presence and absence of 0.185 % BLS at 1.25 mM CaCl$_2$ against *B. subtilis* and *S. aureus*

	MIC (µg/mL)					
	B. subtilis[b]	*B. subtilis*[b]	MSSA[c]	MSSA[c]	MRSA[d]	MRSA[d]
Peptide[a]	- BLS	+ BLS	- BLS	+ BLS	- BLS	+ BLS
Daptomycin	0.5-1	8-16	<0.25	8-16	<0.25	8-16
A5D	2-4	8-16	4-8	8-16	4-8	8-16
A5DKyn	2-4	8-16	1-2	8-16	1-2	8-16
A5DCyh	1-2	8-16	1-2	8-16	1-2	8-16
A5DCyp	1-2	8-16	1-2	8-16	1-2	8-16

[a]Peptide concentrations of 0.5, 1, 2, 4, 8, 16 and 32 µg/mL were used to determine MIC values. Therefore, MIC values are reported as a range. [b]*B. subtilis* 1046. [c]MSSA 25923. [d]MRSA 113.

A5DCyh
MIC = 1-2 µg/mL (*B. subtilis* 1046)

A5DCyp
MIC = 1-2 µg/mL (*B. subtilis* 1046)
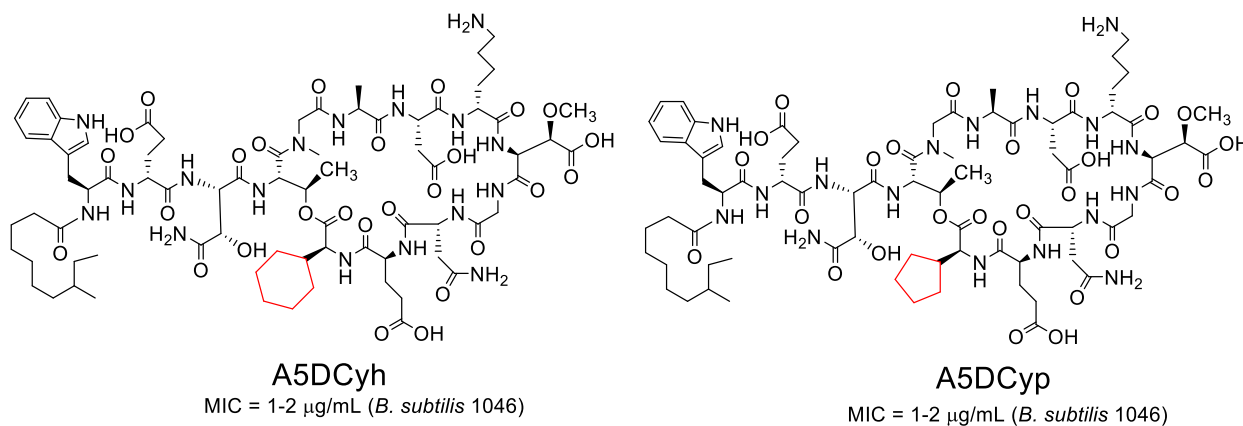
Figure 10.5 The structures of A5DCyh and A5DCyp.

Finally, we determined the fraction of daptomycin and A5DKyn bound to PG in BLS by monitoring the change in Kyn fluorescence as BLS was titrated into a solution of daptomycin or A5DKyn at 1.25 mM Ca^{2+} (Figure 10.6). This study indicates that peptide saturation occurs at approximately 1-2 equivalents of PG in the BLS which further supports our conclusion that the antagonism of daptomycin and A5D by BLS is mainly due to their interaction with PG.
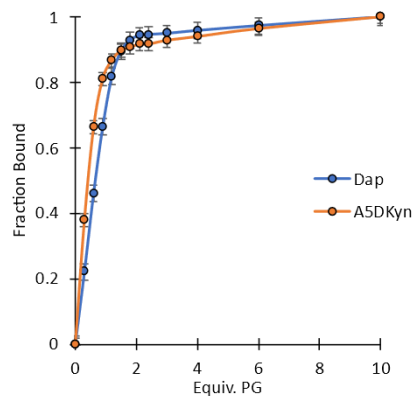
Figure 10.6 The titration of daptomycin (15 uM) or A5D (15 uM) with BLS at 1.25 mM CaCl$_2$.

10.3 Conclusions

In summary, through the synthesis and study of A5D and ent-A5D, we demonstrated that A5D interacts with a chiral target. To determine if the chiral target is PG, the interaction of A5DKyn, an environmentally sensitive fluorescent analog of A5D, with liposomes containing enantiopure PG was studied. Membrane binding studies with A5DKyn demonstrated that membrane affinity is affected by the absolute configuration at both stereocenters of DMPG though the S-configuration at the head group was found to be of particular importance. A5DKyn and DMPG bind stoichiometrically regardless of the absolute configuration at the headgroup of DMPG. CD studies show that the backbone conformation of A5DKyn is impacted by the absolute configuration of DMPG while studies using pyrene-A5D demonstrated that the oligomerization event is contingent on S-absolute configuration at the headgroup of DMPG at physiological calcium concentrations. Based on these findings, we conclude that the chiral target of A5D is 2R,2'S-PG and ent-A5D is not as active as A5D primarily because it cannot oligomerize on bacterial membranes at physiological calcium concentrations. These results are remarkably similar to those reported on daptomycin (chapter 6), suggesting that both of these natural products are accessing a similar structural motif when binding to PG-containing membranes.

287

Although we found that A5D has a lower affinity for 2R,2'S-PG than daptomycin when determined in the context of DMPG:DOPC liposomes, both peptides were completely antagonized by only 1-2 equivalents of 'free' 2R,2'S-PG. This PG stereoisomer was determined to be the only stereoisomer of PG in lung surfactant. These results suggest that complete inhibition of both daptomycin and A5D by BLS should always occur when a quantity of BLS is present such that the molar equivalents of PG in the BLS is approximately 1-2 the molar equivalents of peptide. Indeed, this is what we have found. These results indicate that the antagonism of daptomycin and A5D by BLS is mainly due to their interaction with PG.

Our results on the effect of lung surfactant on the activity of A5D and daptomycin differ in some respects from those reported in the literature by Cubist Pharmaceuticals. In a 2010 paper, researchers at Cubist Pharmaceuticals reported that the presence of 1% surfactant resulted in a 128-fold increase in daptomycin's MIC against *S. aureus* (0.5 µg/mL to 64 µg/mL), while the MIC of A5D increased only 2-fold (2 µg/mL to 4 µg/mL).[16,145] However, in a 2012 publication, they reported that daptomycin's MIC against the same strain of *S. aureus* increased only 8 to 16-fold in the presence of 1% surfactant (1 µg/mL to 16 µg/mL)[357] which is the same difference in MICs that we have found with daptomycin and *B. subtilis* in the absence and presence of surfactant. Nevertheless, even if daptomycin's MIC is increased only 16-fold by surfactant, Cubists report that A5D's MIC is increased only 2-fold by surfactant suggests that A5D is still significantly less effected by lung surfactant than daptomycin. In contrast, our results suggest that A5D is not significantly less susceptible to inhibition by lung surfactant than daptomycin.

One difference between our studies and Cubists' is the surfactant. For our studies, we used a commercial bovine lung surfactant (BLES®) which is obtained by lavaging the bovine lung with a salt solution followed by a series of solvent extractions, centrifugations, and precipitations. For

their studies, Cubist used a commercial semi-synthetic lung surfactant called Survanta® which is obtained by solvent extraction from bovine lung mince supplemented with dipalmitoyl phosphatidylcholine, palmitic acid, and tripalmitoylglycerol. Phosphatidylcholine (PC) makes up the majority of phospholipids in both Survanta® and BLES® and the amounts of PC in these surfactants is very similar.[356] Neither surfactant contains the hydrophilic surfactant protein SP-A, but both contain the hydrophobic surfactant proteins SP-B and SP-C with BLES® containing 12 times more SP-B and 1.6 times more SP-C than Survanta®.[356] Neither surfactant contains quantities of these proteins approaching stoichiometric values at the concentrations used in our investigations. Both surfactants contain PG, though the concentration of PG in BLES® is approximately 5-6 fold greater than in Survanta®.[356] However, by conducting our studies using 5 to 6-fold less surfactant (0.185 % v/v) than that used by Cubist (1% v/v), the amount of PG present in our studies and those conducted by Cubist was essentially the same.

Overall, our results suggest that A5D is not less susceptible to inhibition by lung surfactant than daptomycin. Moreover, our findings suggest that it will be very challenging to develop a safe A5D or daptomycin analog that is highly active in the presence of lung surfactant as such an analog would have to function via a mechanism that is not dependent upon its interaction with PG.

10.4 Experimental
General Methods.

All reagents and solvents were purchased from commercial suppliers. Methylene chloride (DCM) and acetonitrile (MeCN) were dried by distillation over calcium hydride under nitrogen. Tetrahydrofuran (THF) was distilled from sodium metal in the presence of benzophenone under N_2. 2-methylpiperidine was dried over calcium hydride then distilled to give a colorless liquid. Dimethylformamide was dried over barium oxide and distilled under vacuum such that the

temperature of the solution remained below 60 °C throughout the course of the distillation. Chromatography was preformed using 60 Å silica gel.

High resolution positive electrospray (ESI) mass spectra were obtained using an orbitrap mass spectrometer. Samples were sprayed from MeOH: 1% formic acid in H_2O. All spectra were collected in the positive mode. ^{1}H- and ^{13}C-NMR were collected using either a Bruker Avance-300 or a Bruker Avance-500 spectrophotometer. NMR spectra of A5DKyn were collected on a Bruker 600 NMR. Proton Chemical shifts (δ) for samples run in $CDCl_3$ are reported in ppm relative to an internal standard (trimethylsilane, 0 ppm). For samples run in CD_3OD, δ was relative to the solvent peak (3.31 ppm). For ^{13}C-NMR samples run in $CDCl_3$ chemical shifts are reported relative to the solvent peak (77.0 ppm). For samples run in CD_3OD, δ was relative to the solvent peak (49.2 ppm).

Fmoc-D-*threo*-hAsn(TBS)-OH was prepared using our procedure.[352] A5D was prepared according to our procedure.[181] ent-A5D was prepared according to the same procedure but with the absolute configuration at each stereocenter inverted (Figure H.4 for HRMS). Fmoc-L-cyclohexylglycine-OH was purchased from a commercial supplier. Fmoc-L-cyclopentylglycine-OH was prepared from H-L-cyclopentylglycine-OH according to the procedure of Singh et al.[358] Fmoc-L-Kyn(Boc)-OH was prepared using our procedure.[238] Fmoc,DMB-Gly-OH was prepared using the procedure reported by Hart et al.[167] 2R,2'S-, 2R,2'R-, 2S,2'R- and 2S,2'S-DMPG were prepared according to our procedure.[278] (±)-8-methyl decanoic acid was prepared as previously described by Kralt et al.[181] Ligand **10.15** was prepared according to the procedure by Anslyn and coworkers.[267] **R-10.15**, **S-10.15** and **10.15** were prepared from (R)-phenylethylamine, (S)-phenylethylamine and racemic phenylethylamine, respectively. **S-10.11**, **R-10.11**, and **10.12** were

prepared as previously described.[278] $C_{55}P$ was prepared semi-synthetically as described by Cochrane and coworkers.[359]

MIC determinations were performed as previously described.[223]

Liposome preparation.

Large unilamellar vesicles were prepared as previously described.[86,278] DMPC and DMPG were combined in a 1:1 molar ratio in chloroform. The chloroform was removed under an N_2 stream leaving a thin film of lipid coating the interior of a round-bottom flask. Trace chloroform was removed under high vacuum then the lipids were hydrated with a pH 7.4 buffer (20 mM HEPES, 150 mM NaCl). Extrusion through a 100 nm polycarbonate filter yielded a solution of LUVs with a total lipid concentration of 5 mM.

For membrane binding studies involving $C_{55}P$, LUVs consisting of $C_{55}P$/DMPG/DOPC were used.[278] To prepare the LUVs containing $C_{55}P$, commercial DOPC (1,2-di[(8Z)octadecenoyl]-sn-glycero-3-phosphocholine), $C_{55}P$ and DMPG, were dissolved separately in chloroform, then added to a flask and concentrated under an N_2 stream. The lipid film was hydrated and extruded as before which gave a solution of LUVs with a total lipid concentration of 5 mM.

Liposome preparation for Isothermal Titration Calorimetry.

2R,2'S-DMPG and DOPC were combined in chloroform in a 25:75 (DMPG:DOPC) molar ratio and concentrated to a thin film with a stream of nitrogen. The lipid film was hydrated with pH 7.4 buffer (20 mM HEPES, 150 mM NaCl) containing 1.25 mM $CaCl_2$ and then freeze-thawed 5 times before extrusion. This gave a solution of LUVs with a total lipid concentration of 4 mM which were used within three days after extrusion.

291

Titrating a solution of A5DKyn and LUV with CaCl$_2$.

The same procedure reported previously was applied in this study.[278] Briefly, fluorescence was measured in Corning Costar half-area flat bottom black polystyrene 96-well plates using a Tecan Infinite M1000 instrument. 100 µM peptide stocks were diluted with pH 7.4 buffer (20 mM HEPES, 150 mM NaCl) and preheated to 37°C before adding LUVs (see 'Liposome preparation' section) and immediately dispensing 90 µL aliquots into wells pre-loaded with 10µL of buffer containing CaCl$_2$ at 10x the desired calcium concentration (plate had also been preheated to 37°C) giving a final volume of 100 µL in each well. The final concentrations in each well were 3 µM of A5DKyn, and 250 µM of lipid. Fluorescence measurements were timed to allow for a 3-4 minute incubation period at 37°C. Emission spectra were acquired for kynurenine (Excitation: 365 nm, 5 nm bandwidth) intrinsic fluorescence using 100 flashes at 400 Hz and a step size of 3 nm. Emission spectra for blanks containing 250 µM lipid in buffer and 3 µM A5DKyn were also collected.

Circular dichroism studies.

The same procedure reported previously was applied to study A5DKyn in the presence and absence of LUVs.[278] Briefly, circular dichroism (CD) traces were collected using a Jasco J-815 CD spectrometer. The peptide concentration of each solution was 15 µM in 20 mM HEPES buffer (pH 7.4). Samples were measured at room temperature from 210-250 nm at a scan rate of 10 nm min^{-1} with a digital integration time of 2 seconds and a bandwidth 1 nm. A 1 mm quartz cuvette was used. The outputted data was converted to molar ellipticity in units of deg cm^2 dmol^{-1}. For CD traces collected on peptides in the presence of large unilamellar vesicles (LUVs) a LUV concentration of 180 µM and a CaCl$_2$ concentration of 5 mM was used. For these studies, samples were measured once 3 min after mixing and then again after 20 min of mixing to ensure equilibrium was reached. Good agreement with each mixing time was observed in all cases.

Oligomerization studies.

Pyrene-A5D was prepared according to a previously described procedure.[360] Emission spectra were collected using a QuantMaster 4 spectrophotometer (Photon Technology International, London, ON). Samples were excited at 344 nm and the emission between 350 nm and 600 nm was recorded. Bandpasses for emission and excitation were set to 3 nm. Emission spectra were corrected for wavelength-dependent instrument response using a quinine sulfate standard.

Pyrene-A5D (2.5 µM) was incubated in pH 7.4 buffer (20 mM HEPES, 150 mM NaCl) at 37 °C. To this was added $CaCl_2$ in the same buffer until the calcium concentration was 1.25 mM $CaCl_2$. Once the sample had achieved thermal equilibrium, LUVs were added such that a 250 µM total lipid concentration was achieved. This sample was mixed for 3 min then the emission spectra was recorded. This experiment was repeated 3 times, the data presented in Figure 10.3 is a representative spectrum.

Titrating A5DKyn with LUVs or BLS

A5DKyn (15 µM) was incubated in pH 7.4 buffer (20 mM HEPES, 150 mM NaCl) at 37 °C. To this was added $CaCl_2$ in the same buffer until the desired calcium concentration was achieved (0.1, 5 and 10 mM $CaCl_2$ were used). Once the sample had achieved thermal equilibrium, an aliquot of LUV (or BLS) was added, and the sample was mixed for 3 min then the emission spectra was recorded. Samples were excited at 365 nm and the emission between 400 nm and 600 nm was recorded. Bandpasses for emission and excitation were set to 2.5 nm. Emission spectra were corrected for wavelength-dependent instrument response using a quinine sulfate standard. This process was repeated until 10 equivalents of PG were added.

Isothermal Titration Calorimetry

ITC studies were conducted using a MicroCal ITC200 microcalorimeter (Malvern Panalytical Ltd., Malvern, UK). All solutions were degassed for at least 30 minutes prior to loading into the calorimeter. LUVs prepared as described in the *Liposome Preparation for Isothermal Titration Calorimetry* section were loaded into the ITC syringe. The cell was then filled with a solution of lipopeptide (20 µM) in the same buffer that was used to prepare the LUVs (20 mM HEPES, 150 mM NaCl, 1.25 mM CaCl$_2$, pH = 7.4). Titrations were conducted at 25 °C with constant stirring (1000 rpm). The reference power was set to 5 µcal s^{-1} and the feedback was set to 'high'. The volume of the first injection was 0.3 µL, all subsequent injections were 1.5 µL with a 180 s delay between each injection.

The ITC data was post-processed by the proprietary Origin software provided by Microcal. Binding constants were determined from a least-squares analysis of the integrated heat signals using Origin's one-site binding model. Data was collected in triplicate. Heats of dilution were small and constant. These were compared to but not subtracted from the collected data.[72]

In-vitro antagonist studies.

Antagonist studies were done according to the procedure reported by Martin and coworkers with some modifications.[52] In our experiments, the final peptide concentration of each well was 8 µg/mL for daptomycin and 32 µg/mL for A5D. *B. subtilis* 1046 grown in lysogeny broth containing 1.25 mM CaCl$_2$ and diluted to 5 x 10^5 CFU/mL was added to wells containing a solution of peptide and lipid diluted in the same broth. The plates were incubated for 18 hours at 37 °C before growth/no growth was determined visually. A sample (10 µL) from each well was plated onto agar prepared from the same broth and incubated at 37 °C for 18 hours to ensure that the assignment of growth/no growth was correct.

In experiments where the concentration of BLS was varied at a fixed peptide concentration, the PG concentration in BLS was estimated to be 4.9 mM (BLS contains 13% PG (w/w) according to Zhang et al[356] and the average molecular weight of the PG present can be estimated from the composition of fatty acids measured by Possmayer and coworkers[354] which came out to be 719 g/mol) and stocks were diluted in lysogeny broth containing 1.25 mM $CaCl_2$. 50 µL of these lipid stocks were plated and to these wells was added antibiotic (50 µL) diluted in the same broth. 100 µL of bacterial stocks grown in the same broth and diluted to 5 x 10^5 CFU/mL, were added to the wells containing lipid and peptide. The same incubation and analysis procedures were followed as outlined above.

In experiments where the concentration of BLS was fixed and antibiotic concentration was varied, the antibiotic was serially diluted with lysogeny broth containing 1.25 mM $CaCl_2$ and plated (100 µL per well). A solution of bacteria was diluted with the same broth to 5 x 10^5 CFU/mL and BLS (37 µL per 10 mL of diluted bacterial stock) was added immediately before plating this solution with antibiotic (100 µL per well). Since each well contained 100 µL of antibiotic stock and 100 µL of bacterial stock the final concentration of BLS in each well was 0.185% v/v. The same incubation and analysis procedures were followed as outlined above.

Isolating phosphatidylglycerol from BLS and NMR analysis with Ligand 10.15

BLS (3 mL) was lyophilized and resulting solid was dissolved in $CHCl_3$:MeOH:H_2O:NH_4OH (77.5:17.5:2.5:0.1) and this mixture was purified by silica gel column chromatography (90:10:0.1 $CHCl_3$:MeOH:NH_4OH to 77.5:17.5:2.5:0.1 $CHCl_3$:MeOH:H_2O:NH_4OH). This yielded BLS PG as a colorless solid (7 mg). The isolated BLS PG was combined with ligand **10.15** using the procedure previously reported.[278] ^{1}H NMR data of the formed boronic ester **10.16** is presented in Figure H.17.

Hydrolysis of BLS PG and Conversion to the D-camphor ketal (10.9)

BLS PG (5 mg) isolated as described above was hydrolyzed by incubating with 1M KOH/MeOH (930 µL) at room temperature for 30 min. The reaction mixture was worked-up and the resulting phosphatidylglycerol was convert to the D-camphor ketal (**10.9**) using the procedure reported by Tan et al.[355]

Syntheses

Benzyl (((R)-2-phenyl-1,3-dioxolan-4-yl)methyl) diisopropylphosphoramidite (**10.13**)

Oven dried 4 Å powdered molecular sieves (ca. 500 mg), a stir bar and an oven dried flask were placed under high vacuum and further dried heating with a flame for a few minutes. The hot flask was then allowed to cool to room temperature under vacuum and then it was back filled with dry N_2 and charged with **S-10.11** (250 mg, 1.39 mmol, 1.00 equiv) and **10.12** (939 mg, 2.78 mmol, 2.00 equiv.) as a solution in dry, freshly distilled dichloromethane (13.9 mL). In a separate dried flask under N_2, a solution of 4,5-dicyanoimidazole (328 mg, 2.78 mmol, 2.00 equiv.) in freshly distilled, dry acetonitrile (6.2 mL) was prepared. This was transferred by cannula to the flask containing the sieves using a flow of dry N_2. The suspension was allowed to stir over the sieves for 4 hours at room temperature. At this point, the solution was diluted with dry dichloromethane (20 mL) and filtered via cannula. The filtrate was washed with saturate aqueous $NaHCO_3$ (30 mL). The aqueous layer extracted with dichloromethane three times. The combined organic layer was washed with brine, dried over $MgSO_4$, filtered and the concentrated. The crude residue was purified via silica gel column (3% triethylamine/20% ethylacetate /67% hexanes) chromatography giving **10.13** as a colorless oil (287 mg, 50% yield). ^{1}H NMR (300 MHz, CDCl$_3$): δ 7.57-7.29 (10H, m) 6.00-5.86 (1H, m) 4.87-4.70 and 4.31-4.25 (3H, m) 4.52-4.41 (1H, m) 4.15-4.13 (1H, m)

4.05-3.65 (4H, m) 1.29-1.24 (12H, m). ^{31}P NMR (122 MHz, CDCl$_3$) 148.5, 148.5, 148.2, 148.2. ^{13}C NMR (75 MHz, CDCl$_3$): δ 139.4, 139.4, 138.1, 138.0, 137.4, 129.4, 129.2, 128.4, 128.3, 127.3, 127.3, 127.0, 126.7, 126.5, 104.4, 104.0, 103.9, 75.9, 75.8, 75.7, 75.5, 75.4, 68.3, 68.1, 67.9, 65.6, 65.6, 65.4, 65.3, 64.1, 63.9, 63.9, 63.6, 43.2, 43.0, 24.7. HRMS-ESI+ (m/z): [M + H+H$_2$O]$^+$ calculated for C$_{23}$H$_{35}$O$_5$NP,436.22474; found, 436.22365.

Benzyl (((R)-2-phenyl-1,3-dioxolan-4-yl)methyl) (((S)-2-phenyl-1,3-dioxolan-4-yl)methyl) phosphate (**10.14**)

Oven dried 4 Å powdered molecular sieves (ca. 500 mg), a stir bar and an oven dried flask were placed under high vacuum and further dried heating with a flame for a few minutes. The hot flask was then allowed to cool to room temperature under vacuum and then it was back filled with N$_2$ and charged with **R-10.11** (58 mg, 0.322 mmol, 1.00 equiv) and **10.13** (149 mg, 0.357 mmol, 1.10 equiv.) as a solution in dry, freshly distilled dichloromethane (7.2 mL). In a separate dried flask under N$_2$, a solution of 4,5-dicyanoimidazole (56 mg, 0.476 mmol, 1.48 equiv.) in freshly distilled, dry acetonitrile (1.1 mL) was prepared. This was transferred by cannula to the flask containing the sieves using a flow of dry N$_2$. The suspension was allowed to stir over the sieves for 4 hours at room temperature. After cooling the flask (dry ice-acetone bath), a solution of meta-chloroperoxybenzoic acid (62 mg, 0.353 mmol, 1.50 equiv.) dissolved in dichloromethane (1.0 mL) was added dropwise. Cooling was removed and the solution was stirred for 90 min. At this point, the solution was diluted with dry dichloromethane (20 mL) and filtered over a pad of celite which was extracted several times with dichloromethane. The filtrate was washed with saturated aqueous NaHCO$_3$ (50 mL). The aqueous layer extracted with dichloromethane three times. The combined organic layer was washed with brine, dried over MgSO$_4$, filtered and then concentrated. The crude residue was purified via silica gel column chromatography (50% ethylacetate/50 % hexanes then 70% ethylacetate/30% hexanes) giving **10.14** as a colorless oil (80 mg, 48% yield).

^{1}H NMR (300 MHz, CDCl$_3$): δ 7.48-7.39 (15H, m) 5.94-5.80 (1H, m) 5.13 (2H, d, J_{AB} = 11.4 Hz) 4.52-4.34 (1H, m) 4.21-4.02 (7H, m) 3.87-3.76 (1H, m). ^{31}P NMR (122 MHz, CDCl$_3$) -0.81, -0.96. ^{13}C NMR (75 MHz, CDCl$_3$): δ 137.4, 136.8, 135.6, 135.6, 129.6, 129.4, 128.7, 128.4, 128.1, 126.7, 126.4, 104.7, 104.0, 104.0, 74.5, 74.3, 74.2, 69.8, 69.7, 67.6, 67.3, 66.8. HRMS-ESI+ (m/z): [M + H]$^+$ calculated for C$_{27}$H$_{30}$O$_8$P, 513.16728; found, 513.16646.

Sodium (R)-2,3-dihydroxypropyl ((S)-2,3-dihydroxypropyl) phosphate (sodium salt of **10.8**) A suspension of **10.14** (80 mg, 0.156 mmol, 1.00 equiv.) and Pd(OH)$_2$/C (20% w/w; 40 mg, 0.078 mmol, 0.5 equiv.) in tert-butanol (3.1 mL) was stirred under an atmosphere of hydrogen gas for 5 hours at room temperature. The reaction mixture was filtered through a pad of celite which was rinsed several times with chloroform. The resulting solution was concentrated under high vacuum and the residue was concentrate from chloroform three times to remove residual tert-butanol. Once free from organic solvent, the residue was suspended in aqueous sodium acetate (0.030 M; 5.20 mL, 0.156 mmol, 1.00 equiv.), stirred for 30 min at room temperature then frozen and lyophilized. This yielded the sodium salt of **10.8** as a colorless oil. ^{1}H NMR (500 MHz, CDCl$_3$): δ 3.97-3.87 (4H, m) 3.79 (2H, app quintet, J = 5.3, 11.3 Hz) 3.65 (2H, dd, J=11.4, 5.1 Hz) ^{31}P NMR (203 MHz, CDCl$_3$) 2.8. ^{13}C NMR (125 MHz, CDCl$_3$): δ 71.2, 71.1, 66.2, 66.1, 62.4. HRMS-ESI+ (m/z): [M + Na]$^+$ calculated for C$_6$H$_{15}$O$_6$PNa, 269.03968; found, 269.04028.

Scheme 10.5. Synthesis of Fmoc-D-erythro-MeOAsp(t-Bu)-OH
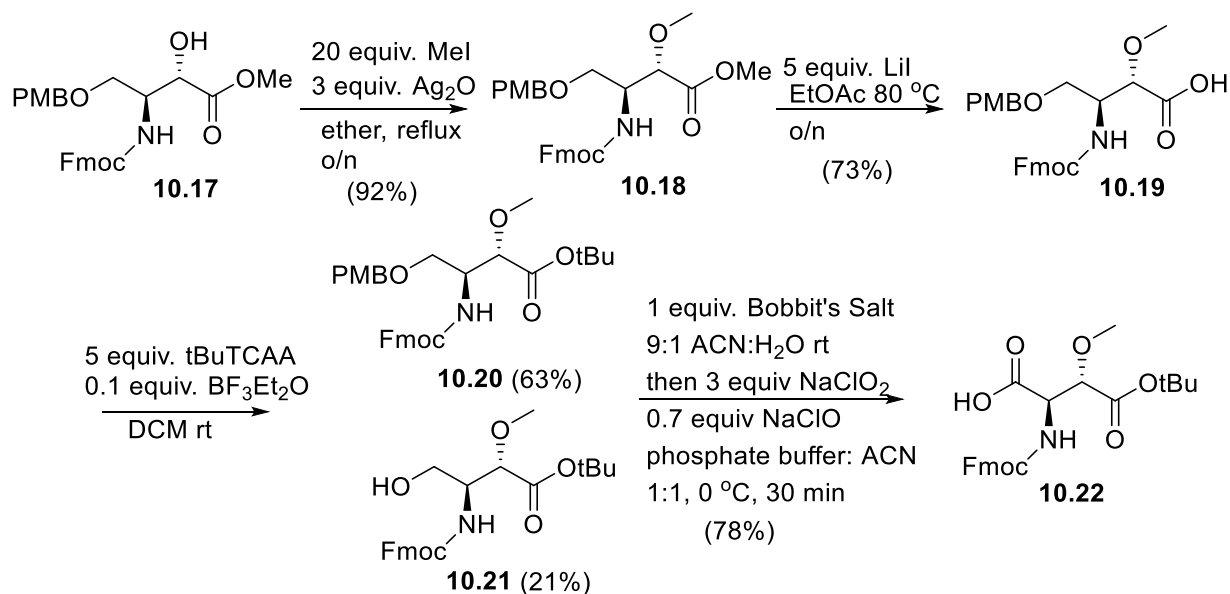
Methyl (2S,3S)-3-(((((9H-fluoren-9-yl)methoxy)carbonyl)amino)-2-methoxy-4-((4-methoxybenzyl)oxy)butanoate (**10.18**)

10.18 was prepared according to our procedure for the methylation of the D-*threo* isomer of **10.17** as outlined in chapter 8 (1.52g, 92% yield).[352] ^{1}H NMR (300 MHz, CDCl₃): (2H, d, *J* = 7.3 Hz) 7.60 (2H, d, *J* = 7.0 Hz) 7.39 (2H, dd, *J* = 7.2, 7.3 Hz) 7.31 (2H, app t, *J* = 7.3 Hz) 7.23 (2H, d, *J* = 7.8 Hz) 6.86 (2H, d, *J* = 8.0 Hz) 5.36 (1H, d, *J* = 9.0 Hz) 4.41-4.22 (6H, m) 3.93 (1H, d, *J* = 4.3 Hz) 3.77 (3H, s) 3.62 (3H, s) 3.62-3.46 (2H, m) 3.42 (3H, s). ^{13}C NMR (75 MHz, CDCl₃): δ 173.7, 162.2, 158.7, 146.8, 146.8, 144.2, 132.8, 132.4, 130.6, 130.0, 128.0, 122.9, 116.6, 82.7, 75.8, 70.8, 70.5, 69.8, 61.9, 58.1, 54.9, 50.1. HRMS-ESI+ (*m/z*): [M + H]⁺ calculated for $C_{29}H_{32}O_7N$, 506.21733; found, 506.21633.

(2S,3S)-3-(((((9H-Fluoren-9-yl)methoxy)carbonyl)amino)-2-methoxy-4-((4-methoxybenzyl)oxy) butanoic acid (**10.19**)

10.19 was prepared according to our demethylation procedure described previously for the D-*threo* isomer of **10.18** as outlined in chapter 3 (1.41 g, 73% yield).[352] ^{1}H NMR (300 MHz, CDCl₃): δ

299

10.51 (1H, br. s) 7.74 (2H, d, J = 7.4 Hz) 7.59 (2H, m) 7.39 (2H, app t, J = 7.3 Hz) 7.30 (2H, app t, J = 7.2 Hz) 7.21 (2H, d, J = 7.7 Hz) 6.84 (2H, d, J = 8.0 Hz) 5.99 and 5.37 (1H, d, J = 8.9 Hz) 4.48-4.36 (5H, m) 4.20 (1H, dd, J = 6.6, 6.7 Hz) 3.95 (1H, d, J = 4.0 Hz) 3.75 (3H, s) 3,61-3.53 (2H, m) 3.41 (3H, s). ^{13}C NMR (75 MHz, CDCl$_3$): δ 177.3, 162.1, 159.0, 146.8, 146.7, 144.2, 132.7, 132.2, 130.6, 130.0, 128.1, 128.0, 122.0, 116.7, 82.6, 75.6, 70.4, 69.9, 62.0, 58.1, 55.0, 50.0. HRMS-ESI+ (m/z): [M + H]$^+$ calculated for C$_{28}$H$_{30}$O$_7$N, 492.20168; found, 492.19980.

*tert-Butyl   (2S,3S)-3-((((9H-fluoren-9-yl)methoxy)carbonyl)amino)-2-methoxy-4-((4-methoxybenzyl)oxy)butanoate (**10.20**)*

10.20 was prepared according to our procedure for the *tert*-butyl esterification of the D-*threo* isomer of **10.19** as outlined in chapter 3 (858 mg of **10.20**, 63% yield and 226 mg of **10.21**, 21% yield).[352] Only **10.20** was fully characterized. ^{1}H NMR (300 MHz, CDCl$_3$): δ 7.75 (2H, d, J = 7.5) 7.61 (2H, d, J = 7.4 Hz) 7.40 (2H, dd, J = 7.3, 7.4) 7.31 (2H, dd, J = 7.3, 7.4 Hz) 7.24 (2H, d, J = 8.4 Hz) 6.86 (2H, d, J = 8.6 Hz) 5.34 (1H, d, J = 9.2 Hz) 4.50-4.39 (4H, m) 4.25-4.20 (2H, m) 3.85-3.74 (4H, m) 3.60 (1H, dd, J = 5.4, 9.6 Hz) 3.50-3.39 (4H, m) 1.45 (9H, s). ^{13}C NMR (75 MHz, CDCl$_3$): δ 172.3, 162.2, 158.7, 146.8, 144.2, 132.9, 132.3, 130.6, 130.0, 128.0, 122.9, 116.7, 85.0, 83.4, 75.6, 70.6, 69.7, 61.6, 58.1, 55.2, 50.1, 30.9. HRMS-ESI+ (m/z): [M + H]$^+$ calculated for C$_{32}$H$_{38}$O$_7$N, 548.26428; found, 548.26271.

*(2R,3S)-2-((((9H-Fluoren-9-yl)methoxy)carbonyl)amino)-4-(tert-butoxy)-3-methoxy-4-oxobutanoic acid (**10.22**)*

10.22 was prepared according to our procedure for the one-pot oxidative cleavage/oxidation of the D-*threo* isomers of **10.20** and **10.21** as outlined in chapter 3 (726 mg, 78% yield).[352] ^{1}H NMR (300 MHz, CDCl$_3$): δ 10.86 (1H, br. s) 7.76 (2H, d, J = 7.4 Hz) 7.60 (2H, d, J = 7.1 Hz) 7.39 (2H,

dd, $J = 7.3$, 7.4 Hz) 7.31 (2H, dd, $J = 7.3$, 7.4 Hz) 5.73 (1H, d, $J = 8.4$ Hz) 4.92 (1H, d, $J = 8.3$ Hz) 4.48-4.40 (2H, m) 4.24 (1H, dd, $J = 6.8$, 6.9 Hz) 3.52 (3H, s) 1.50 (9H, s). ^{13}C NMR (75 MHz, CDCl$_3$): δ 175.6, 171.0, 158.8, 146.7, 146.5, 144.2, 130.6, 130.0, 128.0, 122.9, 86.1, 83.7, 70.3, 62.6, 58.8, 50.0, 30.8. HRMS-ESI+ (*m/z*): [M + H]$^+$ calculated for C$_{24}$H$_{28}$O$_7$N, 442.18603; found, 442.18516.

Fmoc solid-phase synthesis of A5DKyn:

2-chlorotrityl resin loaded with Fmoc-Sar (185 mg, 0.1 mmol) was swollen in DMF (30 min) and then Fmoc-deprotected with 4-methylpiperidine/DMF (20%; 4 x 30 min). After washing the resin with DMF (3 x 5min), a solution of Fmoc-L-Thr-OH (4 equiv.), Hydroxybenzotriazole (4 equiv.) and diisopropylcarbodiimide (DIC, 4 equiv.) in DMF (2 mL) was added to the resin. After rotary agitation for 3 hours at room temperature, the resin containing cartridge was drained and the resin was washed with DMF (3 x 5min). The Thr residue was Fmoc deprotected using 2-MP/DMF (20%; 2 x 1 min) and the Fmoc-L-hAsn(TBS)-OH (2.5 equiv.) was immediately coupled on using DIC (2.5 equiv.) and HOBt (2.5 equiv.). Fmoc-L-MeOAsp(t-Bu)-OH was also coupled on using 2.5 equivalents of amino acids, HOBt and DIC. All other Fmoc deprotections were done using 2-MP/DMF (3 x 8 min). All other couplings, with the exclusion of the ester bond and the cyclization, were done over 3 hours at room temperature using Fmoc-AA-OH (4 equiv.), DIC (4 equiv.) HOBt (4 equiv.). Once Alloc-L-Trp-OH was incorporated, the ester bond was formed by first activating Fmoc-L-Kyn(Boc)-OH (10 equiv.) with DIC (10 equiv.) in dry DCM for 30 min and filtering the solution into the cartridge containing the resin. A precisely measured amount of DMAP (0.1 equiv.) was then added as a solution in DCM and the resulting mixture was agitated for 18 hours at room temperature. After washing the resin with DCM (5 x 3 min) and DMF (5 x 3min), the alloc group was removed over the course of 1 hour at room temperature with 1,3-Dimethylbarbituric

301

acid (10 equiv.) and Pd(PPh₃)₄ (0.2 equiv.) in a continuously deoxygenated (nitrogen stream) solution of 3:1 DCM:DMF. The resin was washed with DCM (3 x 3 min), then a 1.0 % solution of sodium diethyldithiocarbamate trihydrate in DMF (3 x 3 min) to remove excess Pd catalyst, and then DCM (3 x 3 min) and DMF (3 x 3 min). The (±)-8-methyl decanoic acid tail and the remaining amino acid residues were incorporated using DIC/HOBt/DMF as previously described. Once Fmoc-L-Ala-OH was coupled on and Fmoc-deprotected with 2-methylpiperidine/DMF (20%), the peptide was removed from the resin by swelling in DCM (10 min) and then treating with 1% TFA/DCM (6 x 1 min) followed by 1% MeOH/DCM (3 x 1 min). A ninhydrin test was used to determine when all the peptide was removed from the resin. The peptide containing solution was then diluted with toluene and concentrated. The residue was dissolved in dry DMF (100 mL) and to this was added a solution of (7-azabenzotriazol-1-yloxy)tripyrrolidinophosphonium hexafluorophosphate (5 equiv.), 1-hydroxy-7-azabenzotriazole (5 equiv.) and 2,4,6-collidine (10 equiv.) in DMF (5 mL). After stirring at room temperature for 48 hours, the cyclization was determined to be complete by TLC (90:10:1 DCM:MeOH:AcOH). The cyclization solution was concentrated *in-vacuo* and the residue was dissolved in EtOAc (100 mL) and then washed with NaHSO₄ (1M, 2 x 100 mL), saturated aqueous NaHCO₃ (2 x 100 mL) and brine (2 x 100 mL). After drying the organic layer with MgSO₄, filtering it and concentrating the filtrate, the residue was cooled (ice-water bath) and suspended in TFA:TIPS:H₂O (95:2.5:2.5). Cooling was removed immediately after the addition and the resulting solution was stirred for 1.5 hours at room temperature. At this time, the solution was concentrated with a stream of dry N₂. The deprotected peptide was precipitated from the oily residue through the addition of cold ether. The solid was washed with ether 3 times before being dissolved in 3:2 H₂O:MeCN. Pure A5DKyn was isolated from this solution by semi preparative HPLC employing a linear gradient of 30:70 MeCN: H₂O

302

(0.1% TFA) to 45:55 MeCN: H$_2$O (0.1% TFA) over 60 min. A5DKyn containing fractions were combined, concentrated *in-vacuo* and lyophilized from milli-Q H$_2$O to give A5DKyn as a colorless powder (10 mg, 6% yield based on resin loading). HRMS-ESI+ (*m/z*): [M + H]$^+$ calculated for C$_{77}$H$_{111}$O$_{28}$N$_{18}$, 1735.78097; found, 1735.78277. [M + 2H]$^{2+}$ calculated for C$_{77}$H$_{112}$O$_{28}$N$_{18}$ 868.39412; found, 868.39120. See Figure H.3 for analytical R-HPLC trace of purified A5DKyn. See Figure H.5 for HRMS of purified A5DKyn. See Figure H.8 for MS-MS analysis of purified A5DKyn. See Figures H.11-H.15 for NMR spectra of A5DKyn and Table H.1 for our chemical shift assignments

Fmoc solid-phase synthesis of A5DCyp:

A5DCyp was prepared following the route outline for the synthesis of A5DKyn. Fmoc-L-Kyn(Boc)-OH was replaced with Fmoc-L-cyclopentylglycine-OH and the activated solution of this amino acid building block was not filtered prior to adding it the resin-bound peptide. See Figure H.3 for analytical R-HPLC trace of purified A5DCyp. See Figure H.6 for HRMS of purified A5DCyp. HRMS-ESI+ (*m/z*): [M + 2H]$^{2+}$ calculated for C$_{74}$H$_{113}$O$_{27}$N$_{17}$ 835.89904; found, 835.89762.

Fmoc solid-phase synthesis of A5DCyh:

A5DCyh was prepared following the route outline for the synthesis of A5DKyn. Fmoc-L-Kyn(Boc)-OH was replaced with Fmoc-L-cyclohexylglycine-OH and the activated solution of this amino acid building block was not filtered prior to adding it the resin-bound peptide . See Figure H.3 for analytical R-HPLC trace of purified A5DCyh. See Figure H.7 for HRMS of purified A5DCyh. HRMS-ESI+ (*m/z*): [M + 2H]$^{2+}$ calculated for C$_{75}$H$_{115}$O$_{27}$N$_{17}$ 842.90687; found, 842.90374.

Chapter 11 - Summary and Future Work

11 Summary

This thesis aimed to accomplish 3 major goals: (1) establish the chiral target of daptomycin and A54145D; (2) rationalize the apparent difference in the antibiotic activity of daptomycin and A54145D in the presence of lung surfactant; and (3) rationalize resistance mechanisms involving modifications to PG.

The body of work presented succeeds in establishing PG as the chiral target of daptomycin. Preliminary investigation on synthetically accessible daptomycin analogs revealed that daptomycin probably has a chiral target and did seem to recognize the absolute configuration of PG, but further investigation on daptomycin itself were needed to clarify these findings. To this end, extensive developments in the synthetic tools immediately relevant to the synthesis of daptomycin and phosphatidylglycerol were made. The mechanistic work on daptomycin would not have been possible without first developing a highly efficient route to Fmoc-MeGlu(t-Bu)-OH. The developed route is exceptionally efficient proceeding in 6-steps from commercially available and inexpensive starting materials. Although this work could have been completed without investigating a new synthesis of daptomycin, the baseless claims made by the Li group and the Brimble group regarding the reactivity of Fmoc-L-Kyn(CHO,Boc)-OH and Fmoc-L-Kyn(CHO,CHO)-OH begged for further investigation considering that the majority of retrosynthetic considerations center around steps involving these synthons. Rationalizing the reactivity of these synthons proved worthwhile since this led to the development of the first truly efficient synthesis of daptomycin which gave facile access to the unnatural enantiomer of daptomycin and analogs of daptomycin with improved properties. An efficient, operationally simple, and stereospecific synthesis of PG was developed, and this synthesis was used to prepare

all four stereoisomers of DMPG. Bioactivity assays on daptomycin and the unnatural enantiomer unequivocally established that daptomycin interacts with a chiral target as part of its action mechanism. By investigating the interaction of each enantiomer with each stereoisomer of PG individually, the effect of overall peptide and lipid stereochemistry could be determined and resolved from changes in the bulk properties of the model membranes used. This robust experimental framework clearly demonstrated that PG stereochemistry strongly influences membrane affinity, membrane bound state and oligomer formation all of which are predictors of antibacterial activity. These experiments demonstrate that the chiral target of daptomycin is 2R,2'S-PG and that the unnatural enantiomer of daptomycin is nearly inactive against *B. subtilis* primarily because it can not oligomerize to the same extent on the model membranes. Based on these findings, a new daptomycin resistance mechanism was postulated.

Proving that the chiral target of A54145D is 2R,2'S -PG required the development of a solid-phase total synthesis of A54145D. This thesis contributed to that total synthesis by developing an efficient route to Fmoc-L-*threo*-hAsn(TBS)-OH, Fmoc-L-*threo*-MeOAsp(t-Bu)-OH and Fmoc-L-*erythro*-MeOAsp(t-Bu)-OH. The latter two synthons were used to determine the absolute configuration at β-position of MeOAsp9. The primary synthetic tool used to access these building blocks allowed for the synthesis of Fmoc-protected 1,2-aminoalcohols using Sharpless asymmetric aminohydroxylation reaction conditions. The generality of this transformation was thoroughly demonstrated through a scoping study which resulted in the discovery of an olefin substrate well-suited to the synthesis Fmoc-D-*threo*-hAsn(TBS)-OH, Fmoc-D-*threo*-MeOAsp(t-Bu)-OH and Fmoc-D-*erythro*-MeOAsp(t-Bu)-OH with high enantiomeric purity. To date, this synthetic pathway has been used in the synthesis of calcium-dependent antibiotic[361] and malacidin A.[362] These synthons were eventually used to prepare the unnatural enantiomer of A5D

which proved to be nearly inactive against *B. subtilis* demonstrating that A5D interacts with a chiral molecule as part of its action mechanism.

Assaying the interaction of A5D with the 4 stereoisomers of PG proved difficult due to the insensitivity of Trp1 with respect to membrane insertion. Fortunately, previous SAR studies had discovered an analog A5D which bears the environmentally sensitive fluorescent amino acid Kyn at position 13 (A5DKyn) and possess antimicrobial activity both in the presence and absence of lung surfactant that rivals A5D. Using the base-stable Kyn synthon developed in previous chapters, A5DKyn was easily prepared using Fmoc-SPPS and antimicrobial studies revealed that it is just as active as A5D against *B. subtilis*. Experiments with A5DKyn and PG containing model membranes demonstrated that the emission intensity of Kyn13 increases 20-fold upon membrane insertion. Further experiments demonstrated that PG stereochemistry has a substantial influence on the membrane insertion, membrane bound state and extent of oligomerization of A5D. Like daptomycin, A5D was found to strongly prefer 2R,2'S -PG and the unnatural enantiomer of A5D was inactive probably because it cannot oligomerize to the same extant as the natural isomer.

The fact that daptomycin and A5D target the same isomer of PG motivated an investigation into the mechanism of inactivation of each antibiotic by lung surfactant. To this end, the stereochemical content of PG in bovine lung surfactant was determined by a new approach which employs a boronic acid chiral auxiliary to distinguish between 2'R and 2'S isomers of PG by NMR. In combination with a known method to determine the absolute configuration of PG at both the headgroup and tailgroup, PG in LS was determined to be exclusively the 2R,2'S -PG. Isothermal titration calorimetry demonstrated that both peptides should be inactivated by the 2R,2'S -PG present in LS similarly. Antagonism studies revealed that complete inhibition both daptomycin and A5D by LS should always occur when a quantity of LS is present such that the molar

equivalents of PG in the LS is approximately 1-2 the molar equivalents of peptide. These experiments cast doubt on the hypothesis that A5D is less susceptible to inhibition in the presence of LS and suggest that finding an analog A5D or daptomycin that is active in the presence of LS would be very difficult and would be of dubious clinical significance.

The third and final goal of this thesis was to rationalize resistance mechanisms that involve changes in lipid content with a particular emphasis on PG modification. From our studies establishing PG as the chiral target of daptomycin, it became apparent that daptomycin is tightly complexing to this lipid and likely recognizes the lipid headgroup. This observation is contrary to the hypothesis that daptomycin primarily recognizes the negative charge on PG and should insert well into any membrane containing negatively charge phospholipids. To better understand the interaction of daptomycin with PG, we established a structure-activity relationship between these two molecules by making precise alterations to the PG headgroup and PG tailgroup. These studies reveal that daptomycin indeed recognizes the headgroup of PG and possess a binding pocket that uniquely encompasses each hydroxyl group. Modifications to the tailgroup revealed a PG acyl tail chain length of at least 7-8 carbons is required for stoichiometric binding at micromolar peptide concentrations. Daptomycin binds to PG having 8-carbon, linear, unsaturated acyl groups (C8PG) at micromolar concentration and interacts with C8PG in essentially the same manner as when the PG is incorporated into a liposome, and thus preassembly of individual PG moieties is not a prerequisite for binding, structural transition, and oligomerization. The results of this SAR study reveal that daptomycin is sensitive to modification to the PG headgroup and suggest that conversion of PG to lysyl-PG may serve to effectively reduce available binding sites. To explore this hypothesis, a synthesis of isomerically pure lysyl-DMPG was developed. Preliminary studies demonstrated that daptomycin does not readily binding to lysyl-DMPG at physiological calcium

concentrations proving that lysinylation effectively masks PG. The presence of lysyl-DMPG in a DMPG/DMPC was found to insignificantly affect the backbone structure of daptomycin but did increase the extent of oligomerization suggesting that the lipid may impact oligomer structure or localization. It is possible that this effect could confer resistance to daptomycin, but the investigation presented in chapter 7 is currently inconclusive.

11.1 Future work

11.1.1 Broad screening of antimicrobial activity

Many of the studies presented in this thesis use only one or two strains of Gram-positive bacteria to draw broad conclusions about the activity of daptomycin. If indeed daptomycin and A5D target the same stereoisomer of PG then the activity difference between these natural products and their respective unnatural enantiomers should be similar across a wide range of Gram-positive organisms.

11.1.2 Investigations of the unnatural enantiomers of daptomycin and A54145D on bacterial membranes using confocal microscopy

Studies on model membranes suggest that the unnatural enantiomers of daptomycin and A54145D are inactive primarily because they cannot oligomerize to the same extent on model membranes. This claim should be further investigated directly on bacteria using confocal microscopy. Labelling each unnatural enantiomer with BODIPY or some other fluorophore compatible with confocal microscopy should allow for interrogation of the state of each peptide on bacterial membranes.[64,75] Since alterations in the distribution of PG in the bacterial membrane are implicated in the killing action of daptomycin and the oligomerization of daptomycin is likely involved in PG sequestration, the effect each unnatural enantiomer has on the PG distribution should be investigated using FM 4-64.[64,75] Experiments involving FM 4-64 would not involve labelled unnatural enantiomers and would serve to corroborate experiments with the labelled peptides.

11.1.3 Determine how lysyl-PG affects the distribution of daptomycin on model and bacterial membranes

Investigations into the impact of lysyl-PG on the membrane affinity, membrane bound state and oligomerization of daptomycin reveal that conversion of PG to lysyl-PG serves to mask PG, but this explanation seems incomplete. Daptomycin resistant strains have increased lysyl-PG content and reduced PG content, but the change in the content of each lipid often seems too small to explain the difference in antimicrobial activity assuming the conversion of PG to lysyl-PG only serves to reduce binding. It seems likely that lysyl-PG provides additional protection possibly by stabilizing the membrane to the action of daptomycin. To investigate the membrane stabilization hypothesis, the distribution of PG on GUVs containing lysyl-PG should be investigated using confocal microscopy.[234] The same investigation should be done on bacterial strains that possess or lack lysyl-PG while employing a consistent genetic background.[126,129]

11.1.4 Determine how lysyl-PG affects membrane fluidity

Some researchers have observed correlations between changes in membrane fluidity, changes in lysyl-PG content and daptomycin resistance.[122,281,282,363] Considering the work done by Mueller et al, it seems plausible that lysyl-PG stabilizes the membrane to the action of daptomycin by altering membrane fluidity.[64] Therefore, the effect of lysyl-PG on membrane fluidity should be determined. This can be done using a well-characterized fluorescence anisotropy assay which was used to determine the membrane fluidities of daptomycin resistant strains of *S. aureus*.[282,283]

11.1.5 Determining the structure of daptomycin bound to calcium and PG

Currently, there is a dearth in the structural information of daptomycin bound to its target. NMR structures of daptomycin bound to PG are not forthcoming probably because daptomycin aggregates rapidly in the presence of calcium and PG at concentrations needed for analysis by NMR. Based on the SAR established between daptomycin and PG, it may be possible to develop a system suitable for NMR investigation of the daptomycin:PG:Ca complex by employing PGs

with shortened tails or lyso-PGs. Indeed, this approach was used to determine the structure of cinnamycin bound to lyso-phosphatidylethanolamine.[364] Additionally, shortening the tail of daptomycin might also be necessary to control aggregation. X-ray diffraction of the crystallized complex is also a promising approach that might be facilitated by the application of truncated or modified PGs. A similar approach succeeded in producing a crystal structure of laspartomycin bound to calcium and a shortened $C_{55}P$.[52]

11.1.6 Determining the stereochemical content of PG in Gram-positive bacteria

The work presented in this thesis suggests that bacteria could resist daptomycin through altering the headgroup configuration of PG from 2'S to 2'R. Thus, the stereochemical purity of PG extracted from Gram-positive organisms should be determined and a correlation between stereochemical purity and daptomycin resistance should be investigated. The absolute configuration at the headgroup of PG has not been determined in Gram-positive bacteria; however, it should be straightforward to extract and isolate PG from bacteria and determine its stereochemical purity using the boronic acid chiral auxiliary developed in this thesis. It should also be possible to determine whether changes in the diastereomeric purity of PG accompany daptomycin resistance by creating resistant strains in the laboratory or by assaying clinical isolates.

11.1.7 Determining the calcium affinity of daptomycin and A54145

A considerable portion of this thesis dealt with the binding of daptomycin to PG in the presence of calcium and works by others have demonstrated that daptomycin complexes with both calcium and PG. To date, binding analyses have focused on determining the binding constants for daptomycin associating with membranes containing PG. However, considering that daptomycin possess a calcium binding motif, it is likely that the peptide binds calcium in the absence of PG; thus, binding constants describing daptomycin's affinity for model membranes in the presence of calcium are likely a composite.[365] Therefore, it would be informative to determine the peptides

affinity for calcium in the absence of PG. This can be readily accomplished through a competition assay.[366] Analysis of several analogs of daptomycin with varying antibacterial activities using this approach would help to explain changes in activity and would be a step towards a more detailed structure-activity relationship.

Letters of Copyright Permissions
Chapter 1

ELSEVIER LICENSETERMS AND CONDITIONS

Jun 21, 2022

This Agreement between Mr. Ryan Moreira ("You") and Elsevier ("Elsevier") consists ofyour license details and the terms and conditions provided by Elsevier and CopyrightClearance Center.

License Number	5333680558059
License date	Jun 21, 2022
Licensed ContentPublisher	Elsevier
Licensed ContentPublication	Chemistry & Biology
Licensed Content Title	Structural Transitions as Determinants of the Action of theCalcium-Dependent Antibiotic Daptomycin
Licensed Content Author	David Jung,Annett Rozek,Mark Okon,Robert E.W Hancock
Licensed Content Date	Jul 1, 2004
Licensed Content Volume	11

JOHN WILEY AND SONS LICENSETERMS AND CONDITIONS

Jun 21, 2022

This Agreement between Mr. Ryan Moreira ("You") and John Wiley and Sons ("John Wileyand Sons") consists of your license details and the terms and conditions provided by JohnWiley and Sons and Copyright Clearance Center.

License Number	5333680900773
License date	Jun 21, 2022
Licensed ContentPublisher	John Wiley and Sons
Licensed ContentPublication	Molecular Microbiology
Licensed Content Title	Lipid spirals in Bacillus subtilis and their role in cell division
Licensed ContentAuthor	Nada Pavlendová, Peter J. O'Toole, Anthony J. Wilkinson, et al
Licensed Content Date	Apr 22, 2008
Licensed Content	68

312

CCC Marketplace™

This is a License Agreement between Ryan Moreira ("User") and Copyright Clearance Center, Inc. ("CCC") on behalf of the Rightsholder identified in the order details below. The license consists of the order details, the Marketplace Order General Terms and Conditions below, and any Rightsholder Terms and Conditions which are included below.

All payments must be made in full to CCC in accordance with the Marketplace Order General Terms and Conditions below.

Order Date	21-Jun-2022	Type of Use	Republish in a thesis/dissertation
Order License ID	1238821-1	Publisher	AMERICAN SOCIETY FOR MICROBIOLOGY
ISSN	1098-5530	Portion	Image/photo/illustration

LICENSED CONTENT

Publication Title	Journal of bacteriology : JB	Publication Type	e-Journal
Article Title	Daptomycin-mediated reorganization of membrane architecture causes mislocalization of essential cell division proteins.	Start Page	4494
		End Page	4504
		Issue	17
Author/Editor	American Society for Microbiology.	Volume	194
Date	01/01/1916	URL	https://journals.asm.org/journal/jb
Language	English		
Country	United States of America		
Rightsholder	American Society for Microbiology - Journals		

CCC Marketplace™

This is a License Agreement between Ryan Moreira ("User") and Copyright Clearance Center, Inc. ("CCC") on behalf of the Rightsholder identified in the order details below. The license consists of the order details, the Marketplace Order General Terms and Conditions below, and any Rightsholder Terms and Conditions which are included below.

All payments must be made in full to CCC in accordance with the Marketplace Order General Terms and Conditions below.

Order Date	21-Jun-2022	Type of Use	Republish in a thesis/dissertation
Order License ID	1238840-1	Publisher	AMERICAN SOCIETY FOR MICROBIOLOGY
ISSN	0066-4804	Portion	Chart/graph/table/figure

LICENSED CONTENT

Publication Title	Antimicrobial agents and chemotherapy	Publication Type	Journal
		Start Page	2538
Article Title	Correlation of daptomycin bactericidal activity and membrane depolarization in Staphylococcus aureus.	End Page	2544
		Issue	8
		Volume	47
Author/Editor	AMERICAN SOCIETY FOR MICROBIOLOGY., INTERSCIENCE CONFERENCE ON ANTIMICROBIAL AGENTS AN	URL	https://journals.asm.org/journal/aac
Date	01/01/1972		
Language	English		
Country	United States of America		
Rightsholder	American Society for Microbiology - Journals		

ELSEVIER LICENSETERMS AND CONDITIONS

Jun 21, 2022

This Agreement between Mr. Ryan Moreira ("You") and Elsevier ("Elsevier") consists ofyour license details and the terms and conditions provided by Elsevier and CopyrightClearance Center.

License Number   5333710045310

ELSEVIER LICENSE TERMS AND CONDITIONS

Chapter 2

Permission not needed

Chapter 3

SPRINGER NATURE LICENSETERMS AND CONDITIONS

May 02, 2022

This Agreement between Mr. Ryan Moreira ("You") and Springer Nature ("SpringerNature") consists of your license details and the terms and conditions provided by SpringerNature and Copyright Clearance Center.

License Number	5300860180291
License date	May 02, 2022
Licensed ContentPublisher	Springer Nature
Licensed ContentPublication	Amino Acids
Licensed Content Title	Highly efficient and enantioselective syntheses of (2S,3R)-3-alkyl-and alkenylglutamates from Fmoc-protected Garner's aldehyde
Licensed ContentAuthor	Ryan Moreira et al
Licensed Content Date	Jul 3, 2020

Chapter 4

Permission not needed

Chapter 5

JOHN WILEY AND SONS LICENSETERMS AND CONDITIONS

Jun 23, 2022

This Agreement between Mr. Ryan Moreira ("You") and John Wiley and Sons ("John Wileyand Sons") consists of your license details and the terms and conditions provided by JohnWiley and Sons and Copyright Clearance Center.

License Number	5334841003308
License date	Jun 23, 2022
Licensed ContentPublisher	John Wiley and Sons
Licensed ContentPublication	Angewandte Chemie International Edition
Licensed Content Title	The Chiral Target of Daptomycin Is the 2R,2′S Stereoisomer ofPhosphatidylglycerol
Licensed ContentAuthor	Ryan Moreira, Scott D. Taylor
Licensed Content Date	Dec 7, 2021

Chapter 6

Chapter 7

Content not yet published

Chapter 8

Chapter 9

Synthesis of Fmoc-Protected Amino Alcohols via the Sharpless Asymmetric Aminohydroxylation Reaction Using FmocNHCl as the Nitrogen Source

Chapter 10

A54145 Factor D Is Not Less Susceptible to Inhibition by Lung Surfactant than Daptomycin

References

[1]   M. Wainwright, *Mycologist* **1989**, *3*, 21–23.

[2]   R. I. Aminov, *Front. Microbiol.* **2010**, *1*, 1–7.

[3]   E. Chain, H. W. Florey, A. D. Gardner, N. G. Heatley, M. A. Jennings, J. Orr-Ewing, A. G. Sanders, L. F. Peltier, *Clin. Orthop. Relat. Res.* **2005**, *439*, 23–26.

[4]   P. Dadgostar, *Infect. Drug Resist.* **2019**, *12*, 3903–3910.

[5]   A. E. Clatworthy, E. Pierson, D. T. Hung, *Nat. Chem. Biol.* **2007**, *3*, 541–548.

[6]   B. I. Eisenstein, F. B. Oleson, Jr., R. H. Baltz, *Clin. Infect. Dis.* **2010**, *50*, S10–S15.

[7]   P. Fernandes, E. Martens, *Biochem. Pharmacol.* **2017**, *133*, 152–163.

[8]   A. H. Diacon, A. Pym, M. Grobusch, R. Patientia, R. Rustomjee, L. Page-Shipp, C. Pistorius, R. Krause, M. Bogoshi, G. Churchyard, A. Venter, J. Allen, J. C. Palomino, T. De Marez, R. P. G. van Heeswijk, N. Lounis, P. Meyvisch, J. Verbeeck, W. Parys, K. de Beule, K. Andries, D. F. M. Neeley, *N. Engl. J. Med.* **2009**, *360*, 2397–2405.

[9]   G. M. Eliopoulos, C. Thauvin, B. Gerson, R. C. Moellering, *Antimicrob. Agents Chemother.* **1985**, *27*, 357–362.

[10]   V. G. Fowler, H. W. Boucher, G. R. Corey, E. Abrutyn, A. W. Karchmer, M. E. Rupp, D. P. Levine, H. F. Chambers, F. P. Tally, G. A. Vigliani, C. H. Cabell, A. S. Link, I. DeMeyer, S. G. Filler, M. Zervos, P. Cook, J. Parsonnet, J. M. Bernstein, C. S. Price, G. N. Forrest, G. Fätkenheuer, M. Gareca, S. J. Rehm, H. R. Brodt, A. Tice, S. E. Cosgrove, *N. Engl. J. Med.* **2006**, *355*, 653–665.

[11]   F. P. Tally, M. F. DeBruin, *J. Antimicrob. Chemother.* **2000**, *46*, 523–526.

[12]   J. A. Silverman, L. I. Mortin, A. D. G. VanPraagh, T. Li, J. Alder, *J. Infect. Dis.* **2005**, *191*, 2149–2152.

[13]   M. Debono, M. Barnhart, C. B. Carrell, J. a Hoffmann, J. L. Occolowitz, B. J. Abbott, D. S. Fukuda, R. L. Hamill, K. Biemann, W. C. Herlihy, *J. Antibiot. (Tokyo).* **1987**, *40*, 761–777.

[14]   D. S. Fukuda, R. H. Du Bus, P. J. Baker, D. M. Berry, J. S. Mynderse, *J. Antibiot. (Tokyo).* **1990**, *43*, 594–600.

[15]   F. T. Counter, N. E. Allen, D. S. Fukuda, J. N. Hobbs, J. Ott, P. W. Ensminger, J. S. Mynderse, D. A. Preston, C. Y. E. Wu, *J. Antibiot. (Tokyo).* **1990**, *43*, 616–622.

[16]   K. T. Nguyen, X. He, D. C. Alexander, C. Li, J.-Q. Gu, C. Mascio, A. Van Praagh, L. Mortin, M. Chu, J. A. Silverman, P. Brian, R. H. Baltz, *Antimicrob. Agents Chemother.* **2010**, *54*, 1404–1413.

[17]   D. C. Alexander, J. Rock, J.-Q. Gu, C. Mascio, M. Chu, P. Brian, R. H. Baltz, *J. Antibiot. (Tokyo).* **2011**, *64*, 79–87.

[18]   J. H. Lakey, E. J. A. Lea, *Biochim. Biophys. Acta - Biomembr.* **1986**, *859*, 219–226.

[19] J. H. Lake, M. Ptak, *Biochemistry* **1988**, *27*, 4639–4645.

[20] P. Canepari, M. Boaretti, M. M. Lleo, G. Satta, *Antimicrob. Agents Chemother.* **1990**, *34*, 1220–1226.

[21] J. a Silverman, N. G. Perlmutter, M. Howard, H. M. Shapiro, *Antimicrob. Agents Chemother.* **2003**, *47*, 2538–2544.

[22] R. M. Epand, C. Walker, R. F. Epand, N. A. Magarvey, *Biochim. Biophys. Acta - Biomembr.* **2016**, *1858*, 980–987.

[23] R. M. Epand, R. F. Epand, *J. Pept. Sci.* **2011**, *17*, 298–305.

[24] D. Jung, A. Rozek, M. Okon, R. E. . Hancock, *Chem. Biol.* **2004**, *11*, 949–957.

[25] W. Dowhan, *Annu. Rev. Biochem.* **1997**, *66*, 199–232.

[26] P. M. Macdonald, J. Seelig, *Biochemistry* **1987**, *26*, 6292–6298.

[27] W. Zhao, T. Róg, A. A. Gurtovenko, I. Vattulainen, M. Karttunen, *Biochimie* **2008**, *90*, 930–938.

[28] I. Barák, K. Muchová, A. J. Wilkinson, P. J. O'Toole, N. Pavlendová, *Mol. Microbiol.* **2008**, *68*, 1315–1327.

[29] E. Mileykovskaya, W. Dowhan, *Curr. Opin. Microbiol.* **2005**, *8*, 135–142.

[30] D. W. Adams, J. Errington, *Nat. Rev. Microbiol.* **2009**, *7*, 642–653.

[31] S. Furse, H. Wienk, R. Boelens, A. I. P. M. de Kroon, J. A. Killian, *FEBS Lett.* **2015**, *589*, 2726–2730.

[32] Y. Higashi, J. L. Strominger, *J. Biol. Chem.* **1970**, *245*, 3691–3696.

[33] A. M. Seddon, M. Lorch, O. Ces, R. H. Templer, F. Macrae, P. J. Booth, *J. Mol. Biol.* **2008**, *380*, 548–556.

[34] E. M. Bevers, H. H. Wang, J. A. F. Op Den Kamp, L. L. M. Van Deenen, *Arch. Biochem. Biophys.* **1979**, *193*, 502–508.

[35] L. Picas, S. Merino-Montero, A. Morros, J. Hernández-Borrell, M. T. Montero, *J. Fluoresc.* **2007**, *17*, 649–654.

[36] I. Masataka, N. Masateru, K. Michie, K. Makoto, *Biochim. Biophys. Acta - Lipids Lipid Metab.* **1976**, *431*, 426–432.

[37] T. de Vrije, R. L. de Swart, W. Dowhan, J. Tommassen, B. de Kruijff, *Nature* **1988**, *334*, 173–175.

[38] Y. Itabashi, A. Kuksis, *Anal. Biochem.* **1997**, *254*, 49–56.

[39] R. Sato, Y. Itabashi, H. Fujishima, H. Okuyama, A. Kuksis, *Lipids* **2004**, *39*, 1025–1030.

[40] J. N. Hawthorne, G. B. Ansell, *Phospholipids*, Elsevier, Amsterdam, **1982**.

[41] S. F. Yang, S. Freer, A. A. Benson, *J. Biol. Chem.* **1967**, *242*, 477–484.

[42]   A. Joutti, O. Renkonen, *Chem. Phys. Lipids* **1976**, *17*, 264–266.

[43]   S. Kuhn, C. J. Slavetinsky, A. Peschel, *Int. J. Med. Microbiol.* **2015**, *305*, 196–202.

[44]   J. van Heijenoort, *Microbiol. Mol. Biol. Rev.* **2007**, *71*, 620–635.

[45]   H. Barreteau, A. Kovač, A. Boniface, M. Sova, S. Gobec, D. Blanot, *FEMS Microbiol. Rev.* **2008**, *32*, 168–207.

[46]   T. Schneider, M. M. Senn, B. Berger-Bächi, A. Tossi, H.-G. Sahl, I. Wiedemann, *Mol. Microbiol.* **2004**, *53*, 675–685.

[47]   N. Ruiz, *Lipid Insights* **2015**, *2015*, 21–31.

[48]   E. M. Wise, J. T. Park, *Proc. Natl. Acad. Sci.* **1965**, *54*, 75–81.

[49]   N. Allen, *FEMS Microbiol. Rev.* **2003**, *26*, 511–532.

[50]   J. L. Marquardt, E. D. Brown, W. S. Lane, T. M. Haley, Y. Ichikawa, C.-H. Wong, C. T. Walsh, *Biochemistry* **1994**, *33*, 10646–10651.

[51]   T. M. Amorim Franco, L. Favrot, O. Vergnolle, J. S. Blanchard, *ACS Chem. Biol.* **2017**, *12*, 1235–1244.

[52]   L. H. J. Kleijn, H. C. Vlieg, T. M. Wood, J. Sastre Toraño, B. J. C. Janssen, N. I. Martin, *Angew. Chem. Int. Ed.* **2017**, *56*, 16546–16549.

[53]   T. Schneider, K. Gries, M. Josten, I. Wiedemann, S. Pelzer, H. Labischinski, H.-G. Sahl, *Antimicrob. Agents Chemother.* **2009**, *53*, 1610–1618.

[54]   F. Isono, M. Inukai, *Antimicrob. Agents Chemother.* **1991**, *35*, 234–236.

[55]   K. J. Stone, J. L. Strominger, *Proc. Natl. Acad. Sci.* **1971**, *68*, 3223–3227.

[56]   E. Breukink, H. E. van Heusden, P. J. Vollmerhaus, E. Swiezewska, L. Brunner, S. Walker, A. J. R. Heck, B. de Kruijff, *J. Biol. Chem.* **2003**, *278*, 19898–19903.

[57]   T. J. Oman, T. J. Lupoli, T.-S. A. Wang, D. Kahne, S. Walker, W. A. van der Donk, *J. Am. Chem. Soc.* **2011**, *133*, 17544–17547.

[58]   A. Bakhtiary, S. A. Cochrane, P. Mercier, R. T. McKay, M. Miskolzie, C. S. Sit, J. C. Vederas, *J. Am. Chem. Soc.* **2017**, *139*, 17803–17810.

[59]   L. L. Ling, T. Schneider, A. J. Peoples, A. L. Spoering, I. Engels, B. P. Conlon, A. Mueller, T. F. Schäberle, D. E. Hughes, S. Epstein, M. Jones, L. Lazarides, V. A. Steadman, D. R. Cohen, C. R. Felix, K. A. Fetterman, W. P. Millett, A. G. Nitti, A. M. Zullo, C. Chen, K. Lewis, *Nature* **2015**, *517*, 455–459.

[60]   W. Lee, K. Schaefer, Y. Qiao, V. Srisuknimit, H. Steinmetz, R. Müller, D. Kahne, S. Walker, *J. Am. Chem. Soc.* **2016**, *138*, 100–103.

[61]   N. E. Allen, J. N. Hobbs, W. E. Alborn, *Antimicrob. Agents Chemother.* **1987**, *31*, 1093–1099.

[62]   D. Mengin-Lecreulx, N. E. Allen, J. N. Hobbs, J. van Heijenoort, *FEMS Microbiol. Lett.*

1990, *69*, 245–248.

[63] L. J. Wale, A. P. Shelton, D. Greenwood, *J. Med. Microbiol.* **1989**, *30*, 45–49.

[64] A. Müller, M. Wenzel, H. Strahl, F. Grein, T. N. V. Saaki, B. Kohl, T. Siersma, J. E. Bandow, H.-G. Sahl, T. Schneider, L. W. Hamoen, *Proc. Natl. Acad. Sci.* **2016**, *113*, E7077–E7086.

[65] W. Tantibhedhyangkul, E. Wongsawat, S. Matamnan, N. Inthasin, J. Sueasuay, Y. Suputtamongkol, *Antibiotics* **2019**, *8*, 123.

[66] D. Wolf, P. Domínguez-Cuevas, R. A. Daniel, T. Mascher, *Antimicrob. Agents Chemother.* **2012**, *56*, 5907–5915.

[67] H. Hashizume, R. Sawa, S. Harada, M. Igarashi, H. Adachi, Y. Nishimura, A. Nomoto, *Antimicrob. Agents Chemother.* **2011**, *55*, 3821–3828.

[68] M. Boaretti, P. Canepari, M. D. M. Lleò, G. Satta, *J. Antimicrob. Chemother.* **1993**, *31*, 227–235.

[69] M. Boaretti, P. Canepari, *Antimicrob. Agents Chemother.* **1995**, *39*, 2068–2072.

[70] V. Laganas, J. Alder, J. A. Silverman, *Antimicrob. Agents Chemother.* **2003**, *47*, 2682–2684.

[71] F. Grein, A. Müller, K. M. Scherer, X. Liu, K. C. Ludwig, A. Klöckner, M. Strach, H. G. Sahl, U. Kubitscheck, T. Schneider, *Nat. Commun.* **2020**, *11*, 1–11.

[72] I. Kotsogianni, T. M. Wood, F. M. Alexander, S. A. Cochrane, N. I. Martin, *ACS Infect. Dis.* **2021**, *7*, 2612–2619.

[73] V. Sass, T. Schneider, M. Wilmes, C. Körner, A. Tossi, N. Novikova, O. Shamova, H.-G. Sahl, *Infect. Immun.* **2010**, *78*, 2793–2800.

[74] S. D. Taylor, M. Palmer, *Bioorg. Med. Chem.* **2016**, *24*, 6253–6268.

[75] J. Pogliano, N. Pogliano, J. A. Silverman, *J. Bacteriol.* **2012**, *194*, 4494–4504.

[76] S. van Baarle, I. N. Celik, K. G. Kaval, M. Bramkamp, L. W. Hamoen, S. Halbedel, *J. Bacteriol.* **2013**, *195*, 1012–1021.

[77] K. S. Ramamurthi, K. R. Clapham, R. Losick, *Mol. Microbiol.* **2006**, *62*, 1547–1557.

[78] N. Cotroneo, R. Harris, N. Perlmutter, T. Beveridge, J. A. Silverman, *Antimicrob. Agents Chemother.* **2008**, *52*, 2223–2225.

[79] A. Howe, S. Sofou, *J. Phys. Chem. B* **2021**, *125*, 5775–5785.

[80] M.-T. Lee, P.-Y. Yang, N. E. Charron, M.-H. Hsieh, Y.-Y. Chang, H. W. Huang, *Biochemistry* **2018**, *57*, 5629–5639.

[81] R. Taylor, D. Beriashvili, S. Taylor, M. Palmer, *ACS Infect. Dis.* **2017**, *3*, 797–801.

[82] M. A. Kreutzberger, A. Pokorny, P. F. Almeida, *Langmuir* **2017**, *33*, 13669–13679.

[83]   Y.-F. Chen, T.-L. Sun, Y. Sun, H. W. Huang, *Biochemistry* **2014**, *53*, 5384–5392.

[84]   W. E. Alborn, N. E. Allen, D. a Preston, *Antimicrob. Agents Chemother.* **1991**, *35*, 2282–2287.

[85]   N. E. Allen, W. E. Alborn, J. N. Hobbs, *Antimicrob. Agents Chemother.* **1991**, *35*, 2639–2642.

[86]   J. K. Muraih, A. Pearson, J. Silverman, M. Palmer, *Biochim. Biophys. Acta - Biomembr.* **2011**, *1808*, 1154–1160.

[87]   J. K. Muraih, M. Palmer, *Biochim. Biophys. Acta - Biomembr.* **2012**, *1818*, 1642–1647.

[88]   J. K. Muraih, J. Harris, S. D. Taylor, M. Palmer, *Biochim. Biophys. Acta - Biomembr.* **2012**, *1818*, 673–678.

[89]   T. Zhang, J. K. Muraih, E. Mintzer, N. Tishbi, C. Desert, J. Silverman, S. Taylor, M. Palmer, *Biochim. Biophys. Acta - Biomembr.* **2013**, *1828*, 302–308.

[90]   T. H. Zhang, S. D. Taylor, M. Palmer, J. Duhamel, *Biophys. J.* **2016**, *111*, 1267–1277.

[91]   R. Taylor, K. Butt, B. Scott, T. Zhang, J. K. Muraih, E. Mintzer, S. Taylor, M. Palmer, *Biochim. Biophys. Acta - Biomembr.* **2016**, *1858*, 1999–2005.

[92]   M.-T. Lee, W.-C. Hung, M.-H. Hsieh, H. Chen, Y.-Y. Chang, H. W. Huang, *Biophys. J.* **2017**, *113*, 82–90.

[93]   T. Zhang, J. K. Muraih, B. MacCormick, J. Silverman, M. Palmer, *Biochim. Biophys. Acta - Biomembr.* **2014**, *1838*, 2425–2430.

[94]   J. Zhang, K. Scoten, S. K. Straus, *ACS Infect. Dis.* **2016**, *2*, 682–687.

[95]   R. M. Taylor, The Lipopeptide Antibiotic Daptomycin: Its Interaction With Calcium And Membranes And The Effects Of Membrane Lipid Composition On Its Activity, University of Waterloo, Doctoral Thesis, **2017**.

[96]   D. Beriashvili, R. Taylor, B. Kralt, N. Abu Mazen, S. D. Taylor, M. Palmer, *Chem. Phys. Lipids* **2018**, *216*, 73–79.

[97]   D. Beriashvili, Action Mechanism and Structural Studies on the Lipopeptide Antibiotic Daptomycin, University of Waterloo, Masters Thesis, **2019**.

[98]   J. Zhang, W. R. P. Scott, F. Gabel, M. Wu, R. Desmond, J. H. Bae, G. Zaccai, W. R. Algar, S. K. Straus, *Biochim. Biophys. Acta - Proteins Proteomics* **2017**, *1865*, 1490–1499.

[99]   G. Seydlová, A. Sokol, P. Lišková, I. Konopásek, R. Fišer, *Antimicrob. Agents Chemother.* **2019**, *63*, DOI 10.1128/AAC.01589-18.

[100]   F. Zuttion, A. Colom, S. Matile, D. Farago, F. Pompeo, J. Kokavecz, A. Galinier, J. Sturgis, I. Casuso, *Nat. Commun.* **2020**, *11*, 6312.

[101]   N. Cotroneo, R. Harris, N. Perlmutter, T. Beveridge, J. A. Silverman, *Antimicrob. Agents Chemother.* **2008**, *52*, 2223–2225.

[102] B. Mensa, G. L. Howell, R. Scott, W. F. DeGrado, *Antimicrob. Agents Chemother.* **2014**, *58*, 5136–5145.

[103] J. K. Hobbs, K. Miller, A. J. O'Neill, I. Chopra, *J. Antimicrob. Chemother.* **2008**, *62*, 1003–1008.

[104] L. H. Kondejewski, S. W. . Farmer, D. S. Wishart, R. E. W. Hancock, R. S. Hodges, *Int. J. Pept. Protein Res.* **2009**, *47*, 460–466.

[105] T. Kelesidis, R. Humphries, D. Z. Uslan, D. A. Pegues, *Clin. Infect. Dis.* **2011**, *52*, 228–234.

[106] T. Matono, K. Hayakawa, R. Hirai, A. Tanimura, K. Yamamoto, Y. Fujiya, M. Mawatari, S. Kutsuna, N. Takeshita, K. Mezaki, N. Ohmagari, T. Miyoshi-Akiyama, *BMC Res. Notes* **2016**, *9*, 4–9.

[107] H. Hagiya, K. Kimura, H. Okuno, S. Hamaguchi, D. Morii, H. Yoshida, T. Mitsui, I. Nishi, K. Tomono, *J. Infect. Chemother.* **2019**, *25*, 906–908.

[108] A. S. Bayer, T. Schneider, H.-G. Sahl, *Ann. N. Y. Acad. Sci.* **2013**, *1277*, 139–158.

[109] C. Hoischen, K. Gura, C. Luge, J. Gumpert, *J. Bacteriol.* **1997**, *179*, 3430–3436.

[110] M. P. Lechevalier, C. De Bievre, H. Lechevalier, *Biochem. Syst. Ecol.* **1977**, *5*, 249–260.

[111] M. Sandoval-Calderón, D. D. Nguyen, C. A. Kapono, P. Herron, P. C. Dorrestein, C. Sohlenkamp, *Front. Microbiol.* **2015**, *6*, 1–13.

[112] M. C. Zuñeda, J. J. Guillenea, J. B. Dominguez, A. Prado, F. M. Goñi, *Lipids* **1984**, *19*, 223–228.

[113] A.-B. Hachmann, E. Sevim, A. Gaballa, D. L. Popham, H. Antelmann, J. D. Helmann, *Antimicrob. Agents Chemother.* **2011**, *55*, 4326–4337.

[114] A.-B. Hachmann, E. R. Angert, J. D. Helmann, *Antimicrob. Agents Chemother.* **2009**, *53*, 1598–1609.

[115] T. T. Tran, N. N. Mishra, R. Seepersaud, L. Diaz, R. Rios, A. Q. Dinh, C. Garcia-de-la-Maria, M. J. Rybak, J. M. Miro, S. A. Shelburne, P. M. Sullam, A. S. Bayer, C. A. Arias, *Antimicrob. Agents Chemother.* **2019**, *63*, DOI 10.1128/AAC.01531-18.

[116] M. Davlieva, W. Zhang, C. A. Arias, Y. Shamoo, *Antimicrob. Agents Chemother.* **2013**, *57*, 289–296.

[117] K. L. Palmer, A. Daniel, C. Hardy, J. Silverman, M. S. Gilmore, *Antimicrob. Agents Chemother.* **2011**, *55*, 3345–3356.

[118] T. Jones, M. R. Yeaman, G. Sakoulas, S.-J. Yang, R. A. Proctor, H.-G. Sahl, J. Schrenzel, Y. Q. Xiong, A. S. Bayer, *Antimicrob. Agents Chemother.* **2008**, *52*, 269–278.

[119] C. Slavetinsky, S. Kuhn, A. Peschel, *Biochim. Biophys. Acta - Mol. Cell Biol. Lipids* **2017**, *1862*, 1310–1318.

[120] T. T. Tran, J. M. Munita, C. A. Arias, *Ann. N. Y. Acad. Sci.* **2015**, *1354*, 32–53.

[121] T. O. Khatib, H. Stevenson, M. R. Yeaman, A. S. Bayer, A. Pokorny, *Antimicrob. Agents Chemother.* **2016**, *60*, 5051–5053.

[122] N. N. Mishra, A. S. Bayer, *Antimicrob. Agents Chemother.* **2013**, *57*, 1082–1085.

[123] C. J. Slavetinsky, A. Peschel, C. M. Ernst, *Antimicrob. Agents Chemother.* **2012**, *56*, 3492–3497.

[124] R. Rashid, A. Cazenave-Gassiot, I. H. Gao, Z. J. Nair, J. K. Kumar, L. Gao, K. A. Kline, M. R. Wenk, *PLoS One* **2017**, *12*, e0175886.

[125] E. Kilelee, A. Pokorny, M. R. Yeaman, A. S. Bayer, *Antimicrob. Agents Chemother.* **2010**, *54*, 4476–4479.

[126] T. T. Tran, D. Panesso, N. N. Mishra, E. Mileykovskaya, Z. Guan, J. M. Munita, J. Reyes, L. Diaz, G. M. Weinstock, B. E. Murray, Y. Shamoo, W. Dowhan, A. S. Bayer, C. A. Arias, *MBio* **2013**, *4*, e00281-13.

[127] Y. Bao, T. Sakinc, D. Laverde, D. Wobser, A. Benachour, C. Theilacker, A. Hartke, J. Huebner, *PLoS One* **2012**, *7*, e38458.

[128] C. M. Ernst, P. Staubitz, N. N. Mishra, S.-J. Yang, G. Hornig, H. Kalbacher, A. S. Bayer, D. Kraus, A. Peschel, *PLoS Pathog.* **2009**, *5*, e1000660.

[129] C. M. Ernst, C. J. Slavetinsky, S. Kuhn, J. N. Hauser, M. Nega, N. N. Mishra, C. Gekeler, A. S. Bayer, A. Peschel, *MBio* **2018**, *9*, e01659-18.

[130] D. Song, H. Jiao, Z. Liu, *Nat. Commun.* **2021**, *12*, 2927.

[131] V. Pader, S. Hakim, K. L. Painter, S. Wigneshweraraj, T. B. Clarke, A. M. Edwards, *Nat. Microbiol.* **2017**, *2*, 16194.

[132] E. V. K. Ledger, V. Pader, A. M. Edwards, *Microbiology* **2017**, *163*, 1502–1508.

[133] C. J. E. Pee, V. Pader, E. V. K. Ledger, A. M. Edwards, *Antimicrob. Agents Chemother.* **2019**, *63*, DOI 10.1128/AAC.02105-18.

[134] V. M. D'Costa, T. A. Mukhtar, T. Patel, K. Koteva, N. Waglechner, D. W. Hughes, G. D. Wright, G. De Pascale, *Antimicrob. Agents Chemother.* **2012**, *56*, 757–764.

[135] J. A. Karas, G. P. Carter, B. P. Howden, A. M. Turner, O. K. A. Paulin, J. D. Swarbrick, M. A. Baker, J. Li, T. Velkov, *J. Med. Chem.* **2020**, *63*, 13266–13290.

[136] G. Barnawi, M. Noden, J. Goodyear, J. Marlyn, O. Schneider, D. Beriashvili, S. Schulz, R. Moreira, M. Palmer, S. D. Taylor, *ACS Infect. Dis.* **2022**, *8*, 778–789.

[137] R. H. Baltz, V. Miao, S. K. Wrigley, *Nat. Prod. Rep.* **2005**, *22*, 717.

[138] C. Mahlert, F. Kopp, J. Thirlway, J. Micklefield, M. A. Marahiel, *J. Am. Chem. Soc.* **2007**, *129*, 12011–12018.

[139] M. Strieker, F. Kopp, C. Mahlert, L. O. Essen, M. A. Marahiel, *ACS Chem. Biol.* **2007**, *2*, 187–196.

[140] V. Miao, R. Brost, J. Chapple, K. She, M.-F. C.-L. Gal, R. H. Baltz, *J. Ind. Microbiol. Biotechnol.* **2006**, *33*, 129–140.

[141] G. M. Singh, P. D. Fortin, A. Koglin, C. T. Walsh, *Biochemistry* **2008**, *47*, 11310–11320.

[142] J. A. Silverman, L. I. Mortin, A. D. G. VanPraagh, T. Li, J. Alder, *J. Infect. Dis.* **2005**, *191*, 2149–2152.

[143] W. Bernhard, *Ann. Anat. - Anat. Anzeiger* **2016**, *208*, 146–150.

[144] B. Y. Lee, Antimicrobial Peptide Daptomycin and Its Inhibition by Pulmonary Surfactant : Biophysical Studies Using Model Membrane Systems, University of Waterloo, Doctoral Thesis, **2017**.

[145] R. H. Baltz, in *Nat. Prod. Discourse, Divers. Des.*, **2014**, pp. 433–454.

[146] M. Debono, B. J. Abbot, M. R. Molloy, D. S. Fukuda, A. Hunt, V. M. Daupert, F. T. Counter, J. L. Ott, C. B. Carrell, L. C. Howard, L. V. D. Boeck, R. L. Hamill, *J. Antibiot. (Tokyo).* **1988**, *41*, 1093–1105.

[147] D. C. Alexander, R. H. Baltz, P. Brain, M.-F. C. Gal, S. Doekel, X. He, V. Kulkarni, C. J. Leitheiser, V. Miao, K. T. Nguyen, I. B. Park, D. Ritz, Y. Zhang, *Antiinfective Lipopeptides*, **2006**, WO/2006/110185.

[148] D. M. M. Jaradat, *Amino Acids* **2018**, *50*, 39–68.

[149] K. J. Jensen, in *Methods Mol. Biol.*, **2013**, pp. 1–21.

[150] R. B. Merrifield, *J. Am. Chem. Soc.* **1963**, *85*, 2149–2154.

[151] F. Albericio, A. Isidro-llobet, A. Mercedes, *Chem. Rev.* **2009**, *109*, 2455–2504.

[152] M. Meldal, M. A. Juliano, A. M. Jansson, *Tetrahedron Lett.* **1997**, *38*, 2531–2534.

[153] J. T. Lundquist, J. C. Pelletier, *Org. Lett.* **2002**, *4*, 3219–3221.

[154] C. R. Lohani, B. Rasera, B. Scott, M. Palmer, S. D. Taylor, *J. Org. Chem.* **2016**, *81*, 2624–2628.

[155] H. Y. Lam, Y. Zhang, H. Liu, J. Xu, C. T. T. Wong, C. Xu, X. Li, *J. Am. Chem. Soc.* **2013**, *135*, 6272–6279.

[156] X. Li, H. Y. Lam, Y. Zhang, C. K. Chan, *Org. Lett.* **2010**, *12*, 1724–1727.

[157] C. Milne, A. Powell, J. Jim, M. Al Nakeeb, C. P. Smith, J. Micklefield, *J. Am. Chem. Soc.* **2006**, *128*, 11250–11259.

[158] P. Chevallet, P. Garrouste, B. Malawska, J. Martinez, *Tetrahedron Lett.* **1993**, *34*, 7409–7412.

[159] H. Y. Chow, K. H. L. Po, K. Jin, G. Qiao, Z. Sun, W. Ma, X. Ye, N. Zhou, S. Chen, X. Li, *ACS Med. Chem. Lett.* **2020**, *11*, 1442–1449.

[160] D. Lin, H. Y. Lam, W. Han, N. Cotroneo, B. A. Pandya, X. Li, *Bioorganic Med. Chem. Lett.* **2017**, *27*, 456–459.

[161] H. Y. Chow, K. H. L. Po, P. Gao, P. Blasco, X. Wang, C. Li, L. Ye, K. Jin, K. Chen, E. W. C. Chan, X. You, R. Yi Tsun Kao, S. Chen, X. Li, *J. Med. Chem.* **2020**, *63*, 3161–3171.

[162] C. R. Lohani, R. Taylor, M. Palmer, S. D. Taylor, *Org. Lett.* **2015**, *17*, 748–751.

[163] C. R. Lohani, R. Taylor, M. Palmer, S. D. Taylor, *Bioorg. Med. Chem. Lett.* **2015**, *25*, 5490–5494.

[164] M. Pelay-Gimeno, Y. García-Ramos, M. Jesús Martin, J. Spengler, J. M. Molina-Guijarro, S. Munt, A. M. Francesch, C. Cuevas, J. Tulla-Puche, F. Albericio, *Nat. Commun.* **2013**, *4*, 1–10.

[165] P. F. Xu, S. Li, T. J. Lu, C. C. Wu, B. Fan, G. Golfis, *J. Org. Chem.* **2006**, *71*, 4364–4373.

[166] C. T. T. Wong, H. Y. Lam, X. Li, *Org. Biomol. Chem.* **2013**, *11*, 7616–7620.

[167] P. 't Hart, L. H. J. Kleijn, G. de Bruin, S. F. Oppedijk, J. Kemmink, N. I. Martin, *Org. Biomol. Chem.* **2014**, *12*, 913–918.

[168] V. Dianati, A. Shamloo, A. Kwiatkowska, R. Desjardins, A. Soldera, R. Day, Y. L. Dory, *ChemMedChem* **2017**, *12*, 1169–1172.

[169] C. R. Lohani, R. Taylor, M. Palmer, S. D. Taylor, *Bioorg. Med. Chem. Lett.* **2015**, *25*, 5490–5494.

[170] A. Forrest Donnell, R. Kester, Y. Lou, J. Anthony, S. Remiszewski, **2016**, *2*.

[171] M. Ikubo, A. Inoue, S. Nakamura, S. Jung, M. Sayama, Y. Otani, A. Uwamizu, K. Suzuki, T. Kishi, A. Shuto, J. Ishiguro, M. Okudaira, K. Kano, K. Makide, J. Aoki, T. Ohwada, *J. Med. Chem.* **2015**, *58*, 4204–4219.

[172] E. L. Myers, R. T. Raines, *Angew. Chem. Int. Ed.* **2009**, *48*, 2359–2363.

[173] G. Barnawi, M. Noden, R. Taylor, C. Lohani, D. Beriashvili, M. Palmer, S. D. Taylor, *Pept. Sci.* **2019**, *111*, e23094.

[174] V. A. Soloshonok, K. Izawa, *Asymmetric Synthesis and Application of [Alpha]-Amino Acids*, American Chemical Society, Washington, DC :, **2009**.

[175] V. J. Hruby, G. Li, C. Haskell-Luevano, M. Shenderovich, *Biopolymers* **1997**, *43*, 219–266.

[176] Y.-D. Wu, S. Gellman, *Acc. Chem. Res.* **2008**, *41*, 1231–1232.

[177] S. M. Cowell, Y. S. Lee, J. P. Cain, V. J. Hruby, *Curr. Med. Chem.* **2004**, *11*, 2785–2798.

[178] T. M. Wood, N. I. Martin, *Medchemcomm* **2019**, *10*, 634–646.

[179] S. Eliasof, H. B. McIlvain, R. E. Petroski, A. C. Foster, J. Dunlop, *J. Neurochem.* **2001**, *77*, 550–557.

[180] C. Herdeis, H. P. Hubmann, H. Lotter, *Tetrahedron: Asymmetry* **1994**, *5*, 119–128.

[181] B. Kralt, R. Moreira, M. Palmer, S. D. Taylor, *J. Org. Chem.* **2019**, *84*, 12021–12030.

[182] S. Fan, S. Liu, S. Zhu, J. Feng, Z. Zhang, J. Huang, *Org. Lett.* **2017**, *19*, 4660–4663.

[183] K. Suzuki, D. Seebach, *Liebigs Ann. der Chemie* **1992**, *1992*, 51–61.

[184] Y. Tokairin, V. A. Soloshonok, H. Moriwaki, H. Konno, *Amino Acids* **2019**, *51*, 419–432.

[185] B. Hartzoulakis, D. Gani, *J. Chem. Soc. Perkin Trans. 1* **1994**, 2525.

[186] C. Herdeis, B. Kelm, *Tetrahedron* **2003**, *59*, 217–229.

[187] V. A. Soloshonok, H. Ueki, R. Tiwari, C. Cai, V. J. Hruby, *J. Org. Chem.* **2004**, *69*, 4984–4990.

[188] V. A. Soloshonok, C. Cai, V. J. Hruby, *Tetrahedron Asymmetry* **1999**, *10*, 4265–4269.

[189] V. A. Soloshonok, C. Cai, V. J. Hruby, *Angew. Chem. - Int. Ed.* **2000**, *39*, 2172–2175.

[190] V. A. Soloshonok, C. Cai, V. J. Hruby, L. Van Meervelt, *Tetrahedron* **1999**, *55*, 12045–12058.

[191] S. Lou, G. M. McKenna, S. A. Tymonko, A. Ramirez, T. Benkovics, D. A. Conlon, F. González-Bobes, *Org. Lett.* **2015**, *17*, 5000–5003.

[192] B. Xu, Y. Hermant, S. Yang, P. W. R. Harris, M. A. Brimble, *Chem. – A Eur. J.* **2019**, *25*, 14101–14107.

[193] D. Chen, H. Y. Chow, K. H. L. Po, W. Ma, E. L. Y. Leung, Z. Sun, M. Liu, S. Chen, X. Li, *Org. Lett.* **2019**, *21*, 5639–5644.

[194] I. Jako, P. Uiber, A. Mann, C. G. Wermuth, T. Boulanger, B. Norberg, G. Evrard, F. Durant, *J. Org. Chem.* **1991**, *56*, 5729–5733.

[195] S. Ranatunga, C. H. A. Tang, C. C. A. Hu, J. R. Del Valle, *J. Org. Chem.* **2012**, *77*, 9859–9864.

[196] T. Spangenberg, A. Schoenfelder, B. Breit, A. Mann, *European J. Org. Chem.* **2010**, *2010*, 6005–6018.

[197] S. Kumar, C. Flamant-Robin, Q. Wang, A. Chiaroni, N. A. Sasaki, *J. Org. Chem.* **2005**, *70*, 5946–5953.

[198] S. Hanessian, W. Wang, Y. Gai, *Tetrahedron Lett.* **1996**, *37*, 7477–7480.

[199] S. Hanessian, K. Sumi, *Synthesis (Stuttg).* **1991**, *1991*, 1083–1089.

[200] G. Pattenden, N. J. Ashweek, C. A. G. Baker-Glenn, J. Kempson, G. M. Walker, J. G. K. Yee, *Org. Biomol. Chem.* **2008**, *6*, 1478.

[201] D. C. Alexander, R. H. Baltz, P. Brain, M.-F. Coeffet-le Gal, S. Doekel, X. He, V. Kulkarni, C. J. Leitheiser, V. Miao, K. T. Nguyen, I. B. Park, D. Ritz, Y. Zhang, *Antiinfective Lipopeptides*, **2006**, WO/2006/110185.

[202] J. A. Marshall, S. Beaudoin, *J. Org. Chem.* **1996**, *61*, 581–586.

[203] J. Rush, C. R. Bertozzi, *Org. Lett.* **2006**, *8*, 131–134.

[204] K. J. Eash, M. S. Pulia, L. C. Wieland, R. S. Mohan, *J. Org. Chem.* **2000**, *65*, 8399–8401.

[205] P. P. Pradhan, J. M. Bobbitt, W. F. Bailey, *J. Org. Chem.* **2009**, *74*, 9524–9527.

[206] X. Cong, F. Hu, K. G. Liu, Q. J. Liao, Z. J. Yao, *J. Org. Chem.* **2005**, *70*, 4514–4516.

[207] S. Jiang, P. Li, C. C. Lai, J. A. Kelley, P. P. Roller, *J. Org. Chem.* **2006**, *71*, 7307–7314.

[208] G. Han, V. J. Hruby, *Tetrahedron Lett.* **2001**, *42*, 4281–4283.

[209] S. H. Bertz, G. Dabbagh, J. M. Cook, V. Honkan, *J. Org. Chem.* **1984**, *49*, 1739–1743.

[210] S. H. Bertz, G. Dabbagh, A. M. Mujsce, *J. Am. Chem. Soc.* **1991**, 631–636.

[211] S. Takano, Y. Sekiguchi, K. Ogasawara, *Chem. Commun.* **1988**, 449–450.

[212] C. Flamant-Robin, Q. Wang, A. Chiaroni, N. A. Sasaki, *Tetrahedron* **2002**, *58*, 10475–10484.

[213] S. H. Bertz, C. P. Gibson, G. Dabbagh, *Tetrahedron Lett.* **1987**, *28*, 4251–4254.

[214] H. O. House, J. M. Wilkins, *J. Org. Chem.* **1978**, *43*, 2443–2454.

[215] W. H. Chiou, A. Schoenfelder, L. Sun, A. Mann, I. Ojima, *J. Org. Chem.* **2007**, *72*, 9418–9425.

[216] H. O. House, C.-Y. Chu, J. M. Wilkins, M. J. Umen, *J. Org. Chem.* **1975**, *40*, 1460–1469.

[217] J. Grünewald, S. A. Sieber, C. Mahlert, U. Linne, M. A. Marahiel, *J. Am. Chem. Soc.* **2004**, *126*, 17025–17031.

[218] F. Kopp, J. Gru, C. Mahlert, M. A. Marahiel, V. Philipps-uni, *Biochemistry* **2006**, *45*, 10474–10481.

[219] K. T. Nguyen, D. Ritz, J.-Q. Gu, D. Alexander, M. Chu, V. Miao, P. Brian, R. H. Baltz, *Proc. Natl. Acad. Sci.* **2006**, *103*, 17462–17467.

[220] E. M. Scull, C. Bandari, B. P. Johnson, E. D. Gardner, M. Tonelli, J. You, R. H. Cichewicz, S. Singh, *Appl. Microbiol. Biotechnol.* **2020**, *104*, 7853–7865.

[221] N. Mupparapu, Y. C. Lin, T. H. Kim, S. I. Elshahawi, *Chem. – A Eur. J.* **2021**, *27*, 4176–4182.

[222] R. Moreira, G. Barnawi, D. Beriashvili, M. Palmer, S. D. Taylor, *Bioorg. Med. Chem.* **2019**, *27*, 240–246.

[223] G. Barnawi, M. Noden, R. Taylor, C. Lohani, D. Beriashvili, M. Palmer, S. D. Taylor, *Pept. Sci.* **2019**, *111*, e23094.

[224] E. D. Goddard-Borger, R. V. Stick, *Org. Lett.* **2011**, *13*, 2514–2514.

[225] B. Kralt, R. Moreira, M. Palmer, S. D. Taylor, *J. Org. Chem.* **2020**, *85*, 2213–2219.

[226] J. Hirano, K. Hamase, K. Zaitsu, *Tetrahedron* **2006**, *62*, 10065–10071.

[227] D. P. Fairlie, H. N. Hoang, T. A. Hill, *Angew. Chem. Int. Ed.* **2020**, anie.202012643.

[228] C. P. Jones, K. W. Anderson, S. L. Buchwald, *J. Org. Chem.* **2007**, *72*, 7968–7973.

[229] J. Haesslein, I. Baholet, M. Fortin, A. Iltis, J. Khider, M. Periers, J. Vevert, *Bioorg. Med. Chem. Lett.* **2000**, *10*, 1487–1490.

[230] R. Moreira, S. D. Taylor, *Amino Acids* **2020**, *52*, 987–998.

[231] J. C. Pelletier, J. T. Lundquist, *Org. Lett.* **2001**, *3*, 781–783.

[232] D. A. Gray, M. Wenzel, *Antibiotics* **2020**, *9*, 17.

[233] J. Zhang, W. R. P. Scott, F. Gabel, M. Wu, R. Desmond, J. Bae, G. Zaccai, W. R. Algar, S. K. Straus, *Biochim. Biophys. Acta - Proteins Proteomics* **2017**, *1865*, 1490–1499.

[234] M. A. Kreutzberger, A. Pokorny, P. F. Almeida, *Langmuir* **2017**, *33*, 13669–13679.

[235] T. Zhang, J. K. Muraih, N. Tishbi, J. Herskowitz, R. L. Victor, J. Silverman, S. Uwumarenogie, S. D. Taylor, M. Palmer, E. Mintzer, *J. Biol. Chem.* **2014**, *289*, 11584–11591.

[236] D. Beriashvili, R. Taylor, B. Kralt, N. Abu Mazen, S. D. Taylor, M. Palmer, *Chem. Phys. Lipids* **2018**, *216*, 73–79.

[237] R. Moreira, S. D. Taylor, *Amino Acids* **2020**, *52*, 987–998.

[238] R. Moreira, J. Wolfe, S. D. Taylor, *Org. Biomol. Chem.* **2021**, *19*, 3144–3153.

[239] I. Wiegand, K. Hilpert, R. E. W. Hancock, *Nat. Protoc.* **2008**, *3*, 163–175.

[240] P. D'Arrigo, L. de Ferra, G. Pedrocchi-Fantoni, D. Scarcelli, S. Servi, A. Strini, *J. Chem. Soc. Perkin Trans. 1* **1996**, 2657.

[241] E. Baer, D. Buchnea, *J. Biol. Chem.* **1958**, *232*, 895–901.

[242] R. M. Saunders, H. P. Schwarz, *J. Am. Chem. Soc.* **1966**, *88*, 3844–3847.

[243] P. Woolley, H. Eibl, *Chem. Phys. Lipids* **1988**, *47*, 55–62.

[244] M.-C. Gagnon, S. Dautrey, X. Bertrand, M. Auger, J.-F. Paquin, *European J. Org. Chem.* **2017**, *2017*, 6401–6407.

[245] D. R. Kodali, A. Tercyak, D. A. Fahey, D. M. Small, *Chem. Phys. Lipids* **1990**, *52*, 163–170.

[246] R. Wohlgemuth, N. Waespe-Šarčević, J. Seelig, *Biochemistry* **1980**, *19*, 3315–3321.

[247] K. S. Bruzik, G. Salamonczyk, W. J. Stec, *J. Org. Chem.* **1986**, *51*, 2368–2370.

[248] K. Murakami, E. J. Molitor, H. W. Liu, *J. Org. Chem.* **1999**, *64*, 648–651.

[249] P. J. Pedersen, S. K. Adolph, A. K. Subramanian, A. Arouri, T. L. Andresen, O. G. Mouritsen, R. Madsen, M. W. Madsen, G. H. Peters, M. H. Clausen, *J. Med. Chem.* **2010**, *53*, 3782–3792.

[250] P. J. Pedersen, M. S. Christensen, T. Ruysschaert, L. Linderoth, T. L. Andresen, F. Melander, O. G. Mouritsen, R. Madsen, M. H. Clausen, *J. Med. Chem.* **2009**, *52*, 3408–

3415.

[251] S. Burugupalli, M. B. Richardson, S. J. Williams, *Org. Biomol. Chem.* **2017**, *15*, 7422–7429.

[252] Z. J. Struzik, A. N. Weerts, J. Storch, D. H. Thompson, *Chem. Phys. Lipids* **2020**, *231*, 104933.

[253] J. D. Lee, M. Ueno, Y. Miyajima, H. Nakamura, *Org. Lett.* **2007**, *9*, 323–326.

[254] K. Fukase, T. Matsumoto, N. Ito, T. Yoshimura, S. Kotani, S. Kusumoto, *Bull. Chem. Soc. Jpn.* **1992**, *65*, 2643–2654.

[255] A. Plueckthun, E. A. Dennis, *Biochemistry* **1982**, *21*, 1743–1750.

[256] A. M. Kelly, Y. Pérez-Fuertes, J. S. Fossey, S. L. Yeste, S. D. Bull, T. D. James, *Nat. Protoc.* **2008**, *3*, 215–219.

[257] M. T. Lee, W. C. Hung, M. H. Hsieh, H. Chen, Y. Y. Chang, H. W. Huang, *Biophys. J.* **2017**, *113*, 82–90.

[258] S. T. Henriques, H. Peacock, A. H. Benfield, C. K. Wang, D. J. Craik, *J. Am. Chem. Soc.* **2019**, *141*, 20460–20469.

[259] H. S. Martin, K. A. Podolsky, N. K. Devaraj, *ChemBioChem* **2021**, 1–11.

[260] O. M. Schütte, L. J. Patalag, L. M. C. Weber, A. Ries, W. Römer, D. B. Werz, C. Steinem, *Biophys. J.* **2015**, *108*, 2775–2778.

[261] L. H. J. Kleijn, S. F. Oppedijk, P. 't Hart, R. M. van Harten, L. A. Martin-Visscher, J. Kemmink, E. Breukink, N. I. Martin, *J. Med. Chem.* **2016**, *59*, 3569–3574.

[262] M. Boaretti, P. Canepari, *New Microbiol.* **2000**, *23*, 305–17.

[263] K. H. L. Po, H. Y. Chow, Q. Cheng, B. K. Chan, X. Deng, S. Wang, E. W. C. Chan, H. Kong, K. F. Chan, X. Li, S. Chen, *Nat. Sci.* **2021**, *1*, 1–9.

[264] P. L. Yeagle, *Biochim. Biophys. Acta - Biomembr.* **2014**, *1838*, 1548–1559.

[265] J. Lindberg, J. Ekeroth, P. Konradsson, *J. Org. Chem.* **2002**, *67*, 194–199.

[266] R. V. K. Cochrane, F. M. Alexander, C. Boland, S. K. Fetics, M. Caffrey, S. A. Cochrane, *Chem. Commun.* **2020**, *56*, 8603–8606.

[267] S. H. Shabbir, C. J. Regan, E. V. Anslyn, *Proc. Natl. Acad. Sci.* **2009**, *106*, 10487–10492.

[268] D. J. Keith, S. D. Townsend, *J. Am. Chem. Soc.* **2019**, *141*, 12939–12945.

[269] R. H. Baltz, *Curr. Opin. Chem. Biol.* **2009**, *13*, 144–151.

[270] "Critical Micelle Concentrations (CMCs)," can be found under https://avantilipids.com/tech-support/physical-properties/cmcs, **n.d.**

[271] A. M. Thompson, H. S. Sutherland, B. D. Palmer, I. Kmentova, A. Blaser, S. G. Franzblau, B. Wan, Y. Wang, Z. Ma, W. A. Denny, *J. Med. Chem.* **2011**, *54*, 6563–6585.

[272] J. G. Goddard, D. H. Picker, S. R. Umansky, S. Price, J. C. Wijkmans, E. A. Boyd, A. D. Baxter, *Composition Containing Lysophosphatidic Acids Which Inhibit Apoptosis and Uses Thereof*, **2007**, US 7,259.273 B1.

[273] J. C. Sowden, H. O. L. Fischer, *J. Am. Chem. Soc.* **1941**, *63*, 3244–3248.

[274] H. Tateishi, K. Anraku, R. Koga, Y. Okamoto, M. Fujita, M. Otsuka, *Org. Biomol. Chem.* **2014**, *12*, 5006–5022.

[275] I. R. Duclos, *Novel Lipase Inhibitors, Reporter Substrates and Uses Thereof*, **2013**, WO2013177492A2.

[276] T. S. Elliott, J. Nemeth, S. A. Swain, S. J. Conway, *Tetrahedron Asymmetry* **2009**, *20*, 2809–2813.

[277] S. F. Martin, J. A. Josey, Y.-L. Wong, D. W. Dean, *J. Org. Chem.* **1994**, *59*, 4805–4820.

[278] R. Moreira, S. D. Taylor, *Angew. Chem. Int. Ed.* **2022**, *61*, e202114858.

[279] K. Kalyanasundaram, J. K. Thomas, *J. Phys. Chem.* **1977**, *81*, 2176–2180.

[280] C. L. Franklin, H. Li, S. F. Martin, *J. Org. Chem.* **2003**, *68*, 7298–7307.

[281] S. J. Yang, N. N. Mishra, A. Rubio, A. S. Bayer, *Antimicrob. Agents Chemother.* **2013**, *57*, 5658–5664.

[282] N. N. Mishra, J. McKinnell, M. R. Yeaman, A. Rubio, C. C. Nast, L. Chen, B. N. Kreiswirth, A. S. Bayer, *Antimicrob. Agents Chemother.* **2011**, *55*, 4012–4018.

[283] N. N. Mishra, A. Rubio, C. C. Nast, A. S. Bayer, *Int. J. Microbiol.* **2012**, *2012*, 1–6.

[284] R. Rehal, R. D. Barker, Z. Lu, T. T. Bui, B. Demé, G. Hause, C. Wölk, R. D. Harvey, *Biochim. Biophys. Acta - Biomembr.* **2021**, *1863*, 183571.

[285] P. P. M. Bonsen, G. H. de Haas, L. L. M. van Deenen, *Biochemistry* **1967**, *6*, 1114–1120.

[286] J. G. Molotkovsky, L. D. Bergelson, *Chem. Phys. Lipids* **1968**, *2*, 1–10.

[287] P. Fodran, A. J. Minnaard, *Org. Biomol. Chem.* **2013**, *11*, 6919.

[288] J. Tack, R. Wyrwa, T. Laube, M. Schnalbelrauch, J. Weisser, C. Volkel, *Water-Soluble L-DOPA Esters*, **2016**, WO 2016/155888 A1.

[289] J. F. Tocanne, H. M. Verheij, J. A. F. Op Den Kamp, L. L. M. Van Deenen, *Chem. Phys. Lipids* **1974**, *13*, 389–403.

[290] M. J. Martinelli, R. Vaidyanathan, J. M. Pawlak, N. K. Nayyar, U. P. Dhokte, C. W. Doecke, L. M. H. Zollars, E. D. Moher, V. Van Khau, B. Košmrlj, *J. Am. Chem. Soc.* **2002**, *124*, 3578–3585.

[291] K. Neimert-Andersson, E. Blomberg, P. Somfai, *J. Org. Chem.* **2004**, *69*, 3746–3752.

[292] M. Adinolfi, G. Barone, L. Guariniello, A. Iadonisi, *Tetrahedron Lett.* **2000**, *41*, 9305–9309.

[293] M. Govindarajan, *Carbohydr. Res.* **2020**, *497*, 108151.

[294] C. Vargeese, *Nucleic Acids Res.* **1998**, *26*, 1046–1050.

[295] M. A. Blaskovich, G. Evindar, N. G. W. Rose, S. Wilkinson, Y. Luo, G. A. Lajoie, *J. Org. Chem.* **1998**, *63*, 3631–3646.

[296] M. Strieker, M. A. Marahiel, *ChemBioChem* **2009**, *10*, 607–616.

[297] K. Shimamoto, Y. Shigeri, Y. Yasuda-Kamatani, B. Lebrun, N. Yumoto, T. Nakajima, *Bioorg. Med. Chem. Lett.* **2000**, *10*, 2407–2410.

[298] H. Fu, S. H. H. Younes, M. Saifuddin, P. G. Tepper, J. Zhang, E. Keller, A. Heeres, W. Szymanski, G. J. Poelarends, *Org. Biomol. Chem.* **2017**, *15*, 2341–2344.

[299] M. Leuenberger, A. Ritler, A. Simonin, M. A. Hediger, M. Lochner, *ACS Chem. Neurosci.* **2016**, *7*, 534–539.

[300] M. Tsakos, L. L. Clement, E. S. Schaffert, F. N. Olsen, S. Rupiani, R. Djurhuus, W. Yu, K. M. Jacobsen, N. L. Villadsen, T. B. Poulsen, *Angew. Chem. Int. Ed.* **2016**, *55*, 1030–1035.

[301] N. Bionda, M. Cudic, L. Barisic, M. Stawikowski, R. Stawikowska, D. Binetti, P. Cudic, *Amino Acids* **2012**, *42*, 285–293.

[302] G. Cardillo, L. Gentilucci, A. Tolomelli, C. Tomasini, *Synlett* **1999**, 1727–1730.

[303] L. von Eckardstein, D. Petras, T. Dang, S. Cociancich, S. Sabri, S. Grätz, D. Kerwat, M. Seidel, A. Pesic, P. C. Dorrestein, M. Royer, J. B. Weston, R. D. Süssmuth, *Chem. - A Eur. J.* **2017**, *23*, 15316–15321.

[304] Y. Zhang, H. Farrants, X. Li, *Chem. - An Asian J.* **2014**, *9*, 1752–1764.

[305] D. L. Boger, R. J. Lee, P. Y. Bounaud, P. Meier, *J. Org. Chem.* **2000**, *65*, 6770–6772.

[306] W. Jiang, J. Wanner, R. J. Lee, P. Y. Bounaud, D. L. Boger, *J. Am. Chem. Soc.* **2003**, *125*, 1877–1887.

[307] A. Guzmán-Martínez, M. VanNieuwenhze, *Synlett* **2007**, *2007*, 1513–1516.

[308] A. M. Hafez, T. Dudding, T. R. Wagerle, M. H. Shah, A. E. Taggi, T. Lectka, *J. Org. Chem.* **2003**, *68*, 5819–5825.

[309] D. Wong, C. M. Taylor, *Tetrahedron Lett.* **2009**, *50*, 1273–1275.

[310] L. Harris, S. P. H. Mee, R. H. Furneaux, G. J. Gainsford, A. Luxenburger, *J. Org. Chem.* **2011**, *76*, 358–372.

[311] E. Abraham, J. W. B. Cooke, S. G. Davies, A. Naylor, R. L. Nicholson, P. D. Price, A. D. Smith, *Tetrahedron* **2007**, *63*, 5855–5872.

[312] H. Menard, J. Lessard, *J. Chem. Eng. Data* **1978**, *23*, 64–65.

[313] D. Gwon, H. Hwang, H. K. Kim, S. R. Marder, S. Chang, *Chem. - A Eur. J.* **2015**, *21*, 17200–17204.

[314] M. Zhao, J. Li, E. Mano, Z. Song, D. M. Tschaen, E. J. J. Grabowski, P. J. Reider, *J. Org. Chem.* **1999**, *64*, 2564–2566.

[315] J. M. Bobbitt, *TCIMail* **2010**, 2–15.

[316] V. F. Pozdnev, *Tetrahedron Lett.* **1995**, *36*, 7115–7118.

[317] K. Okano, K. I. Okuyama, T. Fukuyama, H. Tokuyama, *Synlett* **2008**, 1977–1980.

[318] X. Xia, P. Toy, *Synlett* **2014**, *25*, 2787–2790.

[319] B. Kralt, Lipodepsipeptide Antibiotics: Total Synthesis and Mechanism of Action Studies Using 19F-NMR, University of Waterloo, Doctoral Thesis, **2020**.

[320] C. R. Lohani, J. Soley, B. Kralt, M. Palmer, S. D. Taylor, *J. Org. Chem.* **2016**, *81*, 11831–11840.

[321] T. Kaneda, *Microbiol. Rev.* **1991**, *55*, 288–302.

[322] T. Wüster, N. Kaczybura, R. Brückner, M. Keller, *Tetrahedron* **2013**, *69*, 7785–7809.

[323] Z. Yang, M. Ma, C. H. Yang, Y. Gao, Q. Zhang, Y. Chen, *J. Nat. Prod.* **2016**, *79*, 2408–2412.

[324] J. A. Bodkin, M. D. McLeod, *J. Chem. Soc. Perkin 1* **2002**, *24*, 2733–2746.

[325] K. L. Reddy, K. R. Dress, K. B. Sharpless, *Tetrahedron Lett.* **1998**, *39*, 3667–3670.

[326] R. Moreira, S. D. Taylor, *Org. Lett.* **2018**, *20*, 7717–7720.

[327] G. Li, H. T. Chang, K. Barry Sharpless, *Angew. Chem. Int. Ed.* **1996**, *35*, 451–454.

[328] D. J. Berrisford, C. Bolm, K. B. Sharpless, *Angew. Chem. Int. Ed. Engl.* **1995**, *34*, 1059–1070.

[329] O. Babot, T. Charvat, Y. Landais, *J. Org. Chem.* **1999**, *64*, 9613–9624.

[330] T. J. Donohoe, P. D. Johnson, M. Keenan, *Chem. Commun.* **2001**, 2078–2079.

[331] T. J. Donohoe, P. D. Johnson, A. Cowley, M. Keenan, *J. Am. Chem. Soc.* **2002**, *124*, 12934–12935.

[332] Z. P. Demko, M. Bartsch, K. B. Sharpless, *Org. Lett.* **2000**, 2221–2223.

[333] D. Raatz, C. Innertsberger, O. Reiser, *Synlett* **1999**, *6*, 1907–1910.

[334] W. P. Griffith, N. T. McManus, A. C. Skapski, A. D. White, *Inorganica Chim. Acta* **1985**, *105*, L11.

[335] V. Nesterenko, J. T. Byers, P. J. Hergenrother, *Org. Lett.* **2003**, 1483–1486.

[336] K. Laxma Reddy, K. Barry Sharpless, *J. Am. Chem. Soc.* **1998**, *120*, 1207–1217.

[337] P. O'Brien, S. A. Osborne, D. D. Parker, *J. Chem. Soc. Perkin Trans. 1* **1998**, 2519–2526.

[338] G. Li, H. H. Angert, K. B. Sharpless, *Angew. Chem. Int. Ed.* **1996**, *35*, 2813–2817.

[339] H. Han, C.-W. Cho, K. D. Janda, *Chem. - A Eur. J.* **1999**, *5*, 1565–1569.

[340] E. C. Shuter, H. Duong, C. A. Hutton, M. D. McLeod, *Org. Biomol. Chem.* **2007**, *5*, 3183–3189.

[341] J. A. Bodkin, G. B. Bacskay, M. D. McLeod, *Org. Biomol. Chem.* **2008**, *6*, 2544.

[342] M. Ito, C. W. Clark, M. Mortimore, J. B. Goh, S. F. Martin, *J. Am. Chem. Soc.* **2001**, *123*, 8003–8010.

[343] I. Duttagupta, J. Bhadra, S. Kr, S. Sinha, *Tetrahedron Lett.* **2016**, *57*, 3858–3861.

[344] W. Wang, J. S. McMurray, *Tetrahedron Lett.* **1999**, *40*, 2501–2504.

[345] K. Tanemura, T. Suzuki, T. Horaguchi, *J. Chem. Soc. Perkin Trans. 1* **1992**, *1*, 2997.

[346] K. C. Nicolaou, A. A. Estrada, M. Zak, S. H. Lee, B. S. Safina, *Angew. Chem. Int. Ed.* **2005**, *44*, 1378–1382.

[347] M. Di Gioia, A. Leggio, A. Le Pera, A. Liguori, F. Perri, C. Siciliano, *European J. Org. Chem.* **2004**, *2004*, 4437–4441.

[348] J. W. Fisher, K. L. Trinkle, *Tetrahedron Lett.* **1994**, *35*, 2505–2508.

[349] I. Ohtani, T. Kusumi, Y. Kashman, H. Kakisawa, *J. Am. Chem. Soc.* **1991**, *113*, 4092–4096.

[350] Y. Kuroda, S. Harada, A. Oonishi, H. Kiyama, Y. Yamaoka, K. I. Yamada, K. Takasu, *Angew. Chem. Int. Ed.* **2016**, *55*, 13137–13141.

[351] H. Zaimoku, T. Taniguchi, H. Ishibashi, *Org. Lett.* **2012**, *14*, 1656–1658.

[352] R. Moreira, M. Diamandas, S. D. Taylor, *J. Org. Chem.* **2019**, *84*, 15476–15485.

[353] P. Thordarson, *Chem. Soc. Rev.* **2011**, *40*, 1305–1323.

[354] S. Yu, P. G. R. Harding, N. Smith, F. Possmayer, *Lipids* **1983**, *18*, 522–529.

[355] H.-H. Tan, A. Makino, K. Sudesh, P. Greimel, T. Kobayashi, *Angew. Chem. Int. Ed.* **2012**, *124*, 548–550.

[356] H. Zhang, Q. Fan, Y. E. Wang, C. R. Neal, Y. Y. Zuo, *Biochim. Biophys. Acta - Biomembr.* **2011**, *1808*, 1832–1842.

[357] Y. He, J. Li, N. Yin, P. S. Herradura, L. Martel, Y. Zhang, A. L. Pearson, V. Kulkarni, C. Mascio, K. Howland, J. A. Silverman, D. D. Keith, C. A. Metcalf, *Bioorg. Med. Chem. Lett.* **2012**, *22*, 6248–6251.

[358] S. Singh, M. W. Pennington, *Tetrahedron Lett.* **2003**, *44*, 2683–2685.

[359] R. V. K. Cochrane, F. M. Alexander, C. Boland, S. K. Fetics, M. Caffrey, S. A. Cochrane, *Chem. Commun.* **2020**, *56*, 8603–8606.

[360] T. Zhang, S. Taylor, M. Palmer, J. Duhamel, *Biophys. J.* **2016**, *111*, 1267–1277.

[361] M. Diamandas, R. Moreira, S. D. Taylor, *Org. Lett.* **2021**, *23*, 3048–3052.

[362] N. Kovalenko, G. K. Howard, J. A. Swain, Y. Hermant, A. J. Cameron, G. M. Cook, S. A. Ferguson, L. A. Stubbing, P. W. R. Harris, M. A. Brimble, *Front. Chem.* **2021**, *9*, 1–11.

[363] V. K. Mishra, J. Buter, M. S. Blevins, M. D. Witte, I. Van Rhijn, D. B. Moody, J. S. Brodbelt, A. J. Minnaard, *Org. Lett.* **2019**, *21*, 5126–5131.

[364] K. Hosoda, M. Ohya, T. Kohno, T. Maeda, S. Endo, K. Wakamatsu, *J. Biochem.* **1996**, *119*, 226–230.

[365] A. Pokorny, T. O. Khatib, H. Stevenson, *J. Phys. Chem. B* **2018**, *122*, 9137–9146.

[366] M. V. Golynskiy, W. A. Gunderson, M. P. Hendrich, S. M. Cohen, *Biochemistry* **2006**, *45*, 15359–15372.

Appendices

Appendix A Supplementary data for Chapter 2
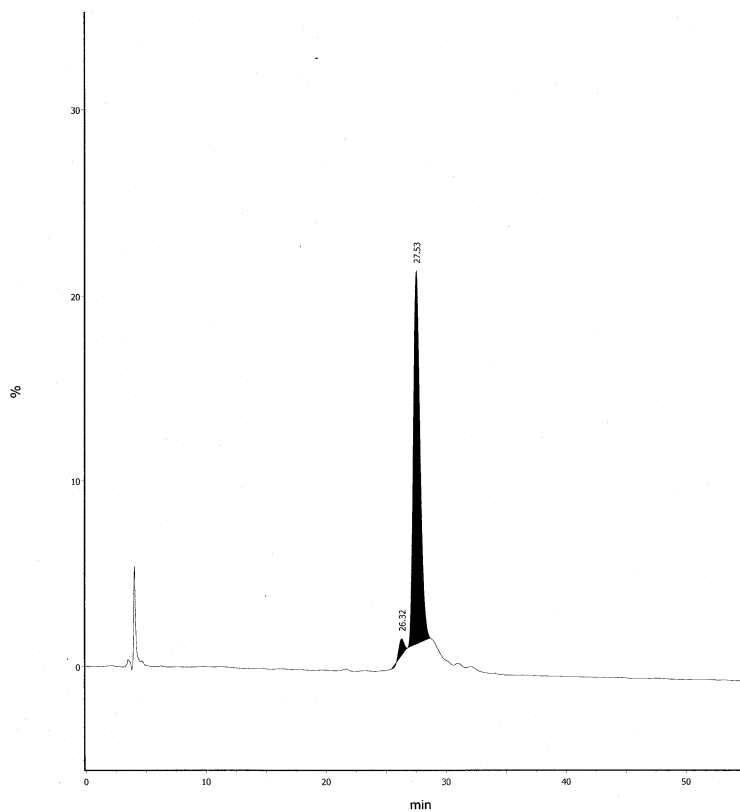
Peak	Fill	Peak Name	t_R	t_S	t_E	H (%)	H_{Norm}	Area	A_{Norm}
1	■		26.32	25.49	26.74	0.89	4.22	24.64	3.01
2	■		27.53	26.74	28.69	20.18	95.78	795.15	96.99
						21.07	100.00	819.79	100.00

Figure A.1. Analytical HPLC trace of peptide **2.1** (90:10 ACN: 0.1 % TFA in H_2O to 10:90 ACN:0.1 % TFA in H_2O over 50 min).
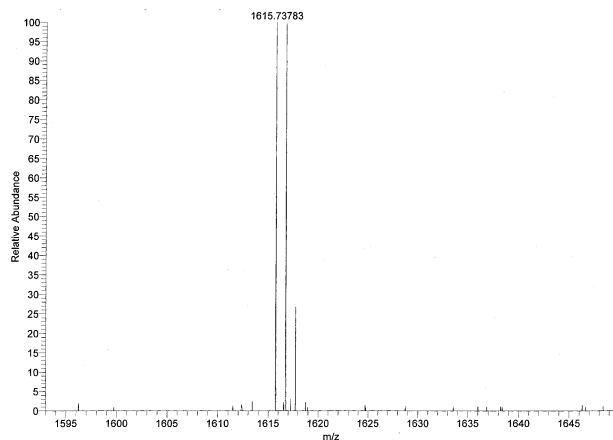
Elemental composition search on mass 1615.73783

m/z= 1610.73783-1620.73783

m/z	Theo. Mass	Delta (ppm)	RDB equiv.	Composition
1615.73783	1615.73871	-0.55	31.5	$C_{73} H_{103} O_{24} N_{18}$
	1615.72614	7.24	32.0	$C_{72} H_{101} O_{24} N_{19}$
	1615.75129	-8.33	31.0	$C_{74} H_{105} O_{24} N_{17}$
	1615.71490	14.19	32.0	$C_{73} H_{101} O_{25} N_{17}$
	1615.76252	-15.28	31.0	$C_{73} H_{105} O_{23} N_{19}$
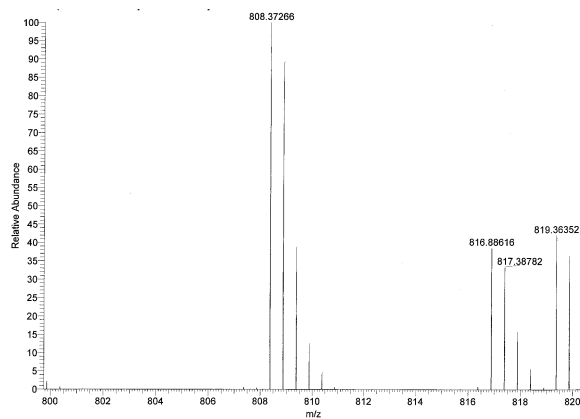
Elemental composition search on mass 808.37266

m/z= 803.37266-813.37266

m/z	Theo. Mass	Delta (ppm)	RDB equiv.	Composition
808.37266	808.37299	-0.41	31.0	$C_{73} H_{104} O_{24} N_{18}$
	808.36671	7.37	31.5	$C_{72} H_{102} O_{24} N_{19}$
	808.36109	14.31	31.5	$C_{73} H_{102} O_{25} N_{17}$
	808.35480	22.09	32.0	$C_{72} H_{100} O_{25} N_{18}$

Figure A.2 HRMS of peptide **2.1**. The spectrum on the left is for the singly charged species and the spectrum on the right is for the doubly charged species. HRMS-ESI$^+$ (m/z) calcd for $C_{73}H_{103}N_{18}O_{24}$ (M+H$^+$), 1615.7387; found, 1615.7378. HRMS-ESI$^+$ (m/z) calcd for $C_{73}H_{103}N_{18}O_{24}$ (M+2H)$^{2+}$, 808.3730; found, 808.3727.
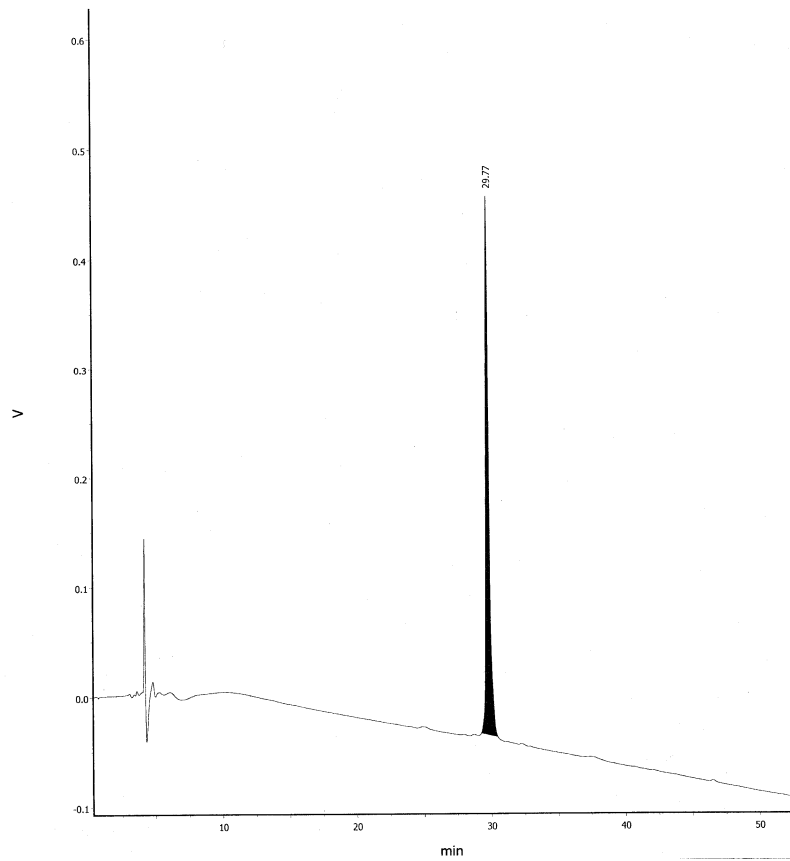
Figure A.3 Analytical HPLC chromatogram of peptide **2.2** (90:10 ACN: 0.1 % TFA in H2O to 10:90 ACN:0.1 % TFA in H2O over 50 min).
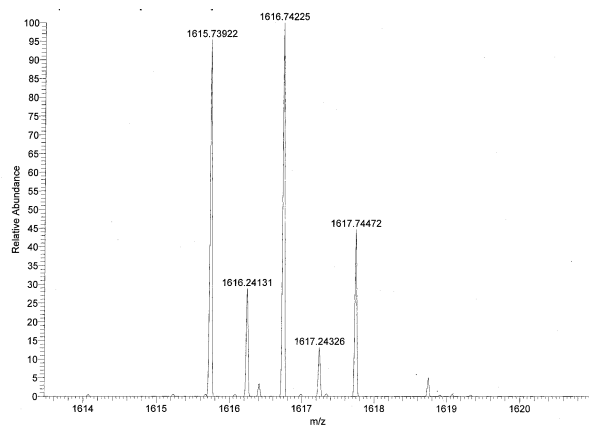
Elemental composition search on mass 1615.73922

m/z= 1610.73922-1620.73922

m/z	Theo. Mass	Delta (ppm)	RDB equiv.	Composition
1615.73922	1615.73871	0.31	31.5	$C_{73} H_{103} O_{24} N_{18}$
	1615.75129	-7.47	31.0	$C_{74} H_{105} O_{24} N_{17}$
	1615.72614	8.10	32.0	$C_{72} H_{101} O_{24} N_{19}$
	1615.76252	-14.42	31.0	$C_{73} H_{105} O_{23} N_{19}$
	1615.71490	15.05	32.0	$C_{73} H_{101} O_{25} N_{17}$
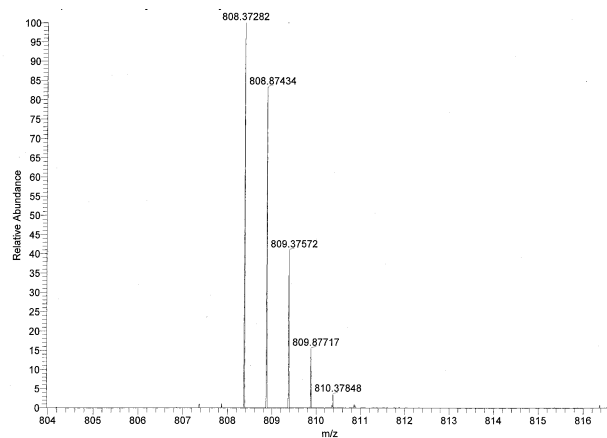
Elemental composition search on mass 808.37282

m/z= 803.37282-813.37282

m/z	Theo. Mass	Delta (ppm)	RDB equiv.	Composition
808.37282	808.37299	-0.22	31.0	$C_{73} H_{104} O_{24} N_{18}$
	808.36671	7.56	31.5	$C_{72} H_{102} O_{24} N_{19}$
	808.36109	14.51	31.5	$C_{73} H_{102} O_{25} N_{17}$
	808.35480	22.29	32.0	$C_{72} H_{100} O_{25} N_{18}$

Figure A.4 HRMS of peptide **2.2**. The spectrum on the left is for the singly charged species and the spectrum on the right is for the doubly charged species. HRMS-ESI+ (m/z) calcd for $C_{73}H_{103}N_{18}O_{24}$ $(M+H)^+$, 1615.7387; found, 1615.7392. . HRMS-ESI+ (m/z) calcd for $C_{73}H_{104}N_{18}O_{24}$ $(M+2H)^{2+}$, 808.3730; found, 808.3728.
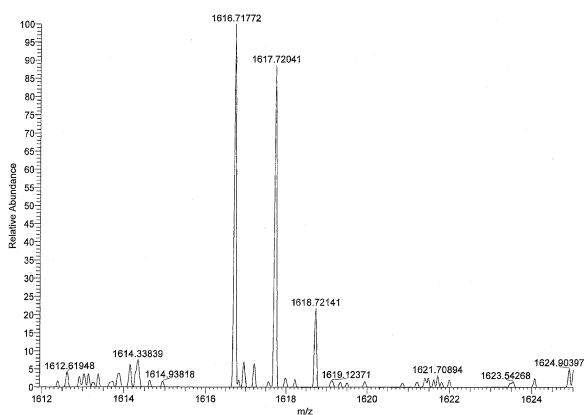
Elemental composition search on mass 1616.71772

m/z= 1611.71772-1621.71772

m/z	Theo. Mass	Delta (ppm)	RDB equiv.	Composition
1616.71772	1616.72138	-2.27	32.0	$C_{71} H_{100} O_{24} N_{20}$
	1616.72273	-3.10	31.5	$C_{73} H_{102} O_{25} N_{17}$
	1616.71149	3.85	31.5	$C_{74} H_{102} O_{26} N_{15}$
	1616.71015	4.68	32.0	$C_{72} H_{100} O_{25} N_{18}$
	1616.73396	-10.05	31.5	$C_{72} H_{102} O_{24} N_{19}$
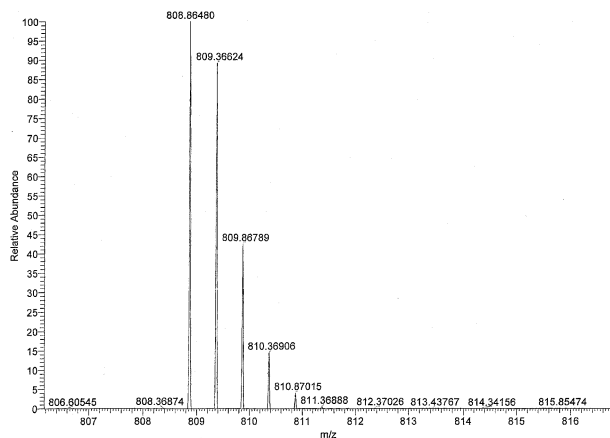
Elemental composition search on mass 808.86480

m/z= 803.86480-813.86480

m/z	Theo. Mass	Delta (ppm)	RDB equiv.	Composition
808.86480	808.86500	-0.25	31.0	$C_{73} H_{103} O_{25} N_{17}$
	808.86433	0.58	31.5	$C_{71} H_{101} O_{24} N_{20}$
	808.85939	6.69	31.0	$C_{74} H_{103} O_{26} N_{15}$
	808.87062	-7.19	31.0	$C_{72} H_{103} O_{24} N_{19}$
	808.85871	7.52	31.5	$C_{72} H_{101} O_{25} N_{18}$

Figure A.5 HRMS for ent-Dap-K6-E12-W13. The spectrum on the left is for the singly charged species and the spectrum on the right is for the doubly charged species. HRMS-ESI+ (m/z) calcd for $C_{73}H_{102}N_{17}O_{25}$ (M+H)+, 1615.7227; found, 1615.7177. HRMS-ESI+ (m/z) calcd for $C_{73}H_{103}N_{17}O_{25}$ (M+2H)2+, 808.8650; found, 808.8648.
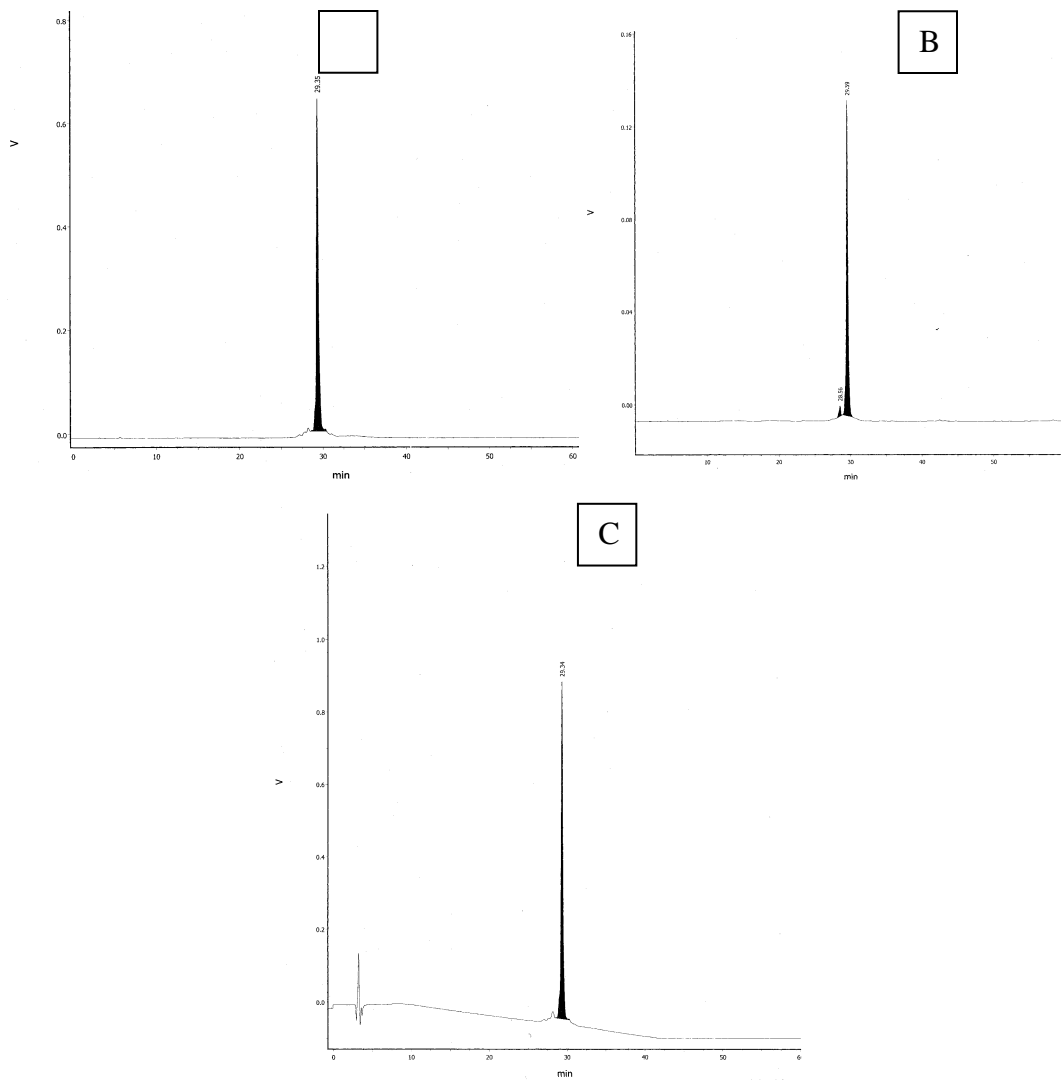
Figure A.6 Analytical RP-HPLC traces of (A), Dap-K6-E12-W13; (B), ent-Dap-K6-E12-W13 and, (C), a coinjection of Dap-K6-E12-W13 and ent-Dap-K6-E12-W13.
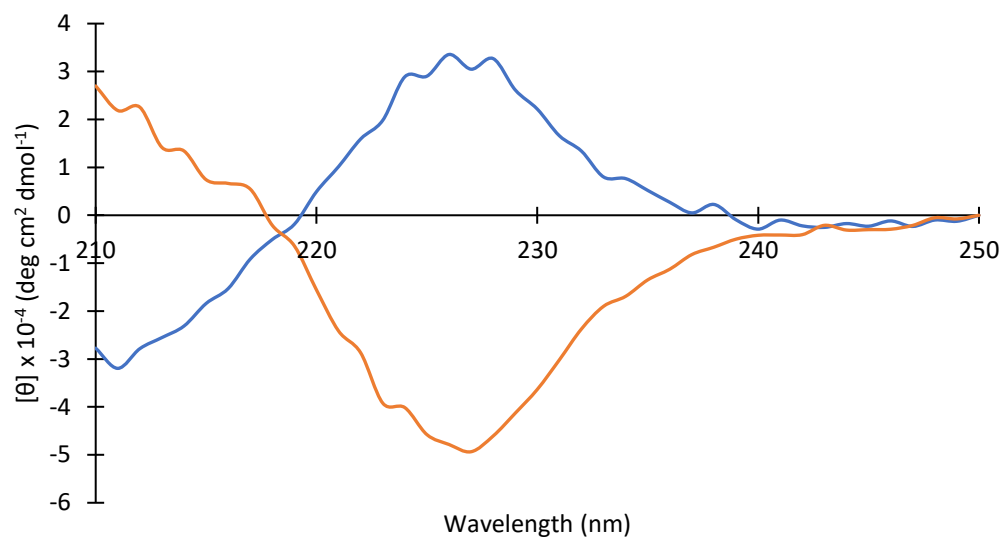
Figure A.7. CD spectra of Dap-K6-E12-W13 (blue line); and ent-Dap-K6-E12-W13 (orange line)

Appendix B Supplementary data for Chapter 4
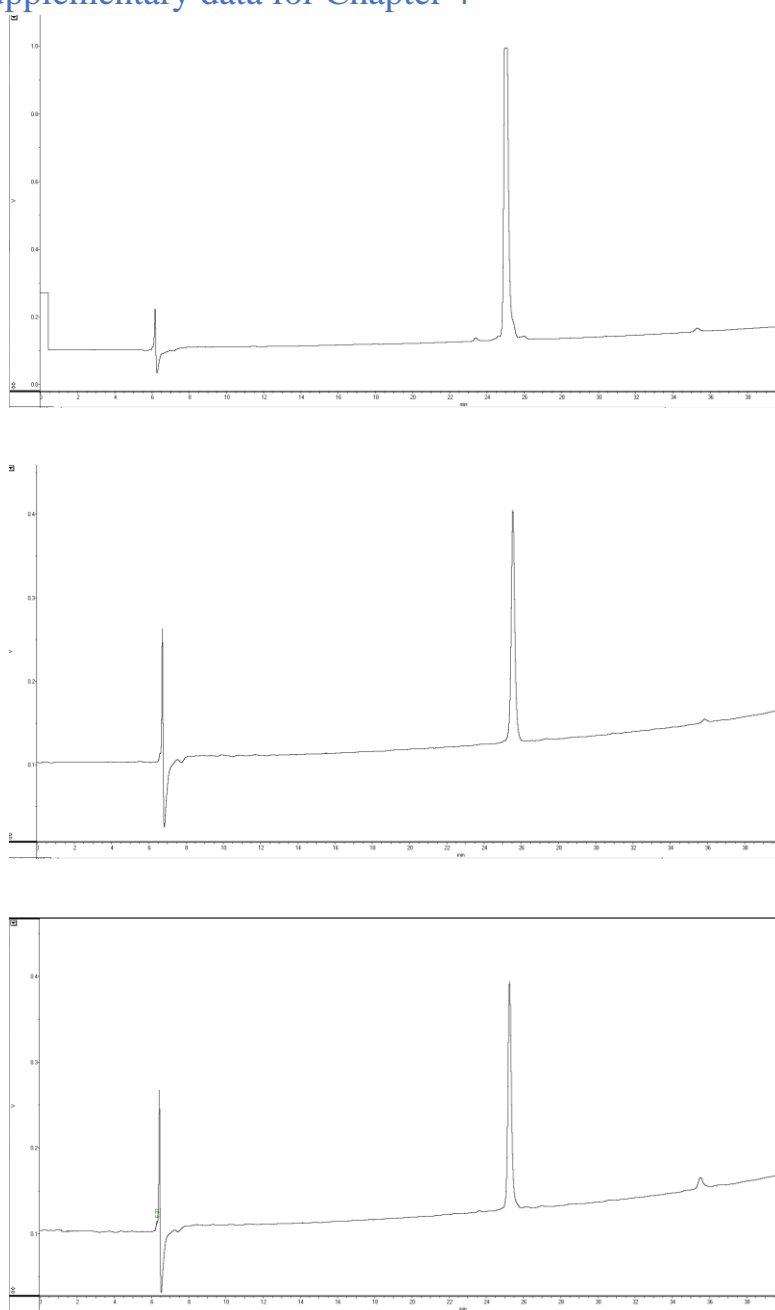
Figure B.1 RP-HPLC chromatograms of authentic daptomycin (top), synthetic daptomycin prepared via Scheme 4.1 (middle) and a mixture of both authentic and synthetic daptomycin prepared via Scheme 4.1 (bottom). A linear gradient 10:90 MeCN: H_2O (0.1% TFA) to 90:10 MeCN: H_2O (0.1% TFA) over 40 min was used. All chromatograms were obtained using λ = 220 nm.
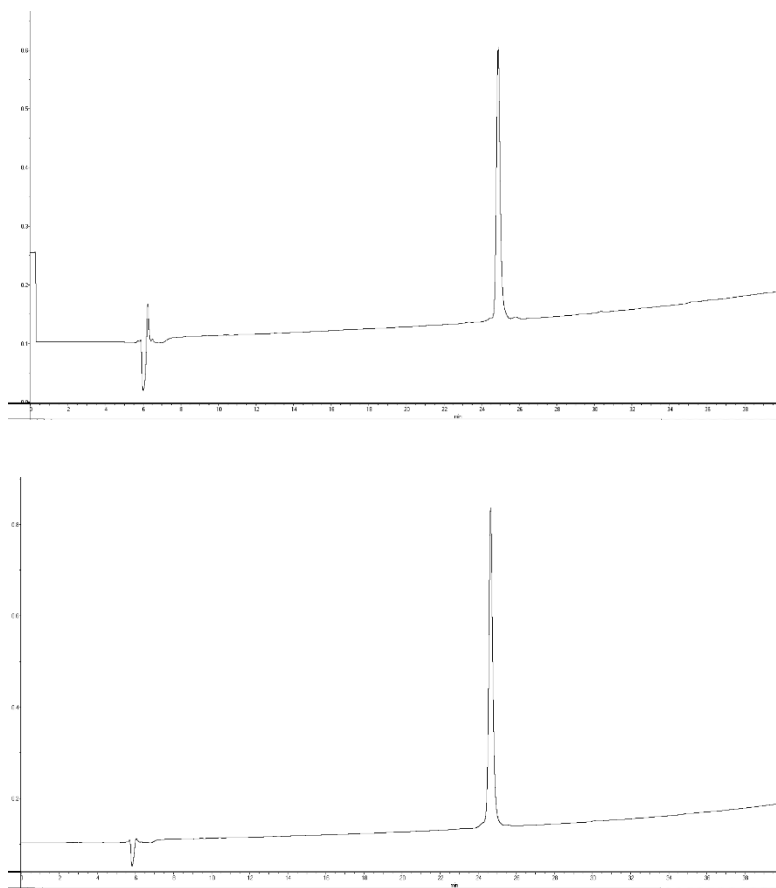
Figure B.2 RP-HPLC chromatograms of synthetic daptomycin prepared via Scheme 4.4 (top) and a mixture of both authentic and synthetic daptomycin prepared via Scheme 4.4 (bottom). A linear gradient 10:90 MeCN: H_2O (0.1% TFA) to 90:10 MeCN: H_2O (0.1% TFA) over 40 min was used. All chromatograms were obtained using λ = 220 nm.
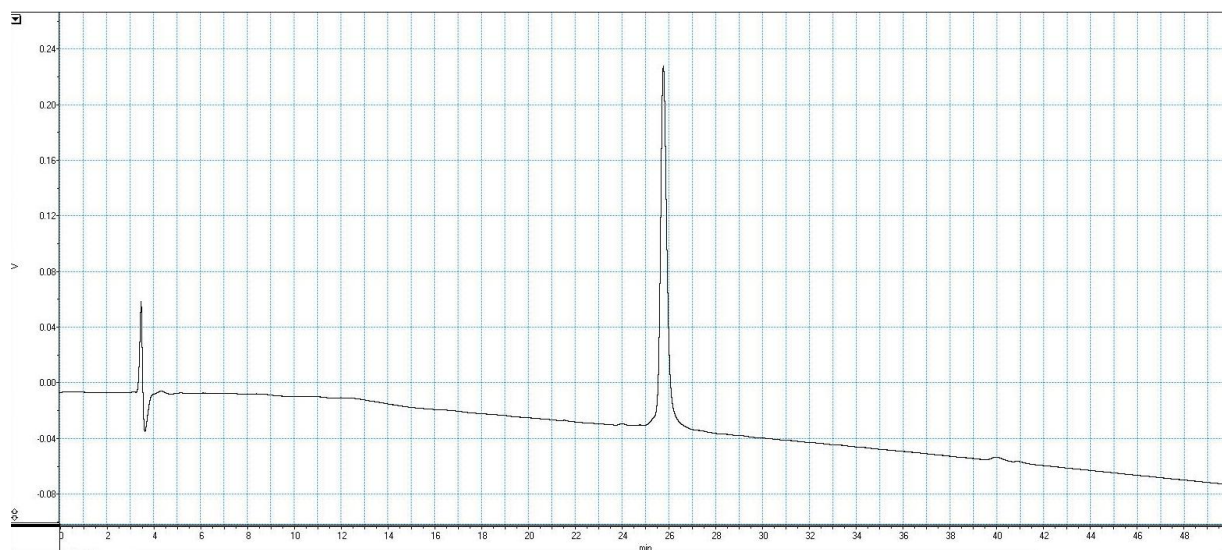
Figure B.3 RP-HPLC chromatogram of peptide **4.7**. A linear gradient of 10:90 MeCN: H_2O (0.1% TFA) to 90:10 MeCN: H_2O (0.1% TFA) over 50 min was used. This chromatogram was obtained using λ = 220 nm.
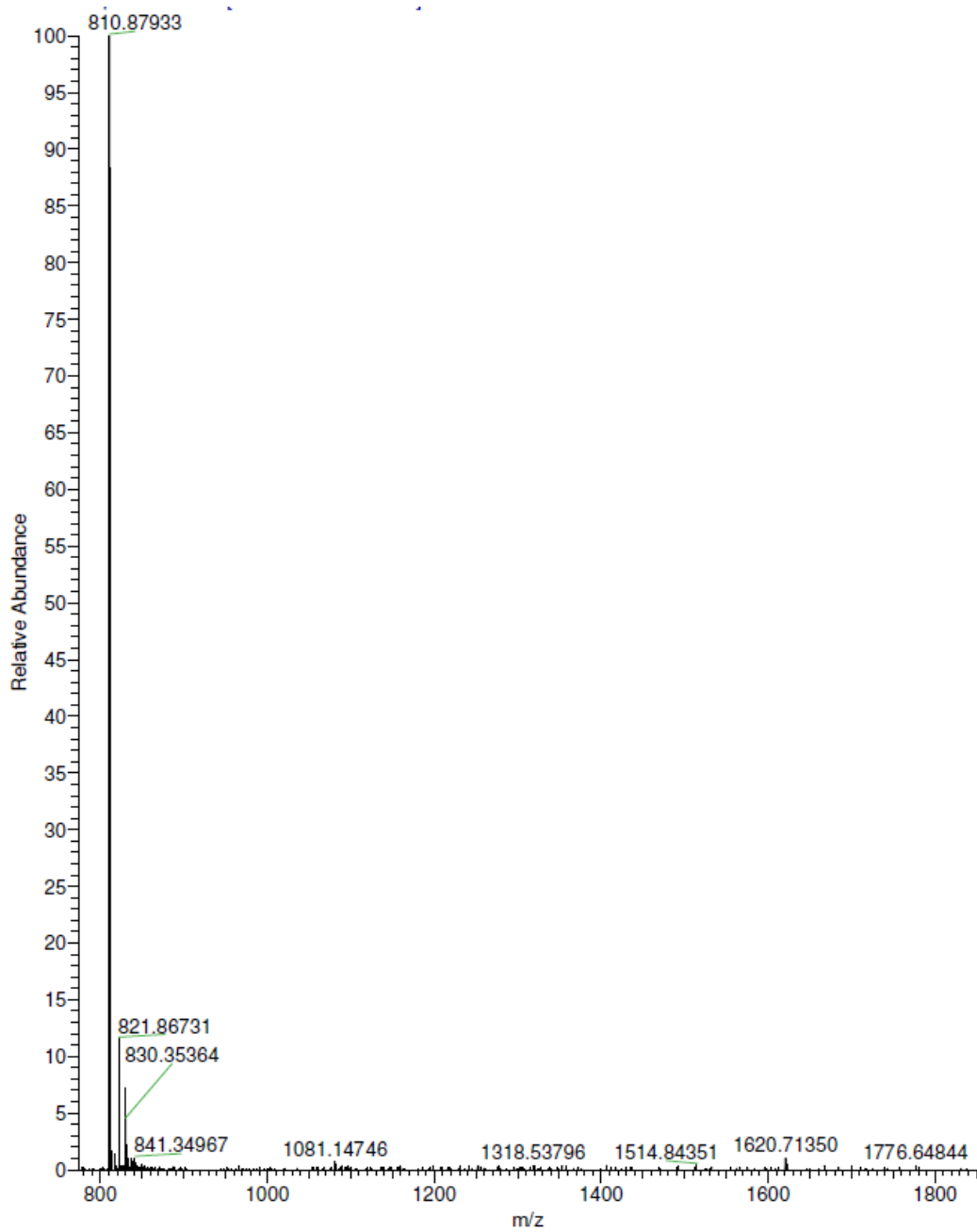
Figure B.4 ESI-MS of synthetic dap prepared via Scheme 4.1 (1:1 MeOH:H_2O + 0.1% formic acid).
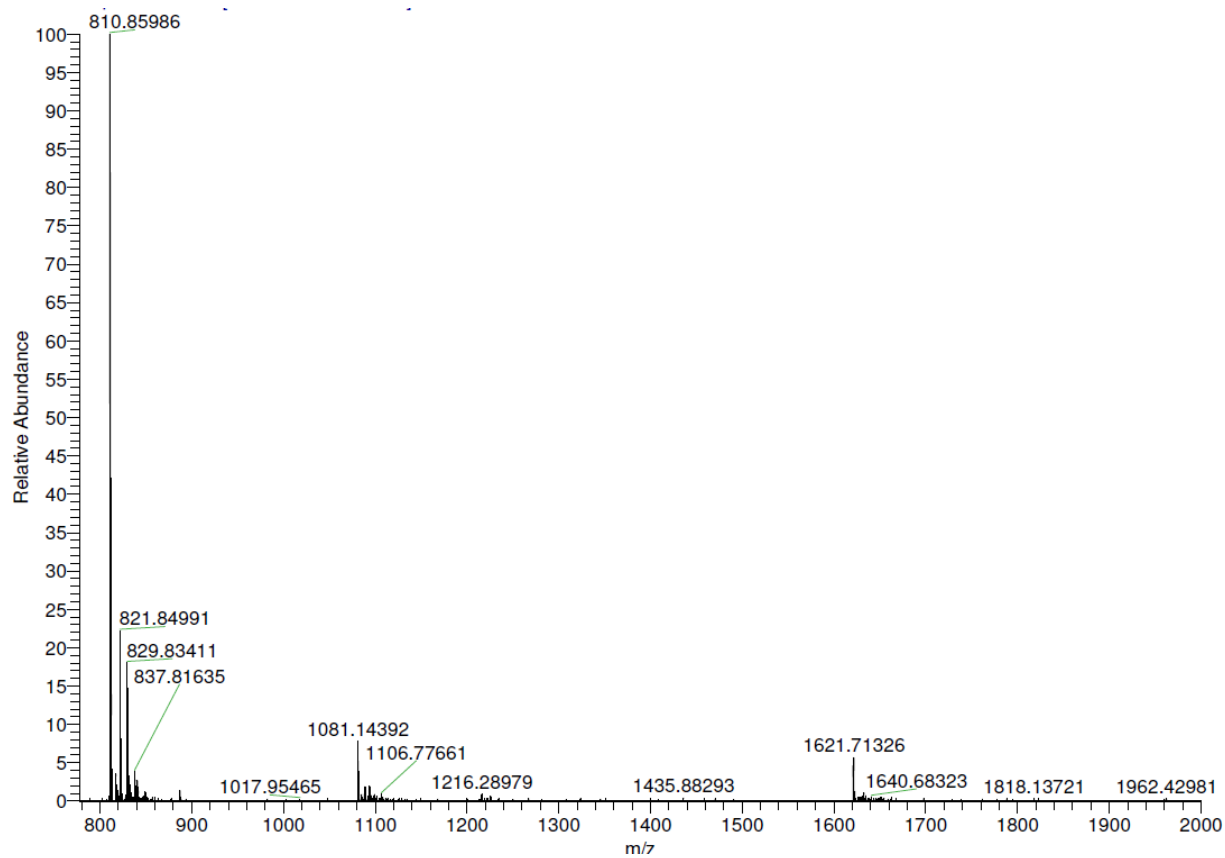
Figure B.5 ESI-MS of synthetic dap prepared via Scheme 4.4 (1:1 MeOH:H$_2$O + 0.1% formic acid).
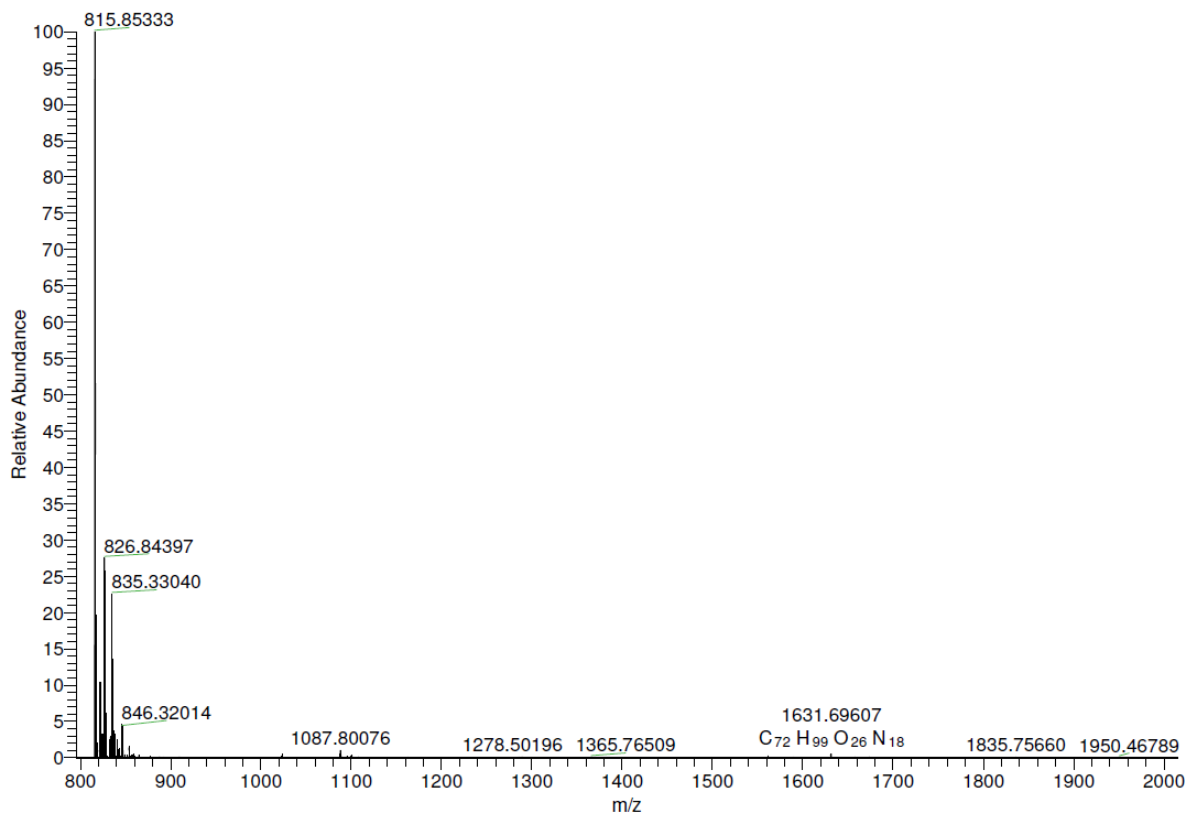
Figure B.6 ESI-MS of peptide **4.7** (1:1 MeOH:H2O + 0.1% formic acid).

Table B.1 MS-MS sequencing of peptide **4.7** following ester bond hydrolysis in 0.1 N LiOH.
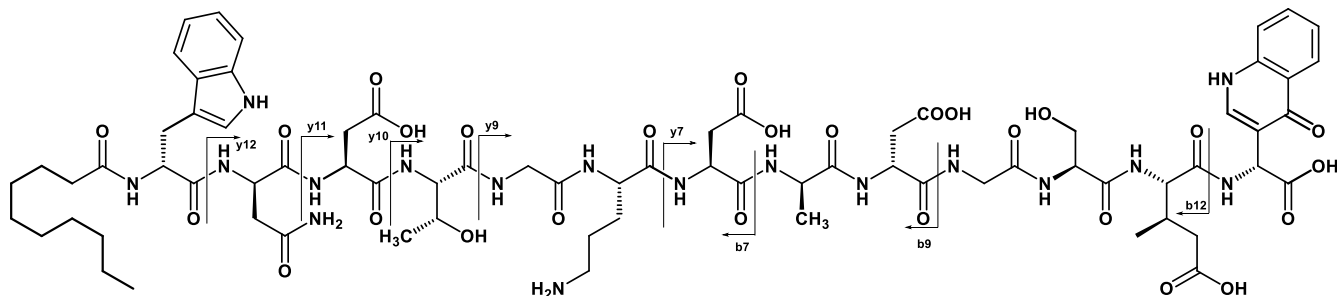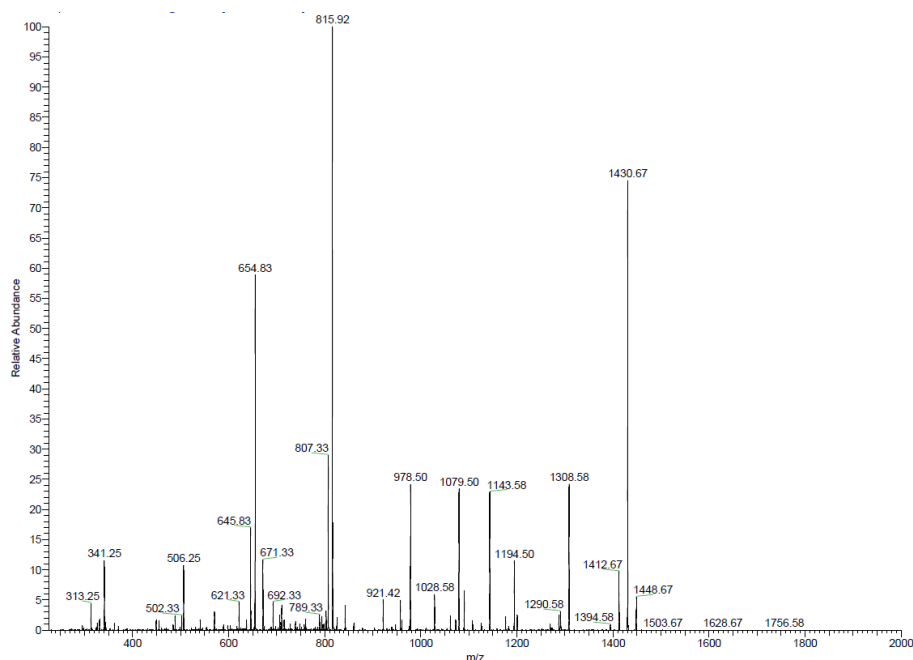
Ion	Molecular formula	Observed fragment (Calculated mass) (Da)	Ion	Molecular formula	Observed fragment (Calculated mass) (Da)
b7	$C_{44}H_{65}N_{10}O_{14}^+$	957.6 (957.5)	y9	$C_{40}H_{56}N_{11}O_{18}^+$	978.5 (978.4)
b9	$C_{51}H_{75}N_{12}O_{18}^+$	1143.6 (1143.5)	y10	$C_{44}H_{63}N_{12}O_{20}^+$	1079.5 (1079.4)
b12	$C_{62}H_{92}N_{15}O_{24}^+$	1430.7 (1430.6)	y11	$C_{48}H_{68}N_{13}O_{23}^+$	1194.5 (1194.5)
y7	$C_{33}H_{43}N_8O_{16}^+$	807.3 (807.3)	y12	$C_{52}H_{74}N_{15}O_{25}^+$	1308.6 (1308.5)
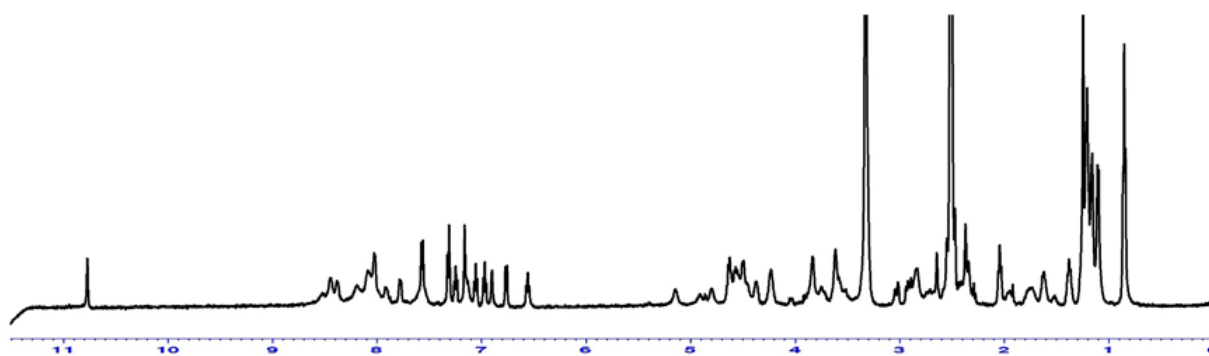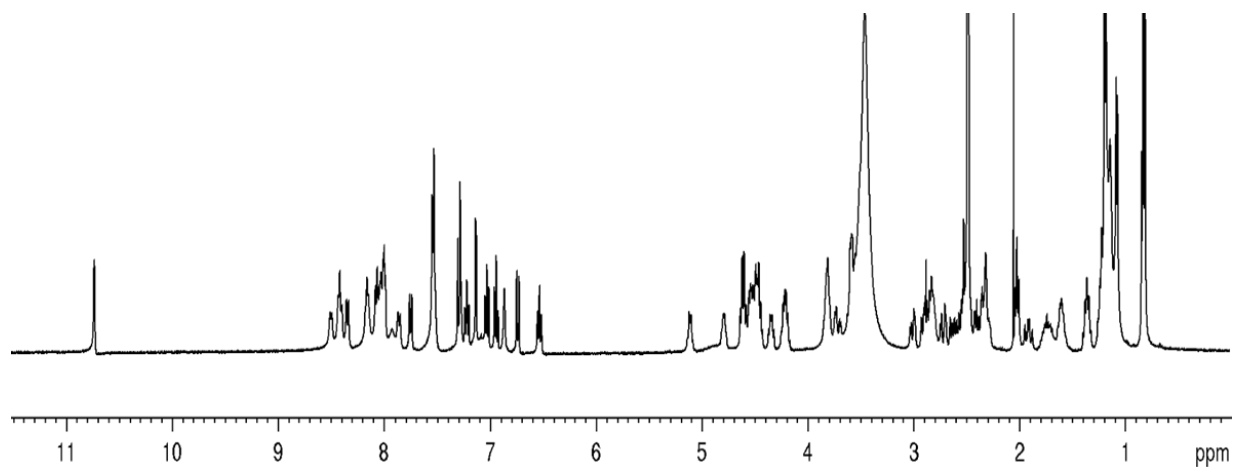
Figure B.7 ^{1}H NMR spectra of Brimble and coworkers' authentic sample of dap in DMSO-d$_6$ (top; 500 MHz NMR, 11.7 mg/mL in DMSO-d$_6$)[192] and the synthetic dap prepared via Scheme 4.1 (bottom; 500 MHz NMR, 5 mg/mL in DMSO-d$_6$).
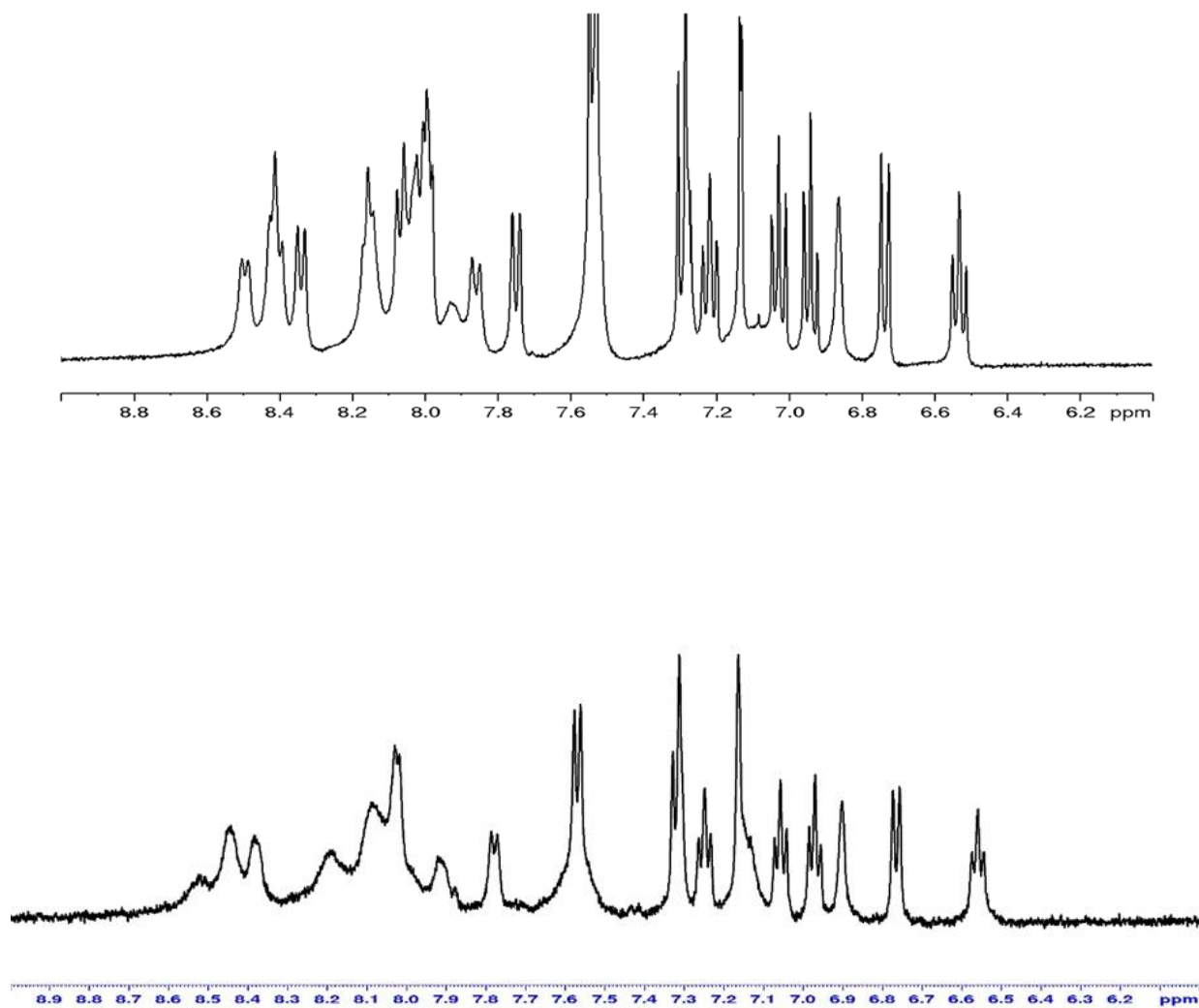
Figure B.8 Amide and aromatic region of the ^{1}H NMR spectra of Brimble and coworkers' authentic sample of dap in DMSO-d_6 (top; 500 MHz NMR, 11.7 mg/mL in DMSO-d_6)[192] and the synthetic dap prepared via Scheme 4.1 (bottom; 500 MHz NMR, 5 mg/mL in DMSO-d_6).
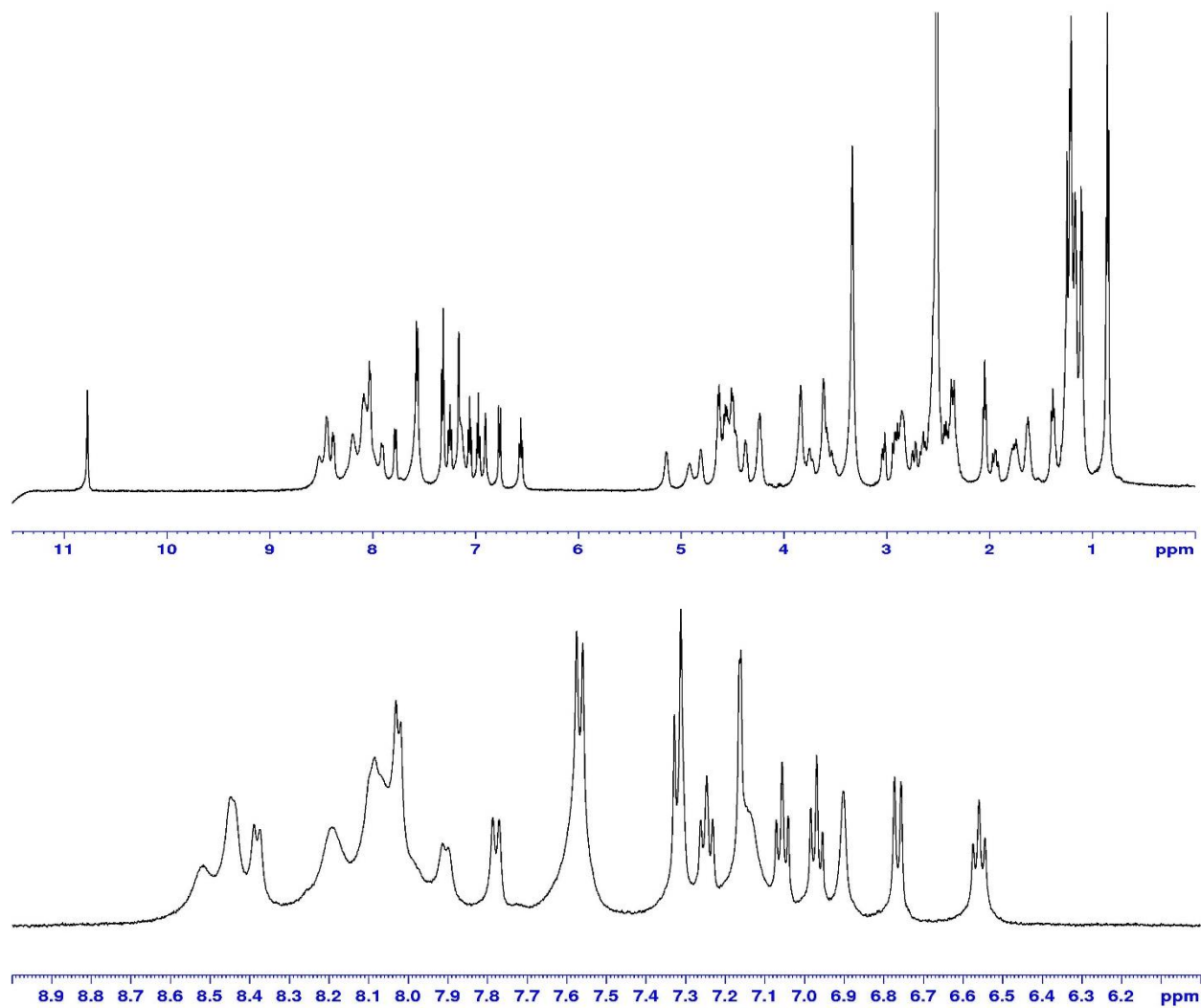
Figure B.9 ^{1}H NMR of synthetic dap prepared via Scheme 4.4 (top; 500 MHz NMR, 8 mg/mL in DMSO-d$_6$). Amide and aromatic region of the same spectra (bottom).
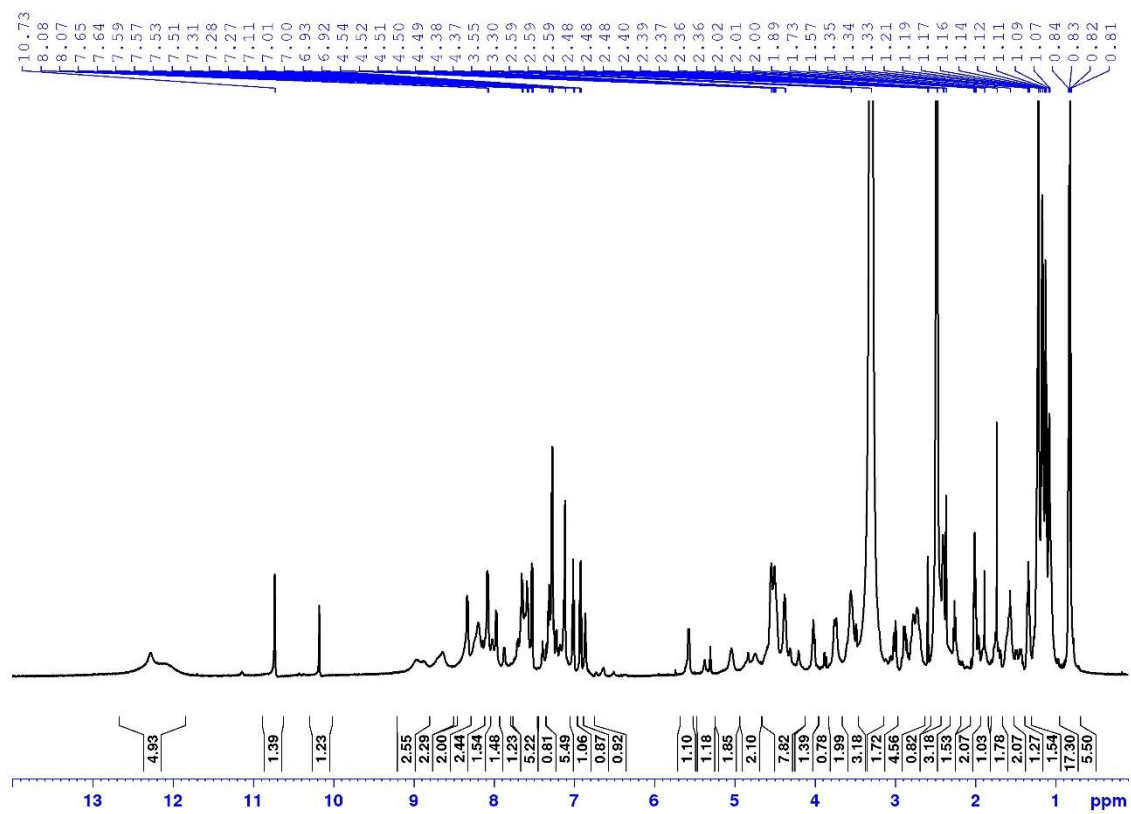
Figure B.10 ^{1}H NMR spectrum of peptide **4.7** in DMSO-d$_6$ (600 MHz NMR).
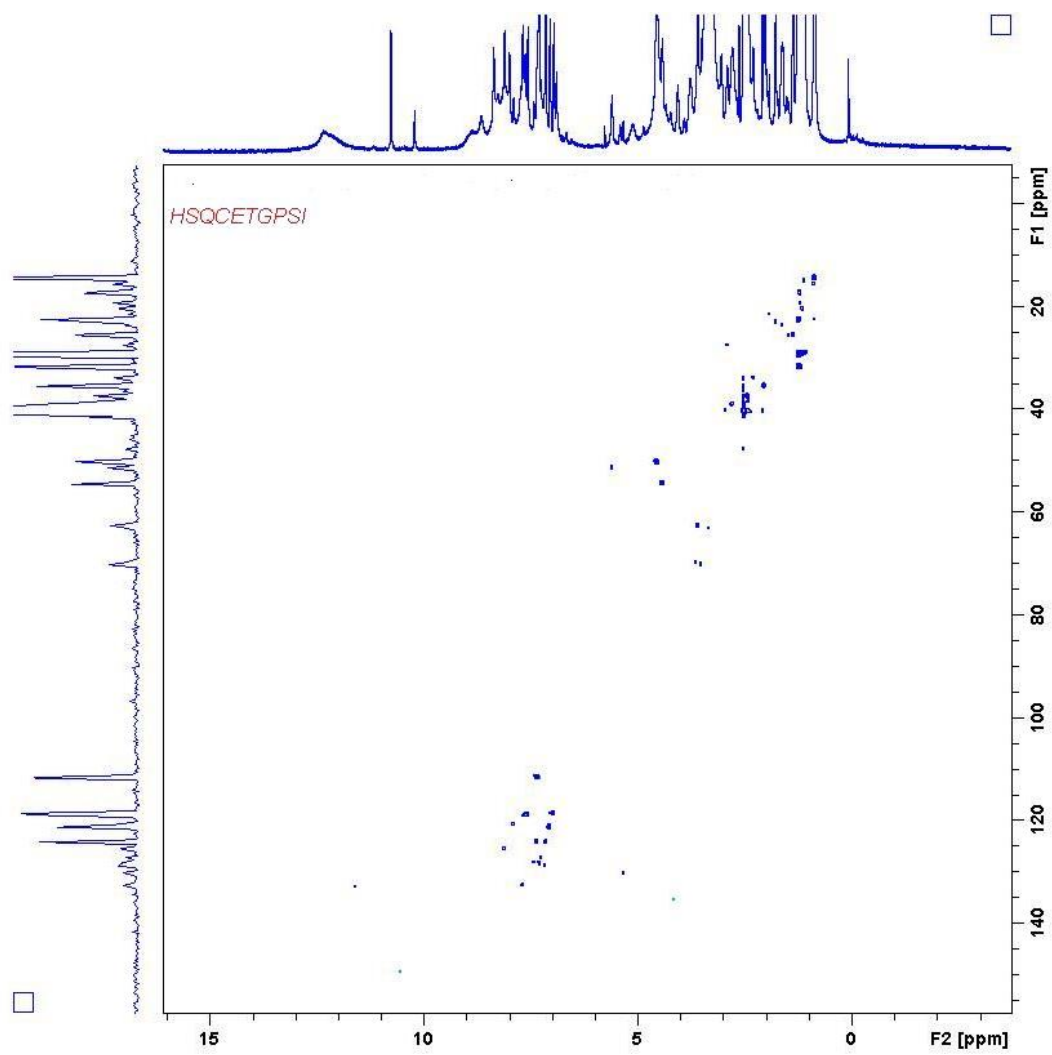
Figure B.11 HSQC of **4.7** in DMSO-d$_6$ (600 MHz NMR)
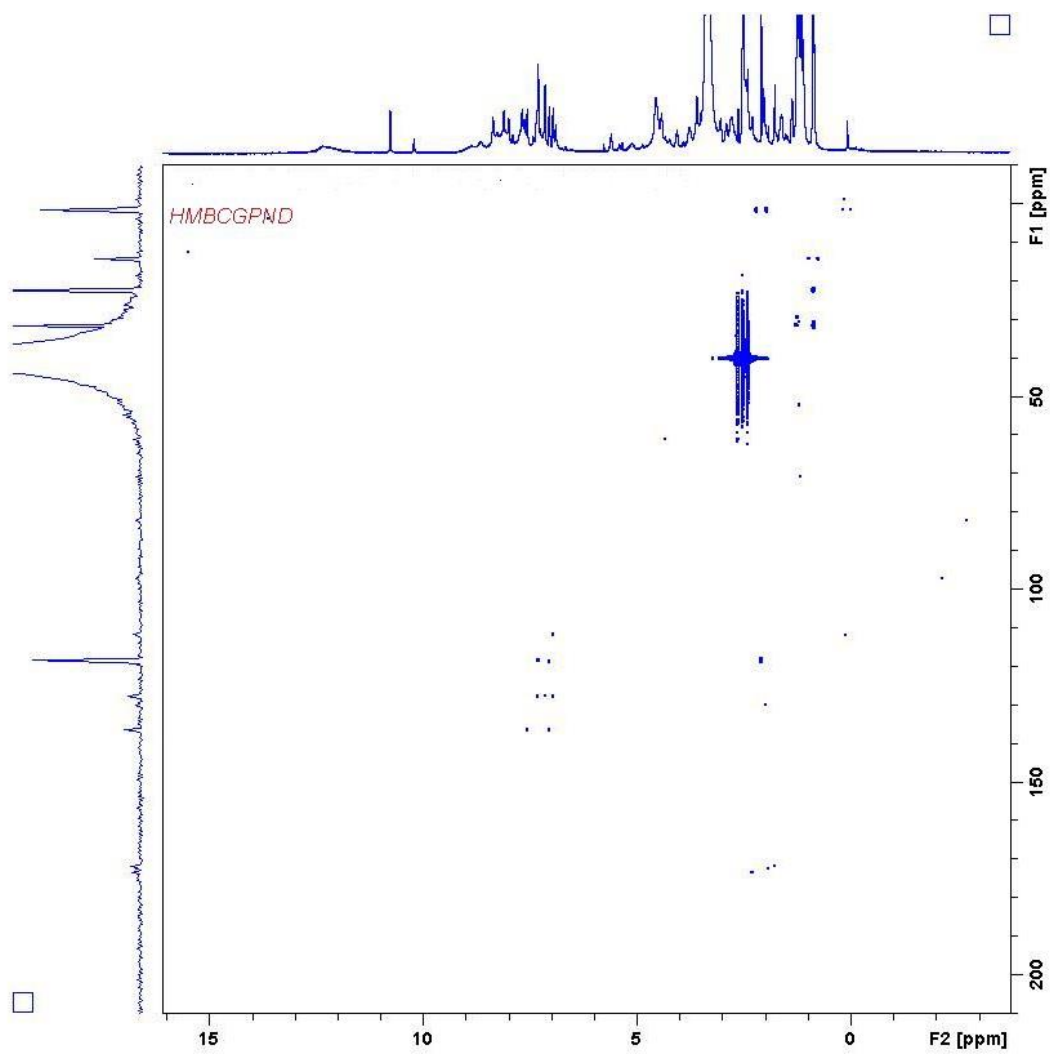
Figure B.12 HMBC of **4.7** in DMSO-d$_6$ (600 MHz NMR).
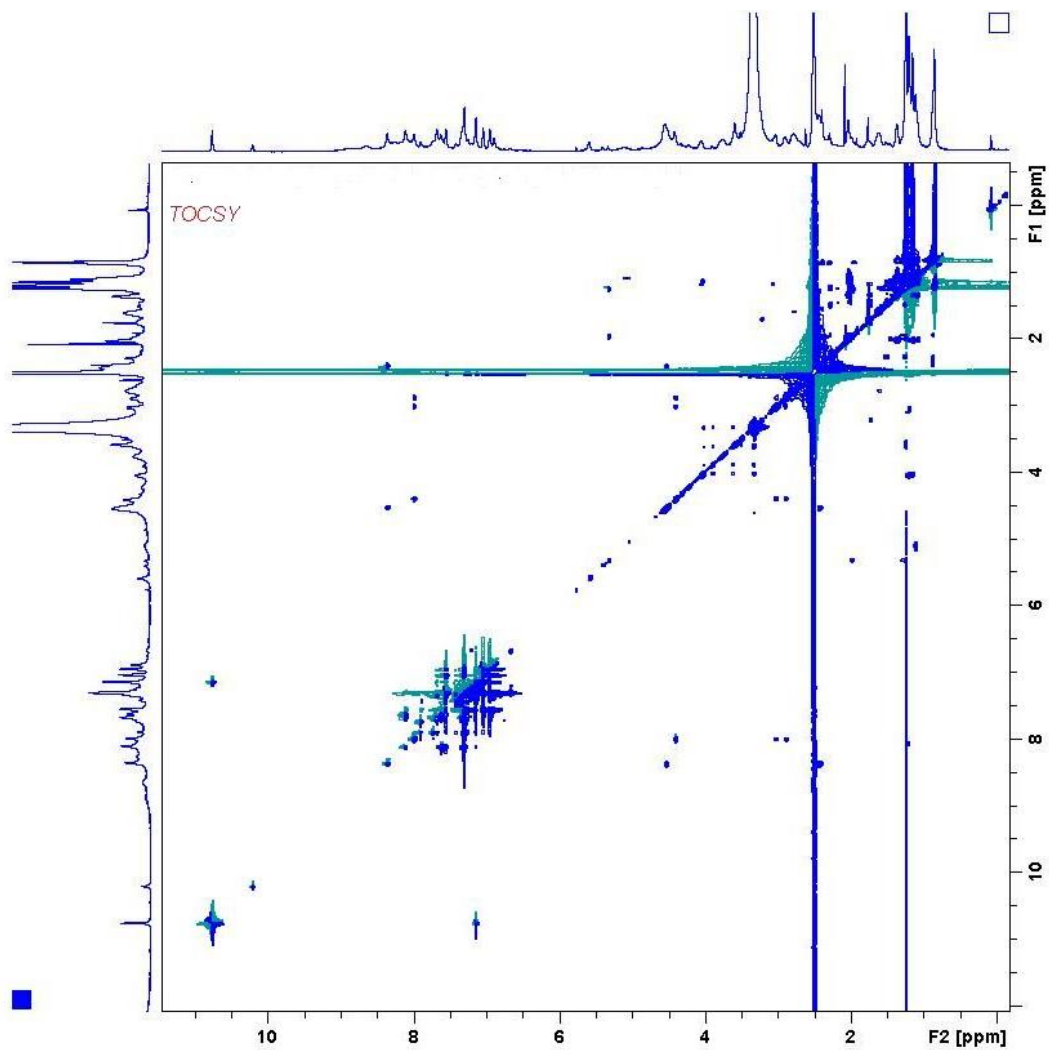
Figure B.13 TOCSY of peptide 4.**7** in DMSO-d$_6$ (600 MHz NMR)
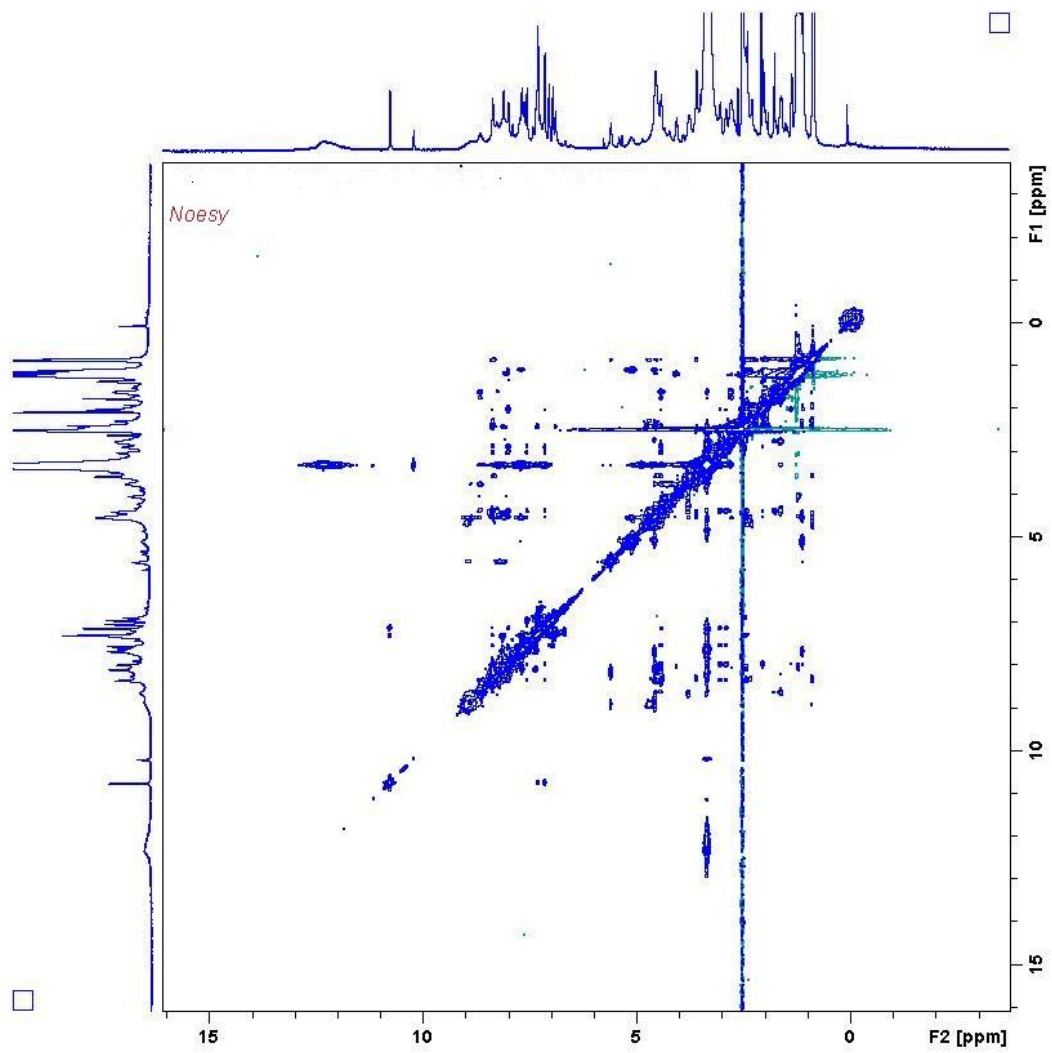
Figure B.14 NOESY of peptide **4.7** in DMSO-d$_6$ (600 MHz NMR)
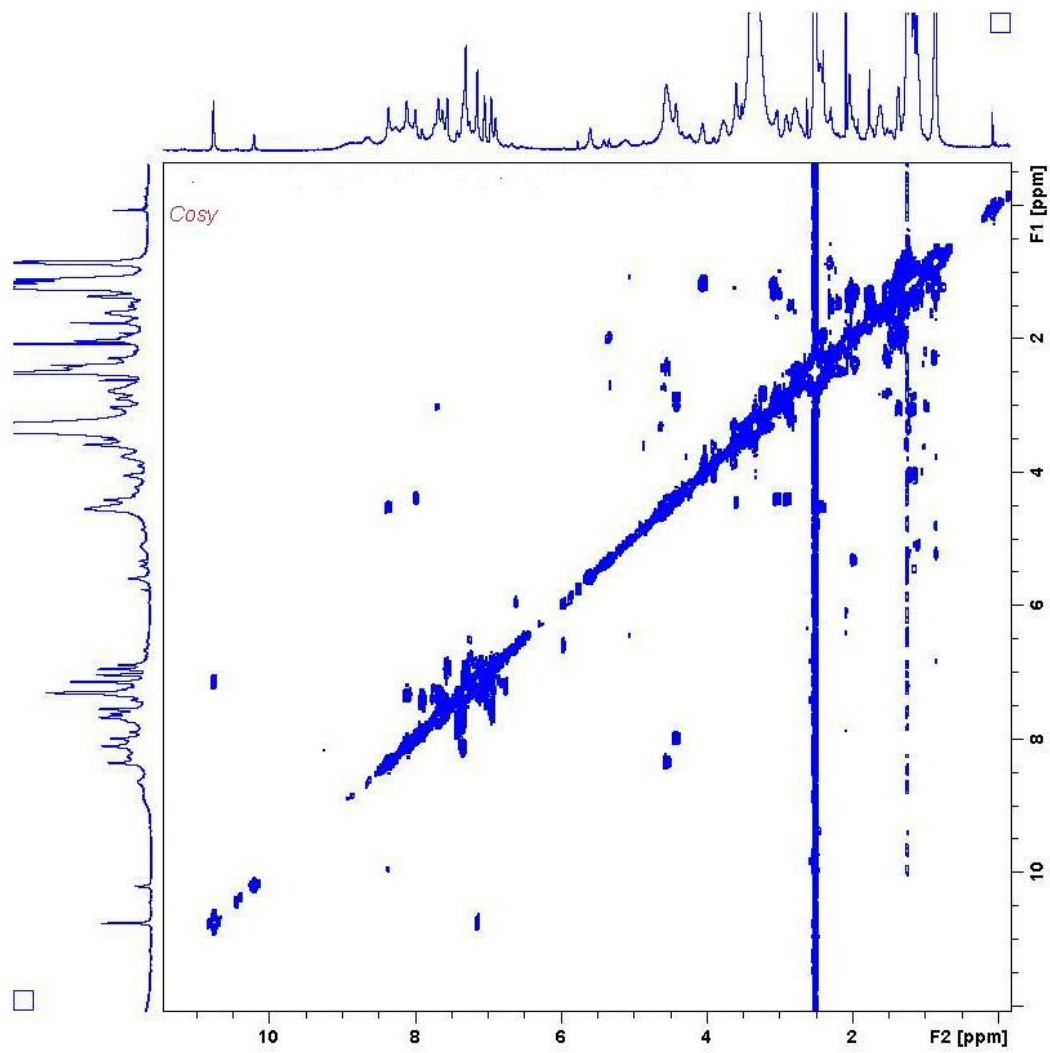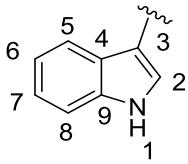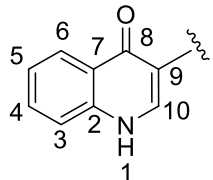
Figure B.15 COSY of peptide **4.7** in DMSO-d$_6$ (600 MHz NMR)

Table B.2 Chemical shift assignment of **4.7**

Residue	Position	δ_C	δ_H (J value, Hz)
Trp1	NH	--	7.99
	α	54.6**	4.41
	β	27.6	3.03, 2.89
	1	--	10.77 s
	2	124.2	7.14 s
	3 (quat)	--	--
	4	118.9	7.55 d (7.3)
	4a (quat)	127.8	--
	5	118.6	6.95 dd (7.1, 7.3)
	6	121.3	7.04 dd (7.5, 7.3)
	7	111.7	7.30 d (7.5)
	7a (quat)	136.6	--
D-Asn2	NH	--	8.35
	α	50.2**	4.55
	β	37.5	2.42, 2.29
	C=O	--	--
	CONH$_2$	--	6.89
Asp3	NH	--	8.35
	α	50.5	4.59
	β	39.0**	2.75, 2.44
	C=O	--	--
	COOH	--	12.32**
Thr4	NH	--	7.46
	α	50.0	4.56
	β	70.5	5.11
	γ	17.5	1.21
	C=O	--	--
Gly5	NH	--	--
	α	42.9**	3.88/3.63**
	C=O	--	--
Orn6	NH	--	8.32
	α	54.5**	4.37/4.41**
	β	--	1.66
	γ	24.7	1.49
	δ	39.0**	2.79**
	NH$_2$	--	--
	C=O	--	--
Asp7	NH	--	7.97
	α	54.5**	4.42
	β	--	2.90
	C=O	--	--
	COOH	--	12.32**
D-Ala8	NH	--	--

	α	49.9	4.06
	β	20.4	1.15
	C=O	--	--
Asp9	NH	--	8.36
	α	50.2**	4.54
	β	38.5	2.41
	C=O	--	--
	COOH	--	12.32**
Gly10	NH	--	--
	α	42.9**	3.88/3.63**
	C=O	--	--
D-Ser11	NH	--	10.20
	α	63.1	3.34
	β	65.9	4.04, 3.90
	OH	--	--
	C=O	--	--
3mGlu12	NH	--	--
	α	--	4.78
	β	34.0	2.31
	γ1	40.5	1.52, 2.07
	γ2	15.8	0.85
	C=O	--	--
	COOH	--	12.32**
4-QO13	NH	--	8.99
	α	51.4	5.59
	1	--	12.32**
	2	--	--
	3	119.0	7.63
	4	132.5	7.66
	5	124.8	7.34
	6	125.5	8.11
	7	--	--
	8	--	--
	9	--	--
	10	135.3	7.65
	C=O	--	--
Decanoic tail	--	--	--

'—'indicates that the signal was not assigned. '**' indicates that the assignment is ambiguous due to overlapping peaks.
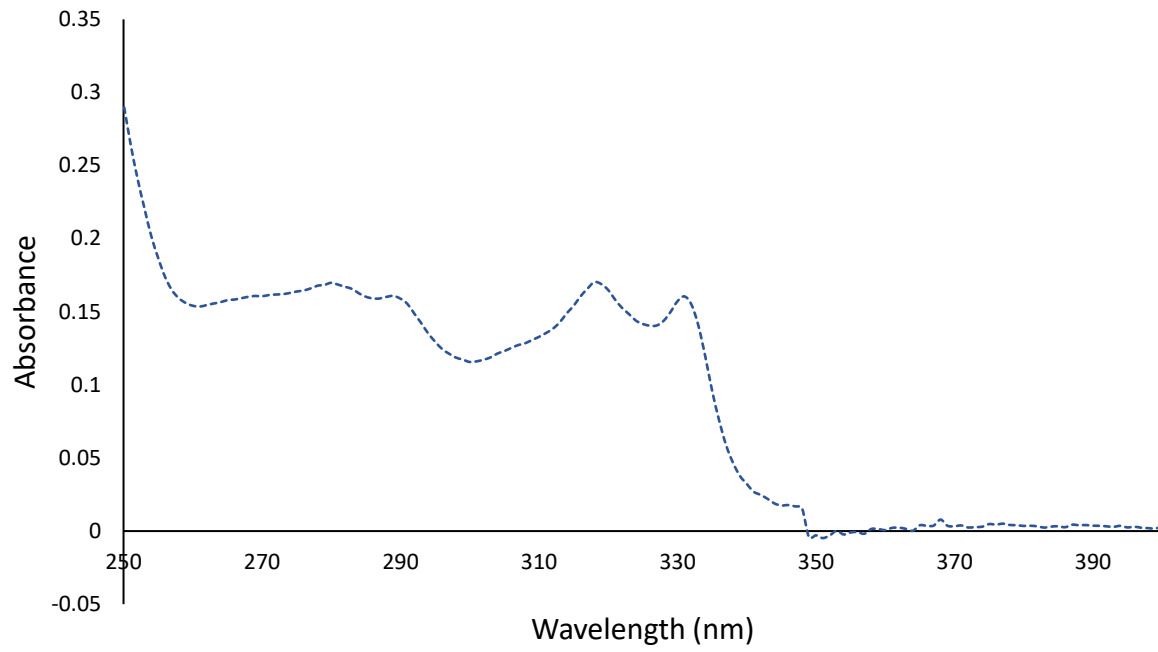
Figure B.16 UV-Vis trace of peptide **4.7** in H_2O at a concentration of 32.5 µg/mL
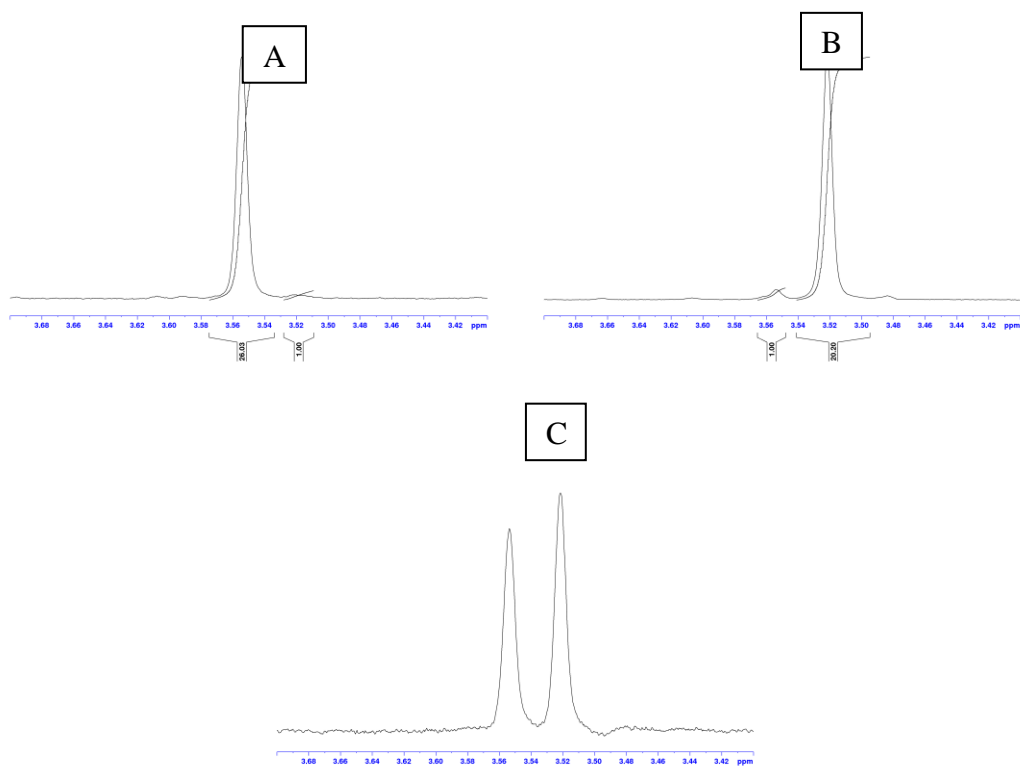
Figure C.1 ^{1}H NMR (500 MHz, C$_6$D$_6$) spectra of the Mosher's esters formed between (A) **R-5.5** and (R)-(+)-α-methoxy-α-trifluoromethylphenylacetic acid; relative integrations show that **R-5.5** possess an ee of 93%; (B) **S-5.5** and (R)-(+)-α-methoxy-α-trifluoromethylphenylacetic acid; relative integrations show that **S-5.5** possess an ee of 91%; (C) a mixture of (A) and (B).
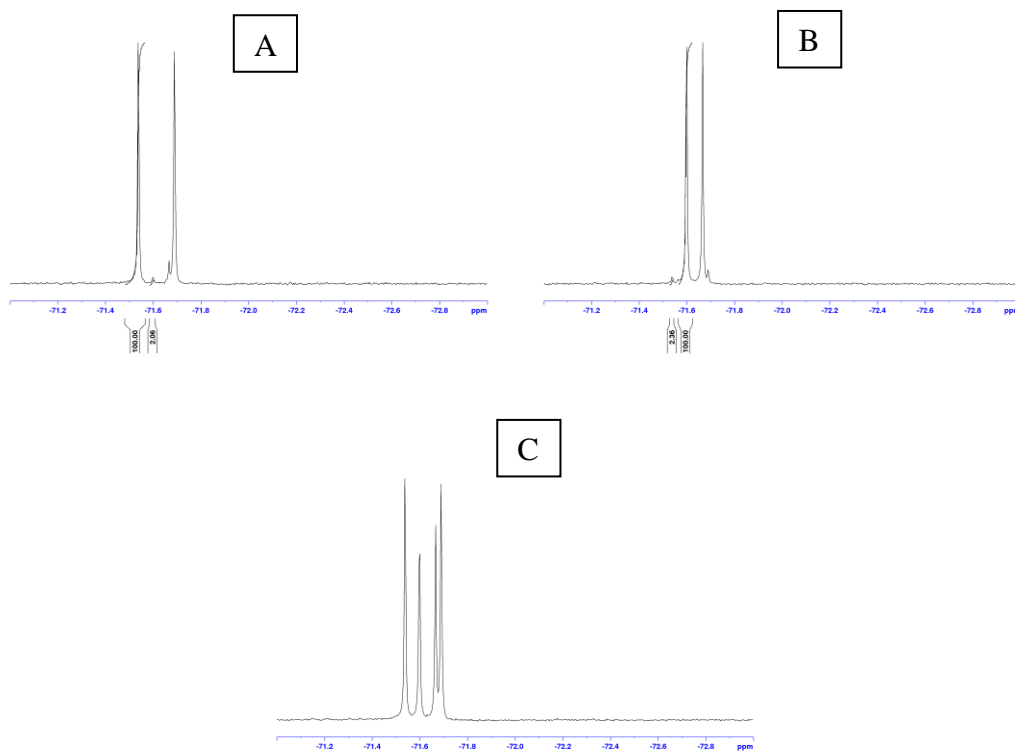
Figure C.2 ^{19}F NMR (470 MHz, CDCl$_3$) spectra of the Mosher's esters formed between (A) **R-5.9** and (R)-(+)-α-methoxy-α-trifluoromethylphenylacetic acid. Relative integrations show that **R-5.9** possess an ee of 96%; (B) **S-5.9** and (R)-(+)-α-methoxy-α-trifluoromethylphenylacetic acid. Relative integrations show that **R-5.9** possess an ee of 95%; (C) a mixture of (A) and (B).
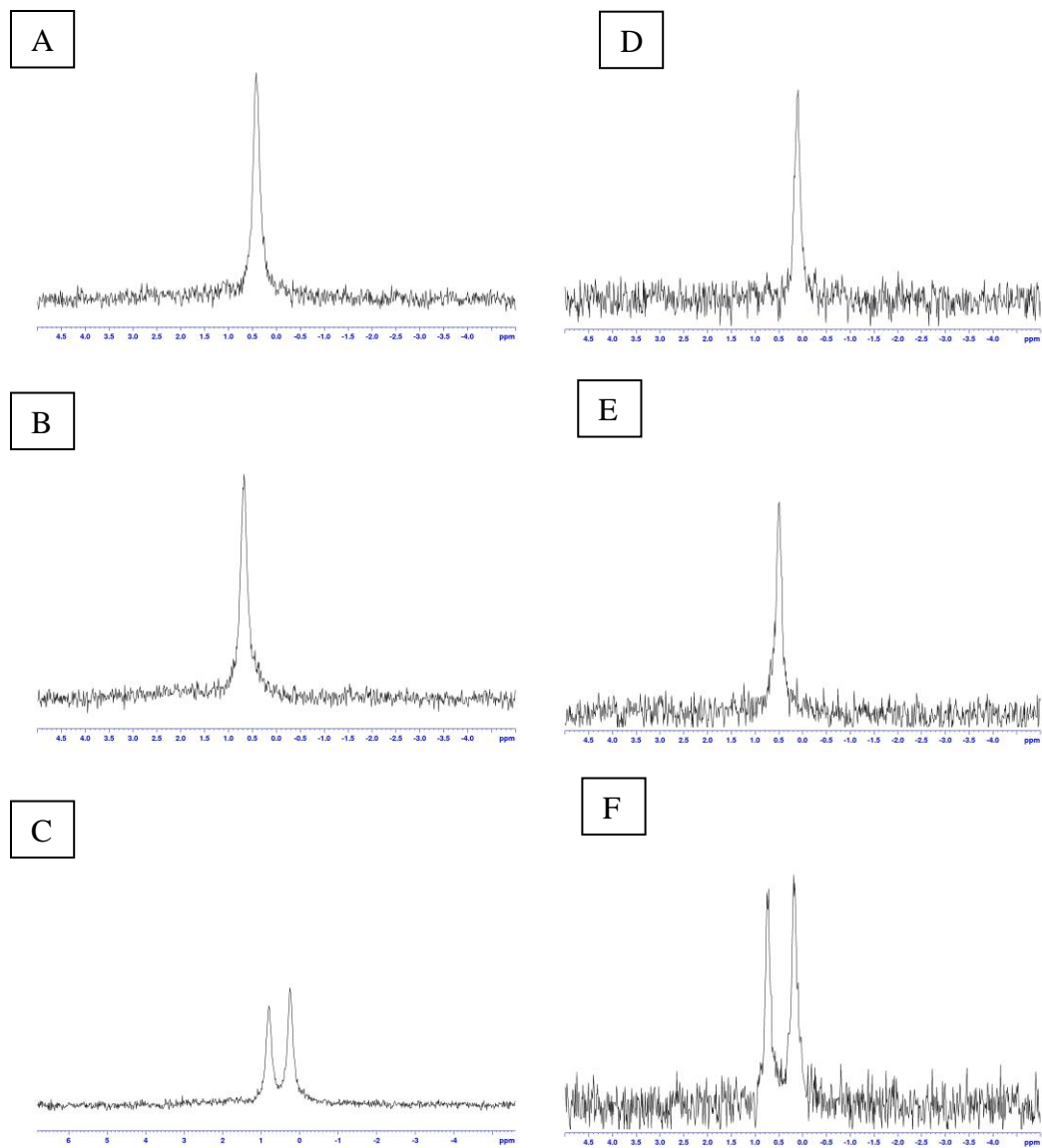
Figure C.3 ^{31}P NMR (202 MHz, CDCl$_3$) spectra of the ester's formed between chiral boronic acid **5.13** (see Scheme S1) and (A) 2R,2'S-DMPG; (B) 2R,2'R-DMPG; (C) 1:1 mixture of 2R,2'S-DMPG and 2R,2'R-DMPG; (D) 2S,2'S-DMPG; (E) 2S,2'R-DMPG; (F) 1:1 mixture of 2S,2'S-DMPG and 2S,2'R-DMPG.
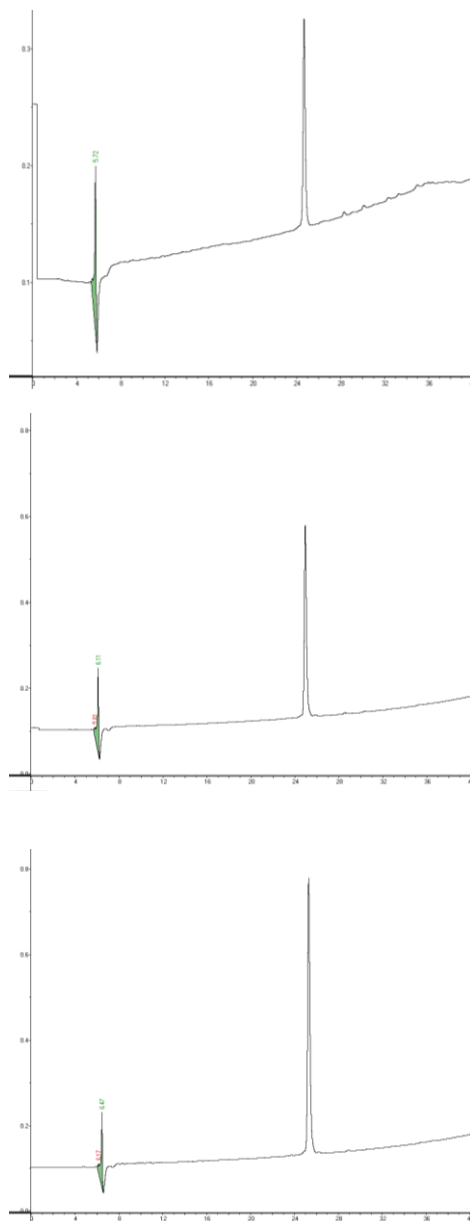
Figure C.4 RP-HPLC chromatograms of authentic daptomycin (top), synthetic ent-dap (middle) and a mixture of both authentic and synthetic ent-dap (bottom). A liner gradient 10:90 MeCN: H_2O (0.1% TFA) to 90:10 MeCN: H_2O (0.1% TFA) over 40 min was used. All chromatograms were obtained using λ = 220 nm.
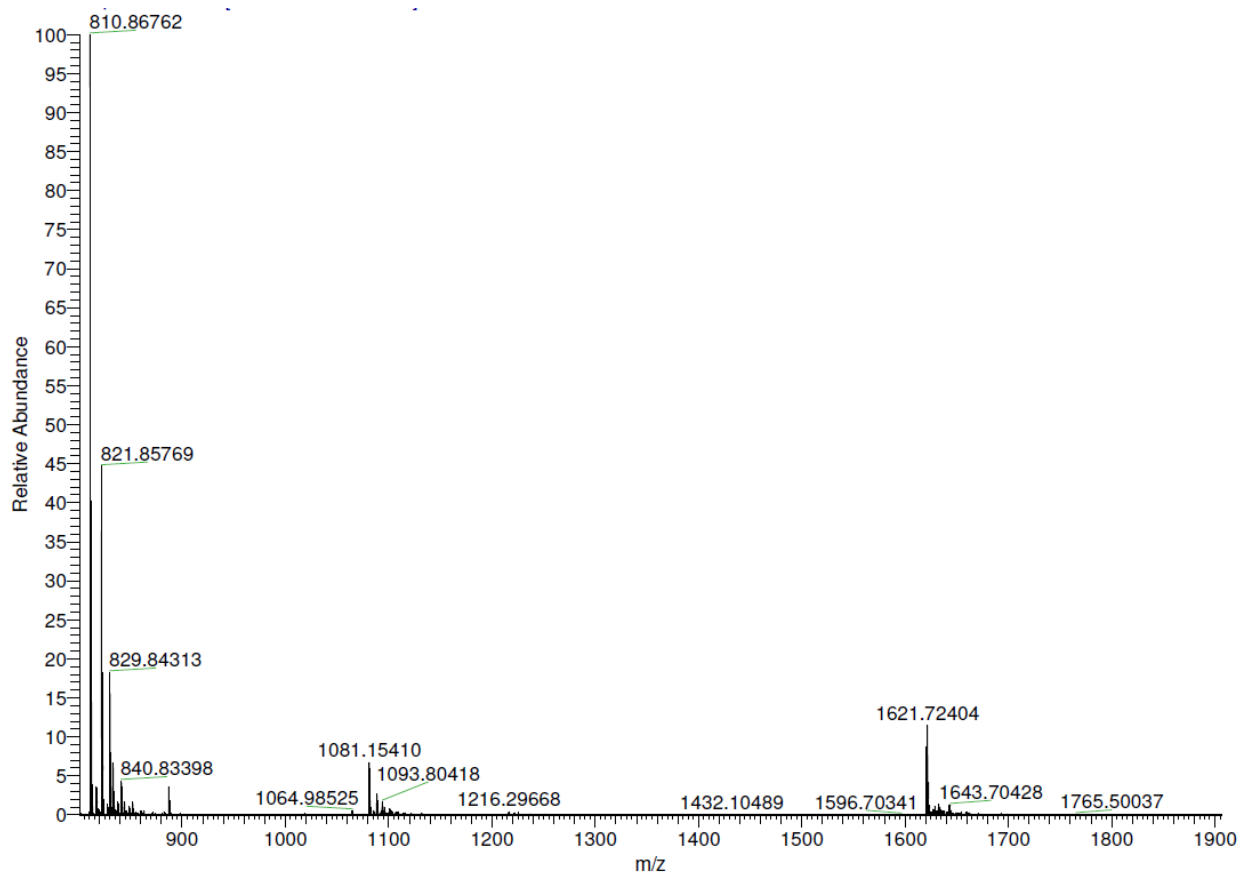
Elemental composition search on mass 810.86225

m/z= 805.86225-815.86225

m/z	Theo. Mass	Delta (mmu)	RDB equiv.	Composition
810.86225	810.86246	-0.21	30.0	$C_{72} H_{103} O_{26} N_{17}$
	810.86179	0.46	30.5	$C_{70} H_{101} O_{25} N_{20}$
	810.86313	-0.88	29.5	$C_{74} H_{105} O_{27} N_{14}$
	810.86380	-1.55	34.5	$C_{75} H_{101} O_{23} N_{18}$
	810.86447	-2.22	34.0	$C_{77} H_{103} O_{24} N_{15}$
	810.85953	2.72	33.5	$C_{80} H_{105} O_{26} N_{10}$
	810.85952	2.73	39.0	$C_{79} H_{99} O_{21} N_{17}$
	810.86514	-2.89	39.0	$C_{78} H_{99} O_{20} N_{19}$
	810.86514	-2.89	33.5	$C_{79} H_{105} O_{25} N_{12}$
	810.85885	3.40	34.0	$C_{78} H_{103} O_{25} N_{13}$

Figure C.5. ESI-MS of ent-dap sprayed from 1:1 MeOH:H_2O + 0.1% formic acid. The peak at m/z 1621 is from the [M + H]$^{+1}$ ion. The peak at m/z 811 is from the [M + 2H]$^{+2}$ ion. The peak at m/z 822 is from the [M + H + Na]$^{+2}$ ion
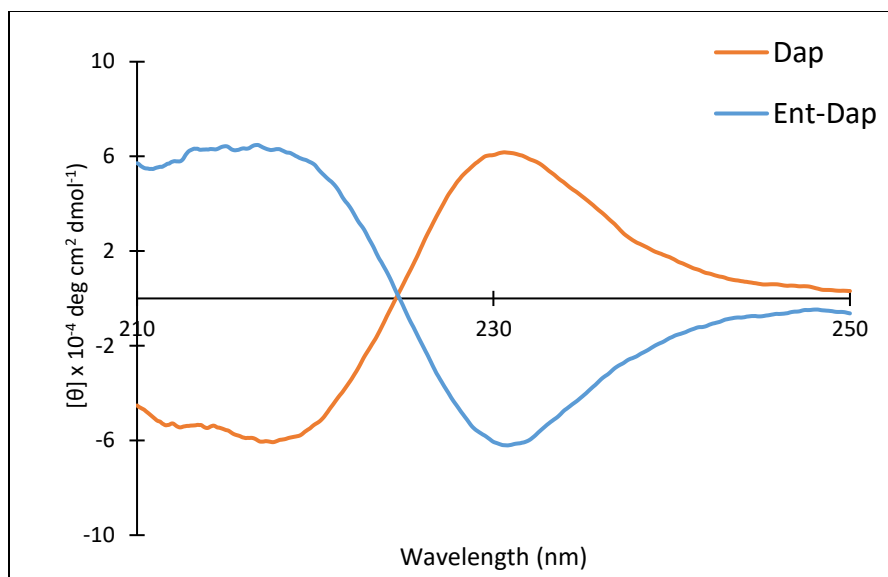
Figure C.6 Circular dichroism spectra of a 15 µM sample of daptomycin or ent-daptomycin in 20 mM HEPES buffer at pH = 7.4 collected at room temperature
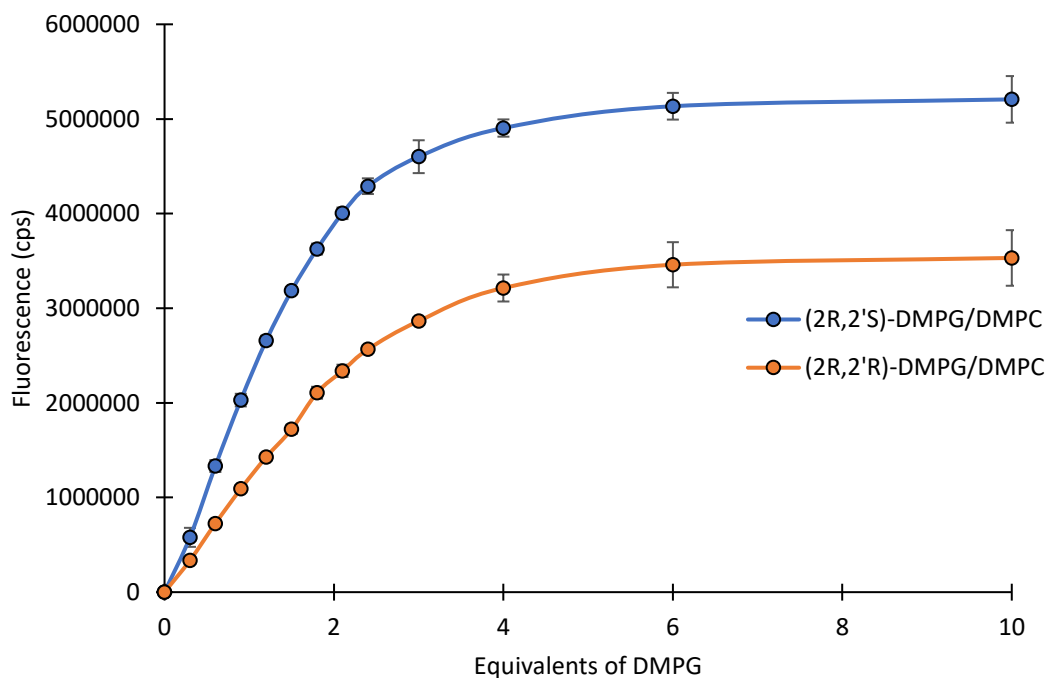
Figure C.7 Titration of a solution of daptomycin (15 μM) with LUVs composed of 1:1 DMPG:DMPC at 37 °C in 20 mM HEPES, 150 mM NaCl (pH 7.4) and 5 mM CaCl$_2$. Maximum fluorescence intensity (not normalized) as a function of DMPG concentration.
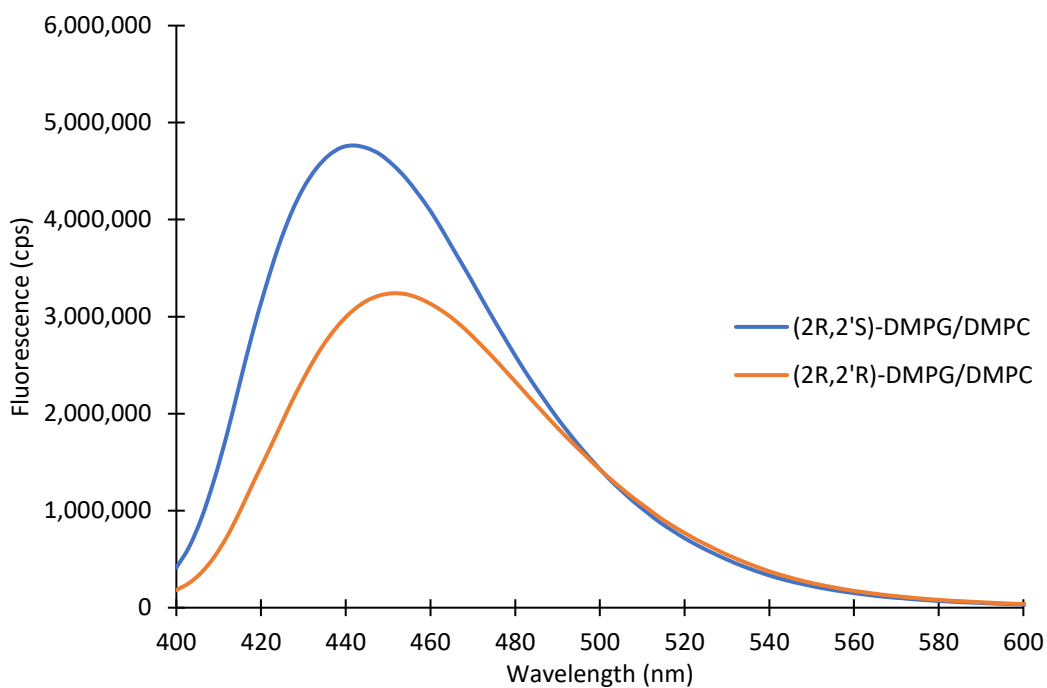
Figure C.8 Emission spectra of a solution of daptomycin (15 μM) and LUVs (300 μM, total lipid concentration) composed of 1:1 DMPG:DMPC at 37 °C in 20 mM HEPES, 150 mM NaCl (pH 7.4) and 5 mM CaCl$_2$.
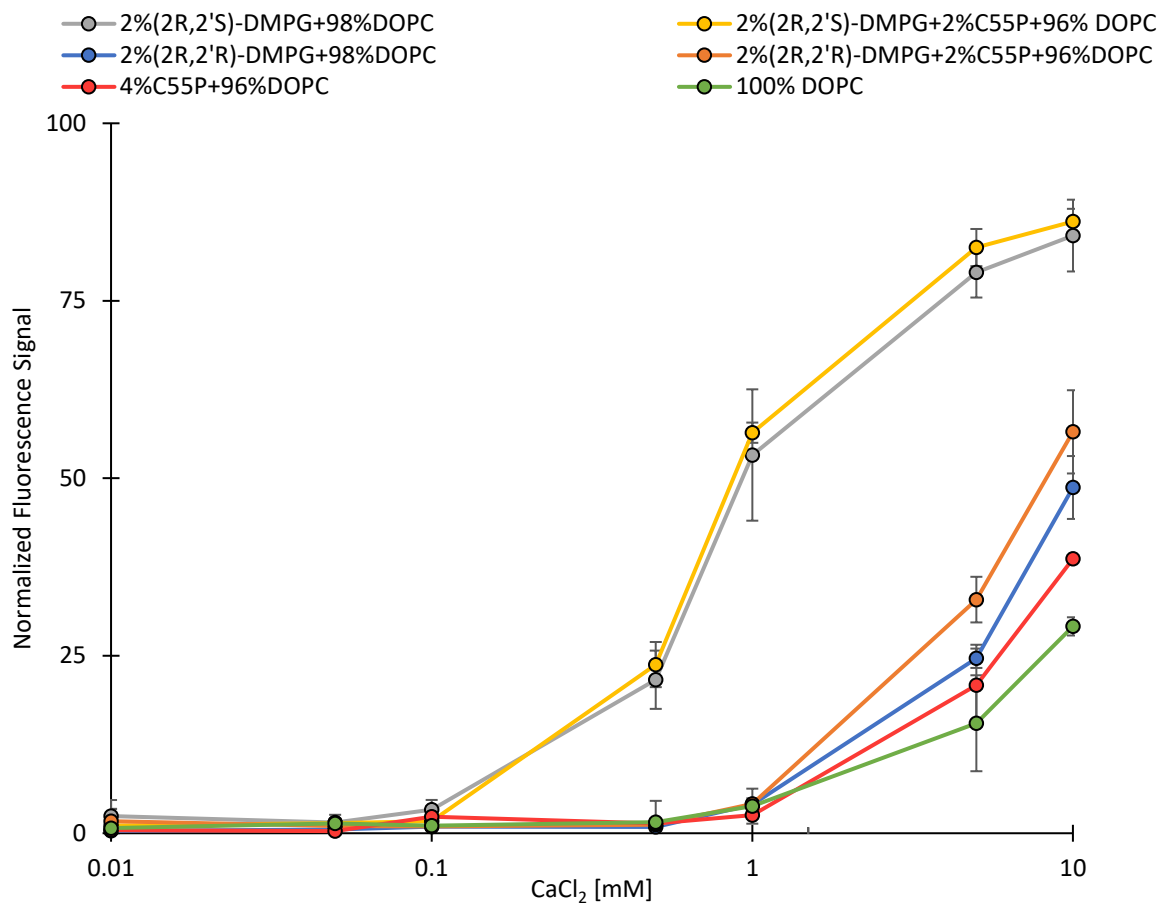
Figure C.9 Membrane binding curves using dap (3 μM) and LUVs composed of DMPG/C_{55}P/DOPC (250 μM total lipid concentration) at 37 ^{o}C in 20 mM HEPES, 150 mM NaCl (pH 7.4).

Appendix D Supplementary data for Chapter 6
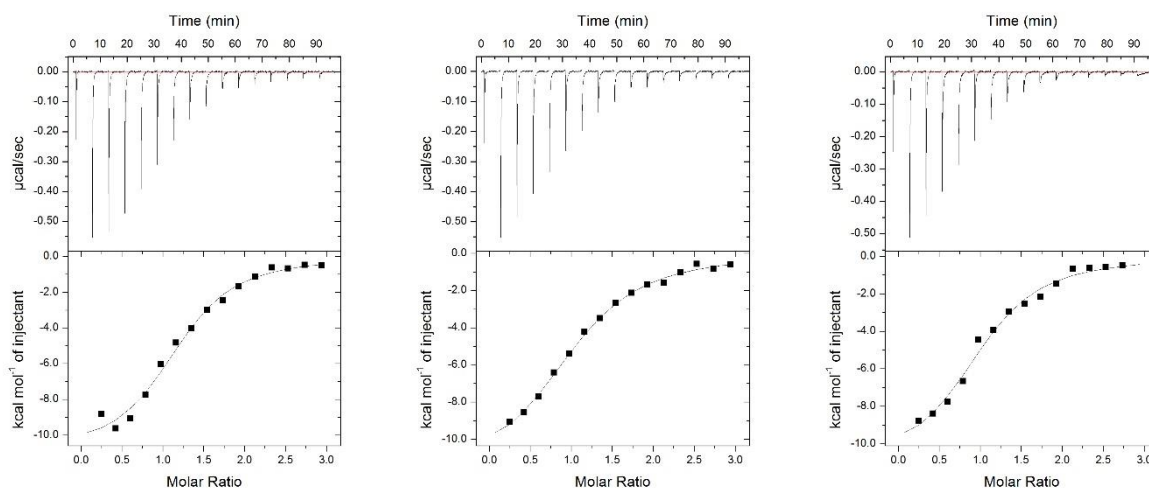
Figure D.1 Thermograms showing the titration of dap (23 μM) with 2R,2'S-C8PG at 5 mM CaCl$_2$
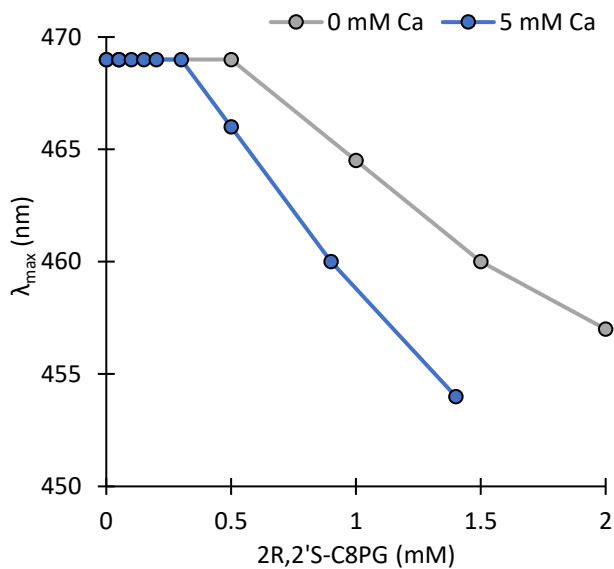
Figure D.2 Determining the CMC of C8PG in buffer (150 mM NaCl, 20 mM HEPES, 1% DMSO, pH = 7.4) with or without 5 mM CaCl$_2$ by observing 1-pyrenecarboxaldehyde emission.
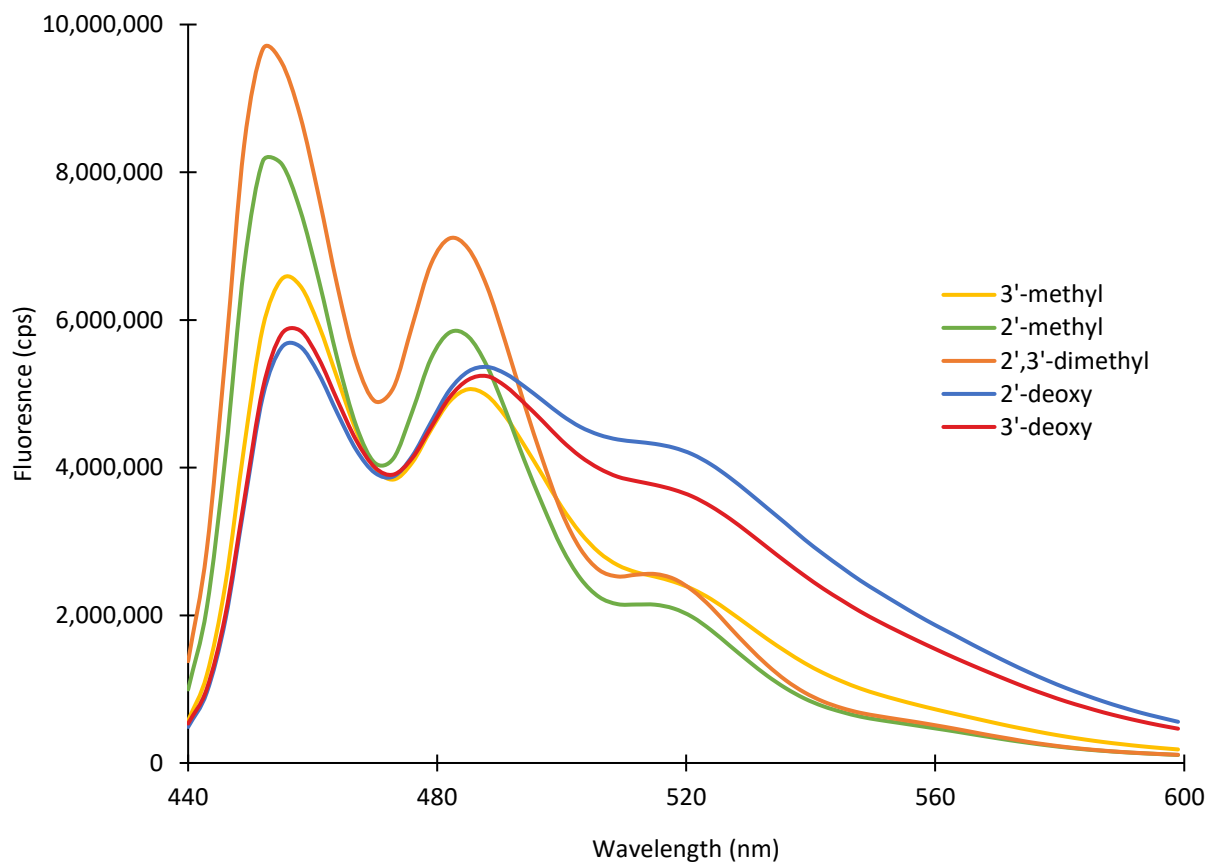
Figure D.3 Fluorescence spectra of perylene-dap (2.5 µM) in the presence of Ca^{2+} (see Table 1) and LUVs composed of 1:1 modified-DMPG:DMPC at 37 ^{o}C in 20 mM HEPES, 150 mM NaCl (pH 7.4).

PMBO⌇⌇OH⌇⌇OTs
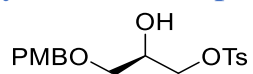
7.6 ^{1}H NMR
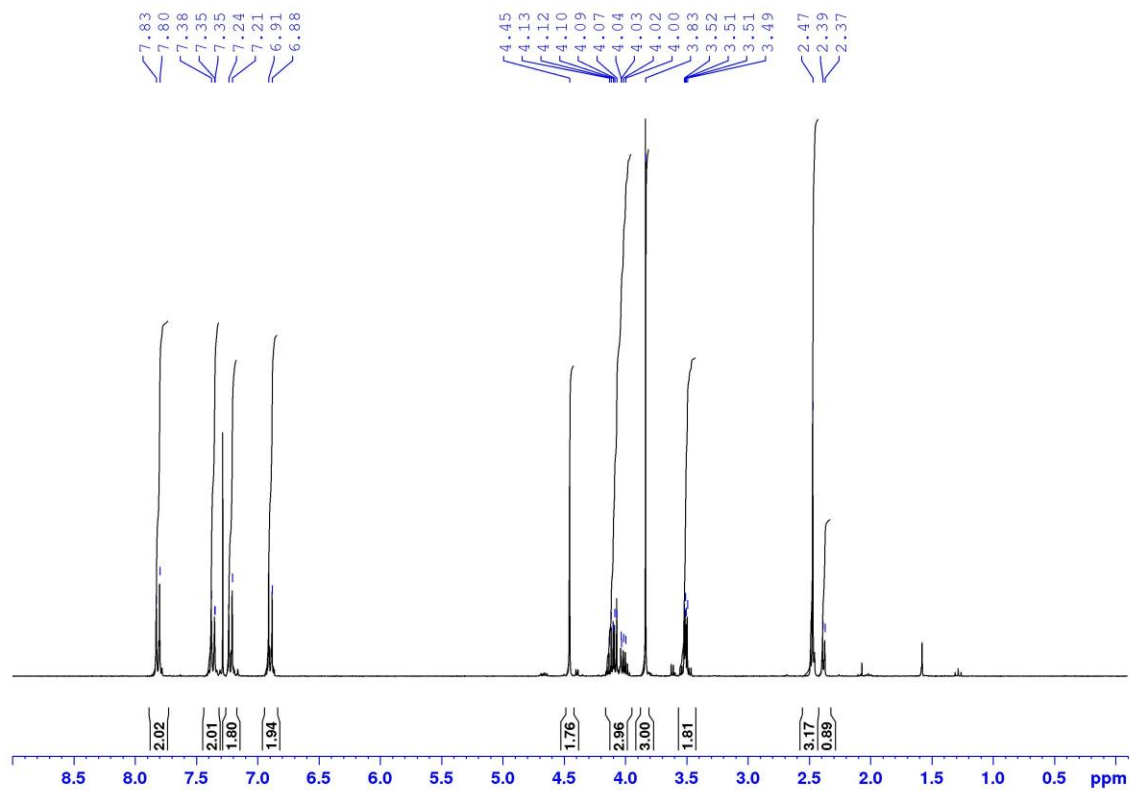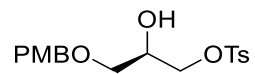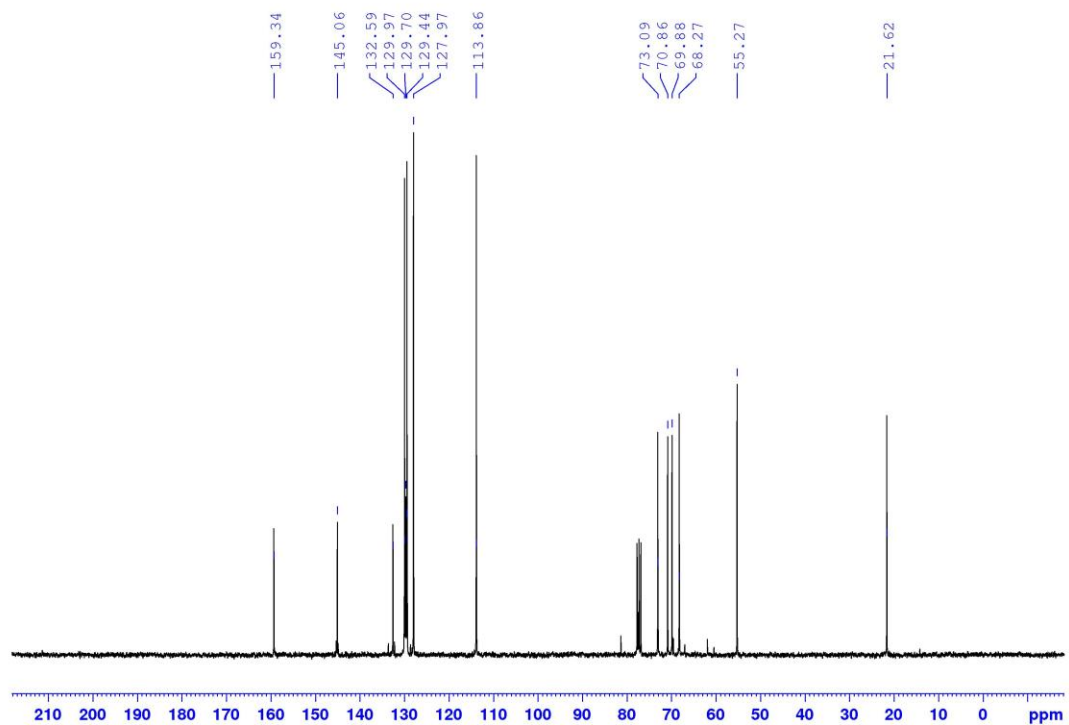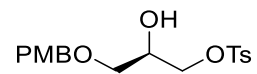
7.6 ^{13}C NMR

7.6 ^{13}C inverse gated NMR
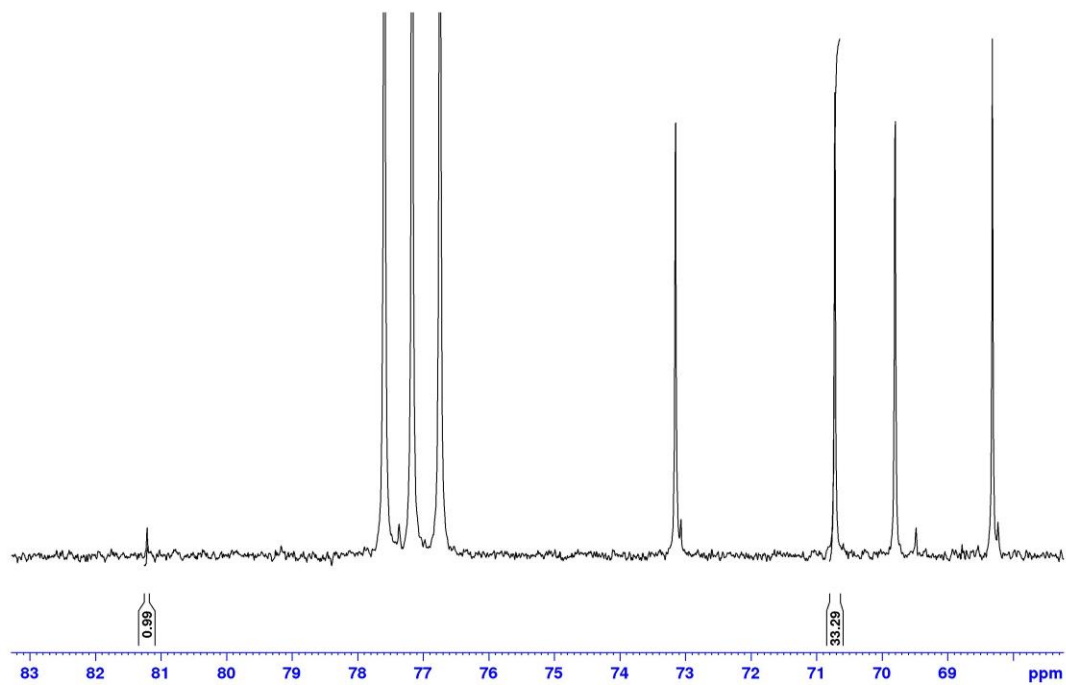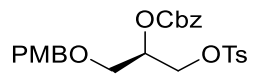
7.7 ^{1}H NMR
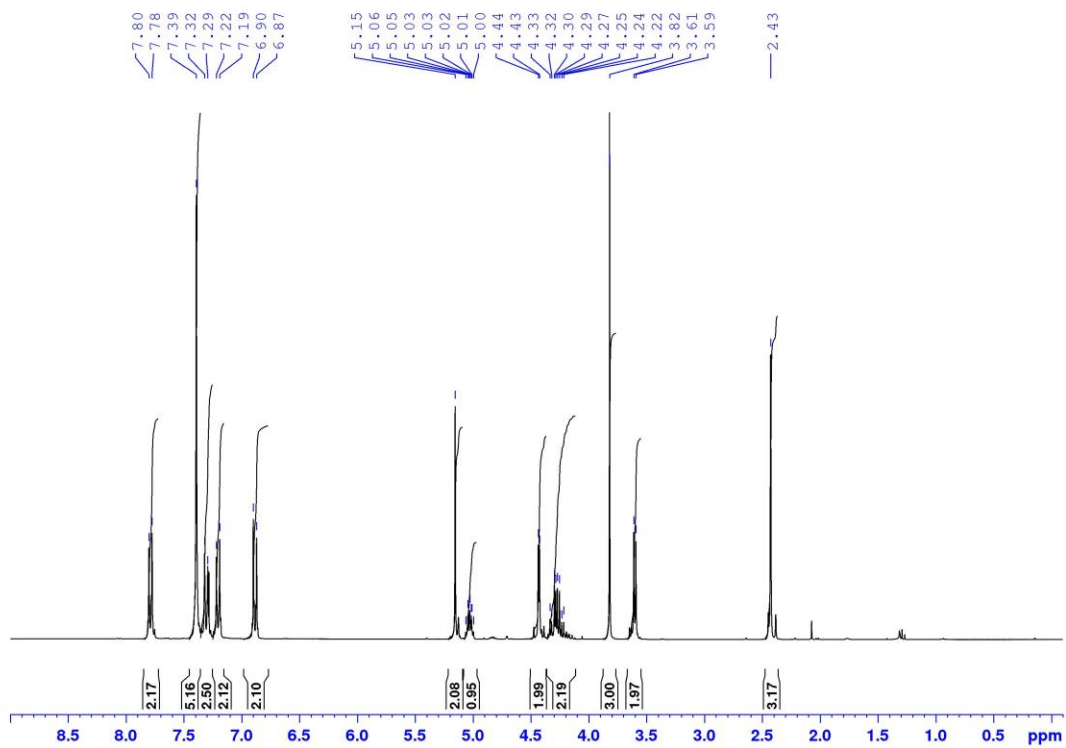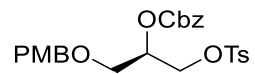
7.7 ^{13}C NMR

7.8 ^{1}H NMR

7.8 ^{13}C NMR

172.15, 172.04, 159.40, 156.60, 156.06, 154.62, 154.57, 136.77, 136.34, 135.10, 135.07, 129.61, 129.43, 129.41, 128.66, 128.57, 128.54, 128.37, 128.31, 128.20, 128.14, 128.09, 113.91, 74.30, 73.07, 69.94, 69.92, 67.54, 67.49, 67.01, 66.57, 63.66, 63.47, 55.28, 53.75, 53.70, 40.48, 31.91, 31.85, 29.28, 22.27, 22.19
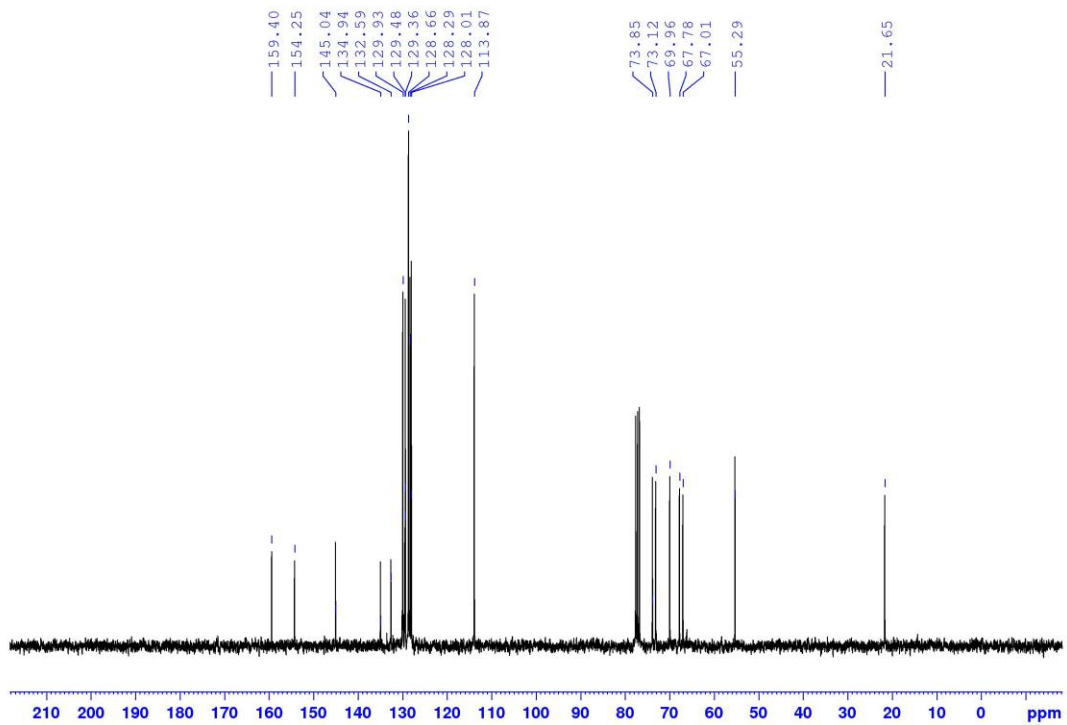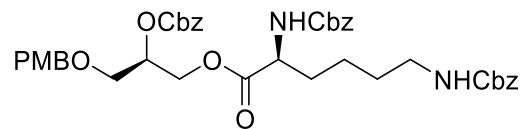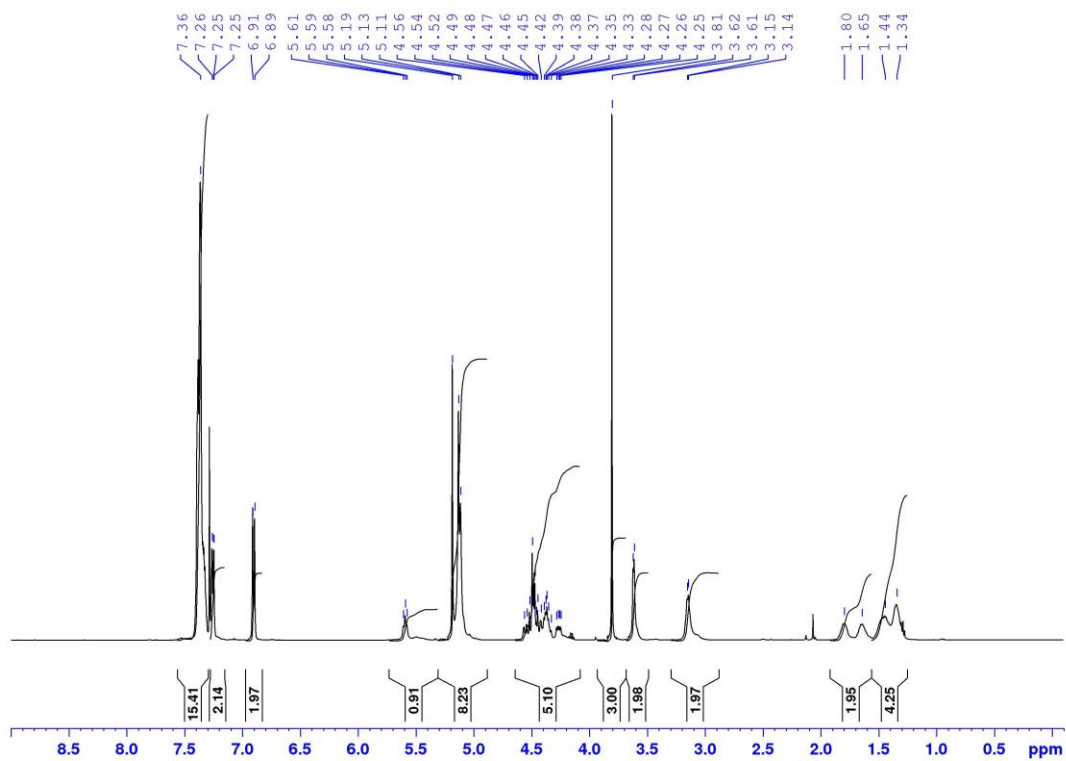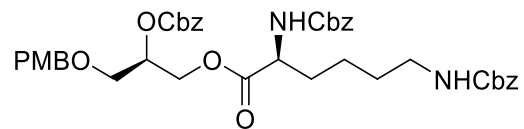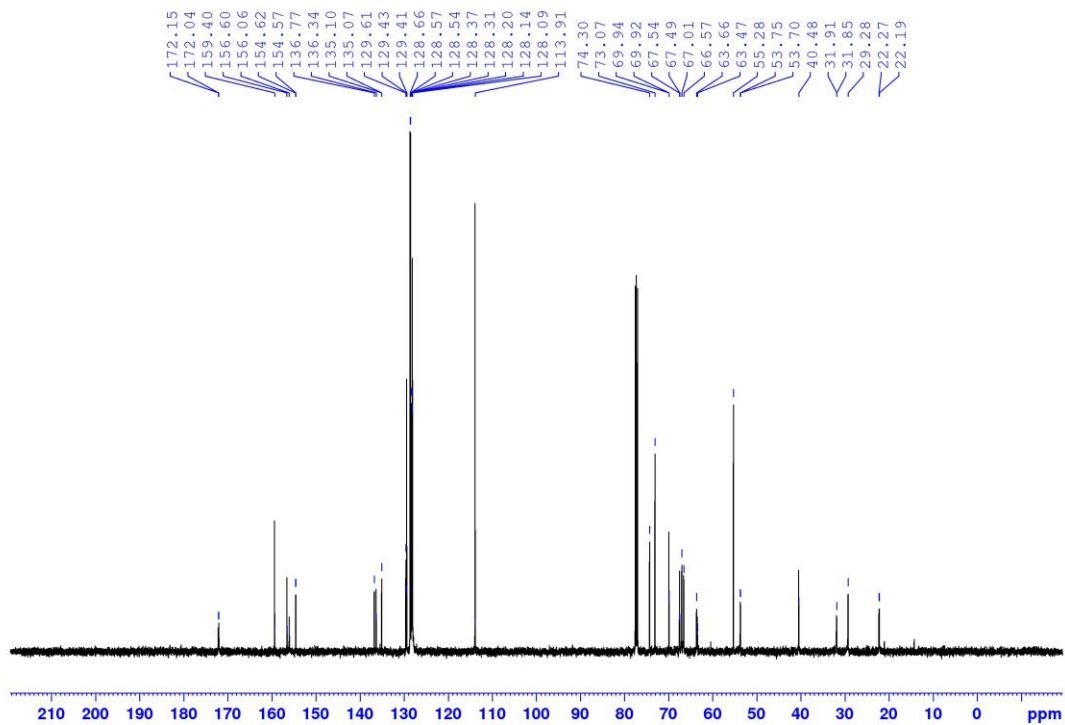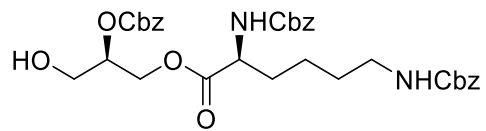
7.2 ^{1}H NMR
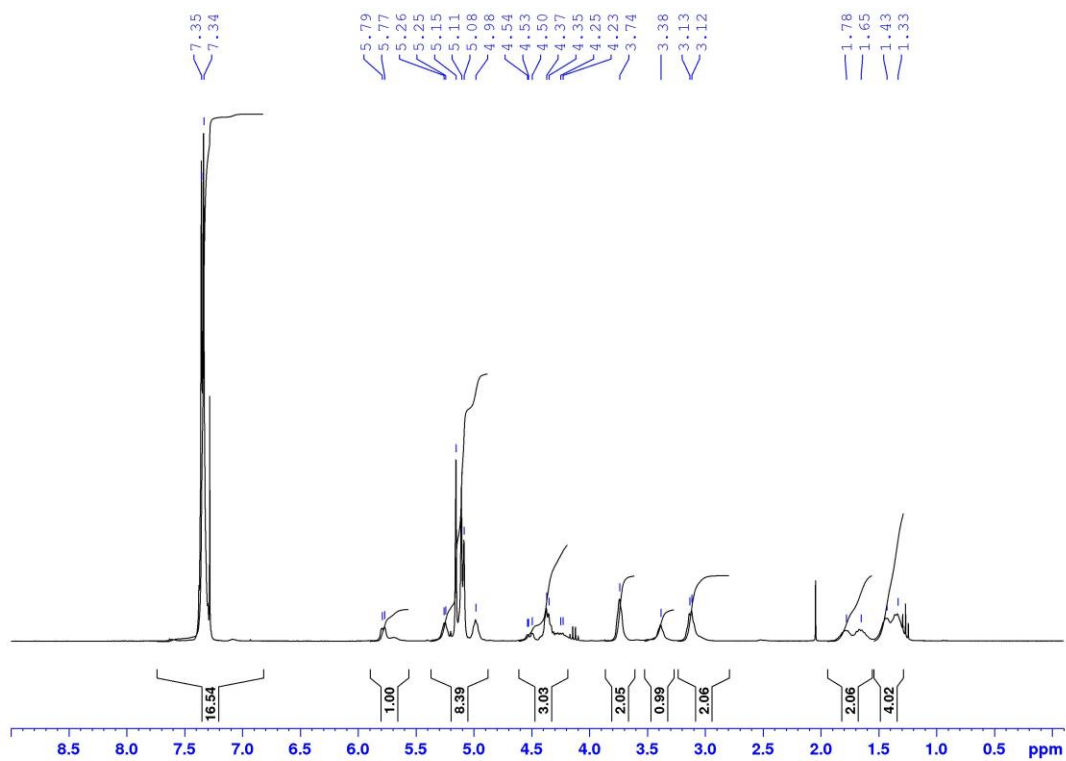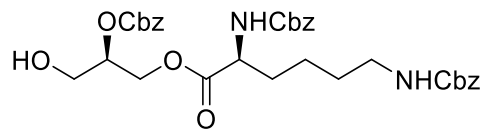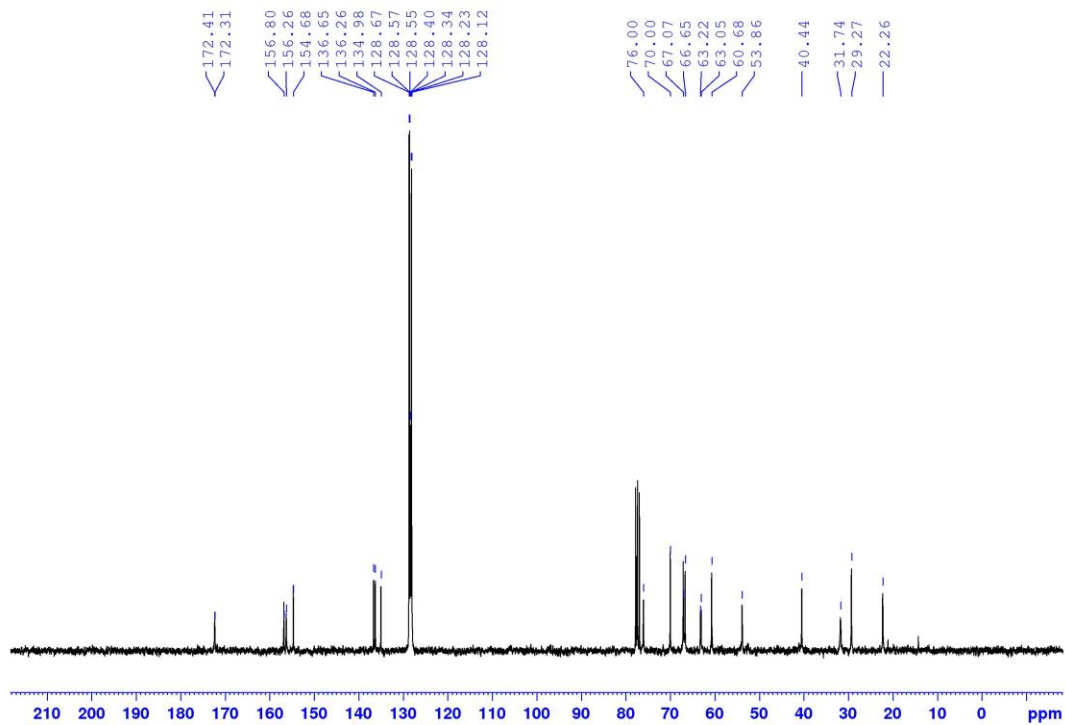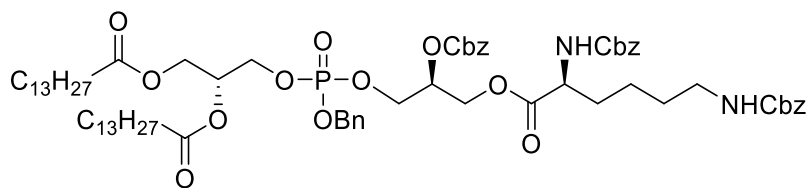
7.2 ^{13}C NMR

7.9 ^{1}H NMR
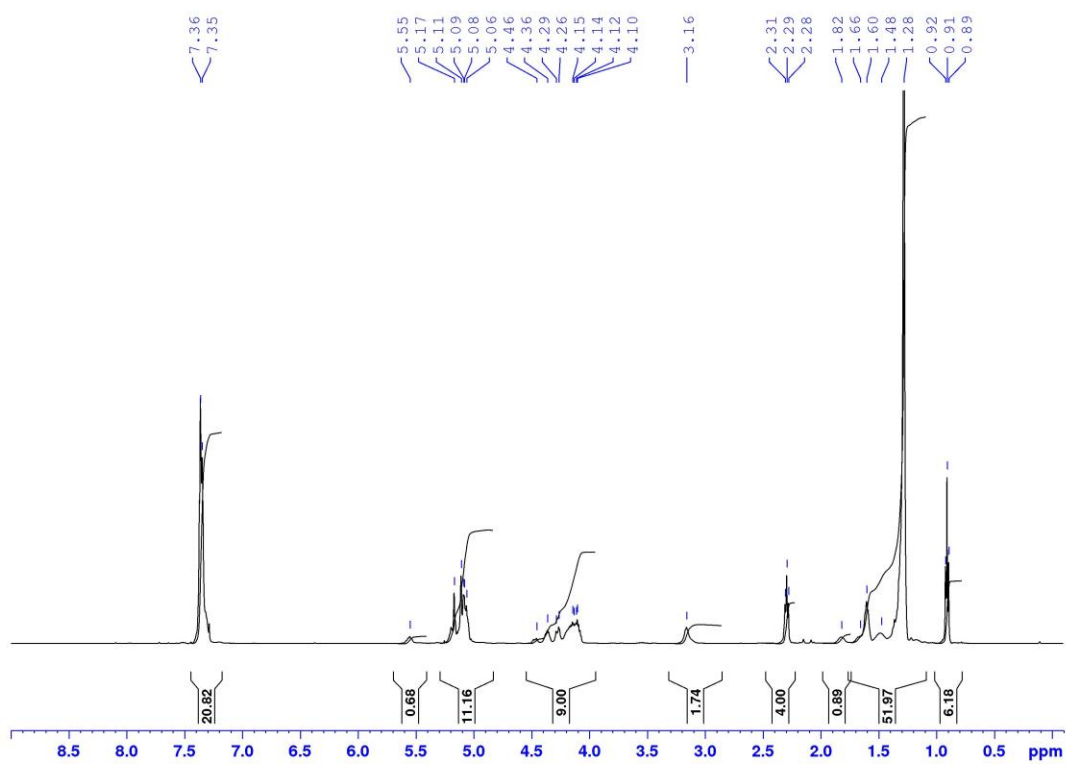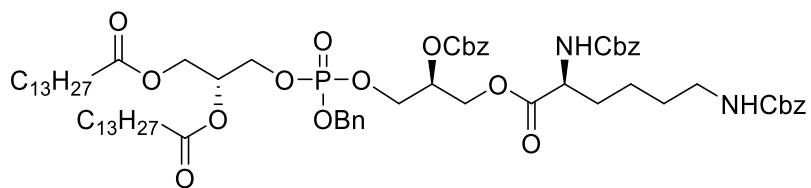
7.9 ^{13}C NMR
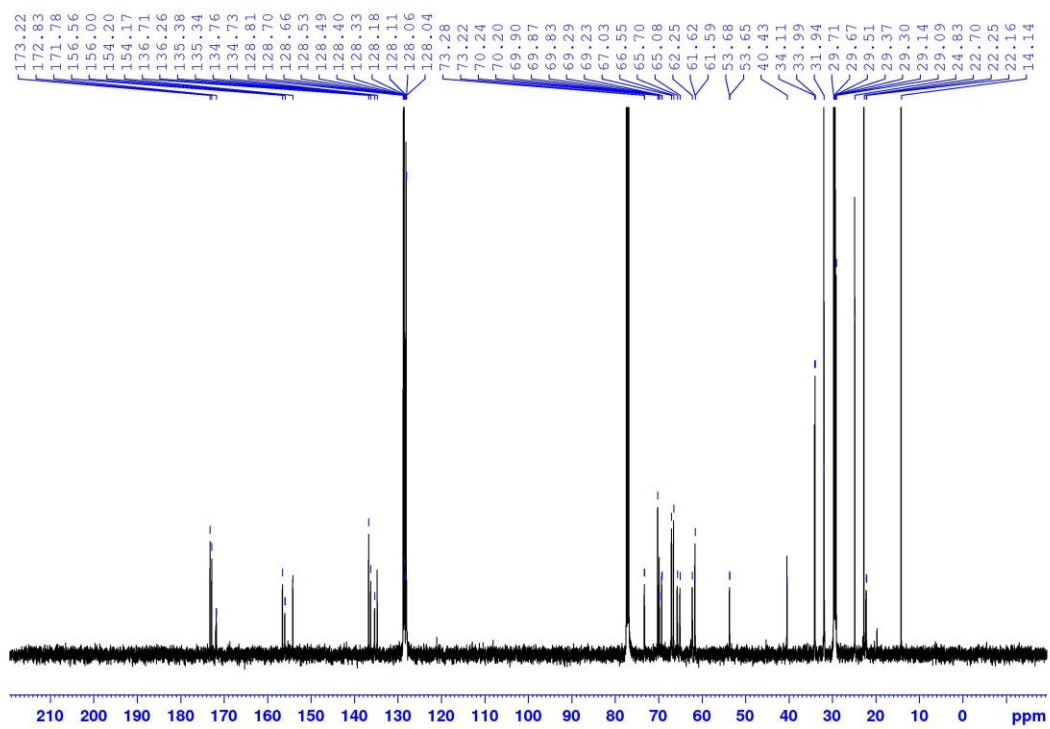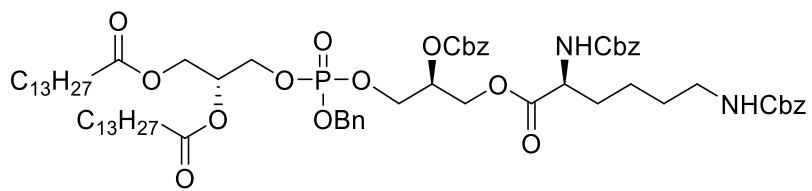
7.9 ^{31}P NMR
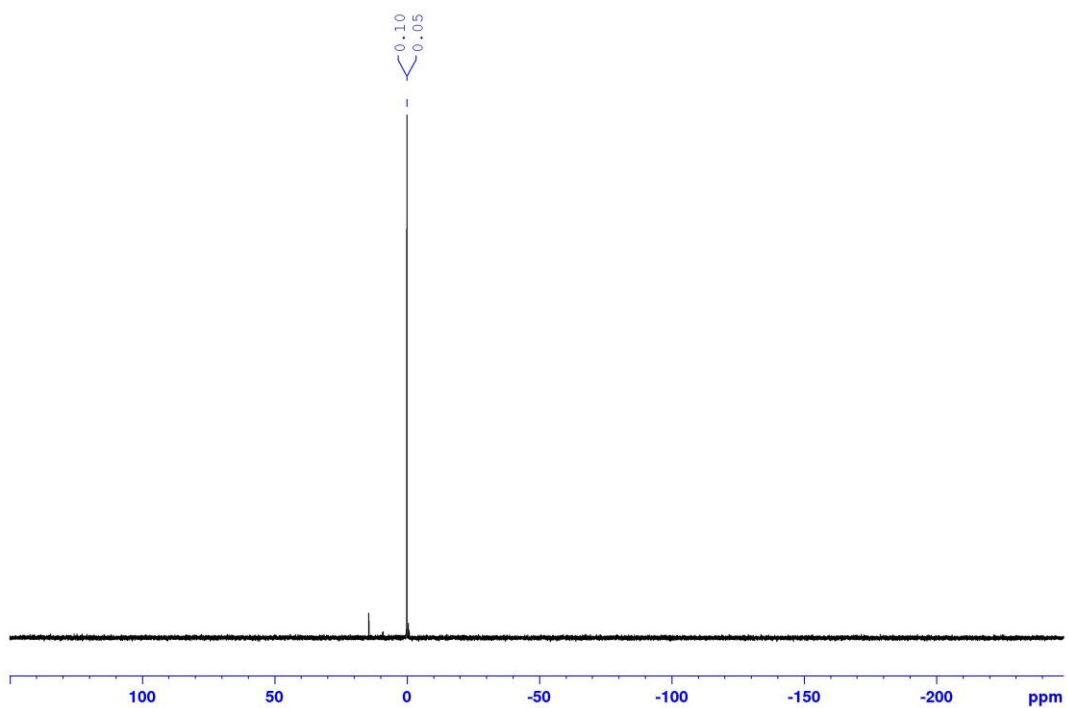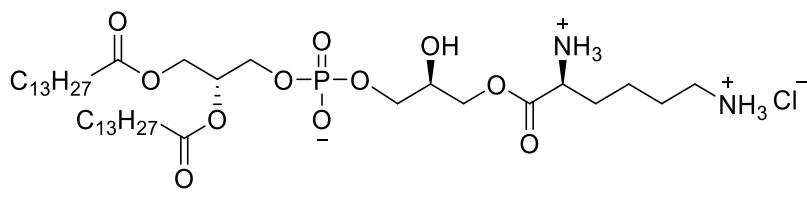
Lysyl-DMPG ^{1}H NMR
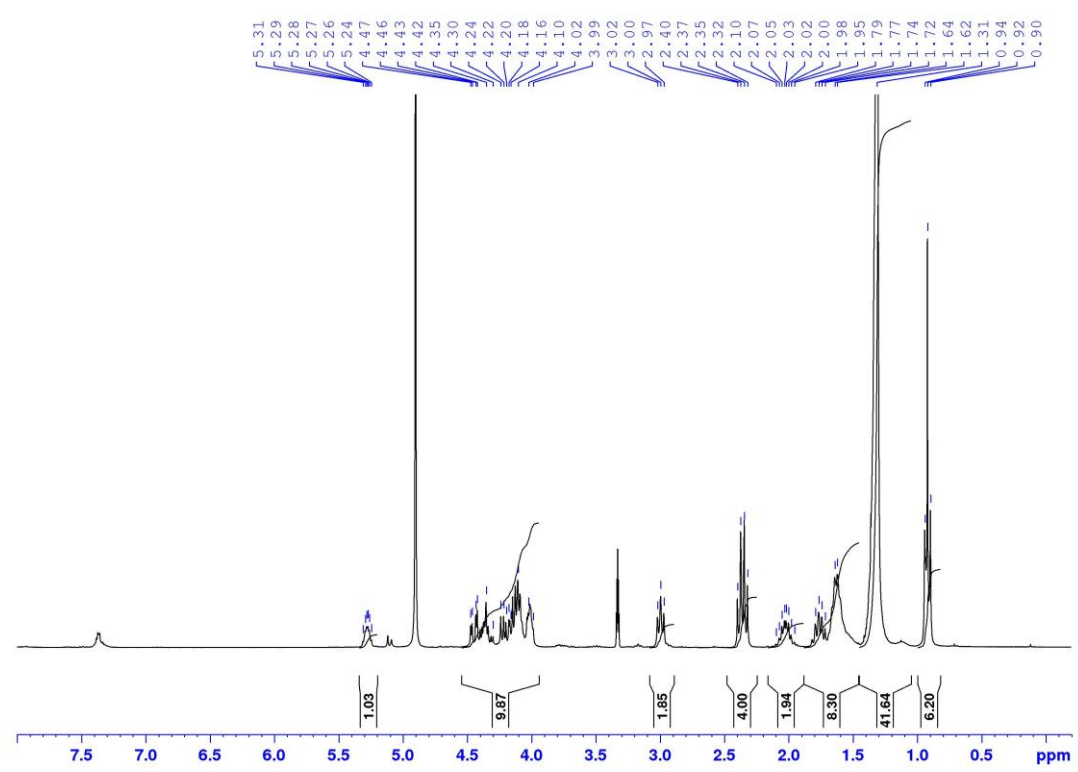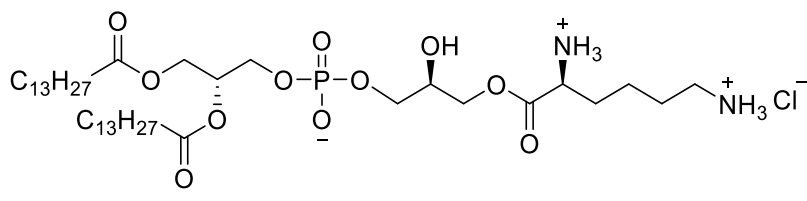
Lysyl-DMPG ^{13}C NMR

Lysyl-DMPG ^{31}P NMR

Appendix F   Supplementary data for Chapter 8
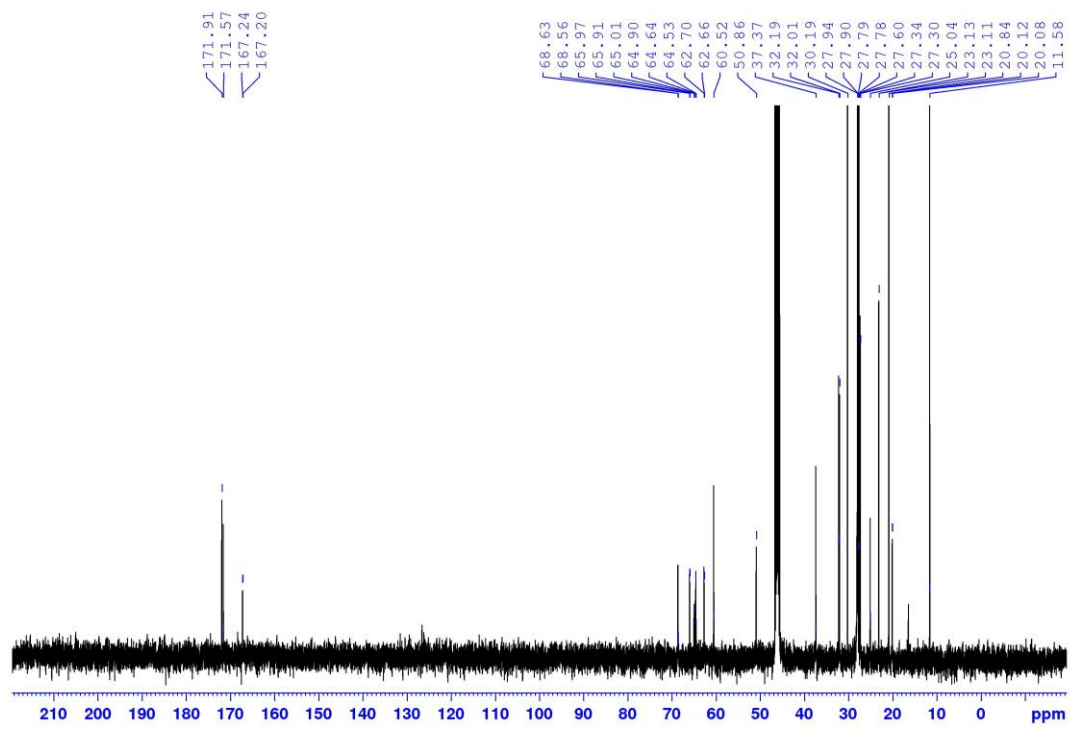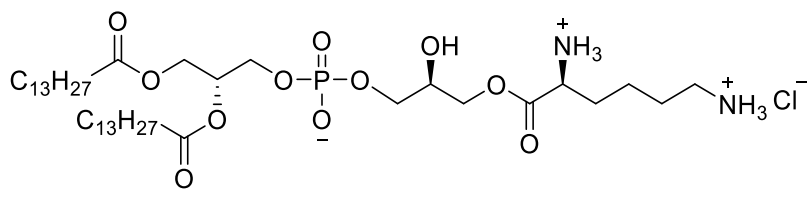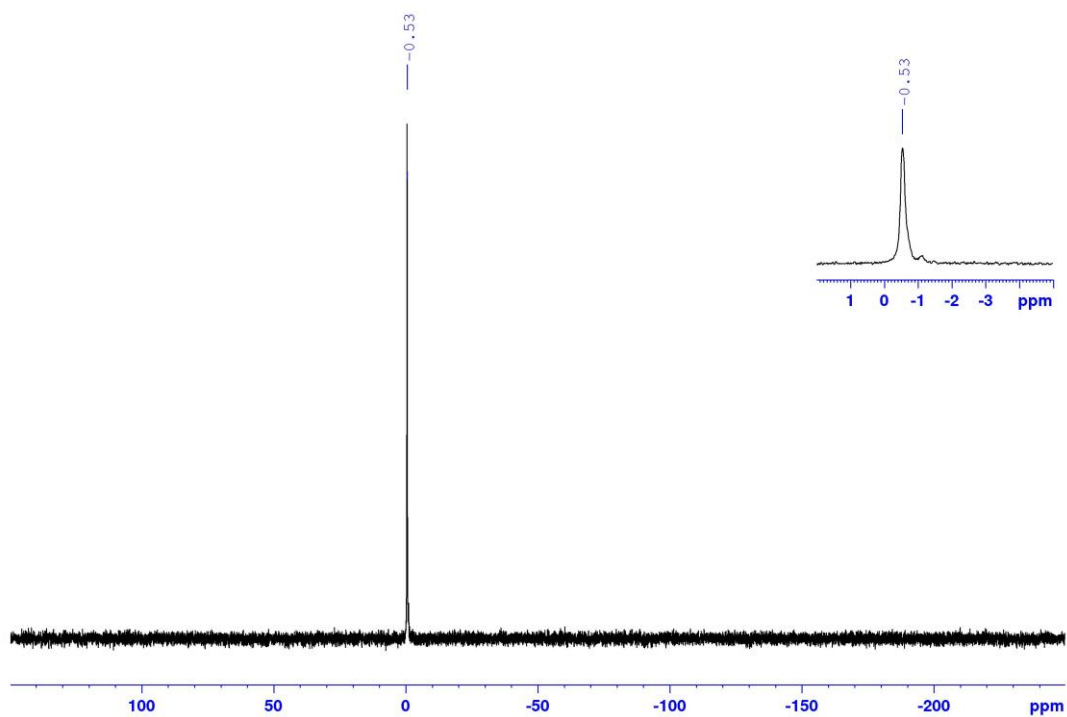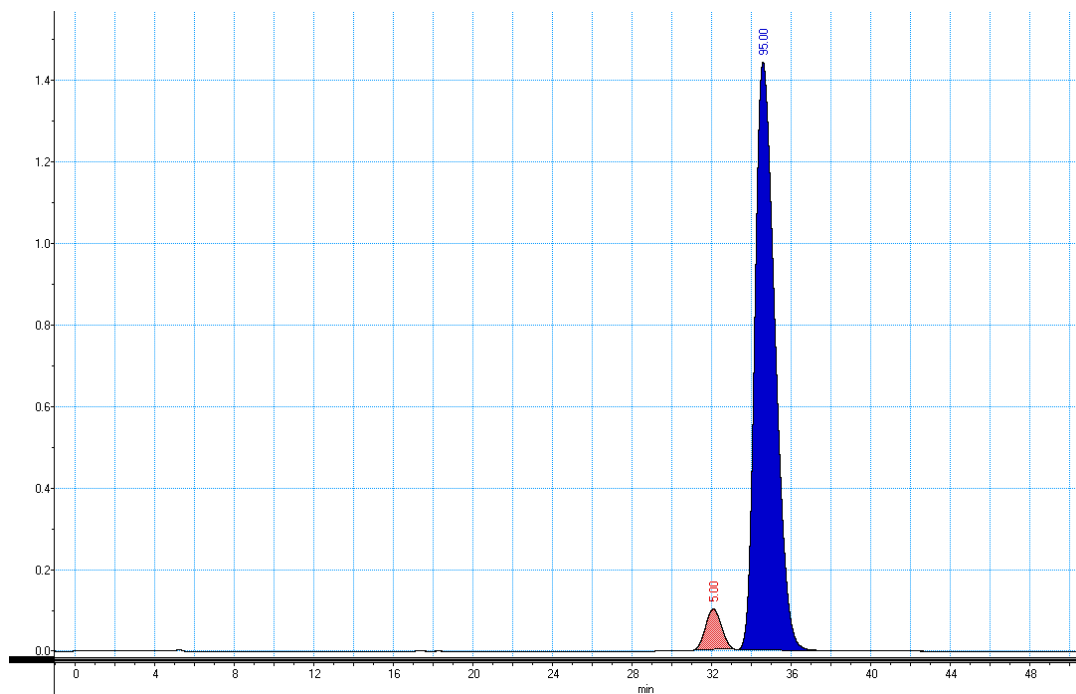
Figure F.1 Chiral HPLC chromatogram of **8.4a** (blue peak, t_r = 34.6 min). The peak with t_r = 32.0 min (red peak) is **ent-8.4a** as determined by injection of an authentic sample. Values above the peaks are the normalized peak areas. Mobile phase: 55% ACN/45% 0.1% TFA in H_2O.
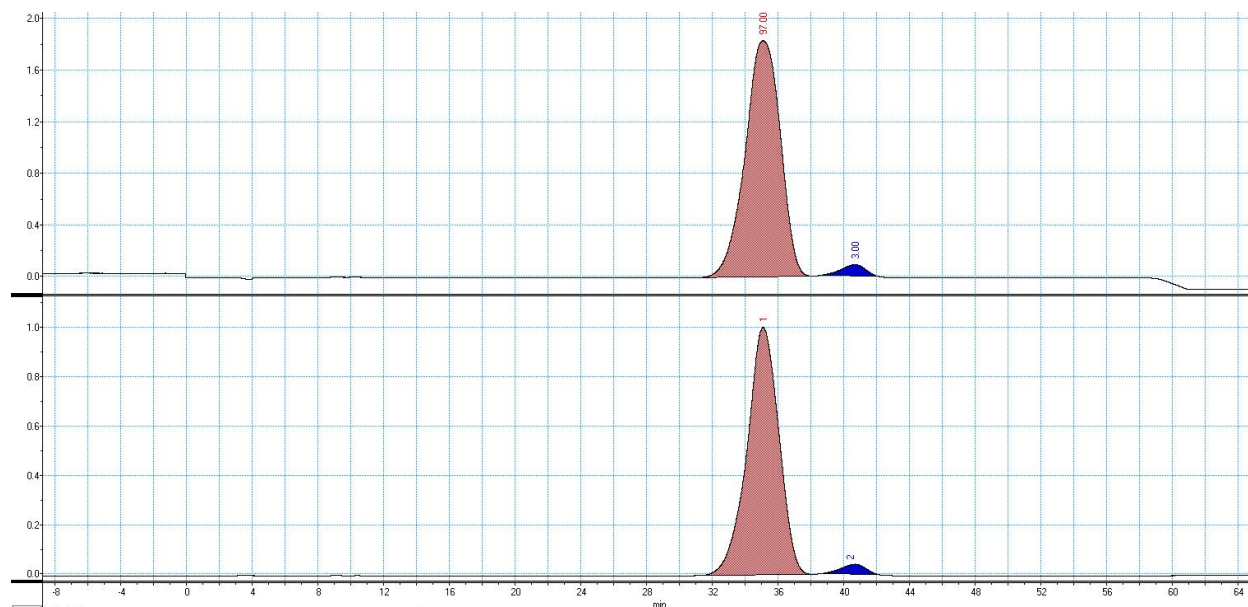
Figure F.2 Chiral HPLC trace of **8.25** showing the er to be 97%. Column: CHIRALPAK AS-RH 5 μm 4.6 mm x 150 mm. Top spectrum: l = 220 nm. Top spectrum: l = 280 nm. Mobile phase: 50:50 MeCN:H$_2$O+0.1% TFA; Flow rate: 0.5 mL/min

Table F.1 Hydrogenolysis conditions that were examined for the attempted conversion of **8.7** to **8.8**.

Catalyst (5 wt %)	Solvent	Hydrogen source	Result
Pd(OH)$_2$	MeOH	H$_2$	removed fmoc selectively
Pd/C	THF, 1% AcOH	H$_2$	removed fmoc selectively
Pd/C	EtOH, 1% AcOH	H$_2$	removed fmoc selectively
Pd/C	Ethyl Acetate, 1% AcOH	H$_2$	removed fmoc selectively
Pd/Ba	THF, 1% AcOH	H$_2$	mixture of desired product, fmoc deprotected SM and fmoc deprotected product observed by MS.
Pd/Ba	EtOH, 1% AcOH	H$_2$	removed fmoc selectively
Pd/Ba	EtOAc, 1% AcOH	H$_2$	mixture of desired product, fmoc deprotected SM and fmoc deprotected product observed by MS.
Pd/C (used 10 wt %)	MeOH	Et$_3$SiH	removed fmoc selectively
Pd/C	EtOH	Et$_3$SiH	removed fmoc selectively
Pd/C	EtOAc	Et$_3$SiH	removed fmoc selectively
Pd/C	ether	Et$_3$SiH	removed fmoc selectively
Pd/C	THF	Et$_3$SiH	removed fmoc selectively
Pd/C	Hexane, 10% EtOAc	Et$_3$SiH	did not proceed
Pd/Ba	EtOH, 1% AcOH	Et$_3$SiH	removed fmoc selectively
Pd/Ba	Acetone, 1% AcOH	Et$_3$SiH	removed fmoc selectively
PdCl$_2$	MeOH	Et$_3$SiH	mixture of desired product, fmoc deprotected SM and fmoc deprotected product observed by MS
Pd/Ba	MeOH	Et$_3$SiH	removed fmoc selectively
Pd(OH)$_2$	MeOH	Et$_3$SiH	removed fmoc selectively
Pd(AcO)$_2$	MeOH	Et$_3$SiH	removed fmoc selectively
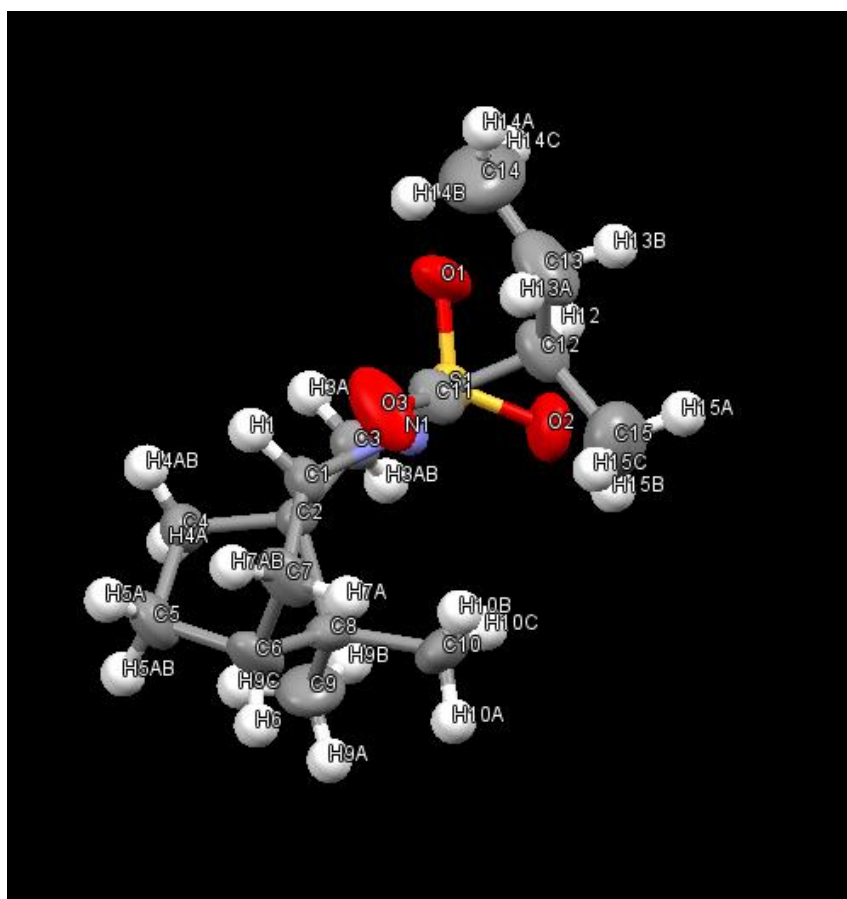
Figure F.3 X-ray crystal structure of **8.28.** Ellipsoid contour probability level is 50 %.

Table F.2 Crystal data and structure refinement for **8.28**

Empirical formula	$C_{15}H_{25}NO_3S$
Formula weight	299.42
Temperature	296(2) K
Wavelength	0.71073 Å
Crystal system	Orthorhombic
Space group	$P2_12_12$
Unit cell dimensions	$a = 14.1638(3)$ Å, $b = 14.8141(3)$ Å, $c = 7.7700(2)$ Å
Volume	1630.33(6) Å^3
Z	4
Density (calculated)	1.220 g/cm^3
Absorption coefficient	0.205 mm^{-1}
F(000)	648
Crystal size	0.240 x 0.110 x 0.090 mm^3
Theta range for data collection	2.621 to 25.996°.
Index ranges	-17<=h<=17, -18<=k<=18, -9<=l<=7
Reflections collected	20875
Independent reflections	3210 [R(int) = 0.0245]
Completeness to theta = 25.242°	99.9 %
Absorption correction	Semi-empirical from equivalents
Max. and min. transmission	0.7460 and 0.7052
Refinement method	Full-matrix least-squares on F^2
Data / restraints / parameters	3210 / 0 / 186
Goodness-of-fit on F^2	1.215
Final R indices [I>2sigma(I)]	R1 = 0.0306, wR2 = 0.0769
R indices (all data)	R1 = 0.0334, wR2 = 0.0785
Absolute structure parameter	0.045(16)
Largest diff. peak and hole	0.237 and -0.176 e.Å^{-3}

Appendix G Supplementary data for Chapter 9
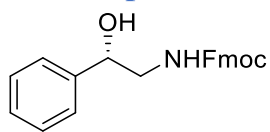
9.8B
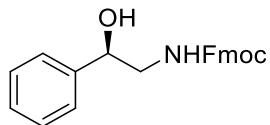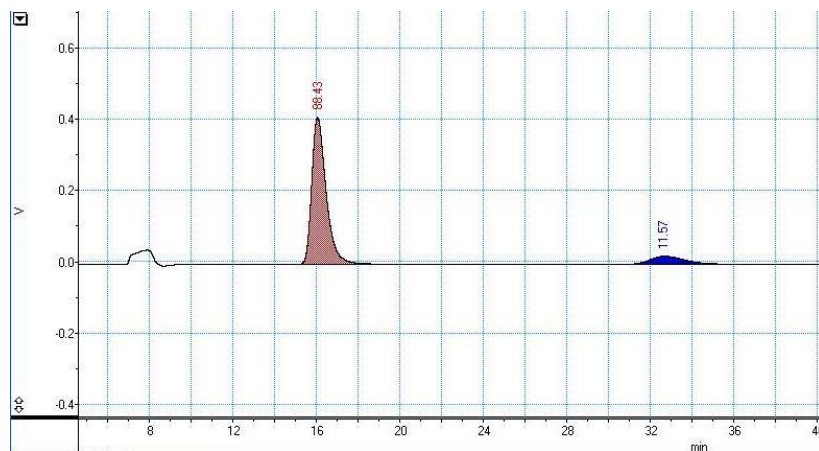
9.8B
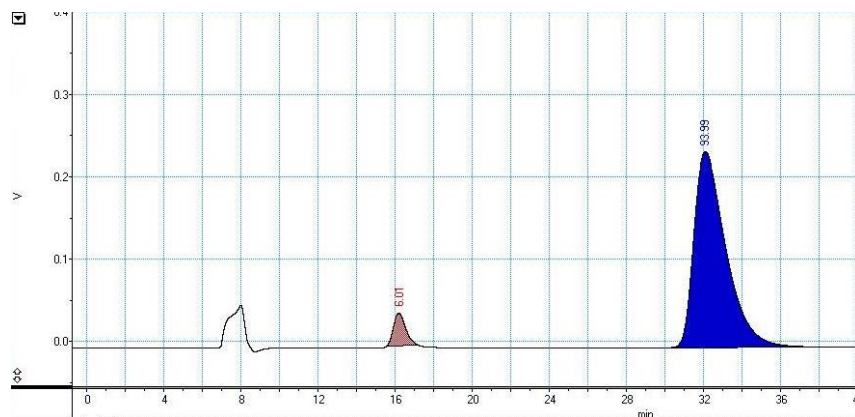
Figure G.1 Both traces collected using CHIRAL PAK OD-H, flow rate = 0.4 mL/min, mobile phase: 10:90 n-hexane:iPrOH. Injection peak at 8 min.
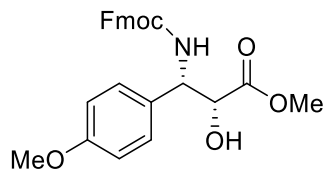
9.14A'
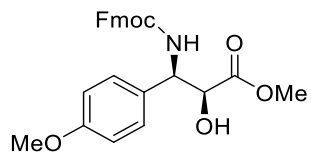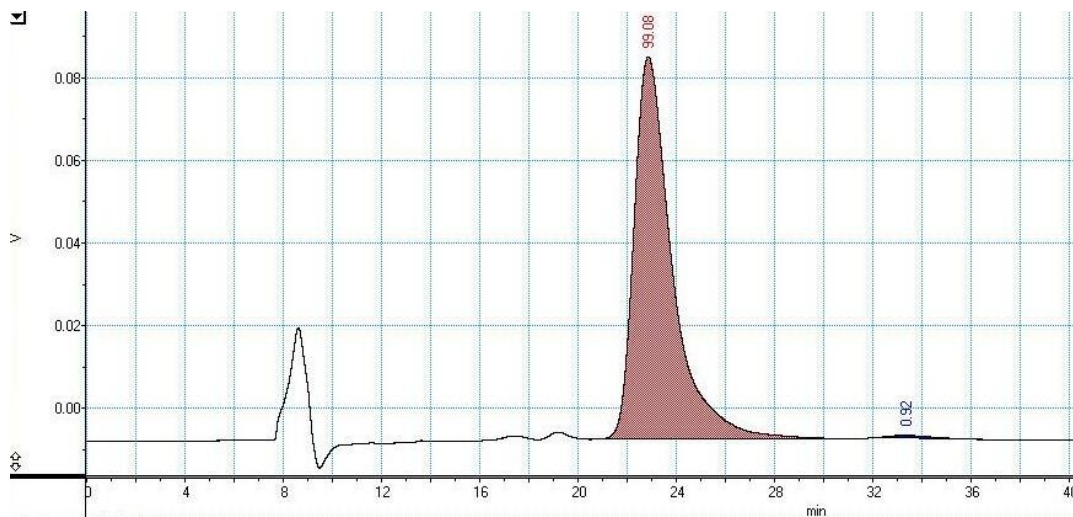
9.14A
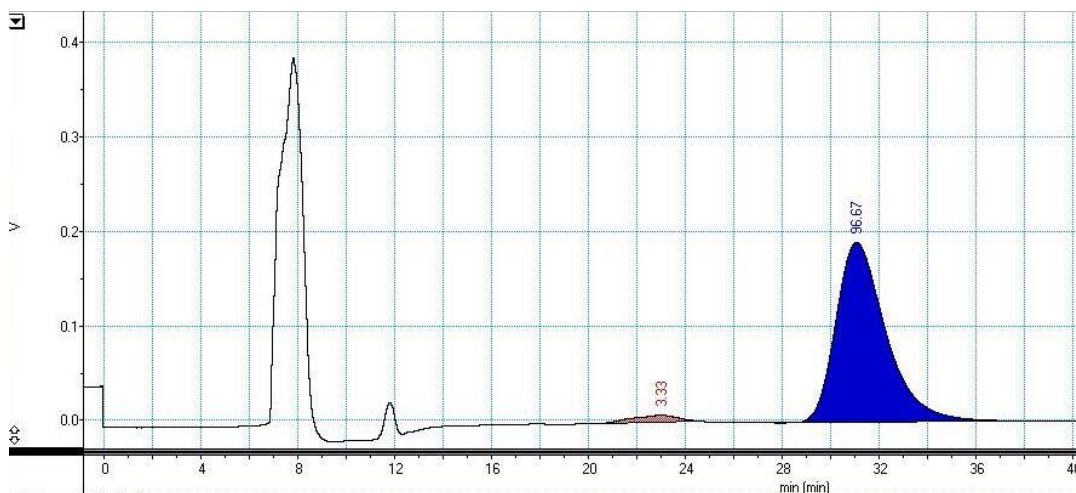
Figure G.2 Both traces collected using CHIRAL PAK OD-H, flow rate = 0.4 mL/min, mobile phase: 10:90 n-hexane:iPrOH. Injection peak at 8 min is due to MeCN used to dissolve the solid sample
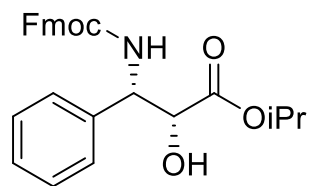
9.16A'
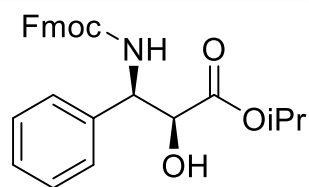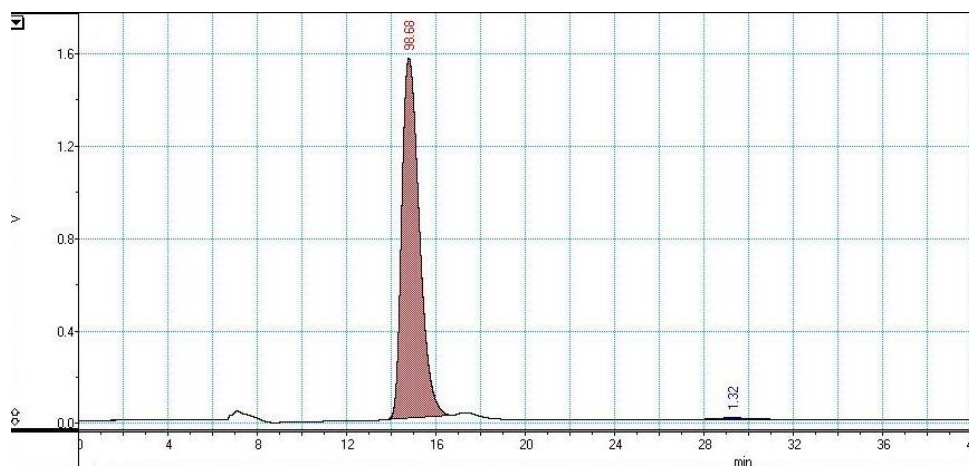
9.16A
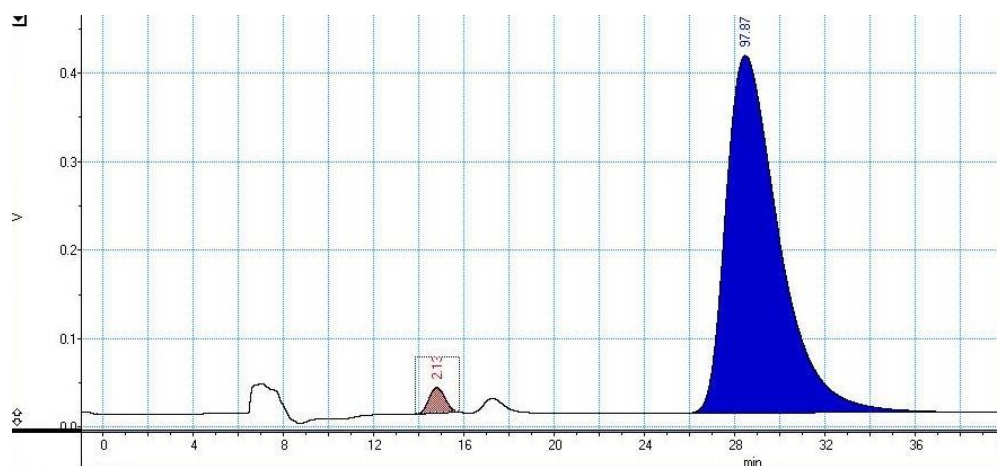
Figure G.3 Both traces collected using CHIRAL PAK OD-H, flow rate = 0.4 mL/min, mobile phase: 10:90 n-hexane:iPrOH. Injection peak at 8 min.
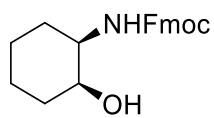
9.18A'
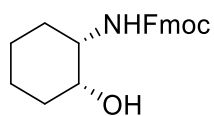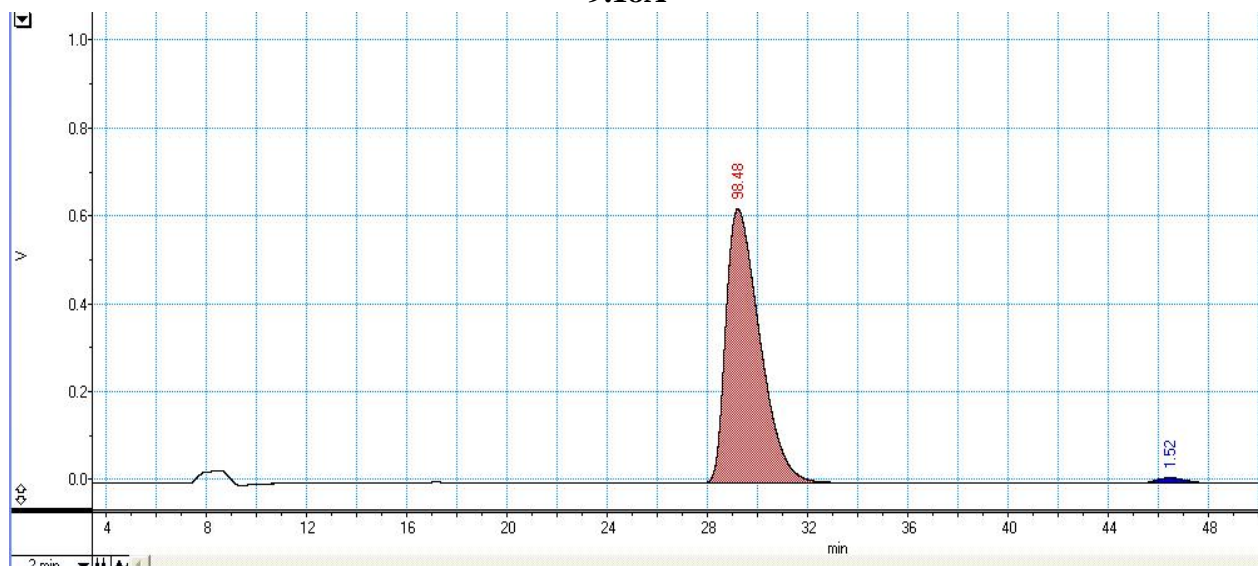
9.18A
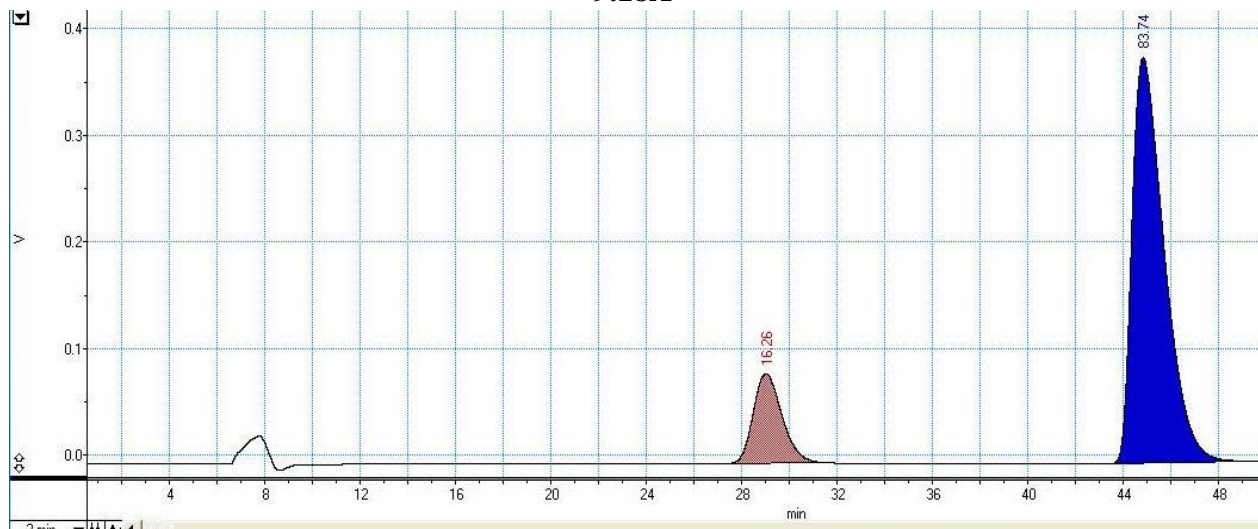
Figure G.4 Both traces collected using CHIRAL PAK OD-H, flow rate = 0.4 mL/min, mobile phase: 10:90 n-hexane:iPrOH for 40 min then 0:100 nhexane:iPrOH for 10min (50 min total). Injection peak at 8 min
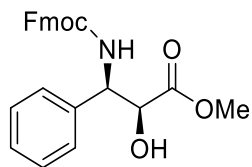
9.21A
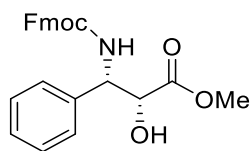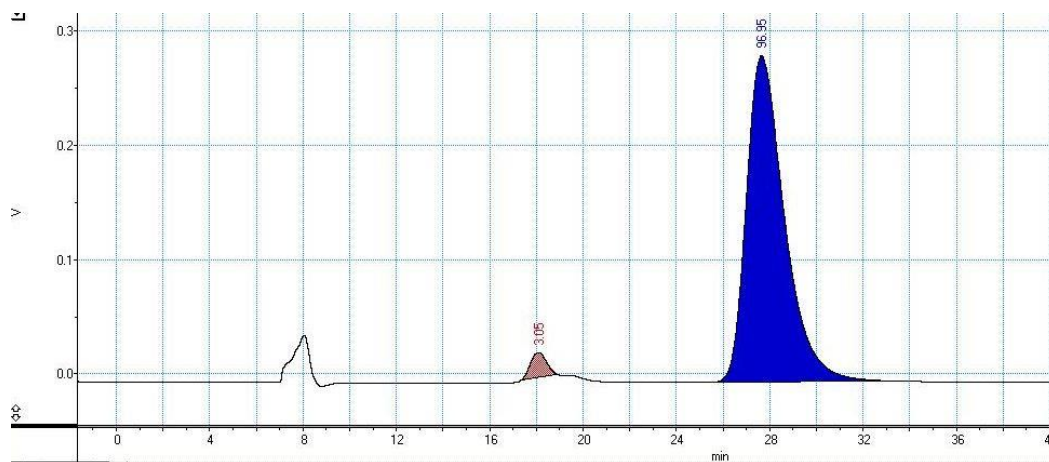
9.21A'
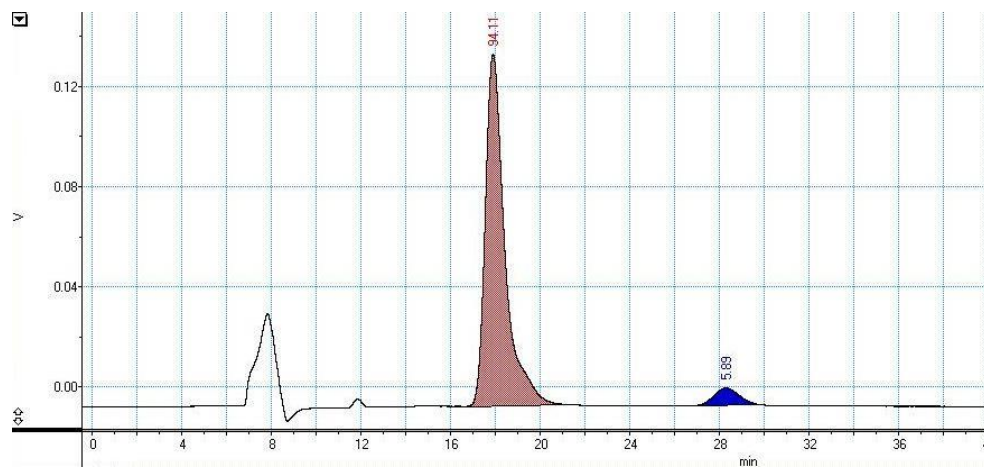
Figure G.5 Both traces collected using CHIRAL PAK OD-H, flow rate = 0.4 mL/min, mobile phase: 10:90 n-hexane:iPrOH. Injection peak at 8 min is due to MeCN used to dissolve the solid sample

9.23A

9.23A'
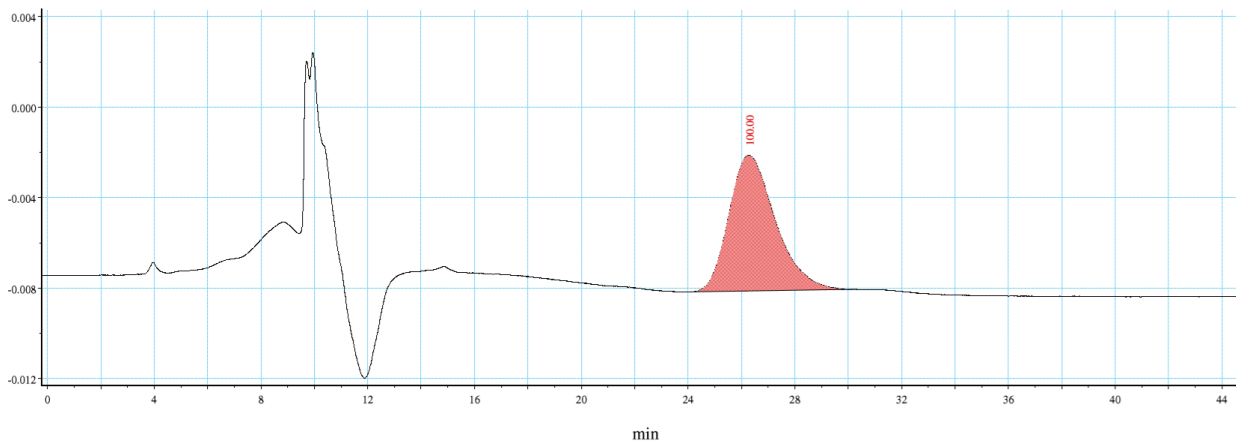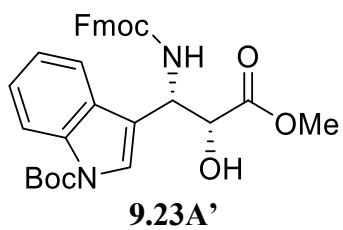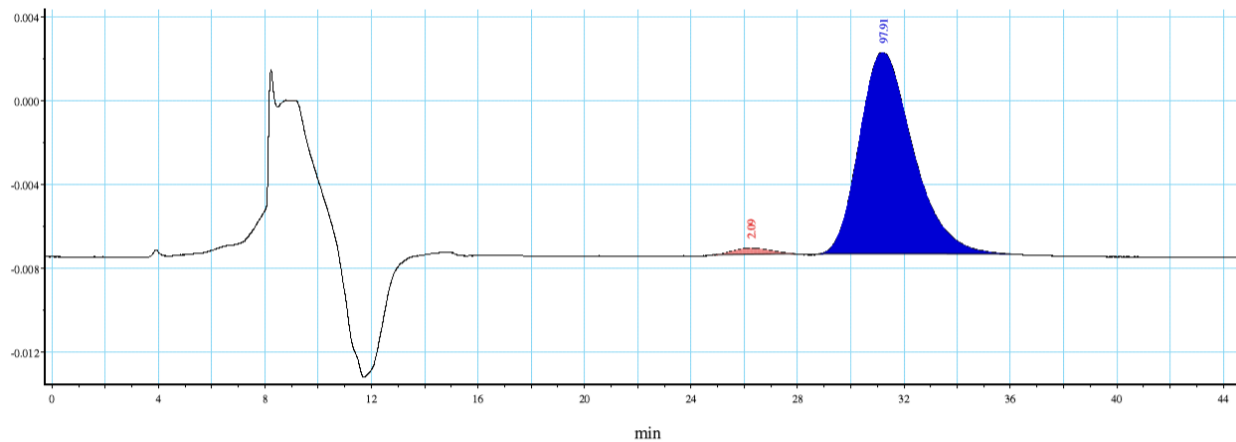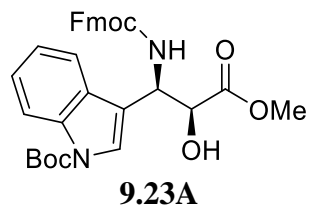
Figure G.6 Both traces collected using CHIRAL PAK OD-H, flow rate = 0.3 mL/min, mobile phase: 100 % iPrOH. Injection peak at 8 min is due to MeCN used to dissolve the solid sample
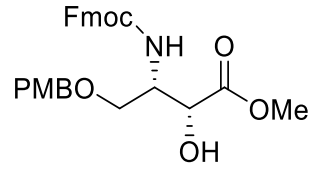
9.25A'
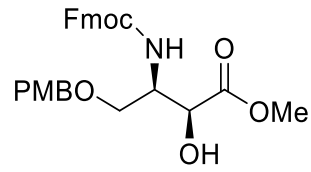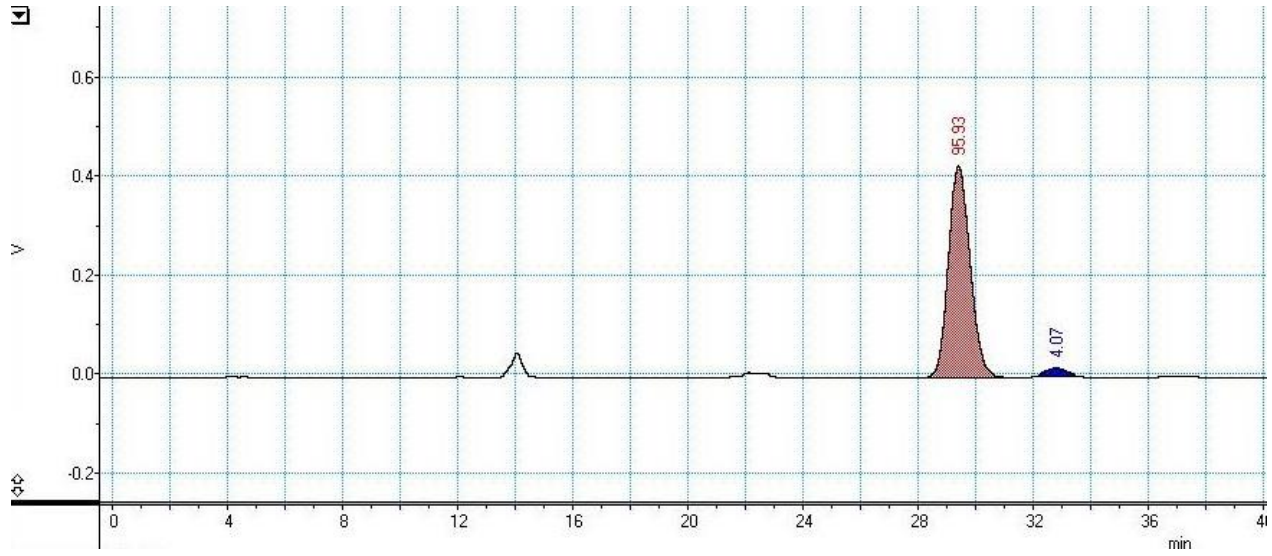
9.25A
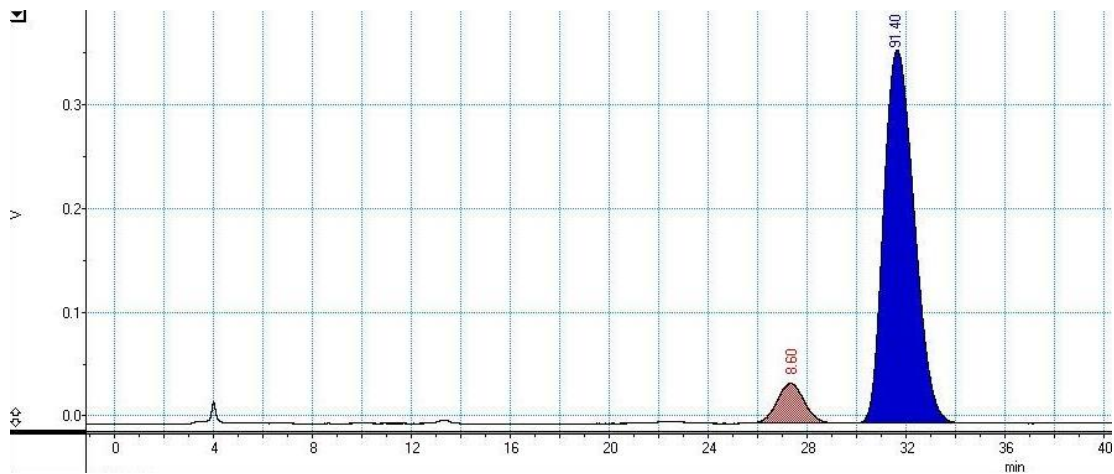
Figure G.7 Both traces collected using CHIRAL PAK AS-RH, flow rate = 0.5 mL/min, mobile phase: 45:55 ACN:H$_2$O+0.1% TFA. Injection peak at 4 min.
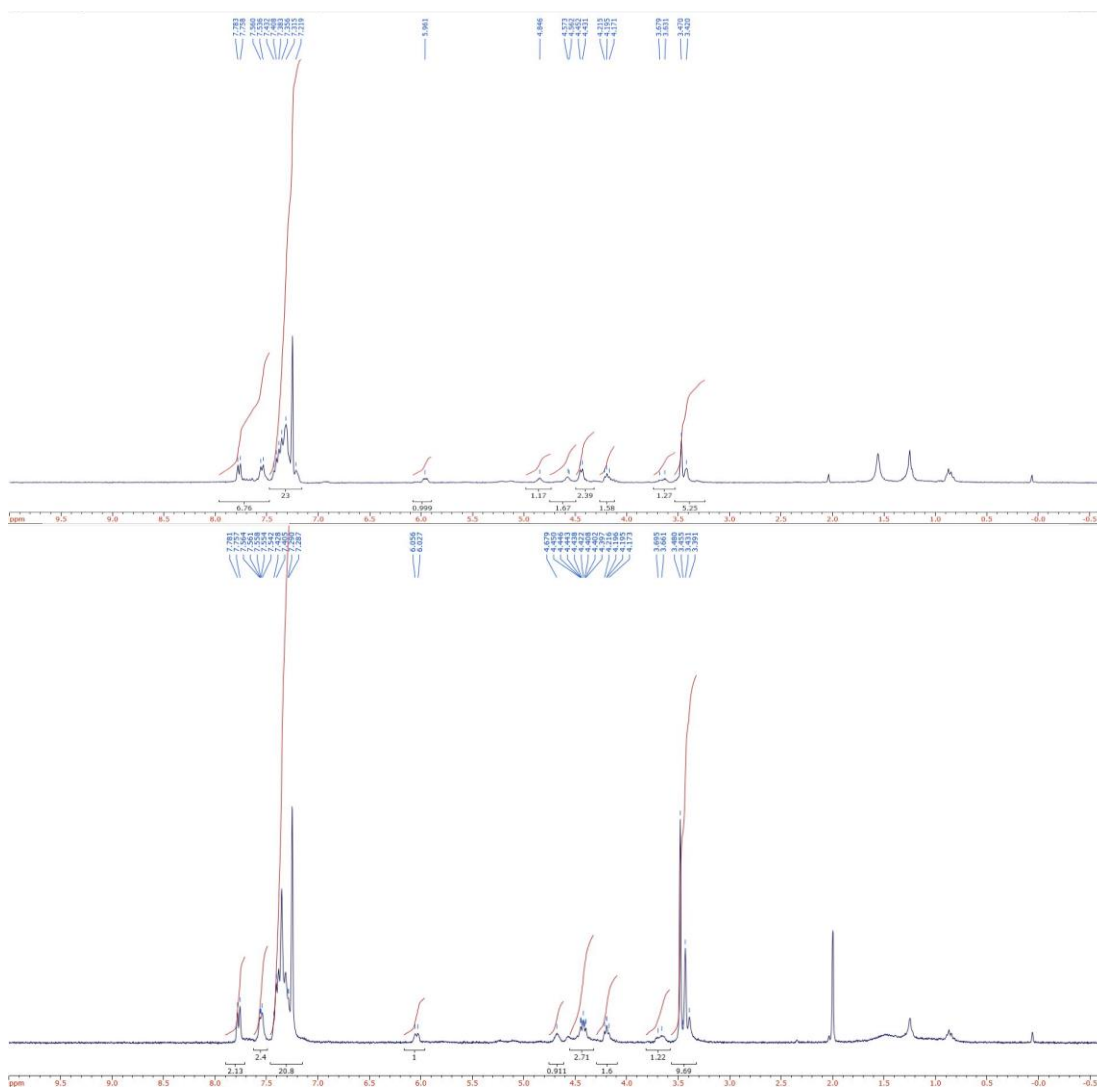
Figure G.8(top) (+)-MTPA ester of **9.8B**. (bottom) (-)-MTPA ester of **9.8B**

Table G.1 Mosher's ester analysis for MTPA-**9.8B**
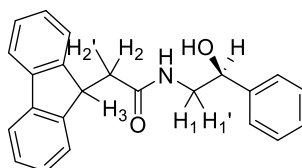
Chemical environment	(+)-MTPA δ	(-)-MTPA δ	Δ δ= δ(-)- δ(+)
1,1'*	3.50, 3.65	3.40, 3.65	-0.1, 0
2,2'*	4.44	4.42	-0.02
3	4.19	4.19	0
N**H**-Fmoc	4.85	4.68	-0.17

*assigned based on COSY

399
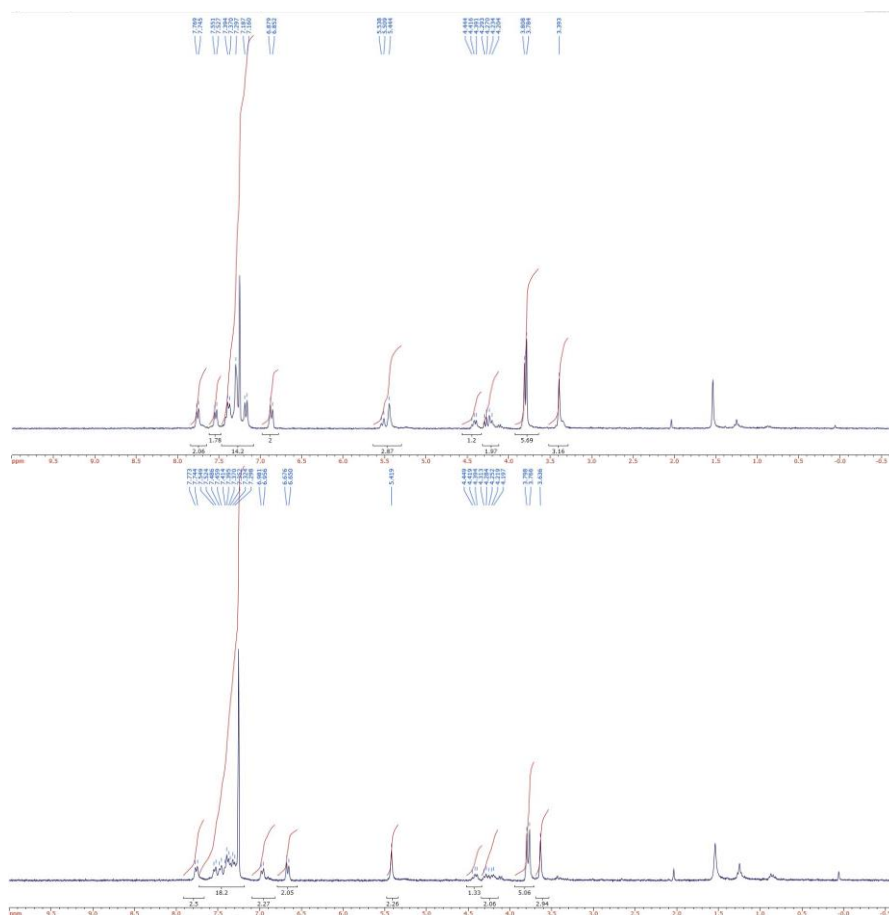
Figure G.9(top) (+)-MTPA ester of **9.14A**. (bottom) (-)-MTPA ester of **9.14A**

Table G.2 Mosher's ester analysis for MTPA-**9.14A**
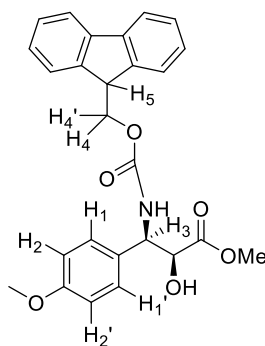
Chemical environment	(+)-MTPA δ	(-)-MTPA δ	Δ δ= δ(-)- δ(+)
1+1',2+2'	7.18(*o*), 6.86(*m*)	6.97 (*o*), 6.67(*m*)	-0.21 (*o*), -0.19 (*m*)
3	5.49	5.41	-0.09
4,4'	4.25	4.25	0
5	4.42	4.42	0
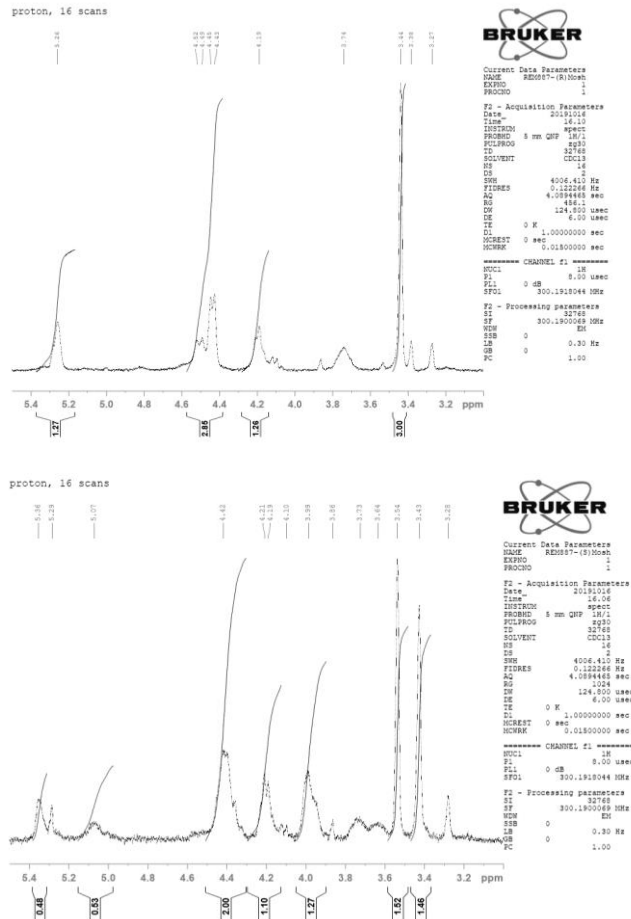
Figure G.10(top) (+)-MTPA ester of **9.18A**. (bottom) (-)-MTPA ester of **9.18A**

Table G.3 Mosher's ester analysis for MTPA-**9.18A**
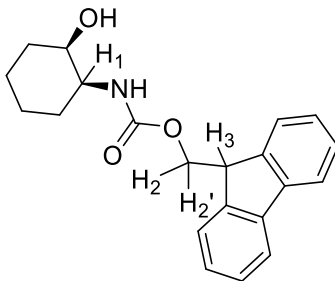
Chemical environment	(+)-MTPA δ	(-)-MTPA δ	Δ δ= δ(-)- δ(+)
1	4.51	4.20	-0.31
2,2'	4.44	4.42	-0.09
3	4.19	3.99	-0.20
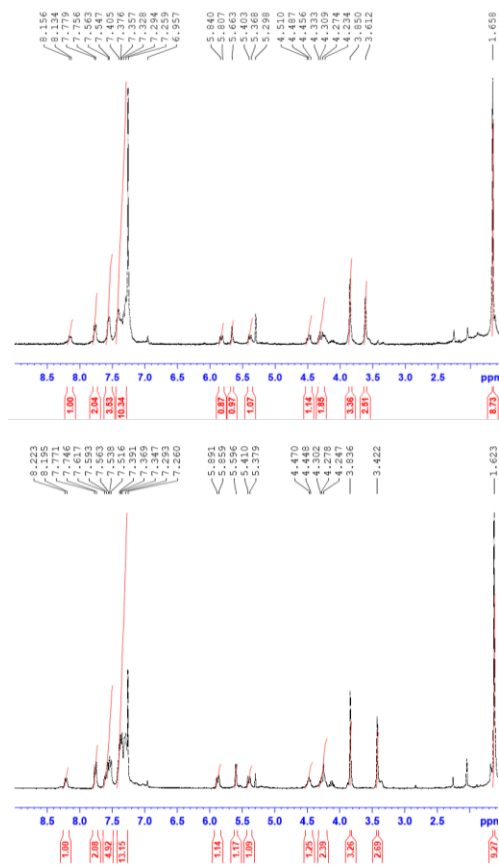
Figure G.11(top) (+)-MTPA ester of **9.23A'.** (bottom) (-)-MTPA ester of **9.23A'.**

Table G.4 Mosher's ester analysis for MTPA-**9.23A'**
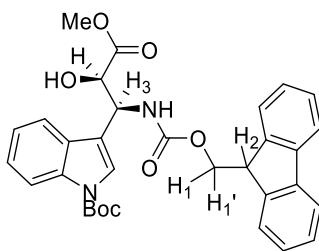
Chemical environment	(+)-MTPA δ	(-)-MTPA δ	Δ δ= δ(-)- δ(+)
NH-Fmoc	5.82	5.87 ppm	0.05 ppm
3	5.37 ppm	5.39 ppm	0.02 ppm
1,1'	4.29 ppm	4.28 ppm	0.01 ppm
2	4.49 ppm	4.46 ppm	-0.05 ppm
COOMe	3.85 ppm	3.84 ppm	-0.01 ppm
Boc	1.66 ppm	1.62 ppm	-0.04 ppm

Scheme G.1 Stability of FmocNHCl in solution

$$\text{FmocNHCl} \xrightarrow[\substack{3:2\ nPrOH:H_2O \\ 0\ ^{\circ}C,\ 3h}]{0.75\ eq.\ NaOH} \underset{(75\%)^*}{\text{FmocNHCl}} \quad \underset{(25\%)^*}{\text{FmocNH}_2}$$
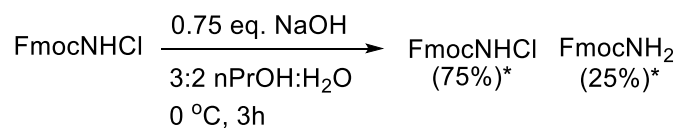
*Estimated from ^{1}H NMR of crude material after usual workup

Table G.5 Analysis of the amount of FmocNHCl and FmocNH$_2$ isolated under various reaction conditions after 3-hour reaction time
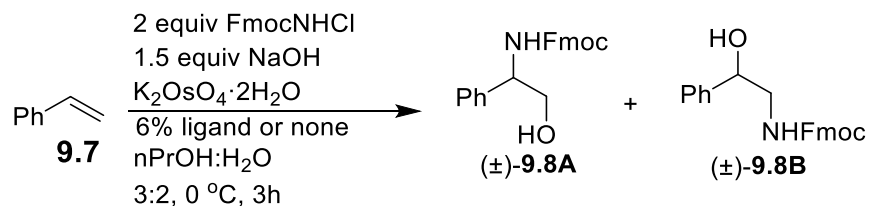
Ligand	Osmate loading (mol %)	FmocNHCl recovered[a]	FmocNH$_2$ recovered[a]	**9.8B** recovered[b]	**9.8A** recovered[b]
none	4%	37%	26%	56%	ND
none	8%	10%	43%	45%	ND
TEA (6 mol%)	4%	35%	29%	61%	ND
(DHQD)$_2$PHAL (12 mol%)	8%	25%	25%	45%	40%

[a]percentage of the total amount of FmocNHCl added [b]percent yield based on alkene starting material added. In all cases, the general procedure outlined in the experimental was followed.
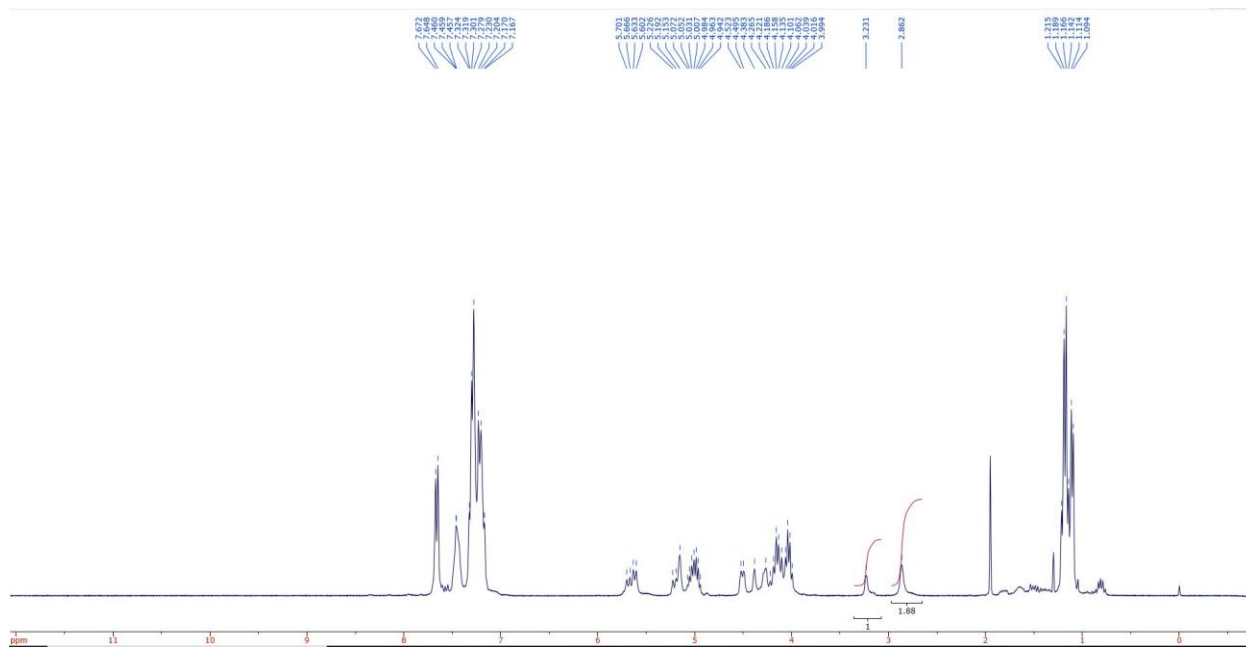
Figure G.12 Regioselectivity of Table 9.2 entry 9
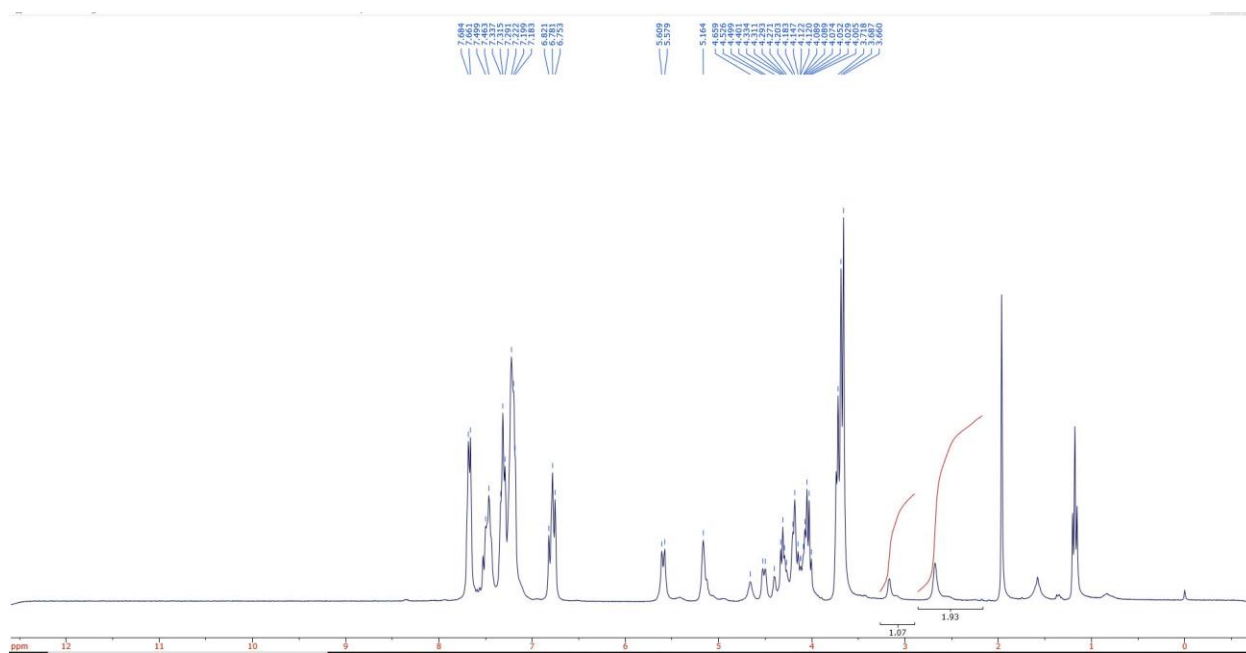
Figure G.13 Regioselectivity of Table 9.2 entry 7
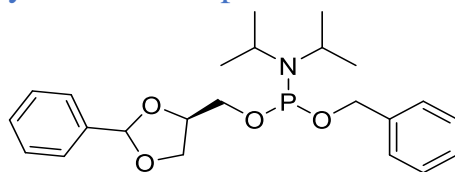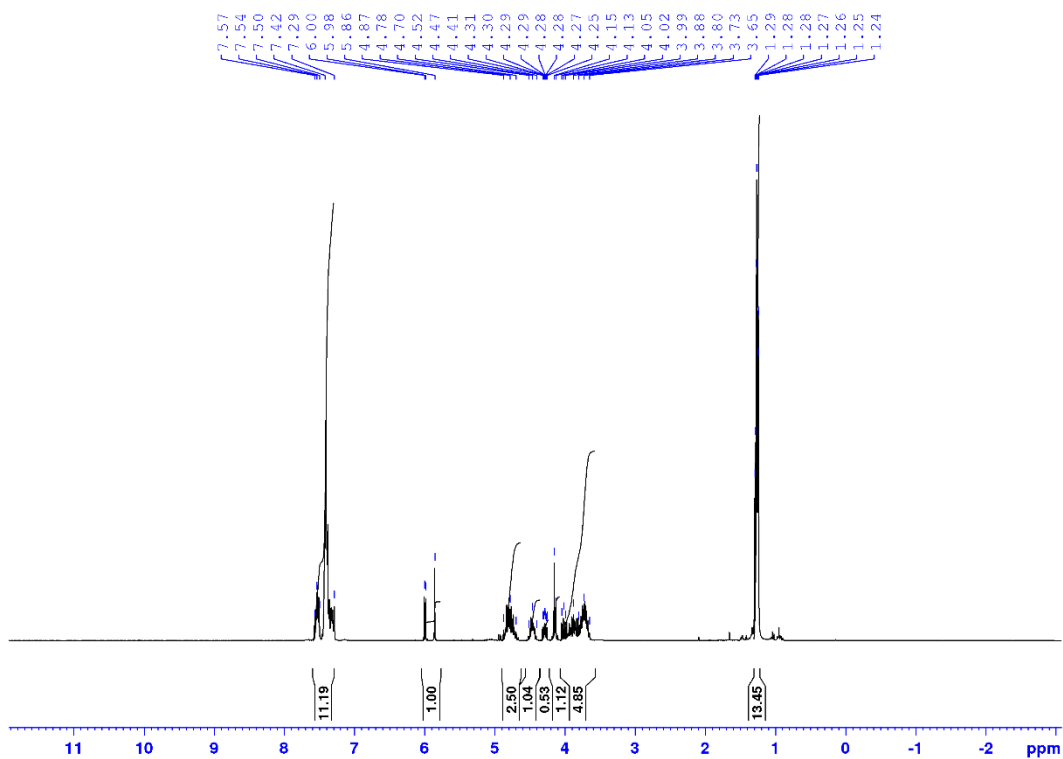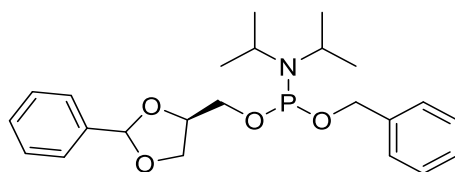
^{1}H NMR of **10.13**

^{1}H NMR of **10.13**

^{31}P NMR of **10.13**

148.52
148.50
148.24
148.20
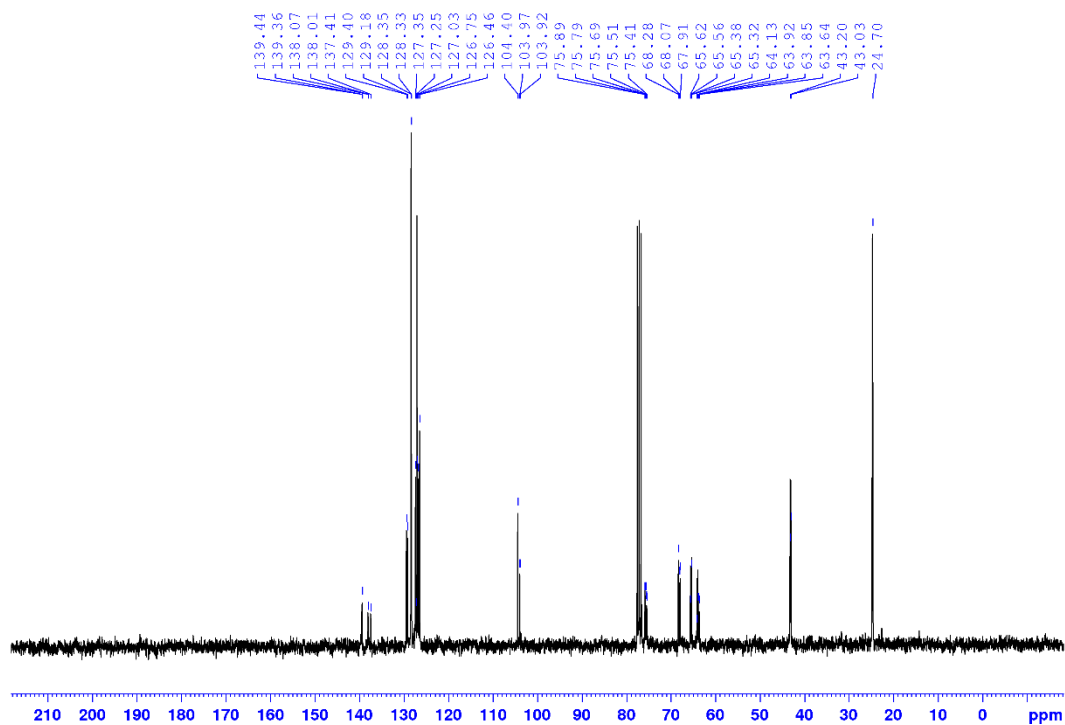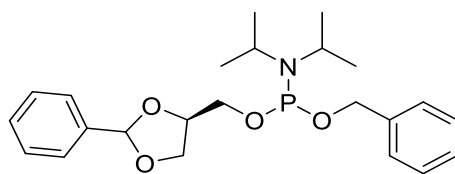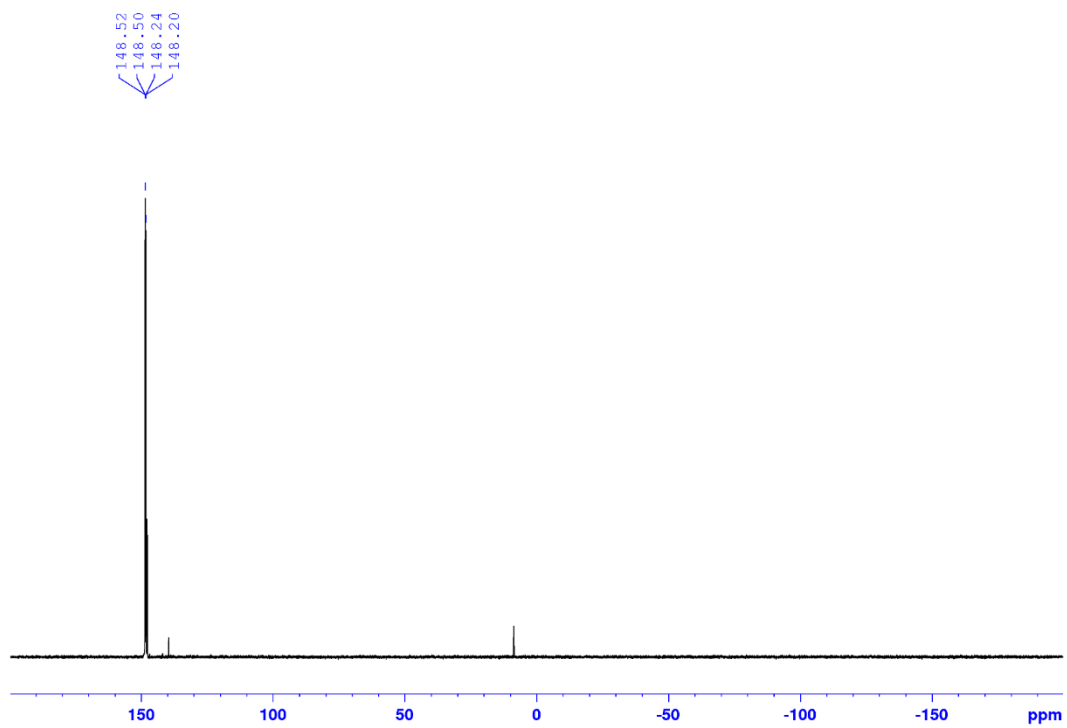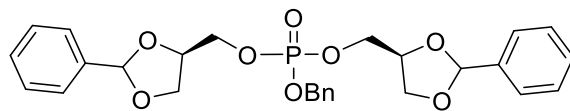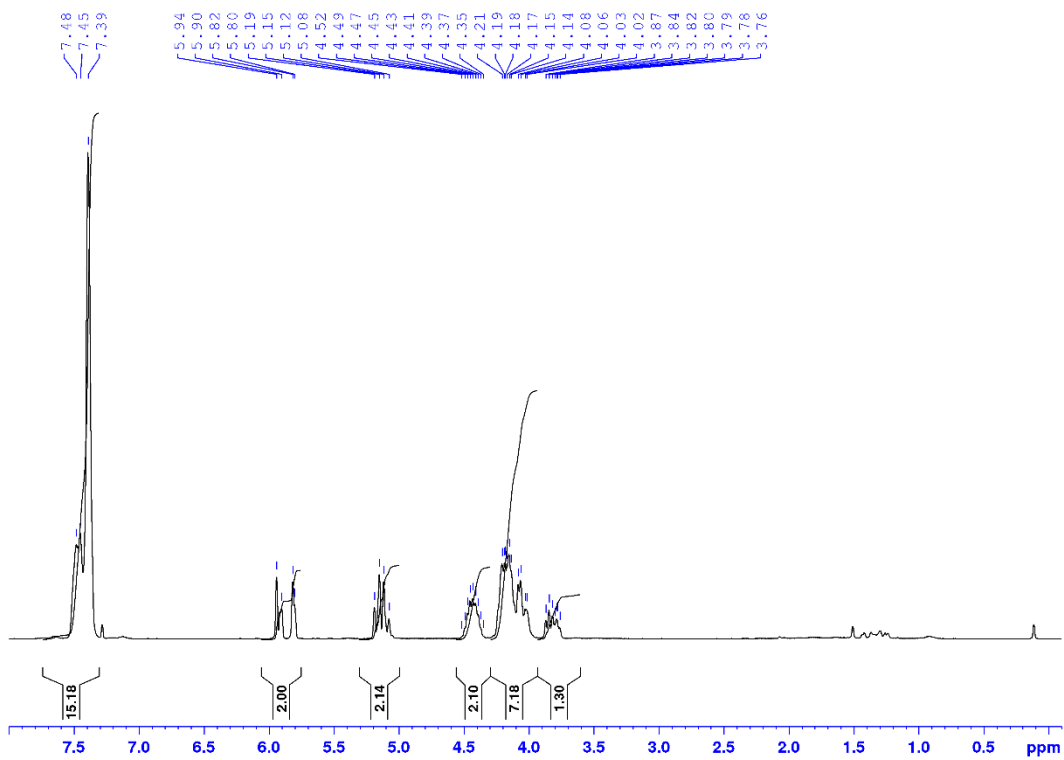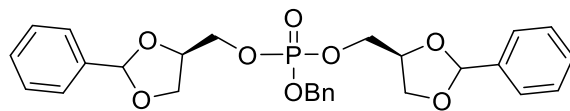
^{1}H NMR of **10.14**

^{13}C NMR of **10.14**
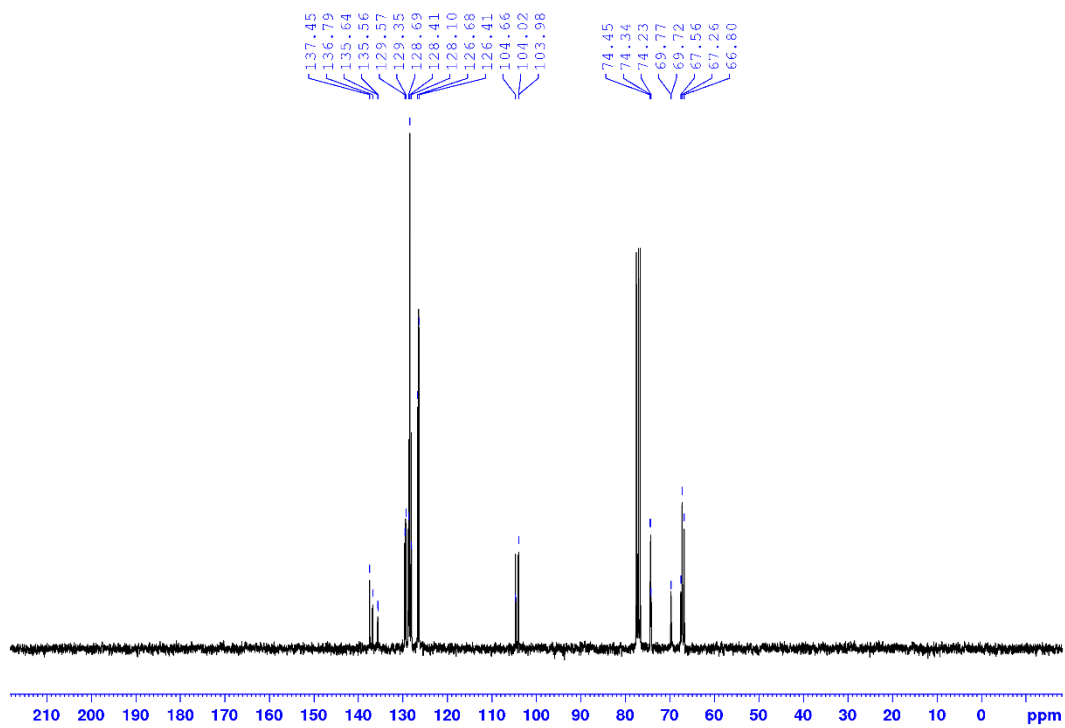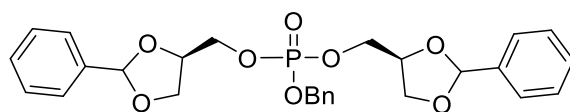
^{31}P NMR of **10.14**
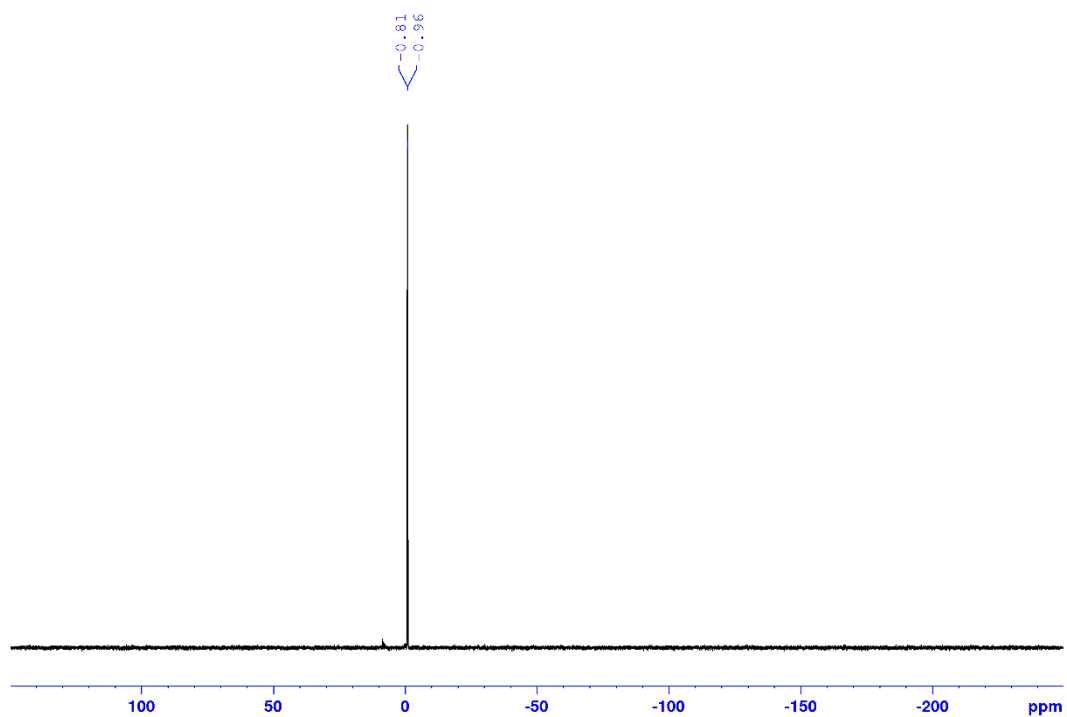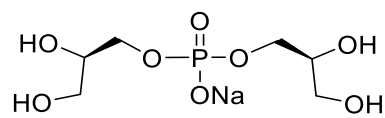
^{1}H NMR of the sodium salt of **10.8**
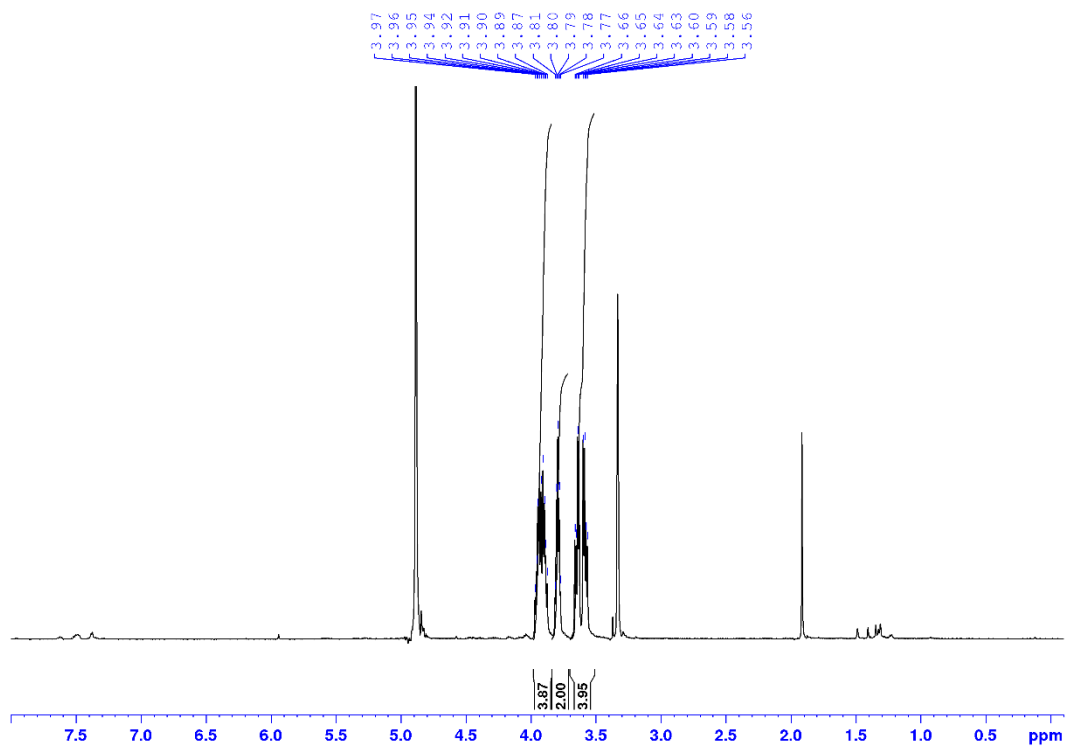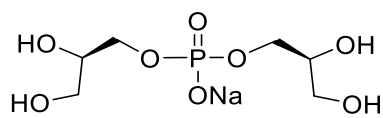
^{13}C NMR of the sodium salt of **10.8**
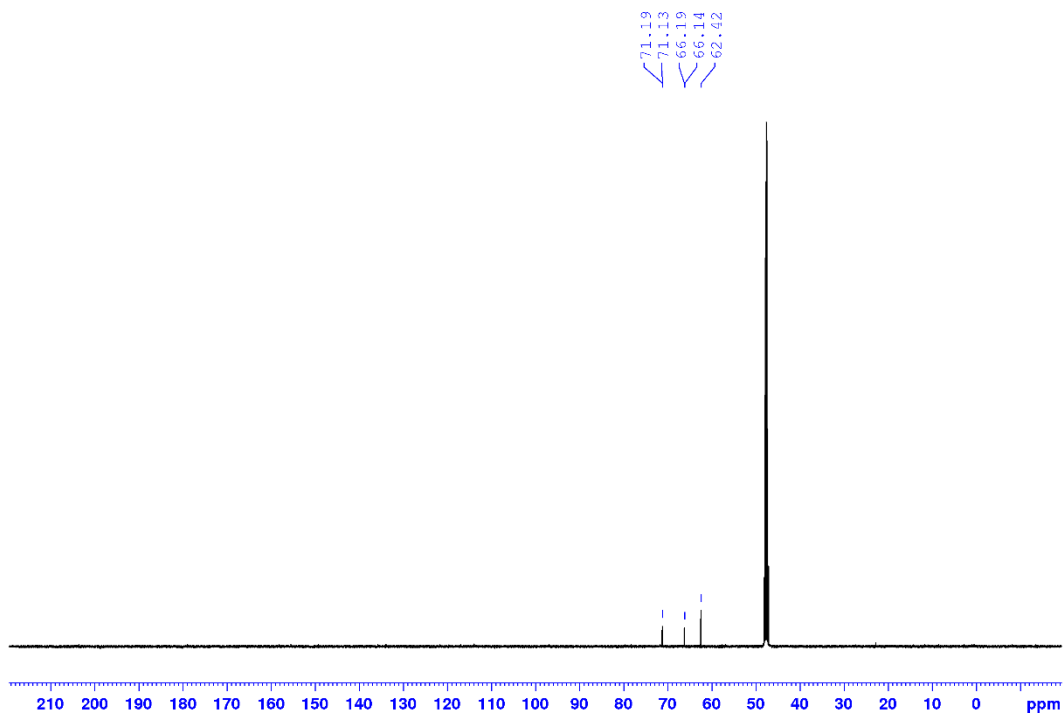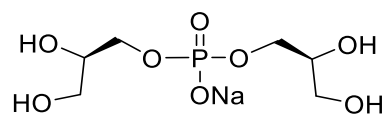
^{31}P NMR of the sodium salt of **10.8**
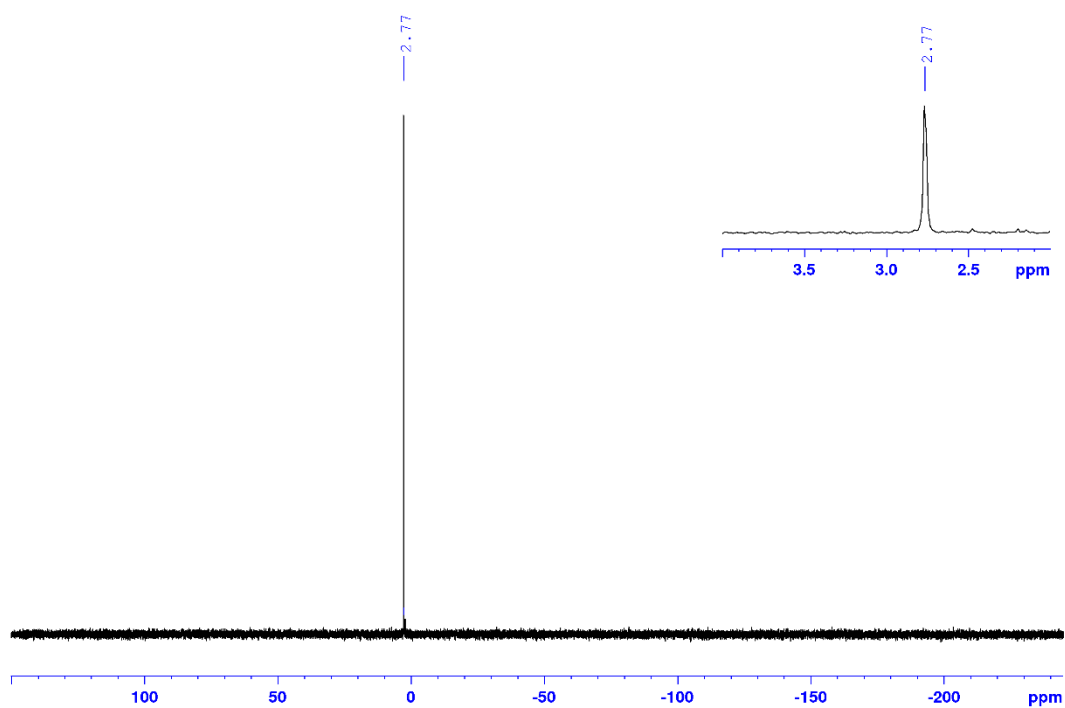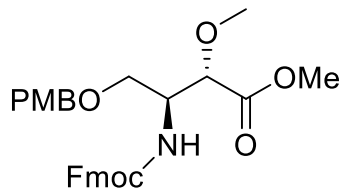
^{1}H NMR of **10.18**
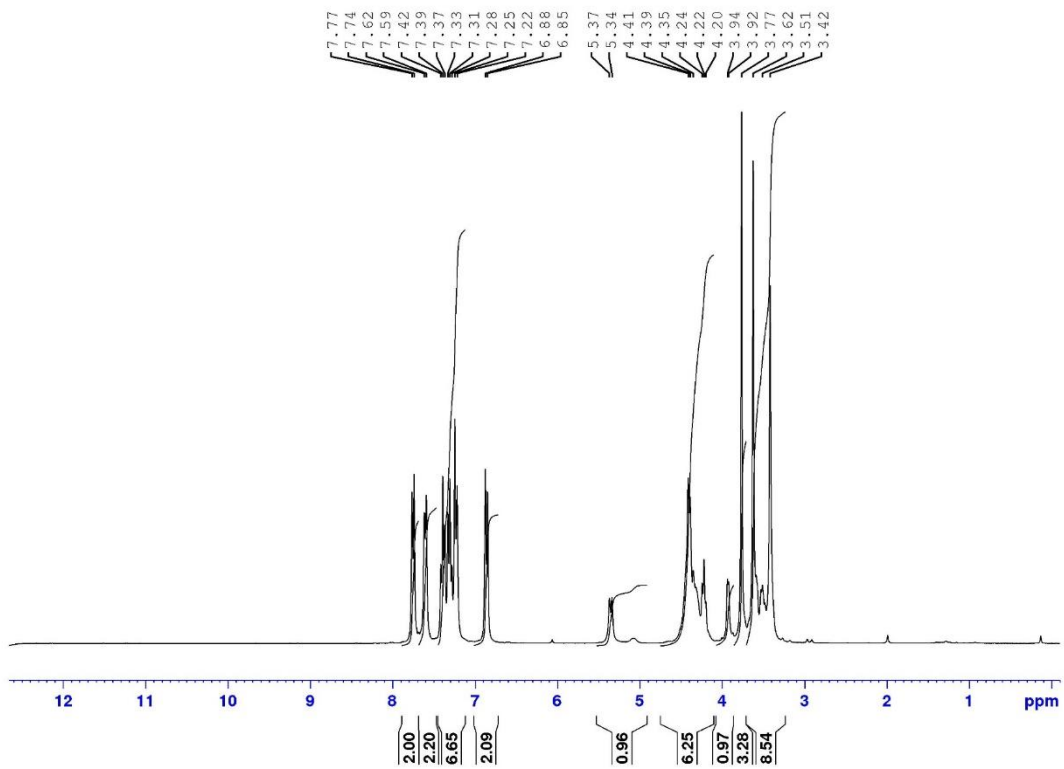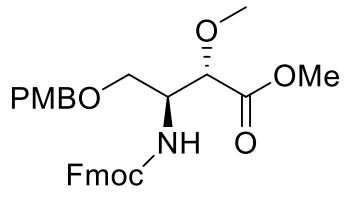
^{13}C NMR of **10.18**
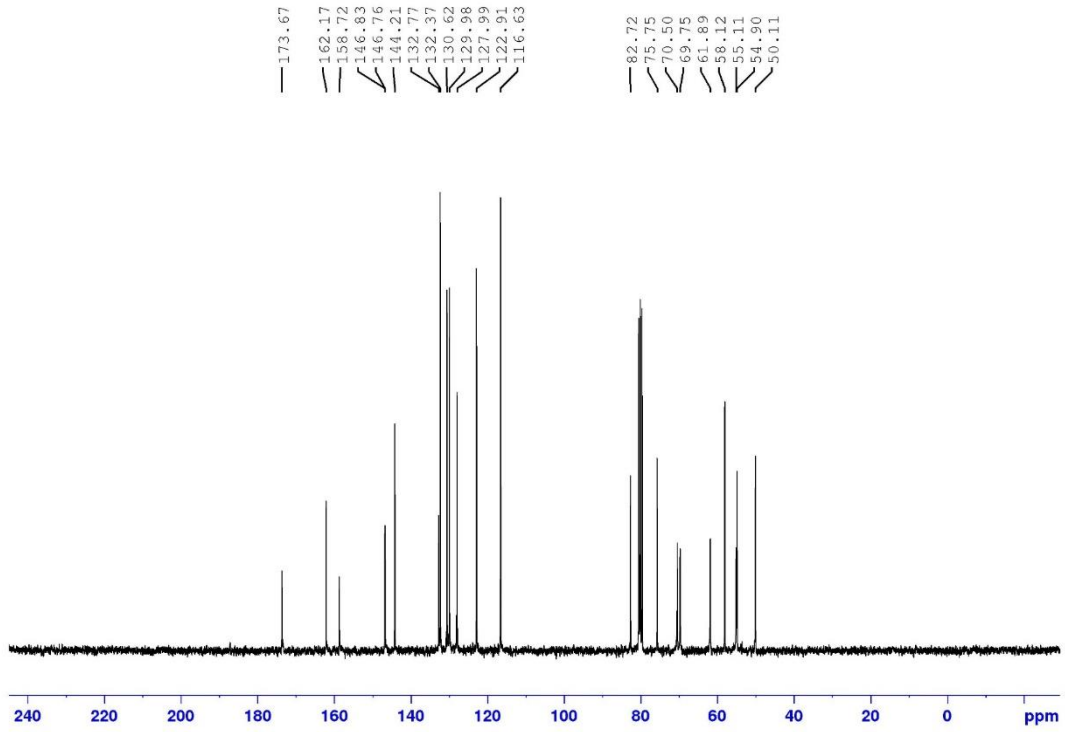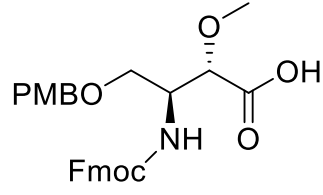
^{1}H NMR of **10.19**
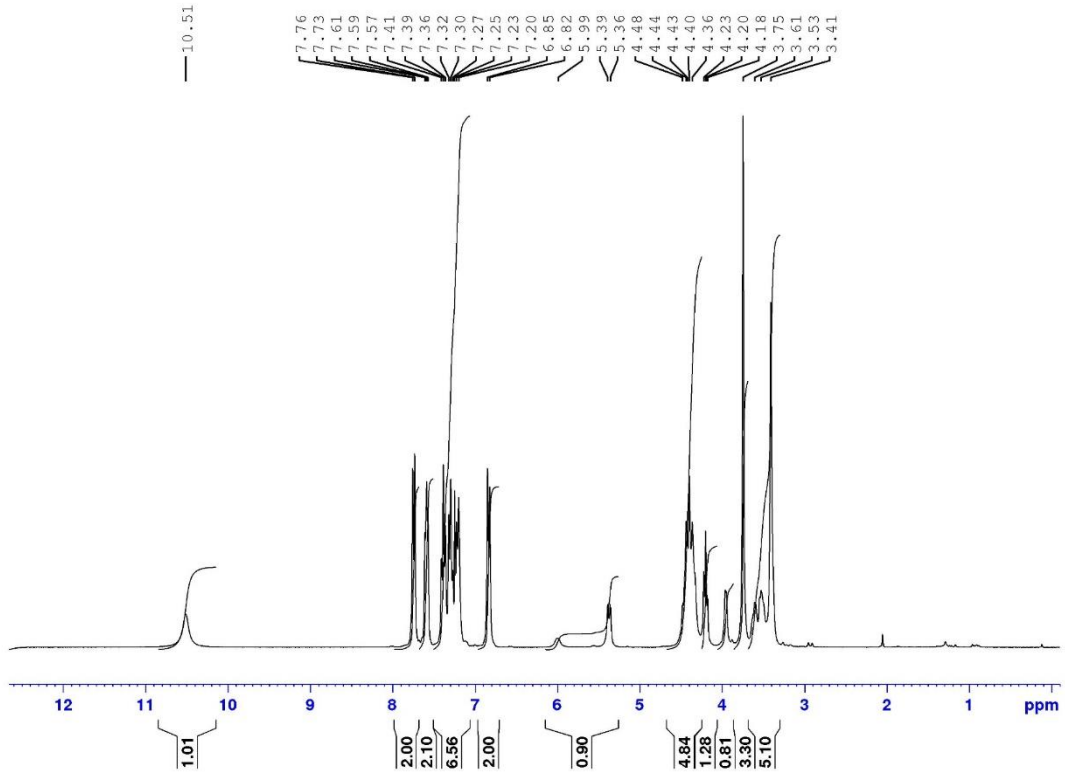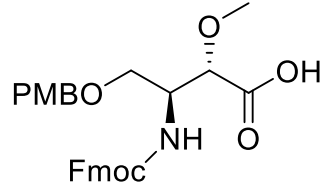
^{13}C NMR of **10.19**
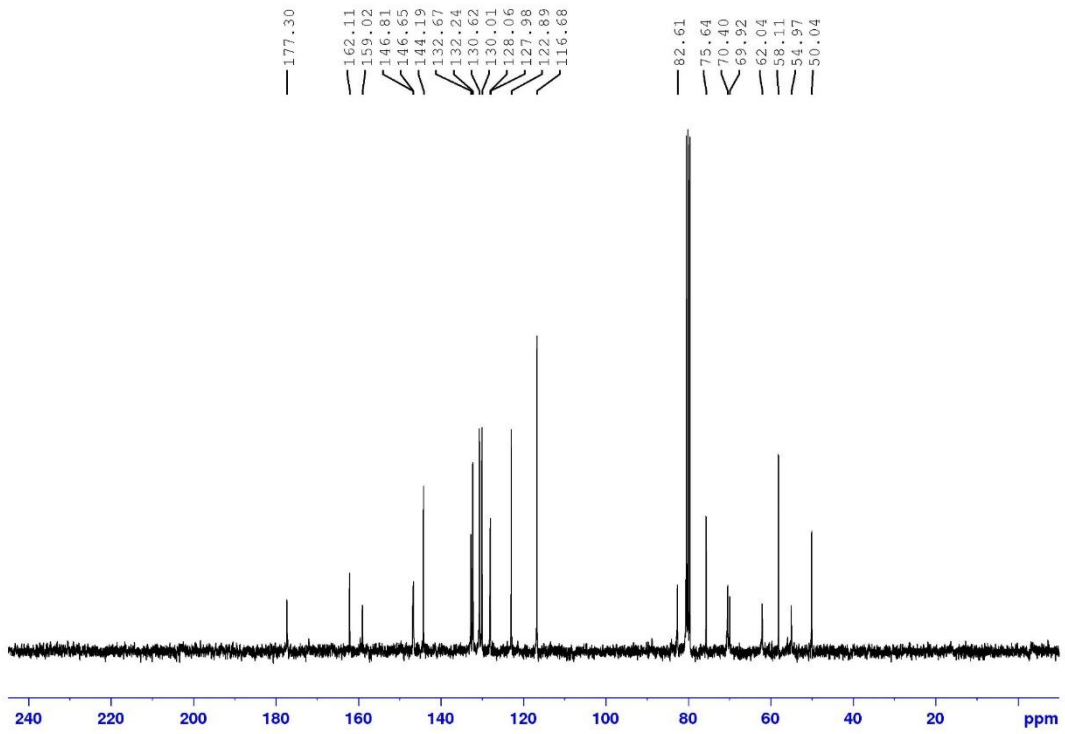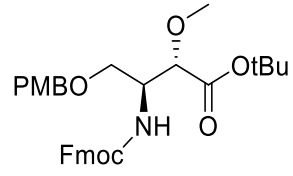
^{1}H NMR of **10.20**
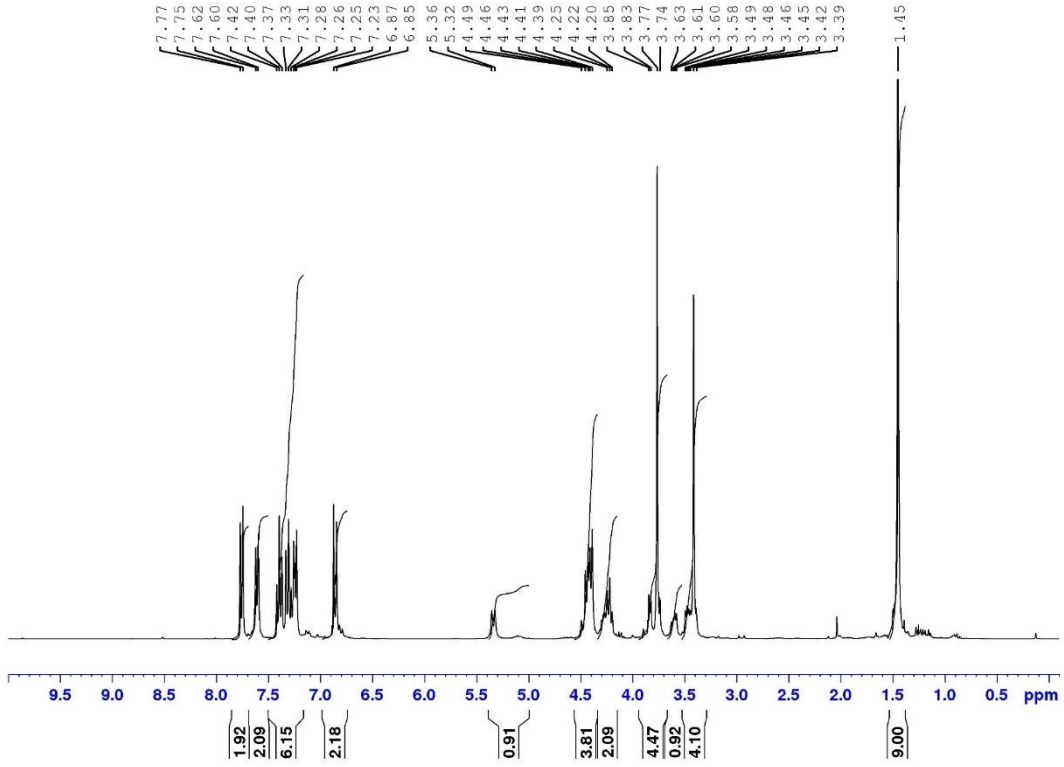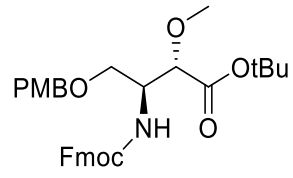
^{13}C NMR of **10.20**
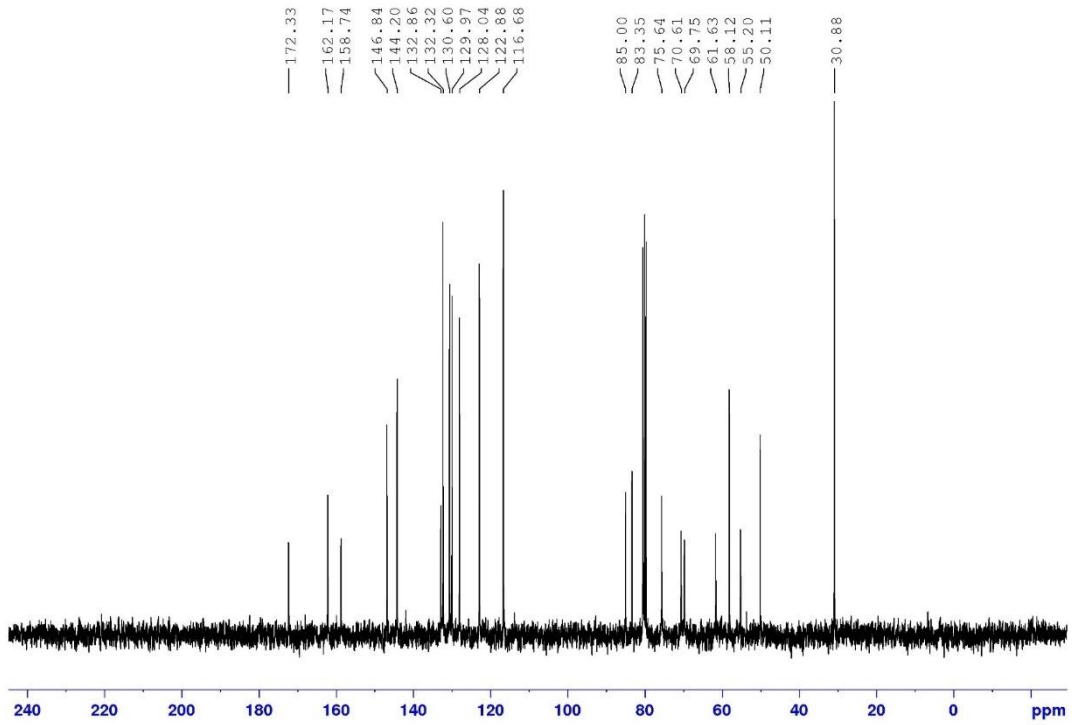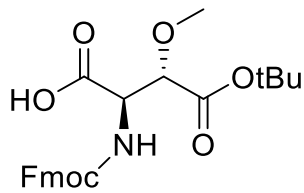
^{1}H NMR of **10.22**
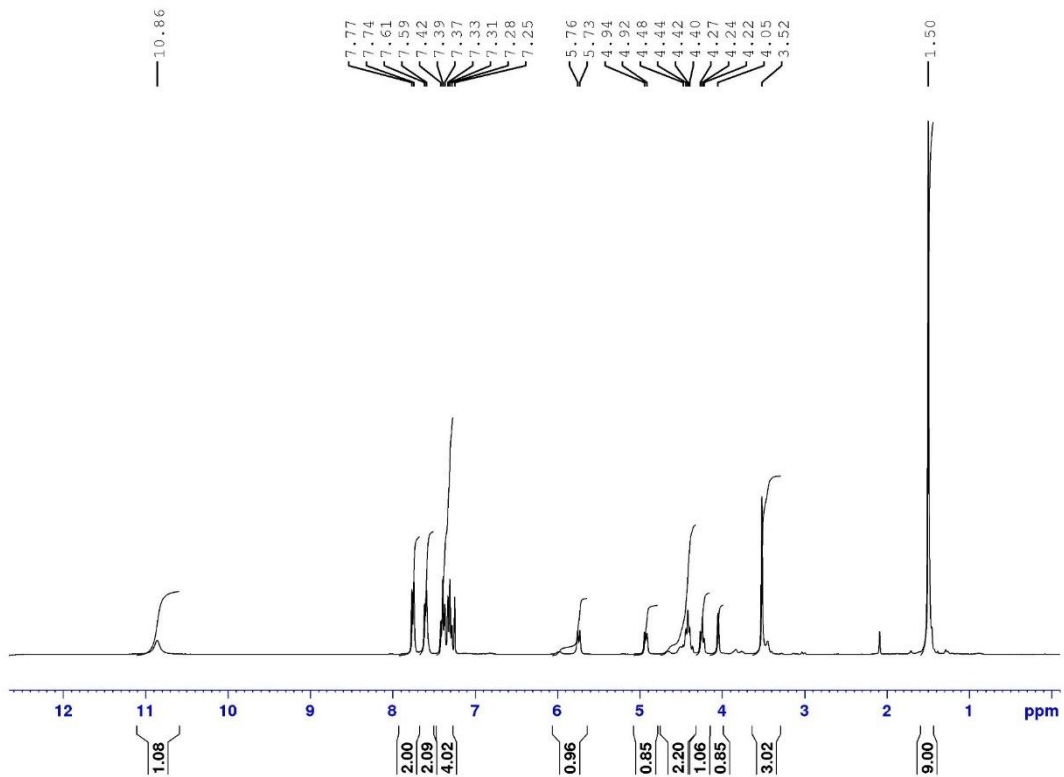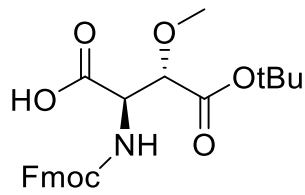
^{13}C NMR of **10.22**
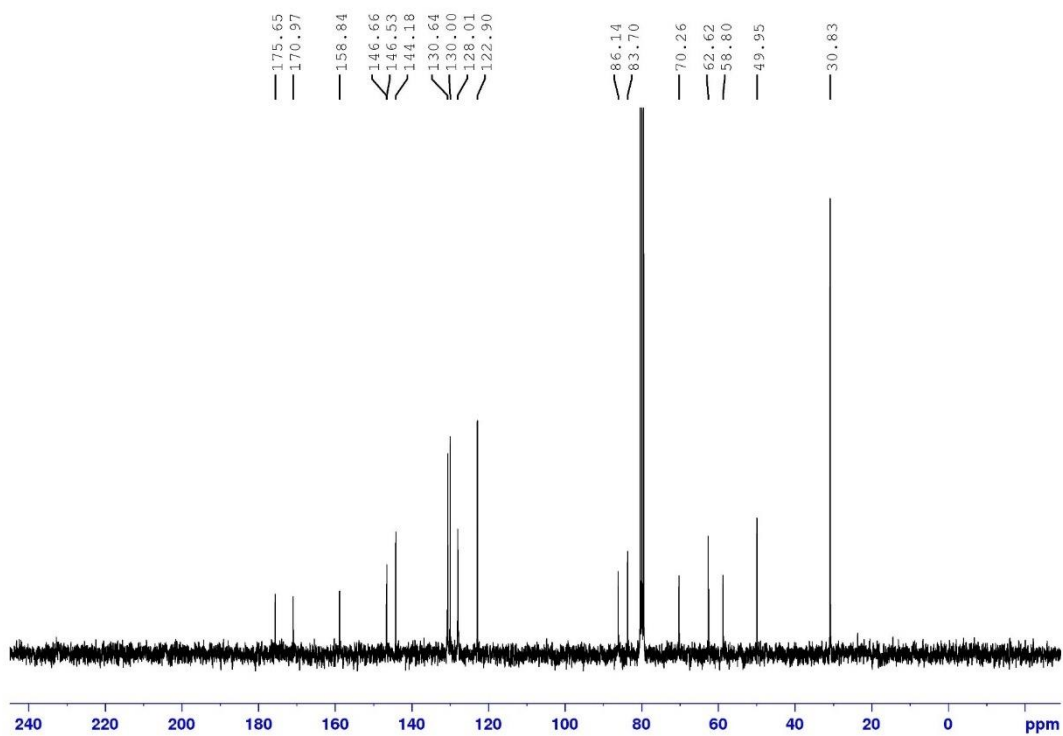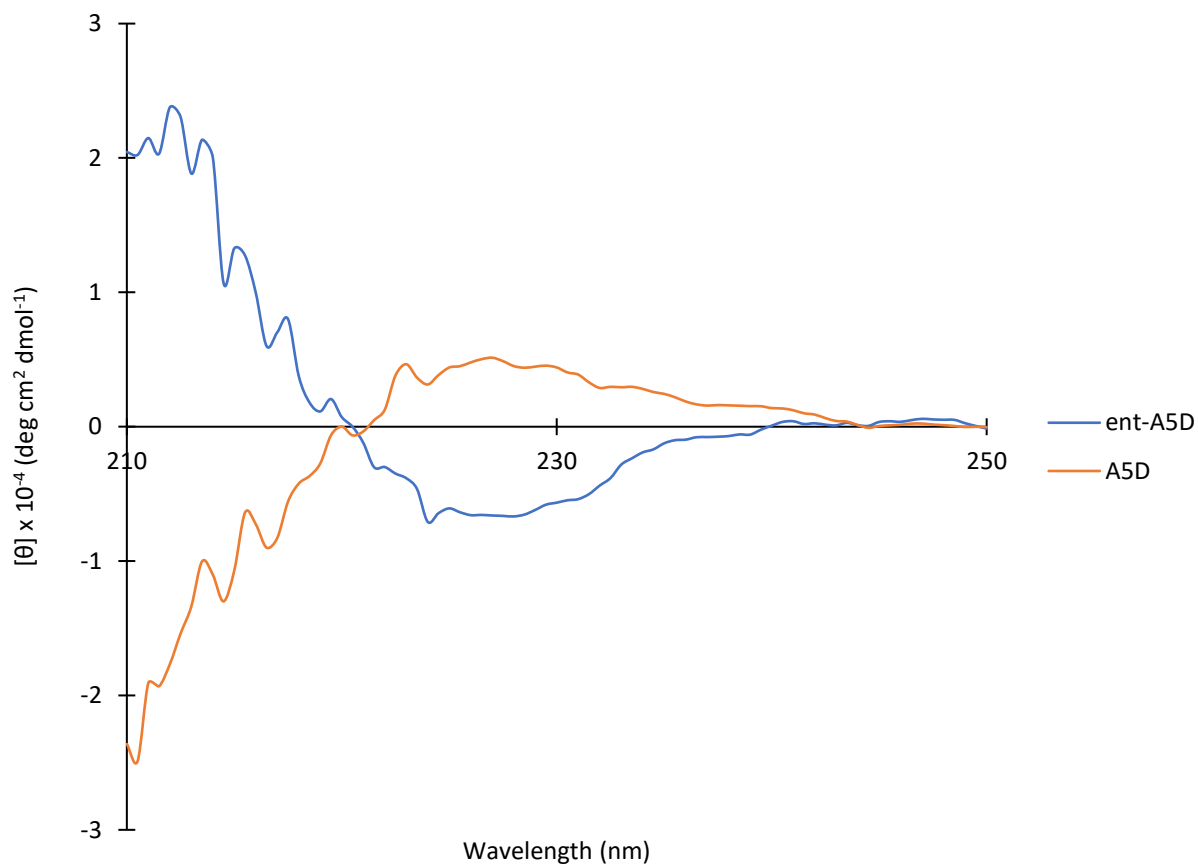
Figure H.1 circular dichroism trace of a 15 μM sample of synthetic A5D or ent-A5D in 20 mM HEPES buffer at pH = 7.4 collected at room temperature
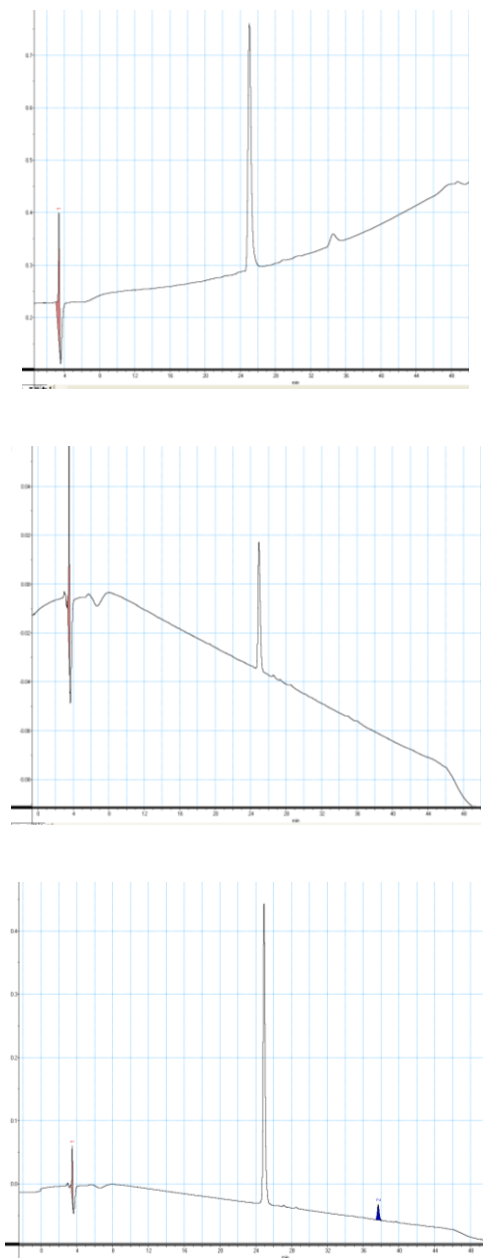
Figure H.2 R-HPLC traces collected on samples of synthetic A5D (top), synthetic ent-A5D (middle) and a mixture A5D and ent-A5D (bottom). A linear gradient 10:90 MeCN: H_2O (0.1% TFA) to 90:10 MeCN: H_2O (0.1% TFA) over 50 min was used. All chromatograms were obtained using λ = 220 nm.
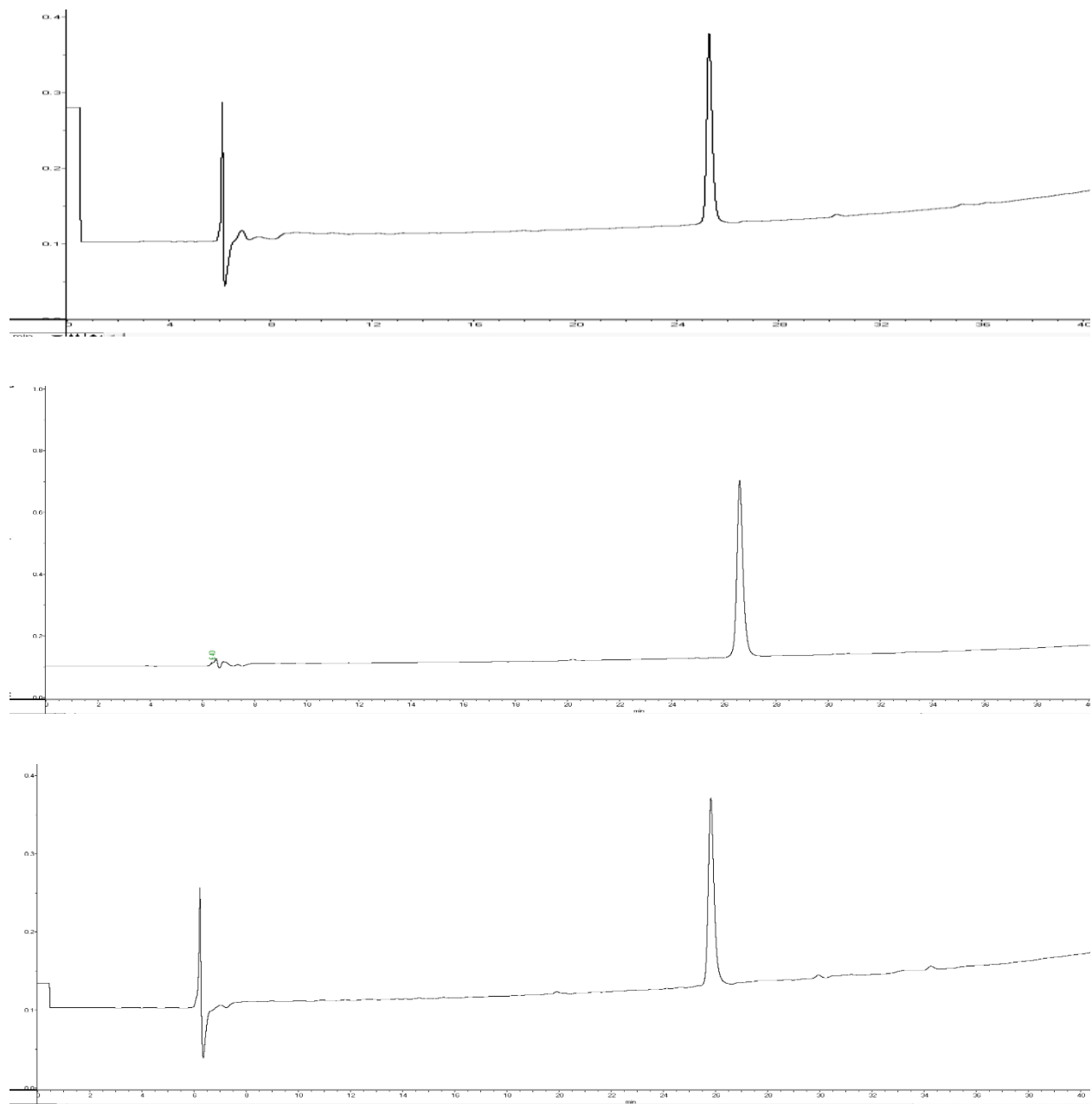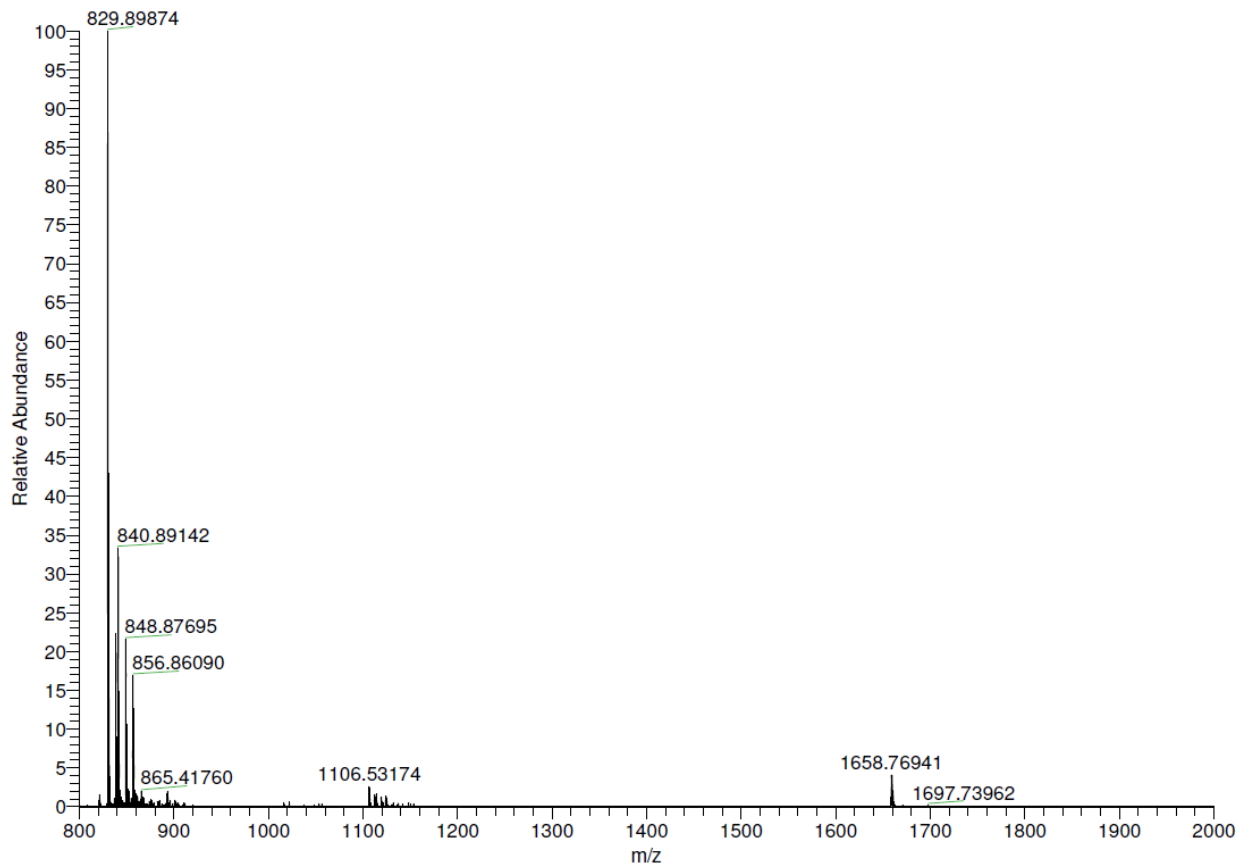
Figure H.3 R-HPLC traces collected on a sample of A5DKyn (top). R-HPLC traces collected on a sample of A5DCyh (middle). R-HPLC traces collected on a sample of synthetic A5DCyp (bottom). A linear gradient 10:90 MeCN: H_2O (0.1% TFA) to 90:10 MeCN: H_2O (0.1% TFA) over 40 min was used. All chromatograms were obtained using λ = 220 nm.

Figure H.4. ESI-MS of ent-A5D sprayed from 1:1 MeOH:H_2O + 0.1% formic acid.

```
Elemental composition search on mass 1658.78760

m/z= 1653.78760-1663.78760                    Elemental composition search on mass 829.89874
    m/z    | Theo. Mass | Delta  | RDB  | Composition
           |            | (mmu)  |equiv.|              m/z= 824.89874-834.89874
1658.78760 | 1658.78813 |  -0.53 | 22.0 |C70 H114 O30 N16     m/z    | Theo. Mass | Delta  | RDB  | Composition
           | 1658.78946 |  -1.86 | 27.0 |C71 H110 O26 N20            |            | (mmu)  |equiv.|
           | 1658.79081 |  -3.21 | 26.5 |C73 H112 O27 N17  829.89874 | 829.89904  |  -0.30 | 26.0 |C73 H113 O27 N17
           | 1658.79215 |  -4.55 | 26.0 |C75 H114 O28 N14            | 829.89837  |   0.37 | 26.5 |C71 H111 O26 N20
           | 1658.78091 |   6.69 | 31.5 |C75 H108 O24 N19            | 829.89971  |  -0.97 | 25.5 |C75 H115 O28 N14
           | 1658.77957 |   8.03 | 26.5 |C74 H112 O28 N15            | 829.89770  |   1.04 | 21.5 |C70 H115 O30 N16
           | 1658.77823 |   9.37 | 27.0 |C72 H110 O27 N18            | 829.89409  |   4.65 | 31.0 |C75 H109 O24 N19
           | 1658.80070 | -13.10 | 21.5 |C71 H116 O30 N15
           | 1658.80204 | -14.44 | 26.5 |C72 H112 O26 N19
           | 1658.80338 | -15.78 | 26.0 |C74 H114 O27 N16
```
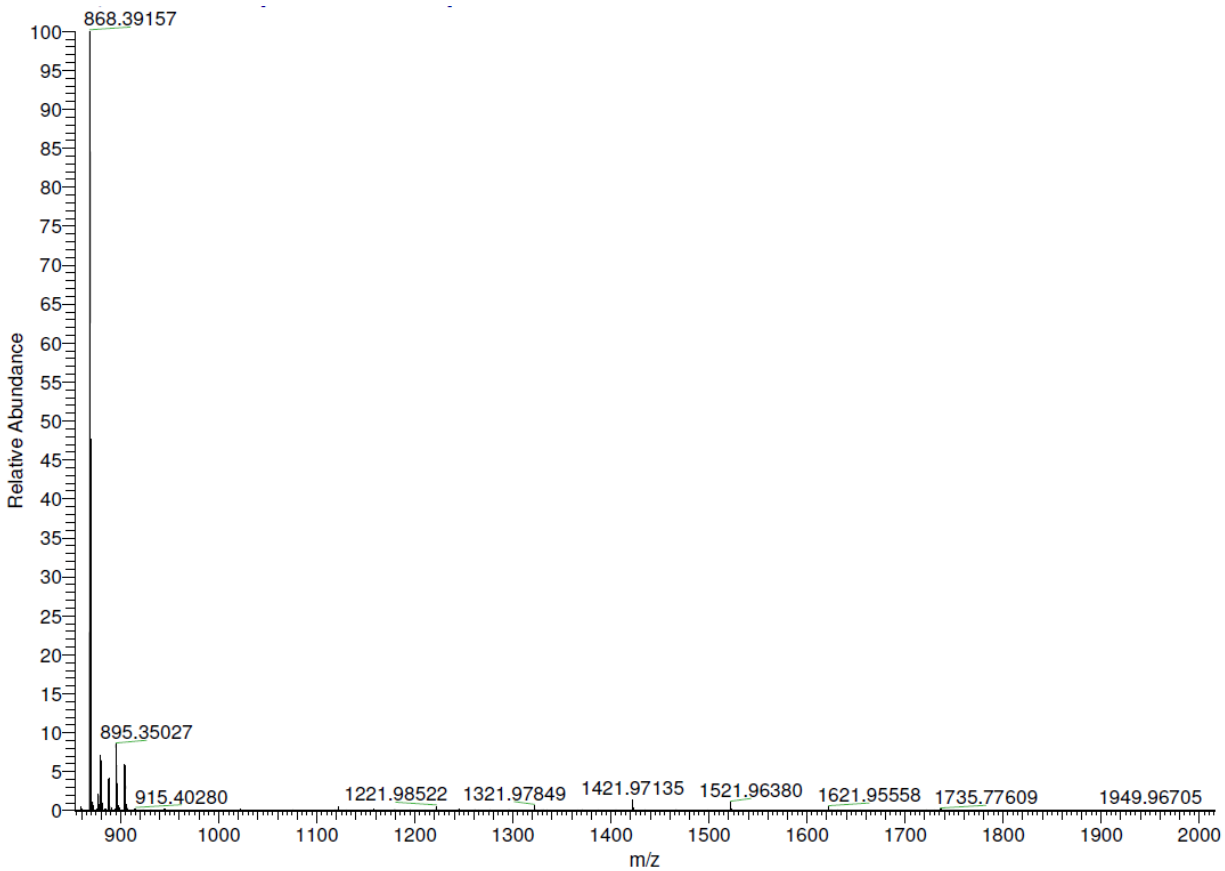
Figure H.5 ESI-MS of A5DKyn sprayed from 1:1 MeOH:H$_2$O + 0.1% formic acid.

Elemental composition search on mass 1735.78277   Elemental composition search on mass 868.39120

m/z= 1730.78277-1740.78277   m/z= 863.39120-873.39120

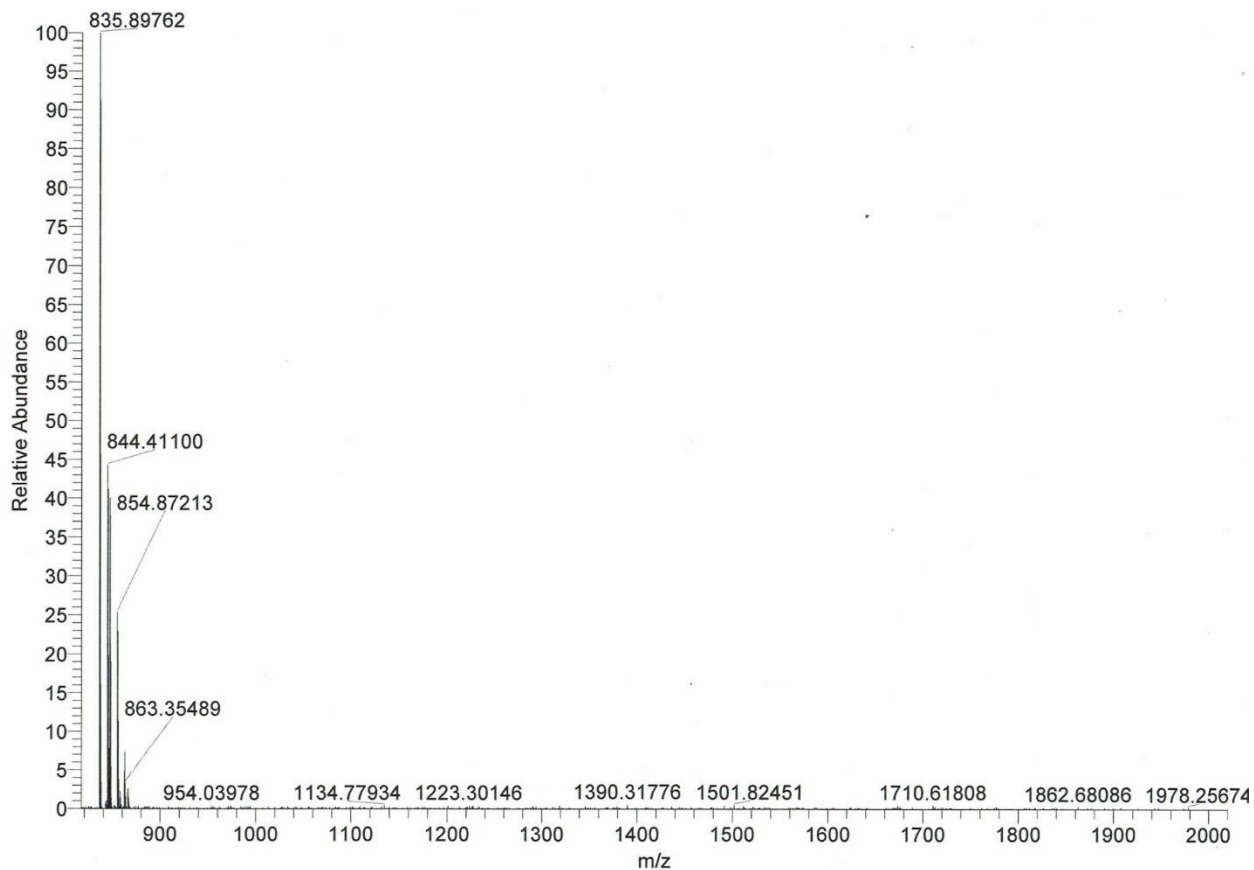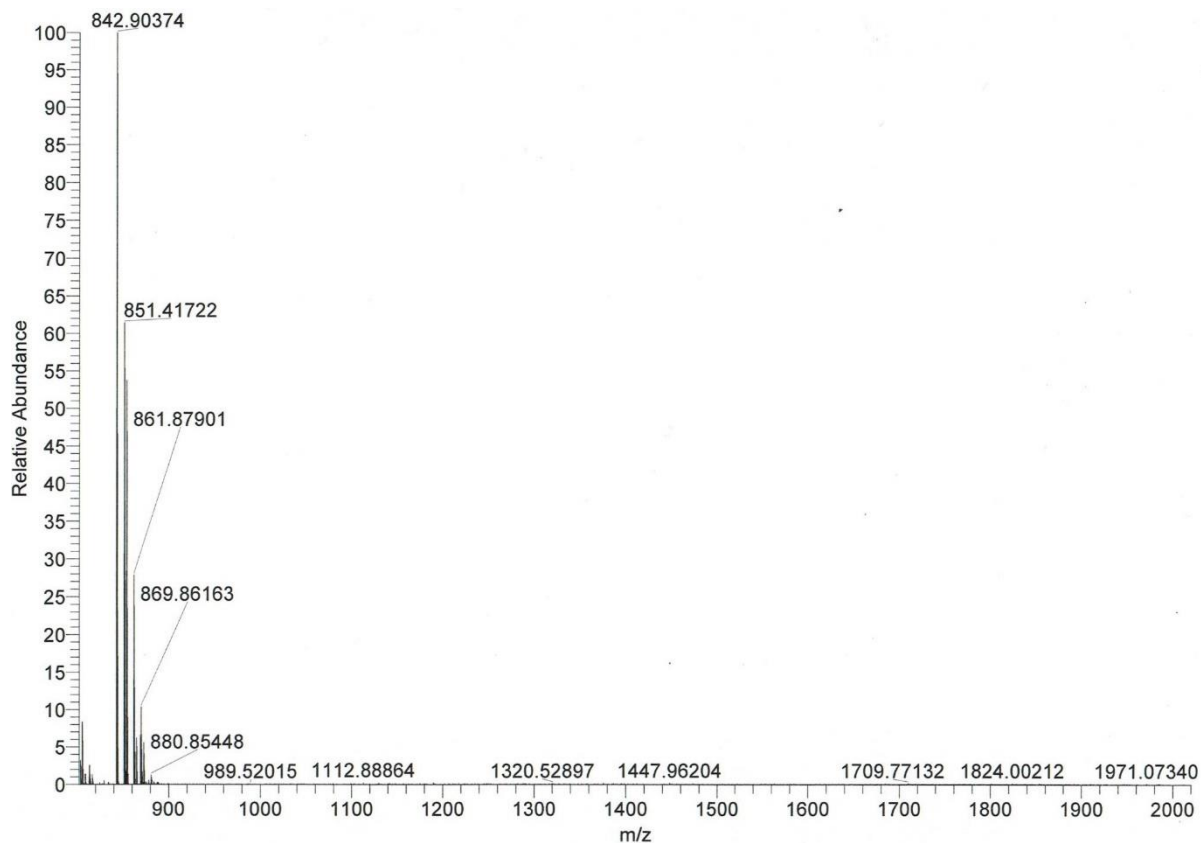| m/z	Theo. Mass	Delta (mmu)	RDB equiv.	Composition	m/z	Theo. Mass	Delta (mmu)	RDB equiv.	Composition
1735.78277	1735.78231	0.46	31.0	$C_{79} H_{113} O_{29} N_{15}$	868.39120	868.38851	2.69	31.0	$C_{78} H_{112} O_{29} N_{16}$
	1735.78097	1.80	31.5	$C_{77} H_{111} O_{28} N_{18}$		868.39412	-2.92	31.0	$C_{77} H_{112} O_{28} N_{18}$
	1735.79220	-9.43	31.5	$C_{76} H_{111} O_{27} N_{20}$		868.38784	3.36	31.5	$C_{76} H_{110} O_{28} N_{19}$
	1735.79355	-10.78	31.0	$C_{78} H_{113} O_{28} N_{17}$		868.39480	-3.60	30.5	$C_{79} H_{114} O_{29} N_{15}$
	1735.76974	13.03	31.5	$C_{78} H_{111} O_{29} N_{16}$		868.39974	-8.54	31.0	$C_{76} H_{112} O_{27} N_{20}$

Figure H.6 ESI-MS of A5DCyp sprayed from 1:1 MeOH:H₂O + 0.1% formic acid.

```
Elemental composition search on mass 835.89762

m/z= 830.89762-840.89762
```

m/z	Theo. Mass	Delta (mmu)	RDB equiv.	Composition
835.89762	835.89770	-0.08	22.5	$C_{71} H_{115} O_{30} N_{16}$
	835.89837	-0.75	27.5	$C_{72} H_{111} O_{26} N_{20}$
	835.89904	-1.42	27.0	$C_{74} H_{113} O_{27} N_{17}$
	835.89477	2.85	31.5	$C_{78} H_{111} O_{25} N_{16}$
	835.90105	-3.43	31.0	$C_{79} H_{113} O_{25} N_{15}$

Figure H.7 ESI-MS of A5DCyh sprayed from 1:1 MeOH:H$_2$O + 0.1% formic acid.

```
Elemental composition search on mass 842.90374

m/z=  837.90374-847.90374
```

m/z	Theo. Mass	Delta (mmu)	RDB equiv.	Composition
842.90374	842.90486	-1.12	23.0	C$_{70}$ H$_{115}$ O$_{29}$ N$_{19}$
	842.90259	1.15	31.5	C$_{79}$ H$_{113}$ O$_{25}$ N$_{16}$
	842.90620	-2.46	27.5	C$_{73}$ H$_{113}$ O$_{26}$ N$_{20}$
	842.90125	2.49	27.0	C$_{76}$ H$_{115}$ O$_{28}$ N$_{15}$
	842.90687	-3.13	27.0	C$_{75}$ H$_{115}$ O$_{27}$ N$_{17}$
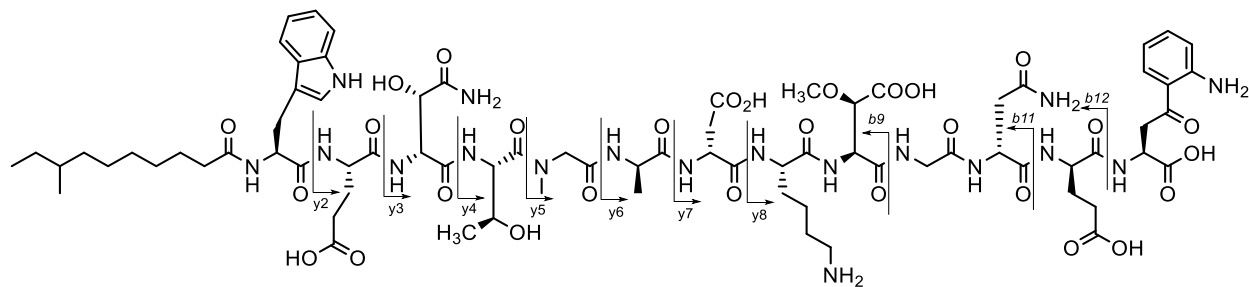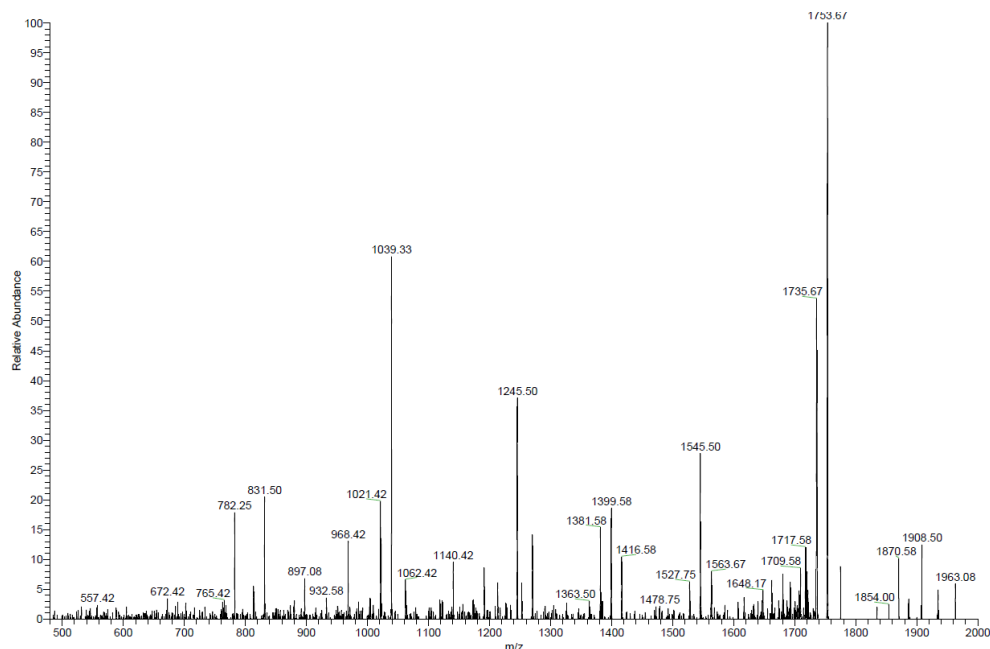
Ion	Molecular formula	Observed fragment (Calculated mass) (Da)
Y2	$C_{55}H_{83}N_{16}O_{27}^{+}$	1399.7 (1399.6)
Y3	$C_{50}H_{76}N_{15}O_{24}^{+}$	1270.4 (1270.5)
Y4	$C_{46}H_{70}N_{13}O_{21}^{+}$	1140.4 (1140.5)
Y5	$C_{42}H_{63}N_{12}O_{19}^{+}$	1039.3 (1039.4)
Y6	$C_{39}H_{58}N_{11}O_{18}^{+}$	968.4 (968.4)
Y7	$C_{36}H_{53}N_{10}O_{17}^{+}$	897.5 (897.4)
Y8	$C_{32}H_{48}N_{9}O_{14}^{+}$	782.3 (782.3)
B9	$C_{56}H_{85}N_{12}O_{20}^{+}$	1245.5 (1245.6)
B11	$C_{62}H_{94}N_{15}O_{23}^{+}$	1416.6 (1416.7)
B12	$C_{67}H_{101}N_{16}O_{26}^{+}$	1545.5 (1545.7)

Figure H.8 MS-MS analysis of hydrolyzed (0.1N LiOH) A5DKyn sprayed from 1:1 MeOH:H_2O + 0.1% formic acid.
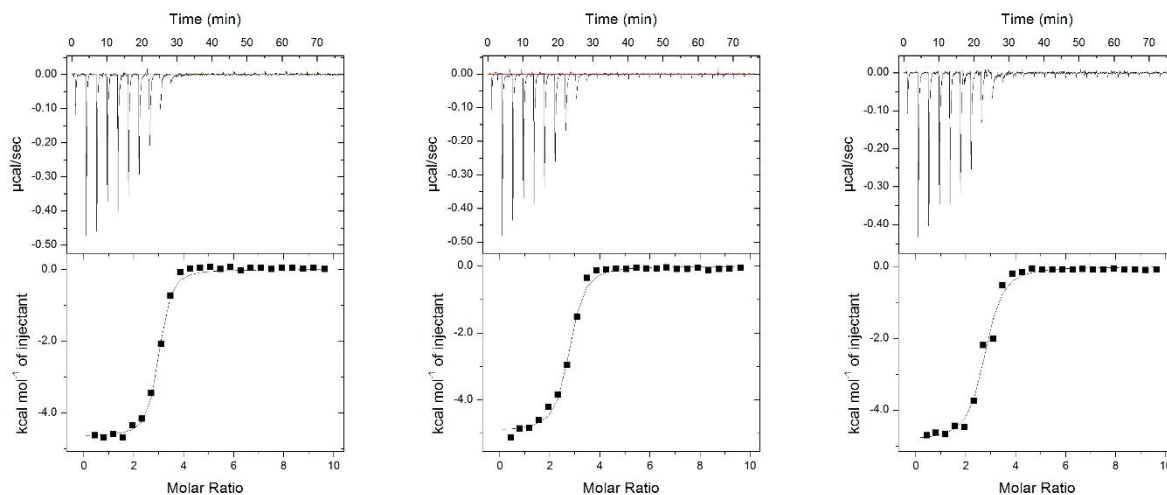
Figure H.9 Binding thermograms for the titration of daptomycin (20 µM) with LUVs composed of 25% 2R,2'S-DMPG/75% DOPC at 1.25 mM CaCl$_2$
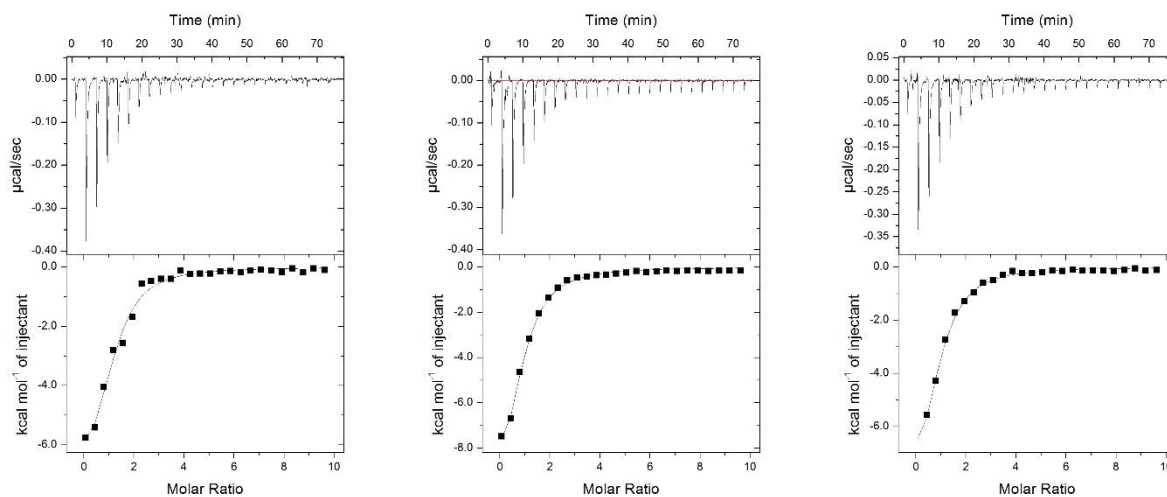

Figure H.10 Binding thermograms for the titration of A5D (20 µM) with LUVs composed of 25% 2R,2'S-DMPG/75% DOPC at 1.25 mM CaCl$_2$
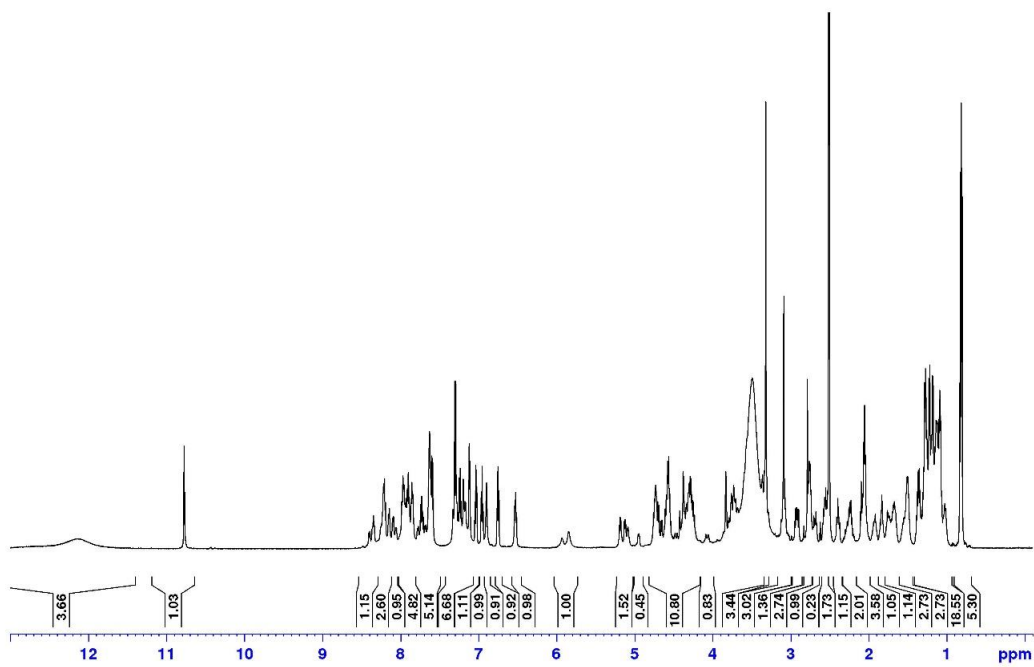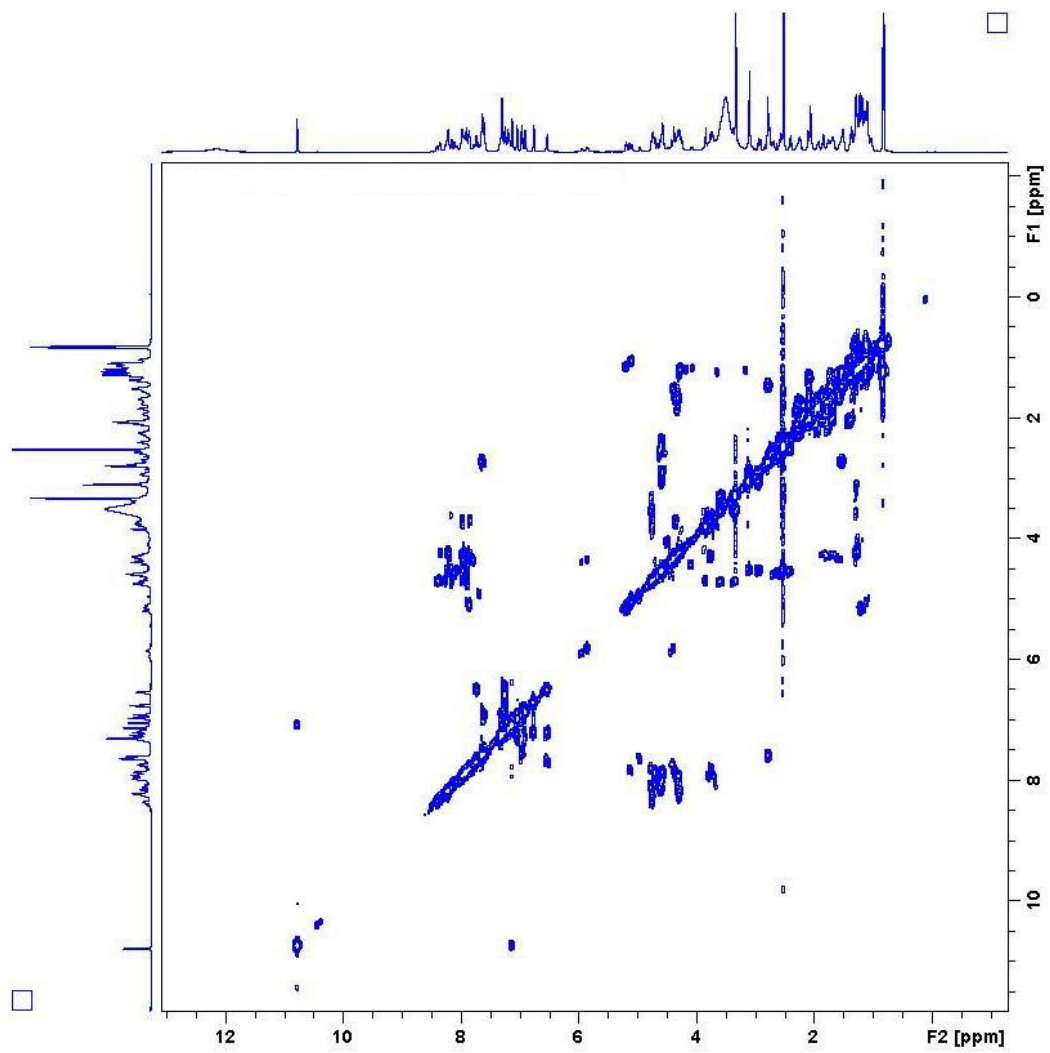
Figure H.11. ^{1}H NMR of A5DKyn in DMSO-d$_6$ (ca. 8 mg/mL)
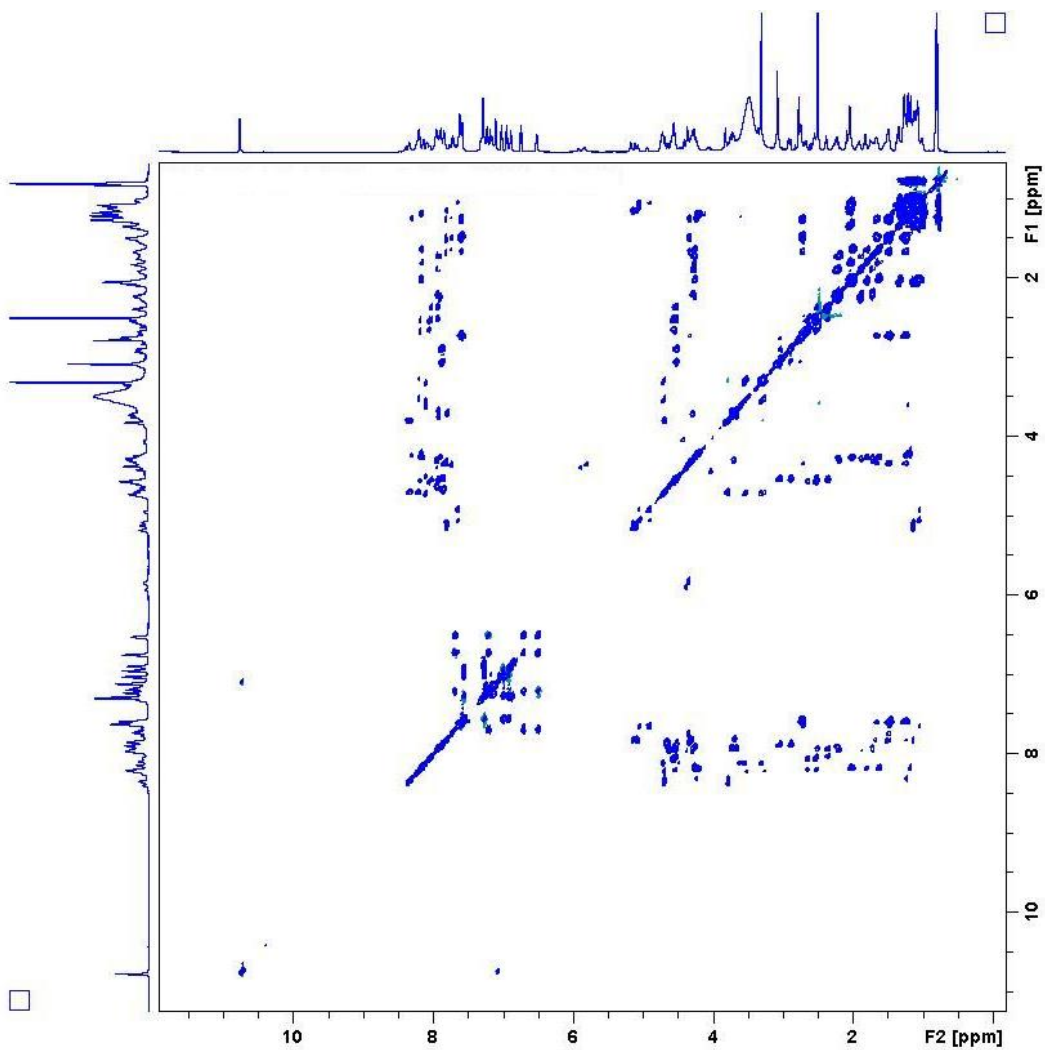
Figure H.12. COSY of A5DKyn in DMSO-d$_6$ (ca. 8 mg/mL)
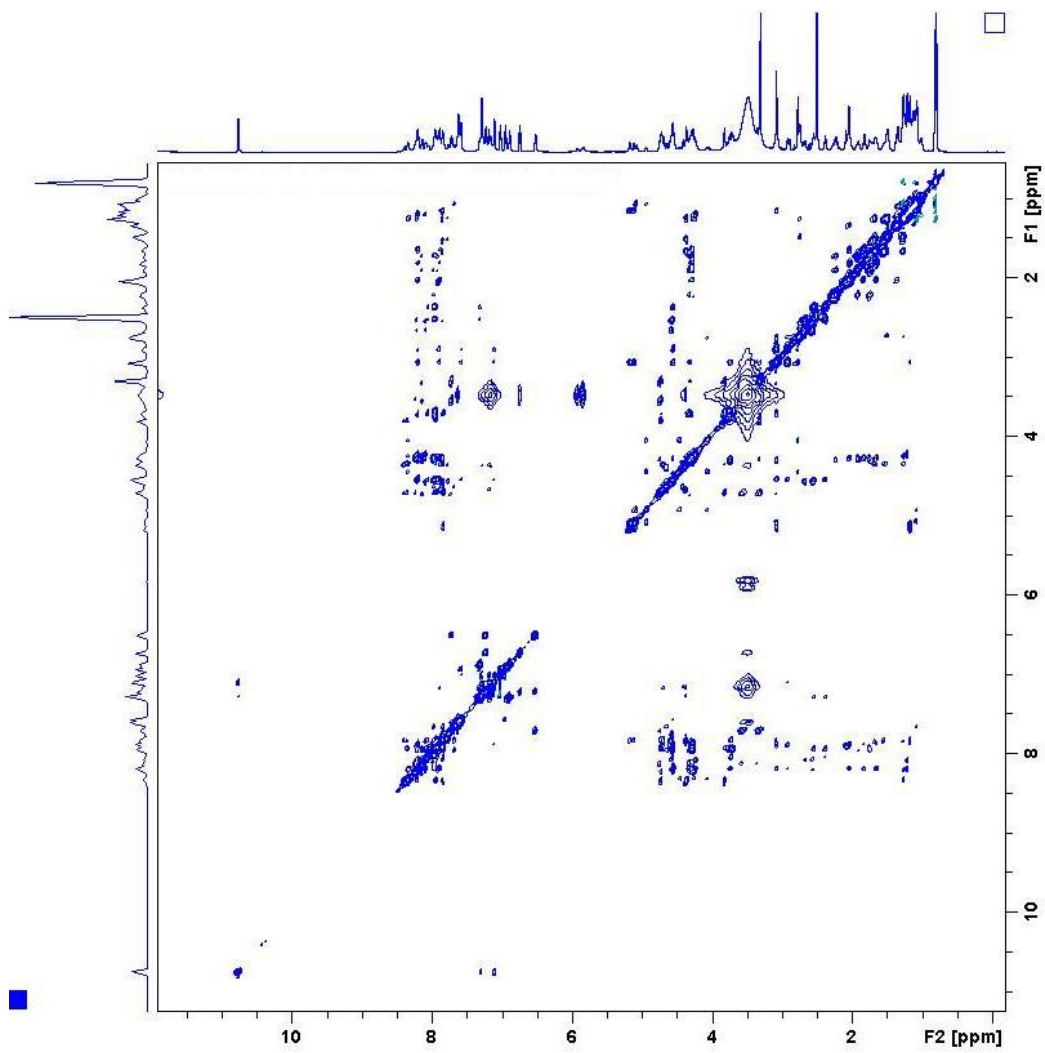
Figure H.13 TOCSY of A5DKyn in DMSO-d$_6$ (ca. 8 mg/mL)
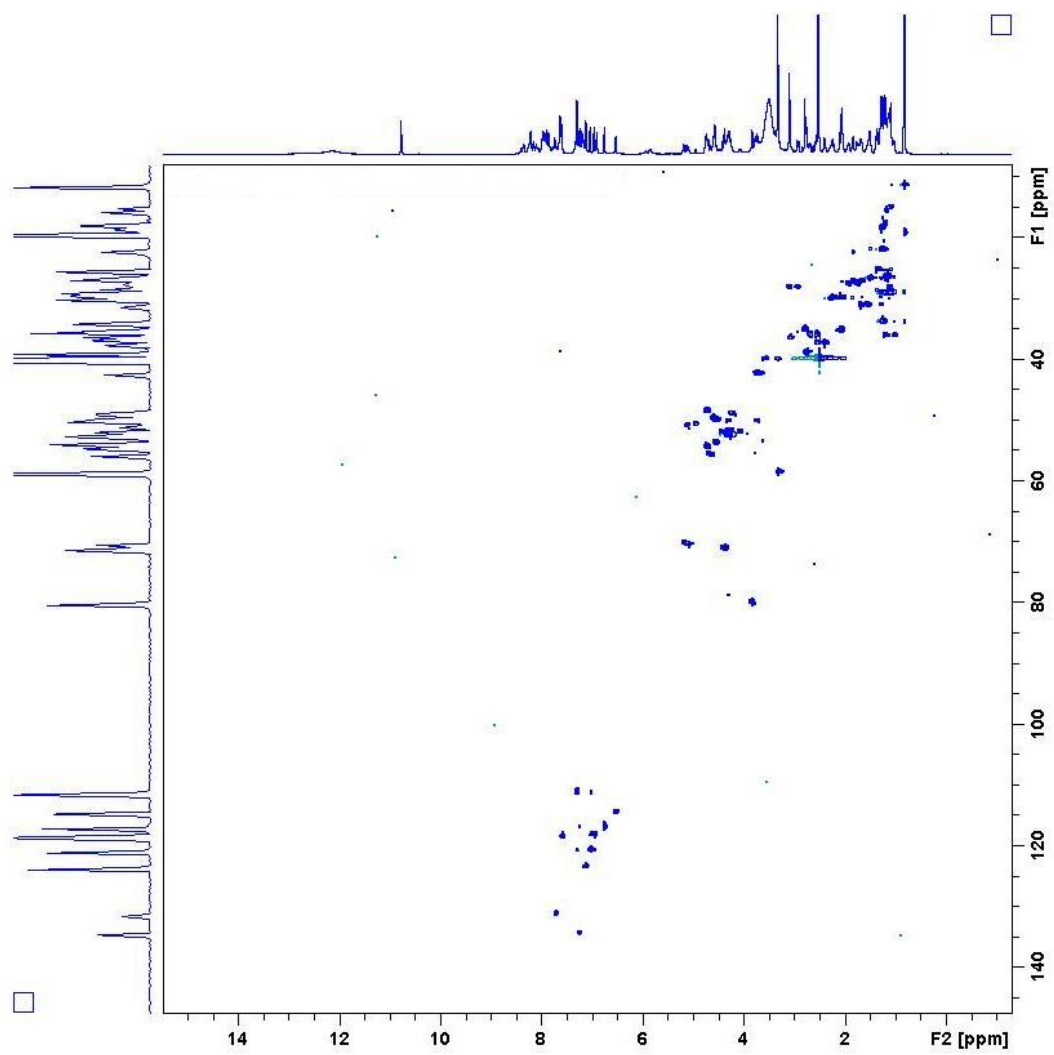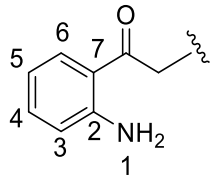
Figure H.14 NOESY of A5DKyn in DMSO-d$_6$ (ca. 8 mg/mL)
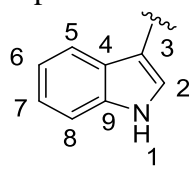
Figure H.15 HSQC of A5DKyn in DMSO-d$_6$ (ca. 8 mg/mL)

435

Table H.1 Chemical shift assignment of A5DKyn

Residue	Position	δ_C	δ_H
Trp1	NH	--	7.88
	α	54.1	4.58
	β	28.4	3.06, 2.90
	1	--	10.77
	2	124.2	7.12, 7.11
	3	--	--
	4	--	--
	5	118.9	7.60
	6	118.6	6.95
	7	121.2	7.04
	8	111.7	7.30
	9	--	--
D-Glu2	NH	--	7.90
	α	49.3	4.26
	β	27.9	1.91, 1.74
	γ	30.4	2.26
	C=O	--	--
	COOH	--	--
hAsn3	NH	--	7.78
	α	52.2	4.42
	β	71.3	4.38
	OH	--	5.33
	C=O	--	--
	CONH$_2$	--	5.79
Thr4	NH	--	7.79
	α	51.2	5.11
	β	70.6	5.16
	γ	15.9	1.16
	C=O	--	--
Sar5	NCH$_3$	36.9	3.09
	α	52.2	4.44, 4.05
	C=O	--	--
Ala6	NH	--	8.23
	α	54.5	4.25
	β	18.7	1.24
	C=O	--	--
Asp7	NH	--	8.06
	α	50.0	4.58
	β	36.5	2.68, 2.55
	C=O	--	--
	COOH	--	--
D-Lys8	NH	--	7.86
	α	49.9	4.35

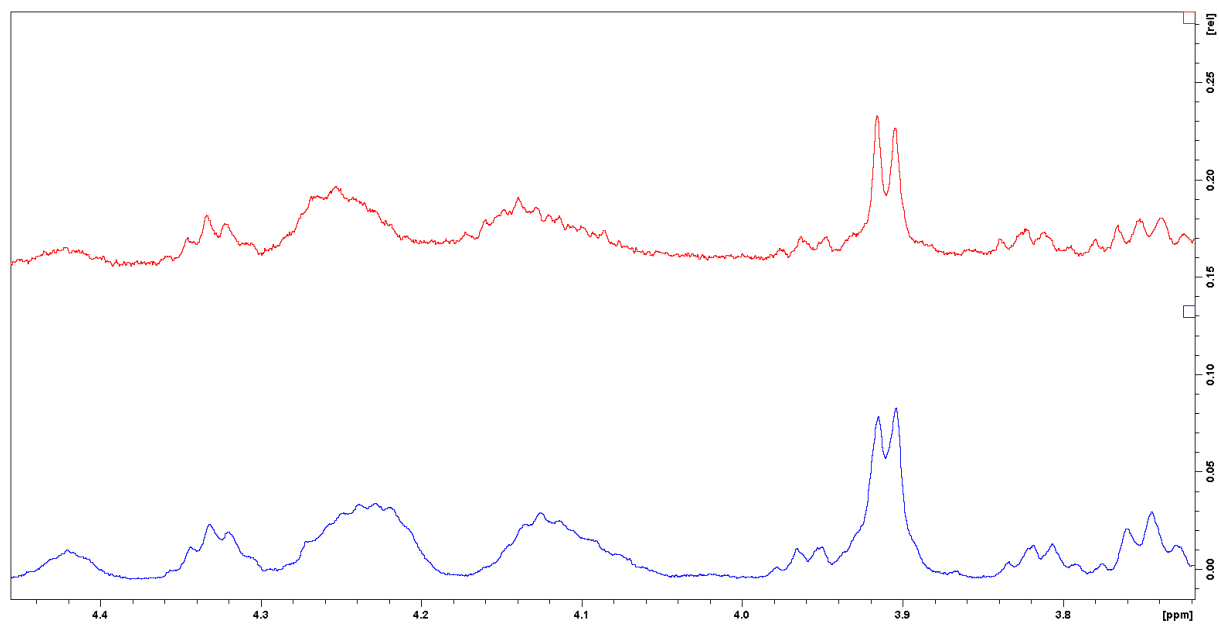|			
	β	20.4	1.67
	γ	18.0	1.26
	δ	27.0	1.49
	ε	39.2	2.72
	NH$_2$	--	7.63
	C=O	--	--
MeOAsp9	NH	--	7.78
	α	56.0	4.73
	β	71.5	4.38
	OMe	58.9	3.32
	C=O	--	--
	COOH	--	--
Gly10	NH	--	7.93
	α	42.6	3.66,3.74
	C=O	--	--
D-Asn11	NH	--	8.02
	α	50.3	4.55
	β	37.7	2.54, 2.39
	CONH$_2$	--	6.90, 7.32
Glu 12	NH	--	7.94
	α	52.8	4.39
	β	27.9	1.90,1.72
	γ	30.3	2.21
	C=O	--	--
	COOH	--	--
Kyn13	NH	--	8.11
	α	54.5	4.72
	β	40.3	3.58,3.34
	1 (NH$_2$)	--	7.00
	2	--	--
	3	117.4	6.75
	4	134.9	7.23
	5	114.9	6.53
	6	131.7	7.74
	7	--	--
	C=O	--	--
(±)-Methyl-Decanoic tail	--	--	--

Figure H.16. ^{1}H NMR spectra of **10.9** derived from PG isolated from BLS (red, top). ^{1}H NMR spectra of **10.9** synthesized via the pathway outlined in Scheme 10.3 (blue, bottom). Both of these traces agree with the sn-3,1' configuration.[355]
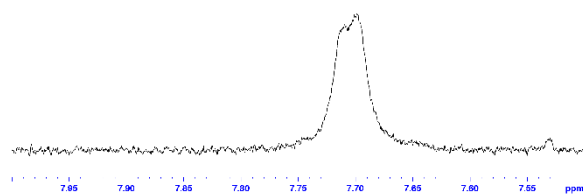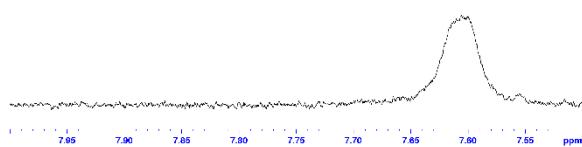
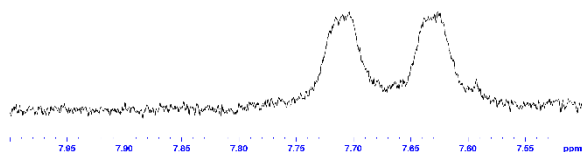Figure H.17 ^{1}H NMR of chiral boronic esters **10.16** formed with BLS PG and (A) **R-10.15** (B) **S-10.15** (C) **10.15**